Proceedings of the ACI-KC Second International Conference, March 12-14, 2007, Kuwait

# **Design and Sustainability**of Structural Concrete in the Middle East with Emphasis on **High-Rise Buildings**

## **Edited by:**

Moetaz M. El-Hawary Naji Al-Mutairi Khaldoun N. Rahal Hassan Kamal

# Organized by:

American Concrete Institute – Kuwait Chapter (ACI-KC)

# Sponsored by:

Kuwait Society of Engineers (KSE) Kuwait Foundation for the Advancement of Sciences (KFAS)

# Co-sponsored by:

Bubiyan Ready-Mix Kuwait University Kuwait Institute for Scientific Research Gulf Consult, Kuwait Kuwait Portland Cement Company American Concrete Institute, International



# **Organizing Committee**

Dr. Naji M. Al-Mutairi (Chairperson)

Prof. Moetaz El-Hawary

Eng. Ebtisam AlKazemi

Mr. Abdul Wahab Rumani

### **Scientific Committee**

Prof. Moetaz El-Hawary (Chairperson)

Dr. Naji M. Al-Mutairi

Dr. Khaldoun Rahal

Dr. Hassan Kamal

# **Advisory Committee**

Prof. M. Naseer Haque

Prof. Amr W. Sadek

Dr. Mohamed Terro

Dr. Saud Al-Otaibi

Copyright © 2007 American Concrete Institute – Kuwait Chapter

All rights reserved. No part of this publication may be reproduced, stored in a retrieval system, or transmitted in any form or by any means, electronic, mechanical, photocopying, recording or otherwise, without the prior written permission of the publisher.

ACI Kuwait Chapter

PO Box 12608, Shamiah 71657, Kuwait

Tel: 2448975 Ext. 312 Fax: 2428148 (Attn: ACI)

info@acikuwait.com www.acikuwait.com

## TABLE OF CONTENTS

Preface	Page No.
Acknowledgements	viii
Keynote Papers	
"Fiber Reinforced Concrete: State of Progress at the Edge of the New Millennium" Prof. Antoine E. Naaman, University of Michigan, Ann Arbor, USA	1
"High Performance Material Applications in Civil Engineering" Prof. Issam E. Harik, University of Kentucky, USA	29
Session 1	
"Comparative Seismic Assessment of Multi-Story Buildings Designed to Latest Design Provisions"	43
Aman Mwafy, University of Illinois at Urbana-Champaign, Illinois, USA	
"Nonlinear Seismic Interaction Behavior of Shear Wall-Frame with Different Stiffness Ratio of Wall and Frame"  A. R. Khaloo, Sharif University of Technology, Tehran, Iran S. A. Taheri, Sharif University of Technology, Tehran, Iran	57
"Top to Toe Mitigation of Progressive Collapse in High Rise Buildings" Fouad A. Kasti, Dar Al-Handasah, Beirut, Lebanon	65
"Response of Upgraded Reinforced Concrete Buildings to Dynamic Lateral Loads" Adnan S. Masri, Beirut Arab University, Lebanon Hisham S. Basha, Beirut Arab University, Lebanon Ziad M. Mousa, Beirut Arab University, Lebanon	77
Session 2	
"Multi-resolution Distributed FEM Simulation of Reinforced Concrete High-Rise Buildings"  Jun Ji, University of Illinois at Urbana-Champaign, Illinois, USA Oh-Sung Kwon, University of Illinois at Urbana-Champaign, Illinois, USA Amr S. Elnashai, University of Illinois at Urbana-Champaign, Illinois, USA Daniel A. Kuchma, University of Illinois at Urbana-Champaign, Illinois, USA	89
"Design and Evaluation of Reinforced Concrete Frames Infilled with Masonry Walls" Ghassan K. Al-Chaar, University of Illinois, USA.	101
"Simplified Method Analysis and Design of Biaxially Loaded Reinforced Concrete Columns"  K. Demagh, University of Batna, Algeria A Chateauneuf University BlaisePascal Clermont France	113

Hisham S. Basha, Beirut Arab University, Lebanon Adnan C. Masri, Beirut Arab University, Lebanon Mohammad A. Sabra, Beirut Arab University, Lebanon	125
"Achieving a Longer Service Life with Durability Modelling" Robert David Hossell, Grace Construction Products, Dubai, UAE	137
Session 3	
"On Flexural Strength and Permeability of Recycled Concrete as Coarse Aggregates" Nayef Z. AlMutairi, Kuwait University, Kuwait Abdullateef M. AlKhaleefi, Kuwait University, Kuwait	153
"Effect of Variant in Concrete Cover and Percentage of Steel Reinforcement on Residual Load Capacity for Reinforced Concrete Columns Exposed to Fire"  M. A. A. El Aziz, Fayoum University, Fayoum, Egypt K. M. Othman, Fayoum University, Fayoum, Egypt A. A. Shahin, Fayoum University, Fayoum, Egypt A. Serag. Fayoum University, Fayoum, Egypt	163
"Evaluation of the Fire Resistance of GFRP Reinforced Concrete Flexural Elements" Moetaz M. El-Hawary, Kuwait Institute for Scientific Research, Kuwait. Amr W. Sadek, Kuwait Institute for Scientific Research, Kuwait. Amr S. El-Deeb, Ain Shams University, Cairo, Egypt.	179
Session 4	
"Improvement in Durability of Concrete with Partial Replacement of Cement by Ground Granulated Blast Furnace Slag"  Saud Al-Otaibi, Kuwait Institute for Scientific Research, Kuwait  Moetaz El-Hawary, Kuwait Institute for Scientific Research, Kuwait  Ali Abdul-Jaleel, Kuwait Institute for Scientific Research, Kuwait	193
"Half-Cell Potential Measurements in Self-Consolidating Concrete" Farzad Arabpour Dahooei, Concrete Research & Education Center (ConREC), Iran A. Maghsoudi, Kerman University, Iran F. Faraji, Kerman University, Iran	201
"Application of High-Strength and Corrosion-Resistant ASTM A1035 Steel Reinforcing Bar in Concrete High-Rise Construction"  S. Faza, MMFX Technologies Corporation, Irvine, California, USA J. Kwok, MMFX Technologies Corporation, Irvine, California, USA O. Salah, Zamil Holding Group, Saudi Arabia	211
"Maximum Allowable In-Plane Shear Stresses in Reinforced Concrete Membrane Elements"  Dr. Khaldoun N. Rahal, Kuwait University, Kuwait	219
"Effect of Unprocessed Steel Slag on the Strength of Concrete when Used as Fine Aggregate"  Hisham Qasrawi, The Hashemite University, Jordan Faisal Shalabi, The Hashemite University, Jordan Ibrahim Asi, The Hashemite University, Jordan	227

# **Session 5**

"Flexural and Shear Behavior of RC Beams Strengthened with CFRP Strips or Mat" Seleem S. E. Ahmad, Zagazig University, Egypt	239
"Repair Work at the Tower-Concrete Structure on the Batllava Lake" Naser Kabashi , Prishtine, Kosovo Cene Krasniqi, Prishtine, Kosovo Fisnik Kadiu, Tirane, Albania	249
"Repairs and Rehabilitation of Town Hall-Calcutta" S.K. Manjrekar, Sunanda Speciality Coatings Pvt. Ltd. Mumbai, India R.S. Manjrekar, Sunanda Speciality Coatings Pvt. Ltd. Mumbai, India	259
"Enhancing the Structural Behavior of Reinforced Concrete Beams Using FRP Systems" Hisham Abdel-Fattah, University of Sharjah, Sharjah, UAE Sameer Hamoush, North Carolina A&T State University, North Carolina, USA	279
Session 6	
"The Behavior of Geopolymer Paste and Concrete at Elevated Temperatures"  B. Toumi, University of Ouem El Bouaghi, Algeria  Z. Guemmadi, University of Constantine, Algeria  H. Houari, University of Constantine, Algeria  H. Chabil, University of Constantine, Algeria	291
"Mechanical Properties of Recycled Aggregate Concrete" Dr. Khaldoun Rahal, Kuwait University, Kuwait	299
"Properties of Recycled Aggregate Concrete" Ali Al-Harthy, Sultan Qaboos University, Oman Ramzi Taha, Sultan Qaboos University, Oman Abdullah Al-Saidy, Sultan Qaboos University, Oman Salim Al-Oraimi, Sultan Qaboos University, Oman	309
"Sustainability - A Duty and Science in the Concrete Industry" O. Kayali, University of New South Wales, Australia M.N. Haque, Kuwait University, Kuwait	319
Session 7	
"Use of Limestone's Filler to Improve the Quality of Algerian Concretes and Cement Paste"  Z. Guemmadi, University of Constantine, Algeria G. Escadeillas, LMDC INSA-UPS Toulouse, France B. Toumi, University of Ouem El Bouaghi, Algeria H. Houari, University of Constantine, Algeria	335
"Influence of Different Admixtures on the Mechanical Behavior of Two-Stage (Pre-Placed Aggregate) Concrete"  Hakim S. Abdelgader, Al-Fateh University, Libya Ahmed E. Ben-Zeitun, Al-Fateh University, Libya Abdurrahman A. Elgalhud, Al-Fateh University, Libya	347

"Recent Practices of Analysis and Design of High-Rise Buildings in Kuwait (Case	359
Study)"	
Tarek Anwar Awida, Ain Shams University, Cairo, Egypt	
"Shear Strengthening of Reinforced Concrete Beams Using Near-Surface Mounted	371
Conventional Reinforcing Bars and CFRP Rods"	3/1
Khaldoun N. Rahal, Kuwait University, Kuwait	
Khaldouh N. Kahai, Kuwah Oliversity, Kuwah	
"Modeling of Cost-Effective Residential Houses in Kuwait"	381
H. Kamal, Kuwait Institute for Scientific Research, Kuwait	
S. Al-Sanad, Kuwait Institute for Scientific Research, Kuwait	
S. Al-Otaibi, Kuwait Institute for Scientific Research, Kuwait	
S. Al-Fulaij, Kuwait Institute for Scientific Research, Kuwait	
• ,	
List of Authors	390

#### **Preface**

Construction is booming in the Middle East and a large number of high-rise buildings are being constructed everyday. In the meantime, the concrete quality needs attention due to the weather conditions and the quality of the work force in the construction industry.

The ACI-KC has the responsibility to improve the local concrete practices and spread awareness of the best techniques that suit our local environment and quality of work force. We encourage technical forums that serve as a platform to exchange experiences and find sound engineering solutions to our specific local problems. We feel that it is our duty to spread knowledge to improve concrete practice and serve our community.

ACI-KC organized the first international conference from September 28-October 1, 2003. The theme of the conference was selected based on the most relevant topic to this region, *Concreting and High Performance Concrete in Hot Weather*. Twenty-five technical papers were presented at the conference.

The second ACI-KC international conference on Design and Sustainability of Structural Concrete in the Middle East with Emphasis on High-Rise Buildings took place on March 12-14, 2007 in Kuwait. The topics covered by the conference include:

- Sustainable Building Materials
- Recycling of Building Materials
- Management and Utilization of Natural Resources
- Design Aspects of Sustainability
- Codes Related to Design and Sustainability
- Maintenance and Repair of Structures
- Durability and Long-lasting Structures and High-Rise Buildings
- Sustainability and Durability of Concrete
- Sustainability and High-Rise Buildings
- Sustainability in Hot Weather

A total of thirty two technical papers from thirteen different countries were accepted for presentation at the conference and are included in the proceedings.

ACI-KC hopes that this document adds to the technical knowledge in the theme of this conference. We look forward to the readers' constructive comments and feedback to improve our future activities.

Dr. Naji M. Al-Mutairi, Chairperson ACI-KC Second International Conference

# Acknowledgement

The success of this conference is attributable to the organizing and scientific committees and the support of ACI-KC Board of Direction. To insure a successful event, members of the committees contributed enthusiastically to the various aspects of the organization of the conference activities for over fourteen months. Without their active participation, determination and dedication, it would not be possible to organize the conference.

ACI-KC highly appreciates the encouragement and help of the Kuwait Society of Engineers' President Eng. Talal Al-Qahtani, Past President Eng. Adel Al-Kharafee, General Manager Eng. Ahmed Al-Dowsari, Eng. Hamoud Al-Zabee and several other colleagues at the society.

We express our deep appreciation to the keynote speakers, the chairpersons of the scientific sessions as well as the distinguished speakers and participants for the effort and contributions they made during the conference activities. Particular thanks are extended to AlKhansaa Al-Hussaini, Melita Alvares, Sheba Mathews, Sunita D'Souza and Nadia Masri for all the assistance provided towards the administrative activities of the conference.

Finally, we wish to extend special thanks to the sponsors of this conference, Kuwait Society of Engineers and Kuwait Foundation for the Advancement of Sciences. The support of the co-sponsors, Bubiyan Ready-Mix, Kuwait University, Kuwait Institute for Scientific Research, Gulf Consult, Kuwait Portland Cement Company and ACI-International is also gratefully acknowledged.

Dr. Naji M. Al-Mutairi, Chairperson ACI-KC Second International Conference

# Fiber Reinforced Concrete: State of Progress at the Edge of the New Millennium

Antoine E. Naaman

Professor of Civil Engineering University of Michigan, Ann Arbor, U.S.A.

email: naaman@engin.umich.edu

#### **Abstract**

The main purpose of this paper is to set the stage, at the beginning of this 21<sup>st</sup> century, for the state of progress in fiber reinforced concrete and, generally, fiber reinforced cement composites. Although fibers have been used in building materials for almost three millennia, the first use of fibers in cement matrices happened only in 1874. Following a dormant period of almost one century, fiber reinforced concrete took off in the early 1960's at a very accelerated pace. The past four decades mark the modern development and broad expansion of fiber reinforced concrete, which led to extensive applications and market penetration worldwide today. Such a success is due in part to significant evolution in the fiber reinforcement, the cementitious matrix, the interface bond between fiber and matrix, fundamental understanding of the mechanics of the composite, and improved cost-effectiveness. Following a brief introduction and definition of fiber reinforced cement composites, conventional (or strain-softening) and high performance (or strain-hardening) FRC composites are addressed. progress in cement matrices and fibers are described, and the key mechanical variables that control composite behavior are explained. Possible near future advances in the use of micro-fibers, fibers with improved interface bond, fabrication processes, and the transition in the function of fiber reinforced concrete from an engineering material to a structural material, are presented. It is concluded that, while stand-alone structural elements using only fiber reinforced concrete can be conceptually built today, such applications are likely to become routine before the end of this century. With the increasing availability of high performance fiber reinforced cement composites, the dream that started more than a century ago, to mix fibers in concrete, like sand or gravel, to achieve a stand-alone structural material is closer today than ever before.

**Note:** This paper was first presented at the 9<sup>th</sup> International Conference on Concrete Engineering and Technology, Concet 2006, (Structural Concrete for the Millennium), Kuala Lumpur, Malaysia, May 2006, and published in the corresponding proceedings by the Institute of Engineers, Malaysia.

#### Introduction

Fiber reinforced cement-based composites have made striking advances and gained enormous momentum since their modern introduction in civil engineering applications during the 1960's. This is due in particular to several developments involving the matrix, the fiber, the fiber-matrix interface, the composite production process, a better understanding of the fundamental mechanisms controlling their particular behavior, and improved cost-effectiveness. Examples of development include:

- 1. The increasing availability for use in concrete of fibers of different types and properties which can add significantly to the strength, ductility, and toughness of the resulting composite.
- 2. The commercial introduction of a new generation of additives (superplasticizers) which allow for high matrix strengths to be readily achieved with little loss in workability.
- 3. The increasing use of active or inactive micro-fillers such as silica fume and fly ash and a better understanding of their effect on matrix porosity, strength, and durability.
- 4. The use of polymer addition or impregnation of concrete which adds to its strength and durability and also enhances the bond between fibers and matrix, thus increasing the efficiency of fiber reinforcement.
- 5. Some innovations in production processes (such as self-consolidation or self-compacting) to improve uniform mixing of high volumes of fiber with reduced effects on the porosity of the matrix. Substantial progress has also been made in modeling the behavior of these composites. A large number of technical studies have been published. Only few particular references are given at the end of this paper.

The attribute "high performance" implies an optimized combination of properties but is limited in this chapter to the particular class of FRC composites that shows strain-hardening behavior in tension after first cracking, accompanied by multiple cracking up to relatively high strain levels [14]. This definition is further explained below in Section 4.

#### **Definition: Fiber Reinforced Cement (FRC) Composites**

For practical purposes and mechanical modeling, fiber reinforced cement (FRC) or concrete composites are generally defined as composites with two main components, the fiber and the matrix (Fig. 1). While the cementitious matrix may itself be considered a composite with several components, it will be assumed to represent, in the context of this paper, the first main component of the composite. The fiber represents the second main component. The fiber is assumed to be discontinuous and, unless otherwise stated, randomly oriented and distributed within the volume of the composite. Both the fiber and the matrix are assumed to work together, through bond, providing synergism for an effective composite. Thus bond is an implied necessary element for the success of the composite. The matrix, whether it is a paste, mortar, or concrete is

assumed to contain all the aggregates and additives specified. Air voids entrapped in the matrix during mixing are assumed to be part of the matrix.

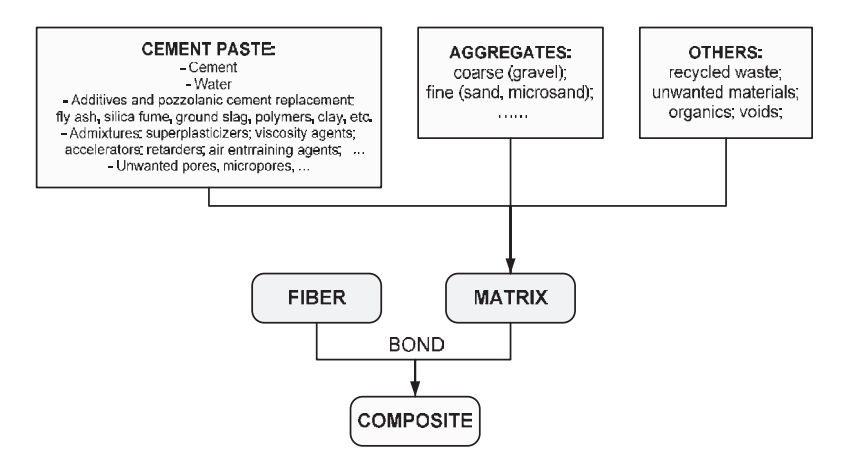


Fig. 1. Composite model considered as a two-component system, (fiber and matrix).

#### **Cement Matrices and Fibers for FRC Composites**

#### Cement or Cementitious Matrices

Cement-based matrices have evolved enormously since the 1960's in particular due to a better understanding of their microstructure and the influence of packing and porosity, as well as the development of mineral and chemical additives to achieve a number of particular properties. Typically, the matrix for fiber reinforced cement composites can be a cement paste, a mortar (that is, essentially a paste with sand), or a concrete (that is, essentially a mortar with coarse aggregates or gravel) (Fig. 1). The cement paste is made of cement and water, and may contain additives, which can be mineral (such as fly ash) or chemical such as air entraining admixtures. The paste itself can be made to have low viscosity, be stiff like clay, or to flow like a liquid; in the latter case, the term slurry or slurry paste is often used to describe the matrix.

The cement powder, which reacts with water to eventually leads to the binder and hardened matrix, may be blended, that is, containing supplementary cementitious materials, such as flash ash, ground furnace slag, micro-silica, and the like (Fig. 1). Indeed, mineral components such as silica fume and fly ash are now commonly used either as additives, to or as replacement of cement. They help provide a denser composite, reduce porosity, improve fresh properties, improve strength, corrosion resistance and durability, control the hydration reaction, etc. Chemical admixtures, such as water-reducing agents, superplasticizers, and viscosity agents, help control and improve a host of other properties in the fresh state to help in the fabrication and manufacturing phase. Today, self-consolidating and self-compacting cementitious mixtures allow us to rethink construction procedures for fiber reinforced cement

composites. Such mixtures, for instance, allow us to use fiber reinforced concrete in congested areas of reinforced concrete structures such as in beam column connections, coupling beams and the like, without losing the penetrating and encapsulating function of the matrix [24, 27 and Chapter 8 of Ref. 13].

The relative cost of the matrix in fiber reinforced cement composites, even when improved with relevant additives, decreases (in comparison to the cost of the fiber) with an increase in fiber content. This is particularly true for high performance fiber reinforced cement composites where the fiber content is relatively high. For instance, in the case of steel fiber reinforced concrete with conventional hooked steel fibers, the cost of the fiber at 2% fiber content by volume may range from about 5 to 15 times the cost of the concrete matrix. Therefore, there is advantage in utilizing the best possible matrix for the conditions of use of the final structure.

The reader may want to refer to a paper parallel to this one at the Concet 6 International Conference, by Prof. C.T. Tam titled "Evolving Concrete for the Millennium" where the main developments in the concrete matrix are reviewed.

#### Fibers for Cement and Concrete Matrices

Short discontinuous fibers used in concrete can be characterized in different ways (Fig. 2). First, according to the geometric properties of the fiber such as length, diameter or perimeter, cross-sectional shape, and longitudinal profile. Second, according to their mechanical properties such as tensile strength, elastic modulus, stiffness, ductility, elongation to failure, surface adhesion property, etc. Third, according to their physical/chemical properties such as density, surface roughness, chemical stability, non-reactivity with the cement matrix, fire resistance or flammability, etc. Fourth, according to the fiber material such as natural organic (i.e., cellulose, sisal, jute, bamboo, etc.); natural mineral (i.e., asbestos, rock-wool, etc.); or man-made (i.e., steel, titanium, glass, carbon, polymers or synthetic, etc). All attributes can be important, some more than others, depending on the application.

Once a fiber material has been selected, such as steel fiber, an infinite combination of geometric properties related to its cross sectional shape, length, diameter or equivalent diameter, and surface deformation can be selected [16]. The cross section of the fiber can be circular, elliptical, rectangular, diamond, square, triangular, flat, polygonal, or any substantially polygonal shape. To develop better bond between the fiber and the matrix, the fiber can be modified along its length by roughening its surface or by inducing mechanical deformations. Thus fibers can be smooth, indented, deformed, crimped, coiled, twisted, with end hooks, end paddles, end buttons, or other anchorage system. Typical examples of steel fibers are shown in Fig. 3. In some fibers the surface is etched or plasma treated to improve bond at the microscopic level. Some other types of steel fibers such as ring, annulus, or clip type fibers (Fig. 3b) have also been used and shown to significantly enhance the toughness of concrete in compression; however, work on these fibers did not advance beyond the research level.

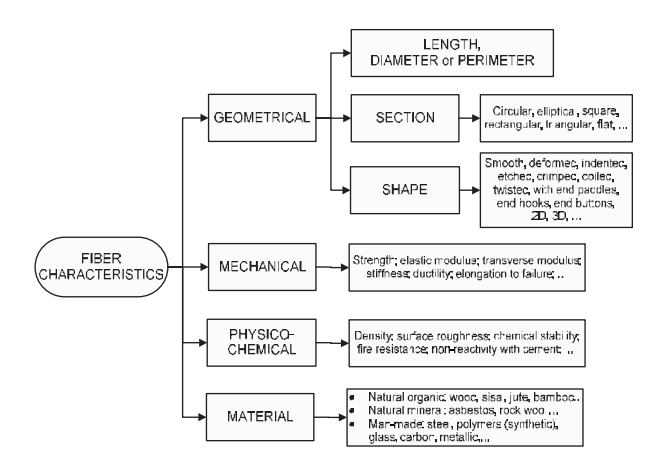


Fig. 2. Main fiber characteristics of interest in fiber reinforced cement composites.

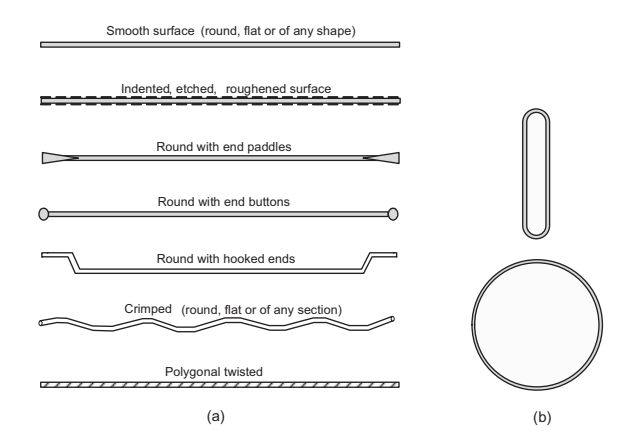


Fig. 3. (a) Typical profiles of steel fibers commonly used in concrete (twisted fiber is new); (b) Closed-loop fibers tried in some research studies.

Table 1. Typical Properties of Some Fibers used in FRC Composites

Material	Specific Gravity (1 for water)	Tensile Strength MPa	Tensile Modulus GPa	Remark
Steel	7.8	Up to 3500	200	The elastic modulus of steel is almost independent of its tensile strength. Yield strength of steel fibers varies widely depending on the fabrication process. The higher the strength the lower the strain capacity to failure.
E-Glass	2.6	Up to 3500	76	Modulus of glass can vary from 33 GPa for A-Glass to 98 GPa for S-Glass. While filament strength remains high from 3300 to 4800 MPa, the strength of a fiber bundle, which is made from a large number of filaments, will have much lower equivalent tensile strength.
Carbon	1.8	Up to 4500	100 to 300	Depending on grade and fabrication, such as pitch carbon or PAN carbon, significantly different properties can be achieved.
Kevlar	1.44	2800	124	Kevlar is a trade name of Dupont. The fiber material source is aramid. Aramid fibers have properties similar to Kevlar.
Spectra	0.97	2585	117	Spectra is a trade-name. The material is an ultra-high molecular weight polyethylene, also termed high performance polyethylene (HPPE). Other similar branded fiber includes: Dyneema.
PVA (PolyVinyl Alcohol)	1.31	880-1600	25 to 40	A large variety of fibers exists with a wide range of tensile strengths and moduli. The higher the diameter, the lower the properties.
PP (Poly- Propylene)	0.91	Up to 800	Up to 10	Strength and modulus depend on the manufacturing process, and heat stretching leading to highly oriented long-chain molecules.

Similar to the geometric properties, a wide variety of fiber materials and corresponding mechanical properties exists. The fibers most commonly used in cement composites at the time of writing this paper are listed in Table. 1 and a range of values is given for

their tensile strength and elastic modulus. While fibers can have equal tensile strengths, the higher modulus fibers are generally more effective for normal weight cement matrices.

#### Microfibers

Short microfibers of carbon, glass, Kevlar, polypropylene, PVA or other polymeric materials are becoming increasingly available for use in cement composites (Table 1). Microfibers offer very large numbers of fibers per unit volume; they induce microtoughness, reduce the size (width and length) of microcracks, and generally improve the tensile strength at cracking (or proportionality limit) of the composite. As fine grain matrices with microfibers can be used to produce manufactured products, the machineability of the product is improved. The use of very fine grain matrices reinforced with short microfibers or combinations of micro- and macro-fibers, in stand-alone applications such as small manufactured products is likely to expand. Figure 4 shows typical examples of macro- and micro-fibers.

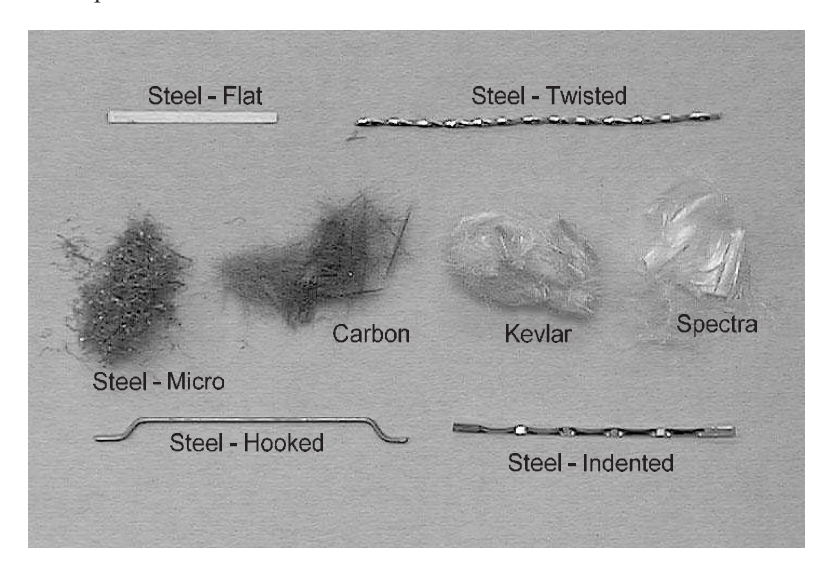


Fig. 4. Photograph illustrating typical fibers and micro-fibers used in cement composites. For scale: the hooked fiber is 30 mm long and 0.5 mm in diameter.

#### Current Range of Fiber Geometric Properties

Most common steel fibers are round in cross-section, have a diameter ranging from 0.3 to 0.8 mm, and a length ranging from 25 to 80 mm. Their aspect ratio, that is, the ratio of length over diameter or equivalent diameter, is generally less than 100, with a common range from 40 to 80. Steel fiber diameters as low as 0.1 mm are available but are much more costly than larger diameter fibers. The length and diameter of synthetic fibers vary greatly. Single filament fibers can be as little as 10 micrometers in diameter such as for Kevlar or carbon fibers, and as large as 0.8 mm such as with some

polypropylene or poly-vinyl-alcohol (PVA) fibers. Generally in concrete applications, the aspect ratio of very fine fibers exceeds several hundred while that of coarser fibers is less than 100. Most synthetic fibers (glass, carbon, Kevlar) are round (or substantially round) in cross section; flat synthetic fibers cut from plastic sheets and fibrillated are suitable when very low volume content is used such as for the control of plastic shrinkage cracking of concrete.

#### **High Performance Fiber Reinforced Cement Composites (HPFRCC)**

Generally the attribute "advanced" or "high performance", when applied to engineering materials, is meant to differentiate them from the conventional materials used, given the available technologies at the time and geographic location considered for the structure. It also implies an optimized combination of properties for a given application and should be generally viewed in its wider scope. Combined properties of interest to civil engineering applications include strength, toughness, energy absorption, stiffness, durability, freeze-thaw and corrosion resistance, fire resistance, tightness, appearance, stability, constructability, quality control, and last, but not least, cost and user friendliness.

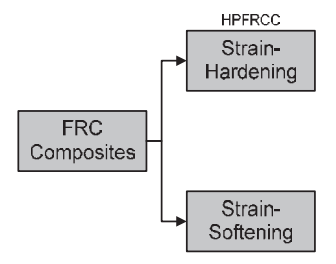


Fig. 5. Simplified general classification of FRC composites based on their tensile stress-strain response.

One approach followed by the author to define whether a fiber reinforced cement composite qualifies as "high performance", is based on the shape of its stress-strain curve in direct tension, that is, whether it can be described as 'strain-hardening" or "strain-softening," as illustrated in Fig. 5. If the stress-strain curve shows strain hardening (or pseudo-strain hardening) behavior such as in Figs. 6b and 7b, then the attribute "high performance" is used [11, 14]. This is equivalent to saying that the shape of the stress-strain curve in tension is at least elastic-plastic or better. Five international symposia have taken place using such a definition [13, 19, 21, 22, 29, 30]. Strain-hardening behavior is a very desirable property; it is generally accompanied by multiple cracking and induces a large energy absorption capacity.

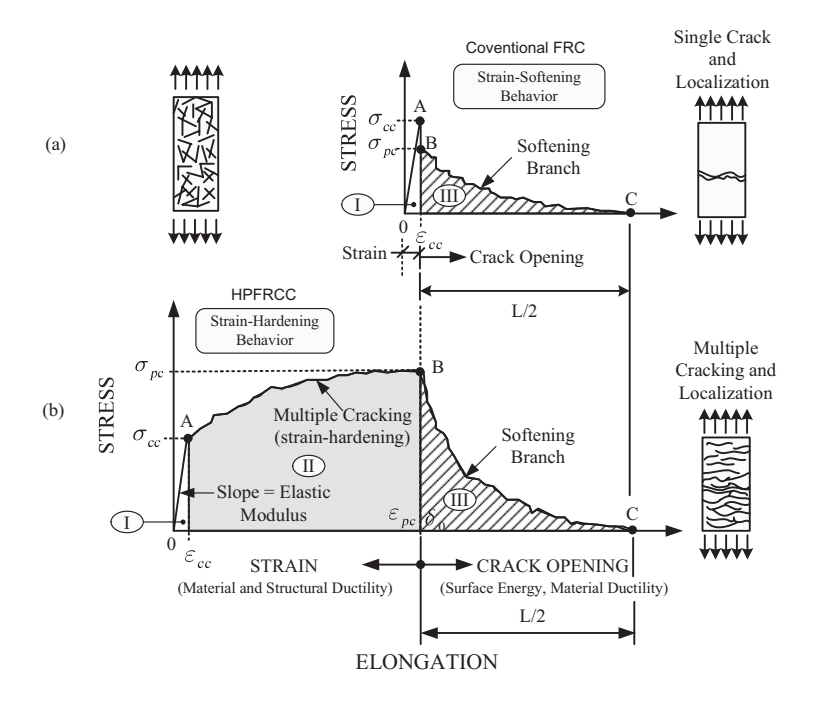


Fig. 6. Typical stress-strain or elongation curve in tension up to complete separation. (a) Conventional strain-softening FRC composite; (b) Strain-hardening FRC composite or HPFRCC [18, 20].

Typically the stress-strain curve of an HPFRC composite (Fig. 6b and 7b) starts with a steep initial ascending portion up to first structural cracking (part I), followed by a strain-hardening branch where multiple cracking develops (part II). The point where first structural cracking occurs is characterized by its stress and strain coordinates ( $\sigma_{cc}$ ,  $\varepsilon_{cc}$ ); the peak point at the end of the strain-hardening branch leads to the maximum post-cracking stress and strain ( $\sigma_{pc}$ ,  $\varepsilon_{pc}$ ). At the peak point, one crack becomes critical defining the onset of crack localization (part III of Fig. 6b); thereafter, the resistance starts dropping; no more cracks can develop and only the critical crack will open under increased straining. Other cracks will gradually unload or become narrower in width.

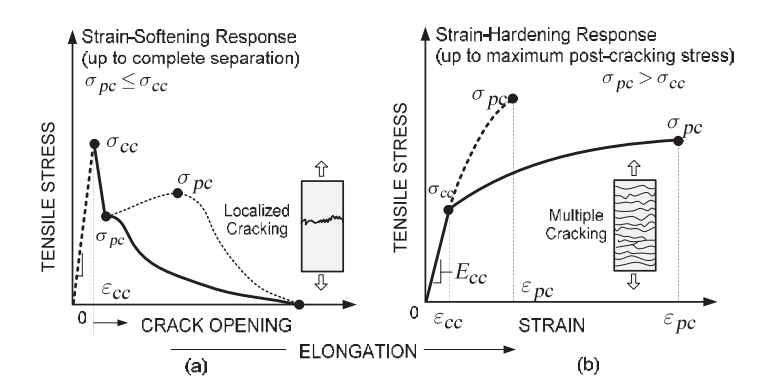


Fig. 7. Typical stress-elongation curves in tension of fiber reinforced cement composites. (a. Strain-softening behavior; (b) Strain-hardening behavior (HPFRCC).

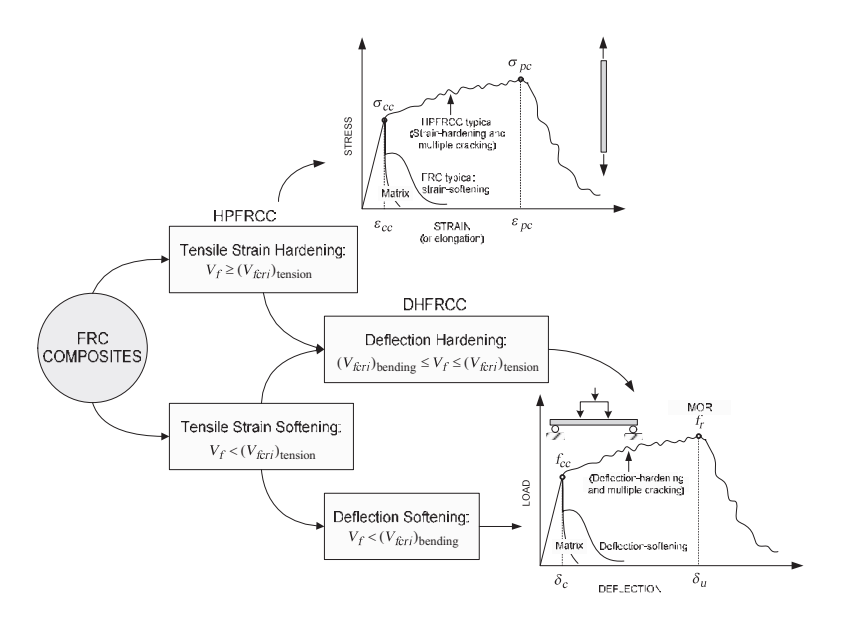


Fig. 8. General classification of FRC composites: ongoing current approach [22, 25].

Following the peak point (Fig. 6b), there is generally a descending branch, which corresponds mainly to the load versus opening of the critical crack (part III). Along that branch fibers can pull-out, fail, or a combination of these phenomena may occur. Also, the cement matrix may partly contribute along that part of the curve up to a certain crack opening.

The stress-strain curve of a conventional strain-softening FRC composite (Fig. 6a and 7a) would start the same way as for a high performance FRC composite; however it will have localization occurring immediately following first cracking; no strain-hardening and multiple cracking occur. After localization the descending branch follows a pattern similar to that of a HPFRC composite.

The classification suggested in Fig. 5 is further extended in Fig. 9 to include behavior of the FRC composite in bending [22, 25]. It is observed that some tension strainsoftening composites can be deflection-hardening while all strain-hardening composites are deflection-hardening as well. It is easier to develop a deflection-hardening composite than a tension strain-hardening one and this is clarified in the next section.

# Composite Mechanics: Fundamental Result on Critical Volume Fraction of Fibers and Other Important Causal Variables

The mechanics of fiber reinforcement of cement matrices can be quite complex whether conventional mechanics or fracture mechanics or damage mechanics approach is used. For the purpose of explaining most common constraints on the behavior of the composite, the results of composite mechanics approach are used next. They best illustrate the importance of causal variables and the trade-offs needed to develop a high performance composite.

#### Strain-Hardening Composite

Prediction equations for the first cracking stress and maximum post-cracking strength (Figs. 6 and 7) of a fiber reinforced cement composite exists essentially since the early 1970's but with slightly modified coefficients [9, 10, 11, 14]. A first attempt to define the condition leading to strain-hardening behavior and multiple cracking in tension was suggested by Naaman in 1987, by setting that the maximum post-cracking stress must be larger than the stress at first cracking [11]. For circular fiber, it led to the following condition on the minimum value of volume fraction of fibers:

$$V_f \ge (V_f)_{cri-ten} = \frac{1}{1 + \frac{\tau}{\sigma_{mu}} \frac{L}{d} (\lambda - \alpha)}$$
 (1)

where:

d = fiber diameter, assuming circular fiber

L = fiber length

L/d = aspect ratio of fiber

 $V_f$  = volume fraction of fibers

 $(V_f)_{cri-ten}$  = critical volume fraction of fibers needed to achieve strain-hardening behavior in tension

product of a number of coefficients dealing with orientation effects,
 distribution, extent of bond mobilized at cracking,...

product of a number of coefficients dealing with orientation efficiency, distribution, expected pull-out length, etc... in the cracked state of the composite

= bond strength at the fiber-matrix interface assumed to be a constant over a minimum slip

 $\sigma_{mu}$  = tensile strength of matrix

τ

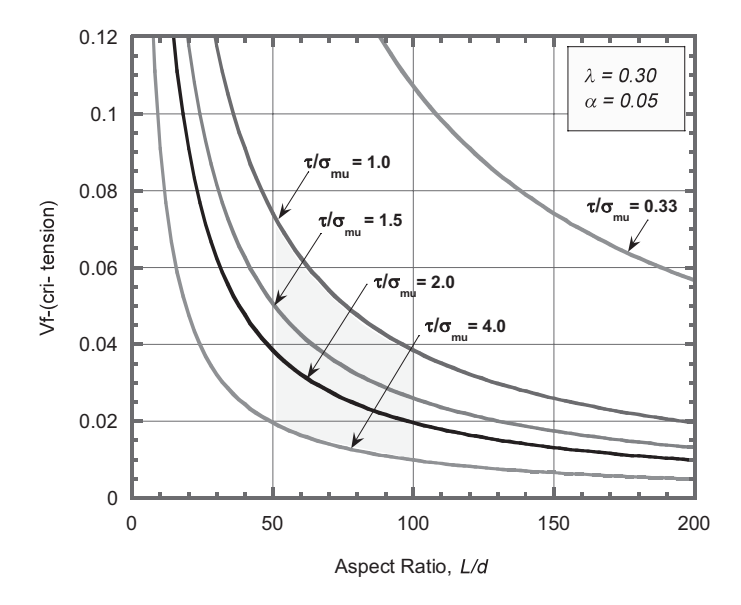


Fig. 9. Example illustrating the critical volume fraction of fibers to achieve strain-hardening behavior in tension.

Figure 9 initially developed in Refs. [11 and 14] illustrates the variation of the critical volume fraction of fiber,  $(V_f)_{cri-ten}$ , versus the aspect ratio of the fiber, L/d, at different values of the ratio of bond strength to tensile strength of the matrix,  $\tau/\sigma_{mu}$ . An estimated value of  $\lambda=0.30$  and  $\alpha=0.05$  for steel fibers is assumed for the numerical results (Eq. 1). Similar figures can be developed for different values of  $\lambda$  and  $\alpha$ . Each curve in Fig. 9 defines a boundary of feasibility above which strain-hardening behavior (such as in Fig. 6b) can be achieved. If, for instance, we assume steel fibers and a value  $\tau/\sigma_{mu}=2$ , Fig. 9 indicates that in order to achieve strain hardening behavior in tension, the volume fraction of fibers needs to exceed about 2% at an aspect ratio of 100, and 4%

at an aspect ratio of 50. These values are almost doubled at  $\tau/\sigma_{mu}=1$ . It is clear that in the range of aspect ratios common for steel fibers for concrete (that is, L/d=50 to 100) one needs a high value of  $\tau/\sigma_{mu}$  in order to actually manufacture a strain hardening fiber reinforced concrete composite. Since it is very hard in the field to mix more that 2% to 3% steel fibers by volume into a concrete mix, the importance of the ratio  $\tau/\sigma_{mu}$  can be easily appreciated from the figure. The figure also illustrates the main causal variables that seem to control the behavior of the composite, namely, the volume fraction of fiber, the aspect ratio of fiber, the bond strength at the fiber matrix interface, and the tensile strength of the matrix. The tensile strength and elastic modulus of the fiber are assumed sufficiently large.

#### **Deflection-Hardening Composite**

In a derivation similar to the one leading to the critical volume fraction of fibers to insure strain hardening behavior, the author has developed an expression leading to the critical volume fraction of fibers for which deflection-hardening is insured [18, 20]. Deflection-hardening implies that the maximum equivalent elastic bending stress (or modulus of rupture, MOR) is larger than the stress at first cracking in bending, and that multiple cracking would generally occur after first cracking. The following solution was obtained:

$$V_{f} \ge (V_{f})_{cri-bending} = \frac{k}{k + \frac{\tau}{\sigma_{mu}} \frac{L}{d} (\lambda - k\alpha)}$$
(2)

where the notation is same as above, and k is a coefficient less than 1. A value of k = 0.4 is recommended for practical applications of steel fiber reinforced concrete.

Figure 10 is similar to Fig. 9 except that it illustrates the conditions for deflection-hardening fiber reinforced cement composites instead of strain-hardening ones. Note that for a typical steel fiber with an aspect ratio of 50 to 100 and reasonable bond strength ( $\tau/\sigma \approx 1$  to 2), deflection hardening can be easily achieved with volume fractions of steel fibers in the range of 0.6% to 2%; such volumes are feasible and practical in actual field applications. For the numerical results of Fig. 10 the following coefficients were used:  $\alpha = 0.05$ ,  $\lambda = 0.30$ , k = 0.40.

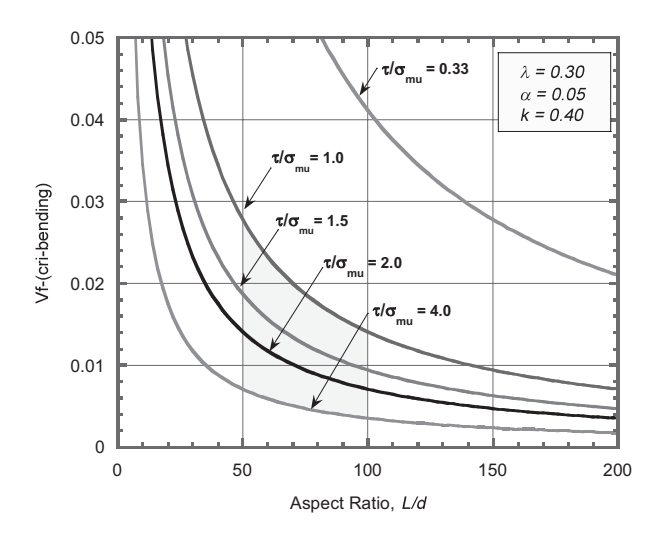


Fig. 10. Example illustrating the critical volume fraction of fibers to achieve deflection-hardening behavior in bending (k = 0.4).

#### **Experimental Observations**

Numerous investigations provide detailed information on experimental tests and experimental results obtained on the mechanical properties of fiber reinforced cement composites. Few selected examples are given for illustration but by no means cover the wide range of responses available. It is noted that experimental tests depend not only on the method of testing but also the size of the specimen, the testing machine, the method of collecting the data, and other important variables. Thus experimental results are significantly affected by the testing procedure; no attempt is made to provide a correlation between the results.

Figures 11 to 15 are taken from different investigations carried out at different times. They illustrate the behavior of fiber reinforced cement composites in tension, bending, and compression and are self-explanatory. Figure 11a illustrates the stress-elongation curve of typical strain-softening FRC composites [17] while Fig. 11b illustrates the stress-strain (strain is valid to the peak load only) of typical strain-hardening FRC composites [34, 35]. Figure 12b shows a comparison between three fibers and fiber materials used under similar conditions [5]; the maximum post-cracking point is indicated by a round marker which represents the limit between strain and crack opening. Figure 12b suggests that size effects can be significant especially for the peak strain values. Figures 13a and 13b describe how the load-deflection (or stress-deflection) response can be changed from deflection-softening to deflection-hardening by increasing the volume fraction of fiber. Figure 14 describes the influence fibers have on the compressive stress-strain response of mortar and concrete matrices; note that the tests shown are for different mixtures but have one common parameter, that is about the same compressive strength.

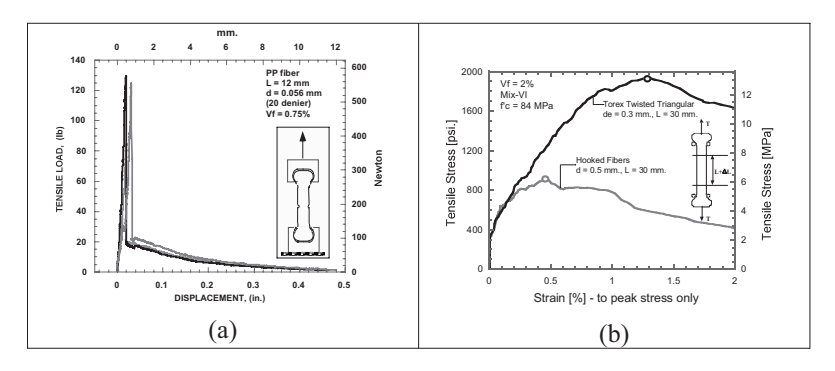


Fig. 11. Typical tensile stress-elongation curve of: (a) Strain-softening FRC composite, and (b) Strain-hardening FRC composite.

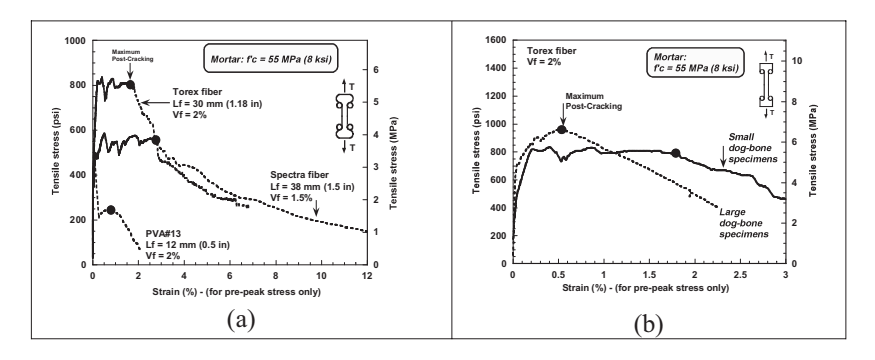


Fig. 12. Typical tensile stress-elongation curve of FRC composites: (a) Fiber comparison, and (b) Size effect.

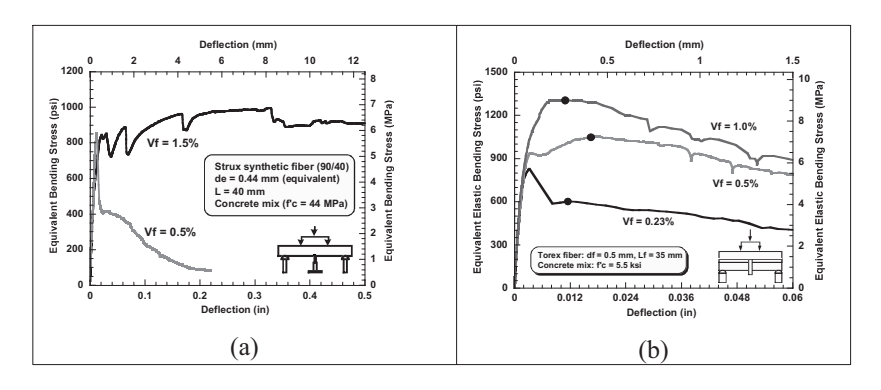


Fig. 13. Typical load-deflection curves comparing deflection-softening and deflection-hardening FRC composites.

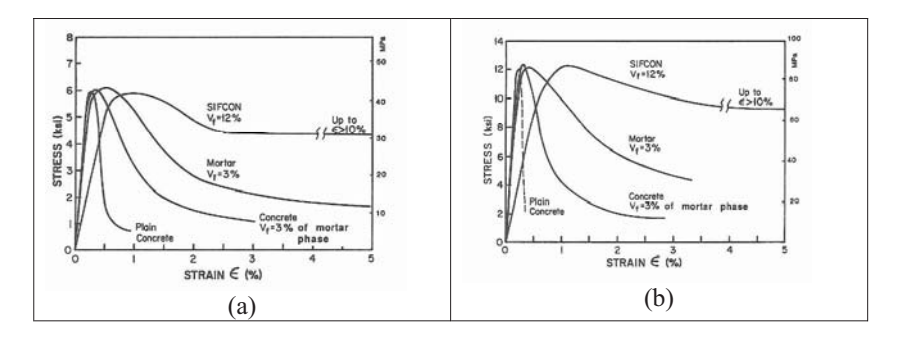


Fig. 14. Typical effect of fibers on the stress-strain curve in compression considering equal compressive strength.

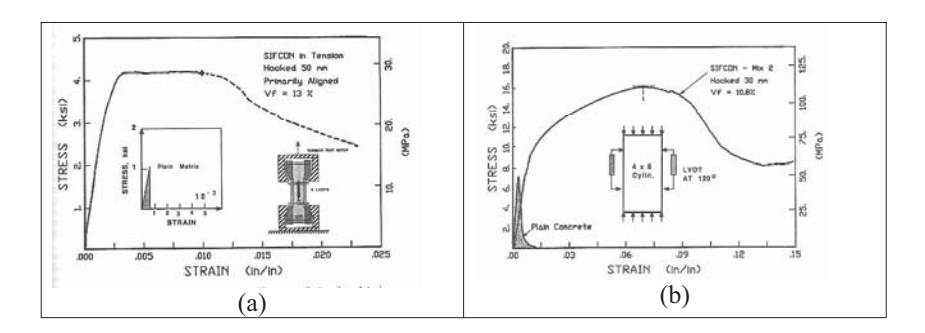


Fig. 15. Typical stress-strain curves of SIFCON in tension (a) and compression (b) compared to the curves of plain concrete without fibers.

Figure 15a describes the tensile stress-strain response of a SIFCON composite in comparison (inset) to the plain matrix. It is noted that while a high tensile strength and strain can be achieved, the volume fraction of fibers needed is very large. Figure 15b describes the compressive stress-strain response of SIFCON in comparison to plain concrete. It is clear that the toughness of SIFCON as measured from the area under the stress-strain curve can be one to two orders of magnitude that of plain concrete.

#### Fiber-Matrix Reinforcing Effectiveness

By its very definition a reinforcement (i.e., the fiber) is supposed to induce an increase in strength in the reinforced material (i.e., the matrix). Both analysis and experimental test results suggest that, in order to be effective in concrete matrices, fibers must preferably have the following properties (Fig. 16): 1) a tensile strength significantly higher than that of concrete (two to three orders of magnitude); 2) a bond strength with the concrete matrix preferably of the same order as or higher than the tensile strength of matrix; and 3) unless self-stressing is used through fiber reinforcement, an elastic modulus in tension is significantly higher than that of the concrete matrix. The Poisson's ratio and the coefficient of thermal expansion should preferably be of the

same order for both the fiber and the matrix. Indeed if the Poisson's ratio of the fiber is significantly larger than that of the matrix, detrimental debonding will occur under tensile load. However, these drawbacks can be overcome by various methods such as inducing surface deformation to create mechanical anchorage.

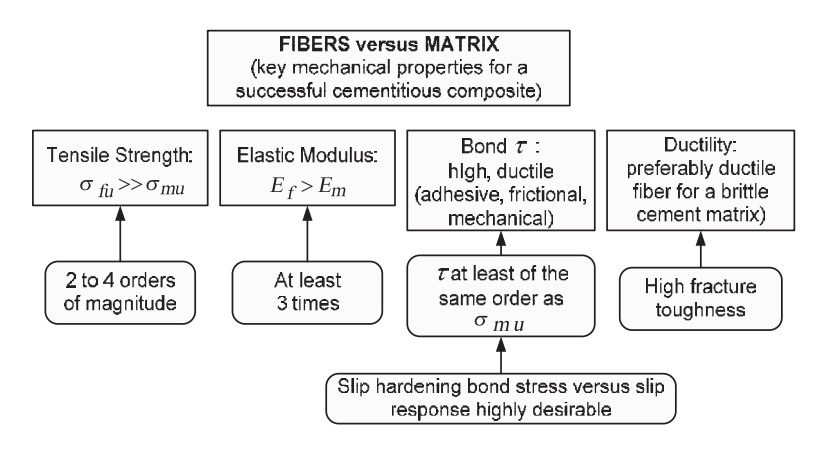


Fig. 16. Desirable fiber versus matrix properties for a successful cementitious composite [16].

#### **Applications**

Fiber-reinforced cement and concrete composites have been used in numerous applications, either as stand-alone or in combination with reinforcing bars and prestressing tendons (Fig. 17). Stand-alone applications include mostly thin products such as cladding, cement boards and pipes, or slabs on grades and pavements. Fibers are also used in hybrid applications to support other structural materials such as reinforced and pre-stressed concrete, and structural steel. Examples include impact and seismic resistant structures, jacketing for repair and strengthening of beams and columns, and, in the case of steel, encased beams and trusses to improve ductility and fire resistance. Particular applications of high performance fiber reinforced cement composites include bridge decks and special structures such as offshore platforms, space-craft launching platforms, super high rise structures, blast resistant structures, bank vaults and other special structures.

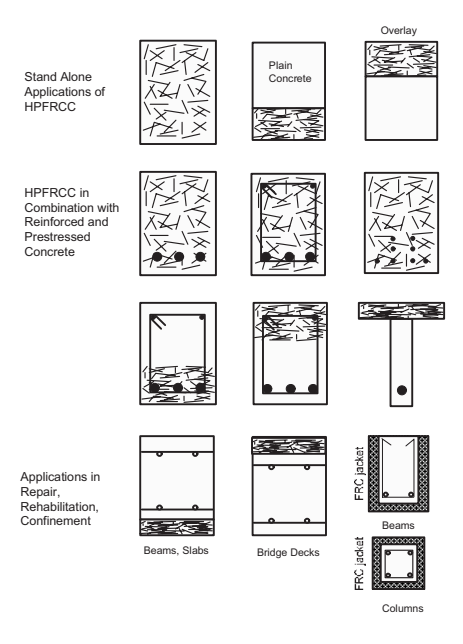


Fig. 17. Examples of applications of FRC composites.

Figure 17 describes a range of typical applications of fiber-reinforced cement composites and Fig. 18 illustrates the particular design property or properties that would call for their use in a particular application.

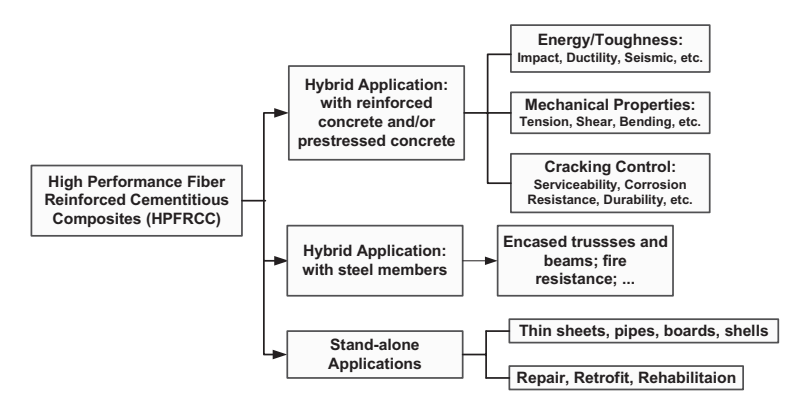


Fig. 18. Advantages of using HPFRC composites in structural applications [16].

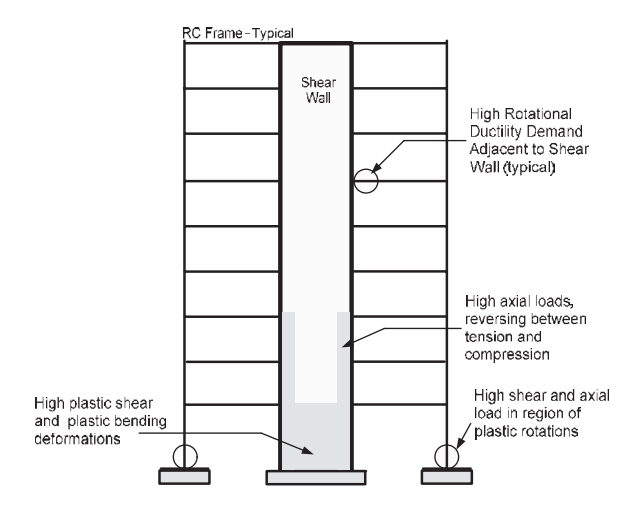


Fig. 19. Selected zones of RC building structure where HPFRC composites can be beneficially used [13].

For economic reasons, fibers do not need to be used in the whole structure but in selected zones of a structure. In such a case their use is often competitive and justifiable. Applications in selected zones of structures include: punching shear zone around columns in two-ways slab systems; end blocks and anchorage zones in prestressed concrete beams; beam to column connections in seismic resistant frames (Fig. 19); beam to shear wall connections (Fig. 19); coupling beams for seismic-cyclic resistance; out-rigger beams; in-fill damping structural elements; lower end of shear walls; tension zone of RC and PC beams to reduce crack widths and improve durability; compression zone of beams and columns to improve ductility; compression zone of RC and PC beams using fiber reinforced polymeric (FRP) reinforcements which improve ductility and take advantage of the strength of FRP reinforcements.

Fibers used in concrete structures are thought first to enhance several material properties, among which cracking and microcracking, resistance in tension and bending, ductility, and energy absorption capacity. Often not mentioned but as important, is their contribution to structural performance in general, such as enhancing bond and the bond versus slip response between reinforcing bars and concrete under monotonic and cyclic loading, preserving the cover of concrete under large deformations, and helping maintain the integrity of the structure by keeping reinforcing bars from buckling in columns.

#### **Typical Fiber Content and Fiber Volume Fraction**

Due to the formulation of the mechanics of the composite (see Section 4), the fiber content in cement matrices is specified by volume fraction, that is, the volume of fibers divided by of the total volume of the composite. The fiber volume fraction in typical fiber reinforced concrete applications is shown in Table 1. Because of fiber materials of

different densities, the same volume fraction of fibers of different materials leads to different weight fractions of fibers. Fibers are purchased by weight but mechanical properties of composites are based on volume fraction, not weight fraction of fibers. Typically a 1% volume fraction of steel fibers in normal-weight concrete amounts to about  $80~{\rm kg/m^3}$  of concrete; however, a 1% volume fraction of polypropylene fibers amounts to about only  $9.2~{\rm kg/m^3}$ .

Table. 1 is purposely kept as general as possible with little reference to trade-type names. However, high performance fiber reinforced cement composites with strain-hardening tensile behavior have been given different names by their developers. Current names include SIFCON (Slurry Infiltrated Fiber Concrete), fiber reinforced DSP (Densified Small Particles Systems), CRC (Compact Reinforced Composite), SIFCA (a form of SIFCON particularly suitable for refractory applications), SIMCON (Slurry Infiltrated Mat Concrete), RPCC (Reactive Powder Concrete Composites), ECC (Engineered Cementitious Composites), Ductal and other proprietary names. They have been shown to develop outstanding combinations of strength (up to 800 MPa in compression for RPC manufactured under temperature and pressure [31]) and ductility or energy absorption capacity (up to 1000 times that of plain concrete for SIFCON), while achieving substantial quasi-strain hardening and multiple cracking behavior.

Table 2. Range of volume fraction of fibers for typical fiber reinforced cement

composites

composites				
Material	Range of $V_f$	Remark		
FRC – Fiber Reinforced Concrete (Strain-softening in tension) or "Conventional FRC"	$V_f \le 2\%$	Fibers are premixed with the concrete matrix. Finer aggregates may be needed.		
HPFRCC – High Performance Fiber Reinforced Cement Composites (Strain-hardening FRC in tension)	$V_f \geq (V_f)_{cri-tension}$	Strain hardening and multiple cracking characteristics in tension. With proper design, critical Vf can be less than 2%.		
DHFRCC - Deflection-Hardening Fiber Reinforced Cement Composites (in bending)	$V_f \geq (V_f)_{cri-bending}$	Deflection-hardening and multiple cracking characteristics in bending. With proper design, critical Vf can be less than 0.8%.		
Shotcrete (steel fibers)	$V_f \le 3\%$	Applications in tunnel lining and repair.		
Spray Technique (glass fibers)	$4\% \le V_f \le 7\%$	Applications in cladding and panels.		
SIMCON (Slurry Infiltrated Mat Concrete – steel mat)	$4\% \le V_f \le 6\%$	A prefabricated steel fiber mat is infiltrated by a cement slurry.		
SIMCON (Slurry Infiltrated Mat Concrete – PVA mat)	$V_f \approx 1\%$	A prefabricated PVA fiber mat infiltrated by a slurry matrix		
SIFCON (Slurry Infiltrated Fiber Concrete)	$4\% \leq V_f \leq 15\%$	Fibers (mostly steel to date) are preplaced in a mold and infiltrated by a fine cementitious slurry matrix.		

#### **Progress and Evolution Since the 1960's**

A summary of the evolution in fiber reinforcement, cement matrices, bond and analytical modeling related to FRC composites has been provided. Other items are briefly addressed below.

#### Evolution in Equipment

Besides the equipment needed to produce a particular fiber, the main challenge for fiber reinforced concrete is to properly mix the fiber in the concrete matrix while achieving uniform dispersion and distribution. Often fibers tend to form "balls" and/or segregate from the bulk of the matrix. Segregation can occur even with properly dispersed fiber simply because of the differential density between fiber and matrix. For instance, in a rather liquid FRC mixture, steel fibers tend to segregate by going down while PP fibers tend to segregate by going up. Horizontal mixers with special shearing action, such as having drums rotating opposite to the mixing blades, provide better mixing, especially when high fiber content is used. Mixers with no blades, but having rubber drum rotating at an angle and vibrating (Omni type mixer), have also been developed for special applications.

Various equipments for spraying (shotcrete, gunite) fiber reinforced cement composites have also been developed and are widely used in tunnel lining. In several research laboratories around the world, special equipment for extrusion of fine grained FRC mixtures is being used and fine tuned [32, 33]. The main idea is to provide thin FRC composite based profiles or products for applications such as in window frames, piping, tubing, light beams, etc.

#### Evolution in Education and Professional Technical Activities

Education and dissemination of information are the main objectives for establishing technical committees. The American Concrete Institute formed ACI Committee 544 on Fiber Reinforced Concrete in mid 1970's. Later RILEM established a similar committee, and ASTM followed up to address testing and quality control of fiber reinforced concrete. The work of these committees have led to state-of-the-art reports and guidelines for design and applications. At time of writing this paper, a large number of symposia proceedings and edited books on fiber reinforced concrete exists. It is estimated that more than 20,000 papers have been written on the subject. A continued series of conferences and symposia dealing with FRC composites was organized by ACI as well as numerous other organizations or universities. Note in particular the series on high performance fiber reinforced cement composites organized under the auspices of RILEM [13, 19, 29, 30]. Universities and research laboratories dealing with studies on fiber reinforced concrete are numerous and can be found worldwide.

Meanwhile, the study of fiber reinforced cement composites appeared in some courses on concrete materials at universities throughout the world and few books specialized on the subject have been published [2, 3, 4, 6]. The author introduced and first taught a graduate level course on fiber reinforced cement composites at the University of

Michigan, in 1985. It may have been the first such graduate level course at a university worldwide, and is still continuing today with expanded material. It is believed that increased focus of education in FRC analysis, design, and construction will continue.

#### Evolution in Guidelines and Codes

Ever since the beginning of modern fiber reinforced concrete, there were requests by users and practitioners for some guidelines or code specification particularly related to it. Generally, codes for reinforced concrete are used, and particular assumptions are made related to a property of interest of FRC such as toughness or crack width. Today, it is possible for researchers and engineering professionals to use accurate non-linear analysis in which the properties of the materials components, steel, concrete or fiber reinforced concrete are input parameters. This implies, for instance, that for fiber reinforced concrete one must at least input the stress-strain (or constitutive) properties in both tension and compression. Surprisingly, even at time of this writing, information on the direct tensile properties of fiber reinforced concrete is rather confusing (see Section 4 about classification) and standard test methods have not been yet developed, although a large number of investigations have addressed the subject. At time of this writing the ACI building code committee is working on introducing a "code language" to allow the use of FRC in structural applications while taking advantage of its particular properties.

In applications where fiber reinforced concrete is used, particularly high performance fiber reinforced cement composites, analytical and experimental investigations have shown that the benefits induced go much beyond initially predicted expectations. For instance, the use of HPFRCCs is expected to lead to a significant decrease in crack width on the tensile side of bending beams, thus leading to reduced corrosion of the continuous reinforcement. However, on the compression side, an increased strain capacity at ultimate, leads to improved ductility, improved energy absorption capacity, and even improved strength since the tensile reinforcement goes well into its strain hardening regime. One of the most important contribution of fiber reinforcement in seismic structures is that the fibers keep the concrete cover from spalling under cyclic load, thus confining the main longitudinal bars and keeping them from premature buckling in compression. Similarly, maintaining the integrity of the concrete cover insures a continuing bond between the reinforcing bars and concrete and helps improve the integrity of the structure under cyclic loading.

It is clear that once started by ACI, provisions for fiber reinforced concrete in a code setting will grow and propagate to other codes as well, and will see numerous modifications and improved versions in the future.

#### **Evolution in Analysis and Modeling**

The initial introduction and subsequent widespread use of computers has affected the analysis, modeling and design of FRC composites to the same extent as other structural materials such as reinforced and pre-stressed concrete. Today, finite element modeling allows detailed analysis accounting for non-linearities at the material level, as well as geometric nonlinearity at the structural level. Static and dynamic analyses are widely used. It is comforting to say that currently available analytical tools allow for modeling

essentially most of what is needed for the current applications of FRC composites. The only drawback is that such analysis are as good as the input information utilized, such as the constitutive properties of the materials. While it is always possible to run an experimental test to determine the constitutive properties of a particular FRC composite for a given application, the analytical prediction of such properties for modeling purposes is still insufficient at time of this writing. Simply imagine how to predict the tensile stress-strain response of a particular fiber reinforced concrete composite; if we refer to Section 4 and Eqs. (1 and 2), it is clear that a large number of assumptions must be made, such as the values of the coefficients alpha and lambda, and the strain at maximum post-cracking,  $\varepsilon_{pc}$ . To this writer's knowledge, only a couple of investigations have addressed the prediction of  $\varepsilon_{pc}$ [36], and yet they require input information more difficult to obtain experimentally that  $\varepsilon_{pc}$  itself.

#### **Evolution in Performance**

The performance of fiber reinforced cement composites has consistently improved over time. While their compressive strength can be directly related to that of the plain matrix, their tensile strength and tensile strain capacity are more specific examples of their advance. Similarly to steel, an increase in tensile strength generally implies a trade-off for a decrease in strain capacity. Figure 20 illustrates examples of stress-strain curves with a wide range of tensile strength and strain capacities. They represent at time of this writing the available range technically possible.

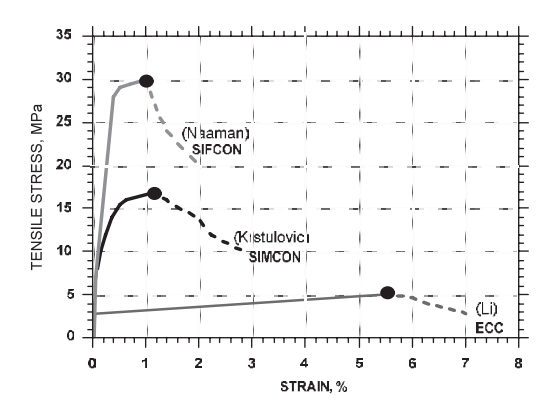


Fig. 20. Typical range of tensile stress-strain curves for HPFRC composites showing the trade-off between strength and strain capacity.

#### **Evolution** in Applications

Traditional applications of FRC composites are numerous and encompass new structures as well as repair and rehabilitation of existing structures. Most important applications are those where other materials cannot compete, that is, specifically energy

absorption capacity. Thus applications in impact and blast resistant structures and seismic structures remain dominant and most competitive. The increasing utilization of high performance matrices and high performance fibers offers opportunities for new applications such as protective panels against projectiles (bullet proof panels) and blast resistant and fire resistant membranes.

#### Looking Ahead

At the pace technology is currently going, it is difficult to predict future developments except for the very near future, with some inference based on current research. Improvements in the fiber, the matrix, the interface bond, and the composite will surely occur.

#### Matrix

It is expected that matrices with finer grains and mineral additives will be increasingly used to improve composite response, especially in thin product applications.

#### Fiber and Interface Bond

Developments in new fibers for concrete will focus on improving fiber efficiency and achieving better bond characteristics, preferably with bond stress-slip hardening behavior. Fiber efficiency will translate in a maximum stress in the fiber under pull-out simulating cracked section conditions, close to the tensile strength of the fiber. Slip hardening behavior will translate into a rather ductile composite. Such behavior would insure the development of high performance fiber reinforced cement composites with an elastic plastic or strain hardening tensile response, accompanied by multiple cracking.

#### Fabrication of Composite

Improved fabrication processes will be increasingly utilized. For thin fiber reinforced cementitious products extrusion for instance allows a better performance than premixing. For bulk fiber reinforced concrete composites, the methodology used in self-compacting or self-consolidating concrete is likely to be increasingly used and accordingly adapted. It is likely that ready-mix truck will routinely deliver fiber reinforced concrete with fiber contents up to 2% by volume.

#### **Hybrid Combinations**

Hybrid combinations, with fibers of different materials (such as steel and PVA) or geometric properties (such as a normal steel fiber and a steel or PVA microfiber), or hybrid combinations of discontinuous and continuous fibers (such as fibers and fabrics), will become increasingly attractive. Such composites cover most of the needs for current applications of thin reinforced concrete products such as cement boards, pipes, corrugated sheets, cladding elements, roofing tiles, etc.

#### Microfibers

The use of very fine grain matrices reinforced with short micro-fibers or combinations of micro- and macro-fibers, in stand-alone applications such as small manufactured products is likely to expand. Short micro-fibers induce micro-toughness, reduce the size (width and length) of microcracks, and improve the tensile strength at cracking (or proportionality limit) of the composite. Because fine grain matrices with micro-fibers

can be used to produce manufactured products, the machine-ability of the product is improved.

#### <u>Improved Function and Market Penetration</u>

During this past century fiber reinforced concrete has played a very important role. It has progressed from an engineering material, such as plain concrete or masonry, to a support material in combination with conventional reinforced or prestressed concrete in new structures or in repair, and finally to a structural material with a stand-alone function, such as in structural elements. However, this last function is really beginning and is expected to develop further in the coming years.

#### **Concluding Remarks**

Fiber reinforced concrete has seen its first patent in 1874. Yet, for all practical purposes, progress in FRC composites has been almost at a standstill for more than 100 years, and picked up at an exceptional pace only during the last four decades. This may be partly due to fundamental research, better understanding of the reinforcing mechanisms of FRC composites, the need for materials with particular properties, developments in advanced materials, economic competitiveness and global circumstances. A solid foundation has thus been built. It is likely that every area mentioned in the above discussion will see progress in the future. However, economic considerations will keep playing a major role.

The dream that started in 1874, to mix fibers in concrete, like sand or gravel, to achieve a stand-alone structural material is closer today than ever before. It is satisfying to know that the next generation of civil engineers will have a structural concrete with a whole spectrum of new possibilities to explore in order to provide better structures for a continually challenging world.

#### Acknowledgments

The research described herein was sponsored by the US National Science Foundation under Grant No. CMS 0408623 and by the University of Michigan. The opinion expressed in this paper are those of the author and do not necessarily reflect the views of the sponsor.

#### References

The following list of references is very limited due to space limitation and does not do justice to the thousands of studies available at the time of writing this paper.

1. Aveston, J., Cooper, G.A., and Kelly, A. "Single and multiple fracture - the properties of fiber composites," *Conference Proceedings of National Physical Laboratory*, IPC, Science and Technology Press, Ltd., 1971, pp. 14-24.

- Balaguru, P., and Shah, S.P., "Fiber Reinforced Cement Composites," McGraw Hill, New York, 1992.
- 3. Bentur, A., and Mindess, S., "Fiber Reinforced Cementitious Composites," Elsevier Applied Science, UK, 1990.
- 4. Brandt, A., Li, V.C., and Marshall, I.H., Editors, "Brittle Matrix Composites 6, BMC-6," Woodhead Publishing Limited, Cambridge and Warsaw, October 2000.
- Chandrangsu, K., and Naaman, A.E., "Comparison of Tensile and Bending Response of Three High Performance Fiber Reinforced Cement Composites," in High Performance Fiber Reinforced Cement Composites (HPFRCC-4), A.E. Naaman and H.W. Reinhardt, Editors, RILEM Publications, Pro. 30, June 2003, pp. 259-274.
- 6. Hannant, D.J., "Fiber Cements and Fiber Concretes" J. Wiley, 1978, 215 pp.
- 7. Li, V.C., & H.C. Wu, "Conditions for pseudo strain-hardening in fiber reinforced brittle matrix composites," *J. Applied Mechanics Review*, V.45, No. 8, August, pp. 390-398, 1992.
- 8. Li, V.C. & C.K.Y. Leung, "Theory of steady state and multiple cracking of random discontinuous fiber reinforced brittle matrix composites," ASCE *J. of Engineering Mechanics*, V. 118, No. 11, pp. 2246 2264, 1992.
- 9. Naaman, A.E., "A Statistical Theory of Strength for Fiber Reinforced Concrete," Thesis presented to the Massachusetts Institute of Technology, Civil Engineering Department in partial fulfillment for the degree of Doctor of Philosophy, Sept. 1972, 196 pp.
- Naaman, A.E., F. Moavenzadeh and F.J. McGarry, "Probabilistic Analysis of Fiber Reinforced Concrete" *Journal of the Engineering Mechanic's Division*, ASCE, Vol. 100, No. EM2, April 1974, pp. 397-413.
- 11. Naaman, A.E., "High performance fiber reinforced cement composites," Proceedings of the *IABSE Symposium on Concrete Structures for the Future*, Paris, France, September 1987, pp. 371-376.
- 12. Naaman, A.E., "SIFCON: Tailored properties for structural performance," in *High Performance Fiber Reinforced Cement Composites*, RILEM Proceedings 15, E. and FN SPON, London, 1992, pp.18-38.
- Naaman, A.E., and Reinhardt, H.W., Co-Editors, "High Performance Fiber Reinforced Cement Composites: HPFRCC 2, RILEM, No. 31, E. & FN Spon, London, 1996, 505 pages.
- 14. Naaman, A.E., and Reinhardt, H.W., "Characterization of High Performance Fiber Reinforced Cement Composites," in "High Performance Fiber Reinforced Cement Composites HPFRCC 2,' A.E. Naaman and F.W. Reinhardt, Editors, RILEM Pub. 31, E. and FN Spon, England, 1996; pp. 1-24.
- Naaman, A.E., "Fibers with Slip-Hardening Bond," in High Performance Fiber Reinforced Cement Composites - HPFRCC 3,' H.W. Reinhardt and A.E. Naaman, Editors, RILEM Pro 6, RILEM Publications S.A.R.L., Cachan, France, May 1999, pp. 371-385.
- Naaman, A.E., "Fiber Reinforcement for Concrete: Looking Back, Looking Ahead," in Proceedings of Fifth RILEM Symposium on Fiber Reinforced Concretes (FRC), BEFIB' 2000, Edited by P. Rossi and G. Chanvillard, September 2000, Rilem Publications, S.A.R.L., Cachan, France, pp. 65-86.
- 17. Naaman, A.E., and Guerrero, P., "A New Methodology to Determine Bond of Micro-Fibers Embedded in Cement Composites," in Brittle Matrix Composites 6,

- BMC-6, Edited by A. Brandt, V.C. Li and I.H. Marshall, Woodhead Publishing Limited, Cambridge and Warsaw, October 2000, pp. 42-51.
- 18. Naaman, A.E., "Toughness, Ductility, Surface Energy and Deflection-Hardening FRC Composites," in Proceedings of the JCI Workshop on Ductile Fiber Reinforced Cementitious Composites (DFRCC) – Application and Evaluation, Japan Concrete Institute, Tokyo, Japan, October 2002, pp. 33-57.
- 19. Naaman, A.E., and Reinhardt, H.W., Co-Editors, "High Performance Fiber Reinforced Cement Composites HPFRCC 4," RILEM Proc., PRO 30, RILEM Pubs., S.A.R.L., Cachan, France, June 2003; 546 pages.
- Naaman, A.E., "Strain Hardening and Deflection Hardening Fiber Reinforced Cement Composites," in High Performance Fiber Reinforced Cement Composites (HPFRCC-4), A.E. Naaman and H.W. Reinhardt, Editors, RILEM Publications, Pro. 30, June 2003, pp. 95-113.
- 21. Naaman, A.E., and Reinhardt, H.W., "Setting the Stage: toward Performance Based Classification of FRC Composites," in High Performance Fiber Reinforced Cement Composites (HPFRCC-4), A.E. Naaman and H.W. Reinhardt, Editors, RILEM Publications, Pro. 30, June 2003, pp. 1-4.
- 22. Naaman, A.E., and Reinhardt, H.W., "High Performance Fiber Reinforced Cement Composites (HPFRCC-4): International RILEM Report," in Materials and Structures, 2003. Also same in Cement and Concrete Composites. 3 pages.
- 23. Naaman, A.E., "Engineered Steel Fibers with Optimal Properties for Reinforcement of Cement Composites," Journal of Advanced Concrete Technology, *Japan Concrete Institute*, Vol. 1, No. 3, November 2003, pp. 241-252.
- 24. Naaman, A.E., "Evaluation of steel fibers for applications in structural concrete," in Fiber Reinforced Concretes BEFIB 2004, Edited by M. di Prisco, R. Felicetti, and G.A. Plizzari, RILEM Proceedings PRO 39, Vol. 1, 2004, pp. 389-400.
- 25. Naaman, A.E., and Reinhardt, H.W., "Fiber Reinforced Concrete: Current Needs for Structural Implementation", Proceedings of US-European Workshop on Fiber Reinforced Concrete from Theory to Practice, Edited by S. Ahmad, M. di Prisco, C. Meyer, G.A. Plizzari, and S. Shah, Bergamo, Italy, Starlink Editrice, September 2004, published in 2005, pp. 151-155.
- 26. Naaman, A.E., and Reinhardt, H.W., "Proposed Classification of FRC Composites Based on their Tensile Response" Proceeding of symposium honoring S. Mindess, N. Banthia, Editor, University of British Columbia, Canada, August 2005. Electronic proceedings, 13 pages. In print in Materials and Structures, Rilem, 2006.
- 27. Parra-Montesinos, G., "High Performance Fiber Reinforced Cement Composites: an Alternative for Seismic Design of Structures," ACI Structural Journal, Vol. 102, No. 5, Sept.-Oct. 2005, pp. 668-675.
- 28. Parra-Montesinos, G., "Proposed Code Changes," personal communication, March 2006.
- 29. Reinhardt, H.W., and Naaman, A.E., Editors, "High Performance Fiber Reinforced Cement Composites," RILEM, Vol. 15, E. & FN Spon, London, 1992, 565 pages.
- Reinhardt, H.W., and Naaman, A.E., Co-Editors, "High Performance Fiber Reinforced Cement Composites - HPFRCC 3," RILEM Proceedings, PRO 6, RILEM Pubs., S.A.R.L., Cachan, France, May 1999; 666 pages.
- 31. Richard, P., "Reactive powder concrete: a new ultra-high strength cementitious material," Proceedings of the 4<sup>th</sup> International Symposium on Ultilisation of High-Strength/High-Performance Concrete, Paris, France, 1996, pp. 1501-1511.

- 32. Shao, Y., Marijunte, S., and Shah, S.P., "Extruded fiber-reinforced composites" Concrete International, Vol. 17, No. 4, April 1995.
- 33. Stang, H., Technical University of Denmark, private communication.
- 34. Sujivorakul, C., and Naaman, A.E., "Tensile Response of HPFRC Composites Using Twisted Polygonal Steel Fibers", in Innovations in Fiber-Reinforced Concrete for Value," N. Banthia, M. Criswell, P. Tatnall, and K. Folliard, Editors, ACI Special Publication, SP216, American Concrete Institute, 2003, pp. 161-179.
- 35. Sujivorakul, C., and Naaman, A.E., "Ultra High-Performance Fiber-Reinforced Cement Composites Using Hybridization of Twisted Steel Fibers and Micro Fibers," in Fiber Reinforced Concretes BEFIB 2004, Edited by M. di Prisco, R. Felicetti, and G.A. Plizzari, RILEM Proceedings PRO 39, Vol. 2, 2004, pp. 1401-1410.
- 36. Tjiptobroto, P., and Hansen, W., "Model for prediction of the elastic strain of fiber reinforced composites containing high volume fractions of discontinuous fibers," *ACI Materials Journal*, V. 90, No. 2, March-April, 1993.

# **High Performance Material Applications in Civil Engineering**

## Issam E. Harik

Raymond Blythe Professor of Civil Engineering, and
Program Manager, Structures and Coatings, Kentucky Transportation Center
University of Kentucky
Lexington, KY 40506-0281, U.S.A.
email: iharik@engr.uky.edu

## Abstract

An overview is presented of the testing conducted on various high performance materials and their deployment in civil engineering structures, primarily concrete bridges. The materials include fiber reinforced polymer composites (FRP), stainless steel clad (SSC) rebars, microcomposite multistructural formable steel (MMFX) rebars, etc. The primary advantage of these materials is their resistance to corrosion and/or their lack of magnetic interference. Corrosion hastens the degradation in civil engineering structures and reduces their life span. This leads to increased costs and frequency of repairs and reduces the monetary return on the investment. The lack of magnetic interference is highly beneficial in the construction of magnetic resonance imaging (MRI) rooms in hospitals, in certain transmission towers, computer chip production facilities, etc. Carbon FRP fabrics and laminates as well as steel reinforced polymer (SRP) fabrics are becoming very popular in the repair and strengthening of existing structural elements. Case studies are presented to highlight the deployment and monitoring of these materials.

## Introduction

The use of high performance materials (HPM) for infrastructure applications offers, in certain applications, both economical and structural advantages, and improved performance. For new structures, the use of HPM provides the advantage of corrosion resistance, and/or high strength to weight ratio, and/or magnetic transparency, etc. For repair and rehabilitation, HPM, especially carbon FRP fabrics and laminates [1,2], are becoming the primary choice for strengthening damaged concrete structural components or for upgrading structures. HPM field applications in concrete bridges are highlighted in this paper.

# The Roger's Creek Bridge Deck - GFRP Rebars

A bridge deck 11.2 m long and 11.0 m wide was constructed in 1997 across Roger's Creek in Bourbon County, Kentucky with GFRP rebars in a region of the top reinforcing mat as shown in Fig. 1 [5]. The remainder of the top mat was reinforced with epoxy coated steel (ECS) bars. The bridge is being monitored on a regular basis (i.e. evaluate crack formation, crack width, crack propagation, etc). To date, no sign of distress has been reported and the bridge is reportedly in excellent condition [6].



Fig. 1. Concrete placement on the Roger's Creek bridge deck.

# The Two Mile Creek Bridge Deck - CFRP Rebars

The Two Mile Creek Bridge is located on Elkin Station Road in Clark County, KY. The 9.45 m (31 ft.) wide and 18.6 m (61 ft.) long bridge in Fig. 2 is reinforced with Carbon Fiber Reinforced Polymer (CFRP) reinforcement [7]. All longitudinal and transverse reinforcements in both the top and bottom mats are CFRP bars (Figs. 3-5). The bridge is being monitored on a regular basis (i.e. evaluate crack formation, crack width, crack propagation, etc). To date, no sign of distress has been reported and the bridge is reportedly in excellent condition [3].

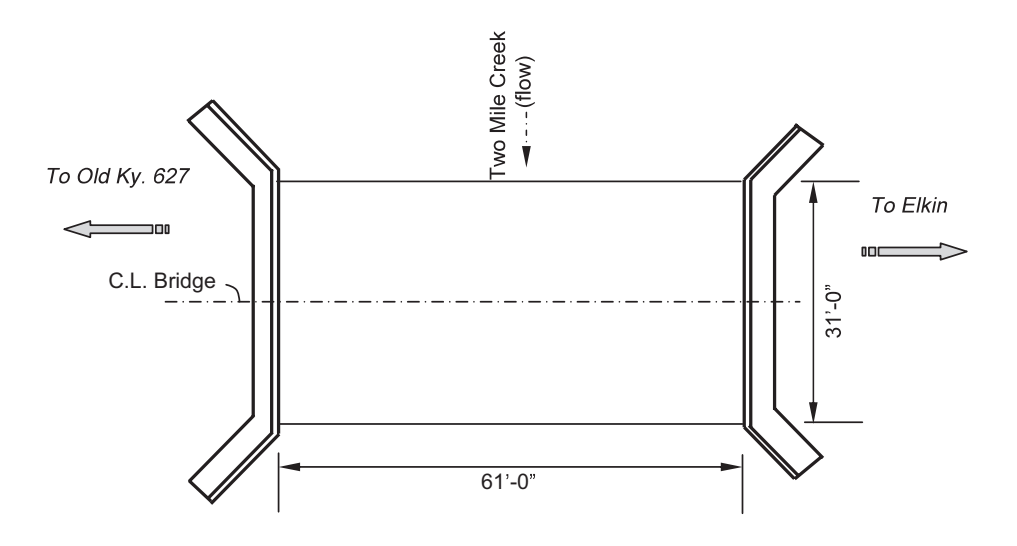


Fig. 2. Plan view of the two mile creek bridge deck.

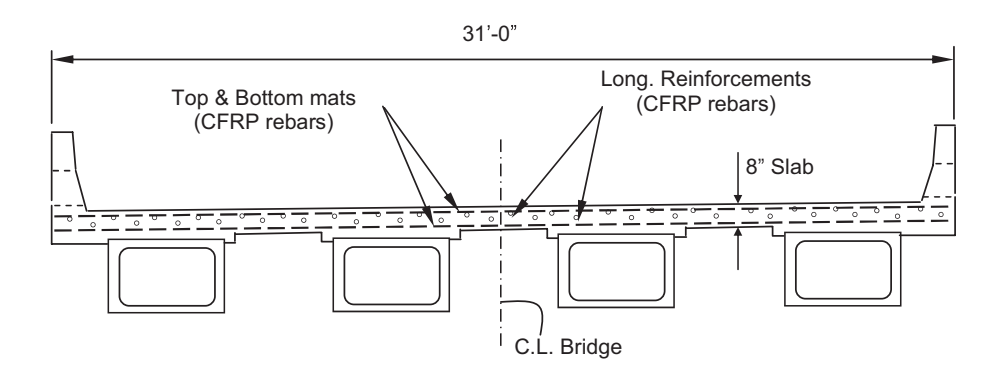


Fig. 3. Typical section of the two mile creek bridge deck.



Fig. 4. The two mile creek bridge deck prior to concrete placement.



Fig. 5. Longitudinal and transverse reinforcements are CFRP rebars in the two mile creek bridge.

# North Elkhorn Creek Bridge Deck - MMFX Rebars

Microcomposite multi-structural formable steel (hereafter referred to as MMFX) bars possess excellent corrosion resistance, according to its manufacturer, due to the steel unique chemical composition; a combination that minimizes the formation of micro galvanic cells which are the source of the electrochemical process in the steel. MMFX bars tested in 2001 at the University of Kentucky [7] had a tensile strength of approximately 180 ksi (1,250 MPa). The stress-strain relationship of MMFX bars is non-linear particularly at high stress levels. Typical stress-strain relationship of a MMFX bar is shown in Fig. 6. In 2001, MMFX bars were used in the construction of one of the two reinforced concrete bridge decks of the CR 5218 Bridge over North Elkhorn Creek on Galloway Road located in Scott County, Kentucky (Fig. 8).

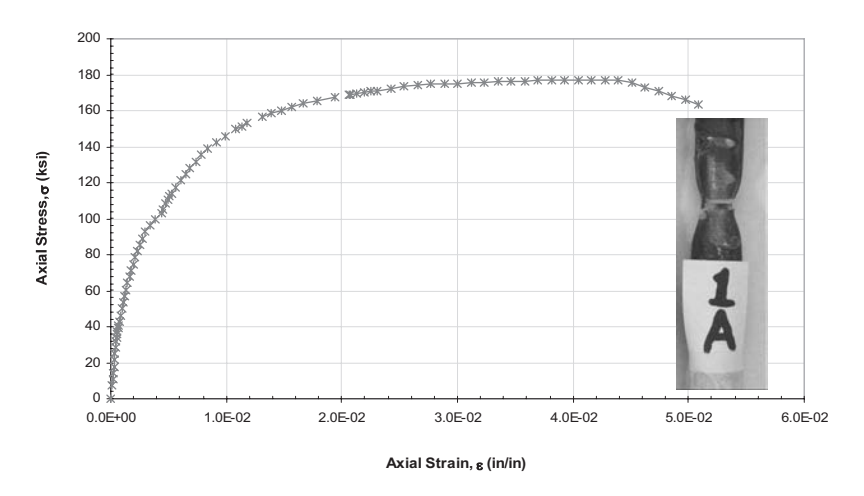


Fig. 6. Stress-strain relationship of a MMFX steel bar.

# North Elkhorn Creek Bridge Deck - SSC Bars

Stainless steel clad (hereafter referred to as SSC) bars are conventional carbon steels (e.g. A615 Grade 40, 60, etc.) with stainless steel serving as exterior protective coating or cladding; much like epoxy coated steels. Stainless steel is essentially a low carbon steel that contains chromium (Cr) at 10% or more by weight. The chromium in steel allows the formation of a rough, adherent, invisible, corrosion-resisting chromium oxide film on the steel surface; this protective film, if damaged, is self-healing. SSC bars are metallurgically bonded by first pressing the carbon steel core into a stainless steel pipe and then hot-rolling the SSC under a specified temperature. Therefore, SSC bars combine most of the advantages of solid stainless steel equivalents and the mechanical properties of their carbon steel core bars. Typical stress-strain relationship of a SSC bar is shown in Fig. 1 [7]. In 2001, SSC bars were used in the construction of one of the two reinforced concrete bridge decks of the CR 5218 Bridge over North Elkhorn Creek on Galloway Road located in Scott County, Kentucky, USA (Fig. 8).

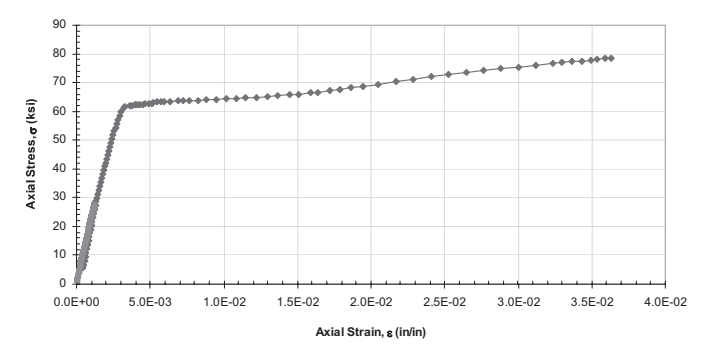


Fig. 7. Stress-strain relationship of a stainless steel clad (SSC) bar.

# The Carter County Bridge

The three-span (21-30-13 m) composite pre-cast pre-stressed concrete box-beam bridge is situated on route KY-3297 crossing the Little Sandy River in Carter County, Kentucky. The bridge was completed in April 1993. A routine inspection conducted in April 1996 found significant diagonal shear cracks that were as wide as 3.2 mm, and 1.8 to 2.4 m long (Fig. 9). The cracks formed in all pre-cast pre-stressed box beams at both ends of Span 2. Subsequent inspections revealed that the shear cracks in Span 2 were propagating at an alarming rate, and new shear cracks were also beginning to develop in Spans 1 and 3. In addition, further evaluation confirmed that the box beams were indeed under-reinforced in shear.

The retrofitting process for the Carter County Bridge began in September 2001, and completed in October of 2001. The process was performed in two phases: (1) crack repairs; and (2) application of CFRP fabric. The goal of crack repairs was to partially restore the capacity of the beams, and the application of CFRP fabric was to strengthen and compensate for shear deficiency. Fig. 10 depicts the retrofitting process: (a) mounting of injection ports in cracks; (b) sealing cracks using epoxy through injection ports; (c) applying two-part resin; and (d) attaching CFRP fabric to concrete. Note that the CFRP fabric is attached to both sides of the concrete beams with a 45-degree angle (see Fig. 10d).

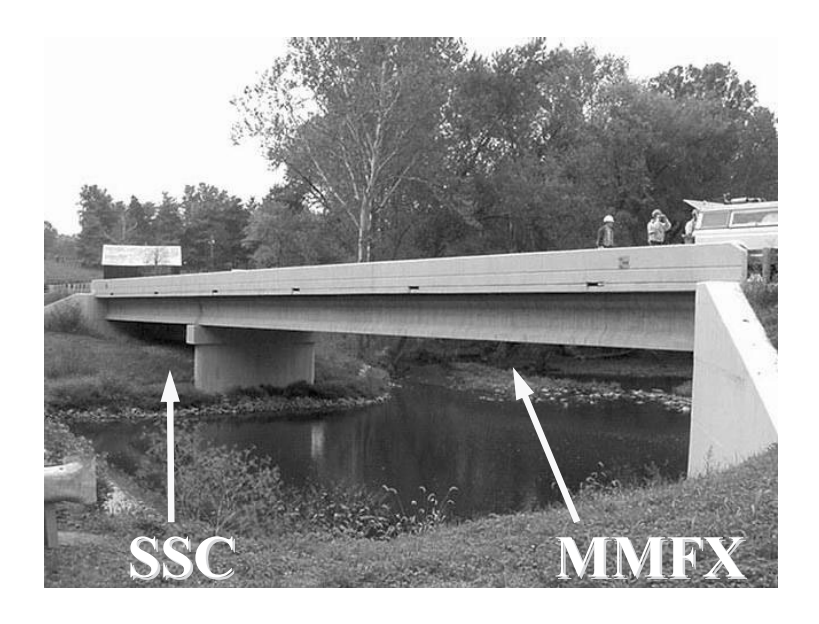


Fig. 8. SSC and MMFX bars were used in the bridge deck of the CR 5218 Bridge in Scott County, Kentucky, USA.

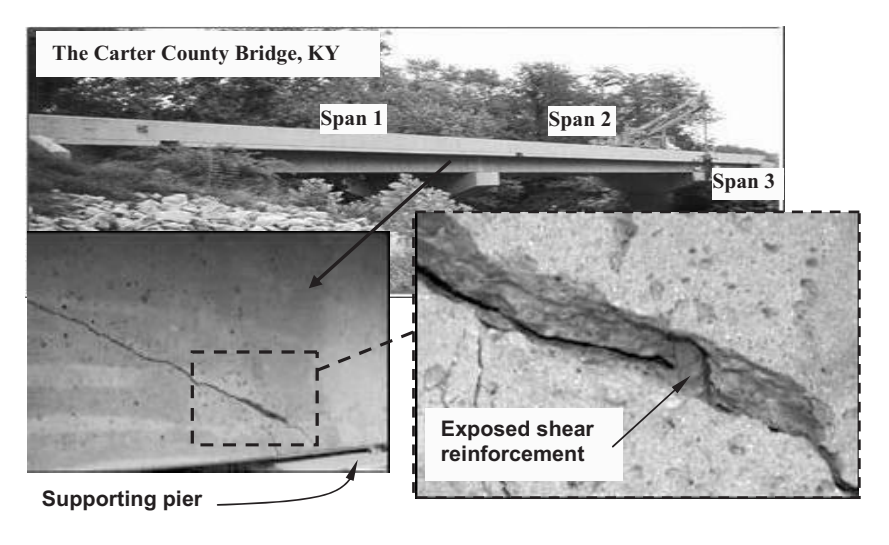


Fig. 9. Diagonal Shear Crack in Span 2 of the Carter County Bridge.

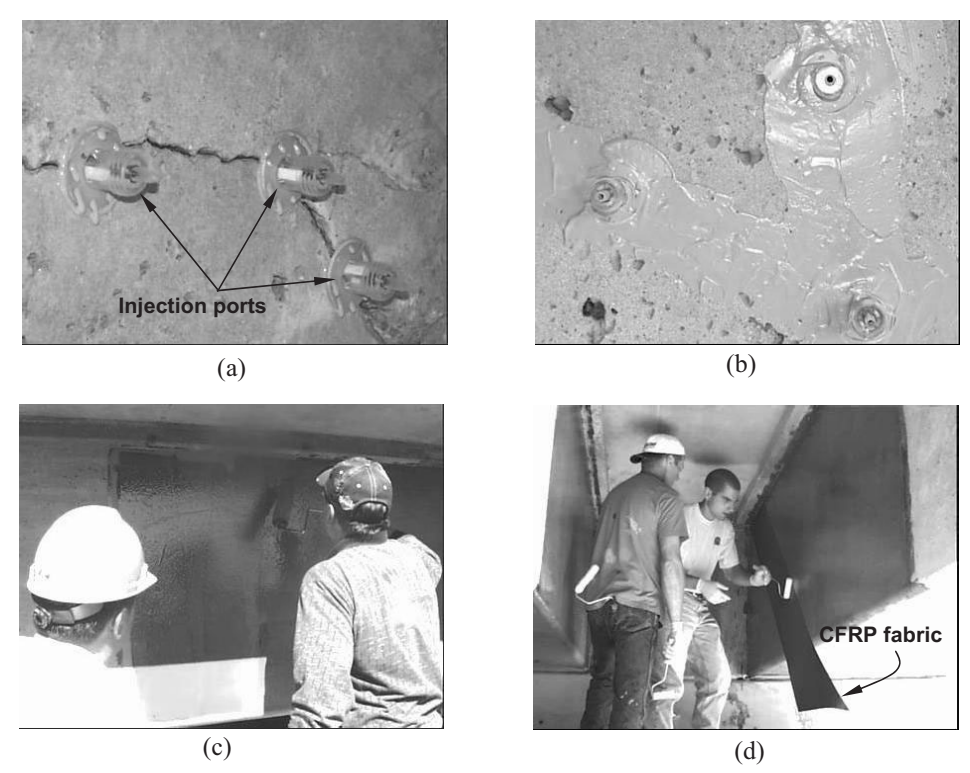


Fig. 10. Retrofitting of concrete box-beams in the Carter County bridge: (a) mounting of injection ports in cracks; (b) sealing cracks using epoxy; (c) applying two-part resin; and (d) attaching CFRP fabric to concrete.

During the retrofitting process, crack monitoring gauges were mounted directly onto the beams over the repaired cracks (Fig. 11). As of September 2003, the repaired beams have shown no indication of distress as zero movement has been registered on these monitoring gauges [8].

The overall success of the project demonstrated that the use of advanced composites can be an effective retrofitting alternative. Additionally, the Kentucky Transportation Cabinet saved approximately \$500 000 by repairing the bridge instead of replacing the entire superstructure as initially planned.

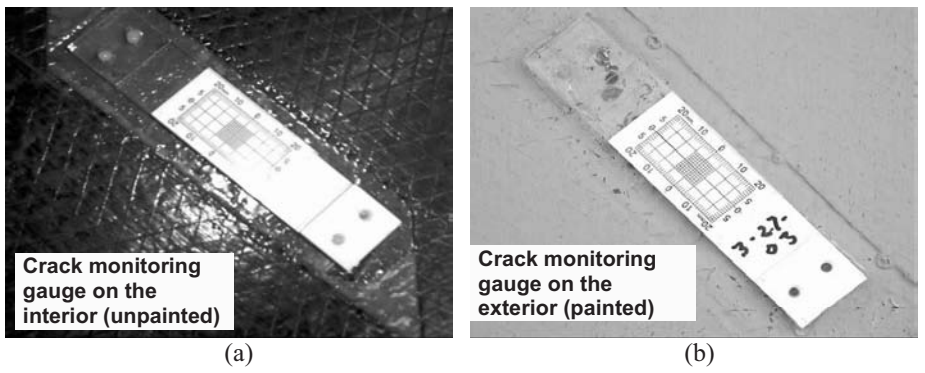


Fig. 11. Crack monitoring gauges mounted on repaired beams in the Carter County bridge.

# The Louisa-Fort Gay Bridge

The Louisa-Fort Gay Bridge is located in a small mining community of Lawrence County in Eastern Kentucky. The multi-span bridge has both steel plate girders and reinforced concrete (RC) girders in the end and middle spans, respectively. A schematic plan view of the middle RC spans (Spans 4-5-6-7) is shown in Fig. 12. Fig. 13 shows a section of the underside of the bridge deck with flexural cracks at the bottom of the girders.

Bridge inspection indicated that flexural cracks developed in the RC girders in Spans 4, 6, and 7 due to heavy coal truck loads. Weigh in motion scales measured trucks weighing in excess to 225 000 lb (1000 kN) [Note: the AASHTO HS20-44 Truck is 72,000 lbs (320 kN)]. For illustrative purposes, moment-curvature analysis, as shown in Fig. 14, reveals how much Girder 4 in Span 4 is being overloaded. The moment-curvature for the strengthened girder 4 in span 4 using CFRP laminates is presented in Fig. 14b. The retrofitting process is similar to the one previously described for the Carter County bridge, except that CFRP laminates are used as shown in Fig. 15.

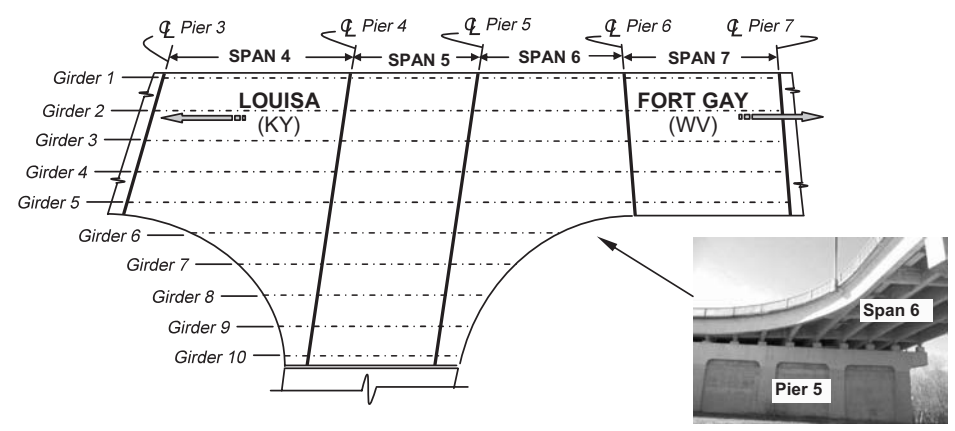


Fig. 12. The reinforced concrete spans of the Louisa-Fort Gay bridge.

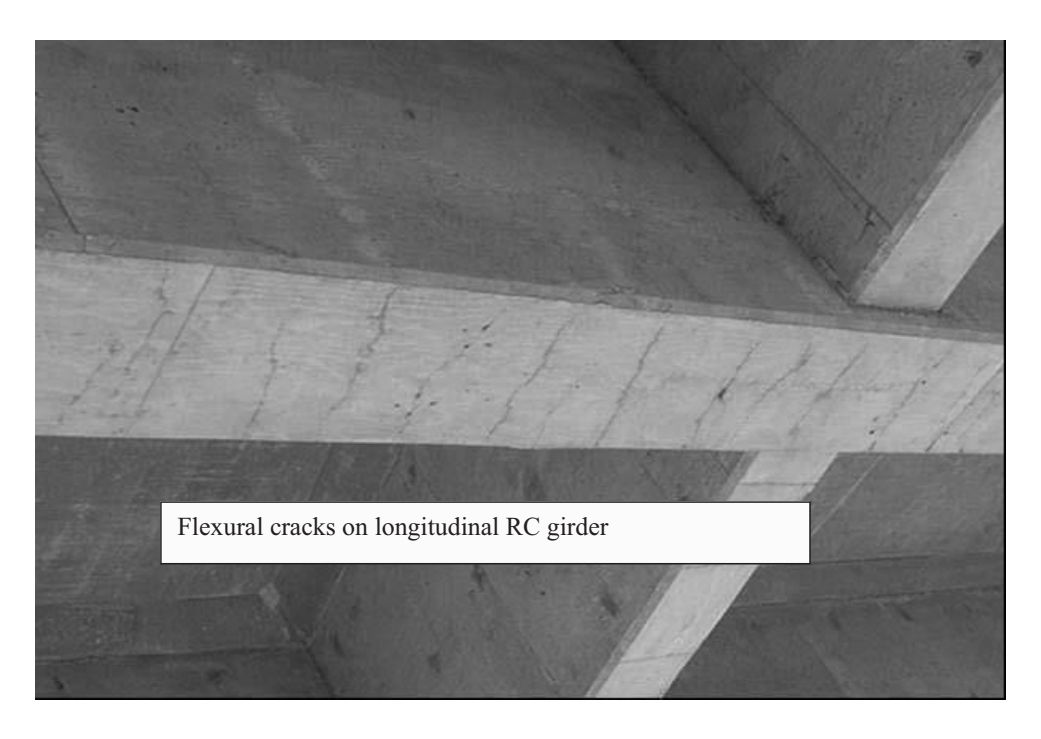


Fig. 13. Flexural cracks on the longitudinal reinforced concrete girders in the Louisafort Gay bridge

# Conclusions

The deployment of high performance materials in concrete bridges is presented herein. The components used in the new bridges were intended for experimental purpose and material evaluation. The two bridge retrofitting projects were chosen because of their economical advantage over other retrofitting alternatives.

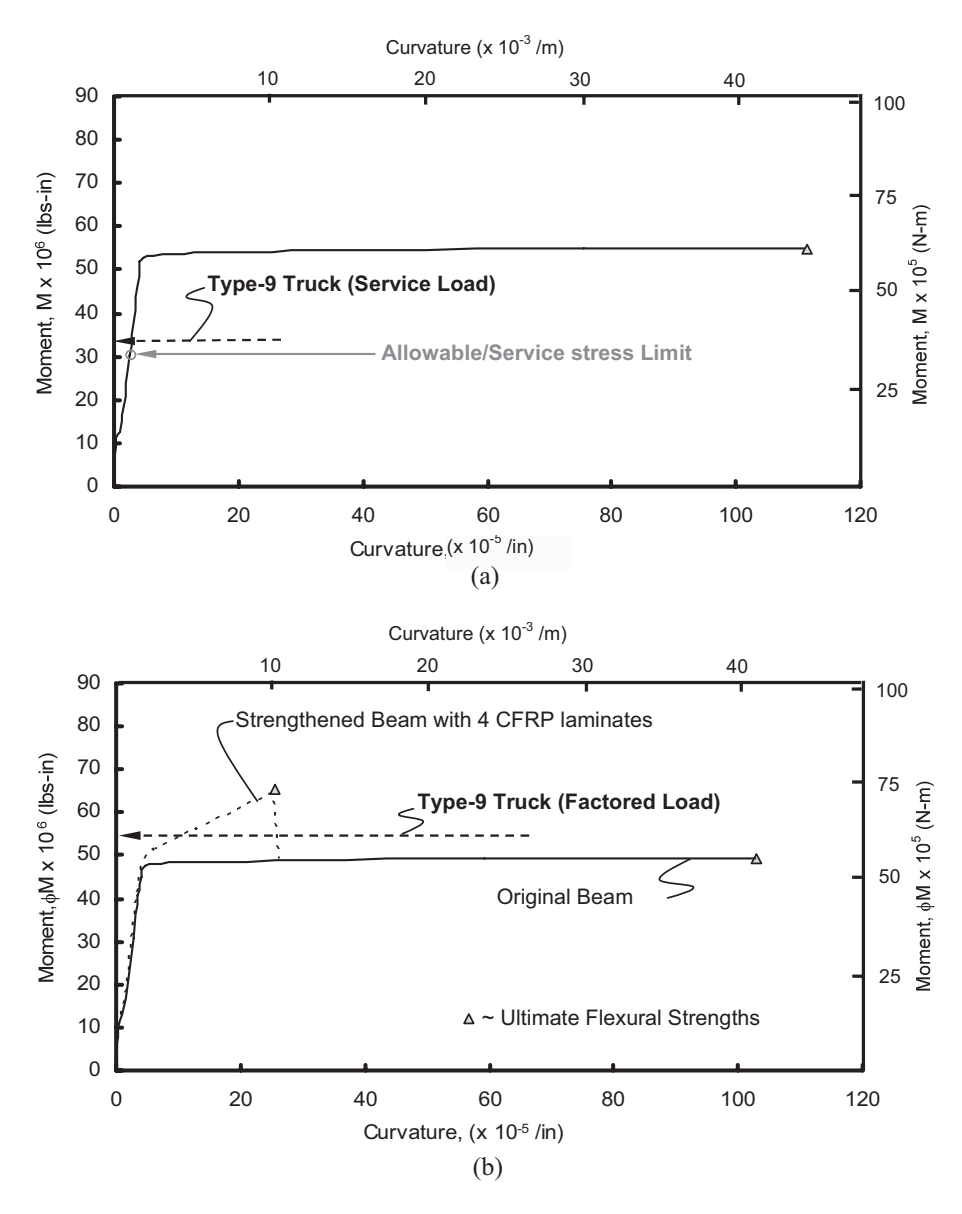


Fig. 14. Moment-curvature analyses of girder 4 in span 4 in the Louisa-Fort Gay bridge

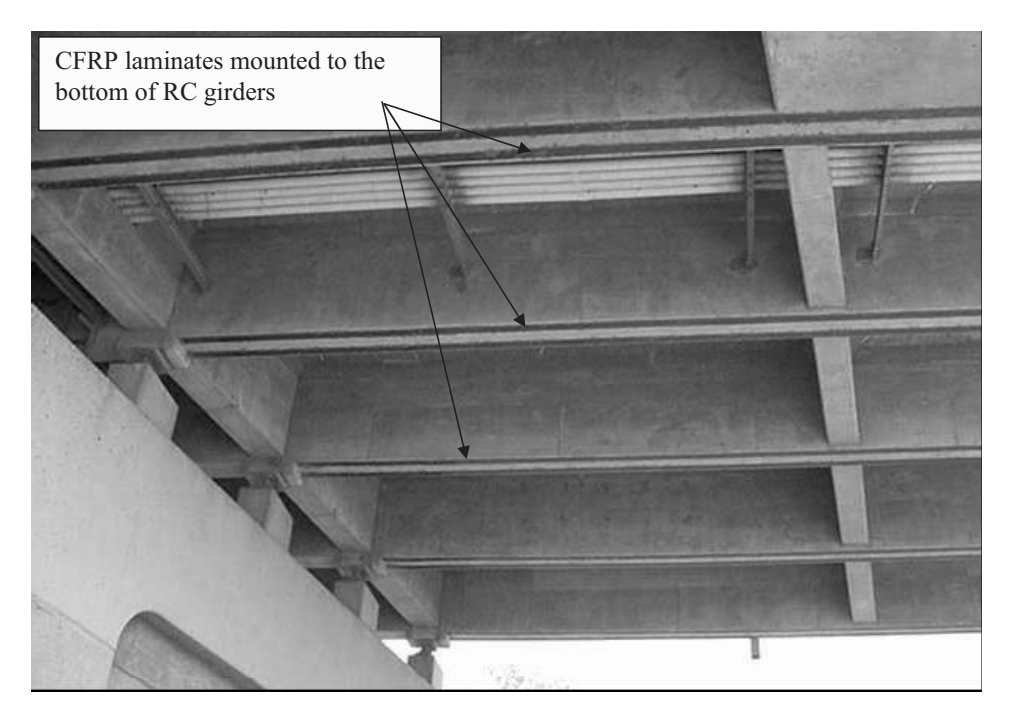


Fig. 12. Girders in span 6 strengthened with CFRP laminates in the Louisa-Fort Gay bridge

# Acknowledgements

The work reported in this article is a summary of research conducted at the University of Kentucky on numerous research projects. The work was conducted by visiting professors, graduate and undergraduate students, staff members from the Kentucky Transportation Center, and staff members from the Kentucky Transportation Cabinet. The projects were funded by the US Department of Defense, the National Science Foundation, the Federal Highway Administration, and the Kentucky Transportation Cabinet.

#### References

- 1. Alagusundaramoorthy, P., Harik, I.E., and Choo, C.C., "Shear Strengthening of R/C Beams Wrapped With CFRP Fabric," *Kentucky Transportation Center Research Report No. KTC-01-1, University of Kentucky*, Lexington, Kentucky, August 2002, 30 pp.
- 2. Alagusundaramoorthy, P., Harik, I.E., and Choo, C.C., "Flexural Behavior of R/C Beams Strengthened With CFRP Sheets or Fabric," *Kentucky Transportation Center Research Report No. KTC-01-2, University of Kentucky*, Lexington, Kentucky, August 2002, 38 pp.

- 3. Choo, C.C., and Harik, I.E., "Inspection and Evaluation of a Bridge Deck Reinforced With Carbon Fiber Reinforced Polymer (CFRP) Bars," *Kentucky Transportation Center Research Report No. KTC 06-06/FRT-102-00-1F, University of Kentucky*, Lexington, Kentucky, March 2006, 18 pp.
- 4. Choo, C.C., and Harik, I.E., "Performance Evaluation of Concrete Bridge decks Reinforced With MMFX and SSC Rebars," *Kentucky Transportation Center Research Report No. KTC 06-02/FRT-113-01-1F, University of Kentucky*, Lexington, Kentucky, January 2006, 39 pp.
- 5. Deitz, D., Harik, I.E., and Gesund, H., "GFRP Reinforced Bridge Decks," *Kentucky Transportation Center Research Report No. KTC-00-9, University of Kentucky*, Lexington, Kentucky, November 1999, 225 pp.
- 6. Harik, I.E., Alagusundaramoorthy, P., Gupta, V., Hill, C., and Choo, C.C., "Inspection and Evaluation of a Bridge Deck Partially Reinforced With GFRP Rebars," *Kentucky Transportation Center Research Report No. KTC 04-21/FRP Deck-1-97-1F, University of Kentucky*, Lexington, Kentucky, August 2004, 102 pp.
- 7. Hill, C., Choo, C.C, and Harik, I.E., "Reinforcement Alternatives for Concrete Bridge Decks," *Kentucky Transportation Center Research Report No. KTC 03-19/SPR-215-00-1F, University of Kentucky*, Lexington, Kentucky, July 2003, 35 pp.
- 8. Simpson, J.W. II, Harik, I.E., and Choo, C.C, "Shear Repair of P/C Box Beams Using Carbon Fiber Reinforced Polymer (CFRP) Fabric," *Kentucky Transportation Center Research Report No. KTC 06-01/FRT-114-01-1F, University of Kentucky*, Lexington, Kentucky, January 2006, 39 pp.

# Comparative Seismic Assessment of Multi-Story Buildings Designed to Latest Design Provisions

# **Aman Mwafy**

Mid-America Earthquake Centre, University of Illinois at Urbana-Champaign, Urbana, Illinois, U.S.A.

## **Abstract**

The paper investigates the inelastic seismic response of contemporary multi-story Reinforced Concrete (RC) buildings to a number of seismic scenarios applicable to medium seismicity regions of the Middle East. Four RC buildings are considered, representing regular and irregular ductile Moment-Resisting Frame (MRF) structures. These are designed and detailed according to two design provisions employed in this region. A verified analytical tool and refined fiber modeling approach able to simulate the cyclic response of structural members are adopted. The seismic response from extensive dynamic collapse analyses is monitored on the member and the structure levels for a diverse set of input ground motions. Investigating the inelastic response of the buildings designed to the two design provisions provides insight into the behavior of structures designed to different levels of force reduction factors. It also offers international calibration to the national design codes in the region and aids in understanding the differences and similarities with international design provisions. This helps to improve the design codes, which is the most effective mean to reduce earthquake losses and increase public safety.

**Key Words:** Seismic design provisions, RC buildings, inelastic dynamic collapse analysis, analytical simulations, medium seismicity regions.

## Introduction

The lack of reliable design codes that account for the latest technology and deep experience alongside local construction practice and simplified requirements has a profound influence on the large human and economic losses observed from recent earthquakes of 2005 Kashmir (Pakistan) and 2006 Yogyakarta (Indonesia). These events have clearly demonstrated the potential for a major catastrophe from future earthquakes, which may hit even more densely populated and industrialized regions than the affected regions (e.g. Durrani et al., 2005). Inadequate design of buildings significantly increases their vulnerability to earthquake damage. Structures which are properly designed on the basis of well-calibrated and extensively verified seismic codes are less vulnerable as a result of their efficient energy dissipation systems. Modern seismic codes and guidelines (EC8, 2004; ASCE, 7, 2005) have been developed based on extensive research related to specific regions and observations of actual damage that has occurred to structures in past events. The continuous update of design codes in the Middle East requires extensive research to calibrate the design provisions and assess the seismic performance of contemporary buildings to mitigate potential earthquake-related losses. The active seismicity of several regions in the Middle East emphasizes the need for calibrating design codes, which is the most effective approach to mitigate seismic hazard in future.

Calibrating design codes can be achieved through extensive assessment of the response of buildings representing the typical structures in the study region. Recent studies on assessment and calibration of modern seismic design codes (Mwafy et al., 2006-a, 2006-b; Mwafy and Elnashai 2001, 2002, 2005, 2006-a, 2006-b) have confirmed the effectiveness of this approach to enhance the level of safety and cost effectiveness of structures. The European codes for design of concrete structures (EC2, 2004) and design of structures for earthquake resistance (EC8, 2004) are currently the official standards for design of RC buildings in different countries in Europe. EC8 adopts a trade-off between strength and ductility by allowing designing to three progressive ductility levels, with increasing capacity design requirements. These standards represent state-of-the-art design provisions, which may be applied to different regions with diversity in structural systems, seismicity and construction techniques. On the other hand, the 2001 version of the Egyptian code for design and construction of concrete structures (ECCS 203, 2001) and the Egyptian code of loads (ECL, 2003) represent typical design provisions adopted in the Middle East. ECCS, 203 has been updated to enhance the ductility by adopting the concept of "capacity design". ECCS, 203 also adopts different levels of reinforcement detailing: (i) structures located in the lowest seismic zone are designed and detailed without additional requirements and (ii) structures located in medium and high seismic zones are designed, dimensioned and detailed either as "non-ductile" or as "ductile", with additional provisions to improve ductility.

Despite the fact that EC8 is the main reference seismic code for ECL (2003), several provisions and design criteria are not uniform. For instance, the force reduction factors (Mwafy and Elnashai, 2002) introduced in the latest version of ECL (2003) are higher than those adopted by EC8. On the other hand, the reference code for ECCS 203 is ACI-318 (2002). This results in notable differences between RC buildings designed to the European and the Egyptian codes. For instance, the length of beam critical regions recommended by ECCS 203 (twice the beam depth) follows the recommendation of

ACI-318 (2002), which is over-conservative compared with the length adopted by EC8, particularly for medium ductility frames. For short beams, this results in employing the stringent ductility requirements of critical regions along the beam length. EC8 (2003) recommends a critical length ranging from 1.0 to 1.5 of the beam depth for design to ductility class Medium and High, respectively. The above discussion emphasizes the pressing need for calibrating of the design provisions adopted in the Middle East.

Contemporary buildings representing characteristics of commonly constructed medium-rise RC buildings in the Middle East are designed to ECCS 203 and ECL. Extensive inelastic analytical simulations are carried out using state-of-the-art assessment methodologies and a diverse set of input ground motions representing the study region. Comparable structural systems designed to EC2 and EC8 are also assessed to compare with those designed to ECCS 203 and ECL. Investigating the seismic response of contemporary structures in the Middle East provides insight into their behavior and offers international calibration to the national design codes (exemplified in this study by the Egyptian code) by comparison with international provisions (represented by the Eurocodes).

# Structural Design and Analytical Modeling

Four RC buildings were selected in the current study to represent characteristics of contemporary medium-rise RC buildings designed to modern seismic codes. The buildings are split into two sets based on their configuration, as shown in Table 1. Within each group, a pair of buildings is considered, representing two different designs. The two configurations are for a twelve story regular frame building and an eight story irregular MRF structure. All beam cross-sectional dimensions are  $0.3\times0.6$  m, while they are  $0.3\times0.8$  m in the ground floor of the 8-story building. Column cross-sections are identical throughout the buildings height. The floor system comprises of a 0.14 m thickness solid slabs. Characteristics of the buildings are described in Fig. 1.

Table 1. Characteristics of the Four Structural Systems Investigated

Group	Reference	Design Code	No. of Stories	Design PGA	T <sub>1</sub> (sec)	T <sub>2</sub> (sec)
A	B8-C1	EC2 and EC8	Eight		0.71	0.23
Λ	B8-C2	ECCS 203 and ECL	Light	0.15	0.71	0.23
D	B12-C1	EC2 and EC8	Twelve	0.13	0.93	0.30
В	B12-C2	ECCS 203 and ECL	Tweive		0.93	0.30

Two of the four investigated buildings (B8-C1 and B12-C1) were designed and detailed in accordance with Eurocode 2 and 8, which represent typical modern seismic codes applicable to more than one country with various levels of seismicity and soil conditions. The selection of this group of buildings was motivated by the desire to include in the study a sample of structures carefully designed and detailed to the modern design practice. The buildings were designed and detailed to the medium ductility requirements of EC8. The design PGA is 0.15g, the soil is medium class (C) and the importance factor is 1.0. The permanent and live loads are 5.5 kN/m² and 2.0 kN/m², respectively. The total gravity loads used in seismic analysis are 36600 kN and 22680 kN for the 12 and the 8-story structure, respectively. The cross-section capacities were computed by

considering characteristic cylinder strength of  $25 \text{ N/mm}^2$  for concrete and a characteristic yield strength of  $500 \text{ N/mm}^2$  for steel.

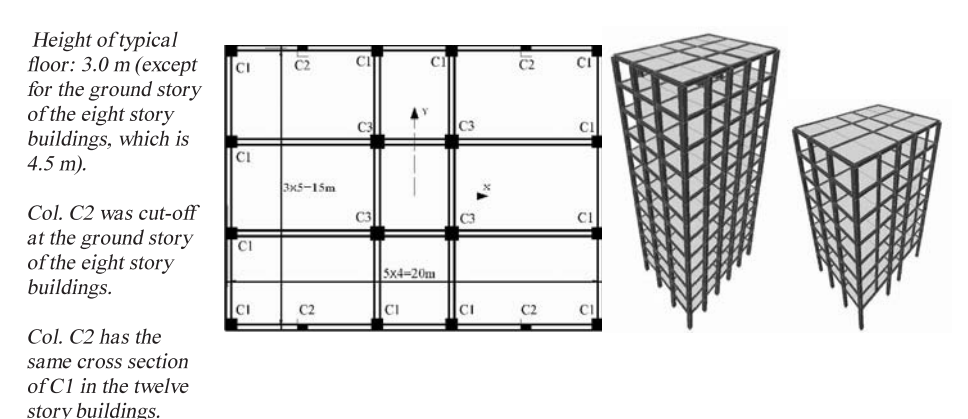


Fig. 1. Description of the investigated buildings.

On the other hand, the design of B8-C2 and B12-C2 buildings were carried out using ECCS 203 (2001) and ECL (2003). The concrete strength is 25 N/mm<sup>2</sup> and steel strength is 400 N/mm<sup>2</sup>. Proportioning of structural members was carried out using the seismic provisions of ductile frames adopted by ECCS 203 (2001). All ductility requirements of ECCS 203 were taken into consideration, including the capacity design provision for columns. The concrete strength used is 25 N/mm<sup>2</sup>, while a steel strength of 400 N/mm<sup>2</sup> was selected since the steel S500 used in design of the European buildings is neither available in the local market nor recommended by the Egyptian code. cross-sections are identical for the pair of buildings of the same height to allow comparisons of the response of buildings designed to different design provisions. Figure 2 shows column and beam sizes and reinforcement details of the two buildings designed to ECCS 203 and ECL. Elastic free vibration analyses of the investigated buildings confirm that the non-cracked fundamental periods of the buildings (0.71 - 0.93) cover a realistic range of medium-rise multi-story buildings, as shown from Table 1. Different building heights (25.5 - 36 meters) and degree of regularity were also taken into consideration to insure that the assessment sample represents contemporary medium-rise RC building.

It is noteworthy that the design base shear of the B8-C2 and B12-C2 buildings is lower than those calculated for the B8-C1 and B12-C1 structures. This is despite the fact that the four buildings were designed to a PGA of 0.15g. The differences in the force reduction factor and the response spectrum used in design are the main source for this discrepancy. The response modification factors (R) adopted by ECL (2003) are notably higher than those recommended by EC8 (2004). This results in an observable difference in seismic design forces and the lateral capacity of the buildings, as confirmed below from pushover analysis results. On the other hand, EC8 (2004) and ECL (2003) employ two different elastic spectra for design. The selection of the shape of the design spectrum is based on the magnitude of earthquakes that contribute most to the seismic hazard rather than on the maximum credible earthquake. The design code recommends that the Type (I)

spectrum is adopted if the earthquakes that contribute most to the seismic hazard have a surface-wave magnitude, Ms, not greater than 5.5. When the earthquakes anticipated at the site are generated by differing sources, the two shapes of the spectra, Type (I) and (II), should be employed to adequately represent the design seismic action. The elastic spectrum Type (I) is the most appropriate for design since the B8-C2 and B12-C2 buildings are assumed at a hypothetical medium seismicity region in the Middle East (e.g. Cairo). The B8-C1 and B12-C1 buildings were designed to the conservative response spectrum (Type II), which has higher amplification in the period range of the buildings compared with the Type (I) spectrum. Nevertheless, it should be pointed out that the most significant source for the difference in seismic design forces is the force reduction factors adopted by the above-mentioned codes.

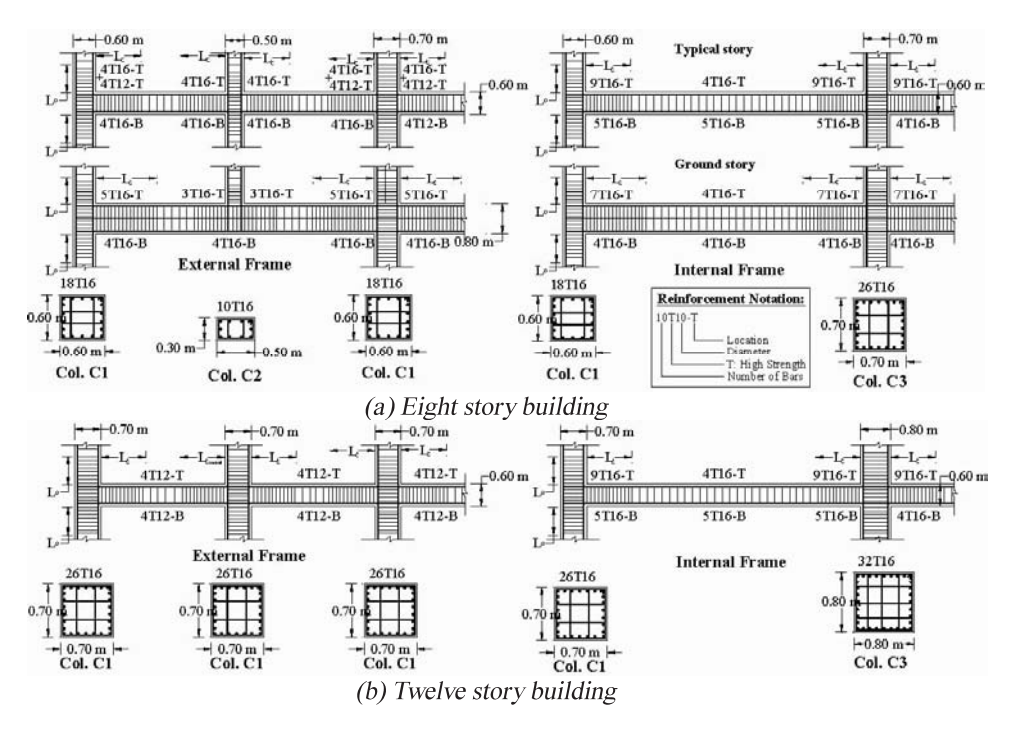


Fig. 2. Sample reinforcement details of the buildings designed to ECCS 203 (2001) and ECL (2003).

The capability to reliably predict the complicated dynamic behavior of structures when subjected to seismic excitations is the key towards improving design provisions. Refined three-dimensional models of the entire buildings employing the fiber approach were therefore assembled for inelastic analysis using ZEUS-NL (Elnashai et al., 2006). This finite element program has been developed and thoroughly verified with full scale test results at Imperial College, UK, and at University Illinois at Urbana-Champaign, USA, to deliver a state-of-the-art inelastic analysis tool for static and dynamic analysis. In this detailed modeling, each structural member is assembled using a number of cubic elasto-plastic elements capable of representing the spread of inelasticity within the

member cross-section and along the member length. Based on anticipated critical response, dynamic analyses are conducted in the longitudinal direction (along the global X-axis).

# **Input Ground Motions for Response History Analysis**

The B8-C2 and B12-C2 buildings are assumed at a hypothetical site in the Middle East (e.g. Cairo) with a PGA of 0.15g. The typical seismic scenario of the site is from shallow earthquakes of magnitude of 5.5. For the inelastic response history analysis, three natural ground motions were selected to match the code spectrum Type (I), which is the most appropriate spectrum for design (ECL 2003). These are Imperial Valley at El Centro Array #1 (USA, 1979), Imperial Valley at El Centro Array #11 (USA, 1979) and Hollister City Hall (USA, 1974). To account for possible earthquakes from other sources, an artificial accelerogram (Art-rec1) was also selected to match the code spectrum Type (II). On the other hand, the two buildings designed to EC2 and EC8 (2004) were assessed under four synthetically generated accelerograms to match the code spectrum Type (II) (Art-rec1-4). Assessment of B8-C2 and B12-C2 under Art-rec1 also allows for comparison of the buildings seismic response.

All records were scaled using the modified Housner spectrum intensity approach (Housner 1952; Mwafy and Elnashai 2001), whereby the code spectra (Type I and II) at the design PGA were taken as references for the two sets of records employed in the analysis (the natural and the artificial records, respectively). The adopted definition of the

spectrum intensity scale is given by:  $\overline{SI} = 1/(T_2 - T_1) \int_{T_1}^{T_2} SV(T,\xi) dT$ , where  $T_1$  and  $T_2$  are the appropriate integration limits for the investigated structures, as shown in Fig. 3. These limits were selected based on the recommendation of Mwafy and Elnashai (2001) and Elnashai and Mwafy (2002). The normalization factors employed to scale input ground motions are summarized in Table 2. The buildings were subjected to the input ground motions with increasing severity, starting from half the design intensity (0.075g) up to the intensity that causes structural failure. The elastic spectra of input ground motions normalized to a PGA of 0.15g are depicted in Fig. 4 along with the design code elastic spectra Type (I) and (II).

# **Inelastic Response of Buildings**

Figure 5 shows the capacity envelops of the four buildings obtained from inelastic pushover analysis using an inverted triangular lateral load distribution. Mwafy and Elnashai (2002) and Mwafy (2001) concluded that this lateral load pattern results in a conservative estimate of initial stiffness and ultimate capacity of medium-rise buildings. The seismic forces used in design of the four buildings are also depicted in Fig. 5. It is clear that the two structures designed to EC2 and EC8 have higher lateral capacity compared with those designed to ECCS 203 and ECL. As mentioned above, B8-C2 and B12-C2 were assigned a force reduction factor of 7.0 according to ECL. This is unlike those designed to EC8 (2004), which imposes an upper limit on the R factor (behavior factor) of 3.9 for frame systems. EC8 also recommends reducing the R factor by 20% for irregular buildings in elevation. This results in a large difference between the design forces and hence the capacities of the buildings designed to the two seismic codes.

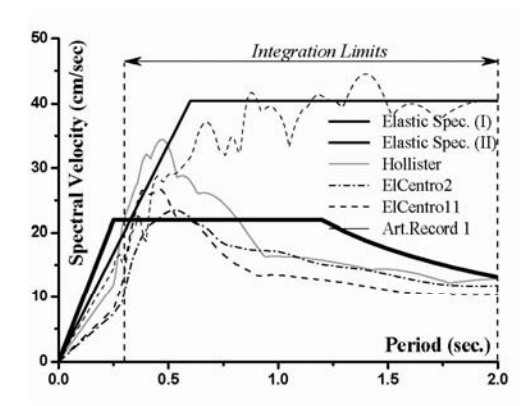


Fig. 3. Velocity spectra and integration limits employed to scale the input ground motions for inelastic analysis

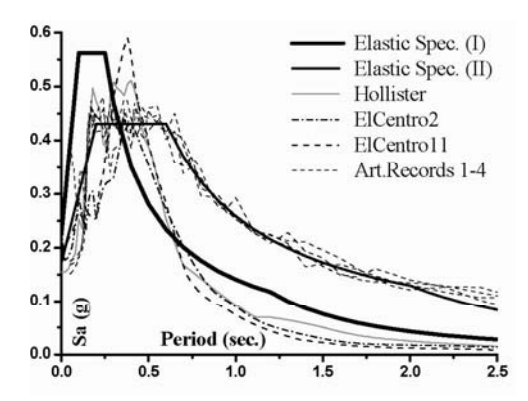


Fig. 4. Acceleration response spectra of input ground motions scaled to a PGA of 0.15g (5% critical damping).

**Table 2. Normalization Factors for Input Ground Motions** 

<b>Ground Motions</b>	El Centro 2 (USA, 1979)	El Centro 11 (USA, 1979)	Hollister City Hall (USA, 1974)	Art. Record
Normalization factors*	1.216	1.321	1.034	1.0

<sup>\*:</sup> the design spectrum type (I) is used as a reference for the natural records, while the code spectrum type (II) is the reference for the artificial records.

It is interesting to note that the two buildings designed to different R factors have the same initial stiffness. The response of the buildings designed to EC2 and EC8 (0-c'-d')

using a force reduction factor R' and those designed to ECCS 203 and ECL (0-c-d) using R is schematically explained in Fig. 6. It is clear that the four structures exhibit high overstrength factors ( $\Omega = V_v/V_d$ ) as a result of the higher contribution of gravity loads compared with seismic actions. Moreover, Fig. 5 shows the sequence of first yielding in beams and columns as well as the global yield and ultimate capacity of the buildings. The sequence of formation of plastic hinges in the external frame columns of B8-C2 and B12-C2 is also depicted in Fig. 7. These external frames are more vulnerable than internal systems as a result of the higher stiffnesses of their beams, which attract higher seismic forces. This sequence is comparable for the pair of buildings of the same configuration. Although first yielding is observed in beams of the four structures, the unfavorable concentration of plastic hinges in the planted columns of the irregular buildings is unfavorable. No indication of a hinging mechanism is detected in the four buildings, even in the soft story of the irregular structures (B8-C1 and B8-C2). The results confirm that ductile frames adequately designed to EC2 and EC8 as well as ECCS 203 and ECL have adequate strength and ductility, and are not likely to develop a collapse mechanism. This is mainly due to the adoption of the capacity design provisions by the design codes.

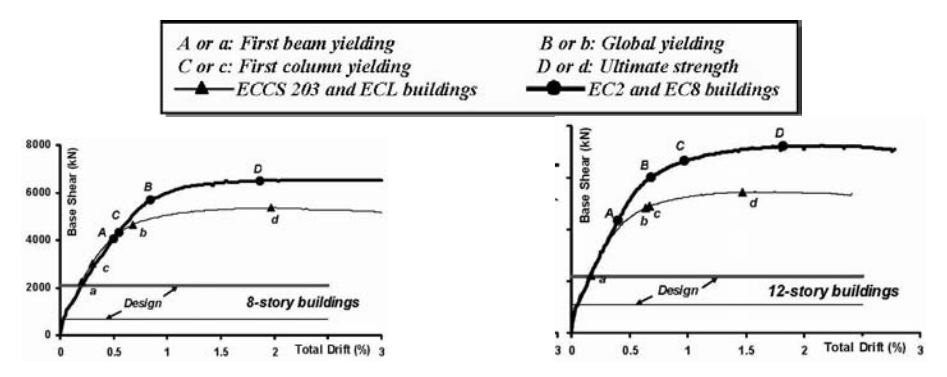


Fig. 5. Base shear vs top displacement response of the four buildings from incremental inelastic static analysis.

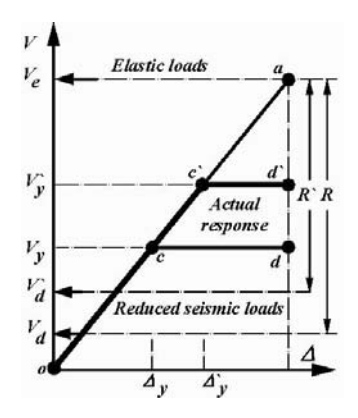


Fig. 6. Comparison of buildings response using different R factors.

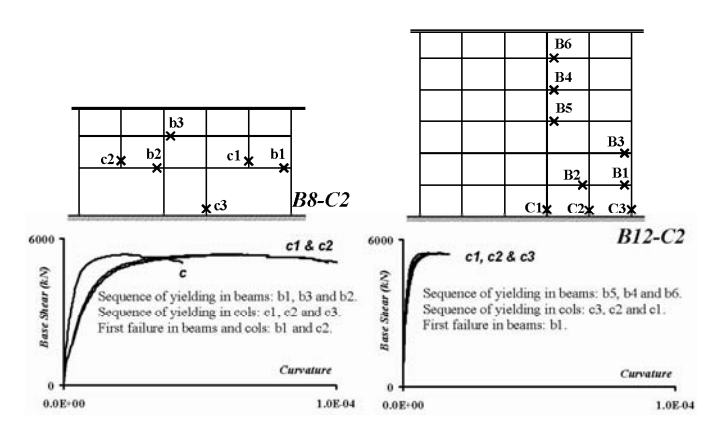


Fig. 7. Sequence of yielding and curvature demands in beams and columns of B8-C2 and B12-C2.

The dynamic response of the buildings is investigated by performing a series of inelastic response history analysis using the progressively-scaled input ground motions mentioned above. For the sake of brevity, only sample results from these extensive analyses are presented for the buildings at various intensity levels. Table 3 shows the local and global response of B8-C2 and B12-C2 for sample records. The variability of the inelastic response is quite significant under different input ground motions. This is more observable when comparing the two seismic scenarios investigated (natural and artificial records), which match two different design spectra. Clearly, the amplification of the artificial records at the period range of both the investigated buildings is higher than the natural records, which results in higher response. Summary of the response of B8-C1 and B12-C1 from four artificial records matching the design spectrum Type (II) is presented in Table 4, while Fig. 8 depicts results of the incremental dynamic collapse analysis of the four buildings.

It is clear that the response of B8-C2 is perfectly elastic while few plastic hinges in beams are observed in B12-C2 under the most probable seismic scenario (natural records). Yielding is observed only in beams under the conservative seismic scenario of the artificial record. At twice the design ground motion, plastic hinges are observed in beams, cut-off columns and at the base of the main columns. With the exception of the cut-off vertical members, yielding in main columns is only observed at the ground level, even under the most conservative seismic scenario. Disadvantages of irregular structural systems are clearly exemplified when comparing response of the irregular buildings with the regular systems. However, since capacity design protects the main columns and prevents any formation of collapse mechanism, the response of both the B8-C2 and B12-C2 buildings is considered satisfactory. As expected, the displacement and base shear demands of the two buildings designed to EC2 and EC8 are higher compared with those designed to ECCE 203 and ECL. This is mainly because the former structures have higher strength, which results in attracting higher seismic demands. Finally, the state of damage of the four buildings at different levels of ground motions is described in Tables 5. This is based on the average curvature ductility demands in beams and columns from all input ground motions. At the design earthquake, the average damage in beams is 'light',

while it is 'negligible' in columns (no yielding). At twice the design earthquake, the average damage in beams and columns is 'light'.

Table 3. Sample Response Results from Dynamic Collapse Analysis of B8-C2 and B12-C2  $\,$ 

EQ	EQ	Top Disp.	Base Shear	Local Response
	Intensity	(mm)	(kN)	
	d	25.9	1469.6	Elastic response (no yielding)
	1.5d	37.1	2682.6	Elastic response (no yielding)
C2 ister	2d	68.8	4034.0	Yielding in several beams and in four cut-off columns.  Total no. of plastic hinges = 120
B8-C2 Hollister	4d	117.4	6024	Yielding in several beams, cut-off columns and at the base of all main columns. Total no. of plastic hinges = 444
	8d	211.7	6487.0	Yielding in several beams, cut-off columns and main columns. Total no. of plastic hinges = 706. Concrete crushing in beams
	d	51.0	2619.0	Twelve plastic hinges in beams
B8-C2 Art. Record	2d	195.3	5391.0	Yielding in several beams, cut-off columns and at the base of all main columns. Total no. of plastic hinges = 502
B8 A Rec	4d	343.8	6268.6	Yielding in several beams, cut-off columns and main columns. Total no. of plastic hinges = 670. Concrete crushing in beams
	d/2	30.6	1564.8	Elastic response (no yielding)
<b>l</b> . [	d	62.6	2861.8	Yielding in beams. Total no. of plastic hinges = 32
B12-C2 Hollister	2d	99.2	5113.4	Yielding in several beams. Total no. of plastic hinges = 510
B12 Hol	4	166.2	7150.0	Extensive yielding in several beams and few columns at the base. Total no. of plastic hinges = 694
	8d	327.0	7466.1	Extensive yielding in beams and in several columns. Total no. of plastic hinges = 894. Permanent deformation.
p.	d/2	75.9	3362.0	Yielding in several beams. Total no. of plastic hinges = 158
B12-C2 rt. Recor	D	141.3	4660.0	Extensive yielding in beams. Total no. of plastic hinges = 458
B12-C2 Art. Record	2d	312.5	6477.6	Extensive yielding in beams and in columns at base. Total no. of plastic hinges = 768
_	4d	728.3	8044.0	Extensive yielding in beams and in several columns. Total no. of plastic hinges = 914. Concrete crushing in beams.

d: design ground motion

Table 4. Sample Response Results from Dynamic Collapse Analysis of B8-C1 and B12-C1 (Average of Four Artificial Records)

EQ	EQ Intensity	Top Disp. (mm)	Base Shear (kN)	Local Response
Ş	d	1238.2	4692	Yielding in beams and I few cut-off columns
<u></u>	2d	248.8	6243	Yielding in several beams, cut-off columns and at the base of all main columns
2	d	158.2	5328	Extensive yielding in beams
B8-	2d	291.6	7937	Extensive yielding in beams and at the base of main columns.

d: design ground motion

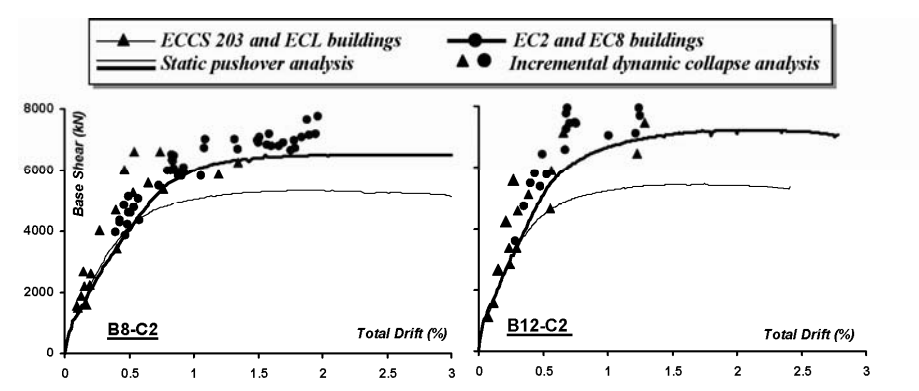


Fig. 8. Incremental dynamic collapse analysis results of the four buildings.

Table 5. Average Damage State Based on the Observed Ductility Demands (average of all input ground motions)

	Design	ı PGA	Twice the Design PGA				
Reference	Damage description in	Damage description in	Damage description in	Damage description in			
	beams	columns	beams	columns			
B8-C1	Light	Light	Light	Light			
B8-C2	Light	Negligible	Light	Light			
B12-C1	Light	Negligible	Light	Light			
B12-C2	Light	Negligible	Light	Negligible			

Negligible: Curvature ductility  $(\mu_{\phi}) \le 1$ , Light:  $1.0 \le \mu_{\phi} \le 3.0$ , Moderate:  $\mu_{\phi} \ge 3.0$ 

Despite the low seismic design forces of B8-C2 and B12-C2, the results confirm the satisfactory performance and the adequate safety margin of the four ductile frame structure investigated in the present study, particularly the regular buildings. This is confirmed even at intensities higher than the design ground motion. This is mainly due to the adequate ductility and lateral strength observed in the buildings. The results clearly confirm the importance of the ductility and capacity design requirements recommended by modern seismic codes for design of multi-story buildings in seismic regions.

## Conclusion

The study assessed the seismic performance of two sets of contemporary RC buildings designed and detailed to two design provisions commonly used in design in the Middle East, namely the European and the Egyptian codes. Designing the same structure to different force reduction factors (R) were exemplified in the investigated case studies since the above-mentioned codes adopt different R factors. Four RC buildings were designed and extensively analyzed using a refined fiber modeling approach and a verified analysis tools. Inelastic pushover and incremental dynamic collapse analyses were undertaken for the four buildings using a diverse set of synthetic and natural ground motions scaled using the spectral intensity scale.

It was confirmed that adequately-designed ductile frame structures can withstand higher levels of earthquake excitations than the design intensity. Demands were satisfactory at the design PGA and acceptable at twice the design ground motion, particularly for the regular frame buildings. This is mainly due to: (i) the high overstrength of the buildings and (ii) the efficient energy dissipation mechanism achieved through the ductility and capacity design provisions of the design codes. Designing to the conservative force reduction factors recommended by EC8 had a marginal effect on improving the response of the investigated buildings. This is due to: (i) the higher design strength of the European buildings, which leads to attracting higher seismic demands and (ii) the higher contribution of gravity loads in design of the investigated structures compared with seismic actions. As intended by the capacity design provisions, inelasticity was observed only at the ground story columns, with acceptably few exceptions in the cut-off columns of the irregular buildings. The comparative study presented in this paper confirmed the adequate safety margins of buildings designed to the latest design provisions. It is therefore highly recommended to adopt the ductility and capacity design requirements of modern seismic codes in design of multi-story buildings, which would render these structures to be more reliable and provided with efficient seismic-resistant mechanisms.

#### References

- ACI-318 (2002), Building code requirements for structural concrete and commentary (318-02), American Concrete Institute, Detroit, Michigan.
- ASCE 7 (2005), Minimum Design Loads for Buildings and Other Structures (ASCE 7-05), American Society of Civil Engineers, Reston, VA.
- Durrani, A.J., Elnashai, A.S., Masud, A., Hashash, Y. and Kim, S.J. (2005), The Kashmir earthquake of October 8, 2005 A quick look report, Mid-America Earthquake Center Report no. 05-04, University of Illinois at Urbana-Champaign.
- EC2 (2004), Eurocode 2: Design of concrete structures Part 1: General rules and rules for buildings, CEN, European Committee for Standardization, Brussels.
- EC8 (2004), Eurocode 8: Design of structures for earthquake resistance Part 1: General rules, seismic actions and rules for buildings, CEN, European Committee for Standardization, Brussels.
- ECCS 203 (2001), The Egyptian Code for Design and Construction of Concrete Structures, Cairo, Egypt.
- ECL (2003), The Egyptian Code for Calculation of Loads and Forces in Structural and Building Work, Cairo, Egypt.
- Elnashai, A.S., Papanikolaou, V. and Lee, D. (2006), Zeus-NL a system for inelastic analysis of structures, User Manual, Civil and Environmental Engineering Department, University of Illinois at Urbana-Champaign, USA.
- Elnashai, A.S. and Mwafy, A.M. (2002), "Overstrength and force reduction factors of multi-storey R/C buildings". The Structural Design of Tall Buildings, Vol. 11, 329–351.
- Housner, G. (1952), "Spectrum intensities of strong-motion earthquakes", Proceedings of the Symposium on Earthquake and Blast Effects on Structures, Los Angeles, California, 20-36.
- Mwafy, A.M., Elnashai, A.S., and Yen, W-H. (2006-a), "Implications of design assumptions on capacity estimates and demand predictions of multi-span curved bridges". ASCE Journal of Bridge Engineering, In Press.

- Mwafy, A.M., Elnashai, A.S., Sigbjörnsson, R., and Salama, A. (2006-b), "Significance of severe distant and moderate close earthquakes on design and behavior of tall buildings". The Structural Design of Tall and Special Buildings, Vol. 15(4), 391-416.
- Mwafy, A.M. and Elnashai, A.S. (2006-a), "Vulnerability of code-compliant RC buildings under multi-axial earthquake loading". Proceedings of the 4th International Conference on Earthquake Engineering, October 12-13, Taipei, Taiwan.
- Mwafy, A.M. and Elnashai, A.S. (2006-b), "Significance of shear modeling in seismic assessment of RC structures". Proceedings of the first European Conference on Earthquake Engineering and Seismology, September 3-8, Geneva, Switzerland.
- Mwafy, A.M., and Elnashai (2005), "Utilization of advanced seismic simulations in design of high-rise buildings". Proceedings of the 7th International Conference on Multi-purpose High-rise Towers and Tall Buildings, December 10-11, Dubai, UAE.
- Mwafy, A.M., and Elnashai, A.S. (2002), "Calibration of force reduction factors of RC buildings". J. of Earthquake Engineering, Vol. 6(2), 239-273.
- Mwafy, A.M., and Elnashai, A.S. (2001), "Static pushover versus dynamic collapse analysis of RC buildings". Engineering Structures, Vol. 23(5), 407-424.

# Nonlinear Seismic Interaction Behavior of Shear Wall-Frame with Different Stiffness Ratio of Wall and Frame

## A.R.Khaloo and S.A.Taheri

Civil Engineering Department, Sharif University of Technology Tehran, Iran email: khaloo@sharif.edu

## Abstract

Most codes recommend a minimum strength for frame, equal to 25% of total lateral force, as an acceptance criterion of shear wall-frame dual action. The purpose of this article is to study nonlinear seismic response of wall-frame structures with constant total stiffness and different stiffness ratio of wall and frames. Four, eight and twelve story RC structures, with different frame-wall stiffness ratio ranging from 10-90 to 80-20, are analyzed nonlinearly under time histories. Stiffness and strength degradation, nonlinear behavior of reinforced concrete sections and their energy dissipation in cyclic loading are taken into account. This study tries to find stiffness ratios for frame in wall-frame structures which lead to safe and best nonlinear performance at different level of hazard. Methods are proposed to define wall, frame and wall-frame stiffness in multistory structures. Based on result of this study the minimum frame strength equal to 25% of lateral forces is not accurate and it could be decreased safely, however the best performance would be possible with higher frame stiffness and strength ratios.

**Key Words:** Shear wall, concrete frame, frame-wall interaction, seismic design, nonlinear analysis

## Introduction

Wall-Frame Interaction under lateral load causes irregularities in lateral force distribution between walls and frames. Figure 1 illustrates a shear wall and a frame, both carrying the same load at a certain height.

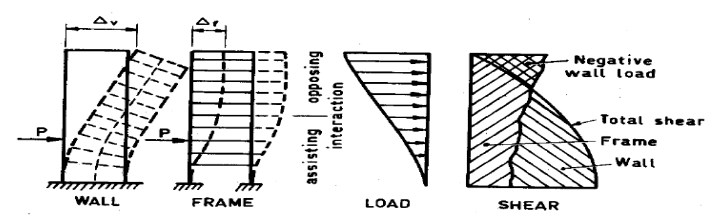


Fig. 1. Frame-Wall interaction (Park and Paulay, 1975).

This load causes the shear wall to suffer bending mode deflections and assume a constant slope above the loaded level. The frame experiences mainly shear mode of deflections and tend to become vertical above the load level. Difference between the modes of deflection causes interaction forces between wall and frames (Park and Paulay, 1975). So lateral load does not distribute between frame and wall at all stories equal to frame-wall stiffness ratio.

Most codes recommend a minimum strength for frame, equal to 25% of total base shear, as an acceptance criterion of shear wall-frame dual action; otherwise this minimum strength does not fully comply with horizontal distribution of load based on stiffness of components, and also with irregularities caused by wall-frame interaction. The criterion of dual action should be based on stiffness of structure instead of its strength, because lateral forces is distributed based on stiffness, and design of frame for 25% of base shear may lead to stiffness higher or lower than 25% of total stiffness. And if designed frame for 25% of base shear provides less than 25% of total stiffness, frame design will be conservative. In addition the minimum required strength, mentioned in most codes is not based on detailed studies and is based mainly on engineers' experience. Also nonlinear dynamic response of frame-wall structure could effect on the all above discussions.

This study attempts to find the best possible and minimum safe strength and stiffness ratio of frame to wall simultaneously by keeping the frame-wall stiffness ratio equal to their design shear ratio.

Four, eight and twelve story frame-wall RC structures with rigid simply connected beam between wall and frames at all stories are modeled. These models with constant total stiffness and different frame- wall stiffness ratio ranging from 10-90 to 80-20 are designed according to linear dynamic procedure of UBC-97. All models are analyzed nonlinearly under time histories to compare different stiffness ratios to find minimum safe and best performance ratios.

# **Model Specification**

The models are two-dimensional because there is no need to take account of the effect of torsion. Shear wall-frame structure is modeled by separate frames and walls which are connected by rigid, simply connected beam at story levels (Fig. 2a). This kind of modeling helps to investigate the interaction of shear wall-frame and also allows defining the accurate stiffness of walls and frames. By modeling wall inside frame (Fig. 2b), separate computation of wall and frame stiffness, which is really important to get the stiffness ratios in this study, would not be possible due to wall and frame influence on each others stiffness.

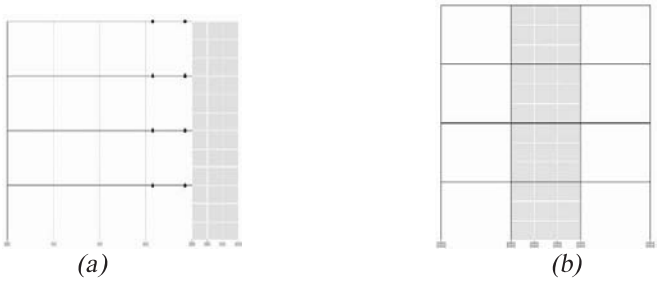


Fig. 2. (a) Frame-wall connected by link beam. (b) Frame-wall.

Nonlinear analysis is performed on three different groups of structures with heights of 12, 24 and 36m. These are four, eight and twelve story structures and include a 3 bay frame with 4m spans and wall with different length.

Models in any groups are defined to have constant stiffness and different stiffness ratio of wall and frame. All other parameters of models like loading, analysis procedure and design specifications, which will be discussed later, are assumed to be constant in structures of any group to allow observing only stiffness and strength ratio of structures.

### Stiffness Calculation

Stiffness of wall, frame and frame-wall structure should be calculated separately as numerical value, in order to obtain the exact stiffness ratio of frame-wall structures. Stiffness of structure calculated for each story which is used for horizontal distribution of lateral load, is not useful for this study because these stiffnesses and their stiffness ratios will differ so much with distributed load on frame-wall models under lateral load. This difference due to frame-wall interaction, leads to define a proper method for computation of stiffness which takes the effect of frame-wall interaction into account. To define stiffness, structures are loaded by reverse triangle loading (Fig. 3) and displacement at different level of stories are obtained by static analysis. Stiffness of each stories are calculated based on story shears and displacement:

$$K_{i} = \frac{V_{i}}{\Delta_{i} - \Delta_{i-1}}$$

$$V_{i} = \sum_{i}^{n} F_{x}$$

$$(1)$$

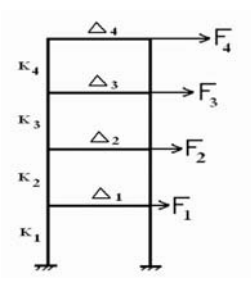


Fig. 3. Loading for stiffness calculation

Stiffness of multistory structure is calculated by story stiffness as numerical value, using simulation of structures to series of spring as shown in Fig. 4.

$$K_{series} = \frac{1}{\frac{1}{k_1} + \frac{1}{k_2} + \frac{1}{k_3} + \frac{1}{k_4}} = \frac{k_1 + k_2 + k_3 + k_4}{k_1 \times k_2 \times k_3 \times k_4}$$
(2)



Fig. 4. Simulation of multi-story structure to series of springs.

To calculate constant stiffness for each group reference structure is defined as follows: a frame is designed for gravity loads only. Then the frame is designed for 25% of base shear. Stiffness of frame will be obtained by the above method. Later a wall with stiffness three times the frame calculated stiffness is defined. The frame and the wall are placed in a model and designed for total base shear.

Stiffness of all models in each group is equal to stiffness of reference structure. Numerous frames and walls are considered and then combined to get different stiffness ratio. For example, a frame with stiffness equal to 10% of constant stiffness (reference structure stiffness) and a wall with 90% of constant stiffness is considered and

combined to have a frame-wall with stiffness ratio 10-90 and total stiffness equal reference structure stiffness.

# **Linear Dynamic Design**

All models are designed according to linearly dynamic procedure of UBC- 97. Gravity load is assumed 4500 kg/m and 1500 kg/m. Structures are assumed to be in high risk zone (zone 4) with distance to nearest fault more than 15 km. Frames are special moment resisting frame (SMRF), so structural system coefficient (R) is assumed 8.5 without consideration of minimum required strength for frame equal to 25% base shear. This assumption allows investigating the 25% of codes. This consistency in design assumption is needed also for comparison of different stiffnesses ratios.

# Nonlinear earthquake analysis

Nonlinear earthquake analysis of structures is performed by modeling in RAM-Perform 3D (Educational version). Structure dimension and properties is just same as linear models. Nonlinear property of material, sections (beam and columns) and shear walls is defined based on section properties and Fema 356 requirements and modeling assumptions. Columns are modeled based on Fema properties and column nonlinear responses are also compared with Fema acceptance criteria for different performance level. The nonlinear behavior of beam is modeled like columns based on Fema. Shear properties of beams and columns are assumed to be linear, and dependent on axial load. Beams and columns are modeled in RAM-Perform by using existing Fema beam and column component in the software. Strength loss, stiffness and strength degradation is also considered in beam and column modeling, by using dissipation factors for hystersis behavior of Fema component.

Shear walls are modeled using fiber sections. Sections with concrete and steel fibers in different coordinates use nonlinear concrete and steel materials behavior. According to the result of the analysis, stress and strain for fiber sections are compared with acceptance criteria of stress and strain.

Based on Fema 356 requirements at least three earthquake records is used for nonlinear earthquake analysis. Three selected earthquake record for this study are North Ridge, Morgan Hill and Landers. These three records are scaled to UBC design spectra based on the Fema 356 procedure. These scale factors are 1.09, 2.03 and 4.15 for North Ridge, Morgan Hill and Landers, respectively. In Fig. 5, the earthquake response spectrum and design spectra is shown before and after scaling records.

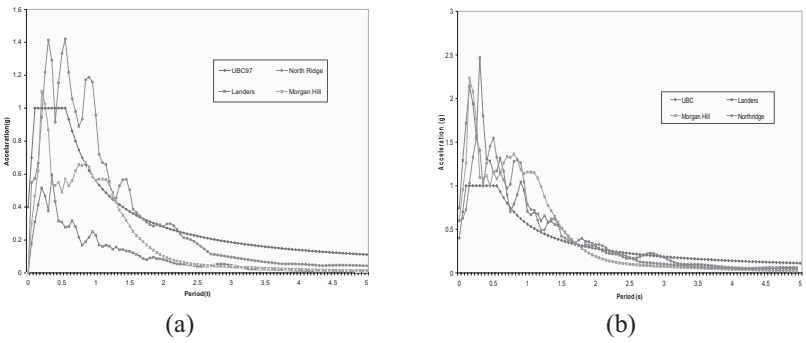


Fig. 5. Earthquakes response spectrum. (a) not scaled (b) scaled.

# Results

Nonlinear analysis result is based on RAM-Perform usage ratios. Usage ratios are maximum demand capacity ratios which are produced by dividing calculated demands by capacities for different level of performance. Any usage ratios are the maximum of demand capacity ratio of defined groups. For example all nonlinear deformation of beams in life safety performance could be sorted as one group and Perform will give the maximum demand/capacity ratio in these beams as one usage ratio.

Different usage ratio of strength, nonlinear deformation and drift are our tools to compare frame-wall structures with different stiffness ratio. These usage ratios are listed in Tables 1, 2 and 3 for four, eight and twelve story structures, respectively.

In tables, usage ratios are listed for different groups. These are beams and columns strength(shear and moment), beams and columns nonlinear deformation, shear wall strain (concrete and steel fibers) and drift which is based on UBC 97 maximum drift equal to 0.025 for period less than 0.7 second, and 0.02 for higher periods.

In four-story structure, stiffness ratios equal or higher than 20-80 have acceptable nonlinear response for performance level 1 (Immediate Occupancy), but 15-85 ratio is not safe for beams in level 1. All ratio response is acceptable for level 3 (Life Safety). The best possible ratio is 60-40.

Beams' response in 8 story structure is not acceptable for level 1 and is acceptable for ratios from 20-80 to 80-20 in level 3. Columns and walls are acceptable for ratios higher than 20-80 for level 3. The best possible ratio is 60-40 in 8 story groups.

Structures in 12 Story group does not perform well in any ratios for level 1 due to beams' response, but are acceptable for ratios higher than 20-80. Shear walls and columns are acceptable for ratios higher than 20-80 even for level 1. The best possible ratios are 50-50 and 60-40.

**Table 1. Four Story Structure Usage Ratios** 

Element		P.				Fran	ne-wall S	e-wall Stiffness Ratio					
Type	Limit State Type	r. L	10~9	15~8	20~8	25~7	30~7	40~6	50~5	60~4	80~2	100~	
Турс		L	0	5	0	5	0	0	0	0	0	0	
Beam	Deformation	1	1.58	1.16	0.84	0.59	0.67	0.60	0.65	0.57	0.56	0.53	
Beam	Deformation	3	0.79	0.58	0.42	0.29	0.34	0.30	0.33	0.29	0.28	0.26	
Beam	Deformation	5	0.54	0.42	0.33	0.23	0.27	0.24	0.26	0.23	0.22	0.21	
Column	Deformation	1	0.87	0.77	0.84	0.54	0.33	0.09	0.00	0.00	0.00	0.27	
Column	Deformation	3	0.30	0.26	0.28	0.18	0.11	0.03	0.00	0.00	0.00	0.09	
Column	Deformation	5	0.22	0.20	0.21	0.14	0.08	0.02	0.00	0.00	0.00	0.07	
Wall	Steel Strain	1	1.27	0.98	0.90	0.89	0.74	0.70	0.71	0.69	0.56		
Wall	Steel Strain	3	0.51	0.39	0.36	0.36	0.29	0.28	0.28	0.28	0.23		
Wall	Steel Strain	5	0.34	0.26	0.24	0.24	0.20	0.19	0.19	0.19	0.15		
Wall	Concrete Strain	1	0.57	0.55	0.57	0.73	0.58	0.59	0.22	0.29	0.17		
Wall	Concrete Strain	3	0.29	0.28	0.28	0.37	0.29	0.29	0.11	0.15	0.08		
Wall	Concrete Strain	5	0.17	0.17	0.17	0.22	0.17	0.18	0.07	0.09	0.05		
Beam	Moment Strength	1	0.94	0.93	0.85	0.83	0.78	0.68	0.65	0.59	0.48	0.41	
Beam	Moment Strength	3	0.85	0.84	0.77	0.75	0.70	0.62	0.59	0.53	0.43	0.37	
Beam	Moment Strength	5	0.71	0.70	0.64	0.62	0.59	0.51	0.49	0.44	0.36	0.31	
Beam	Shear Strength	1	0.77	0.70	0.64	0.58	0.59	0.58	0.55	0.52	0.53	0.54	
Beam	Shear Strength	3	0.69	0.63	0.57	0.52	0.53	0.52	0.50	0.47	0.48	0.49	
Beam	Shear Strength	5	0.57	0.53	0.48	0.43	0.44	0.43	0.41	0.39	0.40	0.41	
Column	Moment Strength	1	1.11	1.11	1.12	1.11	1.27	1.11	0.92	0.90	0.98	1.11	
Column	Moment Strength	3	1.00	1.00	1.01	1.00	1.15	1.00	0.83	0.81	0.88	1.00	
Column	Moment Strength	5	0.83	0.83	0.84	0.83	0.95	0.83	0.69	0.67	0.73	0.83	
Column	Shear Strength	1	0.56	0.56	0.56	0.58	0.80	0.85	0.81	0.96	1.06	1.11	
Column	Shear Strength	3	0.51	0.50	0.51	0.52	0.72	0.77	0.73	0.86	0.95	1.00	
Column	Shear Strength	5	0.42	0.42	0.42	0.44	0.60	0.64	0.60	0.72	0.79	0.84	
Drift	UBC 97		0.45	0.36	0.32	0.25	0.26	0.24	0.24	0.22	0.22	0.20	

**Table 2. Eight Story Structure Usage Ratios** 

Element	Limit State Type	P.L.	Frame-wall Stiffness Ratio									
Type	Limit State Type	r.L.	10~90	15~85	20~80	25~75	30~70	40~60	50~50	60~40	80~20	100~0
Beam	Deformation	1	2.33	2.64	2.01	1.63	1.94	1.31	1.34	1.12	1.32	1.72
Beam	Deformation	3	1.17	1.32	1.00	0.81	0.97	0.66	0.67	0.56	0.66	0.86
Beam	Deformation	5	0.61	0.70	0.64	0.54	0.65	0.48	0.46	0.42	0.42	0.45
Column	Deformation	1	2.32	2.90	0.83	1.26	0.00	0.25	0.81	1.41	1.34	0.40
Column	Deformation	3	0.77	0.97	0.28	0.43	0.00	0.09	0.29	0.51	0.48	0.13
Column	Deformation	5	0.58	0.73	0.21	0.32	0.00	0.07	0.22	0.38	0.36	0.10
Wall	Steel Strain	1	2.32	2.74	2.13	2.38	1.93	1.25	1.27	1.48	1.15	
Wall	Steel Strain	3	0.93	1.10	0.85	0.95	0.77	0.50	0.51	0.59	0.46	
Wall	Steel Strain	5	0.62	0.73	0.57	0.64	0.51	0.33	0.34	0.40	0.31	
Wall	Concrete Strain	1	1.70	2.11	0.47	1.89	0.62	0.74	0.92	1.20	0.61	
Wall	Concrete Strain	3	0.85	1.05	0.24	0.95	0.31	0.37	0.46	0.60	0.30	
Wall	Concrete Strain	5	0.51	0.63	0.14	0.57	0.19	0.22	0.27	0.36	0.18	
Beam	Moment Strength	1	0.68	0.70	0.66	0.64	0.62	0.53	0.49	0.48	0.32	0.22
Beam	Moment Strength	3	0.61	0.63	0.59	0.58	0.56	0.47	0.44	0.43	0.29	0.20
Beam	Moment Strength	5	0.51	0.52	0.50	0.48	0.47	0.39	0.36	0.36	0.24	0.17
Beam	Shear Strength	1	1.03	1.03	0.96	0.90	0.90	0.85	0.86	0.84	1.05	1.30
Beam	Shear Strength	3	0.93	0.93	0.86	0.81	0.81	0.77	0.77	0.75	0.95	1.17
Beam	Shear Strength	5	0.77	0.77	0.72	0.68	0.68	0.64	0.64	0.63	0.79	0.98
Column	Moment Strength	1	1.11	1.11	1.12	1.11	0.93	1.11	1.11	1.11	1.11	1.11
Column	Moment Strength	3	1.00	1.00	1.01	1.00	0.84	1.00	1.00	1.00	1.00	1.00
Column	Moment Strength	5	0.83	0.84	0.84	0.83	0.70	0.83	0.83	0.83	0.83	0.83
Column	Shear Strength	1	0.48	0.47	0.75	0.78	0.80	0.98	1.02	1.05	1.18	1.96
Column	Shear Strength	3	0.43	0.42	0.68	0.70	0.72	0.88	0.92	0.95	1.06	1.77
Column	Shear Strength	5	0.36	0.35	0.56	0.59	0.60	0.74	0.77	0.79	0.89	1.47
Drift	UBC 97		0.66	0.74	0.93	0.82	0.95	0.77	0.73	0.71	0.71	0.68

**Table 3. Twelve Story Structure Usage Ratios** 

Element		P.L				Fram	e-wall S	tiffness	Ratio			
	Limit State Type	r.L	10~9	15~8	20~8	25~7	30~7	40~6	50~5	60~4	80~2	100~
Type		•	0	5	0	5	0	0	0	0	0	0
Beam	Deformation	1	1.85	1.93	2.14	1.90	1.97	1.90	1.63	1.64	1.90	2.00
Beam	Deformation	3	0.93	0.97	1.07	0.95	0.99	0.95	0.82	0.82	0.95	1.00
Beam	Deformation	5	0.53	0.62	0.56	0.58	0.57	0.56	0.51	0.48	0.51	0.50
Column	Deformation	1	0.00	0.00	2.58	0.47	0.00	0.26	1.34	1.57	0.23	0.19
Column	Deformation	3	0.00	0.00	0.86	0.16	0.00	0.09	0.48	0.57	0.06	0.07
Column	Deformation	5	0.00	0.00	0.65	0.12	0.00	0.07	0.36	0.43	0.05	0.06
Wall	Steel Strain	1	0.87	1.01	0.99	0.87	0.95	1.11	0.88	0.98	0.91	
Wall	Steel Strain	3	0.35	0.41	0.39	0.35	0.38	0.44	0.35	0.39	0.36	
Wall	Steel Strain	5	0.23	0.27	0.26	0.23	0.25	0.29	0.23	0.26	0.24	
Wall	Concrete Strain	1	0.80	0.88	0.87	0.85	0.94	1.10	0.71	0.91	0.31	
Wall	Concrete Strain	3	0.40	0.44	0.44	0.42	0.47	0.55	0.35	0.46	0.15	
Wall	Concrete Strain	5	0.24	0.26	0.26	0.25	0.28	0.33	0.21	0.27	0.09	
Beam	Moment Strength	1	0.58	0.70	0.55	0.60	0.49	0.46	0.38	0.37	0.31	0.20
Beam	Moment Strength	3	0.53	0.63	0.50	0.54	0.44	0.41	0.35	0.33	0.28	0.18
Beam	Moment Strength	5	0.44	0.52	0.41	0.45	0.37	0.34	0.29	0.27	0.23	0.15
Beam	Shear Strength	1	1.01	0.97	1.07	1.02	1.07	1.06	1.08	1.10	1.18	1.48
Beam	Shear Strength	3	0.91	0.87	0.96	0.91	0.96	0.96	0.98	0.99	1.06	1.33
Beam	Shear Strength	5	0.76	0.72	0.80	0.76	0.80	0.80	0.81	0.82	0.89	1.11
Column	Moment Strength	1	0.45	0.48	1.12	1.11	1.05	1.11	1.12	1.11	1.22	1.23
Column	Moment Strength	3	0.40	0.43	1.01	1.00	0.95	1.00	1.00	1.00	1.10	1.10
Column	Moment Strength	5	0.34	0.36	0.84	0.83	0.79	0.83	0.84	0.83	0.91	0.92
Column	Shear Strength	1	0.32	0.42	0.53	0.76	0.42	0.98	1.02	1.06	1.14	1.72
Column	Shear Strength	3	0.29	0.38	0.47	0.69	0.81	0.88	0.91	0.95	1.03	1.55
Column	Shear Strength	5	0.24	0.32	0.39	0.57	0.68	0.73	0.76	0.79	0.85	1.29
Drift	UBC 97		0.91	0.87	0.82	0.84	0.87	0.86	0.86	0.65	0.81	0.82

## Conclusions

Based on result of nonlinear analysis it is concluded that:

- 1. It is observed that minimum required strength equal to 25% of total base shear is not satisfying and it should be based on strength and stiffness simultaneously.
- 2. If life safety performance level is assumed to be the code target 20-80 is minimum acceptable ratio, although 15-85 is not so far from acceptance criteria.
- 3. The best possible ratio in any group is 60-40 ratio, but 50-50 and 40-60 is also close to the best possible ratio. So it is concluded that the best performance is obtained at ratios where wall and frame are both carrying almost equal lateral load.

## References

Federal Emergency Management Agency (FEMA 356). (2000), "Prestandard and commentary for seismic rehabilitation of buildings".

Park R. and Paulay T., (1975), Reinforced Concrete Structures, John Wiley & Sons. RAM-Perform 3D User Guide, 2004, Berkeley.

International Conference of Building Officials, Uniform Building code, 1997 Edition, Whittier, California.

# Top to Toe Mitigation of Progressive Collapse in High-Rise Buildings

Fouad. A. Kasti
Dar Al-Handasah, Verdun St.
P.O. Box: 11-7159
Beirut 1107 2230, Lebanon
email: Fouad.kasti@dargroup.co

### Abstract

The ultimate objective of progressive collapse mitigation is to confine losses in load carrying capacity of structural elements to their immediate vicinity particularly in tall and high-rise building structures. A successful and ideal confinement eliminates any propagation in the collapse mechanism that could otherwise lead to catastrophic failure. The concept of progressive collapse mitigation undertaken at design stage to deal with the collapse mechanism in its initial phases offers precious redundancy to indirect measures commonly in place to achieve the same goal. Controlled and limited access policy intended to prevent suspicious human, vehicular and similar elements from physically approaching the structure within a secure periphery is among the latter measures typically considered. Top to toe design stage upgrade of structural elements is required to achieve the concept of progressive collapse mitigation. Proper assessment, upgrade and rehabilitation of each and every structural component throughout the building all the way down to its foundation level are highly emphasized. The concept is valid in retrofitting existing structures as well as new constructions to fulfill the same objectives.

### Introduction

Progressive collapse is typically initiated with a change in system configuration or local member failure. Typical collapse mechanism consists in a three dimensional propagation within or off the current building floor plate. The chain of events is unleashed when amplified strength and ductility demands on structural components such as columns, slabs and beams in the immediate vicinity of a localized failure exceed capacity.

The objective of progressive collapse mitigation (denoted by PCM hereafter) is to prevent the localized failure from fully extending in the horizontal and vertical directions leading to a total catastrophic collapse. The chain reaction of events is initiated with a local structural member failure spinning out into a total and catastrophic loss of the structural system. Progressive collapse is typically accompanied with structural and non-structural damage. The cumulative and extensive damage combines with significant ductility demands to cause further loss in serviceability and human life.

PCM is therefore based on significant redistribution in structural loads and ductility in structural members to maintain the structural strength even at the expense of serviceability. Strength requirements are typically achieved with redundancy which is the ability of the structural system to devise an alternative structural load path to bypass local member failure or system configuration change. Similarly, serviceability requirements are typically achieved with ductility which is the ability to undergo large plastic deformations in order for the alternative load path to be feasible.

The objective of PCM is consequently the ability of a structural system to devise alternative configurations subsequent to cumulative loss of members with significant plastic deformations. Adequate measures to limit further propagation and allow redistribution should be undertaken at design or retrofit phase.

The capacity of structural members should be properly enhanced to allow the structural system to establish the alternative load path. The structural system should be inspected top to toe for potential upgrade in capacity. A number of earlier publications for the author have dealt with mitigation of progressive collapse for structural members located within or off the floor plate within the building system superstructure. The current study particularly focuses on PCM at the soil-structure interface level.

Redistribution due to localized failure will cause substantial overload particularly in vertical structural elements such as columns. Cumulative column overload subsequent to progressive collapse over a number of floor plates will conclude in a significant amplified strength, ductility and serviceability requirements at the soil-structure interface particularly related to structure foundation and underlying soil.

The optimum PCM confines collapse mechanism at initiation to absolutely minimize damage and loss in human life. Such an optimum progressive collapse mechanism cannot theoretically be achieved. Instead, PCM should properly identify deficient top to toe structural components for appropriate strength and ductility upgrade in order to allow the alternative path concept to be a viable option. Along these lines, the structural

system components at the soil-structural level which are typically and critically overlooked should be evaluated for upgrade.

## **Recent Developments**

Progressive collapse is a sequence of events accompanied with severe load redistribution and large plastic deformation. PCM has received special attention with the unfortunate and recent catastrophic failures of special structures particularly tall buildings such as the World Trade Centers in New York and the Alfred P. Murrah Federal Building in Oklahoma City.

Research into and measures against progressive collapse have originally kicked off with external protective measures and general guidance. The protective measures ultimately consisted in limiting vehicle accessibility to a minimum radius away from the structural system. Sophisticated analytical and design tools brought the concept of PCM to a new era. The performance of special structures was investigated for local element structural failures from spinning out into total catastrophic collapse. The current paper falls into the latter class of research perspectives. Recent innovations into progressive collapse research consist in the prevention of the collapse mechanism from even initiating at birth.

The collapse of both the World Trade Centers in New York and the Federal Building in Oklahoma City has been investigated by Astaneh-Asl<sup>1</sup>. A simple, practical and economical approach based on the addition of external cables to a floor system has been proposed for new and existing structures to enhance strength, ameliorate the behavior and prevent progressive collapse. Identical results are obtained with embedded internal cable elements for new construction. Large deformations with substantial inelastic behavior should be expected to induce the catenary actions of the added cables.

An innovative design concept for new and existing special structures, particularly tall buildings has been proposed by Kasti<sup>2</sup>. The strategy is based on the assumption that progressive collapse has been initiated with a local structural failure and the limitation of the extent of progressive collapse within the localized area is the essence. Boundary beam elements added over the line of peripheral columns enhance strength, stiffness and inelastic behavior with similar simplicity and cost efficiency. Such an enhanced performance to existing or new constructions proves to be superior with the enhanced stiffness compared to large deformations required to activate catenary actions of cables.

Another original perspective in PCM has been presented by Kasti<sup>3</sup>. A simple concept has been discussed with the objective to prevent progressive collapse at initiation before the localized structural failure has even taken place. The strength of structural components particularly vertical and other elements should be properly upgraded to accommodate significant demand due to pressure loading from severe remote events such as explosions and vehicular boundary penetration. Strength enhancement will complement and present redundant resolutions to protective measures such as vehicular accessibility limitations.

Sharif, Kasti and Mourad<sup>4</sup> conducted a parametric study on the performance of vertical structural components particularly columns in tall buildings subjected to progressive collapse. Amplified demands on axial forces in column members due to localized failures have been investigated and compared to capacity. Unfortunately, the amplified service strength of columns due to localized failure exceeds ultimate member capacity in an extreme range of conditions. Progressive collapse leading to catastrophic failure will take place unless proper measures are implemented to accommodate such extreme conditions.

Continuity in construction of segmentally erected and tall building concrete structures has been investigated in Kasti<sup>5</sup>. Significant amplification in strength and large plastic deformations are byproducts of progressive collapse. PCM largely consists of accommodating such strength and ductility requirements. Continuity in construction, particularly for tall building structures allows for enhanced redistribution in structural loads due to enhanced structural strength of members and improved ductility.

Progressive collapse due to loss in vertical supports in tall buildings has been discussed by Warn et al.<sup>6</sup>. Gravity and lateral force resisting systems redundancy, continuity and ductility enhance the performance of buildings subjected to progressive collapse.

Dynamic effects on progressive collapse have been investigated by Kaewhulchai and Williamson<sup>7</sup>. Dynamic effects amplify the effects of progressive collapse yielding higher forces, damage and inelastic deformations.

Added robustness and redundancy have been shown to improve the performance of structures with effective alternative load paths, reduced human loss and property damage. Smith et al.<sup>8</sup> have concluded that higher Demand to Capacity Ratio (DCR) indicates higher damage. In the event the DCR value exceeds 1.5 to 2, the corresponding structural element is classified as severely damaged or has already collapsed.

Marjanishvili<sup>9</sup> has evaluated a number of linear-elastic static to nonlinear dynamic analytical methods available for the study of progressive collapse and discussed the advantages and disadvantages of each of these methods.

### Formulation

Progressive collapse is typically a sequence of events initiated with a loss in a vertical support spinning out into a catastrophic failure. The objective of the present study is top to toe mitigation of progressive collapse. The localized failure initiated with a loss in vertical support spills out into a floor system failure in the level above and subsequently into structural load redistribution leading to amplified loads and large plastic deformations in the vicinity of the localized failure including floor slabs and beams, columns as well as foundation.

PCM has normally focused on amplified column loads due to localized failure. Amplified demands in floor components and ultimately in foundations of structural systems have been typically and rarely investigated. Performance of floor components

and vertical column members have been previously discussed in a number of publications by the author referenced above and below. The objective of the current paper is to study the implications of progressive collapse particularly on performance of foundations in tall buildings where maximum amplifications in strength and serviceability is expected.

An innovative design concept for new and existing special structures particularly tall buildings by Kasti<sup>3</sup> has already been referenced above. The simple objective is to prevent progressive collapse at initiation before the localized structural failure has taken place. The resolution provides additional redundancy and protection to other potentially implemented measures such as limited vehicular and periphery accessibility. The concept consists in assessing the remote and impact loading generated from breach in accessibility. The remote pressure or impact concentrated loading on structural components particularly column members is evaluated first and upgrade in member design is undertaken when necessary. The optimum cure for progressive collapse is subsequently achieved when localized member failure before initiation is prevented.

Amplification in vertical member demand has been found to be proportional to the intensity of the remote pressure loading or the concentrated impact loading, the tributary area of the structural member or the point of application of the concentrated load, the dynamic amplification factor and the disintegration factor. Increase in member internal forces such as shear and bending moments has been quantified and needs to be accommodated for, to prevent the initiation of the localized failure. The higher the remote pressure distribution, impact load, tributary area, dynamic or disintegration factors, the more significant the capacity upgrade requirements are.

Another innovation in the mitigation of progressive collapse by Kasti² has also been referenced previously. The proposed enhancement to the performance of structures particularly tall buildings consists in the addition of a boundary beam element spanning over the outer column line grid to assist in the redistribution of loads when a localized failure of a boundary column is caused by a severe loading typically generated with a high pressure or concentrated impact loading. The added boundary beam will bridge out the loss of the vertical column support, stiffen and strengthen the floor plate and allow an alternative load path for the floors above to redistribute to the adjacent columns. The boundary beam element strength and serviceability demands are amplified when loss in column support occurs primarily due to increase in effective span.

Increase in boundary beam demands is largely proportional to span configurations with the investigated column, column tributary area and the number of floors above, the intensity of gravity, dead and live floor loadings, the dynamic amplification and disintegration factors. Increase in strength and serviceability requirements can be evaluated and design revisited when needed, to prevent further propagation in the collapse mechanism. The higher the span lengths adjacent to the studied column, column tributary area and number of floors above, the intensity of the gravity floor loading, the dynamic amplification and disintegration factors, the more pronounced the amplification in the boundary beam strength and serviceability requirements.

PCM used at initiation to avoid local member failure and addition of floor beam element at boundary column lines to allow redistribution of vertical column load to adjacent vertical elements is complemented with a simplified design parametric study on the performance of vertical columns subjected to localized failure by Sharif, Kasti and Mourad<sup>4</sup>. Assuming that alternative load path is feasible and full load redistribution is allowed to the adjacent column, neighboring column demands are subjected to amplification. Localized failure of a vertical column support is therefore investigated and strength enhancement in neighboring columns is sought when necessary to prevent a total catastrophic collapse from being generated.

Amplification in neighboring column demands, particularly axial force, is essentially directly proportional to the span configuration on either side of the lost vertical column support, the tributary area of the lost column, and the dynamic amplification factor. The higher the spans between adjacent columns, the closer the distance to the neighboring columns, the higher the tributary area and the dynamic amplification factor, the higher is the axial force demand on adjacent columns. Localized failure is expected to propagate to the neighboring columns when the amplified axial force at service level exceeds the ultimate capacity of the adjacent columns. The amplified column demands are typically within the ultimate capacity of the member except for extreme situations in span configurations and code ultimate load factors where the member capacity is exceeded and progressive collapse propagation is expected.

A critical conclusion can be drawn from the above studies to the effect that amplification in column demands will increase as columns closer to the foundation level are being investigated for progressive collapse. The level of load redistribution required consists of cumulative gravity loads piled up over the full length of the building structure and the increase in column demand at foundation level is maximized for tall building structures. The present study will be limited to the structural implications of progressive collapse on the performance of foundation design particularly in tall buildings.

PCM will affect foundation design in two aspects. With a mat foundation typical design particularly in tall buildings, amplification in foundation level axial force column demands will spill out in proportional increase in soil bearing stresses and mat foundation design including punching shear, direct shear and bending moment design. The performance of foundation with respect to PCM requires special attention when dealing with soil-structure interaction.

PCM necessitates redistribution of the failed column axial force to the typically adjacent vertical elements columns members as well. Contact soil-structure tributary areas Al and Ar are assumed for left and right columns respectively. The failed column will also be referred as the central column hereafter. The force redistribution is proportional to the central column floor tributary area Ac generally constant over the full height of the structure. To simplify the parametric investigation, the central column axial force Fc amplified with dynamic amplification factor  $\beta$  is assumed to distribute to the left and right columns  $\Delta Fl$  and  $\Delta Fr$  in the ratio of the adjacent left and right spans Ll and Lr. L is the total span between the left and right adjacent columns.

$$\Delta Fl = \beta * Fc * Lr / L \tag{1}$$

$$\Delta Fr = \beta * Fc * L1 / L$$
 (2)

$$Fc = \Delta Fl + \Delta Fr \tag{3}$$

$$L = L1 + Lr \tag{4}$$

The soil bearing pressure at a column is commonly approximated as the ratio of the service level axial force within the column by its contact soil-structure tributary area. The initial bearing pressures in the left and right columns (sol and sor respectively) are simply the ratio of the initial service level axial force in the left column Fol by the left column tributary area Al and the ratio of the initial service level axial force in the right column for by the right column tributary area Ar respectively.

$$\sigma ol = Fol / Al \tag{5}$$

$$\sigma or = For / Ar \tag{6}$$

The increase in left and right columns soil bearing stresses  $\Delta \sigma l$  and  $\Delta \sigma r$  are obtained with the ratio of the increment in axial force due to redistribution of the central column axial force by the corresponding tributary area using Eq. (1) and (2).

$$\Delta \sigma l = \Delta F l / A l \tag{7}$$

$$\Delta \sigma r = \Delta F r / A r \tag{8}$$

Total soil bearing stresses in left and right columns are simply the addition of initial and incremental stresses Eq. (1) through (4). Foundation design requirements dictate that soil bearing pressure should at all times be within the allowable bearing pressure to prevent progressive collapse from leading to catastrophic failure.

$$\sigma l = \sigma o l + \Delta \sigma l \tag{9}$$

$$\sigma \mathbf{r} = \sigma \mathbf{or} + \Delta \sigma \mathbf{r} \tag{10}$$

The left and right columns total design maximum ultimate bending moments Ml and Mr respectively, ultimate direct shear Vl and Vr respectively and ultimate punching shear Sl and Sr respectively could be similarly expressed. The total design maximum ultimate bending moment is simply the initial value incremented with the redistributed contribution due to the localized failure. Similar argument can be presented for ultimate direct and punching shear for left and right columns.

$$Ml = Mol + \Delta Ml \tag{11}$$

$$Mr = Mor + \Delta Mr \tag{12}$$

$$Vl = Vol + \Delta Vl \tag{13}$$

$$Vr = Vor + \Delta Vr \tag{14}$$

$$SI = Sol + \Delta SI \tag{15}$$

$$Sr = Sor + \Delta Sr \tag{16}$$

### Parametric Study

A comprehensive parametric study based on the performance of a typical tall building mat foundation will be undertaken. Mat foundation design generally satisfies serviceability and strength requirements. The former criterion consists in meeting the allowable soil bearing pressure based on service loads at the soil-structure interface. The latter condition necessitates the design of the mat foundation including flexural, direct shear and punching shear based on ultimate loads.

In the event of a progressive collapse mode, the dynamically amplified axial force of a failed column is distributed to the neighboring columns. The increase in neighboring column loads in turn causes simultaneous increase in strength and serviceability requirements in foundation design.

The current study focuses on foundation soil-structure and mat strength design aspect as it is typically the governing requirement in PCM. PCM in foundation design should allow for the increase in soil-structure bearing pressure and mat foundation internal actions including flexural moments, direct and punching shear.

The increase in soil bearing pressure is directly proportional to the axial force in the column at the foundation level. The distribution of the soil pressure is normally non-uniform within the contact tributary area of the column. For the purpose of discussions, the soil bearing pressure will be assumed uniformly distributed within the contact tributary area of the column. The bearing pressure is therefore directly proportional to the service level total axial force in the column which is the sum of its original force incremented with the contribution from the axial force in the failed column amplified with the dynamic factor. The bearing pressure is inversely proportional to the contact tributary area of the column.

The dynamic amplification factor is generally assumed to be in the range of 1.5 to 2. The total service level axial force for a neighboring left or right column Flt and Frt is simply the sum of the initial axial force due to gravity design Fol and For amplified with the contribution from the failing column  $\Delta$ Fl and  $\Delta$ Fr listed in Eq. (1) and (2):

$$Flt = Fol + \Delta Fl \tag{17}$$

$$Fr = For + \Delta Fr \tag{18}$$

For typical design of structural systems with similar geometry and loadings, vertical elements design is practically identical for equal span neighboring groups of columns at a given floor level. For a commonly used value 1.5 of  $\beta$  in progressive collapse

investigations, the amplified service level column load is about 1.75 times the initial service level load and identical to the ultimate load level of the column axial force. The column design remains satisfactory and the column is expected to survive the progressive collapse mode. Special conditions could arise including unfavorable values in the amplification factor, geometry, and loading in which case the amplified service level axial column force exceeds the ultimate column capacity. Column capacity should subsequently be upgraded otherwise progressive collapse mechanism will develop in a catastrophic failure.

$$Flt = Fc^* (1 + \beta * Fc * Lr / L)$$
 (19)

$$Frt = Fc* (1 + \beta * Fc * L1 / L)$$
 (20)

Discussions related to bearing pressure are more pronounced than member structural design. Soil-structure foundation design requires that the allowable bearing be respected. In the event of progressive collapse, the bearing pressure will commonly amplify by a 1.75 factor as well. Assuming that the initial foundation design has matched the allowable bearing capacity, this design requirement is therefore breached. Soil–structure investigations are necessary to evaluate the impact of such breach on the strength and serviceability performance of soil. The breach could be compensated for with a proportional reduction in the allowable bearing pressure used in the traditional design of soil-structure interaction.

The impact of progressive collapse on mat foundation design is subjected to the same thought process presented above. Localized failure amplifies neighboring columns service level axial forces which in turn amplify foundation design parameters including flexural moments, punching and direct shear. The service level axial force in neighboring columns has been found to be the sum of the initial component and the dynamically amplified contribution of the service level of axial force in the failed column.

The performance of the mat foundation will follow similar changes. The service level flexural moment, direct shear and punching shear are respectively proportional to the axial force level in the neighboring column. Amplification in foundation design parameter subsequently follows the same trend observed for axial loads. The service level flexural moment, direct or punching shear in the mat foundation is simply the initial component due to gravity response topped by the amplified component due to load redistribution of the axial force of the failed column. Similar expressions, formulations and conclusions can be derived for the amplified neighboring column axial force.

$$Ml = Mol * (1 + \beta * Lr / L)$$
 (21)

$$Mr = Mor * (1 + \beta * L1 / L)$$
 (22)

$$Vl = Vol * (1 + \beta * Lr / L)$$
 (23)

$$Vr = Vor * (1 + \beta * L1 / L)$$
 (24)

$$S1 = Sol * (1 + \beta * Lr / L)$$
 (25)

$$Sr = Sor * (1 + \beta * L1 / L)$$
 (26)

For typical design of structural systems with similar geometry and loadings, mat foundation design is practically identical for neighboring groups of columns. For a commonly used 1.5 value of  $\beta$  in progressive collapse investigations, the amplified service level foundation load is about 1.75 times the initial service load level and is sensibly identical to the ultimate load level of the mat foundation. For a standard foundation design where capacity of the foundation matches the initial ultimate demand, the mat foundation design remains satisfactory and the mat foundation is expected to survive the progressive collapse mode. Special conditions could arise including unfavorable values in the amplification factor, geometry, loading in which case the amplified service level mat foundation design parameters exceed the ultimate foundation capacity. Mat foundation capacity should subsequently be upgraded otherwise progressive collapse failure will develop in a catastrophic failure.

#### Conclusions

The objective of PCM is to prevent localized failure from spinning out into a total catastrophic structural system loss. The most ideal PCM is in total prevention and initiation. Alternatively, total prevention and initiation may not be practically a viable option in which case strength and serviceability of structural enhancement of various members at all levels should be considered.

Top to toe mitigation of progressive collapse is necessary to eliminate potential weak links in load redistribution and allow alternate viable load paths. All structural elements from the top of the superstructure to the substructure bottom-end should be evaluated for potential overload due to redistribution.

The initiation of progressive collapse is commonly caused by the loss of a structural element particularly a vertical member in the vicinity of the ground floor of tall buildings. PCM of such classes of structures requires that the amplification of strength and serviceability of vertical members, floor plate elements as well as foundation components should be properly addressed.

For common situations and for typical geometry, loading and dynamic amplification factor, the service level overload practically matches the ultimate capacity of vertical structural elements. The ultimate capacity of such classes of members can be exceeded in extreme situations. Such instances should be properly evaluated and the design of members upgraded when necessary.

An innovative concept in the design of floor plate members has been referenced. A beam element located along the boundary of floor plates over column grid lines proves to be superior to the catenary action of exterior or interior cable system. Boundary

beam adds stiffness in addition to strength to the floor plate slab while cable catenary action is based on large deformations.

PCM has rarely addressed amplifications in strength and serviceability of foundation and soil-structure interaction design. Increase in foundation and soil-structure design quantities is similar to the performance of axial force in columns. In soil-structure interaction, soil bearing pressure is magnified beyond allowable limit. Precautionary measures should be adopted to maintain soil bearing pressure within allowable including reducing the allowable value used for standard design. In foundation design, the amplification of the service load level flexural and shear actions remains practically about equal to the ultimate capacity. The progressive collapse mechanism will not generally develop except in extreme situations. In extreme conditions, the capacity of the mat foundation is exceeded and upgraded as required to prevent failure.

### References

- Astaneh-Asl, A. (2003), "Progressive Collapse Prevention in New and Existing Buildings", Proceedings of the 9th Arab Structural Engineering Conference, Emerging Technologies in Structural Engineering, Nov 29 – Dec 1, 2003 Abu Dhabi, UAE.
- 2. Kasti, F. (2005), "Progressive Collapse in High Rise Buildings", Proceedings of the 7th International Conference on Multi-Purpose High-Rise Towers and Tall Buildings, Dubai, U.A.E., December 10-11, 2005.
- 3. Kasti, F. (2006), "Mitigation of Progressive Collapse in High Rise Buildings", Proceedings of the 10th Arab Structural Engineering Conference, Kuwait City, November 13-15, 2006.
- 4. Sharif A., Kasti F., and Mourad S. (2006), "Hazard Mitigation of Progressive Collapse; A Simplified Design Approach for High Rise Building Columns", Proceedings of the CEIS Conference American University of Beirut, Beirut, Lebanon.
- Kasti, F. (2004), "Segmental Construction and Continuity in Concrete Structures", Proceedings of the American Concrete Institute (ACI), International Center for Sustainable development of Cement and Concrete Canada (ICON and CANMET) International Seminar, Beirut, Lebanon September 20-21, 2004.
- 6. Warn, G., Berman, J., Wittaker, A., and Bruneau, M. (2003), "Reconnaissance and Preliminary Assessment of a Damaged High-Rise Building Near Ground Zero", Proceedings of the The Structural Design of Tall and Special Buildings 12, 371-391, 2003.
- 7. Kaewhulchai, G., and Williamson, E. B.(2003), "Dynamic Behavior of Planar Frames During Progressive Collapse" Proceedings of the 16th ASCE Engineering Mechanics Conference July 16-18, 2003, University of Washington Seattle, USA.
- 8. Smith, J. L., Swatzell, S. R., and Hall, B., "Prevention of Progressive Collapse DOD Guidance and Application".
- 9. Marjanishvili, S. M. (2004), "Progressive Analysis Procedure for Progressive Collapse", Journal of Performance of Constructed Facilities, ASCE, Vol. 18, No. 2, 79-85, 2004.

- 10. Aalami, B. and Kasti, F. (1996), "Segmental Analysis and Design Fundamentals, Time Dependent Effects", American Segmental Bridge Institute Seminar, Albany, NY April 22 23, 1996. 34 pages.
- 11. American Concrete Institute (2002), "Building Code Requirements for Structural Concrete ACI 318-02", ACI Committee 318, P.O. Box 9094, Farmington Hills, MI 48333-9094, USA, 2002.

## Response of Upgraded Reinforced Concrete Buildings to Dynamic Lateral Loads

Adnan S. Masri, Hisham S. Basha, Ziad M. Mousa, Beirut Arab University Lebanon

### **Abstract**

Structures are designed to support both gravity and lateral loads. In spite of the fact that Lebanon is vulnerable to strong ground excitations, most of its buildings have been designed for gravity loads with total negligence or inadequate analysis for lateral earthquake forces. To overcome this major structural defect, it is practical and economical to upgrade a seismically weak building rather than demolishing it. The main objective of upgrading is to enhance the dynamic response of the structure. An efficient, rapidly constructed and economic upgrading technique is to use a combination of reinforced concrete and steel jackets. Reinforced concrete jackets are used for the existing RC columns, whereas the RC beams are jacketed by steel plates using epoxygrouted anchors. In this paper, a typical low-rise multistory building is selected for investigation. Using SAP2000, a three-dimensional model for the RC building is subjected to a dynamic time-history analysis using the latest Izmit-earthquake record.

Next, a retrofitting scheme is designed for upgrading two bays of the building. A dynamic time-history analysis is carried on a 3D model representing the upgraded building. An overall comparison and interpretation of results is made between the RC and the upgraded building.

### Introduction

In the development of modern seismic upgrading strategies, very strong emphasis is placed on the criteria that loss of life should be prevented even during the strongest ground shaking. For this reason, the main objective of upgrading is to enhance all structural characteristics: strength, stiffness and ductility, which are in direct relation to acceptable dynamic response.

Upgrading of structures to resist earthquakes is an activity of great significance where the understanding of seismic response concepts plays the central role to improve seismic performance. However, strengthening of reinforced concrete structures by either concrete casing or steel jacketing usually leads to an increase in seismic vulnerability. This is mainly due to their effect on stiffness and strength distribution. Among several strengthening techniques are: addition of reinforced concrete shear walls; addition of steel bracing systems; addition of RC and/or steel jackets; addition of steel sandwich panels.

An attractive and efficient technique is using steel jackets for strengthening of the RC beams, and RC jackets for strengthening of the columns. An existing prototype four-story residential building has been selected for this study. This technique is further selected because of its fast and easy erection specifically when minimum disturbance to occupants is desired.

In this technique steel plates are connected through the top and bottom surfaces of the RC beam by epoxy grouted anchor bolts whilst, the RC columns are jacketed by concrete casing on three or four sides where no bond material is needed between RC columns and the concrete casing. The connections between the vertical reinforced concrete jackets and the horizontal steel jackets are designed and constructed as moment resisting connections in order to assure a frame action that resists lateral forces resulting from earthquakes.

The concrete casing for columns and the steel jacketing for beams is designed to enhance both seismic strength and stiffness of the RC structure. It is also desired to improve the ductility of such brittle structures. This is achieved by designing for a desirable weak-beam strong-column failure mechanism. The objective of this analysis is to determine the lateral load resistance (base shear) of the existing RC building and to compare it to the new resistance when some elements of the building are retrofitted.

## **Description of the Four-Story RC Building**

A typical low-rise four-story residential reinforced concrete building is selected for this study. The building consists of a ground floor and four typical stories. The building total height from ground level to the centerline of roof floor is 16m with 3.2m differences between consequent floors. The framing plan of the building consists of two bays in the short direction and three bays in the long direction. The structural system is designed as a beam-column system, and it consists of RC ribbed slab, concealed RC beams and RC columns. The flooring system consists of 30cm thick ribbed-slab loaded

in the longitudinal direction monolithically cast with concealed beams that are connected to the columns in short direction. A plan view is shown in Fig. 1.

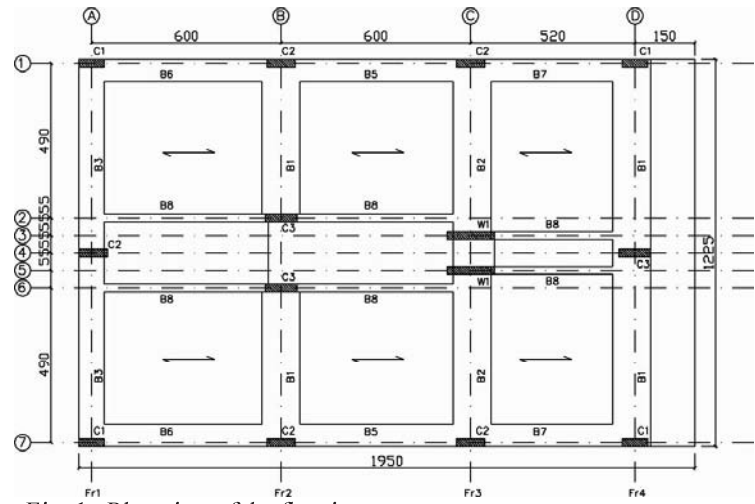


Fig. 1. Plan view of the flooring system.

The building to be retrofitted was designed to resist only gravity loads with beam-column load resisting system. For practical purposes, the two exterior bays along the short direction are selected to be upgraded. Details of the cross section of the exterior and interior columns of bays to be strengthened with concrete jacketing (casing), and the cross section of the embedded beams to be strengthened with steel jacketing is shown in Table 1.

Table 1. Sections and Reinforcement of Columns and Beams

Columns				
Type	Section cm x cm	Reinf.		
C1	25x80	12T14		
C2	25 x90	16T14		
C3	25 x100	16T16		
W1	25 x120	16T16		

	Beams						
Type	Section cm x cm	Top Reinf.	Bot. Reinf.				
B1	30 x120	13T14	13T20				
B2	30 x120	13T20	13T20				
В3	30 x80	8T14	8T20				
B4	30 x80	7T20	7T20				
B5	30 x70	6T12	6T16				
В6	30 x70	6T16	6T16				
B7	30 x70	6T20	6T14				
B8	30 x20	2T12	2T14				

### Seismic Resistance of the RC Building

As the RC building was designed to resist gravity loads only with total negligence to lateral forces caused by earthquakes, the dominant design requirement is therefore the provision of an appropriate structural system that will satisfy established design criteria

as efficiently and economically as possible, while fitting into the architectural layout. A three dimensional (3D) model simulating the RC building is assembled using the structural analysis program SAP2000, Fig. 2. The model is subjected to the ground-acceleration earthquake record which occurred in Izmit-Turkey in 1999, Fig. 3.

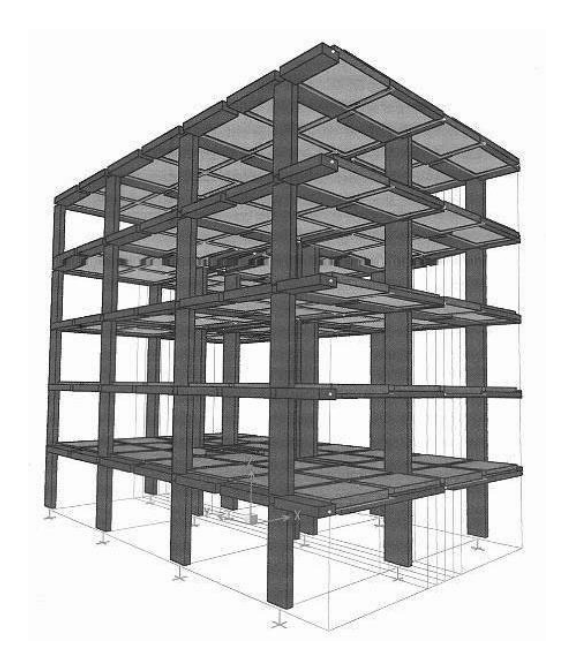


Fig. 2. 3D model of the RC building.

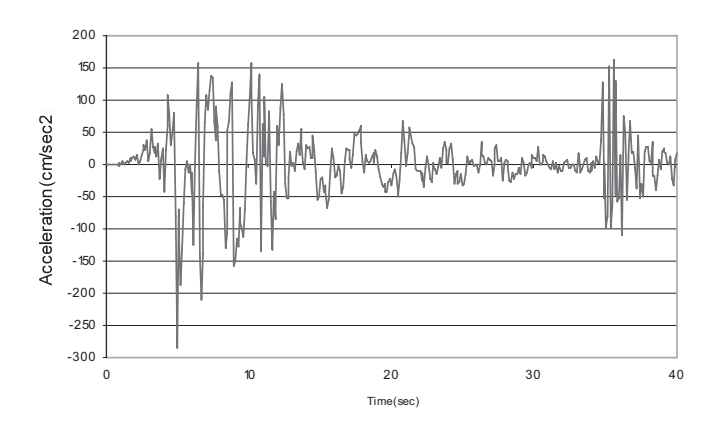


Fig. 3. The N-S component of Izmit earthquake.

A comparison between the acting forces and the section capacities is shown in Table 2. Most columns are inadequate for resisting the forces caused by such earthquake, where the moment capacity of the columns is less than the acting moment.

Table 2. Comparison of Member's Capacity and Acting Internal Forces

			Sections capacity		Internal forces 0.9DL+1.3E		Over-strength Factors	
Membe r	Sectio n cm x cm	Reinf.	M <sub>n</sub> (KNm)	P <sub>n</sub> (KN)	M <sub>u</sub> (KNm)	P <sub>u</sub> (KN)	M <sub>n</sub> /M	P <sub>n</sub> /P <sub>u</sub>
C1	25*80	12T14	144	2859	205	819	0.70	3.50
C2	25*90	14T14	172	3542	227	1136	0.78	3.10
C3	25*100	16T16	200	4042	258	1030	0.81	3.95
W1	25*120	16T16	232	4682	301	875	0.78	5.35
B1	30*120	12T14+12T 20	419	6111	401	-	1.05	-
B2	30*120	12T20+12T 20	484	6553	285	-	1.70	-
В3	30*80	7T14+7T20	269	4005	297	-	0.90	-
B4	30*80	7T20+7T20	290	4156	200	-	1.45	-

The base shear versus time relationship is shown in Fig. 4. The story-drift versus time relationship is shown in Fig. 5. The maximum story drifts are shown in Fig. 6.

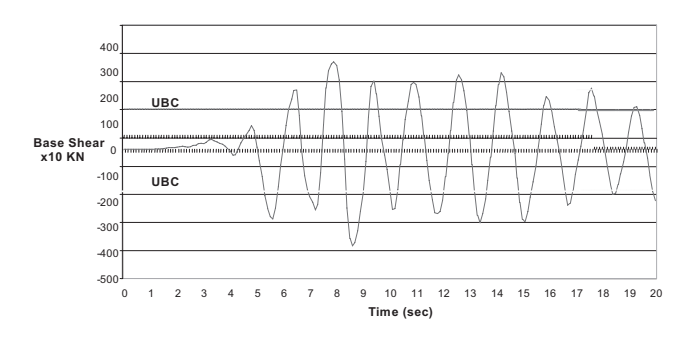


Fig. 4. Base shear vs. time relationship.

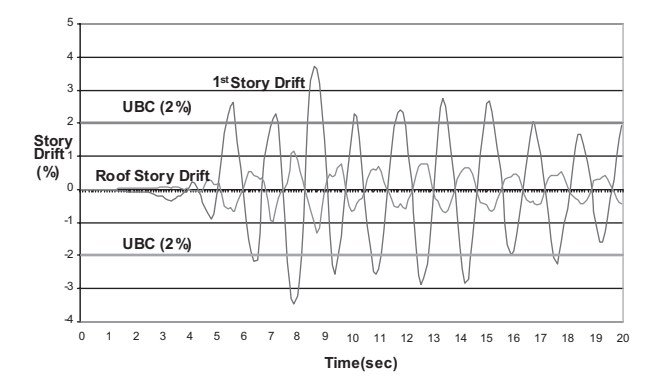


Fig.5. Story drift vs. time relationship.

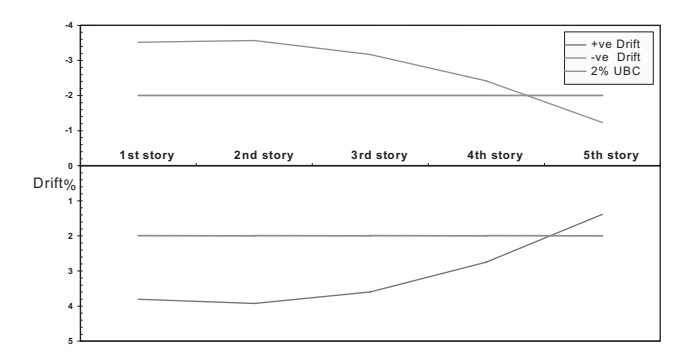


Fig. 6. Maximum story drifts.

The dynamic response of the RC building shows that the structure is not capable of resisting such magnitude of earthquake. The building behavior is elastic during the first five seconds of the record where the maximum resisted base shear is 920 KN and the corresponding first story drift is 0.9%. Large inelastic deformation occurred in the first and second-story members at the occurrence of the first shock at time equal to 5.7 seconds. The first-story drift measured 3.7% and the 3D frame considered unstable. The maximum attained base shear is 373 KN. The maximum attained drifts for the 1<sup>st</sup>, 2<sup>nd</sup>, 3<sup>rd</sup>, 4<sup>th</sup> and 5<sup>th</sup> story was found to be 3.8, 3.9, 3.6, 2.75 and 1.4 % respectively. These drift values exceed the allowed drift recommended by the UBC codes (2%), except the 5<sup>th</sup> floor; due to these values large inelastic deformation occurred in the most building stories, and the building was considered unstable.

### Seismic Resistance of the Upgraded Building

## <u>Jacketing of the Existing RC Columns</u>

One of the most commonly applied methods of strengthening concrete members is the concrete casing. It may be used to enhance stiffness, strength and ductility, and it does not require specialist knowledge. The procedure of strengthening columns is: the concrete is first removed to expose the main reinforcing bars, U shape steel links are then welded to the exposed bars. Weld-able steel is preferable to avoid brittleness. Additional bars are then welded to the U shape links to form the longitudinal reinforcement. These new bars should be adequately anchored to top and bottom columns. Stirrups are added as required and concrete is poured after the erection of timber formwork. The short dimension of each column was increased by 20 cm (10 cm jacket each side) whereas, the long dimension was increased by 10 cm (5 cm jacket each side). Comparison between the capacities of the existing and upgraded columns is shown in Table 3.

Table 3. Capacity of Existing and Upgraded Columns

Exi	cisting section Capacity		y	Upgraded Sect.		Capacity		
	Dimen's cm x cm	Reinf.	P <sub>n</sub> (KN)	M <sub>n</sub> (KN.m)	Dimen's cm x cm	Reinf.	P <sub>n</sub> (KN)	M <sub>n</sub> (KN.m)
C <sub>1</sub>	25x80	12T14	2860	144	45x90	20T32	8865	1063
C <sub>2</sub>	25x90	14T14	3542	172	45x100	24T28	9247	1066
C <sub>3</sub>	25x100	16T16	4024	200	45x110	24T32	8993	930

### Jacketing of the Existing RC Beams

Steel plates are selected for jacketing of the RC beams. This technique is more expensive than the concrete casing, but is faster in erection, more effective, practical and less disturbing to occupants. It is applicable to beams much easier than RC jackets, and it is applied immediately in the site where there is a need for immediate use of the building or where there is a danger from collapse of the structure. If there is a need for thick steel plates (more than 3cm thick), it is advisable to use several thin layers instead, to minimize interfacial shear stresses. The main advantages of this technique are ease and fast erection.

To ensure the weak beam strong column mechanism in the plastic range loading, and based on UBC 1997 requirements; the jacketed beams are designed to satisfy the following nominal moment relationship at the beam-column connection.

$$(\Sigma M_{col}/\Sigma M_{beam} \ge 1.2)$$
 Eq.(1)

Thus, the summation of the beams moment capacities at an interior connection should be 15% less than the summation of the column moment capacities, i.e.;

$$\Sigma M_{\text{beam}} \le 0.85 \text{ x } \Sigma M_{\text{col}}$$
 Eq.(2)

Knowing the moment capacities of the existing RC beams ( $\Sigma M_{RC}$ ), the desired moment capacity to be provided by the steel plates is:

$$\sum M_{\rm pl} = \sum M_{\rm beam} - \sum M_{\rm RC}$$
 Eq.(3)

The plates are designed symmetrical to allow for equal moment resistance at the connections due to reversal moments. The moment capacity of the horizontal steel jacket is determined using:

$$M_{PL} = (A_{PL}.F_Y) \cdot (h_b + t_{PL})$$
 Eq.(4)

where  $A_{PL}$  = cross-sectional area of steel plate.

 $F_Y$ = yield strength of steel plates.

 $h_b = beam depth.$ 

 $t_{PL}$ = plate thickness.

Since the horizontal jackets will be anchored to the RC beams, these jackets are designed for full composite action between the two materials provided that the anchor bolts are designed appropriately to prevent any slippage between the steel jacket and the RC member. Details of the upgraded beams are shown in Table 4.

Table 4. Details of the Upgraded Beams

	Beams						
Type	Section	Top	Bot.	Top PL	Bot. PL		
JI	cm x cm	Reinf.	Reinf.	mm x mm	mm x mm		
<b>B</b> 1	30x120	12T14	12T20	500*12	500*12		
<b>B2</b>	30x120	12T20	12T20	500*12	500*12		
В3	30x80	7T14	7T20	500*12	500*12		
B4	30x80	7T20	7T20	500*12	500*12		

To ensure rigid moment connections between the jacketed beams and columns, the beam plates are welded to similar plates anchored to the RC columns by epoxy grouted bolts as illustrated in the details of an upgraded bay shown in Figure 7.

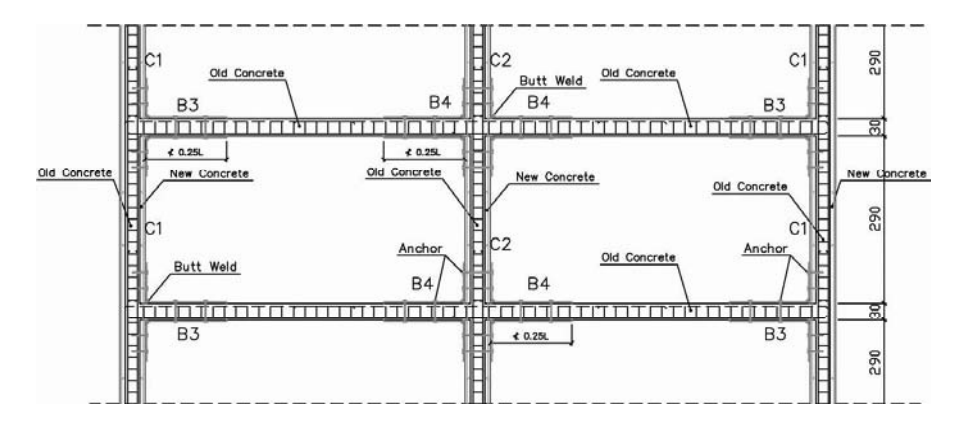


Fig. 7. Details of the upgraded bay along axis-A.

### **Dynamic Time History Analysis**

Using SAP 2000, the 3D model of the upgraded building is subjected to the Izmitearthquake record (Fig. 3), to evaluate its overall dynamic response. For analysis, the mass of the structure (DL) is lumped at the floor levels at six nodes in each floor. For a damping ratio of 3% and using equal time intervals of 0.1 seconds for a total number of output time steps of 200. The peak ground acceleration (PGA) for this record corresponds to 0.3 g value, and the time duration for this dynamic analysis is performed for the first 20 seconds of the record. The 3D model of the structure using SAP2000 is subjected to the above mentioned time-acceleration record. The base shear versus time relationship is shown in Fig. 8. The story-drift versus time relationship is shown in Fig. 9. The maximum story drifts are shown in Fig. 10.

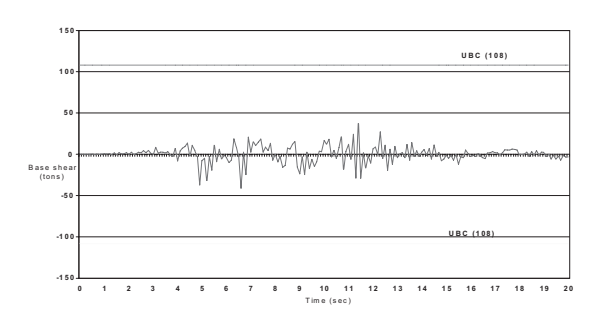


Fig.8. Base shear vs. time relationship.

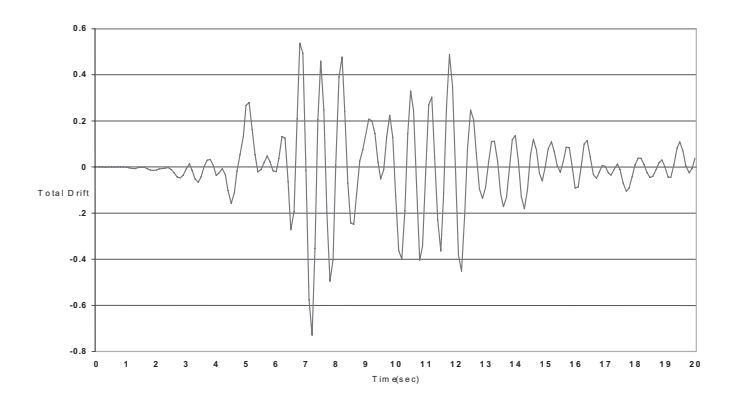


Fig. 9. Drift vs. time relationship.

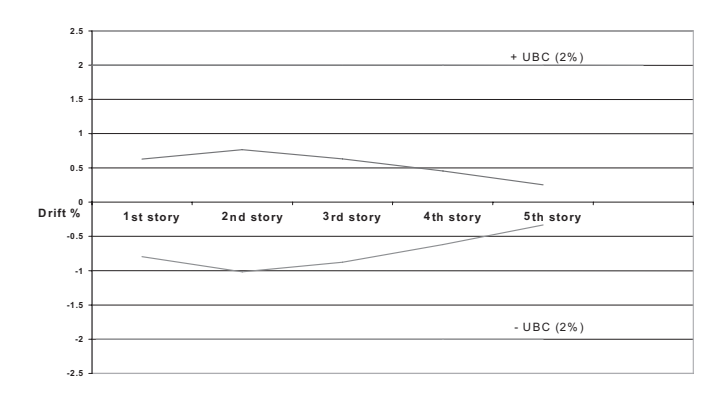


Fig. 10. Maximum story drifts.

At the peak of the first earthquake shock at time equal to 4.9 seconds, the maximum resisted base shear reads 37 tons, and the corresponding total drift is 0.27%. At time equal to 6.6 seconds, the base shear measured 41 tons and the corresponding total drift is 0.53%. The maximum attained drifts for the 1<sup>st</sup>, 2<sup>nd</sup>, 3<sup>rd</sup>, 4<sup>th</sup> and roof stories are found to be 0.8%, 1.02%, 0.88% and 0.34%, respectively. These drift values are within the allowed drift recommended by UBC (2%). The dynamic response of the retrofitted structure after being strengthened by concrete casing and steel jacketing is dramatically improved and able to resist such magnitude of earthquake. The strengthened structure ascertained good strength, stiffness and ductility during the 20 seconds of the record. A comparison between the acting forces and the section capacities is shown in Table 5. All columns have sufficient capacities against the axial forces and bending moments resulting from the earthquake forces.

Table 5. Comparison of Acting Internal Forces and Section's Capacity

Member		al forces L+1.3E	Section's capacity		Over-strength factors	
	P <sub>u(KN)</sub>	M <sub>u(KN.m)</sub>	P <sub>n(KN)</sub>	M <sub>n(KN.m)</sub>	P <sub>n</sub> /P <sub>u</sub>	$M_n/M_u$
C1	1518	909	8865	1063	5.84	1.17
C2	2675	1011	9290	1076	3.47	1.06
C3	1506	1130	10894	1306	7.23	1.16
B1		1288		768		0.59
B2		716		701		0.98
В3		787		768		0.97
B4		797		646		0.81

### **Conclusions**

From the analyses of the results obtained in this study, the following conclusions can be made:

- 1. The dynamic time-history response of the upgraded building is considerably better than that of the existing RC building. The stiffness of the RC building is greatly enhanced after upgrading and the maximum story drifts are significantly reduced from values exceeding 2% to values less than 1%. Besides, the axial and bending strengths of the upgraded columns and beams show its capability to resist the internal forces resulting from such strong magnitude earthquake, which was not the case of the existing RC columns and beams.
- 2. This study shows that the suggested upgrading technique which involves a combination of RC jackets for the columns and steel jackets for the beams is attractive and efficient. It can be rapidly constructed with minimal disturbance to occupants. Special care should be given to design, detailing and erection of the beam-column connections. Further research is required to investigate the possible use of this upgrading technique for medium-rise and high-rise RC buildings.

### References

- 1. Masri, A.C., and Goel, S.C. (1994), "Steel Bracing Systems for Seismic Strengthening of Reinforced concrete slab-column structures", Department of Civil Engineering, University of Michigan, Ann Arbor.
- 2. Jong-wha Bai, (2003) "Seismic Retrofit for Reinforced Concrete Building Structures", Mid-America Earthquake Center, Texas A & M University.
- 3. Elnashai A. S., (1999) "Seismic Capacity Rehabilitation of R.C. Structures", Civil Engineering Department, Imperial College, London, UK.
- 4. American Concrete Institute, (1999) "Building Code Requirements for Reinforced Concrete", Michigan, USA.
- 5. American institute of steel construction, (1999) "Load and Resistance Factor Design Specifications for Structural Steel Buildings", Chicago, USA
- 6. Computers and Structures Inc., "Structural Analysis Program SAP2000", Berkeley-California, USA.

# Multi-Resolution Distributed FEM Simulation of Reinforced Concrete High-Rise Buildings

Jun Ji, Oh-Sung Kwon, Amr S. Elnashai, Daniel A. Kuchma

Mid-America Earthquake Center, Department of Civil and Environmental Engineering University of Illinois at Urbana-Champaign, Urbana, IL 61801, U.S.A

### Abstract

A new analysis framework referred to as multi-resolution distributed FEM simulation is proposed in this study for the analysis of dual-system high-rise RC buildings. Two advanced analysis FE platforms are used to most realistically model high-rise buildings, namely ZEUS-NL with fiber sections to model beam and column members and VecTor2 employing the modified compression field theory to model the RC shear walls. The two different constituent models of skeleton and walls are combined to build an integrated structural realization, using a 'simulation coordinator' referred to as UI-SimCor that seamlessly merges the two components into one structural system. A 54story high-rise building with a dual core wall-frame structural system is selected as the reference application. The results from multi-resolution analysis are compared with those from conventional frame analysis of the whole structure under both static and dynamic loading. The comparison emphasizes that due to shear response considerations, the multi-resolution approach is far superior and more realistic than the conventional frame analysis capabilities. The multi-resolution approach accounts for response limit states including shear-flexure-axial interaction that frame analysis is not capable of capturing. The proposed framework, confirmed by a reference application, avails considerable possibilities for using several FE programs and optimally combining their best features to undertake accurate and efficient inelastic dynamic response assessment under extreme loading scenarios.

### Introduction

Construction of high-rise buildings has become very common all over the world. Especially in newly developing countries, high-rise building construction is gaining momentum due to land shortage, expanding economy and availability of techniques to complete the construction in record time. The use of complex structural systems such as structural walls, tube systems, and composite sections, and advanced construction techniques allow reinforced concrete (RC) structures to be adopted in modern high-rise buildings.

Estimating the capacity preventing failure of low-rise structures has been extensively studied through advanced finite element analyses (FEA), quasi-static experiment or pseudo-dynamic (PSD) simulation of structural components and structural systems, and even shake table tests of full-scale structures. On the contrary, reliable estimation of structural capacity of complex high-rise systems under extreme loading has not been possible due to unavailability of analysis software and lack of computational capacity for refined modeling. Many advanced FEA programs are available for continuum, beam-column joints, or framed elements. Unfortunately, most of them can be applied to limited structural systems due to computational cost and/or lack of results for calibration of the used software.

Complex high-rise systems can be modeled using the above advanced applications with assumptions and approximations. For instance, a wall system is frequently modeled with nonlinear frame element which cannot account for shear deformation and failure. In many practices, the most critical components of a structural system are analyzed with detailed FE model. As boundary conditions of these components are estimated from much less complicated structural models, propagation of failure and redistribution of displacement and force demands between components cannot be accurately accounted for. It is also possible to model a whole complex structure with detailed FEA. However, since such a model would be extremely demanding from the computational point of view then it would not be possible to conduct adequate parametric studies.

The most reliable and computationally efficient method to analyze large complex structures might be modeling the most critical components with detailed FE model and the remaining elements with computationally efficient skeletal elements. Unfortunately, many applications do not include all the best material models or finite elements. It seems natural therefore to consider the use of more than one analysis platform and to make best use of their relative merits.

In this study, a framework for multi-resolution distributed simulation for the FEM analysis (MDFEA) is proposed and used to analyze a complex high-rise RC building. Shear wall of the structure is modeled with concrete continuum element in VecTor2 (Vecchio and Collins, 1986) while remaining frame elements are modeled with fiber section beam-column element in Zeus-NL (Elnashai et al. 2002). The two distinct applications are combined with multi-platform simulation framework, UI-SimCor (Kwon et al. 2005) in a step-by-step fashion in the time domain.

### Reference Structure

A newly constructed high-rise building, Tower C03 of the Jumeirah Beach development in Dubai, United Arab Emirates, is chosen as a reference structure because of its complex core wall systems and interaction with outer frames as shown in Fig. 1. Static pushover analyses and dynamic time history analyses will be performed for Frame F4 along its strong direction. The main features of this building are as shown in Table 1.

Features	Description
Height (m)	184.000
Total Stories	54
Regular Story Height (m)	3.400
Irregular Story Height (m)	4.488
Core Walls	9.43x3.25 (8.48x2.55) (m)
(Exterior and Interior Size)	9.33x3.15 (8.48x2.55) (m)
	9.18x3.05 (8.48x2.55) (m)
Concrete f'c (MPa)	60 (wall); 40 (slab)
Reinforcing Bars fv (MPa)	421 (Grade 60)

Table 1. Main Features of the Reference Structure

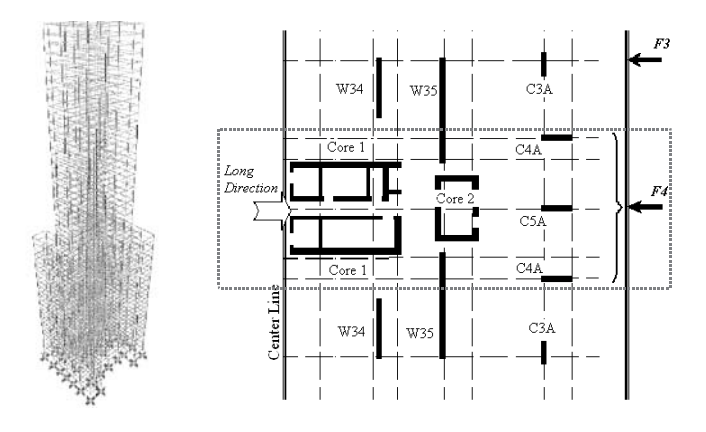


Fig. 1. Configuration of reference structure and half-plane view.

The reference building is divided into two main structural components: box-shaped core wall and outer moment resisting frame. The core walls from the 1<sup>st</sup> through 10<sup>th</sup> stories, which is likely to fail in shear, are modeled using 2D RC continuum elements in VecTor2. Core walls from 11<sup>th</sup> story and above are approximated with fiber section elements in ZEUS-NL. The whole structure is subdivided into three modules as below:

• Module 1:  $1^{st} \sim 10^{th}$  story left wall modeled in VecTor2

This region is modeled in VecTor2. The 10-story wall is meshed in 2D rectangular elements whose behavior is captured using the Modified Compression Field Theory (MCFT). The mesh size is around 200 mm which is

within 10~20 times of aggregate size. Concrete constitutive models are based on Modified Popovics curve (Collins and Porasz, 1989) which considers both prepeak and post-peak concrete behavior. The confinement effects are considered according to Kupfer et al. (1969). The reversed cyclic loading curves of concrete proposed by Palermo and Vecchio (2003) is employed in the analysis.

- Module 2:  $1^{st} \sim 10^{th}$  story right wall in VecTor2
- Module 2 is identical to Module 1.
- Module 3: remaining structure in ZEUS-NL
  Remaining structural components including all frame members and the core
  walls in the 11th story to top story are modeled in ZEUS-NL.

The following section briefly introduces the analysis platforms, VecTor2, ZEUS-NL, and UI-SimCor, followed by details of the substructures and their interfaces.

### **Structural Analysis Platforms**

### ZEUS-NL: Fiber Section 3D Frame Analysis Software

In ZEUS-NL (Elnashai et al. 2002), elements capable of modeling material and geometric nonlinearity are available. The sectional force-displacement and moment-rotation are obtained through the integration of the inelastic material response of the individual fibers describing the section. The Eularian approach towards geometric nonlinearity is employed on the element level. Therefore, full account is taken of the spread of inelasticity along the member length and across the section depth as well as the effect of large member deformations. Since the sectional response is calculated at each loading step from inelastic material models that account for stiffness and strength degradation, there is no need for sweeping assumptions on the moment-curvature relationships required by other analysis approaches. In ZEUS-NL, conventional pushover, adaptive pushover, Eigen analysis, and dynamic analyses are available that have been tested on the member and structural level. Recently, ZEUS-NL was used to steer a full-scale 3D RC frame testing campaign, and the a priori predictions were shown to be accurate and representative of the subsequently-undertaken pseudo-dynamic tests, Jeong and Elnashai, 2004a and b.

### VecTor2: RC Continuum FEM Analysis Software

VecTor2 was developed by Vecchio at the University of Toronto. In VecTor2, the Modified Compression Field Theory (MCFT; Vecchio and Collins, 1986) is adopted in which it assumes that the direction of principal stress and principal strain coincide. The application has been verified with experimental tests to corroborate the ability to predict the load-deformation response of a variety of reinforced concrete structures. The capabilities of VecTor2 have been augmented to model concrete expansion and confinement, cyclic loading and hysteretic response, construction and loading chronology for repair applications, bond slip, crack shear slip deformations, reinforcement dowel action, reinforcement buckling, and crack allocation processes.

### Multi-Platform Distributed Analysis Framework – UI-SimCor

Different state-of-the-art analysis software packages have unique features that other competing packages do not have. Similarly, different research laboratories are equipped with unique experimental facilities that suited best the tasks, time and budget allowed. The main advantage of multi-platform simulation is the use of these unique features of experimental and/or analytical tools in an integrated fashion, the essence of the Network for Earthquake Engineering Simulations (NEES). The concept of multi-platform simulation is implemented using the pseudo-dynamic (PSD) simulation approach combined with sub-structuring. In the latter simulation, a structure is subdivided into several modules that are either physically tested or computationally simulated. UI-SimCor (Kwon et. al. 2005) was developed for this purpose. The Operator Splitting method in conjunction with the α-modified Newmark scheme (α-OS method) is implemented as a time-stepping analysis scheme. The main feature of UI-SimCor is that it is capable of coordinating any number of analysis tools [currently interfaces exist for ZEUS-NL (Elnashai et al., 2002), OpenSees, FedeasLab, VecTor2], any number of testing sites, or a mixture of analysis tools and testing sites. It employs software or hardware supporting NEESgrid Teleoperation Control Protocol as well as TCP-IP connections outside of the NEES system. It is also capable of using the same analysis platform while modeling different parts of the system on the same or different processors, thus minimizing computing run time. In this study, UI-SimCor is used to combine OpenSees and ZEUS-NL to model soil and super-structural systems, respectively, after extensive component verification. In this study, UI-SimCor is used to combine ZEUS-NL and VecTor2 to model the reference structure.

## **Application to Reference Building**

### Interfaces between Sub-Structures

In UI-SimCor there are control points in the sub-structured models, with lumped masses and DOF of interest for applied loads and response displacements. These control points must be defined first in order to form the global mass and stiffness matrices necessary in pseudo-dynamic (PSD) algorithm employed in UI-SimCor, and to serve as the common interfaces between sub-structures. For the interface at control point that has rotational DOF, the method is to simulate the coupling and transfer between control point DOFs and connected plane stress 4-node element nodal DOFs. Here the adjacent 4-node elements 1 and 2 in Fig. 2 are taken into account because of their geometric belonging to the real slab beam region and also the compatibility for the transition of rotation at control point using some constraint equations.

The transition between the different element types and coupling effects are achieved by multi-point constraint equations derived by equating the work done on the beam and continuum side of wall-frame interface. The focus here is on computing the equivalent nodal displacements of continuum elements at the interface connected to the control points.

The derivation of the constraint equations for beam-continuum coupling is explained hereafter. Element 1 and 2, nodes n1, n2, n3 and n4 form the interface region. It is

assumed that the left edges of elements 1 and 2 follow the Bernoulli-Euler beam model, with plane section remaining plane during deformation. The rigid body motion geometric relationships are applied to calculate nodal displacements at left edges.

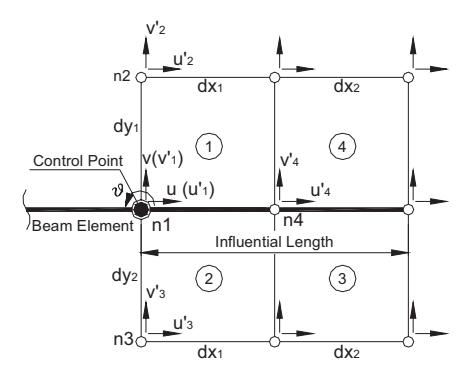


Fig. 2. Beam-wall interface element model and DOFs.

For the nodes along the beam centerline, not all nodes will be considered as being on an interface. Only those within influential length (on account of usual anchorage requirements for rebar) are counted and here the middle node n4 in Fig. 3 is such a node. The right node to n4 is treated as the real fixed end of beam and no displacement effects occur there by the control point. Also for the middle node n4, it is assumed that the horizontal and vertical movements are generated by the control point displacement based on beam shape functions.

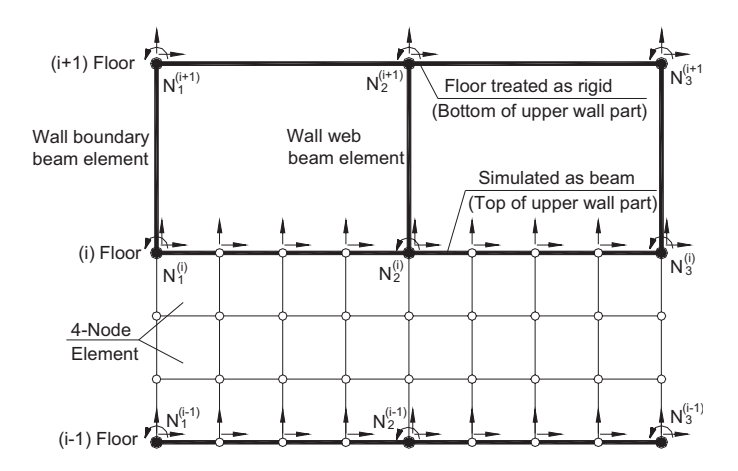


Fig. 3. Upper wall beam and lower wall continuum element interface models.

VecTor2 post-processor allows the interpretation of stress distribution results to obtain nodal forces corresponding to nodes that have displacement control. The lower 10 stories of the wall are modeled using 2D continuum elements in VecTor2, while the

remaining upper parts use beam-column element in ZEUS-NL. There are two types of interfaces: 1) upper- wall frame element and lower-wall continuum element; 2) control point DOFs and wall continuum element DOFs per floor. The modeling of latter one is same as the former situation with identical procedures.

Three control points at the middle and two edge-points for the interface at each floor, as Fig. 3 shows, are used. The upper-wall frame element is divided into three components including two boundary regions and a middle web area, modeled also using fiber analysis with full wall section in ZEUS-NL. The floor system is considered to have some flexibility instead of full rigidity. Instead of rigid body motion (RBM) geometric relationship, beam shape functions are employed for the calculation of the equivalent nodal displacements in the VecTor2 model. In the above approach, the interface floor system is divided into two beams connected with three control points.

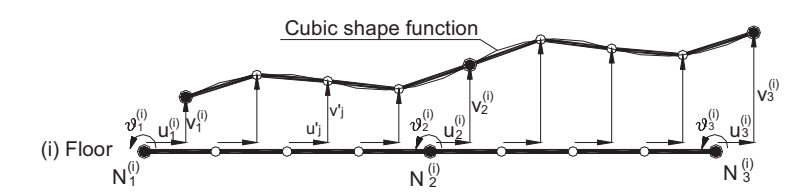


Fig. 4. Wall interface interpolation model and DOFs.

In Fig. 4, control points  $N_1 \sim N_3$  form two beam members with length equal to half of the wall width. Cubic shape functions are used for the interpolation of continuum model nodal displacement loads from  $(u, v, \theta)$  at three control points. The feedback control point reactions are computed from all the nodal force results processed from VecTor2 output, by using equivalent nodal force concept in the beam element model.

### Integrated MDFEA Structural Modeling

The reference high-rise building is sub-structured into three modules as depicted in Fig. 5. Shear walls up to 10<sup>th</sup> floor are modeled in VecTor2. The remaining shear walls at higher stories, which are not subjected to large shear forces, and frame elements, are modeled in Zeus-NL. UI-SimCor coordinates multi-platform simulation of the three components. Each module communicates with UI-SimCor using TCP-IP protocol through the internet. The configuration of multi-platform simulation is presented in Fig. 5. Static analysis and time-history analysis are conducted with the model in Fig. 5. It is noteworthy that there is no requirement that the analysis platforms exist in one geographic location.

## Static Pushover Analysis

Static pushover analysis is conducted for the reference building in order to determine ultimate strength and ductility capacity. In the UI-SimCor framework, static pushover loads are applied as initial loads immediately after the gravity loads application and equilibrium iterations. The pushover results show some differences from the previous results using ZEUS-NL. The comparisons in Fig. 6 show that the lateral drift in the

lower part of the wall has more flexibility and ductility in MDFEA than in the ZEUS-NL analysis. This is mainly due to the much larger shear deformation contributions detected in continuum FEM model. But for high load levels and overall structural responses, the ZEUS-NL model exhibits lower stiffness and strengths than the MDFEA model. This is mainly because the plane section assumption in the fiber approach leads to larger concrete crushing region at the compression side than the continuum model. In the latter approach, load redistribution is repeatedly performed at each load step and concrete confined strength model is functioning especially at the highly two-dimensional compression area. The latter features help to improve the wall resistance capacity and ductility under high load levels even after many cracks are detected. Figure 7 shows the extent of cracking and deformed wall shape and vertical strain distribution along base section at load step 50, as an example. It is observed from Fig. 7a that the wall deforms and is damaged in flexural-shear mode under the incremental pushover loads.

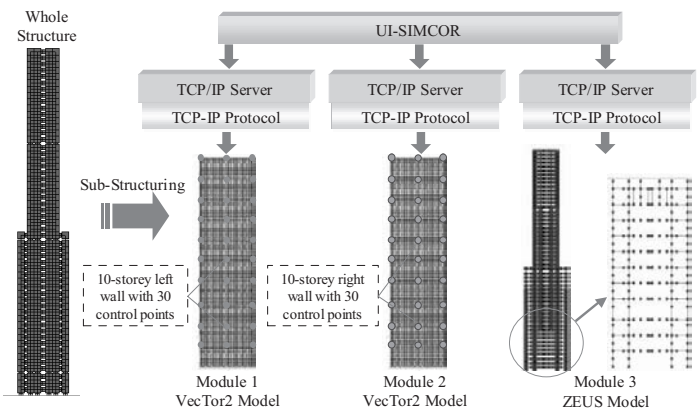


Fig. 5. Multi-resolution distributed simulation for reference building within UI-SimCor.

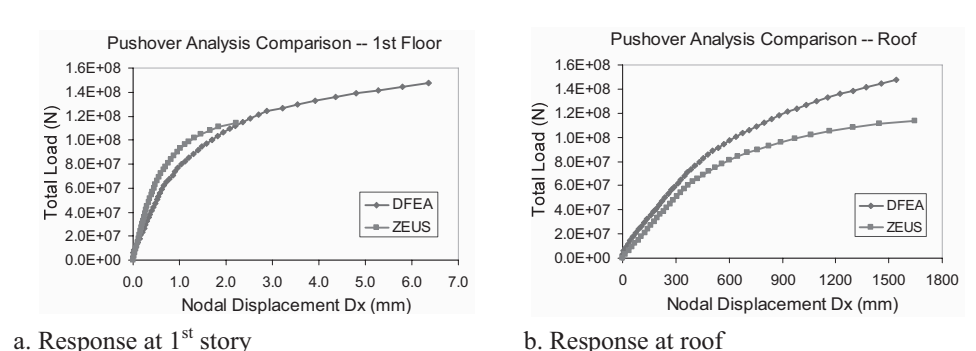
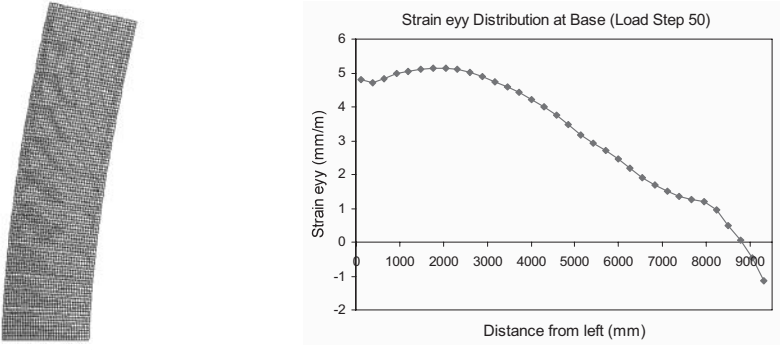


Fig. 6. Pushover comparisons between results from DFEA and pure ZEUS-NL.



a. Cracked Deformed Shape (Step 50, Scale factor: 20)

b. Strain e<sub>yy</sub> Distribution at Wall Base Section (Step 50)

Fig. 7. Pushover comparisons between results from DFEA and pure ZEUS-NL.

## **Dynamic Response History Analysis**

Inelastic dynamic response history analyses are also executed to evaluate the MDFEA for the reference building. The results serve as an investigation of the real building behavior under selected representative ground motion records. Ground motions are selected considering magnitude, distance to source, and site soil conditions. The variation of input ground motion is intended to verify the reliability of the MDFEA algorithm for complex structural system under different types of seismic excitations.

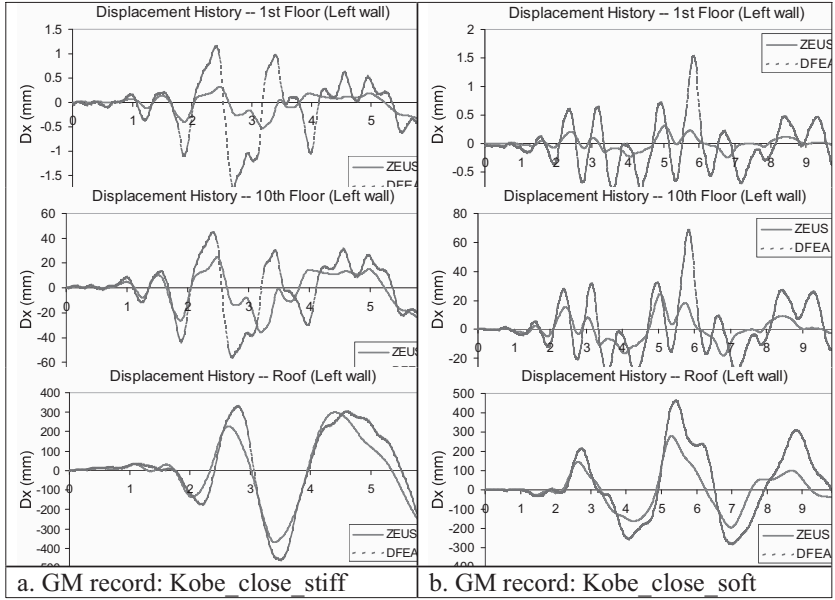


Fig. 8. Sample displacement histories and comparisons between DFEA and ZEUS models.

In Fig. 8, two sets of response history analysis results using both the MDFEA framework and conventional ZEUS-NL model are shown. The left wall displacement responses at different height levels are compared, including total drifts at 1<sup>st</sup> story, 10<sup>th</sup> story (top of the wall VecTor2 models in module 1 and 2) and the roof.

It is evident that the MDFEA results differ from skeletal ZEUS-NL analysis in a significant manner that confirms the importance of the detailed approach that includes shear deformations.

#### **Conclusions and Future Work**

When the use of complex systems in RC high-rise buildings is on the increase, there is a lack of accurate, efficient and reliable analytical approaches for inelastic static and dynamic analyses under extreme loads. In this study, a new approach termed multi-resolution distributed FEM analysis (MDFEA) is proposed and used to analyze a reference RC high-rise building with dual core wall-frame system. The main features of the work are:

- Two advanced analytical platforms ZEUS-NL and VecTor2 are used to accurately
  model the frame and wall separately, based on their unique algorithms and
  functionalities.
- A 'simulation coordinator' UI-SimCor is used to combine the best features of different FEA software for different components within one system. Through sub-structuring, global integration and network data flow, the distributed FEM simulation was successful.
- A real 54-story high-rise building with a dual core wall-frame structural system is selected as the reference application. By using the MDFEA framework, both static pushover and dynamic response history analyses are conducted in a new way that is significantly different than traditional approaches. Multiple modules corresponding to frame and wall components are built in UI-SimCor and analyzed with frame-wall interaction effects fully considered in a step-by-step manner.
- The comparisons from both pushover and response history analysis highlight that
  due to shear deformation and failure, the multi-resolution approach is far superior
  and more realistic than the available frame analysis procedures. The MDFEA
  procedure can account for response limit states including shear-flexure-axial
  interaction.

With the completed and verified functionality of the proposed MDFEA framework, it is practical to extend the application to more high-rise building types other than the reference structure, and the concepts are not restricted to only of ZEUS-NL and VecTor2. Any number of FE packages can be simultaneously integrated and their best features utilized.

## Acknowledgement

This study is a product of project EE-3 'Advanced Simulation Tools' of the Mid-America Earthquake Center. The MAE Center is an Engineering Research Center funded by the National Science Foundation under cooperative agreement reference EEC 97-01785.

### References

- Collins, M. P, and Porasz, A., (1989), "Shear Design for High Strength Concrete." Proceeding of Workshop on Design Aspects of High Strength Concrete, Comité Euro-International du Béton Bulletin d'Information, CEB, Paris (1989) pp. 77–83.
- Elnashai, A. S., Papanikolaou, V. and Lee, D. (2002). Zeus NL A System for Inelastic Analysis of Structures, Mid-America Earthquake Center, University of Illinois at Urbana-Champaign, Program Release Sept. 2002
- Ghobarah, A. and Youssef, M., (1999), "Modeling of reinforced concrete structural walls", Engineering Structures 21(10), pp. 912-923.
- Jeong, S. H and Elnashai, A. S. (2004a), "Analytical assessment of an irregular RC frame for full-scale 3D pseudo-dynamic testing, Part I: Analytical model verification," *Journal of Earthquake Engr.*, 9 (1): 95-128
- Jeong, S. H, and Elnashai, A. S. (2004b), "Analytical assessment of an irregular RC frame for full-scale 3D pseudo-dynamic testing, Part II: Condition assessment and test deployment," *Journal of Earthquake Engr.*, 9 (2): 265-284
- Kupfer, H. B., Hilsdorf, H. K. and Rusch, H., (1969), "Behavior of Concrete under Biaxial Stress", ACI Journal, Vol. 87, No. 2, pp. 656-666
- Kwon, O. S., Nakata, N., Elnashai, A. S., Spencer, B., (2005), "A Framework for Multi-Site Distributed Simulation and Application to Complex Structural Systems", Journal of Earthquake Engineering, Vol. 9, No. 5, pp. 741-753
- Mander J. B., Priestley M. J. N. and Park R. (1988), "Theoretical stress-strain model for confined concrete," Journal of Structural Engineering, Vol. 114, No. 8, pp. 1804-1826
- Palermo, D. and Vecchio, F., (2003), "Compression Field Modeling of Reinforced Concrete Subject to Reversed Loading: Formulation", ACI Str. Journal, V100, No. 5
- Paulay, T., and Priestley M.J.N., (1992), "Seismic design of reinforced concrete and masonry buildings", John Wiley & Sons, Inc., New York, N.Y.
- Popovics, S., (1973), "A Numerical Approach to the Complete Stress-Strain Curve of Concrete", Cement and Concrete Research, Vol. 3, No.5, pp. 583-599.
- Vecchio, F.J. and Collins, M.P., (1982), "Response of Reinforced Concrete to In-Plane Shear and Normal Stresses", Publication No. 82-03, Department of Civil Engineering, University of Toronto, 332 pp.
- Vecchio F. J and Collins M. P., (1986), "The modified compression field theory for reinforced concrete elements subjected to shear", ACI Structural Journal 83(2): 219–31.
- Vecchio, F. J., (1990), "Reinforced Concrete Membrane Element Formulations", Journal of Structural Engineering, Vol. 116, No. 3
- Vecchio, F. J., Wang, P. S., (2002), "VecTor2 & FormWorks User's Manual", University of Toronto

# Design and Evaluation of Reinforced Concrete Frames Infilled with Masonry Walls

Dr. Ghassan K. Al-Chaar

Construction Engineering Research Laboratory University of Illinois, USA.

#### **Abstract**

Extensive research has been done during the last 50 years to determine how the presence of masonry infills influences the in-plane and the out-of-plane behavior of reinforced concrete frame structures. Experimental research on specimens ranging from full size to 1:8 scale with varying numbers of bays and stories, in addition to analytical work ranging from simple mechanics to complex nonlinear finite element analyses, have yielded great insight into infill-frame interaction and behavior. The influence of infills on overall behavior of the structure has been found to change the strength, the stiffness and the dynamic behavior. This study gives guidelines on evaluating the lateral load capacity of infilled panels for in-plane and out-of-plane loading. Further, guidelines are given that account for the effect of out-of-plane loading on in-plane capacity. The guidelines are based on experimental and computational research and include a number of empirically based relationships for estimating strength and stiffness of infill panels subjected to forces applied either normal to or parallel with their plane. The developed evaluating method is proposed for incorporation of "Building Code Requirements for Masonry Structures", ACI 530-05/ASCE 5-05/TMS 402-05, Masonry Infill Structures.

#### Introduction

The in-plane strength and stiffness prediction of infilled frames is complex because it is a statically indeterminate problem. Great efforts have been invested by researcher, both analytically and experimentally, to simplify this problem so it can be resolved using static and dynamic methods. Most researchers agreed that the approach to resolve this problem is to model masonry infilled frames as a diagonal strut that would capture the strength, stiffness, and dynamic characteristics of the masonry. Researchers such as Stafford-Smith (1962), Mainstone (1971), Klingner and Bertero (1978) among others have formed the basis for understanding and predicting infilled frame in-plane behavior.

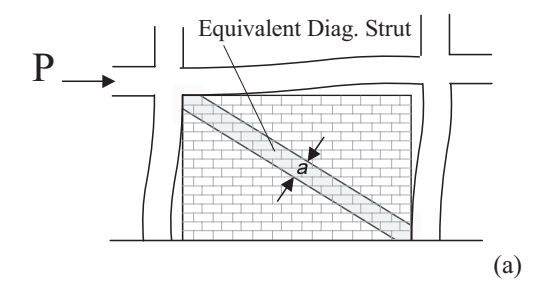
In general, infills can be grouped into two different categories: isolated infills and "regular" infills. This study focuses on the second category, "regular" infills, where the panels act as part of the lateral force-resisting system of the structure. An infill in this category must be fully in tight contact with its confining frame on all four of its sides. Any gaps must be completely filled to guarantee full mortar bonding contact.

The proposed guidelines are based on experimental and computational research and include a number of empirically based relationships for estimating strength and stiffness of infill panels subjected to forces applied either normal to or parallel with their plane. This paper is a synopsis of detailed procedure presented in Al-Chaar (2002) Technical Report. The evaluation process is based on material and geometrical properties of the structure used to calculate in-plane strength and stiffness and the overall capacity of infill-frame lateral-force resisting system. Tests to evaluate mechanical material properties of the masonry infills must be carried out in accordance with Section 7.3.2 (Properties of In-Place materials) of FEMA 273. Evaluation of material properties for the confining frame should be executed in accordance with either Section 6.3.2 (for reinforced concrete frames) or Section 5.3.2 (for steel frames) of FEMA 273. Material properties can also be obtained from building codes or from as-built plans, if available.

# Procedure for Evaluating the Capacity of Infilled Frames Using Pushover Analyses

The proposed method is a pushover analysis of a frame containing eccentric equivalent struts that represent the masonry. Using eccentric struts in this global analysis will yield infill effects on the column directly, which will negate the need to evaluate these members locally. This method relies on the development of plastic hinges to capture the nonlinearities of the structural system. The hinge properties may be calculated using the guidelines given in Section 6.4 of FEMA 273 for reinforced concrete members. Rigid End Offsets (REOs) to the joints of the frame can be assigned as recommended later in this paper. Gravity loads as initial conditions of the pushover analysis are applied in combinations and inertia force distributions be found per FEMA 273 Section 3.3.

Their experimental testing of infilled frames under lateral loads resulted in specimen deformation shapes similar to the one illustrated in Fig. 1a. The equivalent masonry strut of width, a, with same net thickness and mechanical properties as the infill itself is modeled as pinned at both ends to the confining frame as shown in Fig. 1b.



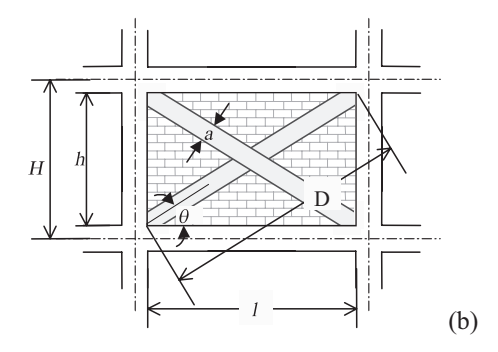


Fig. 1. Deformation shape (a) and equivalent diagonal strut (b)

The following expression used in Eq. (1) recommended by Stafford-Smith and Carter 1969 to determine the relative infill to frame stiffness, have been adopted in this procedure.

$$\lambda_I H = H \left[ \frac{E_m t \sin 2\theta}{4E_c I_{col} h} \right]^{1/4} \tag{1}$$

Also, the Mainstone (1971) is adopted to consider the relative infill to frame flexibility in the evaluation of the equivalent strut width of the panel as shown in Eq. (2).

$$a = 0.175 D(\lambda_1 H)^{-0.4} \tag{2}$$

However, if openings present are and/or existing infill damage, the equivalent strut width must be reduced using Eq. (3).

$$a_{red} = a(R_1)_i (R_2)_i \tag{3}$$

Where  $(R_1)_i$  = reduction factor for in-plane evaluation due to presence of opening defined in the section on perforated panels, and  $(R_2)_i$  = reduction factor for in-plane evaluation due to existing infill damage defined later in this paper.

The equivalent masonry strut is to be connected to the frame members as depicted in Fig. 2. The infill forces are assumed to be mainly resisted by the columns, and the struts are placed accordingly. The strut should be pin-connected to the column at a distance  $l_{column}$  from the face of the beam. This distance is defined in Eq. (4) and is calculated using the strut width, a, without any reduction factors.

$$I_{column} = \frac{a}{\cos \theta_{column}} \quad \tan \theta_{column} = \frac{h - \frac{a}{\cos \theta_{column}}}{I}$$
 (4)

Using this convention, the strut force is applied directly to the column at the edge of its equivalent strut width, a. This concept is illustrated in Fig. 2.

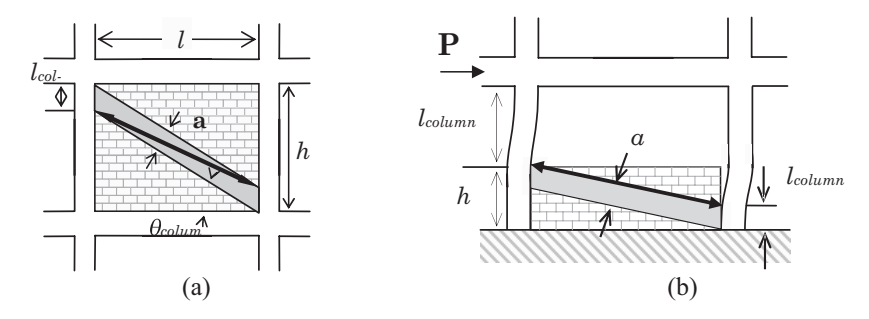


Fig. 2. Placement of strut in full panel (a), in partially infilled wall (b).

In the case of a partially infilled frame, the reduced column length,  $l_{column}$ , shall be equal to the unbraced opening length for the windward column, while  $l_{column}$  for the leeward column is defined as usual (Fig. 2). The strut width should be calculated from Eq. (3), using the reduced infill height for h in Eq. (1). Furthermore, the only reduction factor that should be taken into account is  $(R_2)_i$ , which accounts for existing infill damage.

In the case of a perforated masonry panel, the equivalent strut is assumed to act in the same manner as for the fully infilled frame. Therefore, the eccentric strut should be placed at a distance  $l_{column}$  from the face of the beam as shown in Fig. 3. The equivalent strut width, a, shall be multiplied, however, by a reduction factor to account for the loss in strength due to the opening. The reduction factor,  $(R_1)_i$ , is calculated using Eq. (5).

$$(R_1)_i = 0.6 \left(\frac{A_{open}}{A_{panel}}\right)^2 - 1.6 \left(\frac{A_{open}}{A_{panel}}\right) + 1$$
 (5)

Where:

 $A_{\text{open}}$  = area of the openings (in.<sup>2</sup>) and  $A_{\text{panel}}$  = area of the infill panel (in.<sup>2</sup>) = 1 x h

If the area of the openings  $(A_{open})$  is greater than or equal to 60 percent of the area of the infill panel  $(A_{panel})$ , then the effect of the infill should be neglected, i.e.,  $(R_1)_i = 0$ . Also,

reducing the strut width to account for an opening does not necessarily represent the stress distributions likely to occur. This method is a simplification in order to compute the global structural capacity. Local effects due to an opening should be considered by either modeling the perforated panel with finite elements or using struts to accurately represent possible stress fields as shown in Fig. 3b.

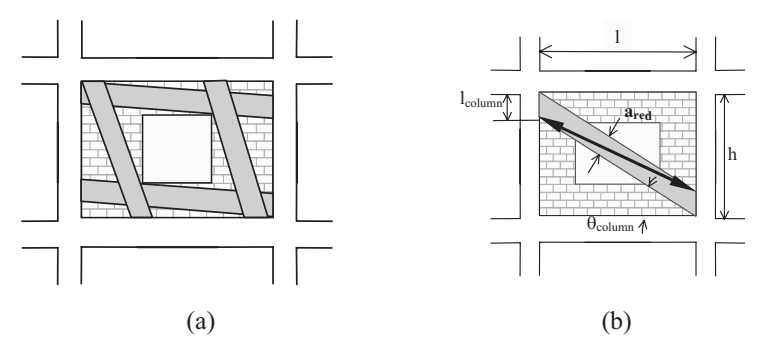


Fig. 3. Possible strut placement for perforated panel.

Existing panel damage (or cracking) must be classified as either: no damage, moderate damage, or severe damage as presented in Fig. 4. If in doubt as to the magnitude of existing panel damage, assume severe damage for a safer (conservative) estimate. A reduction factor for existing panel damage  $(R_2)_i$  must be obtained from Fig. 4. Notice that, if the slenderness ratio (h/t) of the panel is greater than 21,  $(R_2)_i$  is not defined and repair is required. For panels with no existing panel damage, the reduction factor  $(R_2)_i$  must be taken as 1.0.

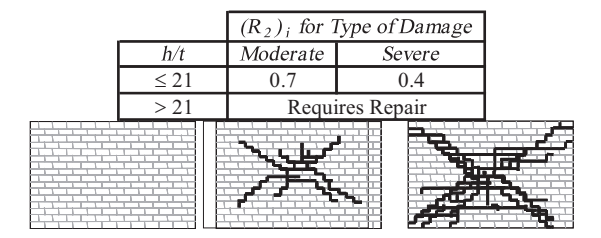


Fig. 4. In-plane damage reduction factor and visual damage classification.

## Load-Deformation Behavior of the Eccentric Equivalent Strut

The eccentric equivalent strut used to model the masonry infill is pin-connected to the frame elements so that no moment transfer occurs. The stiffness of the strut will be governed by the modulus of elasticity of the masonry material ( $E_m$ ) and the cross-sectional area (a x  $t_{eff}$ ). The strength of the strut is determined by calculating the load required to reach masonry infill crushing strength ( $R_{cr}$ ) in Eq. (6) and the load required to reach the masonry infill shear strength ( $R_{shear}$ ) in Eq. (6). The component of these forces in the direction of the equivalent strut will be used to assign the strut a "compressive" strength. This strength is defined as  $R_{strut}$  Eq. (6) and governs the strength of the plastic hinge in the strut.

$$R_{strut} = \min \begin{Bmatrix} R_{cr} \\ R_{shear} / \cos \theta_{strut} \end{Bmatrix} \quad \tan \theta_{strut} = \frac{h - 2I_{column}}{I}$$
 (6)

Where:  $\theta_{\text{strut}}$  = the angle of the eccentric strut with respect to the horizontal, given by Eq. (7). The equivalent strut is assumed to deflect to nonlinear drifts as shown in Fig. 5. The parameter d, which represents the nonlinear lateral drift associated with the infilled panel, is defined in Table 7-7 of FEMA 273.

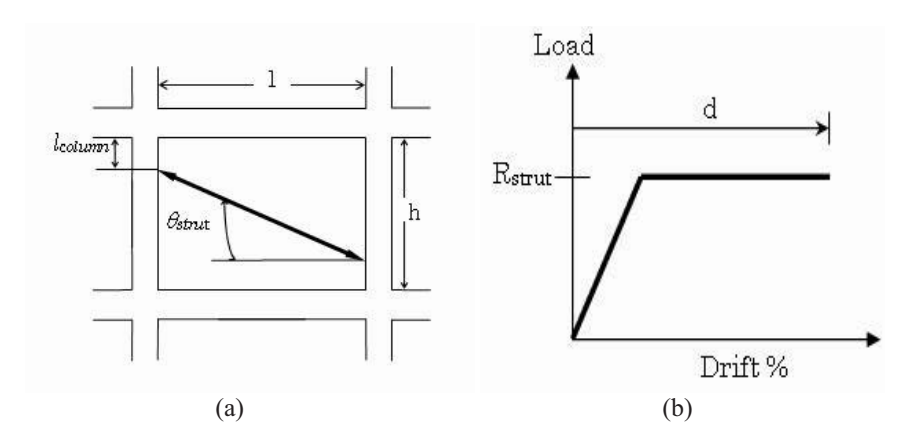


Fig. 5. Geometry of  $\theta_{strut}$  (a) and load deformation (b).

# Masonry Infill Crushing and Shear Strength

The masonry infill crushing strength corresponds to the compressive load that the equivalent masonry strut can carry before the masonry is crushed ( $R_{cr}$ ). The applied load that corresponds to the crushing strength of the infill is evaluated using Eq. (7).

$$R_{cr} = a_{red} t_{eff} f_m' ag{7}$$

Where:  $f_m$  = compressive strength of the masonry (psi),  $t_{eff}$  = net thickness of the masonry panel (in).

The capacity of masonry to shear forces is provided by the combination of two different mechanisms: the bond shear strength and the friction between the masonry and the mortar. Therefore, the horizontal lateral load required to reach the infill shear strength is calculated by Eq. (8).

$$R_{shear} = A_n f_v'(R_1)_i (R_2)_i$$
(8)

Where:  $A_n$  = net cross sectional mortar/grouted area of infill panel along its length (in.<sup>2</sup>), and  $f'_v$  = masonry shear strength (psi).

## Plastic Hinge Placement and Rigid Off Set Placement

Plastic hinges in columns should capture the interaction between axial load and moment capacity. These hinges should be located at a minimum distance  $l_{column}$  from the face of the beam. Hinges in beams need only characterize the flexural behavior of the member. These hinges should be placed at a minimum distance  $l_{beam}$  from the face of the column.

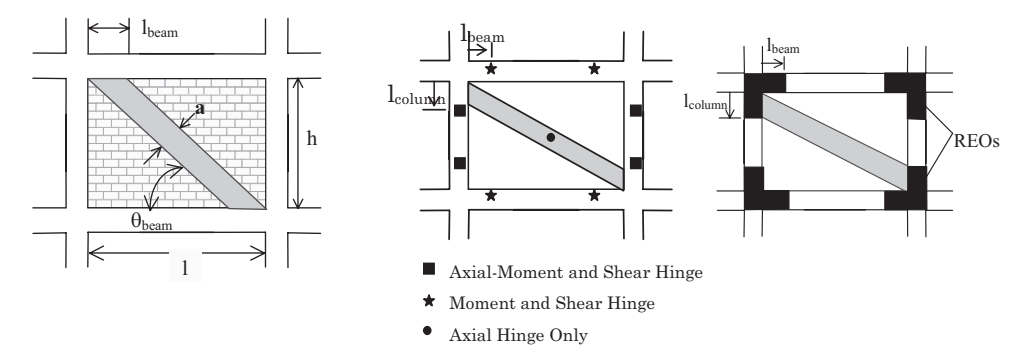


Fig. 6. Distance to beam hinge (a), plastic hinge placement (b) and rigid end offset placement (c)

This distance is calculated from Eq.(9) where  $\theta_{beam}$  is the angle at which the infill forces would act if the eccentricity of the equivalent strut was assumed to act on the beam.

$$I_{beam} = \frac{a}{\sin \theta_{beam}} \quad \text{and} \quad \tan \theta_{beam} = \frac{h}{1 - \frac{a}{\sin \theta_{beam}}}$$

$$(9)$$

Although the infill forces are assumed to act directly on the columns, hinging in the beams will still occur and  $l_{\text{beam}}$  is a reasonable estimate of the distance from the face of the column to the plastic hinge. Shear hinges must also be incorporated in both columns and beams. The equivalent strut, however, only needs hinges at the mid span that represent the axial load. In general, the minimum number and type of plastic hinges needed to capture the inelastic actions of an infilled frame are depicted in Fig. 6b and the rigid end offset placement as shown in Fig. 6c.

#### In-Plane Stiffness Evaluation of URM Infills

The following procedure should be used to resolve the stiffness of structures containing fully infilled panels, partially infilled panels, and/or perforated masonry panels. This method relies on exploiting the pushover curve generated by the structural analysis program for capacity evaluation. The pushover curve must be modified, however, to accurately represent displacements. Modifications must be made in order to increase the initial stiffness and reduce the displacement at ultimate load since the use of an equivalent strut in the pushover analysis yields mathematical models, which are more flexible than experimental models. The slopes of both segments of the bilinear curve are then increased while keeping the "yield" and ultimate loads constant. In effect, the

values for initial stiffness and displacement at ultimate are modified to more reasonable values. The bilinear load-deflection curve is defined by three points; the origin, the "yield" load and displacement ( $V_u$  and  $\Delta_y$ ), and the ultimate load and displacement ( $V_u$  and  $\Delta_u$ ). The bilinear curve is also defined by two stiffnesses,  $K_y$  and  $K_u$ , which are the slopes of the initial and final portions of the curve, as shown in Fig. 7.

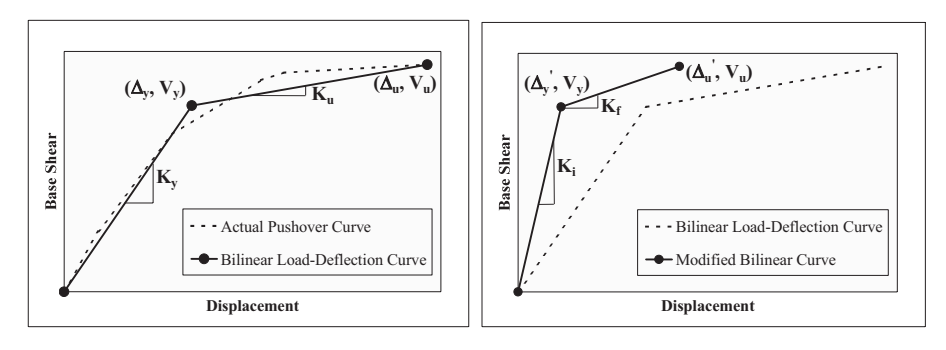


Fig. 7. Bilinear load-deflection curve (left), modified load-deflection curve (right).

The Equation used to calculate the equivalent strut width for determining the capacity of the infill panel is based on a more conservative approach by Mainstone (1971), which establishes a lower bound of the expected elastic stiffness of the infill (shown by the lower curve in Fig. 8). Mainstone (1971) only considered the relative infill-to-frame flexibility in the evaluation of the equivalent strut width of the panel. Upper bound estimates for elastic stiffness, according to Stafford-Smith and Carter (1969), vary not only with the relative infill-to-frame stiffness but also with the aspect ratio of the panel (l/h) as illustrated in Fig. 8.

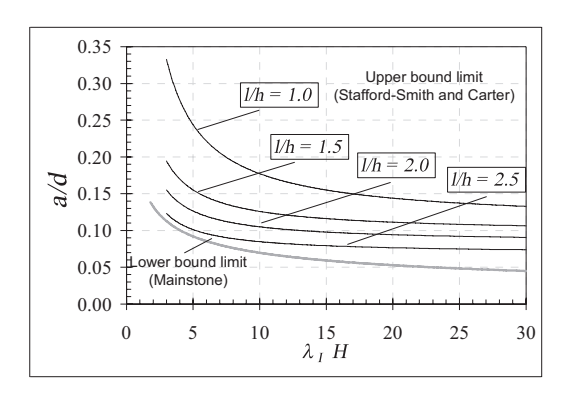


Fig. 8. Upper/lower limit strut width.

The first method increases the existing  $K_y$  by a factor of three, but is applicable only for infill panels with an aspect ratio between 0.67 and 1.5. The second method can be used for any aspect ratio, but must be used for aspect ratios less than 0.67 or greater than 1.5.

This stiffness is referred to as K<sub>SSC</sub> and represents the initial elastic stiffness determined by Stafford-Smith and Carter (1969).

The two methods are summarized in Eq. (11). The final stiffness must also be increased in order to reduce the displacement at ultimate load to more reasonable values. Increasing the secondary stiffness from the pushover,  $K_u$ , by a factor of two along with increasing the initial stiffness to  $K_i$  and keeping the "yield" and ultimate loads constant led to displacement at ultimate load, which matched experimental values fairly well.

$$K_{i} = \begin{cases} 3K_{y} & (0.67 \le \frac{1}{h} \le 1.5) \\ K_{SSC} & (any \quad \frac{1}{h}) \end{cases} \qquad K_{f} = 2K_{u}$$
 (11)

Using the calculated values for  $K_i$  and  $K_f$ , the modified bilinear load-deflection relationship should reasonably predict the initial stiffness  $(K_i)$ , ultimate load capacity  $(V_u)$ , and displacement at ultimate load  $(D_u')$  of the infilled structure.

## **Out-of-Plane Strength and Stiffness Evaluation**

The out-of-plane evaluation procedure for URM infill panels presented in this procedure relies on the development of arching action as the primary lateral-force-resisting mechanism, as presented by Angel (1994). The out-of-plane lateral strength of the panel is evaluated by Eq. (12)

$$W = \frac{2 f_{m}^{\prime} \lambda_{o}}{h_{t}^{\prime}} (R_{1})_{o} (R_{2})_{o} (R_{3})_{o}$$
(12)

Where:  $\lambda_0$  = slenderness parameter as shown in Table 1.  $(R_1)_o$ ,  $(R_2)_o$ ,  $(R_3)_o$  are multiplication factors that consider the presence of openings in the infill, existing panel damage, and flexibility of confining frame.

Table 1. Out-of-Plane Slenderness Parameter

h/t	5	10	15	20	25
λο	0.129	0.060	0.034	0.021	0.013

## **Perforated Panels**

The size and number of openings present in an infill panel can vary its stiffness as well as its strength. A reduction factor  $(R_1)_0$  takes into account the effect of infill openings during the out-of-plane evaluation of infill panels and is evaluated using Eq. (13).

$$\left(R_{1}\right)_{o} = \frac{5}{4} \left(1 - \frac{A_{open}}{A_{panel}}\right) \tag{13}$$

Infills with openings of less than 20 percent of the total area of the panel may be assumed to be fully infilled for the out-of-plane evaluation ( $(R_1)_0 = 1$ ).

## **Existing Infill Damage**

Existing infill damage must be accounted for in the in-plane evaluation. A reduction factor for existing panel damage  $(R_2)_0$  must be obtained from Table 2.

	$(R_2)_o$ for Damage Level					
h/t	Moderate	Severe				
5	0.997	0.994				
10	0.946	0.894				
15	0.888	0.789				
20	0.829	0.688				
25	0.776	0.602				

**Table 2. Damage Reduction Factors** 

# Effect of Out-of-Plane Loading on In-Plane Capacity

The effects of out-of-plane loading cannot be neglected when analyzing the in-plane capacity of an infilled structure. The in-plane capacity can be significantly reduced if large out-of-plane loads exist. Eq. (14) should be used to account for this in-plane capacity reduction. If the out-of-plane demand is less than or equal to 20 % of the out-of-plane capacity, however, the in-plane capacity should not be reduced and Eq. 21 does not apply.

$$\frac{IP_{reduced}}{IP_{capacity}} = 1 + \frac{1}{4} \frac{OP_{demand}}{OP_{capacity}} - \frac{5}{4} \left( \frac{OP_{demand}}{OP_{capacity}} \right)^2$$
(14)

Where:  $IP_{reduced}$  = the in-plane capacity considering out-of-plane loading,  $IP_{capacity}$  = the in-plane capacity found from the section on general procedures for evaluating the capacity of infilled frames using pushover analyses,  $OP_{demand}$  = the out-of-plane demand placed on the infilled frame.  $OP_{capacity}$  = the out-of-plane capacity found from the section on out-of-plane strength evaluation.

## Conclusions

Inspite of the numerous controversies, issues still remain in designing and evaluating of this structural system. The proposed procedure is viewed to be comprehensive and complete, for, it is based on experimental and computational research and include a number of empirically-based relationships for estimating strength and stiffness of infill panels subjected to forces applied either normal to or parallel with their plane. The

modeling procedure is simple and would capture characteristics of the prototypes within acceptable level of accuracy. This procedure was contemplated for wide range of variables that would affect the results.

#### References

- Al-Chaar, G, Evaluating Strength and Stiffness of Inreinfforced Masonry Infill Structures, ERDC/CERL TR-02-1, January 2002.
- Al-Chaar, G., Non-Ductile Behavior of Reinforced Concrete Frames with Masonry Infill Panels Subjected to In-Plane Loading, ERDC-CERL TM 99/18/ADA 360129, Dec. 1998.
- Angel, R., D.P. Abram, D., Behavior of Reinforced Concrete Frames with Masonry Infills, Structural Research Series No. 589, UILU-ENG-94-2005, UOI March 1994
- FEMA 273, NEHRP Guidelines for the Seismic Rehabilitation of Buildings, October 1997.
- FEMA 310, Handbook for the Seismic Evaluation of Buildings A Prestandard, 1998.
- Klingner, R.E., and V. Bertero, "Earthquake Resistance of Infilled Frames," Journal of the Structural Division, ASCE, Vol. 104, June 1978.
- Mainstone, R. J., "On the Stiffness and Strength of Infilled Frames," Proceedings of the Institution of Civil Engineers, 1971.
- Stafford-Smith, B., "Lateral Stiffness of Infilled Frames," Journal of the Structural Division, ASCE, Vol. 88, December 1962.

# Simplified Method for Analysis and Design of Biaxially Loaded Reinforced Concrete Columns

# K. Demagh<sup>1</sup>, A. Chateauneuf<sup>2</sup>

<sup>1</sup>Department of Civil Engineering, University of Batna, Algeria <sup>2</sup>Laboratory of Civil Engineering, University Blaise Pascal, Clermont, France

#### Abstract

In this paper, a simple analysis and design formula to predict the resisting capacity of biaxially loaded short reinforced concrete (RC) columns with square cross-section is introduced. Based on the numerical analysis, the resisting capacity factor which represents the ratio of P–M interaction diagrams in uniaxial loading column to biaxial loading column is proposed. The relationships between the resisting capacity factor and all design variables are established by regression, and the required P-M interaction diagram of biaxial RC column can be easily constructed without conducting additional non linear finite element analyses. The ultimate resisting capacities calculated from the proposed formula are compared with the BS simplified methods and some experimental data, in order to establish the efficiency of the proposed method. The good results obtained show that the proposed model can represent the ultimate resisting capacity of RC columns subjected to biaxial bending and axial load.

**Key Words:** RC columns, biaxial bending, interaction diagram, resisting capacity factor, design formula.

### Introduction

A reinforced concrete column is always subjected to axial load and biaxial bending due to geometry, cross-section shape or eccentricity from imperfect alignment. Due to the combination of axial load and bending moment, the column cross-section must be designed to ensure that the forces acting on a member fall inside the P-M interaction diagram representing the resisting capacity of the column. For biaxially loaded columns, many studies have been carried out on the interaction surface of the cross-sections. Particular mention may be made to the research by Brondum (1982-83) and Yen (1991), who presented methods for the analysis of arbitrary cross-sections, but using a rectangular stress block. In addition, Kawakami (1985) presented a complete algorithm for the analysis of RC members, including the effect of both regular and prestressed reinforcements, but their method was very difficult to implement in a computer program. Subsequently, Rodriguez-Gutierrez and Dario Aristizabal-Ochoa (1999) presented a method to determine the biaxial interaction diagrams for any orientation of the neutral axis of RC column with any geometry, obtaining analytical closed form expressions for equilibrium forces. Recently, Fafitis (2004) developed a method for computation of the interaction surface of RC concrete cross-sections subjected to axial load and biaxial bending based on Green's theorem. On the other hand, there has been considerable interest in developing simplified design methods for analysis and design to be included in the codes of practice. Due to the complex nature of the design relationships for columns cross-sections, simplifications have been adopted almost universally. According to current practice, the calculation of reinforcement steel area and the checking of the capacity of standard uniaxial column cross-sections have been usually carried out by using the interaction diagrams provided by the codes of practice's BS8110 (1985), CP110 (1972) and Eurocode (2004). Hence, the construction of a correct P-M interaction diagram for RC columns would require a sophisticate analysis considering material nonlinearities. However, non linear analysis is time consuming, and its use in design practice requires much experience. To solve this problem in practice and to consider all the nonlinear effects in design, a simplified analysis and design method for short RC columns is proposed in this paper. The ultimate resisting capacity factor, which represents the ratio of P-M interaction diagrams of uniaxial loading to biaxial loading, is proposed for regression. Based on the proposed factor, the required P-M interaction diagram of biaxial loaded RC column can be easily constructed without conducting additional sophisticated analyses. The ultimate resisting capacities calculated by the proposed formula are compared with those calculated by numerical analysis and BS methods, as well as some experimental results, in order to establish the efficiency of the proposed formula.

## **Design Methods**

#### Load Contour Method

The CP110 adopted a simplified "load contour" approach proposed by Bresler (1961) with certain modifications. The main concept behind this method is that for a given constant ultimate axial load P, the following design formula is applied:

$$\left(\frac{M_x}{M_{ux}}\right)^a + \left(\frac{M_y}{M_{uy}}\right)^a \le 1.0$$
(1)

Where  $M_x$ ,  $M_y$  are the applied moments about x and y axes and  $M_{ux}$ ,  $M_{uy}$  are the corresponding ultimate moments.

The only modification to the "load contour" method proposed by the CP110 was a simplified formula to calculate the value of  $\alpha$  (the common exponent in the load contour formula). The proposed formula was based on the ratio of the applied axial load P to the ultimate resistance in pure axial load  $N_{uy}$ , the value of  $\alpha$  lies between 1 and 2 as:

$$\alpha = \frac{2}{3} + 5 \frac{5P}{3N_{uv}} \tag{2}$$

The EC2 (2004) gives the values of  $\alpha$  based on the axial load level; it varies from 1 to 2 with linear interpolation:

N <sub>sd</sub> / N <sub>Rd</sub>	0.1	0.7	1
α	1	1.5	2

Where  $N_{Sd}$  is the applied axial load and  $N_{Rd} = A_{cfcd} + A_{sfyd}$  is the axial resistance capacity, with  $f_{cd}$  and  $f_{vd}$  are the material's resistances.

# Design Method in the BS

The demands for a simplified approach, which would cover most practical columns led to a simplified approach. This method was initially proposed by Beeby (1978) and later adopted for BS8110. A similar simplified method is proposed by Gouwens (1975). The simplified approach increases the design moment about the main bending axis in such way that the design is carried out only under uniaxial bending. The moment about the dominant axis is given by:

If 
$$\frac{M_x}{h'} > \frac{M_y}{b'}$$
 then  $M_{xm} = M_x + \gamma M_y \left(\frac{h'}{b'}\right)$  (3)

If 
$$\frac{M_y}{b'} > \frac{M_x}{h'}$$
 then  $M_{ym} = M_y + \gamma M_x \left(\frac{b'}{h'}\right)$  (4)

Where b'and h' are the effective width and depth of the cross-section respectively; The proposed empirical formula for the value of  $\gamma$  is given in the BS8110 by:

$$\gamma = 1 - \frac{7}{6} \left( \frac{P}{bhf_c'} \right) \tag{5}$$

Where f'<sub>c</sub> is the characteristic strength of concrete;

The proposed approach is more suitable for small column cross-sections with reinforcement bars located at the four corners of the cross-section but for any other bar arrangement the method is not valid (Rafik 1995). Although in the BS approach, the design moment about the dominant axis is increased, the simplified stress block does not represent the true status of the stress and strain within the cross-section essentially when the neutral axis is out of the cross-section (i.e. full compression). The BS8110 simplified approach may give a reasonable approximation of the biaxial bending for cases where the bending moment about the dominant axis is much larger than the moment about the other axis (Rafik 1995).

## **Proposed Formula**

# Strength capacity factor

Since the ultimate resisting capacity of RC column is governed by many variables and is gradually reduced as the degree of axial load increases ( $P/A_g f^*_c$ ), it is necessary in many cases to conduct refined numerical analysis that considers material nonlinearities to accurately predict the ultimate strength of biaxial RC column. However, the nonlinear analyses are time consuming and costly, they are not suitable for everyday designers needs. To directly analyse and design biaxial RC column, a resisting capacity factor is introduced to evaluate the resistance from the strength under uniaxial loading. If the dimensions of the concrete cross-section and the material properties have been selected, the interaction diagrams for uniaxial loading are easily constructed then by introducing the strength capacity factor one can easily obtain the interaction diagrams for biaxial loading with any angle of resultant bending moment  $M_{\rm BIA}$ . The strength capacity factor is defined as the ratio of the distance from the origin (eccentricity) for uniaxial interaction diagram to biaxial loading interaction diagram at the same degree of axial load level ( $P/P_0$ ) (Fig. 2.):

$$P_{UNI} = P_{BIA} \tag{6a}$$

$$M_{UNI} = K M_{BIA} = K M_n = \sqrt{M_x^2 + M_y^2}$$
 (6b)

Then

$$K = \frac{M_{UNI}}{M_{RIA}} = \left(\frac{OA}{OB}\right) \tag{7}$$

Where K is the strength capacity factor,  $M_{UNI}$  is the resistance for uniaxial loading, MBIA is the resistance for biaxial loading and  $M_n$  is the resultant moment for biaxial loading.

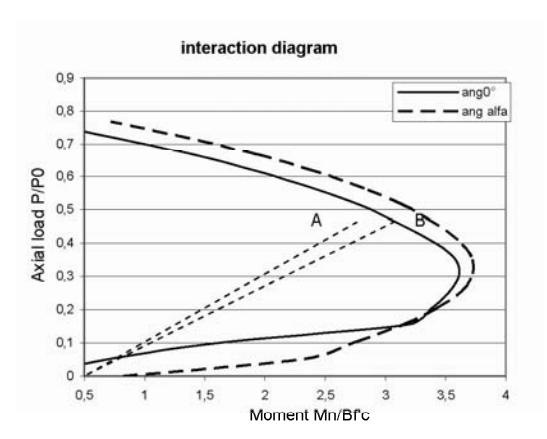


Fig.1. Determination of the strength resisting factor K.

However, to introduce a formula for the strength capacity factor some difficulties must be overcome because the interaction diagrams must be determined for biaxial and uniaxial cross-section with the same design variables, the value of the factor changes according to the reinforcement ratio, the concrete strength, the axial load level and the angle of loading. Also an infinite number of possible RC sections can be selected for the same set of applied external forces. Hence, in determining RC interaction diagrams, all the variables need to be assumed on the basis of practical limitations and the design code requirements. The commonly used compressive strength of concrete and stress of steel for design are  $f_{\rm c}\!=\!25,\,30$  and 40MPa for normal concrete and  $f_y\!=\!400$ MPa respectively. In addition, the steel ratio ranges from 1% to 4% in current zones (R.P.A. 2003). Due to the symmetry of the section and the reinforcement, the angle of loading is supposed to vary from  $0^\circ$  (uniaxial) to  $45^\circ$  (biaxial) with an increment of  $15^\circ$ . Table1 gives the range of variables adopted for the design of experiment plans to be included in the analysis.

**Table 1. Parameters Variation** 

Parameters	Values
Cross-section shape	Square
Biaxial bending angle ( $\alpha$ ) with respect to the	α=0°, 15°, 30°, 45°
strong axis	
Reinforcement distribution	Uniformly distributed at four faces
Axial load P/P <sub>0</sub> where P <sub>0</sub> =f' <sub>c</sub> A <sub>g</sub>	10 values from 0,1P <sub>0</sub> to 0,7P <sub>0</sub>
Compressive concrete strength	f' <sub>c</sub> =25, 30, 40 MPa
Steel strength	$f_y = 400 Mpa$
Geometrical reinforcement ratio	$\rho_s = 1\%, 2\%, 4\%$

The influence of the different parameters on the interaction diagrams are depicted in Figs. 2 to 4. We can observe that:

- The cross-section capacity increases with the increase of the concrete strength in the same proportion, especially in the region  $0.1 < P/P_0 < 0.7$ , Fig. 2;

- The section capacity increases with the increase of steel ratio over the length of the curves, Fig. 3;
- The section capacity decreases when the angle of loading increases over the curve especially in the region of tension control and until P/P0= 0.6, over this value the resistance capacity is the same for the different angles, Fig. 4.

The calculated capacity factors K for the different parameters chosen is depicted in Figs.5 to 7.

Nine typical results of the strength capacity factor K calculated with 3 ratios, 3 angles and 3 types of concrete with a range of axial load equal  $0.1\ P_0$  to  $0.7\ P_0$  are obtained. Figures 5 to 7 show that the strength capacity factor K:

- Decreases with large values of compression strength especially in the region of tension control  $P \leq 0.4 \ P_0$ . In the compression control region, the factor decreases proportionally to large axial load values;
- Increases with large values of steel ratio but the values of K are lower in the region of compression control;
- Increases with large values of loading angle especially in the region of tension control.

To determine a reasonable regression formula, the effect of each design variable was studied, Figs. 5 to 7. Consequently, it was found that the variation of compressive concrete strength  $f'_c$ , steel ratio  $\rho_s$ , loading level  $P/P_0$  and loading angle  $\alpha$  have the greatest effects on the variation of K. Since the factor coefficients are gradually increased or decreased according to changes in each design variable and represent a nonlinear characteristic, a second order polynomial is assumed in term of design variables. On the basis of the strength capacity, K is calculated according to the change in each design variable, the regression formula represented in Eq.8 is finally chosen.

$$K = a_0 + a_1 f_c' + a_3 \left(\frac{P}{P_0}\right) + a_4 \alpha + a_5 f_c'^2 + a_6 \rho_s^2 + a_7 \left(\frac{P}{P_0}\right)^2 + a_8 \alpha^2 + a_9 f_c' + a_{10} f_c' \left(\frac{P}{P_0}\right) + a_{11} f_c' \alpha + a_{12} \rho_s \left(\frac{P}{P_0}\right) + a_{13} \rho_s \alpha + a_{14} \alpha \left(\frac{P}{P_0}\right)$$

$$(8)$$

Where  $f_c$  is the compressive strength of concrete (MPa), P/P0 the loading level of axial force,  $\rho_s$  the steel ratio (100.A<sub>st</sub>/A<sub>c</sub>) and  $\alpha$  the loading angle ( $\alpha^{\circ}$ ).

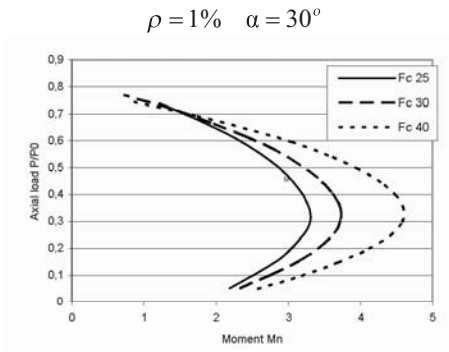


Fig. 2. Interaction diagram in accordance with compressive strength.

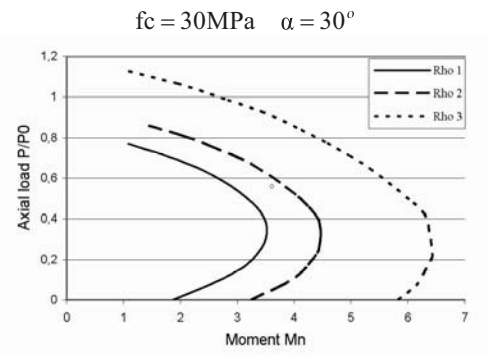


Fig.3.Interaction diagram in accordance with steel percentage.

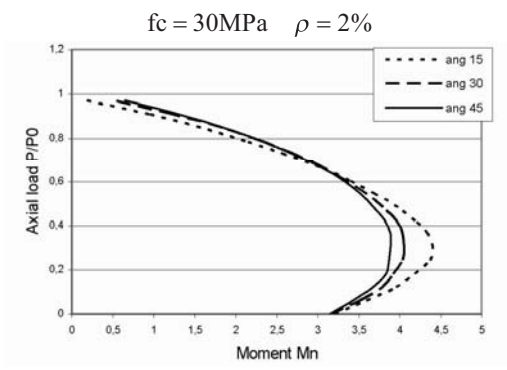


Fig. 4. Interaction diagram in accordance with angle of loading.

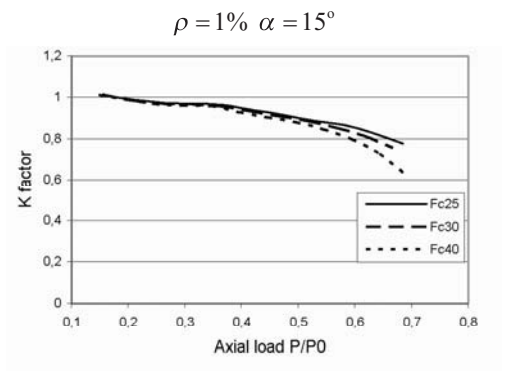


Fig. 5. Variation of K factor in accordance with compression strength.

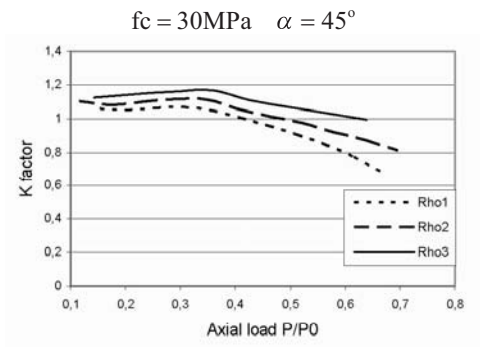


Fig. 6. Variation of K factor in accordance with steel percentage.

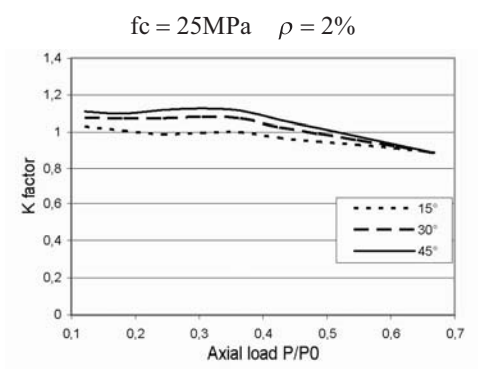


Fig. 7. Variation of K factor in accordance with angle of loading.

## Validation of the Proposed Formula

## Numerical Validation

To verify the effectiveness of the proposed formula typical, RC square sections are analysed with different steel ratios, compressive concrete strengths and loading angles. The comparison is done between: the exact solution  $M_{\rm exact}$ , the proposed  $M_{\rm K}$  and the BS method  $M_{\rm BS}$ . The numerical results are presented in Tab.2 and the variation of the strengths is depicted in Figs.8-10. The proposed formula provides results that are reasonably close to those obtained from sophisticated biaxial analysis through the entire range of axial load level P/P<sub>0</sub>, the maximum error of 3.8% is obtained for low reinforcement ratio. The BS method gives good agreement and it is more conservative especially for low axial load level (P/P<sub>0</sub>< 0.4), the maximum error is equal to 9 % through the range P/P<sub>0</sub>=0.1 to 0.4 but non conservative for great reinforcement ratio (4%) and high level of axial load (P/P<sub>0</sub>>0.4), the maximum error is equal to 20% through the range P/P<sub>0</sub>=0.4 to 0.7.

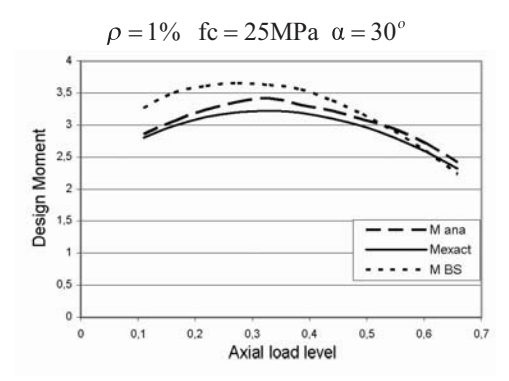


Fig.8. Comparison of design moments.

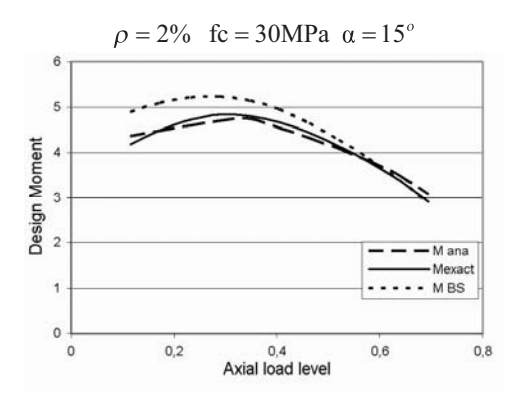


Fig. 9. Comparison of design moments.

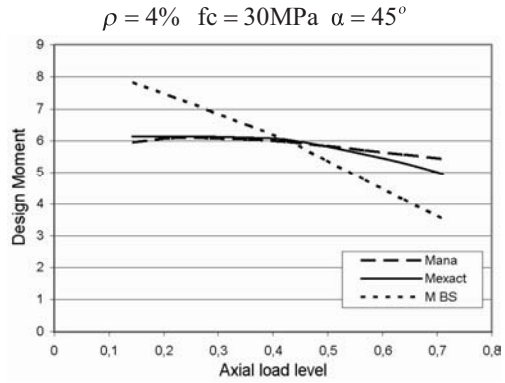


Fig. 10. Comparison of design moments.

## **Experimental Validation**

An experimental study is carried out in order to compare the numerical results obtained by the proposed formula with those obtained by some experimental data. For this purpose we calculated the strength capacity factor with the Eq. (8) and with static from the data for the specimens selected, and then we took a comparison. Table 2 shows the comparison with the experimental data in reference (Hsu 1988); it seems that the proposed formulation gives good results: error of 7% for the specimens governed by tension control and 6% for the specimens governed by compression control, with a deviation of 3%.

#### Conclusions

A numerical model to simulate the strength capacity of biaxial loading RC square columns is presented in this paper, and the proposed model is verified by comparison with the exact analysis, the BS simplified method and some experimental results. A simple but effective regression formula is presented with a strength capacity factor K to simulate an equivalent analysis and design for a biaxial loaded column is proposed. Although accurate numerical methods will play an increasingly important role and may become the standard for the final design checks, the simple formula introduced in this paper can effectively be used in determining an accurate analysis and design for common RC columns. Moreover, to reach a more rational and general approach; extensive studies for other cross-section aspects need to be followed. The results of this limited investigation shows that the proposed method gives good accuracy with the exact analysis and experimental data (<7%) and permit simple construction of biaxial interaction diagrams. The proposed formula is easily applicable for the analysis and design for the engineers in comparison of the utilization of the biaxial interaction diagrams. This study shows that the BS simplified proposed gives good agreement with the exact method in general but uneconomic for the low ratios of steel ( $\rho_s$ <2%) and unsafe for high ratios at high level of axial load ( $P/P_0 > 0.4$ ). The proposed method may be easily extended to other shapes of cross sections.

Table 2. Comparison with Experimental Data, Hsu 1988

Experiment investigator	Column Specimen	Values from Tests K <sub>test</sub>	Values from Formula K <sub>K</sub>	Ratio K <sub>test</sub> / K <sub>K</sub>	%				
Tension Control									
	U-1	1,025	1,102	0,930	7				
Hsu	U-2	1,024	1,122	0,913	9				
пѕи	U-3	1,015	1,138	0,892	11				
	U-6	0,859	0,912	0,942	6				
	B-3	1,061	1,081	0,98	2				
Domomunthy	B-4	1,086	1,095	0,992	0				
Ramamurthy	B-7	1,032	1,123	0,919	8				
	B-8	1,03	1,151	0,895	10				
average									
	C	Compression Co	ontrol						
	S-1	1,198	1,092	1,097	10				
Hsu	S-2	1,118	1,084	1,031	3				
	U-4	1,047	1,148	0,912	9				
D	B-1	0,97	0,995	0,975	2				
Ramamurthy	B-6	1,063	1,151	0,923	8				
	BR-3	1,108	1,059	1,046	5				
	BR-4	1,173	1,059	1,107	11				
	CR-3	1,164	1,131	1,026	3				
Heimdahl and	CR-4	1,184	1,134	1,044	4				
Bianchini	ER-1	0,946	1,042	0,907	9				
	ER-2	1,09	1,055	1,033	3				
	Fr-1	1,054	1,124	0,938	6				
	Fr-2	1,13	1,154	0,979	2				
average 6%									

#### References

Beeby, A.W. (1978), "The design of sections flexure and axial load according to CP110". Cem. Conc. Assoc., Development Report 2.

Bresler, B. (1961), "Design Criteria for Reinforced Concrete Columns Under axial load and Biaxial Bending". ACI Jour. Vol. 32 (8), 481-490.

Brondum-Nielsen, T. (1982), "Ultimate Limit States of Cracked Arbitrary Concrete Sections Under Axial Load and Biaxial Bending". ACI Concrete Inst. Vol. 4(11), 51-55.

Brondum-Nielsen, T. (1983), "Ultimate Flexure Capacity of Partially or Fully pre-stressed Cracked Arbitrary Concrete Sections under Axial Load Combined with Biaxial Bending". ACI Concrete Inst. Vol. 5(11), 75-78.

Fafitis, A. (2004), "Analysis of Biaxial Bending of Reinforced Concrete Columns Using Green's Theorem". FASCE, Civil and Environmental university, Tempe AZ 85287-5306.

Furlong, R.W. (1961), "Ultimate Strength of square columns under axial load and biaxial bending". ACI Jour. Vol. 32 (9), 1129-1140

Hsu, C.T.T. (1988), "Analysis and Design of Square and Rectangular Columns by Equation of Failure Surface". ACI Struc. Jour. Tech. paper, No 85-S20, 167-179.

- Parme, A.L., Nieves J.M., Gouwens A. (1966), "Capacity of Reinforced Concrete Rectangular Members Subjected to Biaxial Bending". ACI Jour. Vol. 63(9), 911-923.
- Kawakami, M. T., Kagaya, M., Hirata, M. (1985), "Limit States of Cracking and Ultimate strength of Arbitrary RC Sections under Biaxial Loading", ACI Jour. Vol. 82(1), 203-212.
- Rodriguez, J.A, Dario Aristizabal-Ochoa, J. (1999), "Biaxial Interaction Diagrams for Short RC Columns of Any Cross section", Jour. Struc. Eng. Vol. 125(6), 672-683.
- Rafiq, M.Y., Southcombe C. (1995), "Genetic Algorithm in optimal Design and Detailing of RC Biaxial Columns Supported by Declarative Approach for Capacity Checking". Comp. Struc., V.69, 443-457.
- Yen, J. R. (1991), "Quasi-Newton Method for RC Column Analysis and Design", Jour. Struc. Eng. ASCE, Vol. 117(3), 657-666.
- Pannell, F.N., "Design Charts for Members Subjected to Biaxial Bending and Trust". London: Concrete Publishing, 1966.
- Gouwens, A.J. (1975), "Biaxial Bending Simplified". Symp. Reinforced Concrete Columns. ACI Publication SP-50, 233-261.
- Demagh, K. Chabil H. (2004), "Analysis of reinforced concrete columns subjected to biaxial loads", 7th inter. Conf. Concrete technology in developing countries, 5-8 Oct 04, Kuala Lumpur, Malaysia, proc. 7 ICCT M-13, 145-156.
- Demagh, K. Chabil, H. (2005) "Analysis of Reinforced Concrete Columns Subjected To biaxial Loads", Concrete For Transportation Infrastructure, Dundee, Scotland, UK, 5-7 July, proc. 433-440.
- BS8110. Structural use of concrete: part 1. London: British Standards Institutions 1985.
- CP110. Code Practice for Structures use of Concrete. London: British Standards Institutions 1972.
- R.P.A 99-V03, Règlement Parasismique Algérien, C.G.S. 2003, Alger, (Algerian code) in French.
- Eurocode 2, Design of Concrete Structures, General Rules and Rules for Buildings, BSI, 2004.

# **Behavior of Axially Loaded Concrete-Filled Steel Tubes**

Hisham S. Basha, Adnan C. Masri and Mohammad A. Sabra Beirut Arab University, Lebanon

#### Abstract

This paper presents an integrated experimental and analytical study on the behavior of short circular concrete filled steel tube columns concentrically loaded in compression. Twenty-four specimens were tested to investigate the post-yield strength of CFT columns and study the effect of steel wall thickness on the ultimate strength of composite columns. Confinement of the concrete core provided by the circular tube shape was also addressed. Depth to tube wall thickness ratios between 30<D/t<40 and length to tube depth ratio of 2<L/D<5 were investigated. The ratio between ultimate to yield strength was also investigated for different sections. Results from this study showed a good agreement between analytical and experimental results. The results also indicate that circular tubes offer substantial post-yield strength and stiffness as well as better ductility; and therefore considered a good candidate as a structural element in an earthquake resisting system. Ultimate strength results indicate that CFT columns possess higher strengths through the composite action represented by concrete confinement and steel interaction, than the algebraic summation of concrete and steel strength. A comparison between CFT and conventional circular reinforced concrete columns with spiral reinforcement shows that CFT offers higher capacity and reduction in area, an attribute strongly recommended in design of heavily loaded columns located at lower stories in high-rise buildings.

#### Introduction

There has been a growing interest in utilizing composite construction worldwide, in particular, high-rise buildings susceptible to extreme wind intensities or seismic forces. The use of concrete-filled tube (CFT) columns is increasingly entailed in common engineering practices; CFT possesses favorable characteristics in terms of strength, stiffness, and ductility; and therefore recommended to be used in high-rise buildings and mega structures (Fig. 1), where smaller column cross sections can support more stories than with conventional structural systems of steel reinforced concrete and steel columns. Another advantage of the system is the natural formwork provided by the steel tube.

This paper presents an experimental study on the behavior of the circular CFTs loaded in compression. The results suggest that all circular tubes exhibited significant strain-hardening behavior and offer substantial post-yield strength and stiffness as well as better ductility and therefore considered a good candidate as a structural element in an earthquake resisting system. Results indicate that CFT offers higher capacity and reduction in area an attribute strongly recommended in design of heavily loaded columns located at lower stories in high-rise buildings.



Fig. 1. CFT construction.

#### **Previous Research**

Tests to investigate the axial strength of CFT columns have been performed on a variety of cross-sectional shapes; the diameters of the steel tube to the wall thickness ratio (D/t) as well as the height to diameter ratio (L/D) were the primary parameters studied in previous researches as well as the bond effect (Roeder, 1999) and use of high-strength concrete in CFT (Varma, 2002).

A study (Knowles, 1996) on 12 circular and seven square columns with D/t ratios of 15, 22, and 59, and L/D ratios ranging from 2 to 21 was conducted. It was concluded that larger than expected capacity for composite columns with L/D<11 was due to the

increase of concrete strength resulting from triaxial confinement effects. However, this increase was noted for circular tubes only, not for square or rectangular shapes. Furthermore, CFT columns with large L/D ratios failed by column buckling before reaching the strains necessary to cause an increase in concrete core volume.

In another study (Schneider, 1998), a total of 14 test specimens were constructed and tested under concentric axial compression. Of these 14 CFT specimens, three were circular, five square cross-sections, and six were rectangular steel tube shapes. D/t ratios in the study ranged from 17 to 50.8, and L/D ratios ranged between 4 and 5. It was concluded that circular steel tubes offer much more post-yield axial ductility than the square or rectangular tube sections. The confinement effect was not significant until the axial load reached almost 90% of the column yield strength.

## **Objectives**

Results from previous research demonstrated that slender columns did not exhibit the beneficial effects of composite behavior, in which the concrete strength was greater than that of the cylinder strength due to core confinement, which make it suitable for columns at lower stories in high-rise buildings. Short columns, however, exhibited greater than predicted capacity, generally associated with the higher concrete strength due to the confinement offered by the steel tube. It was concluded that concrete-steel interaction was not fully understood by the common practice. The focus of this research is to experimentally investigate the effect of the circular steel tube shape and the wall thickness on the yield strength of the CFT and the confinement of the concrete core. Another objective is to examine the factors that influence the post yield strength of CFT. Analytical modeling of CFT is also an important issue in this research, however due to space limitation analytical results are addressed in separate publication; nevertheless a brief discussion on analytical results was presented in this paper. Also, to investigate the advantages of using CFT columns over conventional ordinary and spiral reinforced concrete columns in terms of strength and cross-sectional dimensions. This was carried through an integrated experimental and analytical program.

## **Experimental Program**

The compressive strength of concrete calculated from tests of concrete cylinders is  $200 \text{ kg/cm}^2$  and the yield stress of the steel tube is  $3170 \text{ kg/cm}^2$ . A total of 24 specimens (12x2; i.e., two specimens of each of the twelve different sizes) of different D/t and L/D ratios were tested. Three steel tube diameters of type A, B, and C, were selected for the experimental analysis as shown in Table 1.

Table 1. Experimental Test Specimens

Type	Diameter (mm)	D/t	L/D
A	145	36.25	Variable
В	115	46	Variable
C	90	36	Variable

The specimens were tested using a compressive testing machine of 1000 KN maximum load cell capacity. Column loads were applied at a very slow rate in order to carefully observe any local buckling behavior of the CFT specimens, if any.

For type [A] the ultimate load capacity of the specimen was greater than the axial capacity of the loading machine (1000 KN). From the data acquisition readings the specimen type [A] has reached only its yield capacity. Very smooth corrugations are observed on the external surface of the steel tube. These corrugations are observed on the whole surface of the specimen. For type [B], the yield and the ultimate load capacity of the specimen were reached. Figure 2 shows the deformations on the external surface of the steel tube at ultimate load. Tests were stopped just as the axial machine readings started to decline.

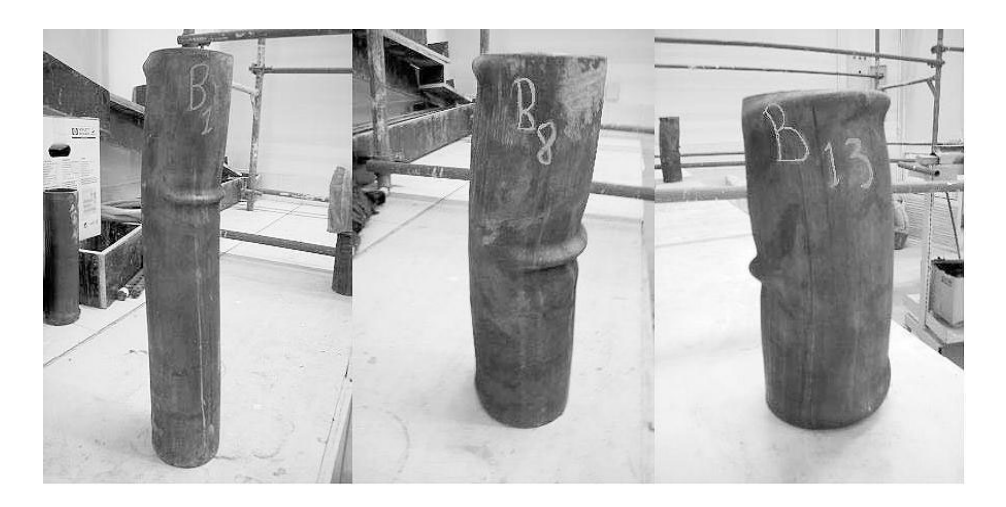


Fig.2. CFT Type [B] Tested Specimens (Diameter = 11.5 cm).

Figure 3 shows the load displacement relation for test specimens of type [B], as well as the normalized load/displacement curves of the specimens. In each graph, the load capacity of the concrete core alone and the total load capacity of the concrete core and the steel tube are shown.

Tested specimens of type [C] are shown in Fig. 4. The trend of deformation at failure was almost identical to that of CFT-type [B], in spite of the fact that the two sets have different width-to-thickness ratio as well as length-to-diameter ratio. Figure 5 shows the load displacement relation for test specimens of type [C], as well as the normalized Load/displacement curves of the specimens.

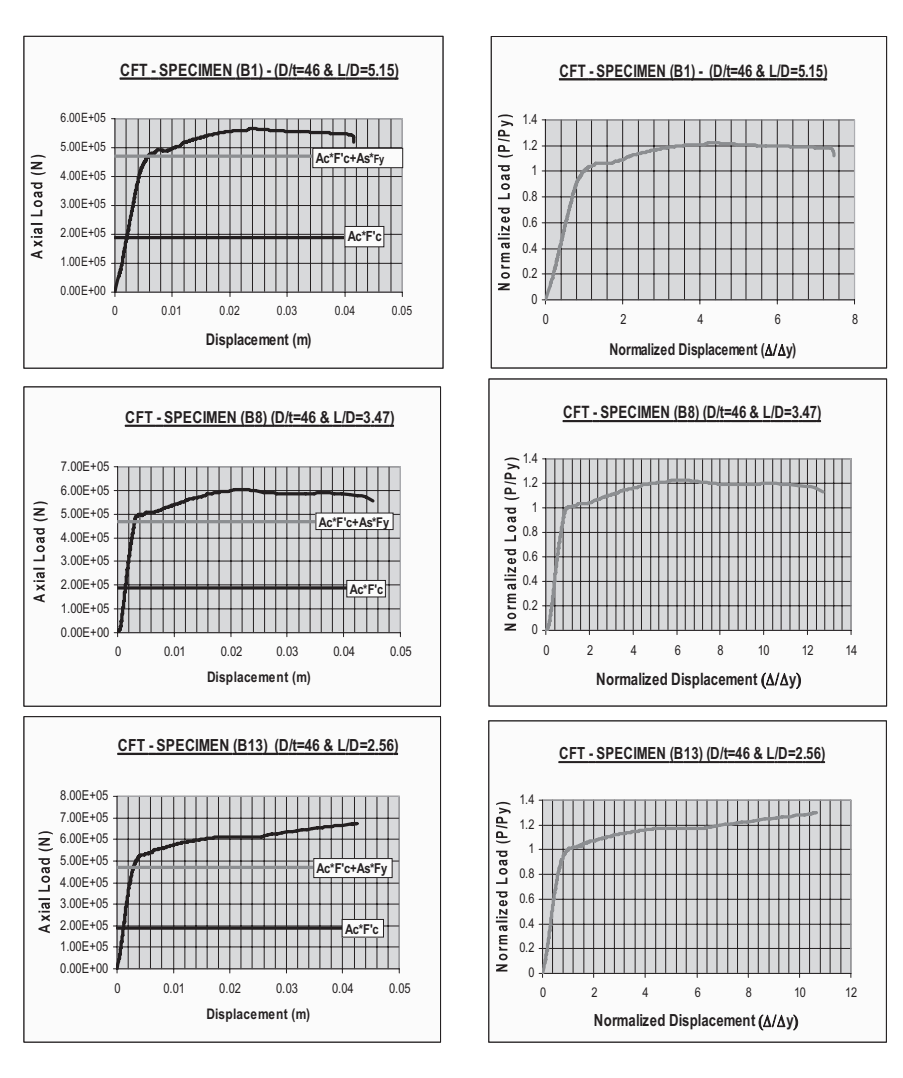


Fig.3. CFT-specimens type [B] - load displacement relationship.

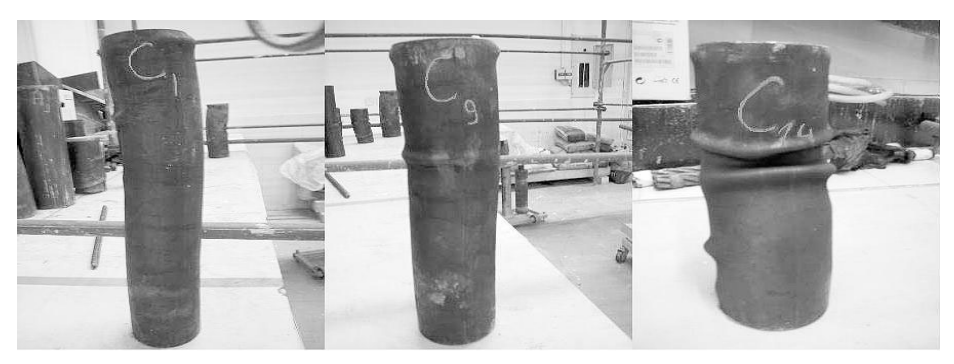


Fig.4. CFT type [C] tested specimens (diameter = 9.0 cm).

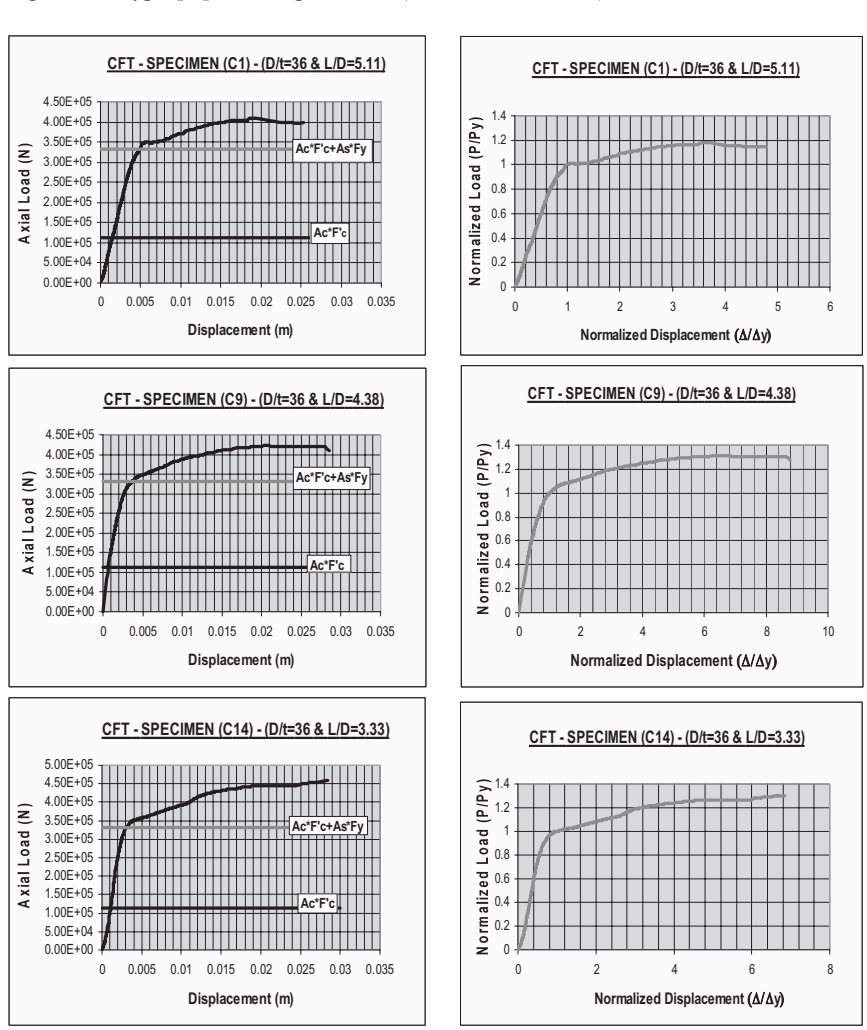


Fig.5. CFT-specimens type [C] - load displacement relationship.

As was done for specimens [B] the two horizontal lines on the plots are drawn showing the load capacity of the concrete core alone and the total load capacity of the concrete core and the steel tube. It is well noticed that the ultimate load capacities of the composite CFT column for all the specimens of either set [B] or [C] are greater than the total loads of both the steel tube and the concrete core. The reserve post-yield strength and the extensive ductility of the specimens before the ultimate load capacity is reached are extremely beneficial in high-rise buildings and those particularly subjected to seismic forces.

The structural behavior of CFT is considerably affected by the difference between the Poisson's ratios of the steel tube and concrete. In the initial stage of loading, the Poisson's ratio for the concrete is lower than that of the steel. Thus, the steel tube has no confining effect on the concrete. As longitudinal strain increases, the lateral expansion of concrete gradually becomes greater than expansion of steel tube. At this stage, the concrete becomes tri-axially stressed and steel tube bi-axially stressed. The steel tube under a bi-axial state of stress cannot sustain the normal yield stress, causing a transfer of load from the steel tube to the concrete. In the first stage of loading, the steel tube sustains most of the load until it yields. At this point, there is a load transfer from the steel tube to the concrete. The steel tube exhibits a gradual decrease in load sharing until the concrete reaches its maximum compressive strength. After this stage of loading there is a redistribution of load from concrete to the steel tube. The steel exhibits a hardening behavior with almost the same slope as in the uniaxial stress-strain hardening relationship.

It has been observed form Figures 3 and 5 that the ultimate axial capacity  $(P_u)$  of CFT columns is larger than the sum of uncoupled steel and concrete failure loads  $(P_y)$ , ranging between 1.2 and 1.3. The increase in the failure load is caused by the confining effect of steel tube on the concrete. This 20% to 30% increase in ultimate strength is very beneficial as discussed earlier. Test results from this study indicate that larger ratios of (D/t) from 36 to 46 results in no significant change in post yield strength but rather more ductile behavior. On the other hand, for specimens of same (D/t) ratios and different (L/D) ratios, results indicate that smaller (L/D) ratio results in higher post-yield strength and better ductility.

For the two types of specimens [B] and [C] the mode of failure of the concrete filled specimens resembles to some extent the mode of failure of the unfilled specimens having the similar properties of L/D and D/t ratios.

The manner in which CFT is loaded affects confinement, i.e., loading the concrete alone tends to induce confinement at lower load levels than loading both materials simultaneously. In contrast, loading steel alone, as may be done if a girder frames into a CFT with a simple connection, causes localized friction in the connection region, but confinement is not induced until sufficient load is shed to the concrete core.

## **Strength Provisions for Circular CFT-Columns**

Task Group 20 of the Structural Stability Research Council (SSRC, 1979) proposed guidelines for the design of composite members, which were adopted by the LRFD

specification (AISC-LRFD, 1993). This specification provides design guidelines for elements in which the area of the steel tube comprised at least 4% of the total composite cross-sectional area. The axial strength of a composite element is computed similar to that of a structural steel column, except the material yield strength and stiffness are modified to account for the steel and concrete components in the composite column.

Table 2 shows the code calculated critical load for the test specimens and recorded values of yield and ultimate loads. A comparison between the code critical load and the recorded yield load of the test specimens shows that the code is always conservative.

For type [A] specimens, only the code critical load is calculated. The ultimate compressive load recorded for both types [B] and [C] is about 35% greater than the yield load. Table 2 also shows a comparison between the yield and ultimate deformations of the test specimens. For test specimens type [B], and [C] the ultimate load deformation is in no case less than 4 times the yield load deformation. For test specimens of Type [A] no values are recorded. The ultimate deformation to yield deformation for the test specimens ranged between 4 and 9; recall that previous researches have shown that this range can go up as much as 10.

Table 2. Code and Experimental Test Results

Tube type	Fcr (N/m²)	P <sub>cr</sub> (N)	P <sub>y</sub> (N)	P <sub>u</sub> (N)	P <sub>y</sub> /P <sub>cr</sub>	P <sub>u</sub> /P <sub>cr</sub>	Δ <sub>y</sub> (mm)	∆ <sub>u</sub> (mm)	$\Delta_u/\Delta_y$
A1	4.53.E+08	8.03.E+05							
A4	4.54.E+08	8.05.E+05							
A9	4.55.E+08	8.07.E+05	Va	lues not Red	corded		Valu	es not Rec	orded
A11	4.57.E+08	8.10.E+05							
В9	4.96.E+08	4.38.E+05	4.70E+05	5.90E+05	1.07	1.35	0.00276	0.0234	8.5
B1	4.91.E+08	4.34.E+05	4.63E+05	5.66E+05	1.07	1.3	0.00557	0.0244	4.4
B8	4.96.E+08	4.38.E+05	4.92E+05	6.03E+05	1.12	1.38	0.00355	0.023	6.5
B13	4.98.E+08	4.40.E+05	5.21E+05	5.21E+05 6.12E+05 1.18 1.39				0.022	5.5
C6	4.50.E+08	3.09.E+05	3.23E+05	4.15E+05	1.04	1.34	0.00276	0.0213	7.7
C1	4.50.E+08	3.09.E+05	3.47E+05	4.09E+05	1.12	1.32	0.0052	0.0207	4
C9	4.52.E+08	3.10.E+05	3.22E+05	4.21E+05	1.04	1.36	0.00325	0.0231	7.1
C14	4.54.E+08	3.12.E+05	3.52E+05	4.45E+05	1.13	1.43	0.00415	0.0204	4.9

## **Analytical Verification**

Two dimensional nonlinear finite-element models were developed to study the axial load behavior of the circular CFTs. Analytical models simulating test specimens were developed using ADINA software (ADINA, 2000). The concrete core and the steel tube are modeled using 4-node 2-D solid axisymmetrical elements. The interface between both the steel tube and concrete core is modeled by defining contact surfaces (2D- axisymmetrical contact surfaces). A proper constitutive model describing the concrete behavior under confining condition is a challenging task for developing an accurate finite element model. The developed material model for finite element

analysis of concrete structure using "ADINA" software can be employed with the 2-D solid, as adopted in this study, and 3-D solid elements. The analytical material model developed is not discussed in this paper due to space limitation; a separate publication will be devoted for that part.

The finite element model was verified by simulating the experimental tests of circular CFT columns of type B and C tested under concentric axial compression. Figure 6 shows the load-displacement relation for both the experimental test models B8 and C6 and the analytical simulating models. From the figures we noticed a close matching of the load displacement curves for both the experimental tests and the analytical ones. Based on the outcome the finite element model is justified.

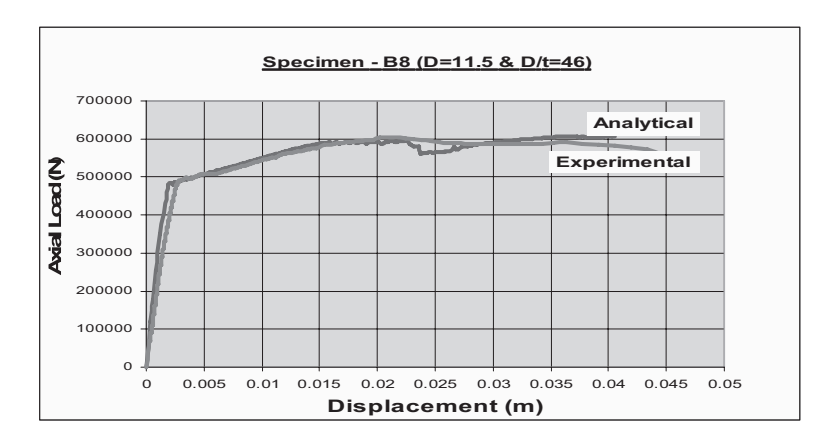


Fig. 6. Finite element verification with experimental test of CFT (B8) & (C6).

## Comparison between Spiral R/C and CFT Columns

The code provisions (ACI 318-99) for design of spirally reinforced concrete columns is presented in this section. The capacities of conventional reinforced concrete columns of certain diameter are compared to the capacity of CFT columns of the similar diameters. It should be noted that when comparing CFT columns to conventional reinforced concrete circular columns the same percentage of steel is used in both columns of same diameters, so as to reflect cost. The ACI code states that the minimum volumetric ratio of spirals to be used in designing spirally reinforced columns,  $\rho_s$ , is given by Eq.(1):

$$\rho_{s} \ge 0.45 \left[ \frac{A_{g}}{A_{core}} - 1 \right] \cdot \frac{f_{c}'}{f_{y}}$$
(1)

This minimum ratio is used to ensure that after crushing of concrete shell the column can sustain additional load resulting from confining effect of concrete core, where:

 $A_g$  = gross area of concrete,

 $A_{core}$  = area confined by the spiral reinforcement,

 $f'_c$  = unconfined concrete strength,

 $f_y$  = yield strength of steel.

The confined concrete strength is given by:

$$[f'_c]_{conf} = f'_c + 4.1 f_l$$
 (2)

Where:  $f_l$  = splitting strength of concrete that may be computed from:

$$f_l = (1/2) \rho_s f_v$$
 (3)

The ultimate load capacity of spirally reinforced concrete circular that could be attained in this case due to confinement is computed from:

$$P_{ou} = 0.85 [f'_c]_{conf} (A_{core} - A_{st}) + A_{st} f_v$$
(4)

The following Table 3 shows a comparison between different column diameters. CFT columns having D/t ratio of 70 (maximum) is used in the comparison and a minimum volumetric ratio of spirals is used for the reinforced concrete columns. The use of minimum volumetric ratio of spirals is justified, as it requires less workmanship complexity and the use of maximum D/t ratio is justified due to the savings in material attained for higher D/t ratios.

Table 3. Comparison of CFT and Spirally Reinforced Columns

D(mm)	t(mm)	Pu (N)	ρ% <u>(</u> spiral)	$f_l$	$(f_c)_{conf}$	$(f_c)_{conf}/f_c$	$\rho$ %( $A_s$ )	$P_{ou}$	$P_u/P_{ou}$
400	5.7	7.29E+06	2.06	3272934	4.4E+07	1.43	4.01	4.64E+06	1.57
600	8.6	1.57E+07	1.24	1964124	3.9E+07	1.26	2.71	9.50E+06	1.65
800	11.4	2.77E+07	0.88	1401806	3.7E+07	1.19	2.05	1.60E+07	1.73
1000	14.3	4.33E+07	0.69	1089516	3.5E+07	1.14	1.65	2.42E+07	1.79
1200	17.1	6.21E+07	0.56	890925	3.5E+07	1.12	1.38	3.40E+07	1.83

The plot (Fig. 7) shows comparison between the capacities of CFT and spirally reinforced circular columns of the same diameter.

It is clear that the use of CFT column is more practical and requires less cross sectional area about 60% of the area of conventional spirally reinforced concrete columns. It is also noted that for larger column diameters the required cross sectional area is less, since the capacity ratio  $P_{u'}P_{ou}$  is higher for same diameters.

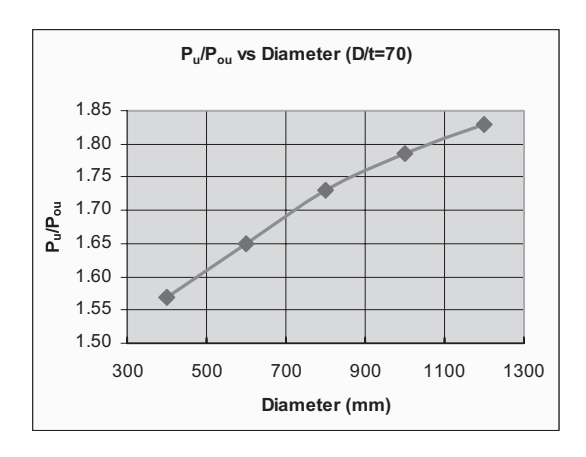


Fig. 7. Ratio of CFT to spirally reinforced column strength vs diameter.

#### **Conclusions**

Major findings of this study are summarized by the following four points:

- Post-Yield load-deformation relationship in circular CFT columns is linear and increases at a constant rate.
- The ultimate axial capacity  $P_u$  of CFT columns is larger than the sum of uncoupled steel and concrete failure loads  $P_y$ , ranging between 1.2 and 1.3. The increase in failure load is caused by confining effect of steel tube on the concrete.
- Results indicate that larger ratios of (D/t) from 36 to 46 results in no significant change in post-yield strength but rather more ductile behavior. On the other hand, for specimens of same (D/t) ratios and different (L/D) ratios, results indicate that smaller (L/D) ratio results in higher post yield strength and better ductility.
- When CFT columns are compared to conventional spirally reinforced concrete columns, of the same diameter and amount of material used, the results show that CFT columns carries 50% to 80% more load for columns of 400mm to 1200mm. The load capacity ratio of CFT columns to spirally reinforced concrete columns "Pu/Pou" is higher for larger column diameters.

In summary, results from this study indicate that all circular tubes exhibited significant strain-hardening behavior, which offers substantial post-yield strength and stiffness as well as better ductility and therefore considered a good candidate as a structural element in an earthquake resisting system. Results indicate that CFT offers higher capacity and reduction in area; an attribute strongly recommended in design of heavily loaded columns located at lower stories in high-rise buildings.

#### References

- ADINA (2000), "Automatic Dynamic Incremental Nonlinear Analysis", Theory and Modeling Guide, Report ARD 00-1, Watertown, MA, USA.
- American Concrete Institute -ACI 318-99 (1999), "Building Code Requirements for Structural Concrete", Farmington Hills, Michigan.
- American Institute of Steel Construction, AISC (1999), "Manual of Steel Construction, Load and Resistance Factor Design (LRFD)", Specifications for Structural Steel Buildings, Chicago.
- Knowles, R.B. and Park, R. (1996), "Strength of Concrete Filled Steel Tubular Columns", Journal of Structural Engineering, ASCE, American Society of Civil Engineering, Vol. 95(ST12), 2565-2597.
- Roeder, C.W., Cameron. B., and Brown, C. (1999), "Composite Action in Concrete Filled Tubes", Journal of Structural Engineering, ASCE, American Society of Civil Engineering, Vol. 125(5), 477-484.
- Schneider, S.P. (1998), "Axially Loaded Concrete-Filled Steel Tubes", Journal of Structural Engineering, ASCE, American Society of Civil Engineering, Vol. 124(10), 1998-1138.
- Varma, A.H., Ricles, J.M., Sause, R., and Lu, L., (2002), "Experimental Behavior of High Strength Square Concrete-Filled Steel Tube Beam-Columns", Journal of Structural Engineering, ASCE, American Society of Civil Engineering, Vol. 128(3), 309-318.

# Achieving a Longer Service Life with Durability Modelling

Robert David Hossell, MICT Grace Construction Products, Dubai, UAE

#### **Abstract**

To obtain longer service lives, today's owners and designers are utilising additional corrosion protection measures. However, the science of corrosion protection can be very complex and is often confusing. Therefore it is necessary to use a modelling process that can make sense of it all. The durability modelling process (DMP) provides a uniform, technical-based evaluation method to compare available protection products and systems.

A common corrosion prevention measure in the Arabian Gulf is the addition of calcium nitrite-based corrosion inhibitors. The DMP can now be used to provide designers with clear requirements for calcium nitrite addition to protect any structure in any chloride environment to the requested design life. In fact, the benefit deriving from the presence of calcium nitrite either as a single corrosion protection system or in conjunction with other systems can now be quantified in terms of extended service life (calcium nitrite functions by increasing the critical chloride concentration for corrosion initiation).

The DMP uses engineering, scientific, and business principles to evaluate the available corrosion protection products. It is divided into two parts consisting of corrosion protection and economic performances. Modelling each part within a single process provides both an engineering and business solution to designing for chloride exposure durability.

The whole process accommodates the exposure condition and all other physical and economic parameters particular to a given concrete element within a structure. Consequently, it has been frequently applied to the Middle East conditions, where imported design codes and standards have found to be inadequate.

## Introduction

Concrete in marine and saline environments is subjected to severe chloride intrusion, which results in corrosion of the embedded steel. One means of combating chloride-induced corrosion is to decrease the concrete permeability. This is recognised by the American Concrete Institute (ACI) in the Building Code (1) and in its guide to offshore structures (2). These documents call for a maximum water-to-cement ratio (w/c) of 0.4 and for a minimum of 65 mm cover in a marine environment. The use of pozzolans further reduces the concrete permeability. If no other protection methods at the reinforcing steel level are used, corrosion will occur when the chloride reaches a certain concentration at the steel surface. Calcium nitrite corrosion inhibitor is widely used to remedy this situation; it functions by increasing the critical chloride concentration for corrosion initiation. Epoxy-coated rebars have also been used to this end. Their performance depends on the integrity of the coating being maintained during transport, fabrication, and concrete placement.

Very often, no one corrosion protection system is sufficient in very severe environments to achieve a service life of say 30-60 years in the Middle East. In this case, a combination systems approach is sometimes required such as the use of pozzolans in the presence of corrosion inhibitors.

The ingress of chloride into the concrete is of particular concern because chloride ions are aggressive and promote corrosion of the reinforcing steel. When the chloride concentration in the vicinity of the steel reinforcing reaches a critical value, corrosion commences and will subsequently increase in rate as the chloride concentration increases. A concentration of approximately 0.9 kg/m<sup>3</sup> is sufficient to initiate corrosion and major damage can be expected (3-5).

# **Durability Modelling Process (DMP)**

In this paper we present a methodology that compares the life-cycle cost of several corrosion protection options. The key performance features are predicting future chloride profiles, the effects of the corrosion protection systems on chloride threshold levels and corrosion rates, and the estimated times of repairs. A Net Present Value (NPV) cost analysis is then utilized to provide the engineer with an estimate of the costs associated with various protection systems.



DMP uses engineering, scientific, and business principles to evaluate the available corrosion protection products. The modeling process is divided into two sections consisting of corrosion protection and economic performances. Modeling both sections

within a single process provides both an engineering and business solution to designing for chloride exposure durability.

## **Corrosion Protection Performance**

The performance of corrosion protection can be measured by categorising the proposed corrosion protection systems into three distinct and inclusive engineering performance criteria. Figure 1 depicts these three criteria; the product/system effects upon concrete permeability, impact on corrosion threshold, and finally the effect on corrosion rate after initiation.

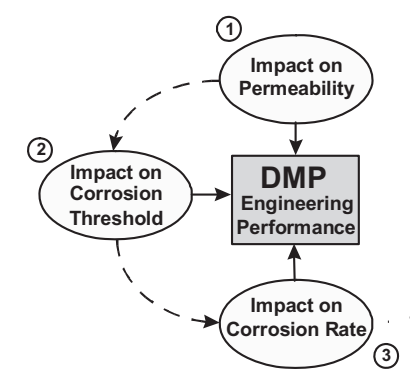


Fig. 1. Example of marine quaywall.

The DMP will be applied to a theoretical quaywall to demonstrate the application of this analysis program. This exemplary location will be arbitrarily chosen to be somewhere in the lower Gulf and will require a thirty-year service life. The average 365 day/year and 24 hours/day temperature for this location from sea temperature records is 27°C. The concrete will be exposed to severe seawater splashing and tidal fluctuations. The concrete will be modelled with a base concrete design consisting of a 0.40 water-to-cement ratio, a 75mm reinforcing cover, and a 500mm thick section. By following the DMP described below, one can determine the lowest or several low life cycle cost corrosion protection alternatives to specify on this exemplary marine project.

# **Concrete Permeability**

The exact rate of chloride diffusion through concrete cannot be calculated due to the heterogeneous nature of concrete and the differences between concreting materials. However, an approximate value can be obtained with sufficient accuracy for estimating the ingress of chloride into concrete structures in the field as a function of exposure conditions.

The diffusion of chlorides through a porous medium follows Fick's second law of diffusion (3, 6-21). This correlation can be used to calculate an effective diffusion coefficient,  $D_{\mbox{eff}}$ , if the chloride concentration at any time is known as a function of depth. A more rigorous approach would determine chloride binding and calculate the

diffusion coefficient independent of chloride binding (22). To minimize effects of sorption, longer test periods are also recommended (23). However, work in our lab (24-26) and by others (16-20) showed that the effective diffusion coefficient can be used to accurately estimate future chloride profiles, when it is determined from data on chloride concentration at various depths, measured after one to two years of exposure, since this exposure allows opportunity for both sorption and diffusion processes to occur.

While sampling, field concrete gives the most reliable information; ponding tests are used to obtain chloride profiles of various types of concrete. The concrete type should be representative of field specified concrete and should be run in solutions of 3 to 15% Cl-, according to AASHTO T259 (27). The chloride concentration at various depths is obtained by analyzing crushed samples using ASTM C 1152 (28). Comparison of treated concretes to control specimens yields the percent reduction of the diffusion coefficient values of treated concretes.

Diffusion through the concrete cover region is predicted using the solution to Fick's second law:

$$C(x,t)$$
  $C_{x,t} = C_o \left[ 1 - Error Function \left[ \frac{x}{2\sqrt{t} D_e} \right] \right]$ 

C(x,t) = Chloride content in kg/m<sup>3</sup> at depth x at time t.

 $C_o$  = Surface chloride concentration in kg/m<sup>3</sup>.

x = Depth into concrete. Usually the design concrete cover.

t = Time in years.

D<sub>e</sub> = Effective diffusion coefficient.

Error Function = Mathematical standard error function.

If chlorides are building up on the concrete surface (changing  $C_{\rm o}$ ), as is the case in airborne chloride exposure, the estimation of chloride ingress becomes somewhat more complex but can still be handled by the DMP. The most important variable is the effective diffusion coefficient as it reflects the concrete permeability. If a proposed corrosion protection system claims to reduce chloride ingress, test results should provide a reduction factor to the base diffusion coefficient.

From the equation shown above, the chloride content for every year up to the desired service life of the structure can be estimated and a plot of the results can be made. A sample chloride profile is provided in Fig. 2. The horizontal axis reflects the time in years and the vertical axis represents the estimated chloride content at a given 75mm depth into concrete. The top curve represents a base concrete performance and the lower curve represents the effect of reducing the effective diffusion coefficient by 37%. This would approximate a 0.40 W/C concrete with a pozzolan to achieve a Rapid Chloride Permeability Value of 1000 Coulombs (29).

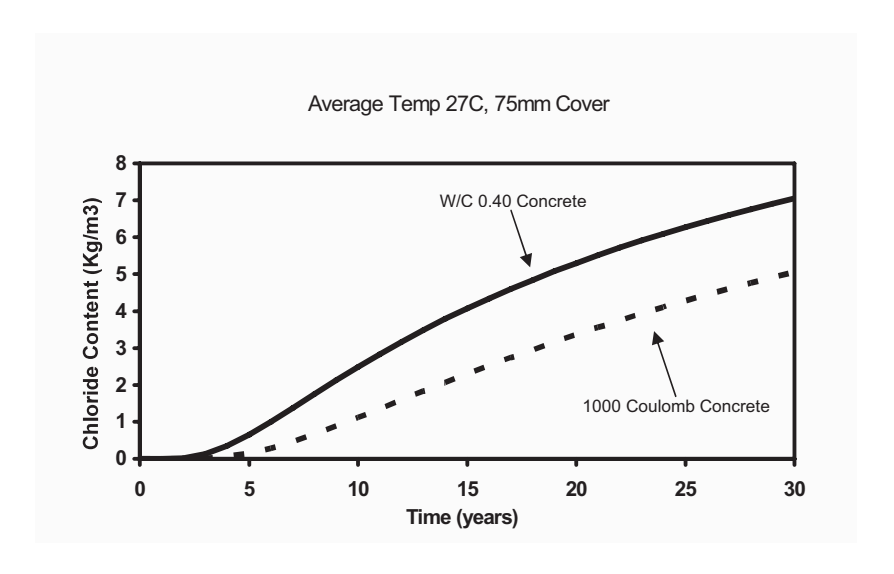


Fig. 2. Estimated Quaywall Diffusion Curves.

Corrosion protection systems with surface barrier mechanisms will also reduce chloride ingress. These systems may be surface applied sealers or membranes. This is currently dealt with by shifting the estimated chloride profiles to the right. The number of years that one shifts the curve should represent the effective life of the individual surface treatment. Future modeling programs should include the ability to represent the reduction in surface treatment effectiveness over time.

# **Impact on Corrosion Threshold**

The high alkalinity of reinforced concrete provides a chloride ion corrosion threshold for black steel of approximately  $0.9~{\rm Kg/m^3}$  ( $\sim 0.2\%$  by weight of cement). This means that it will take a concentration of  $0.9~{\rm Kg}$  of chloride ion per cubic metre, at the reinforcing steel, to initiate corrosion activity. Some corrosion protection products/systems can significantly elevate this threshold. Calcium nitrite corrosion inhibitor when added to concrete will protect reinforcing steel from corrosion initiation to various levels of chloride ion content depending on the volume of admixture added. The mechanism by which calcium nitrite prevents corrosion of reinforcing steel is exhaustively described (30-32). In summary, the use of calcium nitrite results in the creation and maintenance of a stronger, flawless and stable passive film on steel embedded in concrete, even in the presence of chloride levels much higher than the critical chloride concentration for corrosion onset for conventional concrete. In the Arabian Gulf, calcium nitrite has been widely used for more than 15 years on a large scale in more than 600 structures (33).

Table 1 provides the established corrosion thresholds for calcium nitrite admixture (30% calcium nitrite solids) determined through extensive laboratory and field testing (34).

Table 1. Calcium Nitrite Corrosion Thresholds

Dosage (30% Solids) (Litres/m³)	Corrosion Threshold (Kg/m³)
0	0.9
10	3.6
15	5.9
20	7.7
25	8.9

Corrosion thresholds can be overlaid on the estimated chloride profiles by placing a horizontal line representing the chloride content of the corrosion threshold. The intersection of the chloride profile curve and horizontal corrosion threshold line indicates the estimated corrosion initiation point. The relationship to the x-axis represents the time to corrosion initiation. Figure 3 depicts the overlay of corrosion thresholds on to the sample chloride profile previously shown in Fig. 2.

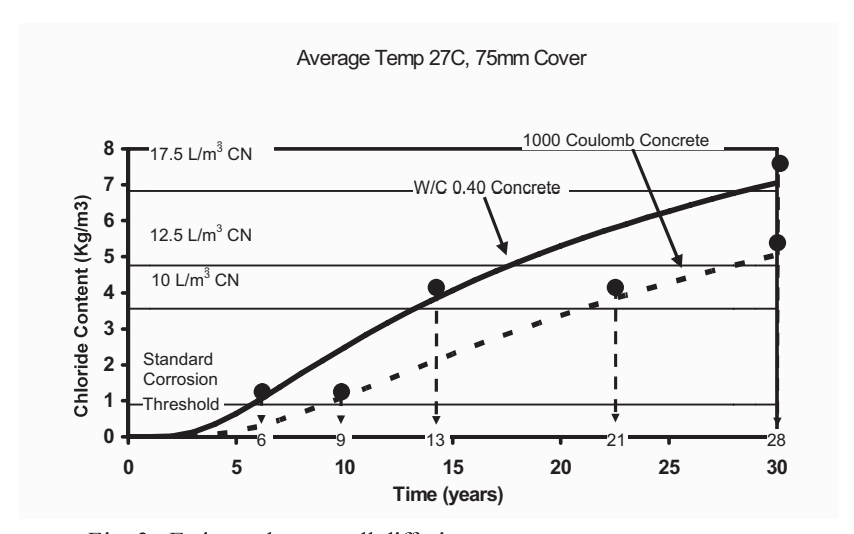


Fig. 3. Estimated quaywall diffusion curves.

## **Impact on Corrosion Rate**

The corrosion rate after corrosion initiation affects the time it takes from initiation to time-to-repair (T-T-R). This is called the corrosion propagation time. The lower the corrosion rate, the longer the time until required repairs. Some corrosion protection systems reduce the corrosion rate. This criterion will require significant long-term test results (5 to 10 years). In 1994, the Strategic Highway Research Program (SHRP)

found that the typical time on bridge decks from corrosion initiation to corrosion damage averages 2.5 to 5 years (6). If a corrosion protection system claims a reduced corrosion rate, the value of this criterion should be expressed as a percent reduction to a base corrosion rate or in estimated years. In the absence of other information, the typical time between corrosion initiation and corrosion damage for black bars in normal concrete has been assumed to be 3 years for this example.

The propagation time in years used by a product/system reducing corrosion rate can be expressed by the following equation:

Propagation Time = 3.0 years x 
$$\frac{1}{(1 - \%Reduction)}$$

Epoxy-coated reinforcing (FBECR) is a corrosion protection system that in principle reduces the corrosion rate over a given length of rebar. Coated reinforcing steel protection mechanism is by the reduction to corrosion rate alone. The likely damages to the coating leaves unprotected steel areas that will corrode similar to steel areas on uncoated rebars. Calcium nitrite has been shown to be fully compatible with FBECR, providing protection at both flawed edges and flaws which are unavoidable in actual service conditions (35-36). The corrosion protection benefits of epoxy-coated reinforcing could be integrated into the DMP by applying a corrosion rate reduction factor, on the basis that the coating has not debonded from the bar when the chlorides arrive (37).

Sealers and membranes may also reduce the corrosion rate if the concrete is capable of significant drying. The moisture content within the concrete must be lower than 70% relative humidity. This low humidity within concrete is difficult to achieve in the Gulf Environment.

It should be noted here how, in addition to increasing the threshold value for corrosion initiation, several laboratory tests show that calcium nitrite reduces corrosion rates after corrosion initiation (38). Therefore, such a combined effect should lead to significantly improved times to repair in reinforced concrete structures subjected to chlorides.

# **Impact on Cracked Concrete**

The corrosion performance in cracked concrete is an important criterion. Concrete will crack, so there is a value if products/systems can extend the time to repair. No corrosion protection system used in concrete alone will stop corrosion at cracks, especially if these cracks go directly to the reinforcing steel. Some systems will significantly reduce the corrosion activity in cracked concrete. Calcium nitrite (39), stainless steel, epoxy-coated bars, membranes, and other corrosion inhibitors have demonstrated significant improvement in corrosion protection in cracks. If cracks are numerous or exceed the ACI 224 (40) guidelines pertaining to crack size, the cracks should be repaired regardless of corrosion protection system. Cracked concrete is

outside the capabilities of this DMP, however, a review of a corrosion protection system performance in cracked concrete is prudent.

# Time-To-Repair (T-T-R)

It is possible to estimate the total time it takes with any concrete and corrosion protection system(s) for a structure exposed to aggressive chlorides to reach a point of repair (T-T-R). The process follows:

- 1. Determine the estimated chloride profiles.
- 2. Overlay the corrosion threshold(s).
- 3. Determine the intersection point (corrosion initiation time).
- 4. Add the propagation time (from corrosion rate effects).

Some products/systems will meet the desired service life without major repairs. Other products/systems will not meet the desired service life without repair and therefore require life cycle cost analysis to address the cost associated with those needing repairs.

For the quaywall case, the time to corrosion initiation and time-to-repair (T-T-R) are provided in Table 2. This table compares the performance of the base 0.40 W/C concrete, a 1000 Coulomb concrete and calcium nitrite at various dosages. Individual manufacturers may have long-term research data, which could require the above assumptions to be modified. These assumptions have been selected for example purposes only.

Table 2. Estimated Time-To-Repair Performance Summary

<b>Protection Systems</b>	Initiation Time (Years)	Propag. Time (Years)	Time To Repair Repair
Base Case	6	3	9
1000 Coulomb Concrete	9	3	12
10L/m³ Calcium Nitrite	13	3	16
17.5L/m <sup>3</sup> Calcium Nitrite	28	3	31
$1000 \text{ C} + 10 \text{L/m}^3 \text{ CN}$	21	3	24
$1000 \text{ C} + 12.5 \text{L/m}^3 \text{ CN}$	28	3	31

## **Economic Performance**

The second half of the material selection modeling process is based on economic performance. Many past evaluations pertaining to corrosion protection has been focused solely on the first cost of products/systems. Two primary reasons for this are:

1. Contractor pressure for low in-place costs;

2. Inability of some manufacturers to quantify time to corrosion initiation.

Comparing first construction costs has nothing to do with long-term corrosion protection performance. This method of evaluation may result in lower cost construction but may lead to high future costs for maintenance and repairs. Today, many of the owners, designers, and contractors are moving towards the use of life cycle cost analysis (LCCA) to determine the lowest net present value (NPV) of the corrosion protection investment. This would incorporate the first cost and all subsequent costs associated with obtaining the desired service life.

There are many other tangible and intangible costs associated with repair and such lost revenue and the poor image the client suffers. Sometime the "other" costs are more important than first and repair costs.

# **Life Cycle Cost Analysis (LCCA)**

The DMP will apply a simple LCCA to the various corrosion protection investment alternatives to reach a desired service life. The LCCA incorporates the first cost and all future repair cost brought back to present cost.

The LCCA equation is:

Repeat as Necessary

The future cost of repairs will be influenced by the inflation rate. The present value of the future cost considers both the inflation rate and the return on capital in invested funds. This return on capital is usually higher than the inflation rate, which leads to a discount rate that is positive. Positive discount rates result in the present value of future repair costs which are less than current repair costs. In Fig. 4 this relationship between the increasing future cost due to inflation and the decreasing cost due to a positive discount rate is demonstrated. The example uses a 4% inflation rate and a 4% positive discount rate.

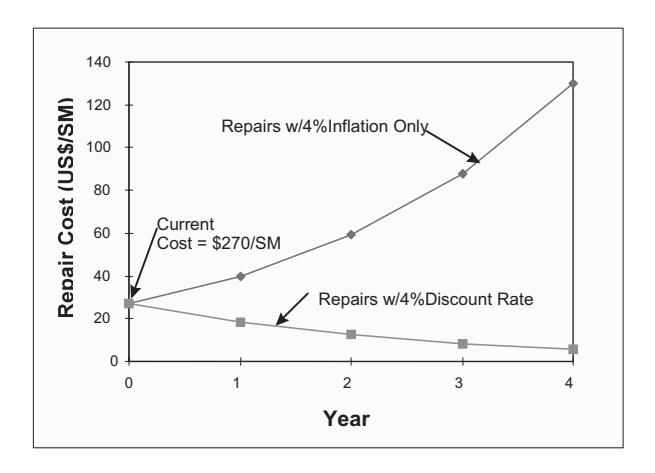


Fig. 4. Example of future cost of repairs.

The economic results of the example quaywall will incorporate the modeling performance data found in Table 2. Then a life cycle cost analysis is conducted to determine the lowest cost solution to the 30-year service life. The life cycle cost analysis will sum the first cost and the net present value of the anticipated future repairs. The first cost will be determined by applying an estimated constructed cost to a variety of corrosion protection systems to the quaywall. The various corrosion protection systems compared are not inclusive of all available alternatives; however, all other alternatives must be able to be applied to the DMP analysis.

The net present value of the future repairs were determined by taking the estimated Time-To-Repair (T-T-R) for the various corrosion protection systems and comparing this time to the projects required 30 year service life. If the T-T-R is less than the required service life, a repair cycle is applied to this system. For the use of this example analysis we applied repairs over 10% of the element surface and used an average patching repair cost of \$200 per square metre. Of course, these costs will vary depending on project location and size. A discount rate of 4% was used which represents an 8% return on capital and a 4% inflation rate. If repairs on a corrosion protection system occurred well before the desired service life, additional repairs would be likely. For the sample economic modelling, we applied additional repairs on a 5-year cycle until the desired service life was met.

The results of the economic analysis are summarized in Table 3 below. The total cost is the most important value to compare, since this represents the estimated owners' total cost for each protection system in current dollar rates.

Figure 5 provides the total cost for each system and is plotted from lowest cost to highest cost.

Table 3. Quaywall Example-Economic Performance

<b>Protection Systems</b>	First Cost (\$/m²)	NPV of Repairs (\$/m²)	Total Cost (\$/m²)
Base Case	0	49.30	49.30
1000 Coulomb Concrete	5.00	38.14	43.14
10L/m <sup>3</sup> Calcium Nitrite	5.00	26.67	31.67
17.5L/m <sup>3</sup> Calcium Nitrite	8.75	0	8.75
$1000 \text{ C} + 10 \text{L/m}^3 \text{ CN}$	10.00	14.21	24.21
$1000 \text{ C} + 12.5 \text{L/m}^3 \text{ CN}$	11.25	0	11.25

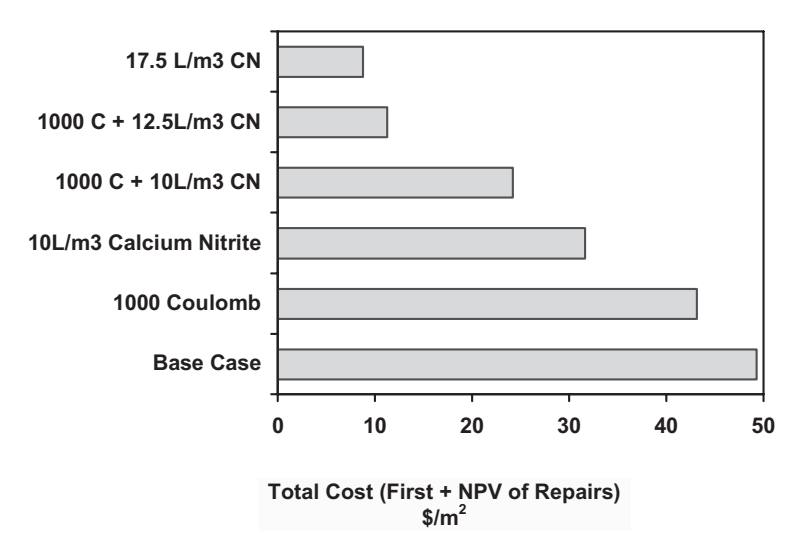


Fig. 5. Quaywall example-ranking of NPV costs.

# **Specifications**

The final result of the analysis is to incorporate the engineering and economic performance results of the various corrosion protection alternatives into a construction specification. Most commonly the preferred method would be to specify the lowest net present value alternatives after the design engineer conducts a durability assessment. However, the owner and designer could ask for a durability assessment in the bid tender (tender price + estimated repair cost to meet service life = Actual project cost). The specifier can simply set the repair cost, discount rates, percent of repair area, and the repair frequency to provide bidders with a common comparison variables.

In the sample quaywall project, a designer could conduct this DMP on the project specifics and write into the specification the lowest two corrosion protection alternatives.

# **Specific Project Analysis**

Each construction project or structural element may require a separate durability analysis with input variables respective of the chloride exposure, corrosion protection products/systems, construction costs, repair costs, and service life requirements. The actual process has been outlined by the following flow chart (Fig. 6).

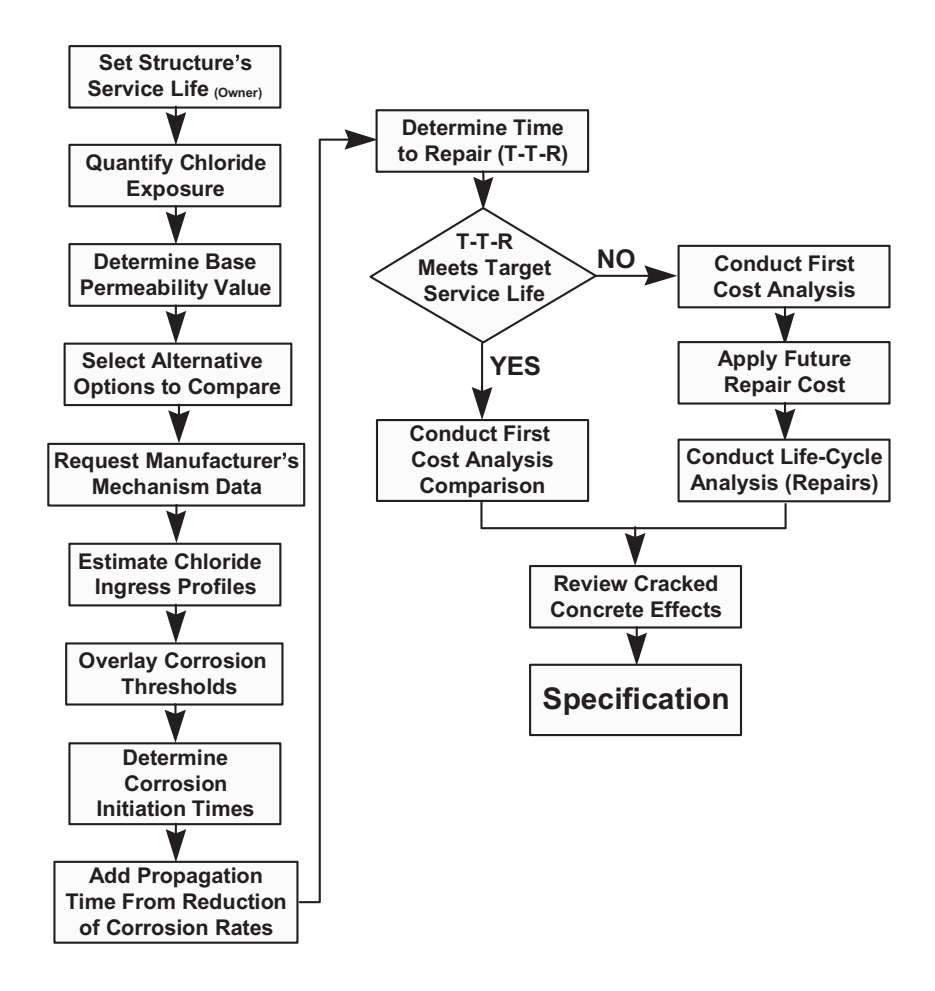


Fig. 6. DMP flow chart.

# References

 ACI 318, "Building Code Requirements for Reinforced Concrete," American Concrete Institute, Detroit, 1995.

- 2. ACI 357, "Guide for the Design and Construction of Fixed Offshore Concrete Structures," American Concrete Institute, Detroit, 1991.
- 3. Y. Gau and I. Cornet, "Penetration of Hardened Concrete by Seawater Chlorides With and Without Impressed Current," Corrosion, Vol. 41, No. 2, pp 93-100, February 1985.
- 4. R. D. Browne, "Design Prediction of the Life for Reinforced Concrete in Marine and Other Chloride Environments." Durability of Building Materials, 1 (1982), pp. 113-125.
- P. D. Cady and R. E. Weyers, "Chloride Penetration and the Deterioration of Concrete Bridge Decks," Cement, Concrete and Aggregates, CCAGDP, Vol. 5, No. 2, Winter 1983, pp. 81-87.
- Strategic Highway Research Program, Report No. SHRP-S-668, National Research Council, Washington DC, 1994.
- 7. N. S. Berke, "Resistance of Microsilica Concrete to Steel Corrosion, Erosion, and Chemical Attack," Third International Conference on the Use of Fly Ash, Silica Fume, Slag and Natural Pozzolans in Concrete, ACI SP114, V. Malhotra Ed., American Concrete Institute, pp 861-886, 1989.
- 8. N. S. Berke and T. G. Weil, "World Wide Review of Corrosion Inhibitors in Concrete," Advances in Concrete Technology, CANMET/ACI, Montreal, 1992, pp 899-924.
- 9. S. W. Yu and C. L. Page, "Diffusion in Cementitious Materials: 1. Comparative Study of Chloride and Oxygen Diffusion in Hydrated Cement Pastes," Cement and Concrete Research, Vol. 21, pp 581-588, 1991.
- S. Goto and D. M. Roy, "Diffusion of lons Through Hardened Cement Pastes," Cement and Concrete Research, Vol. 11, No.5/6, pp 751-757, 1981.
- 11. C. L. Page, N. R. Short and A. El Tarras, "Diffusion of Chloride lons in Hardened Cement Pastes," Cement and Concrete Research, Vol. 11, No. 3, pp 395-406, 1981.
- 12. S. Tangtermsirikul, T. Maruya and Y. Matsuoka, "Chloride Movement in Hardened Concrete. Part 1: Modeling," Cement, Concrete and Related Building Materials, Vol. 24, pp. 377-382, 1991.
- 13. T. Maruya, S. Tangtermsirikul and Y. Matsuoka, "Chloride Movement in Hardened Concrete. Part II: Experiment and Verification," Cement, Concrete and Related Building Materials, Vol. 24, pp 383-388, 1991.
- 14. K. Uji, Y. Matsuoka and T. Maruya, "Formulation of an Equation for Surface Chloride Content of Concrete due to Permeation of Chloride," Corrosion of Reinforcement in Concrete C. L. Page, K. W. J. Treadaway and P. B. Bamforth Eds., pp 258-267, May 1990.
- 15. R. K. Dhir, M. R. Jones, H. E. H. Ahmed and A. M. G. Seneviratne, "Rapid Estimation of Chloride Diffusion Coefficient in Concrete," Magazine of Concrete Research, Vol. 42, No. 152, pp 177-185, September 1990.
- 16. S. Chatterji and M. Kawamura, "A Critical Reappraisal of lon Diffusion Through Cement Based Materials. Part 1: Sample Preparation, Measurement Technique and Interpretation of Results," Cement and Concrete Research, Vol. 22, pp 525-530, 1992.
- 17. E. J. Garboczi, "Permeability, Diffusivity, and Microstructural Parameters: a Critical Review," Cement and Concrete Research, Vol. 20, pp 591-601, 1990.

- 18. E. C. Bentz, C. M. Evans and M. D. Thomas, Chloride Diffusion Modelling for Marine Exposed Concretes", Fourth International Symposium on Corrosion of Reinforcement in Concrete Construction, C. Page, P. Bamforth, and J. Figg Eds., SCI, Cambridge, UK, 1996, pp 136-145.
- 19. N. R. Short and C. L. Page, "The Diffusion of Chloride lons through Portland and Blended Cement Pastes," Silicates Industriels 1982-10, pp 237-240.
- 20. P. B. Bamforth, "Definition of Exposure Classes and Concrete Mix Requirements for Chloride Contaminated Environments", Fourth International Symposium on Corrosion of Reinforcement in Concrete Construction, C. Page, P. Bamforth, and J. Figg Eds., SCI, Cambridge, UK, 1996, pp176-188.
- 21. N. S. Berke and M. C. Hicks, "Estimating the Life Cycle of Reinforced Concrete Decks and Marine Piles using Laboratory Diffusion and Corrosion Data," Corrosion Forms and Control for Infrastructure, ASTM STP 1137, Victor Chaker, Ed., American Society for Testing and Materials, Philadelphia, 1992
- 22. C. J. Pereira and L. L. Hegedus, "Diffusion and Reaction of Chloride Ions in Porous Concrete", 8th International Symposium on Chemical Reaction Engineering, Edinburgh, Scotland, 10-13 September, 1984.
- 23. M. D. A. Thomas and J. D. Mathews, "Chloride Penetration and Reinforcement Corrosion in Fly Ash Concrete Exposed to a Marine Environment", ACI SP-163-15, pp 317-338, Proceedings of the Third CANMET/ACI International Conference on Concrete in Marine Environments, Canada, 1996.
- 24. N. S. Berke, D. W. Pfeifer and T. G. Weil, "Protection Against Chloride Induced Corrosion," Concrete International, Vol.10, No. 12, pp. 45-55. 1988.
- 25. N. S. Berke and M. C. Hicks, "Predicting Chloride Profiles in Concrete", Corrosion, Vol. 50, No. 3, pp 234-239, 1994.
- 26. N. S. Berke, M. C. Hicks and R. J. Hoopes, "Condition Assessment of Field Structures with Calcium Nitrite", Philip D. Cady International Symposium, Concrete Bridges in Aggressive Environments, P. Cady and R. Weyers Eds., SP-151-3, American Concrete Institute, Detroit, MI, 1994.
- 27. AASHTO T 259, "Resistance of Concrete to Chloride Ion Penetration", American Association of State Highway and Transportation Officials, Washington DC.
- 28. ASTM C 1152, "Standard Test Methods for Acid-Soluble Chloride in Mortar and Concrete", American Society for Testing and Materials, Philadelphia, PA.
- 29. ASTM C1202, "Standard Test Method for Electrical Indication of Concrete's Ability to Resist Chloride Ion Penetration", American Society for Testing and Materials, Philadelphia, PA.
- 30. Berke, N.S., Gianetti, F., Tourney, P.G., Matta, Z.G., "The Use of Calcium Nitrite Corrosion Inhibitor to Improve the Durability of Reinforced Concrete in the Arabian Gulf", 4th Int. Conf. on Deterioration and Repair of Reinforced Concrete in the Arabian Gulf, G.L. Macmillan ed. Manama, BAHRAIN (1993).
- 31. Berke, N.S., Hicks M.C., "Protection Mechanism of Calcium Nitrite", International Conference on Understanding Corrosion Mechanisms in Concrete Massachusetts Institute of Technology, Cambridge, MA (27-31 July 1997).
- 32. F. Gianetti, "Understanding Calcium-Nitrite-Based Corrosion Inhibitors", Concrete Engineering International, Vol. 2, No. 2, pp. 31-35. March 1998.

- 33. Matta, Z.G., Gianetti, F., "The Use of Calcium Nitrite Admixtures Inhibitor in the Arabian Gulf', Second Regional Concrete Conference on Concrete Durability in the Arabian Gulf, Bahrain 19-21 March 1995, pp 157-171.
- 34. COST 509 European Commission (Co-operation of Science and Technology), "Corrosion Protection of Metals in Contact with Concrete", Final Report. April 1997.
- 35. Berke, N.S., Hicks, M.C., "Calcium Nitrite Corrosion Inhibitor With and Without Epoxy-Coated Reinforcing Bar for Long Term Durability, in the Gulf", Second Regional Concrete Conference on Concrete Durability in the Arabian Gulf, Bahrain 19-21 March 1995. pp 119-132.
- 36. Berke, N.S., Hicks, M.C., Abdelrazig, B.I., Lees, T.P., "A Belt and Braces Approach to Corrosion Protection", International Conference on Corrosion and Corrosion Protection of Steel in Concrete, University of Sheffield (24-29 July 1994).
- 37. R. E. Weyers, W. Pyc, M. M. Sprinkel, "Estimating the Service Life of Epoxy-Coated Reinforcing Steel", ACI Materials Journal, pp 546-557, Sep-Oct 1998
- 38. N.S. Berke, M.C. Hicks and P.G. Tourney, "Predicting Long-Term Durability of Steel Reinforced Concrete with Calcium Nitrite Corrosion Inhibitor in the Arabian Gulf Environment", 5th International Conference, Deterioration and Repair of Reinforced Concrete in the Arabian Gulf, Bahrain 27-29 October 1997. Supplementary paper.
- 39. P. Schiessl, J. Moersch, "Effectiveness and Harmlessness of Calcium Nitrite as a Corrosion Inhibitor", RILEM international Symposium on the Role of Admixtures in High Performance Concrete, Monterrey, Mexico, March 21-26 1999
- 40. ACI 224, "Control of Cracking in Concrete Structures", American Concrete Institute, Detroit. 1990.

# On Flexural Strength and Permeability of Recycled Concrete as Coarse Aggregates

Nayef Z. AlMutairi and Abdullateef M. AlKhaleefi

College of Engineering and Petroleum, Kuwait University, Kuwait

## **Abstract**

Recycling of construction materials plays a growing role in construction industries nowa-days. The relatively high cost of the building materials combined with the environmental awareness worldwide has helped in the use of the recycled construction materials. Due to the escalating growth in construction in Kuwait and the limitations of the available lands for landfill it is essential to rely on recycled materials. Demolished concrete can be used as coarse aggregates since it occupies huge areas of landfills. Lands are very scarce in a developing country like Kuwait with limited areas for all types of construction projects. In this research the flexural strength of concrete mixes in which crushed recycled concrete was used as coarse aggregate is investigated. Beams made with 100%, 50% and 0% recycled coarse aggregate were tested for flexural strength. Results were compared with ACI Code requirements and found to be within the acceptable range. The permeability (water penetration) tests were conducted. Slabs were made with 100%, 50% and 0% recycled aggregates. The statistical analysis of the permeability tests are discussed. It is suggested that the recycled concrete can be used as a coarse aggregate in concrete mixes.

Key Words: Aggregate, Crushed Concrete, Flexural Strength, Permeability

## Introduction

Now-a-days the construction and demolition (C&D) rates are considered a major source of environmental concern. Not only C& D wastes occupy significant areas that can be utilized for better use otherwise, but also many components of the wastes can be recycled and used in the construction industry. For example, ferrous metals, aggregates, demolished concrete and wood can be reprocessed and recycled. Such approach will help in reducing both the areas of lands allocated for landfills and the natural resources as well. In countries like Kuwait, in particular, there is a scarcity in the lands available for use as landfills. Due to the limited area of the country and the vast oil fields which occupy huge portions of the country a further look at reducing landfills areas should be given top priority. In reality, the C&D wastes have surpassed the available landfills areas in Kuwait. No further delay can be considered and immediate actions should be taken to avoid any future crisis regarding where to dump C&D wastes. Given the fact that 40% of C&D wastes can be utilized as recycled materials, the landfill areas can be reduced.

There has been a great deal of research regarding the recycled aggregates (Banthia 2000, Fraaij 2002, Metha 1999, Metha 2001). It is intended to investigate the use of crushed concrete as coarse aggregate. The emphasis of this particular research is to provide appropriate scheme to determine the flexural strength and the permeability (water penetration) of the recycled concrete when used as a coarse aggregate in a concrete mix. Needless to say that C&D wastes have been investigated widely in the research and industry (Ajdu Reiwiez 2002, DIN 1978, Hendriks 2001, Metha and Burrows 2001, Simpson 1999). From this approach it is worth looking at the properties of some of the "valuable" wastes to find out how the industry can benefit from these wastes. Given the huge amounts of C&D wastes due to the continuous development of Kuwait and the growth in the public and the private sector construction projects, a closer look at the C&D wastes is required. By utilizing the "valuable" C&D wastes materials, the landfills areas are reduced and the resources are optimized.

# **Materials and Sample Preparation**

The concrete mix contains fine aggregate which is dry local washed sand, virgin coarse aggregate which is dry Gabro aggregates of sizes 3/4 in. and 3/8 in. brought from the United Arab Emirates. The recycled coarse aggregate is chunks of demolished concrete that were crushed to sizes 3/4 in. and 3/8 in. The water used is cold tap water. The admixture in the mix is Caplast/R which allows lowering of the water-cement ratio (w/c) while keeping the workability unchanged. It was bought from a local materials company.

Four different mixes were designed with a target water-cement ratio of 0.53, except for Mix. No 4, as shown in Table 1. Two of the mixes were control mixes and the other two mixes were developed by keeping all the mix design parameters constant except for the aggregate constituents.

Table 1. Mix Quantities Used in the Standard Reference Mix  $(Kg/M^3)$ 

W/C ratio	0.53
Cement	$380 \text{ kg/m}^3$
Washed sand (dry)	$670 \text{ kg/m}^3$
3/4" Aggregates (dry)	$770 \text{ kg/m}^3$
3/8" Aggregates (dry)	$380 \text{ kg/m}^3$
Water	200 litres/m <sup>3</sup>
Caplast/R (superplasticiser)	3.1 litres/m <sup>3</sup>

The cement content, the water-cement ratio and the aggregate weight were kept constant. The recycled aggregates replaced an equal aggregate by weight. In summary, the mixes are classified as follows:

- a) Mix no. 1: 100 percent recycled coarse aggregate crushed to 3/4 in. and 3/8 in. The mix was very dry and showed very low workability.
- b) Mix no. 2: 50 percent recycled coarse aggregate with 3/4 in. and 3/8 in. sizes. The other half was virgin coarse aggregate. The mix had better workability than Mix no. 1.
- c) Mix no. 3: No recycled aggregates. Rather, virgin aggregate. The mix was used as a control mix for comparison purposes. It was very liquid with poor workability which implied the need for another control mix (Mix no. 4).
- d) Mix no. 4: No recycled aggregate but with controlled slump. Coarse virgin aggregates were used and water was added gradually, unlike other mixes where water was constant, until an adequate workability was reached.

Table 2 lists the contents of the mixes 1 to 3 of the first concrete batches mixed. Table 3 lists the composition of the second concrete patches mixed. Three beams from each mix were cast for flexural strength tests. Three slabs from each mix were cast for permeability tests.

Table 2. Batch Quantities (kg) and the Characteristics of the Fresh Concrete for the First Batch

Material	Mix 3-R100	Mix 2 – R50	Mix 1 – R0
Cement	17.1	17.1	17.1
Sand	30.15	30.15	30.15
19 mm Virgin coarse aggregates	-	17.32	34.65
10 mm Virgin coarse aggregates	-	8.55	17.1
19 mm Recycled coarse aggregates	34.65	17.32	-
10 mm Recycled coarse aggregates	17.1	8.55	-
Water (litres)	9	9	9
Caplast/r (litres)	0.14	0.14	0.14
Slump (mm)	85	70	185
Density (kg/m <sup>3</sup> )	2285	2360	2450

Table 3. Composition of the Second Concrete Batches Mixed

Material	Mix 1	Mix 2	Mix 3	Mix 4
Cement (kg)	9.5	9.5	9.5	21.66
Sand (kg)	16.75	16.75	16.75	38.19
3/4 in. Virgin coarse aggregates (kg)	-	9.625	19.25	43.89
3/8 in. Virgin coarse aggregates (kg)	-	4.75	9.5	21.66
3/4 in. Recycled coarse aggregates (kg)	19.25	9.625	*	*
3/8 in. Recycled coarse aggregates (kg)	9.5	4.75	*	*
Water (litres)	5	5	5	9.58
Caplast/R (litres)	0.0775	0.0775	0.0775	0.1767
Volume of concrete (m <sup>3</sup> )	0.025	0.025	0.025	0.057
Slump (mm)	85	70	185	100

## Flexural Strength Testing and Results

The modulus of rupture is defined as the flexural tensile stress at which a crack forms in plain concrete beams. The flexural test, determines the modulus of rupture. A plain concrete beam is loaded at the third point at a rate of 0.5 KN/Sec. Figure 1 shows the third point loading in this test. When the beam fails due to tensile stresses produced from the bending moment (failure immediately follows the formation of tensile cracks) the modulus of rupture (tensile strength) is calculated. Figure 2 shows the test apparatus and a tested sample beam. The equation used to calculate the modulus of rupture is in accordance with the ACI specifications 78-94 in this regard as follows:

$$R = PL / pd^2$$
 (1)

where:

R: modulus of rupture, MPa;

P: maximum applied load, N;

L: spam length (m);

b: average width (m);

d: average depth (m);

The span length, width and depth of each beam were measured at three different locations of the beam. The average values were used in Eq. (1) above. The tests were performed based on 28-day strength of the concrete. Three beams from each of the four mixes were tested. Tables 4, 5, 6 and 7 show the results for mixes 1, 2, 3 and 4 respectively. Table 8 summarizes the results of all the tested beams. The results were analyzed using ANOVA1 (MATLAB 2002) as shown in Fig. 3.

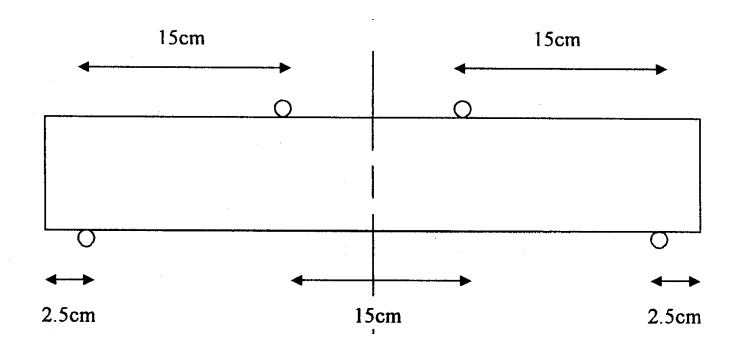


Fig. 1. A sketch of the apparatus for flexure test (third-point loading).

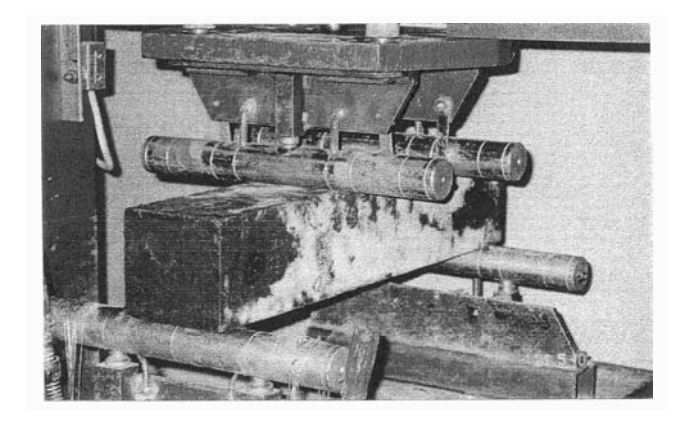


Fig. 2. Sample placement in the apparatus.

Table 4. Mix No. 1 – Day 28 with 100% Recycled Aggregate

Beam No.	Age of sample (days)	AVG, L (mm)	AVG, b (mm)	AVG, d (mm)	Max. load, P (kN)	Location of fracture initiation	Modulus of rupture, R (MPa)	Modulus of rupture, R to the nearest 0.05 MPa
1	28	500	100.2	100.9	9.65	Middle	4.72985	4.7
1						L/3		
2	28	499	102.5	101.4	9.99	Middle	4.73006	4.75
						L/3		
3	28	499	102.7	101.9	10.02	Middle	4.68867	4.7
						L/3		

Table 5. Mix No. 2 – Day 28 with 50% Recycled Aggregate

Beam No.	Age of sample (days)	AVG, L (mm)	AVG, b (mm)	AVG, d (mm)	Max. load, P (kN)	Location of fracture initiation	Modulus of rupture, R (MPa)	Modulus of rupture, R to the nearest 0.05 MPa
1	28	499	102.1	99.8	8.91	Middle L/3	4.37211	4.4
2	28	499	101.3	100.6	10.11	Middle L/3	4.92092	4.9
3	28	499	100.7	101.5	9.54	Middle L/3	4.58868	4.6

The average modulus is 4.2 MPa. From Fig. 3 it can be seen statistically that the modulus of rupture for the four mixes is at a 5% level of significance. The ACI code (American Concrete Institute, 2002) states that the flexural strength of concrete is 10 to 15 % of the compressive strength. The target compressive strength for the mixes is 30 MPa (AlKhaleefi, 2006). In Table 8 the average flexural strength for each mix is within the ACI range.

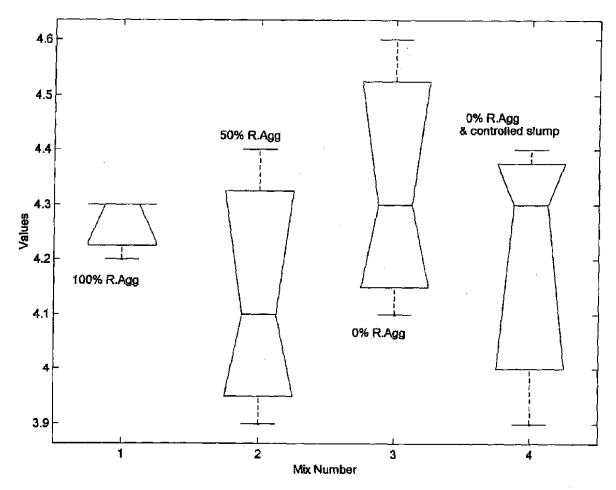


Fig. 3. Modulus of Rupture (MPa), p = 0.7278.

Table 6. Mix No. 3-Day 28 with 0% Recycled Aggregate

Beam No.	Age of sample (days)	AVG, L (mm)	AVG, b (mm)	AVG, d (mm)	Max. load, P (kN)	Location of fracture initiation	Modulus of rupture, R (MPa)	Modulus of rupture, R to the nearest 0.05 MPa
1	28	499.5	101.6	101.4	9.43	Middle L/3	4.50897	4.5
2	28	499.0	102.0	100.6	10.66	Middle L/3	5.15302	5.15
3	28	500.0	100.5	100.8	9.81	Middle L/3	4.80343	4.8

Table 7. Mix No. 4 – Day 28 with 0% Recycled Aggregate and Controlled Slump

Beam No.	Age of sample (days)	AVG, L (mm)	AVG, b (mm)	AVG, d (mm)	Max. load, P (kN)	Location of fracture initiation	Modulus of rupture, R (MPa)	Modulus of rupture, R to the nearest 0.05 MPa
1	28	501.3	101.4	101.13	9.9	Middle L/3	4.78401	4.8
2	28	500.3	101.9	103.12	9.4	Middle L/3	4.34109	4.35
3	28	500.3	100.5	101.66	10.2	Middle L/3	4.91353	4.9

Table 8. The Modulus of Rupture for the Four Mixes (MPa)

		Mix 1 100% recycled aggregate	Mix 2 50% recycled aggregate	Mix 3 0% recycled aggregate	Mix 4 0% recycled aggregate
	Beam 1	4.7	4.4	4.5	4.8
	Beam 2	4.75	4.9	5.15	4.35
R	Beam 3	4.7	4.6	4.8	4.9
	Average	4.72	4.63	4.82	4.68
	ACI Spec. 10-15% fc'	3.7 – 5.6	4.1 – 6.0	4.0 – 6.2	4.75 – 7.0

It should be noted here that since the mix design was based on the required strength of K 300 it is anticipated that the tests show values of 300 kg/cm<sup>2</sup> which is equivalent to a 30 MPa compressive strength as a minimum.

# **Water Penetration Testing and Results**

The ease with which water can pass through the concrete is defined as permeability. The absorption is defined as the ability of concrete to draw water into the voids. Concrete tends to be porous when air voids are not removed during compaction. For fully compacted concrete the permeability decreases with decreasing water-cement ratio. The permeability is also influenced by the fineness and the chemical composition of the cement. Coarse cements have the tendency to produce pastes with relatively high porosity. Aggregates with low porosity have significant effect on the permeability of the concrete. Also, when the constituent materials of the concrete are segregated this will have adverse effect on the permeability and consequently the strength of the concrete.

The German Method was used in the water permeability tests. Three slabs  $200 \times 200 \times 120$  mm in dimension from each of the four mixes were cast. After being cured for 28 days in room temperature water tanks, each sample was placed in the machine. Water was then released upwards from under the sample at a certain pressure for a fixed time period. Each sample was placed at a pressure of 1 bar for 24 hours and then 3 bars for 48 hours followed by 7 bars for 24 hours. The samples were split open

thereafter. The distance travelled upwards by the water inside the concrete were taken at different locations. The results are listed in Table 9. The average for each sample was calculated for comparison and listed in table 10. ANOVA1 (MATLAB 2002) was used to analyze the averages. Figure 4 shows the results.

Table 9. Results of Water Penetration of the Mixes (mm)

Mix No.	Slab No.	Left end	R1	R2	R3	R4	R5	Right end	Max. R	AVG	AVG. to the nearest 0.5 mm
	1	26.9	43.1	55.2	63.2	59.0	51.5	27.0	63.2	49.8	50.0
1	2	23.9	56.1	70.4	75.7	73.3	43.7	15.9	75.7	57.2	57.0
	3	26.0	18.0	33.0	56.0	62.0	48.0	31.0	62.0	40.5	40.5
	1	30.4	61.6	71.4	68.5	48.3		31.9	71.4	52.0	52.0
2	2	23.8	36.7	50.3	46.7	32.4		17.0	50.3	34.5	34.5
	3	21.0	31.6	53.5	71.0	60.1		24.0	71.0	43.5	43.5
3	1	23.8	41.7	69.4	87.5	77.4	48.5	26.3	87.5	58.0	58.0
3	2	8.4	17.4	25.4	21.3	26.84	18.9	11.5	26.84	19.7	20.0
	3	18.0	26.7	47.0	39.0	30.9	24.0	18.0	47.0	30.9	31.0
4	1	28.0	35.0	38.0	42.0	36.0	32.0	26.0	42.0	35.2	35.0
	2	29.0	33.0	39.0	26.0	32.0	27.0	*	39.0	31.8	32.0
	3	19.0	24.0	34.0	36.0	33.0	29.0	17.0	36.0	29.2	29.0

Table 10. Comparison between the Water Penetration Results for the Three Concrete Mixes (mm)

	Mix 1	Mix 2	Mix 3	Mix 4
	100%		0%	0%
	recycled	recycled	recycled	recycled aggregate &
	aggregate	aggregate	aggregate	controlled slump
Slab 1	50.0	52.0	58.0	35.0
Slab 2	57.0	34.5	20.0	32.0
Slab 3	40.5	43.5	31.0	29.0
Average to the				
nearest 0.5	49.2	43.3	36.3	32.0
mm				

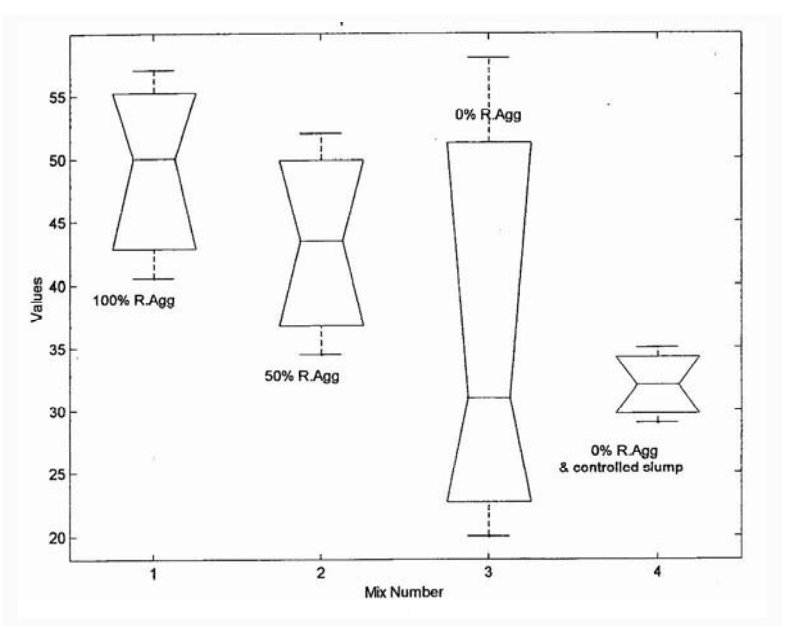


Fig. 4. Permeability Test: distance travelled up in the concrete (mm), p=0.3438.

The results indicated that mix No. 1 (100 % recycled aggregates) has higher permeability than mix No. 2 (50 % recycled aggregates). Mix No. 2 has higher permeability than the control mixes (mixes No. 3 and 4). Stronger the concrete the denser it is and a less permeable concrete is expected. The difference between the samples was not large. The average water penetration ranged between 32 and 49.2 mm. The results were found to be statistically similar to a 5% level of significance.

## **Conclusions and Recommendations**

In this study the emphasis is on the flexural strength and water penetration of the recycled concrete when used as a coarse aggregate. The following can be concluded:

- i) The modulus of rupture which measures the flexural strength was not affected by the introduction of the recycled aggregates to the mix.
- ii) The permeability of the concrete was not affected significantly by the introduction of the recycled aggregates.

The study recommends the following:

i) Based on the test result obtained so far, the use of the recycled aggregates can be brought to the attention of the concerned parties. However, it is recommended to apply the tests to specimen that are 3 months, 6 months, and one year old to clarify the suitability of using the recycled aggregates further.

- ii) It is recommended to conduct a study on using saturated surface dry (SSD) aggregate instead of the dry aggregates. It is anticipated that such study will produce different yet better results.
- iii) Due to the short time of the study it is recommended to conduct tests related to time-dependent effects such as drying, shrinkage and creep.

# Acknowledgment

The authors express their gratitude to Mrs. Mini Kora and Mrs. Estella Fernandez for their valuable assistance in producing this manuscript.

## References

- Ajdu Riewicz, A. and Klisz Czewicz, A. (2002), "Influence of recycled aggregates on mechanical properties of HS/HPC". Cement and Concrete Composites, Vol. 24(2), 268-279.
- AlKhaleefi, A.M. and AlMutairi N.Z. (2006), "Strength of concrete made with crushed concrete as coarse aggregate". The 31<sup>tst</sup> International Conference on Our World in Concrete and Structures, Singapore, August 16 17.
- Banthia, N. and Chan, C. (2000), "Use of recycled aggregate in plain and fiber-reinforced shotcrete". ACI, Concrete International, Vol. 22 (6), 41-45.
- Building Code Requirements for Structural Concrete, (2002). ACI 318-02, American Concrete Institute, Detroit, MI, USA.
- Deutsches Institut Fur Normung, (1978), Test methods of concrete impermeability to water, DIN, Germany, 1048, December.
- Fraaij, A.L.A., Pietersen, H.S and Vries, J.DE. (2002), "Performance of concrete with recycled aggregates, sustainable concrete construction". Editors: Dhir, R.K.; Dyer, T.D.; Halliday, J.E. and Thomas Teford, pp. 187-198.
- Hendriks, C.F. and Janssen, G.M. (2001), "Application of construction and demolition waste". HERON, Vol. 46(2), 95-108.
- MATLAB (2002), MathWorks, Natick, MA, USA.
- Metha, P.K. (1999), "Advancements in concrete technology". ACI, Concrete International, Vol. 21(6), 69-76.
- Metha, K. and Burrows, R.W. (2001), "Building durable structures in the 21<sup>st</sup> century". ACI, Concrete International, Vol. 23(3), 57-63.
- Metha, K. (2001), "Reducing the environmental impact of concrete". ACI, Concrete International, Vol. 23(10), 61-66.
- Simpson, D. (1999), "Recycled aggregates in concrete". Concrete, Vol. 33(6), 17.

# Effect of Variant in Concrete Cover and Percentage of Steel Reinforcement on Residual Load Capacity for Reinforced Concrete Columns Exposed to Fire

M. A. A. El Aziz, K. M. Othman, A. A. Shahin, A. Serag Fayoum University, Egypt.

### **Abstract**

This paper presents the effect of variant in concrete cover and percentage of steel reinforcement for reinforced concrete scaler models column residual load capacity under fire exposure using finite element analysis program (Ansys10). The temperature distribution in the section of concrete columns according to *ISO-834 Standard Fire* curve at 600°C and at 30 mi. of fire time, which is then input in F.E.A program ANSYS. Forty-five scaler models under investigation were classified according to columns model cross-sections to three groups. The effective parameters presented in this study are concrete cover and percentage of steel reinforcement of concrete column cross-section. The variance of the concrete cover are 1, 2 and 3cm of concrete cover, the variance of percentage of steel reinforcement nearly 1, 2 and 3% of concrete column cross-section. The procedure has been found the high effect of concrete cover and percentage of steel reinforcement on columns residual load capacity after fire.

**Key Words**: ANSYS, F.E.A, Reinforced Concrete, Columns, Concrete Cover, Steel Percentage

### Introduction

Reinforced concrete structure is the common structural system used all over the world. Thus, the behavior of reinforced concrete structures and its failure modes has been extensively studied. Fire is the main problem affecting is the combustibility of contents and failure of the structure. The extent of ensuing damage depends primarily on structural performance of building both during and after the fire. The behavior of concrete elements exposed to fire depends on its mix composition, size of cross section, concrete cover, percentage of reinforcement, and thermal properties. It has been determined by complex interactions during heating process. The modes of concrete failure under fire exposure have been varied according to the nature of the fire, the loading system, and the type of structure.

Fire resistance of building elements such as columns is described by the time during which the specimen can withstand the fire without loss of bearing load or ability to act as a barrier to spreading of fire. Currently, it is determined mostly by the fire tests prescribed in *ISO* 834(1985).

Due to high temperature shrinkage may be formed in the material, and expansion may cause buckling or crushing of the concrete structure; for these reasons the building codes and regulations in Europe and U.S.A have relied on standardized test methods [2, 3] to specify fire endurance requirements. The primary objective of the test method is to determine the length of time that a structural assemblage will withstand exposure to the test conditions.

Effect of fire on the structural elements in the fire compartment mainly depend on intensity of the fire and thermal properties of the structural material such as thermal conductivity, specific heat, and diffusivity. Changes in physical and chemical properties of reinforced concrete occur as a result of an increase in the temperature, which in turn affect its mechanical properties [1]. Strength, physical properties and stiffness of the concrete and steel mainly have a considerable change by effects of heating and some of the changes are not recoverable after subsequent cooling. Chemical changes may also occur, especially in siliceous aggregate concrete. Finally, prediction or assessment of the performance of reinforced concrete elements during fire and subsequent cooling must consider all changes in materials properties which will be presented in the following subsections.

In recent years many researches put much effort to develop a calculation method to predict fire resistance and residual load capacity of concrete columns.

Anderberg and Thelandersson [2] pointed that, not only the thermal expansion of concrete is influenced by cement, water content, aggregate type, and age but also affected by the stress level.

Khoury [3] studied the transient thermal strain behavior of concrete during elevated temperature up to 600 °C under load. The results showed that, free thermal strain of concrete was nonlinear function of temperature, dominated by the aggregate type and content, it was increased progressively for light weight concrete, basalt, limestone, and gravel concrete with concrete containing quartz expanding markedly above 550 °C. They also investigated the effect of different load of thermal expansion of a siliceous-aggregate concrete heated at rate

of 5°C per minute, and they found that thermal expansion was strongly reduced as the stress level increased.

Osman [5] investigated the bond strength between different types of steel and concrete at high temperature. The results of his study showed that, the bond strength not only depends on the temperature level but also depends on the test procedure and the shape of the bars. The losses of the bond strength for ribbed bars at constant elevated temperature is of the same order of the magnitude as the losses in the compressive strength of concrete. At the same temperature, the plain round bars showed a sharper decrease in the bond strength.

University of Ghent and Laboratory of Bridges and Structural Engineering at the University of Liege [6] showed the effect of different parameters on the behavior of reinforced concrete columns under fire conditions. The dimensions of the cross–sections and the values of concrete cover are the only factors conditioning the fire resistance, while it is logical to think that other parameters may have aggregate non–negligible influence. They also intended to develop aggregate simple approach to study effect of different parameters, which were published widely [7,8]. One of the observations made during test action, is that after failure of the columns, buckling of some individual longitudinal reinforcements occurs between two stirrups. Therefore, decreasing the spacing between stirrups might modify the behavior of the column under fire conditions. They studied the effect of load level, dimensions of the cross–section, column height, main reinforcement, the concrete cover and load eccentricity.

# Verification of Analytical Model

# Experimental Test

Several experiments were undertaken by Khalil and Mohammed [9] and [10]. Biaxial compression test was carried out with five square specimens. The dimensions and details of reinforcement for all specimens, load eccentricities and the material properties are shown in Table 1 and Fig. 1.

**Table 1. Details of Tested Specimens** 

Col No.	x-sec	Height (cm)	f <sub>cu</sub> (kg/cm <sup>2</sup> )	Rft.	Stirrups	Fire Exposure Time	
C1	10x10	100	254.3	4 φ 6	ф2.7@7cm	At 10 min At 20 min	
C2	10x40	100	254.3	14 φ 6	φ2.7@7cm	At 10 min At 20 min	
C3	10x25	100	254.3	10 ф 6	φ2.7@7cm	At 5 min At 10 min At 15 min At 20 min	
C4	15x15	100	300	4 <b>#</b> 10	ф6@10cm	At 15 min	
C5	15x15	100	375	4 <b>#</b> 10	ф6@10cm	At 15 min	
С6	15x15	100	300	4 <b>#</b> 12	ф6@10cm	At 15 min	

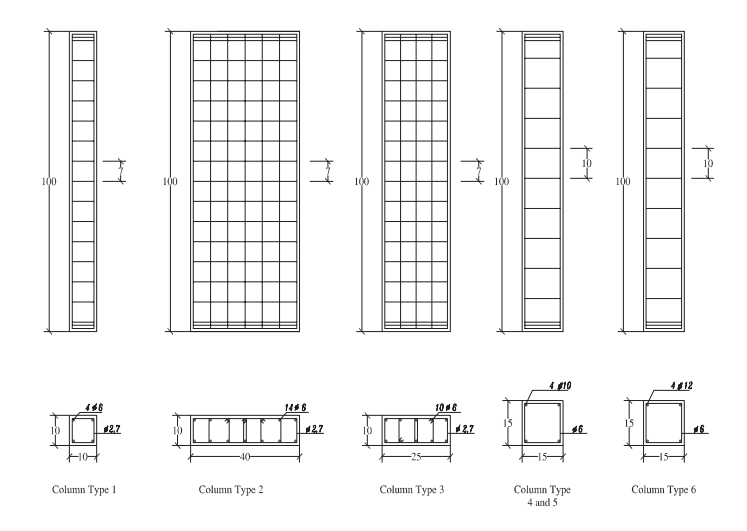


Fig. 1. Cross section and reinforcement details for tested columns.

# **Analytical Model**

# Elements and their material properties

ANSYS codes are used to model reinforced concrete columns subjected to fire. The purpose of this section is to give an explanation to all the steps involved in the ANSYS code as well as to give a brief overview of the entire code. All of the specimens were simulated with ANSYS (version 10), which offers a series of very robust nonlinear capabilities for designs and analyses and is popularly utilized in engineering. In this paper, three solid elements are used to define them in ANSYS code; the reinforced concrete adopted SOLID65, the thermal element adopted SOLID70 which convert to structural element SOLID45, the reinforced steel bars adopted LINK8 and the thermal element adopted LINK33 which convert to structural element LINK8 [11].

# Meshes for concrete and steel for the study cases

Figure 2 shows meshed columns. It is an assumption that all joints of elements satisfy displacement coordination.

## Output Data

Column load and column residual load were exposed to high temperatures at each load step. Temperature distribution or temperature gradient, first crack loads, deformed shape and failure mode are obtained for each column at failure load. Load-time curves were obtained at mid-height of the columns.

# Comparisons between numerical and experimental results

Table 2 shows the results of the crushing load failure before fire and residual load capacity of fire exposed columns model from experimental and theoretical test.

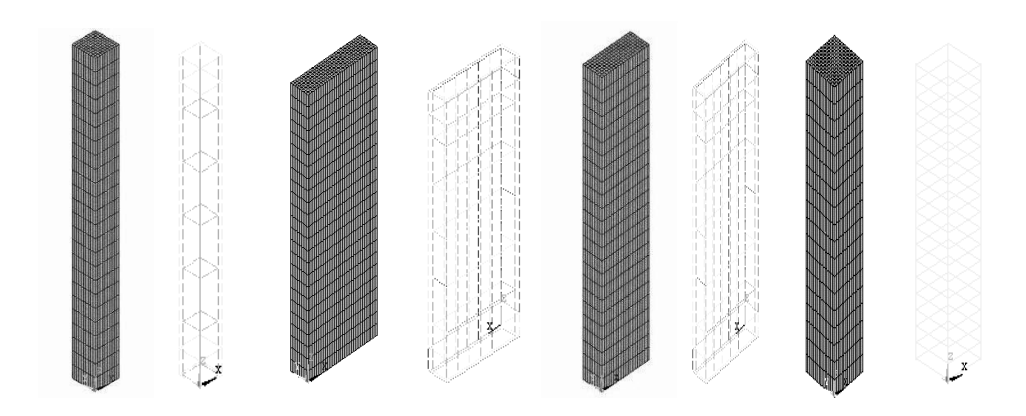


Fig. 2. F.E. Meshed columns models for concrete and steel bars for the modeled columns.

Table 2. Comparison between Theoretical and Experimental Results.

Column No.	Exposure Time	Experimental Results	Theoretical Results (ANSYS)	% Error
	Actual Load	26.8	26.1	-2.611
C1	At 10 min	15.7	15.605	-0.6051
	At 20 min	10.6	11.214	5.794
	Actual Load	103.3	101.098	2.132
C2	At 10 min	70.5	67.345	-0.6051
	At 20 min	46.9	49.3768	5.281
	Actual Load	66.70	65.384	-0.002
	At 5 min	51.40	50.056	-2.605
C3	At 10 min	36.60	37.412	2.219
	At 15 min	34.90	34.214	-1.966
	At 20 min	26.50	24.839	-6.266
C4	Actual Load	70.50	72.00	2.13
(Reference)	At 15 min	56.50	53.61	-5.12
C5	Actual Load	84.50	87.68	3.76
	At 15 min	58.00	60.63	4.53
C6	Actual Load	86.00	80.79	-6.06
	At 15 min	70.00	69.45	-0.79

Figure 3 shows the % Error Ratio of Comparison between Experimental Tests and ANSYS Results. Figure 4 shows the residual load capacity, deformed shape, and the first crack of some sample tested column models.

By analyzing Fig 3, we found that the maximum % error ratio of the comparative study between experimental test results and finite element analysis study by using ANSYS program is 6.27, which revealed good agreement with test results.

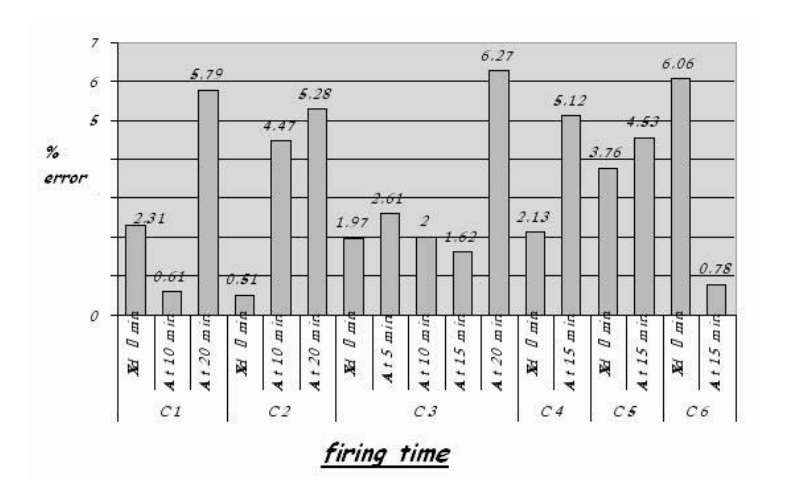


Fig. 3. Total % Error Ratio for Comparison between Experimental Tests and ANSYS Results.

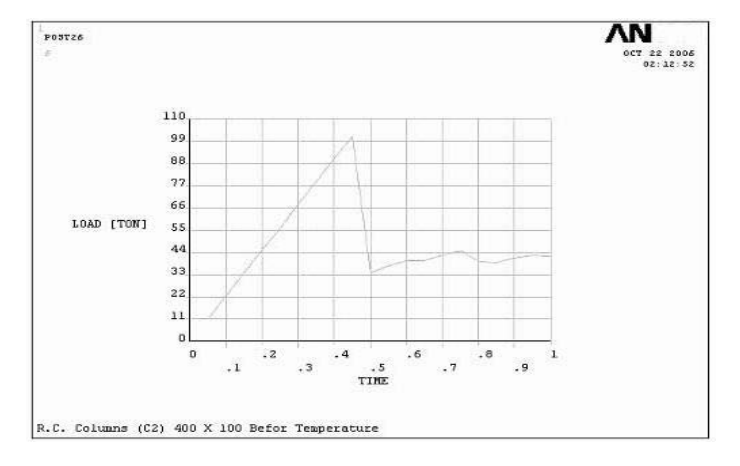


Fig 4a. Residual load capacity for column no C2 before exposure to fire.

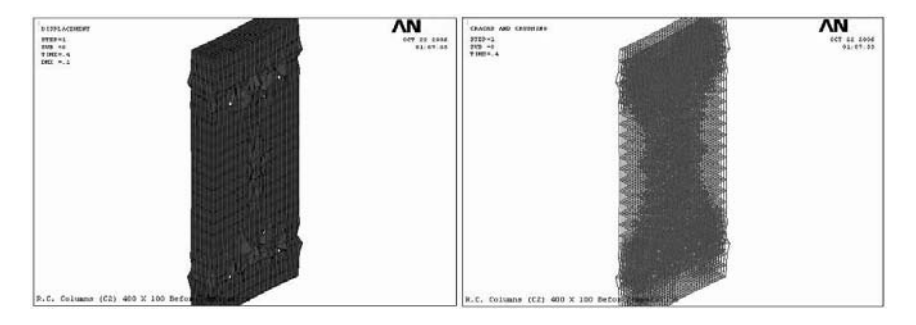


Fig. 4b. Deformed shape and first crack for column no C2 before exposure to fire.

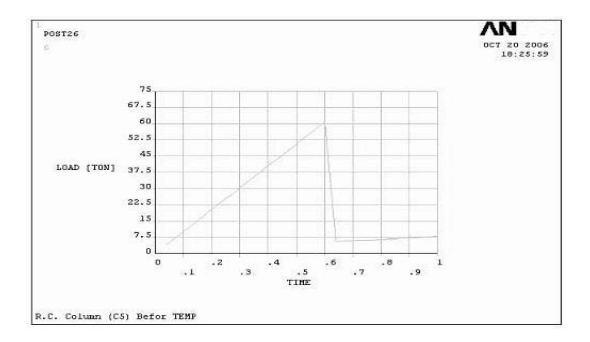


Fig. 4c. Residual load capacity for column no C5 15 min. after fire.



Fig. 4d. Deformed shape and first crack of column no. C5 15 min. after fire.

# **Parametric Study**

Based on the verification of the analytical model and due to the expensive cost of the experimental and field tests and the tedious procedure to evaluate a detailed and complex structure. The finite element analysis makes it possible using computers. Due to these reasons, extensions for the proposed model are given to study the residual load capacity of reinforced concrete columns exposed to fire.

# Parameters of the Finite Element Analysis

The key variables to be investigated were:

- 1. Column dimensions (C1=10x15 cm, C2=15x15 cm, and C3=15x20 cm).
- 2. Fire duration (at temperature 600°C and after 20 min heating).
- 3. Percentage of main steel reinforcement and steel diameter ( $\mu = 1\%$ , 2%, and 3%).
- 4. Concrete column cover (concrete cover = 1 cm, 2 cm, and 3 cm).

Column load and column residual load due to exposure to elevated temperature were obtained at each load step. Temperature distribution or temperature gradient, first crack loads, deformed shape and failure mode are obtained for each column at failure load. Load-time curves were obtained at mid-height of the columns.

Sixty-three reinforced concrete scale model columns (1/3 models) were analyzed under the effect of axial compression load and the effect of high temperature. Specimens are classified to three groups according to specimen cross-section (Group "C1= 10x15 cm", Group "C2= 15x15 cm", Group "C3= 15x20 cm"), and all specimens had a height of 90 cm. Each group was sub-classified into three subgroups according to the following parameters study (concrete cover, concrete characteristic strength and percentage of main steel reinforcement). Finally, each sub-group was divided into three sections according to fire exposure time (in air condition, at 600°C and at 20 min exposed to temperature) (Fig. 5).

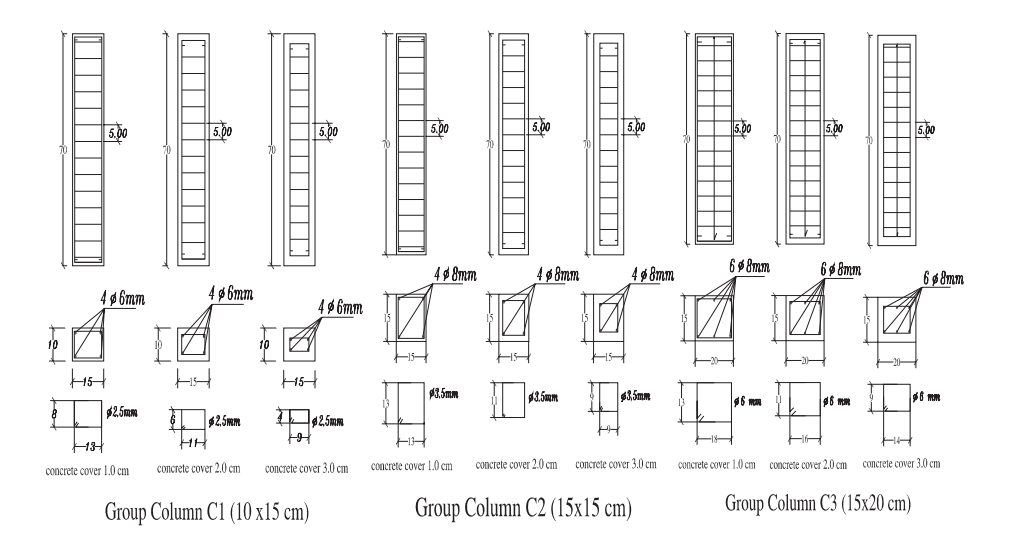


Fig. 5. Columns model dimensions, reinforcement and material properties.

The column had a clear height of 70 cm and 90 cm overall height including corbels heads, while the top and bottom were cross section x 10 cm in dimensions. The corbels heads were introduced to prevent premature failure.

Table 3 shows columns model dimensions, reinforcement and material properties for all specimens.

**Table 3. Columns Model Dimensions, Reinforcement and Material Properties** 

Group No.	Column. No.	Column. Dim. cm	Concrete Cover.cm	Fcu kg/c m <sup>2</sup>	% μ	RFT.	Stirrups	Para- metric Study
	C11	10 X 15	1	250	1.1	6 <b>\$</b> 6	ф2.5	Referenc e
C1	C12	10 X 15	2	250	1.1	6 <b>#</b> 6	ф2.5	Cover
GROUP CI	C13	10 X 15	3	250	1.1	6∯ 6	ф2.5	Cover
GR	C14	10 X 15	1	250	2.0	4 <b>\$</b> 10	ф3.5	Steel
	C15	10 X 15	1	250	3.0	<b>4₽</b> 12	ф 6	Steel
	C21	15 X 15	1	250	0.9	4 <b>\$</b> 8	ф 3.5	Referenc e
C2	C22	15 X 15	2	250	0.9	4 <b>\$</b> 8	ф3.5	Cover
GROUP C2	C23	15 X 15	3	250	0.9	4 <b>\$</b> 8	ф3.5	Cover
GR	C24	15 X 15	1	250	2.0	4 <b>#</b> 12	ф 6	Steel
	C25	15 X 15	1	250	3.1	2 <b>#</b> 14+2 <b>#</b> 1	ф 6	Steel
	C31	15 X 20	1	250	1.0	6 <b>\$</b> 8	ф 3.5	Referenc e
C3	C32	15 X 20	2	250	1.0	6 \$8	ф3.5	Cover
GROUP C3	C33	15 X 20	3	250	1.0	6 \$8	ф3.5	Cover
	C34	15 X 20	1	250	2.0	8 <b>#</b> 10	ф6	Steel
	C35	15 X 20	1	250	3.0	8 <b>#</b> 12	ф6	Steel

# Temperature Effect and Equivalent Model Exposure Time

Figure 6 shows the *ISO-834 standard time-temperature curve* which was used in this study. The time-temperature relationship on the boundary member is defined in equation (1) and shown graphically in Fig. 6.

$$T_{b} = 345 \times \log_{10} (8t + 1) + T_{0}$$
Where
$$t \quad \text{is time [min].}$$

$$T_{0} \quad \text{is ambient temperature [°C].}$$

$$T_{b} \quad \text{is boundary temperature [°C].}$$

Figure 7 shows the temperature distribution at temperature 600°C and after 20 min of fire time, as per ANSYS program for different column model.

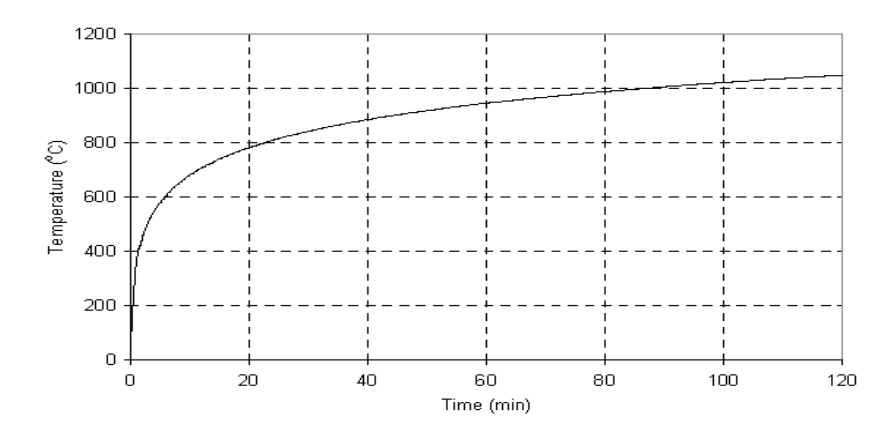
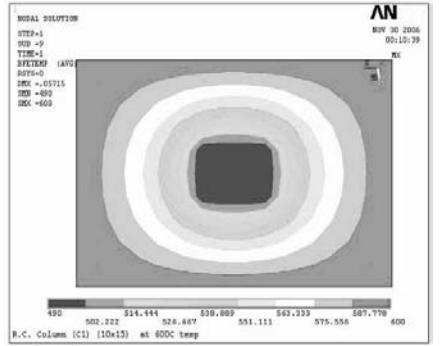
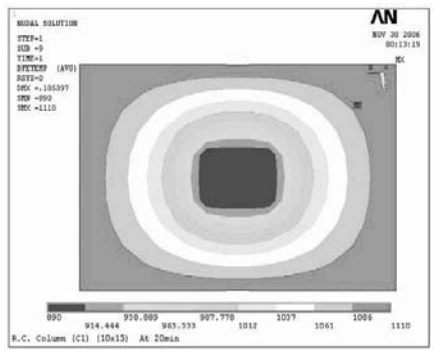
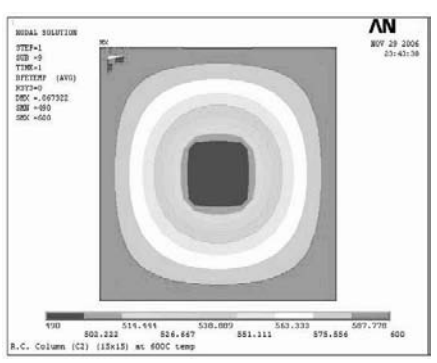


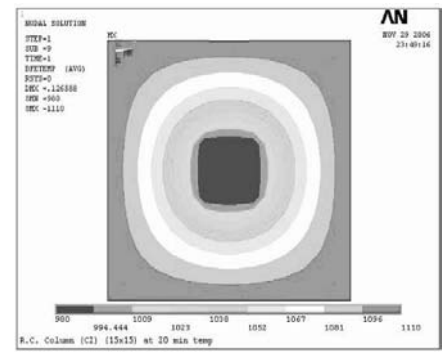
Fig. 6. Standard ISO 834 Fire Curve.



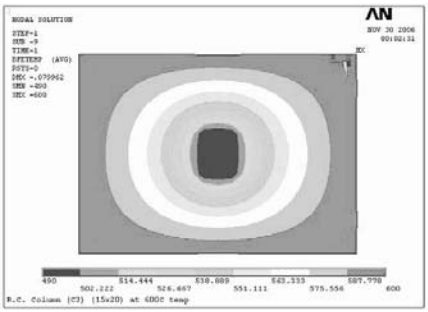


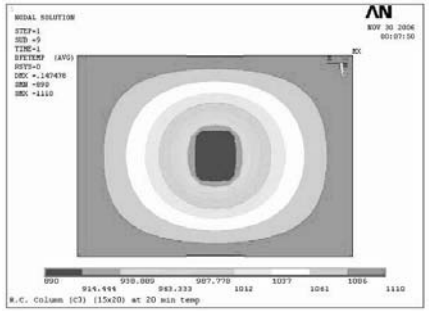
At Temperature 600°C 20 min After Fire (a)Temperature Distribution for Column C1 (10 x 15 cm).





At Temperature 600°C 20 min After Fire (b)Temperature Distribution for Column C2 (15 x 15 cm).





At Temperature 600°C 20 min After Fire (c)Temperature Distribution of Column C3 (15 x 20 cm).

Fig. 7. Temperature distribution of tested column groups.

#### **Results and Discussions**

## Results

All the tested models were classified to three cases of fire exposure; the reference case was at normal condition while second and third cases were at temperature 600°C, and after 20 min of fire, as mentioned before.

Figures 8 and 9 show the load capacity and residual load capacity percentage of studied columns before and after exposure to elevated temperature for all tested columns models. It concluded that, all reference specimens gives crushing load capacity higher than specimens exposed to fire.

From Figs. 8 and 9 the following can be observed:

- The column load capacities were decreased by increasing the concrete cover. On the other hand, the residual load capacity for specimens exposed to fire were increased with the increase of the concrete cover.
- For all fire effect the column load capacity and the residual load capacity were increased by increasing the percentage of main steel reinforcement.
- Column load capacity for square cross section columns was more than the column load capacity for rectangular cross section columns.

Figure 10 shows the residual load capacity, deformed shape, and the first crack for some sample tested column models.

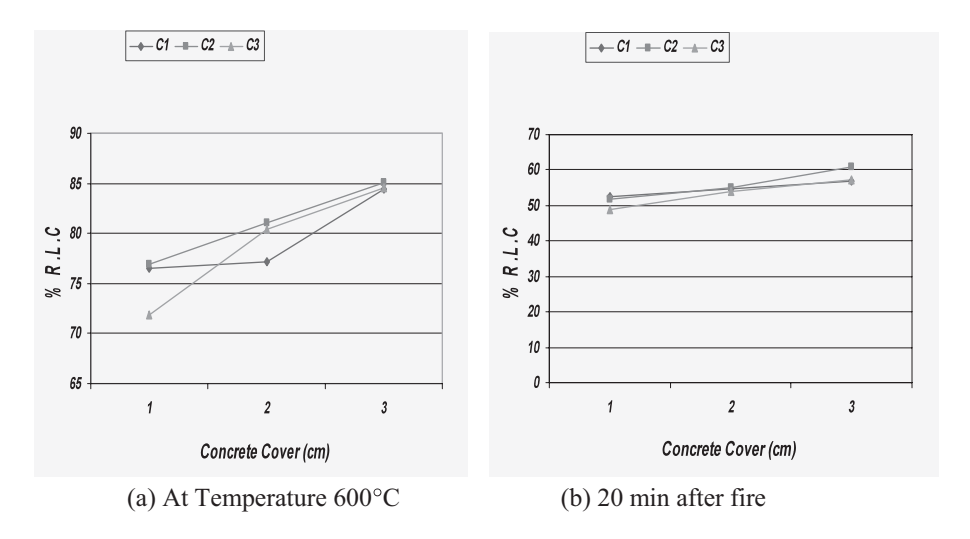


Fig. 8. The residual loads capacity of columns C1, C2, and C3 with different concrete cover.

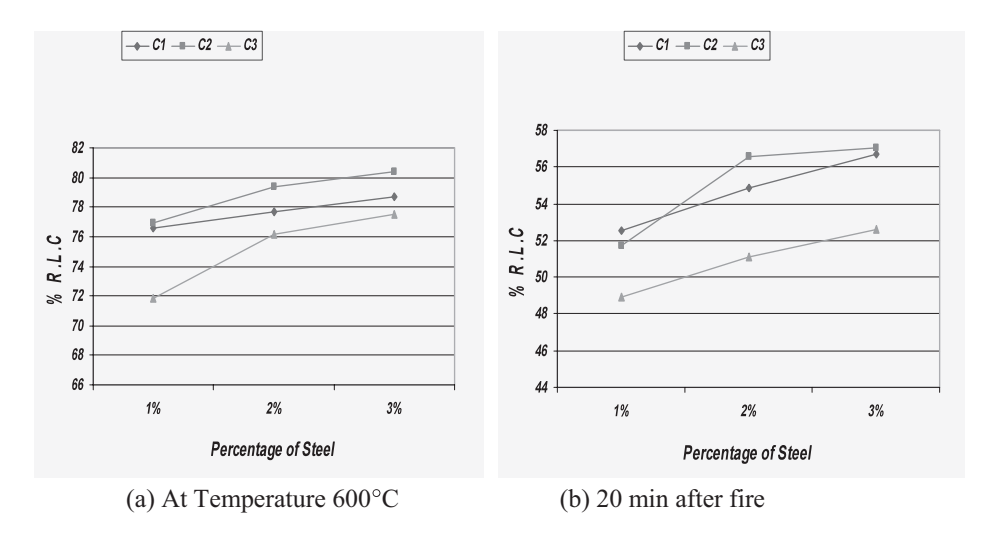


Fig. 9. The residual loads capacity of columns C1, C2, and C3 with different percentage of steel.

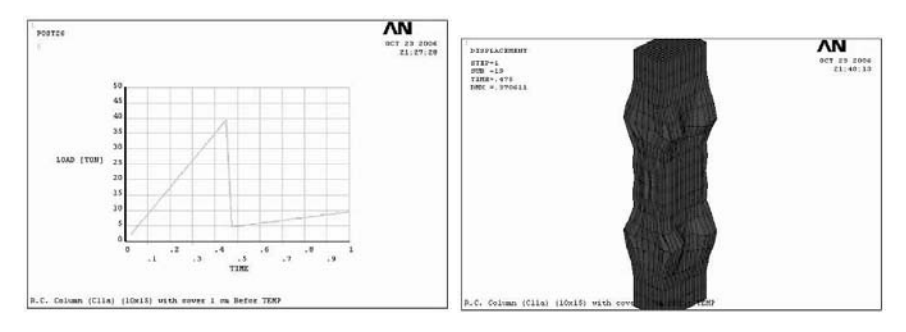


Fig. 10a. Residual load capacity and deformed shape of model (C11a) before exposure to fire.

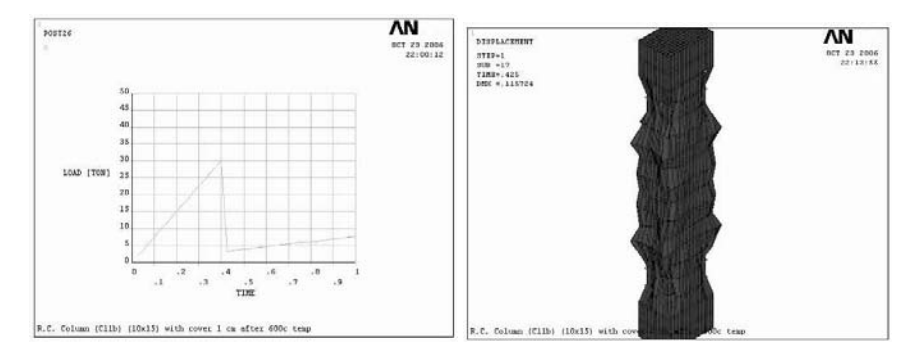


Fig 10b. Residual load capacity and deformed shape of model (C11b) after exposure to temperature 600°C.

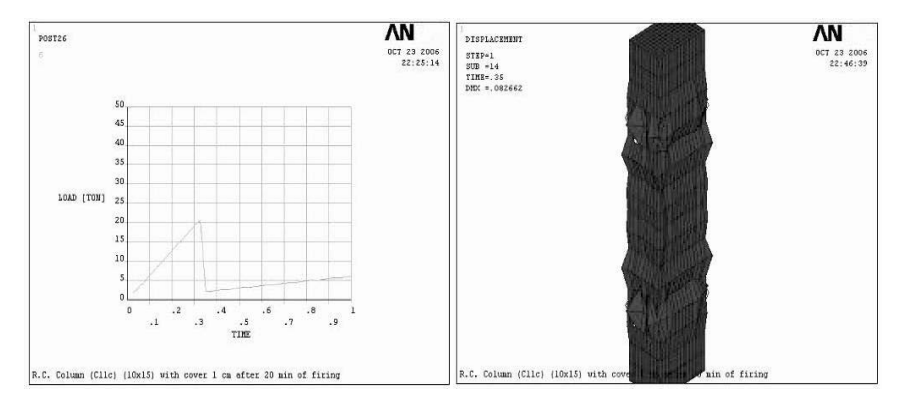


Fig. 10c. Residual load capacity and deformed shape of model (C11b) 20 min after fire.

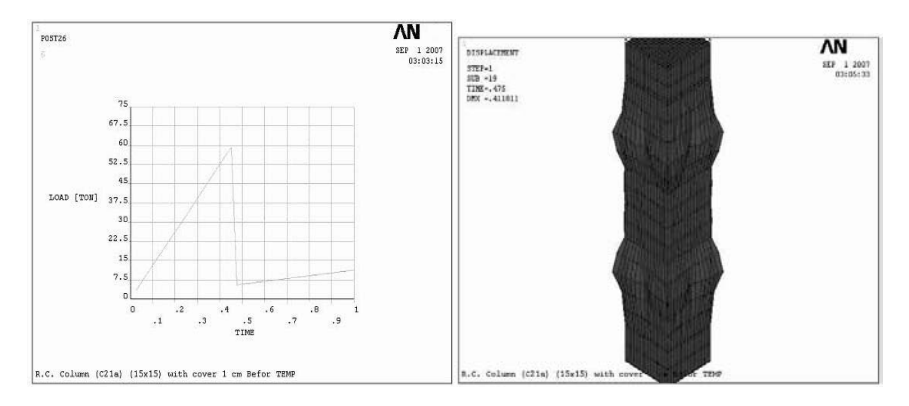


Fig. 10d. Residual load capacity and deformed shape of model (C21a) before exposure to fire.

## Conclusion

In this study, numerical investigation was undertaken to study the effect of fire exposure on residual load capacity of short columns. From numerical results, the following conclusions were obtained:

- 1. FEM was found to be an effective method for analyzing the behavior of reinforced concrete columns subjected to elevated temperature with different concrete cover, and percentage of reinforcement ratio.
- 2. Columns residual crushing loads after fire are function in fire exposure time.
- 3. Crushing loads of columns before exposure to fire were decreased by increasing the concrete cover. This was attributed to the increase in confined concrete area within the core area of the column cross-section.
- 4. Residual load capacity after fire were increased by increasing concrete cover. This might be explained as when concrete cover increases, the temperature effect on the reinforcing steel decreases, then the steel expansion decreases. Hence, the expansion difference between column concrete and reinforcing steel is minimum.

- 5. The residual load capacity increases when the percentage of main steel reinforcement increases. This might be explained as when percentage of main steel reinforcement increases, the temperature effect on them decreases, then the steel expansion decreases. Hence, the expansion difference between column concrete and reinforcing steel is minimum.
- 6. Columns cross-section rectangularity ratio affect the residual crushing loads of different modeled columns after fire. The square cross-section model (group No. C2 15x15cm) have residual load capacity more than other two group, C1 (10x15 cm) and C3 (15x20 cm). This might be explained as the perimeter which was exposed to fire in square column cross-section is less than the rectangular column perimeter.

#### References

- 1. James A.M. (1999), "Analytical Method to Evaluate fire Resistance of Structural Members", Journal of Structural Engineering, pp.1179-1187.
- 2. Anderberg, Y. and Thelandersson, S., (1976), "Division of Structural Mechanics and Concrete Construction", Bulletin 54, Lund Institute of Technology, Lund, Sweden.
- 3. Khoury, G.A., Grainger, B.N., and Sullivan, P.J., (1985), "Strain of Concrete During First Heating to 600°C Under Load", Magazine of Concrete Research, Vol. 37, No.133, December, pp. 195-215.
- 4. Morly, P.D., and Royles, R., (1983), "Response of the Bond in Reinforced Concrete at High Temperature", Magazine of Concrete Research Vol. 35, No.123, pp.67-74.
- 5. Osman, K.M., (1994), "Finite Element Modeling of Concrete Slab Exposed to High Temperature", M. Sc. Thesis Cairo University, Faculty of Engineering.
- Dotreppe, J. C., Franssen, J. M., Bruls, A., Baus, R., Vandevelde, R., Van Nieuwenburg, D., and Lambotte, H., (1997), "Experimental Research on the Determination of the Main Parameters Affecting the Behavior of Reinforced Concrete Columns Under Fire Conditions," Magazine of Concrete Research, V. 49. No. 179. Thomas Telford Ltd, London, pp. 117-127.
- Anderberg. Y., 1993), "Concrete structure and fire. Computer simulations and design method for fire".
- 8. Hertz. K., (1993),"Simplified calculation method for fire exposed concrete structures." Supporting document for CEN pr-ENV 1992-1-2. Technical University of Denmark, Lyngby.
- 9. Khalil, U.F., (2002), "Experimental study for the residual load capacity of short modeled columns fired in a fire furnace", Ph.D. Thesis Cairo University, Faculty of Engineering.
- 10. Mohamed, B.M., (2004), "Behavior of reinforced concrete columns exposed to fire", M. Sc. Thesis Cairo University, Faculty of Engineering.
- 11. ANSYS<sup>®</sup>. Manual, Version 10.

# **Evaluation of the Fire Resistance of GFRP Reinforced Concrete Flexural Elements**

Moetaz M.El-Hawary<sup>1</sup>, Amr W. Sadek<sup>1</sup>, Amr S. El-Deeb<sup>2</sup>

<sup>1</sup>Kuwait Institute for Scientific Research, Kuwait

<sup>2</sup>Ain Shams University, Cairo, Egypt

#### Abstract

The present paper investigates experimental testing of fire resistance of concrete flexural elements (beams and slabs) reinforced by GFRP rebars. Three beam specimens were used in the fire exposure testing with emphasis on their ability to sustain loads under fire exposure. One specimen was reinforced with ordinary steel rebars and the other two specimens were reinforced with GFRP rebars. The effect of concrete quality on fire resistance was examined. Sustained loads on beams specimens under fire exposure testing were 60% of the ultimate loads. Behavior of the beams up to failure was observed. Large reduction in fire resistance due to the use of GFRP rebars was observed. Three slabs were also tested and evaluated.

**Key Words:** Fire resistance, GFRP, beams, rebars.

#### Introduction

Fiber Reinforced Plastic (FRP) is an advanced composite made of fibers embedded in a polymeric resin under high temperatures. The material has several potential benefits over conventional steel reinforcement. One of the main concerns of structural engineers regarding fiber reinforced polymers (FRP) rebars as main reinforcement in concrete constructions, is their fire resistance characteristics and performance under fire exposure. This issue has precluded the widespread employing of FRP rebars in building constructions. The present paper investigates the performance of concrete beams reinforced by FRP rebars under fire exposure with emphasis on their carrying capacity and ability to sustain loads under fire exposure.

The data available on the behavior of FRP under fire exposure and at high temperature are very scarce. ACI committee 440 in its two documents reported only values on the coefficient of thermal expansion of some types of FRP along with some design data related to the minimum reinforcement for temperature and shrinkage [1, 2]. ISIS Canada, Design Manual 3 [3], and the fire testing data by Abbasi and Hogg [4] are some of the few reports and articles that include data on the effect of high temperature on some types of FRP rebars. A model for predicting the behavior of FRP reinforced beams under simulated fire is also available [5].

The purpose of the present experimental investigation is to study the fire resistance and the performance of beams reinforced with glass FRP (GFRP) rebars when subjected to fire and to compare the results to specimens reinforced with conventional steel reinforcement. The specimens were loaded (i.e. load is sustained on the specimens) during the exposure to fire (i.e. fire endurance test).

The study is part of an ongoing project conducted by Kuwait Institute for Scientific Research (KISR) and funded by Kuwait Foundation for the Advancement of Sciences (KFAS) to examine the feasibility of employing FRP rebars as reinforcement in concrete constructions.

## **Testing Program**

The testing program focused on the fire resistance of structural members reinforced with FRP bars. As no codes or design data are available regarding the fire resistance of structural members reinforced with FRP, it was decided to evaluate the fire resistance through subjecting members to a standard fire according to the recommendation of ASTM E119 [6] and ISO 834 [7].

## **Test Specimens**

The experimental program included three beams. One beam was reinforced with steel reinforcement and the other two beams were internally reinforced by GFRP bars. Table 1 gives the configuration of the tested beams. Figure 1 shows the reinforcement details. The simply supported beams were loaded by a point load in the beam mid span (clear span = 100 cm).

**Table 1. Configuration of Tested Beams** 

Beam	Concrete Grade	Section (om)		Concrete Cover	Bottom	Тор	Stirrups		
I.D.		(cm)	Rft.	Rft.					
B1	25	15	25	25 2.5		2Ф10	7 φ 8		
DI	23	13	25	2.3	Steel	Steel	Steel		
B2	25	15	25	2.5	3 # 4	2Ф10	7 φ 8		
DZ	23	13	23	23	23		GFRP	Steel	Steel
В3	15	15	25 2.5	2.5	3 # 4	2Ф10	7 φ 8		
ВЗ	13	13		2.3	GFRP	Steel	Steel		

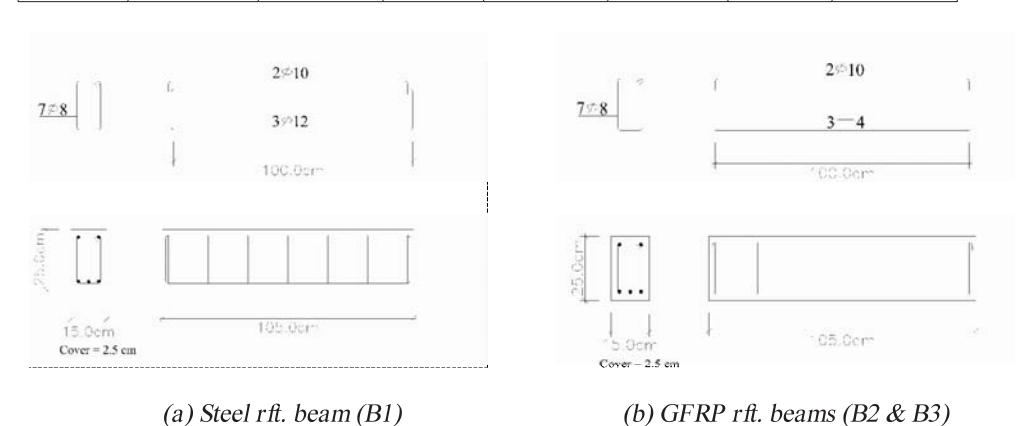


Fig. 1. Reinforcement details of beams.

In addition, three slabs with thickness of 10cm were included in the experimental program. One slab was reinforced by steel reinforcement and the other two with GFRP bars. The 4 sides simply supported slabs were loaded by a load applied on a loading area of 20x20cm at the center of the slabs (clear span = 100 cm). Slab S3, had spliced GFRP reinforcement in one direction with an overlap length of 35cm. The reinforcement details of the three slabs are shown in Table 2.

## **Material and Mixture Proportions**

Ordinary Portland cement was used in the concrete mixes. Natural siliceous sand with fineness modulus of 2.6 was used. Crushed stone (i.e. dolomite) with nominal maximum size of 28mm, absorption 1.3%, and Los Angles value of 26.2% was used in the concrete mixtures. The fresh concrete had a slump value ranging from 60mm to 80mm. Table 3 gives the proportions for the two concrete mixtures used in the investigation. The compressive strength, the splitting tensile strength and the modulus of elasticity for the used concrete mixtures are given in Table 4. The modulus of elasticity was measured according to ASTM C469. The measured modulus is the Secant Modulus between a stress of 0.5MPa and 1/3 of the compressive strength of the concrete.

**Table 2. Configuration of Tested Slabs** 

Slab I.D.	Concrete Grade (MPa)	Slab Thickness (cm)	Concrete Cover (cm)	Type of Rft	Remarks
S1	25	10	2.5	Steel	No splice
S2	25	10	2.5	GFRP	No splice
S3	25	10	2.5	GFRP	Middle Splice

**Table 3. Ingredients Proportions of Concrete Mixtures** 

Ingredient	Concrete Grade 15 MPa	Concrete Grade 25 MPa
Cement (kg/m <sup>3</sup> )	250	350
Sand (kg/m <sup>3</sup> )	663	630
Stone (kg/m <sup>3</sup> )	1209	1149
Water (lit/m <sup>3</sup> )	201	205

**Table 4. Properties of Concrete Mixtures** 

Concrete Grade	Compressive Strength (MPa)	1 0	Modulus of Elasticity (GPa)
15 MPa	20	1.69	21.2
25 MPa	30	2.3	26.7

The tensile strength of the type of steel used for reinforcement is 518 MPa, while the yield strength is 412 MPa. The nominal tensile strength for the GFRP bars was given by the manufacturer as 600 MPa, while the modulus of elasticity is 40.8 GPa.

Thermocouples of Type K were inserted inside the specimens at different locations during casting in order to monitor the temperature inside the specimens during the fire test. Seven thermocouples were used for each beam. Figure 2 shows the locations of the thermocouples inside the specimens.

## **Test Setup**

Beams (B1 and B2) were loaded by a point load up to 60 kN, while beam B3 was loaded by a point load up to 40 kN before being exposed to fire. The load was sustained on the tested beams during fire exposure and up to the beams' failure. The sustained load for beams (B1 and B2) was selected to represent about 60% of the ultimate load of beam B1 (see Table 5). The sustained load for beam B3 also represents about 60% of the ultimate load for that beam. Figure 3 shows the testing setup of the beams.

Slabs S1, S2 and S3 were loaded using a steel plate of dimensions 20x20cm up to 30kN before being exposed to fire. The load was sustained on the tested slabs during fire exposure and up to the slabs' failure. The sustained load for all slabs was selected to represent about 60% of the ultimate load of slab S1

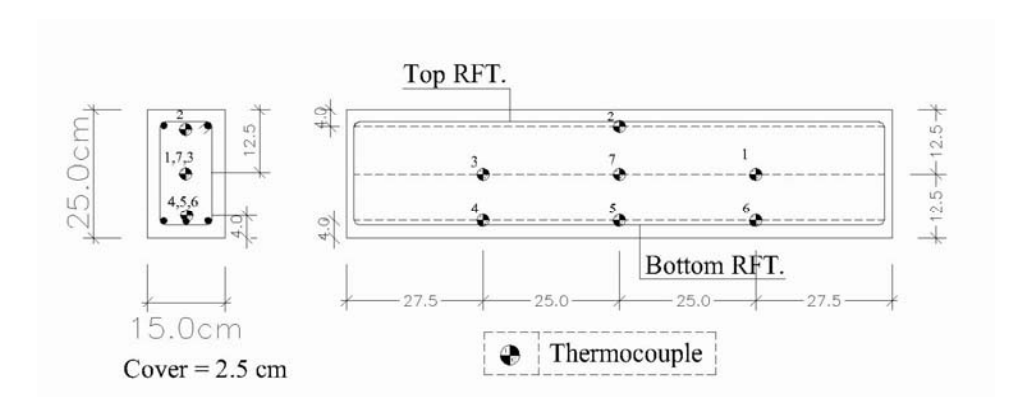


Fig. 2. Location of thermocouples inside the specimens.

Beam	f'c (MPa)	f <sub>u</sub> (MPa)	fy (MPa)	A <sub>s</sub> (mm <sup>2</sup> )	P <sub>ult</sub> (kN)
B1	25	518	420	339	103
B2	25	600	-	389	80
B3	15	600	_	389	68

**Table 5. Ultimate Loads of Beams Specimens** 

The deflection of the tested specimens was planned to be measured using dial gauges but due to the very high temperature around the specimens it could not be recorded.

The fire temperature inside the oven (i.e. furnace) followed the recommendation of ASTM E119 (ASTM, 1983) and ISO 834 (ISO, 1999). The maximum temperature that could be reached inside the oven was 1000°C. The temperature inside the oven (i.e. temperature measured underneath the tested specimens) and temperature inside the tested specimens were recorded every 5 minutes and up to failure of the specimens. Figure 4 shows typical measured fire temperature inside the oven.

#### **Test Results and Discussion**

During the fire test of beams (B1) and (B2), the sheath protecting thermocouples number 4, 5 and 6 (located at the bottom reinforcement along the beam) was damaged, and the thermocouples did not record temperature measurements.

Figure 5 shows one of the beams during fire testing while Fig. 6 shows the temperature measurements inside beam (B1) with steel reinforcement versus time up to failure. Temperature measurements showed fluctuations during the first 50 minutes, which could be attributed to lack of sufficient protection to the thermocouples from the surrounding high temperature (i.e. beam B1 was the first specimen to be tested). The beam started to fail at 85 minutes with excessive deflection and cracking. The beam totally failed at 90 minutes. The average oven temperature at failure was 980°C. The temperature inside the beam (i.e. at 12.5cm from the bottom surface of the beam) at failure ranged between 400 and 500°C.

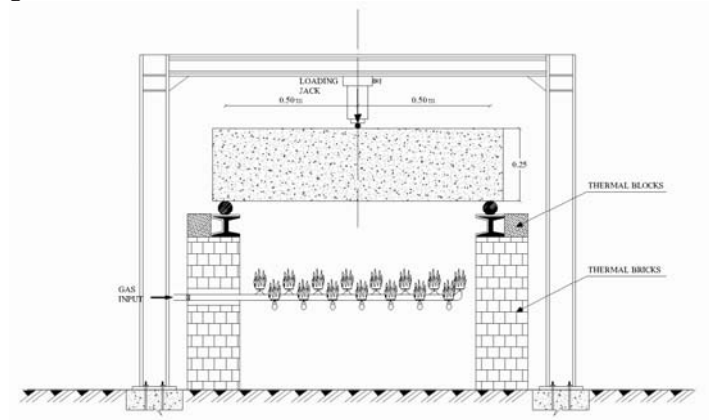


Fig. 3. Test setup of beams.

Figure 7 shows the temperature measurements inside beam (B2) with GFRP bars with time up to failure. Similar to Beam (B1), thermocouples number 4, 5, and 6 located at the bottom reinforcement did not record any measurement due to the damage of the sheathing around the thermocouple. Slight fluctuation in the measured temperatures was observed as thermocouples were protected in order to reduce the fluctuation in the measured temperatures. The beam started to fail at 40 minutes with excessive deflection and cracking (Fig. 8). The beam totally failed at 45 minutes. The average oven temperature at failure was 870°C. The average temperature inside the beam (i.e. at 12.5cm from the bottom surface of the beam) at failure ranged from 100 to 160°C. With the increase in temperature, the beam color got darker and wide cracks were formed. Because of extensive wide cracks at failure, the bottom GFRP bars were locally burnt at the location of the wide cracks and liquid polymer seeped out.

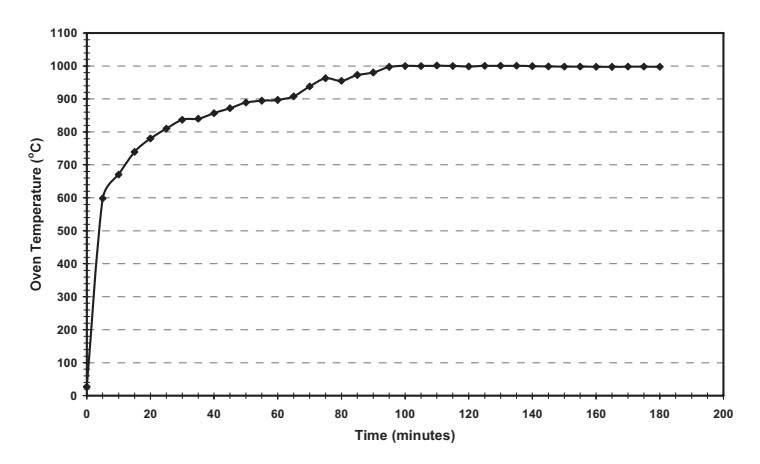


Fig. 4. Typical measured fire temperature inside the oven.

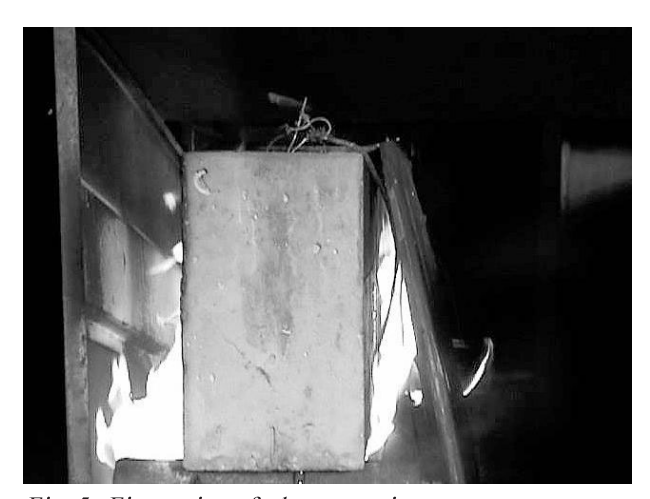


Fig. 5. Fire testing of a beam specimen.

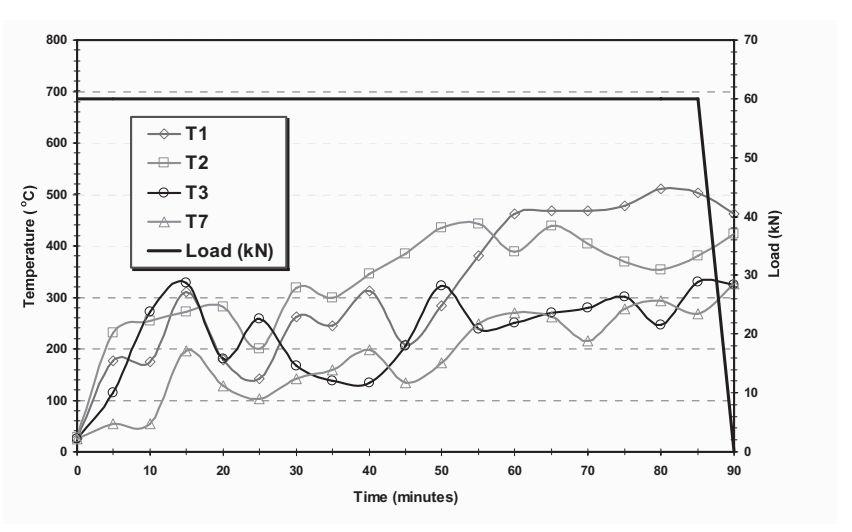


Fig. 6. Temperature measurements inside beam B1 with time.

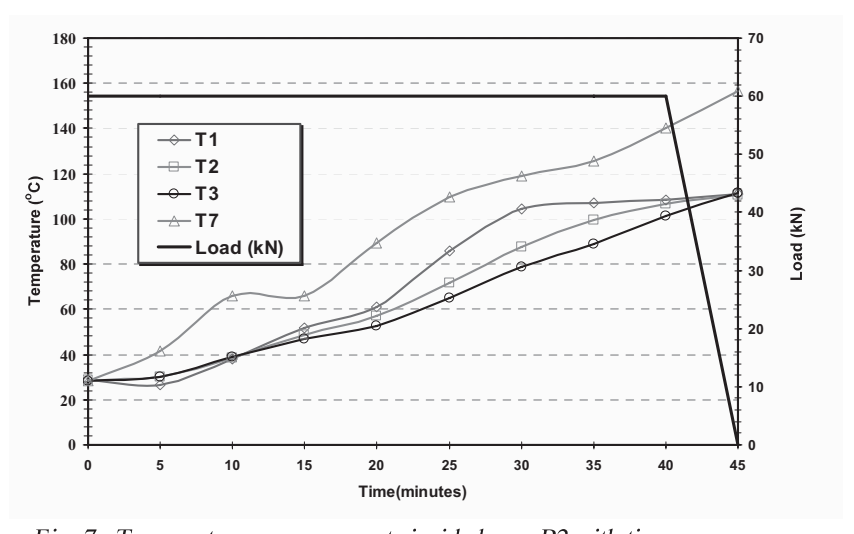


Fig. 7. Temperature measurements inside beam B2 with time.

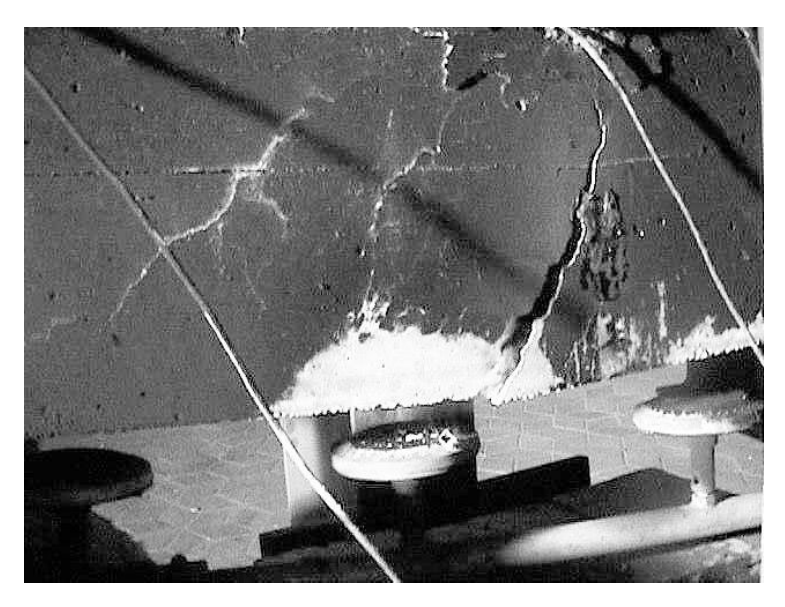


Fig. 8. Fire penetrating cracks in a beam specimen.

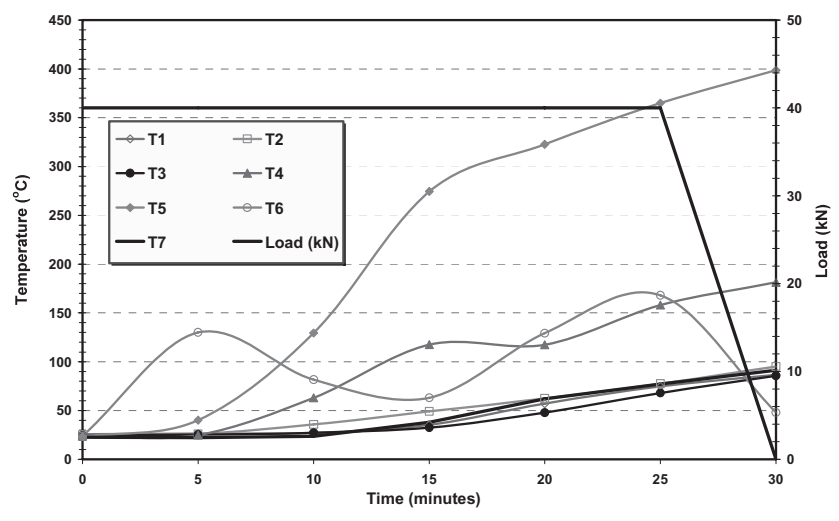


Fig. 9. Temperature measurements inside beam B3 with time.

Figure 9 shows the temperature measurements inside beam (B3) with GFRP bars with time up to failure. In this test, the bottom thermocouples were better protected to prevent the damage of the sheath around the thermocouple. Yet, thermocouples number 4 and 6 showed fluctuation in the measured temperature. The beam started to fail at 25 minutes with excessive deflection and cracking. The beam totally failed at

30 minutes. The average oven temperature at failure was 830°C. The temperature at 4.0cm from the bottom surface of the beam at failure was about 400°C. The average temperature inside the beam (i.e. at 12.5cm from the bottom surface of the beam) at failure ranged between 100 and 160°C. As for beam B2, the beam got darker in color and wide cracks were formed at lower temperatures compared to beam B2, due to the lower grade concrete. Because of these extensive wide cracks at failure, the bottom GFRP bars were locally burnt at the location of the wide cracks. Figure 10 shows the burnt bars.



Fig. 10. GFRP bars after fire.

Table 6 gives the summary of the tested beams. The steel reinforced beam (B1) sustained the applied load under the exposure of fire more than the GFRP reinforced beam (B2), despite the average oven temperature (i.e. fire temperature) at which the steel reinforced beam (B1) failed at was higher than that for the GFRP reinforced beam (B2). On the other hand, comparing GFRP beams (B2) and (B3), it was found that reducing the concrete grade from 25 MPa to 15 MPa reduced the time needed to reach failure under the sustained load, taking into consideration the difference in the applied load. The average oven temperature at which both beams (B2) and (B3) failed was almost the same.

The replacement of steel reinforcement by GFRP bars resulted in a reduction in the fire resistance of beams by 50%. This is mainly attributed to the formation of wide cracks which facilitated the way for the fire to reach the easily burned GFRP bars. The use of lower grade concrete resulted in a reduction in fire resistance of about 33% as the lower grade concrete is easily cracked which in turn attributed to the spread of fire inside the beam and the burning of the GFRP bars.

It must be also noted that while the same sustained loads for beams B1 and B2 were used, the ultimate loads for the two beams are different, which makes the sustained load reach 60% for beam B1 and about 75% for B2 from the load carrying capacity of the two beams, respectively. This in turn attributed to the large reduction in the fire resistance of B2 compared to B1.

**Table 6. Test Results of Tested Beams** 

Beam I.D.	Concrete Grade (MPa)	Sustained Load (kN)	Type of Rft.	Time to failure (minutes)	Average Oven Temp. at Failure (°C)
B1	25	60	Steel	90	980
B2	25	60	GFRP	45	870
В3	15	40	GFRP	30	830

Figure 11 shows the fire chamber for slabs while figure 12 shows the temperature measurements inside slab (S1) with steel reinforcement versus time up to failure. Temperature measurements for thermocouple number 1 showed slight fluctuation. The slab started to fail at 175 minutes with excessive deflection and cracking. The slab totally failed at 180 minutes. The average oven temperature at failure was about 1000°C. The temperature inside the slab (i.e. at about 4.0cm from the bottom surface of the slab) at failure ranged between 300 and 450°C. The temperature at 2.0cm under the top surface of the slab (thermocouple number 2) at failure was 200°C.

Table 7 gives summary of the tested slabs. The steel reinforced slab (S1) sustained the applied load under the exposure of fire more than the GFRP reinforced slabs (S2 and S3), also the average oven temperature (i.e. fire temperature) at which the steel reinforced slab (S1) failed at was higher than that for the GFRP reinforced slabs (S2 and S3). On the other hand, comparing GFRP slabs (S2) and (S3), it was found that introducing splices in the GFRP reinforcement slightly reduced the time needed to reach failure under the sustained load. The average oven temperature at which both slabs (S2) and (S3) failed was almost the same.



Fig. 11. Fire chamber for slabs.

Table 7. Test Results of Slabs

Slab I.D.	Concrete Grade (MPa)	Sustained Load (kN)	Type of Rft.	Time to failure (minutes)	Average Oven Temp. at Failure (°C)
S1	25	30	Steel	180	1000
S2	25	30	GFRP	50	890
S3	25	30	GFRP	45	870

The average fire resistance of the slabs reinforcement with GFRP is only about 26% of that of the slab reinforced with conventional steel reinforcement. The main reason for that is the formation of wide cracks which facilitated the way for the fire to reach the easily burned GFRP bars. The gel resulted from the burning of the polymer part of the GFRP may be seen in most cases. Even at failure, the temperature at top fibers of slab S2, figure 15, only reached 100°C and the bottom fibers reached about 300°C. This enhances the conclusion that failure was due to the burning of GFRP bars through the formed wide cracks and not due to thermal failure of concrete which can not take place at those relatively moderate temperatures. The use of spliced GFRP bars did not result in a noticeable additional reduction in the fire resistance.

As for the beams, it must be also noted that while the same sustained load for all slabs was maintained, the ultimate loads for the three slabs are different, which makes the sustained loads reach higher percentages of the load carrying capacities of slabs S2 and S3 than for S1. This in turn attributed to the large reduction in the fire resistance of S2 and S3 compared to S1.

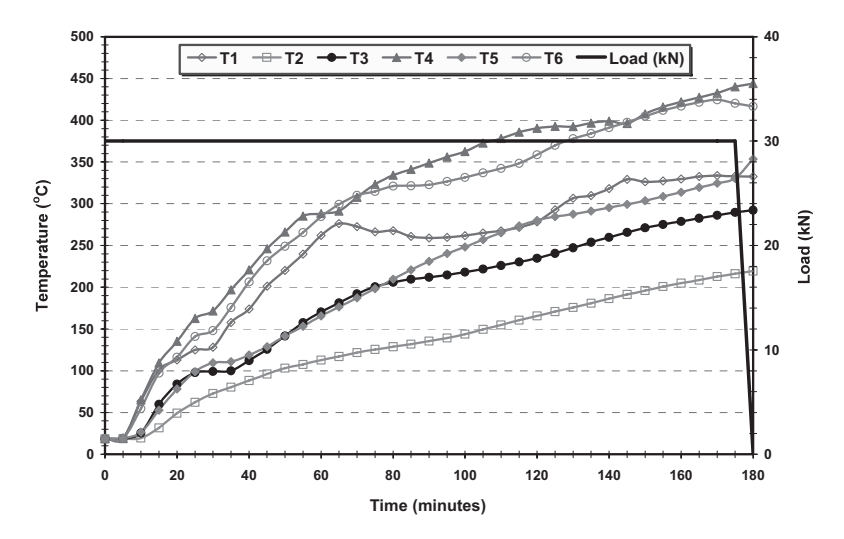


Figure 12. Temperature measurements in slab S1 versus time.

#### **Conclusions**

Fire tests of concrete beams and slabs reinforced with GFRP bars and with conventional steel bars for comparison were performed. Fire resistance and temperature distribution through samples were determined. Sustained loads were maintained during testing to represent actual behaviour of structural members during service. Behaviour of the beams up to failure, including cracks formation, changes in colour and types of failure, was observed. Effect of using concrete of different compressive strength was also investigated. The following may be concluded:

- Large reduction in fire resistance due to the use of GFRP was observed. The reduction reached 50% for beams.
- Failure was mainly due to fire penetration through the wide cracks developed during testing. This resulted in the burning of the GFRP matrix. This in turn caused interface cracking and debonding of bars and eventually failure.
- Due to the reduction in the fire resistance, failure may take place at relatively low temperatures compared to the actual furnace temperature. In one of the tests, failure took place while the temperature at top fibers was only 100°C.
- Using lower quality concrete resulted in additional reduction in the fire resistance as more and wider cracks were formed resulting in faster burning of the GFRP bars.
- In order to assure the required fire resistance, GFRP bars should be protected. This may be achieved by using thicker denser concrete covers. Special materials may be applied to increase the fire resistance. Compartmentation may be also applied.
- Additional research may be needed to investigate different approaches to increase the fire resistance of concrete members reinforced with FRP in order to meet necessary requirements.

### References

- ACI Committee, September 2000, "Guide for Design and Construction of Externally Bonded FRP Systems for Strengthening Concrete Structures" Reported by ACI Committee 440.
- 2. ACI Committee, January 2001, "Guide for Design and Construction of Concrete Reinforced with FRP Bars" Reported by ACI Committee 440.
- 3. ISIS Canada, 2001 "Reinforcing Concrete Structures with Fiber Reinforced Polymer", Design Manual 3.
- 4. Abbasi, A. and Hogg, P.J., 2006, "Fire Testing of Concrete Beams with Fibre Reinforced Plastic Rebars", Composites, Part A: Applied Science and Manufacturing, Vol. 37, Issue 8, PP 1142-1150.
- 5. Abbasi, A. and Hogg, P.J., 2005, "A Model for Predicting the Properties of the Constituents of Glass Fibre Rebar Reinforced Concrete Beam at Elevated Temperature Simulating a Fire Test", Composites, Part B: Engineering, Vol. 36, Issue 5, PP 384-393.
- 6. ASTM-E119, 1983,"Methods of Fire Tests of Buildings Construction and Materials", American Society for Testing and Materials.
- ISO 834, 1999 "Fire-resistance Tests- Elements of Building Construction", International Organization of Standards.

# Improvement in Durability of Concrete with Partial Replacement of Cement by Ground Granulated Blast Furnace Slag

Saud Al-Otaibi, Moetaz El-Hawary, Ali Abdul-Jaleel Division of Environmental and Urban Development, Kuwait Institute for Scientific Research, Kuwait

## **Abstract**

The Kuwaiti environment, defined as hot marine environment, is a very aggressive environment for concrete. One of the main reasons for the apparent premature deterioration of concrete structures in Kuwait is exposure to chlorides, available in soils, ground water and seawater that may even reach inland structures through water laden wind. Chlorides cause corrosion in steel reinforcement. The replacement of certain percentages of cement with some a supplementary cementitious material such as ground granulated blast furnace slag can assist in improving the durability of concrete.

This paper presents the results of an investigation on the use of slag-blended cements in the production of normal-strength concrete with nominal strengths of 40 MPa. Slag replacement levels studied were 0%, 50%, 60%, and 80%. This investigation studied the chloride permeation resistance properties of slag concretes. The results show that good compressive strength can be obtained with different slag levels replacing ordinary cements as all the mixes reached 40 MPa at 90 days and maintained the same strength at later ages. The water curing (WC) clearly gives higher strength values than dry curing (DC) which shows the importance of curing for concrete and more important in slag blended concrete mixes. Slag concrete is highly resistant to chloride permeability.

**Key Words:** Ground granulated blast furnace slag; Durability; Chloride; Permeability.

#### Introduction

The severe environmental conditions in Kuwait resulted in many cases of concrete deterioration as reported by several researchers. The need for a more durable concrete is very clear. The deterioration of concrete in general is caused by different factors. Some related to the exposure conditions that concrete faces such as high temperature, the salt laden environment, etc. Others related to the concrete constituent materials, which could be contaminated or may be of poor quality. Improving the quality of concrete can be achieved by improving the concreting practices on workmanship, in addition to the proper selection of concrete materials.

The weather in Kuwait, in general, is characterized as hot marine environment. Due to these special characteristics, concrete is subjected to chlorides responsible for the corrosion of reinforcement. The use of supplementary cementitious materials, in which part of cement is replaced by pozzolanic materials, increases the concrete resistance to chloride ingress. Among those useful, supplementary cementitious materials available is granulated blast furnace slag which is generally by-product resulting from the steel industry.

GGBS has been used in composite cements and as a cementitious component of concrete for many years. The first industrial commercial use (about 1859) was the production of bricks using unground GBS. In the second half of the 19th century the cementitious properties were discovered and by the end of 19<sup>th</sup> century the first cements containing GBS were produced. Since the late 1950's the use of GGBS as a separately ground material added at the concrete mixer together with Portland cement has gained acceptance. World-wide, it can be expected that the expansion of GGBS use will continue for the foreseeable future (Euroslag, 2003). As an example, in the year 2000 GGBS accounted for about 10%, of the total cementitious material used throughout UK (Higgins et al. 2001).

The use of GGBS is now specified in the following international standards:

- European Standard EN 197-1: Cement Part 1, Composition, specifications and conformity criteria for common cements (2000)
- British Standard BS 6699: Ground granulated blastfurnace slag for use with Portland cement (1992)
- ASTM C 989: Ground granulated blast-furnace slag for use in concrete and mortars (1999).

The reduction in chloride penetration achieved by GGBS has been confirmed by many different investigators and would appear to be due to two mechanisms. Firstly, GGBS reduces the permeability of the concrete; secondly, it binds the chloride adsorptively and thus interrupts the concentration of gradient needed for diffusion (Page, *et al.*, 1981, Arya and Xu, 1995, Al-Bahar, *et al.* 1998, Roy *et al.* 2000, Leng *et al.*, 2000, Pal *et al.*, 2002 Al-Otaibi, 2002).

## Methodology

## **Concrete Mixing**

A set of normal and high-strength mixes incorporating slag in four different levels of cement replacement (0, 50, 70, 80) were designed and patched following the ACI manual of concrete practice (ACI: Part 1, 211.1-91, 211.4R-93, 363R-92 and ACI 233R-95, 2001).

The details of the materials and mixes are presented in the following sections:

*Materials:* The same type of ordinary Portland cement, ground granulated blast-furnace slag, fine and coarse aggregates have been used throughout the investigation. Details of each material used are given below.

- **Cement** Ordinary Portland cement, from Kuwait Cement Company, conforming to the requirements of BS 12:1996 class 42.5 N, was used in this investigation. The chemical and physical properties of the cement, as provided by the manufacturer, are given in Table 1.
- **Slag.** The ground granulated blast-furnace slag (GGBS) used was obtained from the Falcon Cement. It complied with BS 6699:1992. Typical chemical and physical properties provided by the manufacturer are shown in Table 2.
- **Aggregates.** Medium graded sand and 20-mm and 10-mm crushed gravel complying with BS 882:1992 were used in this investigation.
- **Admixtures.** A high performance concrete superplasticiser based on modified polycarboxylic ether was used to get the desired workability.
- Water. Potable tap water available at the laboratory was used throughout the investigation.
- Concrete Mixes. The proportioning of a concrete mixture is based on determining the quantities of the ingredients which, when mixed together and cured properly will produce reasonably workable concrete that has a good finish and achieves the desired strength when hardened. This involves different variables in terms of water to cement ratio, the desired workability measured by slump (60-100 mm) and cement content and aggregate proportions. Several trial batches were made to arrive at mix proportions that achieve the designated targets in terms of strength (35- 40 MPa) and workability. The mixes that were selected are presented in Table 1.

Table 1. Chemical and Physical Properties of Cement

Oxide	Percent	Physical Properties
$SiO_2$	20.7	Specific Surface: 331 m <sup>2</sup> /kg
$Al_2O_3$	5.7	Average particle size: 10 m
Fe <sub>2</sub> O <sub>3</sub>	2.3	Coarse particles (>45 m): 11.2%
CaO	64.8	Specific gravity: 3.14
MgO	1.1	Loss on ignition: 0.92%
SO <sub>3</sub>	3.21	Colour: Steel grey
Na <sub>2</sub> O	0.19	
K <sub>2</sub> O	0.6	

Table 2. Chemical and Physical Properties of GGBS

Oxide	Percent	Physical Properties
SiO <sub>2</sub>	37	Specific Surface: 401 m <sup>2</sup> /kg
$Al_2O_3$	12	Specific gravity: 2.91
Fe <sub>2</sub> O <sub>3</sub>	0.55	Colour: White
CaO	41	
MgO	8	
$SO_3$	0.1	
N <sub>2</sub> O	0.35	
K <sub>2</sub> O	0.5	

**Table 3. Mix Proportions** 

Mix No.	Slag kg/m <sup>3</sup>	OPC kg/m <sup>3</sup>	Admix. ml	Water kg/m <sup>3</sup>	Fine Agg. kg/m <sup>3</sup>	10 mm kg/m <sup>3</sup>	20 mm kg/m <sup>3</sup>	w/b %
NSC and SRN	0	390	0	210.6	522	401.94	816.06	0.54
SG50	195	195	0	179.4	522	401.94	816.06	0.46
SG60	246	164	3280	176.3	550	405.9	824.1	0.43
SG70	301	129	4300	172	590	402.6	817.4	0.40
SG80	360	90	5850	166.5	590	402.6	817.4	0.37

#### **Results and Discussion**

## Physical and Mechanical Properties

Concrete specimens were cast and cured under moist and dry curing condition. They were tested at different ages for compressive strength using 100mm cubes. The results are presented in Fig. 1. These results indicate that good compressive strength can be obtained with different slag levels replacing ordinary cements as all the mixes reached 40 MPa at 90 days and maintained the same strength at later ages. The water curing (WC) clearly gives higher strength values than dry curing (DC) which shows the importance of curing for concrete and more important in slag blended concrete mixes.

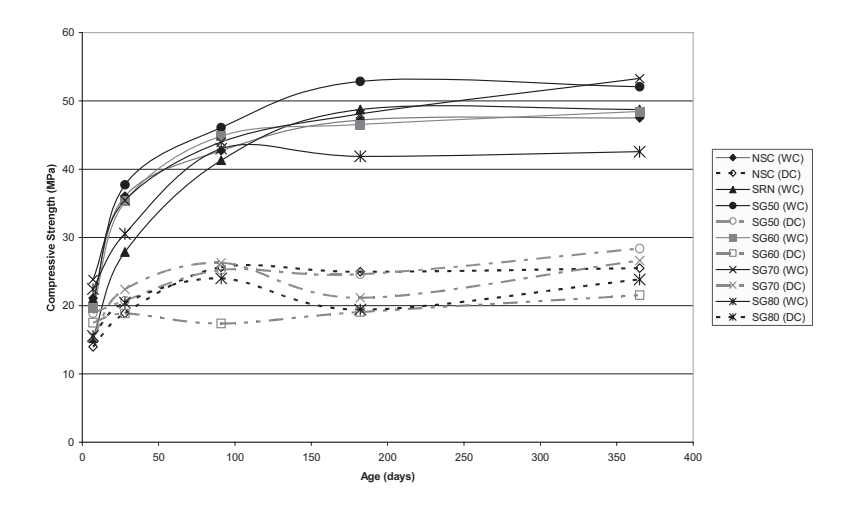


Fig. 1. Development of compressive strength.

**Chloride penetration test:** The test was conducted according to ASTM: C 1202 - 91. This test is convenient, known as Standard Method of Test for Electrical Indication of Concrete's Ability to Resist Chloride Ion Penetration. The results presented in Fig. 2 indicate the high resistant of slag concrete to chloride permeability.

**Chloride ponding test:** Chloride content was measured by taking drilled specimens from the concrete slabs at depths from 1 to 3 cm. The results shown in Fig. 3 indicate the lower concentration for the slag concrete specimens.

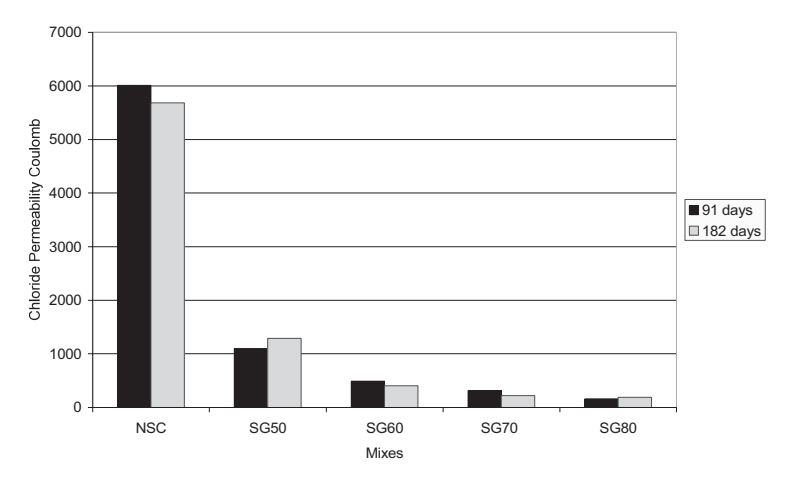


Fig. 2. Chloride permeability.

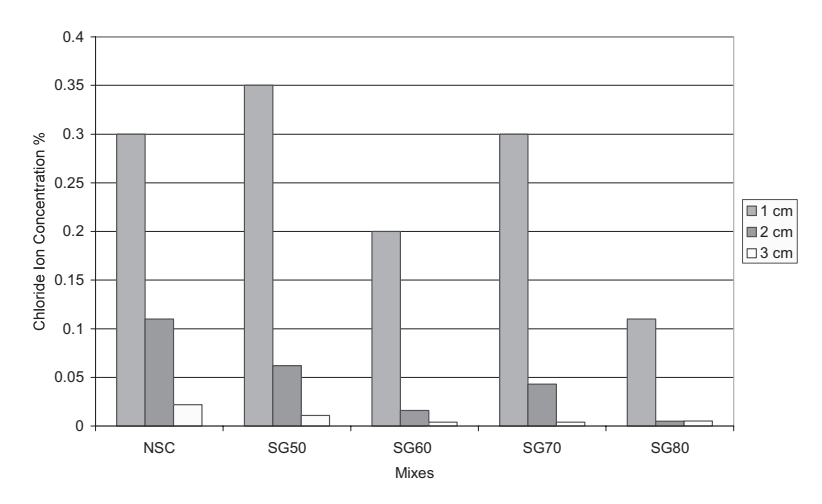


Fig. 3. Chloride ion concentrations.

## Cost-Benefit Analysis

Cost estimates were carried out based on collected information from the local market. The details of those estimates are presented in Tables 4 and 5 using the lowest and the highest prices respectively for both fine aggregate and admixtures. It is shown that on average slag concrete costs 8% higher that normal OPC concrete. The good performance justifies, in certain exposure conditions, the extra cost incurred.

Table 4. Cost Estimates Using the Lowest Prices of both Fine Aggregate and Admixtures

Mix	Price	Price	Price	Price	Price	Price		Total
Type	slag	cement	Water	Fine	10mm	20mm	Admix.	Price
	K.D./m <sup>3</sup>							
NSC	0	10.53	0.043	0.363	2.643	5.222	0	18.800
SG50	8.25	5.265	0.037	0.363	2.643	5.222	0	21.780
SG60	12.3	4.428	0.036	0.382	2.669	5.274	0.328	25.417
SG70	15.05	3.483	0.036	0.410	2.647	5.231	0.43	27.287
SG80	18	2.43	0.035	0.410	2.647	5.231	0.585	29.338

Table 5. Cost Estimates Using the Highest Prices of both Fine Aggregate and Admixtures

Mix Type	Price slag	Price cement	Price Water	Price Fine	Price 10mm	Price 20mm	Admix.	Total Price
	K.D./m <sup>3</sup>							
NSC	0	10.53	0.043	0.394	2.643	5.222	0	18.831
SG50	8.25	5.265	0.037	0.394	2.643	5.222	0	21.811
SG60	12.3	4.428	0.036	0.415	2.669	5.274	0.82	25.942
SG70	15.05	3.483	0.036	0.445	2.647	5.231	1.075	27.967
SG80	18	2.43	0.035	0.445	2.647	5.231	1.4625	30.250

#### Conclusions

- 1. Good compressive strength can be obtained with different slag levels replacing ordinary cements as all the mixes reached 40 MPa at 90 days and maintained the same strength at later ages.
- 2. The water curing (WC) clearly gives higher strength values than dry curing (DC), which shows the importance of curing for concrete and more importantly in slag blended concrete mixes.
- 3. Slag concrete is highly resistant to chloride permeability.
- 4. Slag concrete costs 8% higher that normal OPC concrete. The good performance justifies, in certain exposure conditions, the extra cost incurred.

#### References

- ACI 233R-95, (2001), 'Ground Granulated Blast Furnace Slag as a Cementitious Constituent in Concrete', ACI Manual of Concrete Practice, Part 1: Materials and General Properties of Concrete, Detroit, Michigan.
- ACI 211.1-91, (2001), 'Standard Practice for Selecting Proportions for Normal, Heavyweight, and Mass Concrete', ACI Manual of Concrete Practice, Part 1: Materials and General Properties of Concrete, Detroit, Michigan.

- Al-Bahar, S., Abduljaleel, A. and Abdul-Salam, S., (1998), "Performance of Slag Concrete" Kuwait Institute for Scientific Research, Report No. KISR5264, Kuwait.
- Al-Otaibi, S. (2002), 'Performance of alkali-activated slag concrete', PhD Thesis, University of Sheffield.
- Arya, C. and Xu, Y., (1995), "Effect of Cement Type on Chloride Binding and Corrosion of Steel in Concrete", Cement and Concrete Research, Vol. 25, No. 4, pp 893-902.
- ASTM C 989 (1999), 'Ground granulated blast-furnace slag for use in concrete and mortars', American Society for Testing and Materials, USA.
- BS 6699 (1992), 'Specification for Ground Granulated Blastfurnace Slag for Use with Portland Cement', British Standard Institution, London.
- European Standard EN 197-1: Cement Part 1, (2000) 'Composition, specifications and conformity criteria for common cements'
- Euroslag, (2003), 'Granulated blast-furnace slag', Technical leaflet.
- Higgins, D., Parrott, L., Sear, L., (2002), 'Effects of ground granulated blastfurnace slag and pulverised fuel ash upon the environmental impacts of concrete', Available at www.concemsus.info.
- Leng, F., Feng, N. and Lu, X., (2000),"An Experimental Study on the Properties of Resistance to Diffusion of Chloride Ions of Fly Ash and Blast Furnace Slag Concrete", Cement and Concrete Research, Vol. 30, pp 989-992.
- Page C.L., Short N.R. and El Taras A., (1981) "Diffusion of Chloride Ions in Hardened Cement Pastes", Cement and Concrete Research, Vol. 11, pp 395-406.
- Pal, S. C., Mukherjee, A. and Pathak, S. R., (2002) "Corrosion Behaviour of Reinforcement in Slag Concrete", ACI Materials Journal, November-December, pp. 521-527.
- Roy, D. M., Jiang, W., and Silsbee, M. R., (2000), "Chloride Diffusion in Ordinary, Blended and Alkali-activated Cement Pastes and its Relation to Other Properties", Cement and Concrete Research, Vol. 30, pp 1879-1884.

## Half-Cell Potential Measurements in Self-Consolidating Concrete

## Farzad Arabpour Dahooei

Concrete Research and Education Center (ConREC)
Tehran, Iran
email: info@aciiranchapter.org

### A. A. Maghsoudi

Kerman University, Kerman, Iran email: maghsoudi.a.a@mail.uk.ac.ir

## F. Faraji,

Kerman University, Kerman, Iran, email: <a href="mailto:ftmfji@yahoo.com">ftmfji@yahoo.com</a>

#### **Abstract**

Marine seawater corrosion has caused severe concrete deterioration over the past decades. Major industrial buildings such as power generation plants, desalination plants and off-shore structures and oil or water piers deteriorate severely in the marine industrial seawater environment due to the deleterious effect of chloride ions.

The half-cell potential technique was used in this study for the evaluation of chloride corrosion of rebar in Self-Consolidating Concrete (SCC) with two different amounts of cement (300 and 500 kg/m³). In addition, the rebars were coated with 3 types of coating: i) epoxy, ii) zinc-rich and iii) zinc-aluminum-rich and were compared with the bare rebar. The SCC specimens were placed in macrocell design according to ASTM G109-92. The open circuit potential of anode and macrocell current were measured for every cycle under alternate wetting and drying conditions to find out the values of rebar corrosion

It can be concluded that the use of SCC with 500 kg/m<sup>3</sup> cement decrease chloride corrosion rate of rebar. Meanwhile, the epoxy was better than other coatings against corrosion.

Key Words: Self Consolidating Concrete, Coated Rebar, Half-Cell Potential.

#### Introduction

Marine seawater corrosion has caused severe concrete deterioration over the past decades. Major industrial buildings such as power generation plants, desalination plants and off-shore structures and oil or water piers deteriorate severely in the marine industrial seawater environment due to the deleterious effect of chloride ions.

Twenty years of investigation and research on the performance of reinforced concrete in the Persian Gulf region concluded that corrosion prevention measures must be an essential and integral part of any concrete practices, and certain corrosion protection systems must be included in new concrete structures [1].

The main frequent cause of corrosion of reinforcement in reinforced concrete structures is chloride attack. Chlorides come from several sources and they can diffuse into concrete as a result of sea salt spray and direct sea water wetting. Further, they can diffuse into concrete due to the application of chloride de-icing salts and at the storage of chloride substances in concrete tanks and like wise [2]. A survey of the condition of a reinforced concrete structure is the first step towards its rehabilitation. A rapid, cost-effective and non-destructive condition survey offers key information on the evaluation of corrosion, and aids in the quality assurance of concrete repair and rehabilitation and in the prediction of remaining service life [3].

The half-cell potential measurement is an electrochemical technique commonly used by engineers to assess the severity of corrosion in reinforced concrete structures. This update explains how various factors can affect the reliability of the data obtained [3].

Self-Consolidating Concrete (SCC) is a new type of concrete. SCC is expected to flow by only its own weight, without influence from external forces or vibration. It is because of that ability, it fills the formwork completely without any voids, it joins to the reinforcement, and it desecrates and levels itself without segregation. To fulfill this request, concrete needs to have special properties in the fresh state. The advantages of SCC offers many benefits to the construction practice; the elimination of the compaction work results in reduced costs of placement, equipment needed on construction, shortening of the construction time and improved quality control [4,5].

## **Experimental Study**

#### Materials Used

The concrete mixtures investigated in this study were prepared with Portland cement type II (Table 1). Continuously graded aggregate with nominal particle size of 12.5 mm and well-graded sand with a fineness modulus of 2.87 were employed. The particle size distributions of both coarse and fine aggregates were within ASTM C-33 limits as shown in Table 2. The relative density values of the coarse and fine aggregates were 2.68 and 2.57 and their absorption rates were 0.6% and 2%, respectively. The superplasticizer used in all mixtures, was Poly-Carboxylic Ether (PCE) and had a specific gravity of 1.03 and PH of 7. In addition, Limestone Powder (LSP) with maximum size of 0.3 mm and relative density of 2.65 was employed.

Table 1. Typical Analysis of Portland Cement

SiO <sub>2</sub>	21.74		
$Al_2O_3$	5.0		
Fe <sub>2</sub> O <sub>3</sub>	4.0		
CaO	63.04		
MgO	2.0		
$SO_3$	2.3		
C1	0.035		
Na <sub>2</sub> O+0.658K <sub>2</sub> O	1.0		
$C_3S$	45.5		
$C_2S$	28.0		
C <sub>3</sub> A	6.5		
C <sub>4</sub> AF	12.2		
Loss on ignition	1.3		
Insoluble Residue	0.6		
Free CaO	1.4		
Fineness (cm <sup>2</sup> /gr)	2900		
Residue on 90 µm sieve	4.0		
(%)			

Table 2. Particle Size Distribution of Coarse and Fine Aggregates (By Mass)

Screen Size (mm)	Coarse Aggregate (% Passing)	Fine Aggregate (% Passing)
19	100	
12.5	99	
9.5	89	100
4.75	4	96
2.36		85
1.18		60
0.6		42
0.3		26
0.15		6

## Properties of Fresh SCC

There is yet no universally accepted standard for characterizing of SCC. Nevertheless, a few testing methods seem to reappear several times in literature and tend to become internationally recognized as suitable methods to characterize the self compatibility of a concrete [6]. The same testing methods such as slump flow, J-ring, L-box and V-funnel tests were prepared in this research (Figs. 1 to 4) and obtained results are shown in Table 3.



Fig. 1. Slump flow test.



Fig.2. J-ring test.



Fig. 3. L-box test.



Fig. 4. V-funnel test.

## Specimens' Preparation and Mix Design

To produce the SCC, the following two mixes, i) SCC with 300 kg/m<sup>3</sup> cement, as the control mix "SC" and ii) SCC included 500 kg/m<sup>3</sup> cement, "SCH" were selected. The properties of concrete mixes design of SCC and compressive strength at 7 and 28 ages are shown in table 3.

For the purpose of macro cell corrosion studies, the concrete specimens of size  $28 \times 11.4 \times 15.2$  cm were designed as per ASTM G109-92. As shown in Fig. 5, in each specimen three reinforced bars of 12 mm diameter with 36 cm length were used as both anode and cathodes.

Table 3. Mixes design of SCC

Mix Labels Material	SC	SCH			
Cement (Kg)	300	500			
Water (Kg)	181	210			
LSP (Kg)	225	100			
Coarse Aggregate (Kg)	750	720			
Fine Aggregate (Kg)	870	800			
PCE (Liter)	3.15	2.50			
W/P*	0.345	0.35			
Fresh Properties					
Slump Flow (mm)	710	690			
L-Box $(h_2/h_1)$	0.89	0.87			
Slump Flow + J-Ring (mm)	7				
V-Funnel, 1 minute (s)	4	3.5			
Compressive Strength (MPa)					
7 days	21	32			
28 days	26	39			

\* P: Cement+LSP



Fig. 5: Concrete specimens according to ASTM G 109-92

#### Potential Measurement Method

By using a high impedance voltmeter and Saturated Calomel Electrode (SCE) as reference electrode, the open circuit potential of steel anode was measured for every cycle under alternate wetting and drying conditions. The duration of every wetting and drying cycle is 14 days.

#### Corrosion Current Measurement Method

Macrocell current flow between anode and cathodes was measured using high-impedance voltmeter. The top and the bottom mat rebar were connected by a  $100\Omega$  resistor and macrocell current was obtained from the relation I=V/100.

## **Total Integrated Current Measurement**

The total integrated current for each coating was calculated based on ASTM G 109-92 by Eq. (1).

$$TC_{i}=TC_{i-1}+[(t_{i}-t_{i-1})\times(i_{i}+i_{i-1})/2]$$
(1)

Where TC= total corrosion (coulombs),  $t_j$  = time (seconds) at which measurement of macro cell current is carried out and  $i_i$  = macrocell current (amps) at time  $t_i$ .

#### **Results and Discussion**

Results of open circuit potential (OCP) of anodes in SC and SCH concrete are shown in Figs. 6 and 7. As we can see in both figure bare rebar has the lowest potential in SC and SCH concrete and epoxy coated rebar has highest potential among other coatings till 5 cycles in SC concrete but after 5 cycles zinc-Al rich coated rebar has the highest potential. In SCH concrete epoxy coated rebar has the highest potential after 8 cycles.

ASTM C 876 gives the criteria that if the corrosion potential is more positive than -120 mV versus the SCE reference electrode, there is less than 10% probability to corrode, and the potential is more negative than -270 mV versus the SCE reference electrode, there is less than 90% probability to actively corrode. For the corrosion potential between -120 mV and -270 mV, the corrosion reaction is uncertain.

Potential of the rebar in both concrete is between -120 mV and -270 mV, so the corrosion reaction is uncertain. This is because the concentration of chloride ions did not reach to threshold value for initiation corrosion reaction.

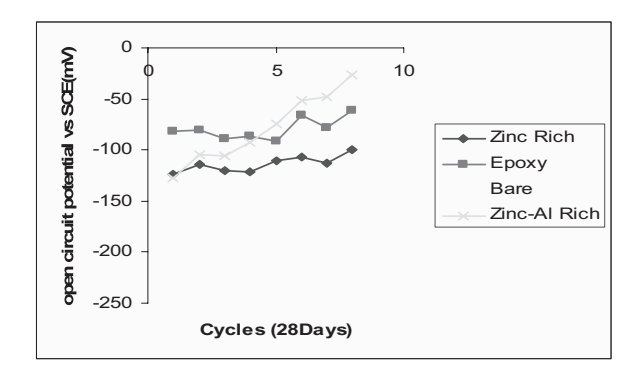


Fig. 6. Open circuit potential of anode rebar in SC.

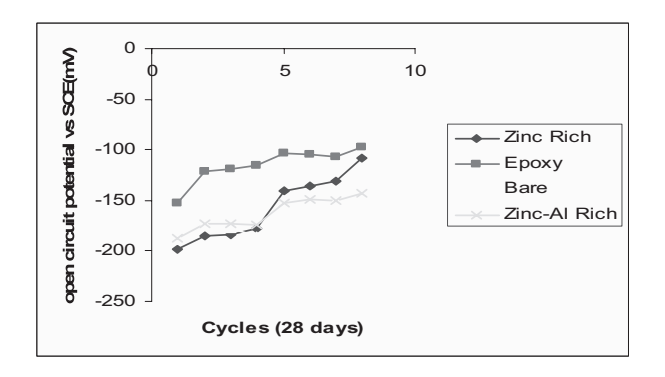


Fig. 7. Open circuit potential of anode rebar in SCH.

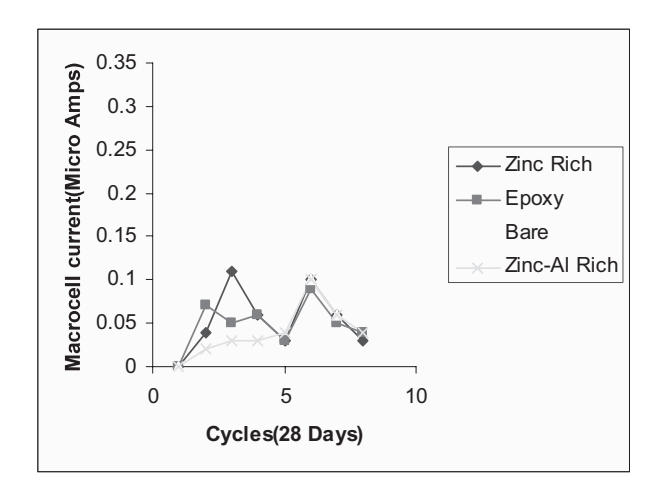


Fig. 8. Macrocell current of rebar in SC concrete.

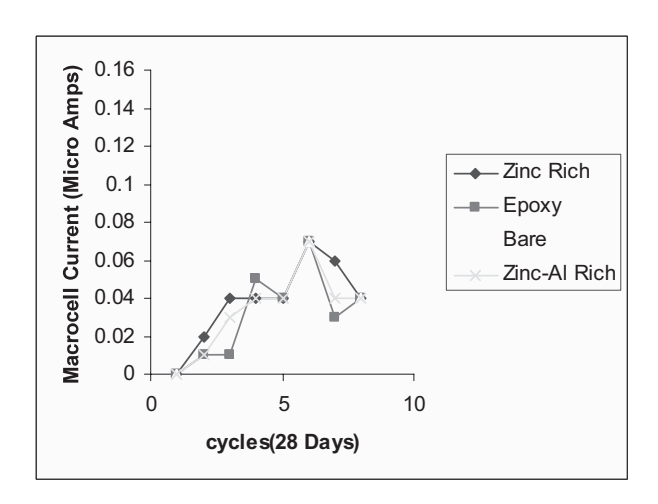


Fig. 9. Macrocell current of rebar in SCH concrete.

Figures 8 and 9 show the macrocell current in SC and SCH. According ASTM G109-92 when the macrocell current is  $10\mu A$  or greater, corrosion is certain. As we can see in both figures, bare rebar has the highest current and this current tends to decrease by time, this behavior can be related to formation of passive layer on the surface of rebar and can be concluded again that concentration of chloride ion does not reach to threshold value for initiation corrosion. In concretes, epoxy and zinc-Al coated rebar have the lowest macrocell current till 5 cycles but after 5 cycles all of the coated rebar has approximately same current value.

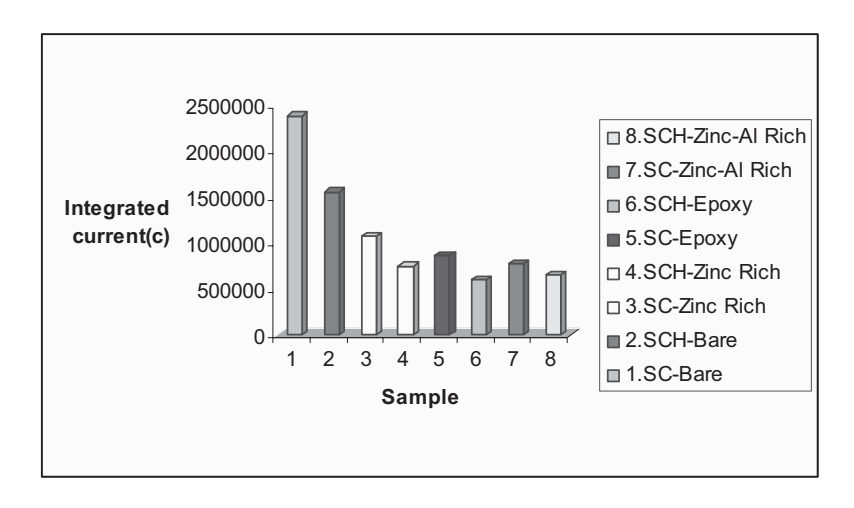


Fig. 10. Integrated current of rebar in SC and SCH.

Figure 10 shows the integrated current which calculated according to Eq. (1). The current of rebar in SC concrete is more than SCH concrete. This is because SCH concrete has more cement than SC concrete in its mix design, so the concrete became more compact and porosity is reduced thus aggressive ions cannot easily diffuse and more time is needed for reaching to threshold concentration.

#### References

- 1. Al-Amoudi, ACI Mat. J., 92(3) (1995) 236–245.
- 2. Zivica, V., "Corrosion of Reinforcement Induced by Environment Containing Chloride and Carbonation", Bull. Mater Sci., Vol. 26, No. 6, Indian Academy of Sciences, October 2003, pp. 605-608.
- 3. Ping Gu and J.J. Beaudoin, "Obtaining Effective Half-Cell Potential Measurements in Reinforced Concrete Structures", Journal of National Research Council of Canada, No. 18, July 1998.
- 4. Takada, K., Pelova, G. I. and Walraven, J. C., "Influence of Mixing Efficiency on the Mixture Proportions of General Purpose Self-Compacting Concrete", *Proceedings of the International Symposium on High-Performance and Reactive Powder Concretes*, University of Sherbrooke, 1998, Volume 1, pp. 19-39.
- Saria, M., Prat, E. and Labastire, J. F., "High-Strength Self-Compacting Concrete, Original Solutions Associating Organic and Inorganic Admixtures", *Proceedings of* the International Symposium on High-Performance and Reactive Powder Concretes, University of Sherbrooke, Canada, 1998, Volume 2, pp. 317-329.
- 6. M. Poppe and G. De Schutter, "Influence of the Nature and the Grading Curve of the Powder on the Rheology of Self-Compacting Concrete," Proceedings of the Fifth CANMET/ACI International Conference Recent Advances in Concrete Technology, Singapore, 2001, pp. 399-414.

# Application of High-Strength and Corrosion-Resistant ASTM A1035 Steel Reinforcing Bar in Concrete High-Rise Construction

S. Faza<sup>1</sup>, J. Kwok<sup>1</sup> and O. Salah<sup>2</sup>

<sup>1</sup>MMFX Technologies Corporation, Irvine, California, U.S.A.

<sup>2</sup>Zamil Holding Group, Saudi Arabia

#### **Abstract**

Concrete reinforcing steel congestion in high-rise structures is a major concern to design engineers. Congestion of the reinforcing steel decreases the efficiency of construction and adds greatly to the cost of construction of high-rise structures. MMFX Microcomposite steel bars (MMFX 2), conforming to ASTM A1035 specification, have high-strength properties that can be utilized to combat this problem. In addition, ASTM A1035 steel bar's distinct microstructure technology provides an answer for the worldwide corrosion problem. The technology that gives ASTM A1035 steel bar its mechanical properties also makes it very corrosion resistant. Independent tests show that the chloride threshold of this uncoated steel is 5 to 6 times greater than that of conventional A615 steel bars and 1.75 greater than 2101 solid stainless steel bars. This paper presents the economical analysis done on the design and construction of different high-rise structures and make recommendations to designers on where cost savings can be realized. The use of ASTM A1035 steel bar reduced the amount of steel in some areas by up to 40% while providing a reduction in the installed cost of the material by 15-25% in the highly congested areas.

#### **Current High-Rise Construction Issues**

#### Reinforcing Steel Congestion

One of the major issues currently facing the concrete construction industry is the congestion of reinforcing steel in structural components. Rebar congestion complicates steel placement, hinders concrete placement, and as a result leads to improper consolidation of concrete around rebar, affecting the integrity of the structure.

#### Reinforcing Steel Corrosion

Another major issue currently facing the concrete construction industry is the corrosion of steel reinforcing in concrete members subjected to corrosive environment. Corrosion of steel reinforcing leads to reduction in strength of the concrete member and causes the deterioration of the surrounding concrete, further damaging the concrete member. Repair and maintenance cost is enormous to address the corrosion issue.

#### Proposed Resolution

Utilizing the higher yield strength at the mat foundation rebar would reduce the amount of reinforcing steel required and this will reduce the congestion. Reduced congestion facilitates concrete consolidation around the rebar and results in safer structures.

Besides the ease of placement of rebar and concrete, the use of higher strength steel reinforcing can be an economical method of construction, by reducing the total tonnage of steel reinforcing, the placement labor, time, etc.

The inherent corrosion resistance property of ASTM A1035 reinforcing steel would also improve the long-term durability of the structure. If water penetrates the waterproofing membrane or if the top of the mat is exposed to water, the water can reach the reinforcing through the anticipated micro-cracks that are inevitable with concrete. ASTM A1035 rebar provides much better performance under these conditions.

#### **ASTM A1035 Steel Rebar Solution**

#### ASTM A1035 Steel Rebar

The strength of ASTM A1035 steel rebars far surpasses conventional steel. The high-strength corrosion-resistant steel bars are produced in 12 and 18m (40 and 60 ft) stock lengths. Alternatively, longer lengths can be produced by using mechanical splices that develop the full strength of the reinforcing bars. Stock 12 and 18 m (40 and 60 ft) length material is generally available in bar sizes [#10 (#3) through #36 (#11)]. Stock material for #10 (#3) through #15 (#5) bars are available in coils commonly used by fabricators for fabrication of ties and spirals. Bar sizes #43 (#14) and #57 (#18) are generally available but these bar sizes are not usually kept in fabricator's inventory.

#### Material Composition

One of the unique features of the ASTM A1035 steel rebar is the chemical composition. The maximum chemical constituent requirements of the ASTM A1035 reinforcing bars are illustrated in Table 1.

Table 1. Maximum Chemical Constituents (Weight %)

Element	Carbon	Chromium	Manganese	Nitrogen	Phosphorus	Sulfur	Silicon
ASTM A1035 Maximum Amount *	0.15%	8 to 10%	1.5 %	0.05%	0.035%	0.045%	0.50%
Typical MMFX 2	0.08%	9%	0.5%				

<sup>\*</sup>Maximum unless range indicated.

#### **Tensile Properties**

The ASTM A1035/A1035M steel bars are of a single minimum yield strength level of 690 MPa [100 000 psi]. The yield strength is determined by the offset method (0.2 % offset), described in Test Methods and Definitions ASTM A 370 (ASTM 2004). In addition, the stress corresponding to a tensile strain of 0.0035 shall be a minimum of 550 MPa [80 000 psi]. The mechanical properties are summarized in Table 2.

Table 2. Tensile Properties of ASTM A1035 High Strength Steel Bars

Tensile strength, min, MPa [psi]	1030 [150
	000]
Yield strength (0.2 % offset), min, MPa [psi]	690 [100
	000]
Stress corresponding to an extension under load	550 [80 000]
of 0.0035 mm/mm. (0.0035 in/in), min, MPa [psi]	
Elongation in 203.2 mm [8 in.]	min. %:
#10 through #36 [#3 through #11]	7
#43, #57 [#14, #18]	6

#### Corrosion Properties

Many highly credible institutions and government agencies have tested the corrosion resistance of ASTM A1035 steel bars. Substantial documented test results have been published to validate the corrosion resistance of this innovative steel product. The high-corrosion resistance provides increased service life to the steel before its structural carrying capacity has dissipated leading to reduced serviceability of reinforced concrete structures, damage to structural load carrying capacity or loss of aesthetic appeal. ASTM A1035 steel bars' corrosion resistance is 5 to 6 times better than the corrosion resistance of conventional carbon steel (ASTM A615) as measured by its critical chloride threshold level, CCTL (Clemena, G.G. 2004).

#### **ASTM A1035 Rebar Application In High-Rise Construction:**

#### Flexural Tension Application

Practical application of ASTM A1035 steel rebars to high-rise construction includes but is not limited to, tension piles, mat foundations, shear walls and moment frames, etc. These structural components designed with the higher yield strength property of ASTM

A1035 steel rebars have been demonstrated to be cost-effective, improve constructability and shorten construction schedules.

The design of concrete members reinforced with ASTM A1035 steel rebars for flexure is analogous to the design of concrete reinforced with conventional steel bars. Experimental data of concrete members reinforced with ASTM A1035 steel bars show that flexural capacity can be calculated based on similar assumptions for members reinforced with ASTM A615 carbon steel rebars, taking into account the higher strength of the ASTM A1035 steel bars.

Designers need to be aware that typical design standards limit the design strength to 550 MPa [80,000 psi] and that the use of deformed reinforcing bar with a material specified yield strength  $f_y$  exceeding 420 MPa [60,000 psi] is permitted, providing  $f_y$  is the stress corresponding to a strain of 0.35%. Based on the experimental results and the analysis conducted, the design of a concrete section reinforced with ASTM A1035 steel bars can be simplified by using the ACI 318 design philosophy and 690 MPa [100,000 psi] in tension, while limiting the stresses in compression up to 550 MPa [80,000 psi]. However, well-confined concrete, such as that used in seismic-resisting columns and shear walls, has a compressive strain capacity much greater than that of unconfined concrete. So, the 80,000 psi and 0.35 percent limits in steel compression strength may be unnecessary for well-confined concrete.

Calculations involved in control of cracking should be made for the service load level. Research have shown that, in spite of service load steel stresses as high as 60,000 psi, the width of individual cracks can be held down to hair-line size by proper distribution of the bars (Malhas, F. 2002, El-Hasha, R. and Rizkalla, S. 2002). The strength characteristics of high quality concretes along with the high corrosion resistance properties of the high strength steel will complement the structural properties of the ASTM A1035 steel bars, thus facilitating design development of attractive and economical structures.

#### Transverse Reinforcing

One of the applications that high-strength reinforcing steel achieved code recognition and market acceptance is for use as shear reinforcement in columns and comparable vertical elements. There are indications worldwide that increased design requirements for transverse reinforcing steel especially in concrete columns and piles, are either exceeding the practical capacity of mild steel reinforcing bars, or are causing such a great amount of steel congestion that correct placement and consolidation of concrete is becoming complex.

There are further indications that this burden is adversely affecting the market for such reinforced concrete structures by making them prohibitively more expensive. As a result, alternative members such as structural steel rolled sections have replaced reinforced concrete as the material of choice. It appears that in some regions, design engineers are seriously questioning the ability of reinforced concrete members utilizing mild steel reinforcement to perform with structural integrity under certain types of

anticipated loading conditions. In one state in the United States, pre-stressed concrete piles are no longer usable under the current code restraints.

As a result, the newly published American Concrete Institute, ACI, 318-05 building code includes a new provision for allowing the use of higher design stresses for spiral transverse reinforcement in section 10.9.3 of the building code.

The American Concrete Institute's ACI 318-05 building code commentary provides the following explanation for the acceptance of the use of the high strength steel bars with yield strength of 100,000 psi for spiral reinforcement: "Confinement reinforcement often creates congestion in reinforced concrete structures. Research shows that 690 MPa (100,000 psi) yield strength reinforcement can be used for confinement (ACI, 2005). This will reduce congestion, thereby making structures safer, because concrete can be consolidated more easily and will make structures more economical".

#### Structures Exposed to Corrosive Environment

The corrosion-resistant ASTM A1035 steel rebars are also ideal for structural members and systems exposed or in direct contact with corrosive environment, such as humid atmosphere, high foundation water table, and corrosive soil condition. Possible application would be in foundation piles, foundation systems, exposed balconies, etc. Structural systems reinforced with ASTM A1035 steel rebars have shown to provide extended service lives of 75 to 100 years, depending on the severity of the exposure.

#### **Lowest Construction System**

The effectiveness of reinforcement in strengthening a concrete member is generally almost proportional to the product of bar area and yield strength,  $A_s f_y$ . The economies of high strength steels may therefore be estimated in terms of costs per ton per psi yield strength. Relative costs of reinforced concrete structures depend on several factors, in addition to the cost of reinforcing steel. The reduction of steel area which accompanies an increase in  $f_y$  often facilitates concrete placement by eliminating steel congestion.

The technology behind ASTM A1035 steel bars can change the way high-rise buildings are designed. ASTM A1035 steel products provide the designer with higher grade steel along with the corrosion-resistant properties, at a lower overall cost. The added strength of ASTM A1035 steel rebars results in an incremental decrease in the amount of conventional steel necessary to accomplish the same task. High-rise structures can be designed with less congestion without adding additional concrete cover. By specifying ASTM A1035 steel rebar, the high-rise owner will experience upfront cost savings, as well as lower life cycle costs.

Projects using ASTM A1035 steel rebars can be completed with up to 40% less steel resulting in less congestion and up to 50% lower labor costs (Fig. 1). Stronger, more corrosion resistant, and with faster construction times, ASTM A1035 steel bar is truly a key component of the lowest cost construction system.



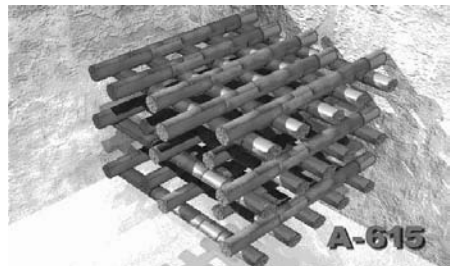


Fig. 1. Side by side MMFX vs. A615.

Practical example 1: Parking structure in Las Vegas, NV (mat foundation application)
The proposed project is located in Las Vegas, Nevada, U.S.A. The structure consists of 12 levels of steel parking decks, supported on a 5' thick concrete mat. The original design was completed using ASTM A615 Grade 60. A preliminary redesign was performed using ASTM A1035 steel bars using 690 MPa [100 ksi] design to provide the equivalent steel strength in the mat. The redesign led to significant savings in total weight of reinforcing, pieces of steel to be placed, as well as overall installed cost. A summary of the potential savings is listed in the Table 3.

Table 3. Potential project savings (A1035 vs. A615) – Mat Foundation.

Bar Type	Cost (\$)	Weight (tons)	Placing (pieces)
A615 Gr. 420 [60 ksi]	\$1,793,572	1,121	13,478
A1035 690 MPa [100ksi]	\$1,570,622	714	10,874
Savings	\$222,950	407	2,604
	12%	36%	19%

Further analysis was performed to include the use of high-strength mechanical couplers in reinforcing splice locations. The purpose of the exercise was to illustrate further potential savings by eliminating long reinforcing splices and replacing with mechanical couplers. Again, the result of the analysis indicated further savings as illustrated in Table 4 below:

Table 4. Potential project savings (A1035 w/ couplers vs. A615) – Mat Foundation.

Bar Type	Cost (\$)	Weight (tons)	Placing (pieces)
A615 Gr.420 [60 ksi]	\$1,793,572	1,121	13,478
A1035 690 MPa [100ksi]	\$1,521,533	644	9,765
w/couplers			
Savings	\$272,039	477	3,713
	15%	43%	28%

### Practical example 2: High-rise condominium tower in Las Vegas, NV (shearwall application)

The proposed project is a 50 story tall condominium tower in Las Vegas, Nevada. The building system consists of post-tensioned concrete flat plates, concrete shearwalls, and mat foundation. The high aspect ratio of the building causes the flexural reinforcing, also known as jamb reinforcing, to be very substantial with Grade 420 [60] reinforcing. Due to the high flexural reinforcing and congestion in the shear wall boundary zones, an alternate reinforcing scheme was considered using ASTM A1035 steel reinforcing. Shear walls of the tower were redesigned using ASTM A1035 steel from foundation through the roof level. The use of ASTM A1035 in the flexural reinforcing of the tall shear walls effectively reduced the amount of congestion in the shear wall boundary zones. The following Table 5 illustrates the savings realized:

Table 5. Potential project savings (A1035 vs. A615 Grade 60) Shearwall Jamb Reinforcing.

Bar type	Cost (\$)	Weight (tons)
A615 Grade 420 [60]	\$2,709,290	1,500
A1035 690 MPa [100ksi]	\$2,160,540	1,097
Savings	\$548,750	403
	20%	27%

The savings shown in the table only include the effect of ASTM A1035 reinforcing substitution for flexural reinforcing of the walls. With less flexural reinforcing, the boundary zone transverse reinforcing ties are also significantly reduced, leading to further installation savings.

#### Mat Foundation Application

The mat foundation was also redesigned using ASTM A1035 steel reinforcing to reduce the amount of horizontal flexural reinforcing. To further utilize the high strength property of ASTM A1035 steel bars, the total thickness of the mat foundation system was reduced by 3 feet on average. As a result, there is a total savings of more than 4,000 cubic yard of concrete. In additional to the steel reinforcing savings, there is significant reduction in excavation, dirt haul-out, concrete pour back, as well as construction schedule. Table 6 summarizes the savings incurred on the project by utilizing ASTM A1035 steel reinforcing:

Table 6. Potential project savings (A1035 vs. A615 Grade 60) – Mat Foundation w/ Reduced Thickness.

Bar type	Cost (\$)	Weight (tons)
A615 Grade 420 [60]	\$1,739,040	1,449
A1035 690 MPa [100ksi]	\$1,695,050	1,097
Concrete Savings	\$1,200,000 Estimated	4,000 cubic yard
Total Foundation Savings	\$1,243,990 (plus 2 week	ks saving in excavation time)

As illustrated in the examples above, the use of ASTM A1035 steel reinforcing is very effective in reducing overall project cost. The above examples only consider the effect

of direct substitution of reinforcing. However, there are other potential savings areas including less reinforcing congestion, less placement difficulties, less plasticizer in concrete mix, more effective concrete pour and ultimately, overall project time and cost savings.

#### Conclusions

Concrete reinforcing steel congestion in high-rise structures can be addresses utilizing the high-strength corrosion-resistance MMFX 2 steel bars produced in accordance with the ASTM A1035 specification. It is apparent that the use of ASTM A1035 steel bar is extremely effective in reducing the total weight of steel for the project, providing flexibility in structural design, and at the same time achieving tremendous time and labor savings.

#### References

- ACI Committee 318, 2005. Building Code Requirements for Structural Concrete (ACI 318-05) and Commentary (ACI 318R-05). Farmington Hills: American Concrete Institute.
- ASTM A1035, 2005 "Standard Specification for Deformed and Plain, Low-carbon, Chromium, Steel Bars for Concrete Reinforcement", ASTM International, 100 Barr Harbor Drive, PO Box C700, West Conshohocken, PA 19428-2959, United States
- ASTM A370, 2004 "Test Methods and Definitions for Mechanical Testing of Steel Products", ASTM International, 100 Barr Harbor Drive, PO Box C700, West Conshohocken, PA 19428-2959, United States.
- El-Hacha, R. and Rizkalla, S. 2002. Fundamental Material Properties of MMFX Steel Rebars. Retrieved February 5, 2004, from the MMFX Technologies Corporation Web site:
  - http://www.mmfxsteel.com/technical resources/Default.asp.
- Malhas, F.A. 2002. Preliminary Experimental Investigation of the Flexural Behavior of Reinforced Concrete Beams Using MMFX Steel. Retrieved February 5, 2004, from the MMFX Steel Corporation of America Web site <a href="http://mmfxsteel.com/technical\_resources/Default.asp">http://mmfxsteel.com/technical\_resources/Default.asp</a>
- Clemenea, G. and Virmani, P. Comparing the Chloride Resistance of Reinforcing Bars", Concrete International, November 2004, Farmington Hills, American Concrete Institute.
- S.K. Ghosh 2006. Application of ASTM A1035 MMFX Steel Reinforcement in Building Application: An Appraisal.

#### Maximum Allowable In-Plane Shear Stresses in Reinforced Concrete Membrane Elements

#### Khaldoun N. Rahal

Civil Engineering Department, Kuwait University, Kuwait e-mail: rahal@civil.kuniv.edu.kw

#### Abstract

Thin structural elements such as shear walls, silos and plates and shells can be analyzed as assemblages of thin membrane elements subjected to in-plane shearing and normal stresses. The shear provisions of building and bridge codes such as the ACI building code and the AASHTO LRFD bridge specifications and EC2 are commonly used in the design of such elements. An upper limit on the shear stress is set to avoid crushing of the concrete before the yielding of the reinforcement. The ACI upper limit is a function of the square root of the specified concrete strength  $f_c$  while those of AASHTO LRFD Specifications, the Danish code and the European Code are related directly to  $f_c$ , and the difference between these limits is considerable especially at higher concrete strengths. This article provides a critical review of this upper limit, and proposes an alternative limit based on experimental results. This limit is compatible with the results of an analytical model named the modified compression field theory (MCFT).

#### Introduction

Numerous structural elements such as box and I- bridge girders, shear walls, silos and other thin shell and plate structures can be modeled as thin membrane elements subjected to in-plane shearing and biaxial normal stresses. Figure 1 shows two examples of such structural elements. The analysis of such structures is typically based on elastic models such as the Finite Elements Method or more conventional structural analysis methods, while the design of the membrane elements is based on their non-linear behavior. Orthogonal reinforcement is typically provided as shown in the membrane element in Fig. 2.

Design codes such as the ACI Building code (ACI, 2005) and the AASHTO LRFD Bridge Specifications (AASHTO, 2004) give shear design equations. It is to be noted that these equations were developed over the past century from the experimental results of tests on reinforced and pre-stressed concrete beams subjected to shear and bending moments, and not for thin membrane elements. The Danish Code (1984) and EC2 (1991) give equations based on the Plasticity Theory (Braestrup, 1974).

To ensure that the reinforcement yields before brittle crushing of the concrete, an upper limit is set on the shear stress that is applied to the element. The following section summarizes the code provisions for this maximum stress.

#### **ACI Upper Limit**

The ACI code equations are based on the 45° truss model modified with a concrete contribution. For membrane elements, the concrete contribution stress  $v_c$  can be based on the web cracking as given in ACI 11.4, calculated using a shear stress of  $0.33\sqrt{f_c^c}$  MPa. The steel contribution  $v_s$  (as a stress) is calculated as  $\rho_y f_y$  where  $\rho_y$  and  $f_y$  are the ratio of reinforcement and its yield stress respectively. Using the yield stress requires that the section is under-reinforced, i.e. the steel yield before crushing of the concrete. This is ensured by limiting that the steel  $v_s$  to  $0.66\sqrt{f_c^c}$  MPa as per ACI 11.5.7.9. The total shear strength is hence limited to  $(0.33+0.66)\sqrt{f_c^c} = 0.99\sqrt{f_c^c}$ :

$$v_{ACI} = 0.99\sqrt{f_c'}$$
 Eq. (1)

It is to be noted that the upper limit on the shear stress was imposed by ACI to limit crack widths at service load, and this limit was also found to be an adequate safeguard against concrete crushing before yielding of the reinforcement.

The ACI Clause 11.1.2 requirement to limit the term  $\sqrt{f_c}$  to 8.3 MPa is equivalent to limiting the usable compressive strength to 69 MPa. This limit is not applicable if an ample amount of transverse reinforcement given in ACI clause 11.5.6 is provided. It is to be noted that slightly higher concrete contribution is allowed in pre-stressed members and in members subjected to significant compressive axial loads.

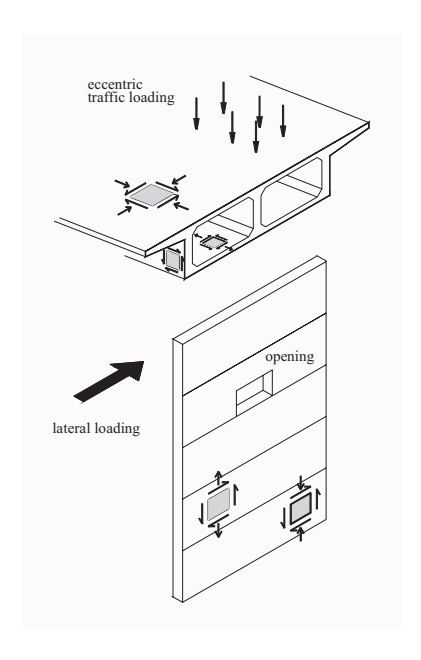


Fig. 1. Examples of membrane elements in structures.

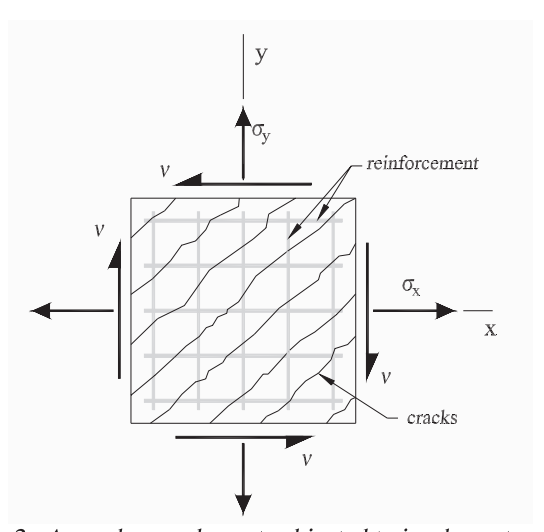


Fig. 2. A membrane element subjected to in-plane stresses.

#### **AASHTO LRFD Upper Limit**

The General Procedure of the AASHTO LRFD specifications is based on a variable angle truss model modified with a concrete contribution. To ensure yielding of the transverse reinforcement, the maximum attainable shear stress is taken as a function of the concrete strength as follows:

$$V_{IRFD} = 0.25 f_c'$$
 Eq. (2)

In explaining the development of the General Procedure, Rahal and Collins (1999) showed that larger maximum values are possible in members where the longitudinal strain in the cross section and relatively low or compressive. The limit shown in Eq. (2) was however maintained for its simplicity.

#### EC2 and the Danish Code Upper Limit

The Plasticity Theory, the Danish Code and EC2 assume that the maximum attainable shear stress decreases with higher concrete strengths. The Plasticity Theory gives the following equation:

$$v_{p_L} = 0.4 - \frac{f_c'}{100}$$
 Eq. (3)

Equation (3) is a central estimate. For code values, the maximum allowable stress in EC2 and the Danish code was reduced to.

$$v_{PL} = 0.35 - \frac{f_c}{100}$$
 Eq. (4)

Equation 4 unduly penalizes higher strength concrete. For this reason, a lower limit of 0.25 and 0.2 was set in the Danish Code and the EC2 respectively, giving

$$v_{EC2} = 0.35 - \frac{f_{c}^{'}}{100} \ge 0.25$$
 Eq. (5)

$$v_{Danish} = 0.35 - \frac{f_c}{100} \ge 0.20$$
 Eq. (6)

Note that the material reduction factors are not shown in all the equations presented above.

#### Comparison between Code Upper Limit

Figure 3 shows the relationship between the maximum shear strength (normalized with respect to  $f_c$ ) and the concrete compressive strength from the equations 1, 2, 5 and 6. The maximum shear stress in the North American ACI Code and AASHTO Specifications are significantly different especially at medium and higher concrete strengths. For a 65 MPa (9500 psi) concrete, the AASHTO LRFD Specifications allows twice the shear strength that the ACI code allows.

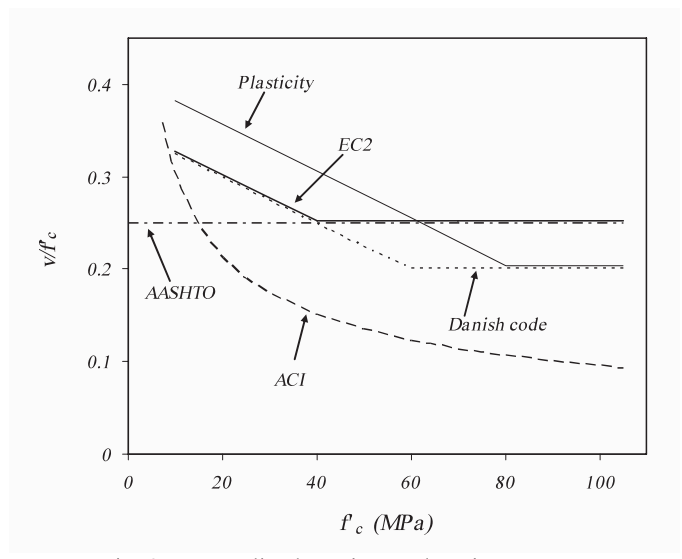


Fig. 3. Normalized maximum shearing stresses.

#### **Experimental Evidence**

The mode of failure of forty one reinforced concrete panels subjected to pure in-plane shear was available [Vecchio and Collins, (1986), Vecchio et al., (1994), Pang and Hsu, (1995), Hsu and Zhang (1998), Hsu and Zhang, (1997), Khalifa, (1986), Kirschner, (1986), Porasz, (1989)]. Seven of these specimens failed in concrete crushing before yielding of any of the reinforcement, while the remaining panels failed in a partially or fully under-reinforced mode, with the reinforcement in one or two directions yielding before concrete crushing. Figure 4 shows these test results.

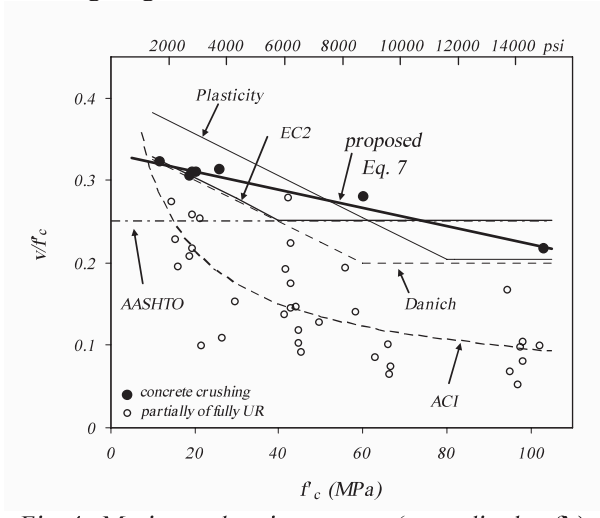


Fig. 4. Maximum shearing stresses (normalized to  $f'_c$ ).

The figure shows a clear trend in decrease in the maximum attainable shear stress at higher  $f'_c$  values. The ACI and the Danish and the EC2 codes assume a decrease in  $v/f'_c$  at higher concrete strengths. A good fit of the experimental points representing the strength of over-reinforced specimens is given as:

$$\kappa = \frac{1}{3} - \frac{f_c'}{900}$$
 (MPa) Eq. (7-a)

$$\kappa = \frac{1}{3} - \frac{f_c'}{13000}$$
 (psi) Eq. (7-b)

Figure 4 shows that the ACI code equation is considerably conservative over a wide range of practical concrete strengths while the AASHTO LRFD and the EC2 equations are slightly non-conservative at concrete strengths larger than 80 MPa (11,500 psi). The Plasticity Model is slightly non-conservative for concrete strengths below 30 MPa (4300 psi).

#### **Theoretical Evidence**

The equations of the Modified Compression Field Theory (Vecchio and Collins, 1986) were also used to further support the trend of decrease of the normalized shear strength at higher concrete strength. The software MEMBRANE was used to develop the relationship between the maximum shearing stresses for panels of equal orthogonal reinforcement at various concrete compressive strengths. For a specific concrete strength, the amount of equal orthogonal reinforcement was increased to change the mode of failure from under-reinforced to over-reinforced. The amount of reinforcement where the shift in mode of failure takes place was recorded and plotted in a graph versus the concrete strength. Figure 5 shows the results, along with the seven over-reinforced specimens and the proposed Eq. 7. The figure shows an acceptable correlation of the proposed Eq. 7 with the MCFT results.

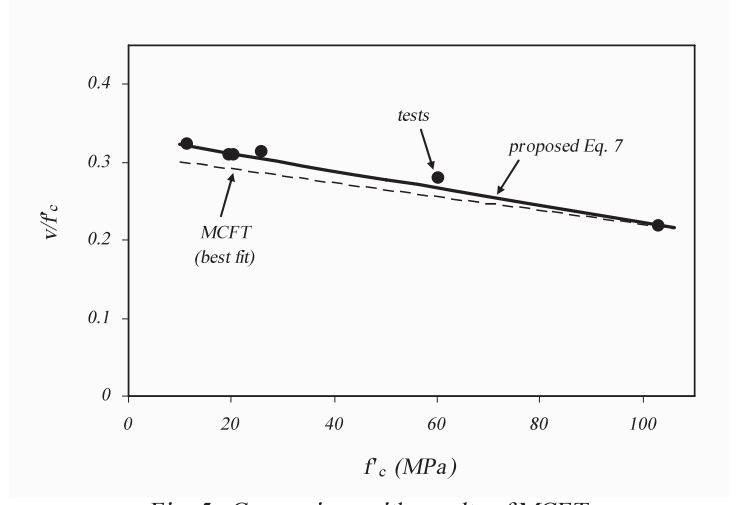


Fig. 5. Comparison with results of MCFT.

#### **Conclusions**

A new equation for the crushing shear strength of reinforced concrete membrane elements subjected to shear is proposed. The equation assumes a constant decrease in the maximum attainable shear stress with an increase in concrete strength. The equation is a lower bound of the test results from seven over-reinforced membrane elements. The trend was confirmed using the equations of the modified compression field theory.

The experimental results were also compared to the equations proposed by the ACI, Danish, EC2 codes and the AASHTO LRFD Specifications. It was found that the proposed equation provided the best fit of the data, while the ACI equation was significantly conservative, especially at relatively higher concrete strength.

#### **Notations**

 $f'_c$  = compressive strength of concrete  $f_y$  = yield strength of reinforcing steel v = shear stress in membrane element

 $v_{ACI}$  = maximum allowable shear stress (ACI code)

 $v_c$  = concrete contribution in ACI Code

 $v_{Danish}$  = maximum allowable shear stress (Danish code)  $v_{EC2}$  = maximum allowable shear stress (EC2 code)

 $v_{LRFD}$  = maximum allowable shear stress (LRFD Bridge Specifications)

 $v_{PL}$  = maximum allowable shear stress (Plasticity model)

 $v_s$  = steel contribution in ACI Code

 $\rho_{v}$  = ratio of reinforcement

proposed maximum allowable shearing stress

#### References

ACI Committee 318, 2005, "Building Code Requirements for Reinforced Concrete and Commentary ACI 318M-05," American Concrete Institute, Detroit, 436 pp.

AASHTO LRFD, 2004, "Bridge Design Specifications and Commentary," 3<sup>rd</sup> Edition, American Association of State Highway and Transportation Officials, Washington D.C., 1264 pp.

Bræstrup, M. W., 1974, "Plastic Analysis of Shear in Reinforced Concrete," Magazine of Concrete Research, V. 26, No. 89, Dec. 1974, pp. 221-228

Danish Standards Institute, 1984, "Code of Practice for the Structural Use of Concrete," DS41, 3<sup>rd</sup> Edition, (Translation Edition April 1986), Copenhagen, Denmark, 101 pp.

"Design of Concrete Structures-Part 1: General Rules and Rules for Buildings," ENV 1992-1-1, CEN, Brussels, Belgium, Dec. 1991, 253 pp.

Rahal, K. N., and Collins, M. P. (1999), "Background of the 1994 CSA-A23.3 General Method of Shear Design." Canadian Journal of Civil Engineering, Vol. 26, No. 6, pp. 827-839.

Vecchio, F.J. and Collins, M.P., 1986, "Modified Compression Field Theory for Reinforced Concrete Elements Subjected to Shear," ACI Journal, Vol. 83, No. 2, pp. 219-231.

- Vecchio, F.J., Collins, M.P., and Aspiotis, J, 1994, "High-Strength Concrete Elements Subjected to Shear," ACI Structural Journal, Vol. 91, No. 4, pp. 423-433.
- Pang, X. and Hsu, T.T.C., (1995), "Behavior of Reinforced Concrete Membranes in Shear," ACI Structural Journal, V. 92, No. 6, pp. 665-679.
- Hsu, T.T.C., and Zhang L., 1998, "Behavior and Analysis of 100 MPa Concrete Membrane Elements," Journal of the Structural Division, Vol. 124, No. 1, pp. 24-34
- Hsu, T.T.C., and Zhang L., 1997, "Nonlinear Analysis of Membrane Elements by Fixed Angle Softened-Truss Model," ACI Structural Journal, Vol. 94, No. 5, pp. 483-492.
- Khalifa, J, 1986, "Limit Analysis of Reinforced Concrete Shell Elements," Ph.D. Thesis, Department of Civil Engineering, University of Toronto, Toronto, Ontario, Canada, 312 pp.
- Kirschner, U, 1986, "Investigating the Behavior of Reinforced Concrete Shell Elements," Ph.D. Thesis, Department of Civil Engineering, University of Toronto, Toronto, Ontario, Canada.
- Porasz, A, 1989, "An Investigation of the Stress-Strain Characteristics of High Strength in Shear," M.A.Sc. Thesis, Department of Civil Engineering, University of Toronto, Toronto, Ontario, Canada, pp. 173.

## Effect of Unprocessed Steel Slag on the Strength of Concrete when used as Fine Aggregate

Hisham Qasrawi, Faisal Shalabi, Ibrahim Asi Civil Engineering, Faculty of Engineering, Hashemite University, Zarqa 13115, JORDAN

E-mail: gasrawi2@yahoo.com

#### Abstract

Steel slag, which is produced locally in great amounts, creates problems for the environment when disposed. Since the quality of concrete depend on the materials used, waste materials may have a positive or negative effect on concrete properties. Local steel slag has a low CaO content and hence it has no pozzolanic activity. Therefore, it is necessary to test the possibility of using the slag in the concrete industry. In this research, local unprocessed steel slag is introduced in concrete mixes. Various mixes with compressive strength ranging from 25 to 45 MPa are studied. The slag is used as fine aggregate replacing the sand in the mixes, partly or totally. Ratios of 0 to 100% are used. Depending on the grade of concrete, the compressive strength is improved if steel slag is used for low replacements (up to 30 %). The tensile strength of concrete is improved by 1.7 to 2.4 times depending on the replacement ratio and the grade of concrete. The best results are obtained for replacement ratios of 30 to 50 %. Therefore, the use of steel slag in concrete would enhance of the strength of concrete, especially the tensile strength, provided the correct ratio is used.

**Key Words:** Aggregate, concrete, steel slag, strength.

#### Introduction

Locally, waste materials from the steel industry are produced in high amounts and shapes ranging from large boulders to dust. They are considered "a headache" for both the factories and the environment. The factories have to pay huge amounts for the disposal of these materials. The disposal of these materials will have a negative impact on the environment. The final properties of concrete, such as strength, durability and serviceability depend mainly on the properties and the quality of the materials used. Therefore, the use of waste materials, such as steel slag, in concrete may have a positive or negative effect. Utilizing steel slag for concrete construction has proved to be useful in solving some of the problems encountered at sites. Steel slag can be used in conventional concrete to improve its mechanical, physical, and chemical properties. The slag produced from local resources have been divided into three types:

- 1. The coarse materials that need to be cut into smaller ones in order to be disposed.
- 2. The fine material, which is called locally "scrap" and can be used directly in concrete mixes without any modifications.
- 3. The very fine materials, dust, which may need further processing before use in concrete
- In this research, the unprocessed fine material has been introduced as fine aggregate in normal concrete mixes in order to evaluate its use in normal concrete mixes.

#### **Use of Steel Slag Aggregate in Concrete Mixes**

Slag, the by-product of steel and iron producing processes, has been used in civil engineering before many decodes (Geiseler, 1999; Neville, 1996; Neville and Brooks 2002; Alizadeh et. al., 1996, Asi et al 2005). Portland granulated ground blast furnace slag cement, which is produced from rapidly water-cooled blast furnace slag, has been successfully used in concrete due to the high amount of lime (40 -50%), which posses pozzolanic activity (Neville, 2002; Alizadeh et. al., 1996). Electric arc furnace slag (EAFS) that contains low percentage of amorphous silica and high content of ferric oxides and consequently has low, or no, pozzolanic activities in comparison with blast furnace slag (BFS), is not appropriate to be used in blended cement production (Kamal et. al. 2002). Although many studies have been conducted on the evaluation of steel slag to be used in road construction, there are rare researches regarding the utilization of steel slag in concrete (Kamal et. al. 2002). ASTM C33 gives specifications for the use of blast furnace slag as aggregates in concrete, while there is not such a standard for steel slag. Alizadeh et. al., (1996) results of the experiments which were carried out on hardened concrete, indicated that slag aggregate concretes achieved higher values of compressive strength, tensile strength, flexural strength and modulus of elasticity, compared to natural aggregate concretes. Shekarchi et. Al., (2004, 2003) introduced a comprehensive research on the utilization of steel slag as aggregate in concrete. In the study, Shekarchi (2004) concluded that the use of air-cooled steel slag with low amorphous silica content and high amount of ferric oxides it unsuitable to be employed in blended cement. On the other hand, utilization of steel slag as aggregate is advantages when compared to normal aggregate mixes. Maslehuddin et. al., (2003) presented a comparative study of steel slag aggregate concrete and crushed limestone concrete. In the study, only part of the coarse aggregate has been replaced by slag aggregate. The study concluded that the compressive strength of steel slag aggregate concrete was marginally better than that of crushed limestone aggregate concrete. Moreover, no significant improvement was noted in the tensile strength. Manso et al., (2004) presented a study in which electricity has been used to obtain concrete of better quality. It was concluded that steel slag can be used to enhance concrete properties. However, according to the authors, special attention must be paid to the mixes of concrete to achieve a suitable fine aggregate, which can be obtained by mixing fine slag with filler material.

#### Materials

Graduation of normal aggregates from local sources was obtained using ASTM C136. The aggregate was well-graded and conforms to ASTM C33 grading requirements for coarse aggregate of nominal maximum size 25 to 4.75 mm. The results of the sieve analysis of both the fine aggregate and the fine steel slag are shown in Table 1, together with ASTM C33 and BS 882 grading limits. The sand used is natural sand, known locally as desert sand. Although this sand is relatively fine, it is known to be good quality and is commonly used in concrete mixes. The fineness modulus of the sand was 1.56 and that of the slag was 1.50. As shown in Table 2, both of them can be classified as fine and are not within the limits of the ASTM C 33-92 standard limits. However, the natural sand is within the limits of BS 882: 1992 standards and is classified as "F" (fine aggregates). The slag contains high amounts of material passing sieve # 100, but this value is reduced to the half at sieve # 200.

Table 1. Sieve Analysis of Fine Aggregates

Sieve size	ASTM	Sand	nd Slag ASTM		BS Gra	ding Requi	rements
(mm)	Designation	% Passing	% Passing	limits	BS - C	BS - M	BS - F
9.5	3/8"	100	100	100	100	100	100
4.75	# 4	99.9	99	100	89-100	89-100	89-100
2.360	# 8	99.6	95.6	95 - 100	60-100	65-100	80-100
1.180	# 16	98.9	85.4	80 - 100	30-90	45-100	70-100
0.600	# 30	91.3	72.1	50 - 85	15-54	25-80	55-100
0.300	# 50	45.1	56.2	25 - 60	5-40	5-48	5-70
0.150	# 100	8.6	40	10 -30	0-15*	0-15*	0-15*
0.130	π 100	0.0	10	10-30	0-20^	0-20^	0-20^
0.075	# 200	1	20.5	NA	NA	NA	NA

<sup>\*</sup> Natural aggregate

Slag was intended to be used "as received" from the factory without any further screening. The locally available desert sand from near-by sources was intended for use. This choice would be the most economical for use in concrete mixes when accounting for the costs of transporting and screening. The specific gravity and absorption of the aggregates were measured using ASTM C 127-88 and ASTM C 128-88. In each case,

<sup>^</sup> Crushed aggregate

ASTM. The apparent specific gravity of the coarse aggregate, sand and steel slag were 2.69, 2.6 and 3.25 and the absorption was 1.65, 0.4 and 0.8% respectively. It is clear that the specific gravity of the steel slag is higher than that of normal aggregate. Also, it is clear that the absorption is small (< 1 %). These results are acceptable for use in concrete structures, keeping in mind that higher density is expected. Dry-rodded unit weight of the coarse aggregate was obtained using ASTM C29-90 specifications and was 1528 kg/m³. Chemical analysis of steel slag is shown in Table 2. It is clear that the slag has low CaO content indicating that no pozzolanic activity is expected.

Table 2. Chemical Analysis of the Slag Used in the Study

Oxides	Fe <sub>2</sub> O <sub>3</sub>	MnO	TiO <sub>2</sub>	SiO <sub>2</sub>	MgO	CaO	C	S
%	97.05	1.07	0.01	0.8	0.4	0.4	0.23	0.21

#### **Experimental Program**

In order to study the effect of the use of steel slag as fine aggregates, several concrete mixes have been prepared and tested in the laboratory. The following steps summarize the program that has been followed:

- 1. Conventional concrete mixes of 25, 35 and 45 MPa cube strength were designed and tested in the laboratory. In addition to the strength requirement, all mixes were prepared and adjusted to obtain concrete of medium workability (slump 8 to 12 cm). This workability is the most desired one in local concrete sites, especially during hot summer.
- All mixes were tested for workability using the slump test described in ASTM C 143
- 3. Several cubes of 100 mm side length were prepared and cured in the laboratory in a water bath under a temperature of  $20 \pm 2^{\circ}$  C; then tested at the ages of 3, 7, 28 and 90 days for compressive strength. At each age, a minimum of three cubes were randomly chosen and tested in saturated surface dry condition.
- 4. Several standard prisms of  $100 \times 100 \times 500$  mm were prepared and cured in the laboratory in a water bath under a temperature of  $20 \pm 2^{\circ}$  C, then tested at the ages of 7, 28 and 90 days for flexural tensile strength. At each age, a minimum of three prisms were randomly chosen and tested in saturated surface dry condition.
- 5. Steel slag concrete mixes were prepared by replacing certain amount of sand by slag, while keeping all other variables constant. The ratio of slag used was 15, 30, 50 and 100 percent by weight of sand.
- 6. Steel slag concrete cubes and prisms were prepared and tested as in steps 2, 3 and 4.

#### **Results and Discussions**

**Workability**: Figure 1 shows the relationship between the slump of concrete and the ratio of slag used. It is clear that the use of slag reduced the workability of concrete. It is clear from the graph that rations up to 50 % replacement have only marginal effect and the concrete can still be classified as concrete of medium workability. The mixes

containing 100 % slag were sticky rather than dry. All these mixes lacked mobility and hence resulted in low slump values. The reduction in workability is attributed to the fact that the sand has been replaced by a finer material. The more the fines, the less the workability is as shown in Fig. 1. Also, the slag has more angular shapes when compared with normal sand.

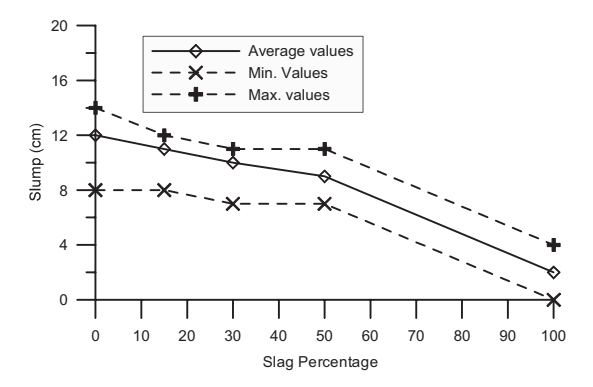


Fig. 1. Effect of steel slag on workability.

**Compressive strength:** The results of the compressive strength of the tested samples are shown in Fig. 2. Plots for 25 and 35 MPa concrete only are shown<sup>1</sup>. From the figures, the following observations are obtained:

- 1. The strength of concrete increases with age for all mixes.
- Mixes containing slag showed higher compressive strength in the early ages (the first seven days).
- 3. The mix containing 100 % slag produced compressive strengths less than the normal concrete mix at the ages of 28 and 90 days.
- 4. The lower the slag ratio, the higher the compressive strength of concrete at the ages of 28 and 90 days.
- 5. Mixes containing 50% slag produced lower strength than the control mixes.
- 6. Mixes containing 15 % and 30% both produced strength values at later ages more than the control mix.

oto of 45 MDs communicative atmomath above

<sup>&</sup>lt;sup>1</sup> (Concrete of 45 MPa compressive strength showed similar trends and was omitted for the sake of space)

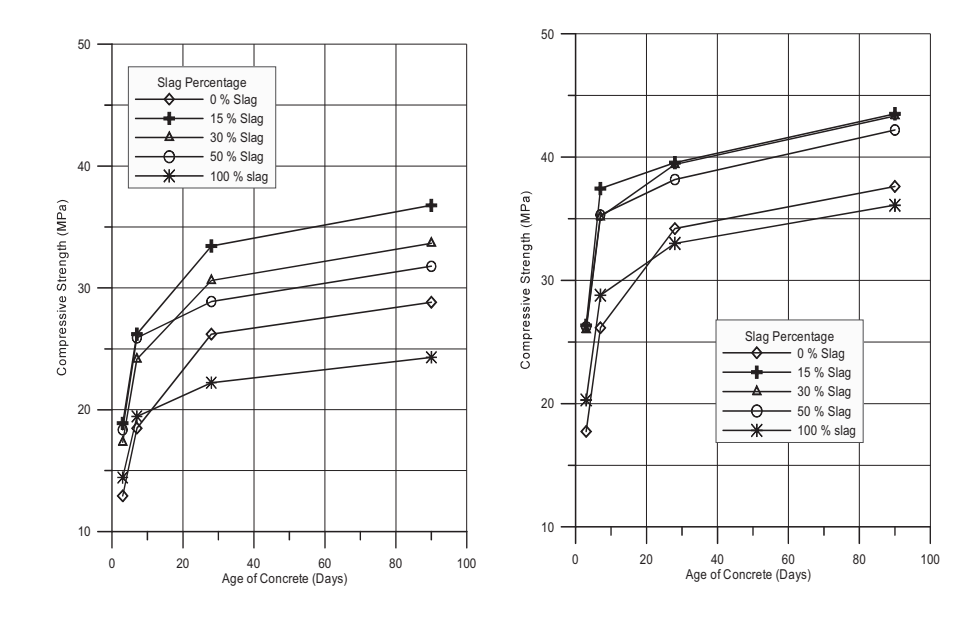


Fig. 2. Relationship between age of concrete and its compressive strength for various slag replacements (25 and 35 MPa concrete).

Furthermore, the relationship between the slag replacement percentage and the strength of concrete for the ages of 7, 28 and 90 days is plotted in Fig. 3. In all figures and for all grades of concrete it can be seen that a peak exists between 10% to 30 % sand-slag replacements. The increase in strength is expected because of the higher angularity of steel slag particles compared to those of sand. However, when high ratios are used, the cement would not be sufficient to coat all particles because of the higher specific surface area of slag particles. This is clear in the grading shown in Table 1.

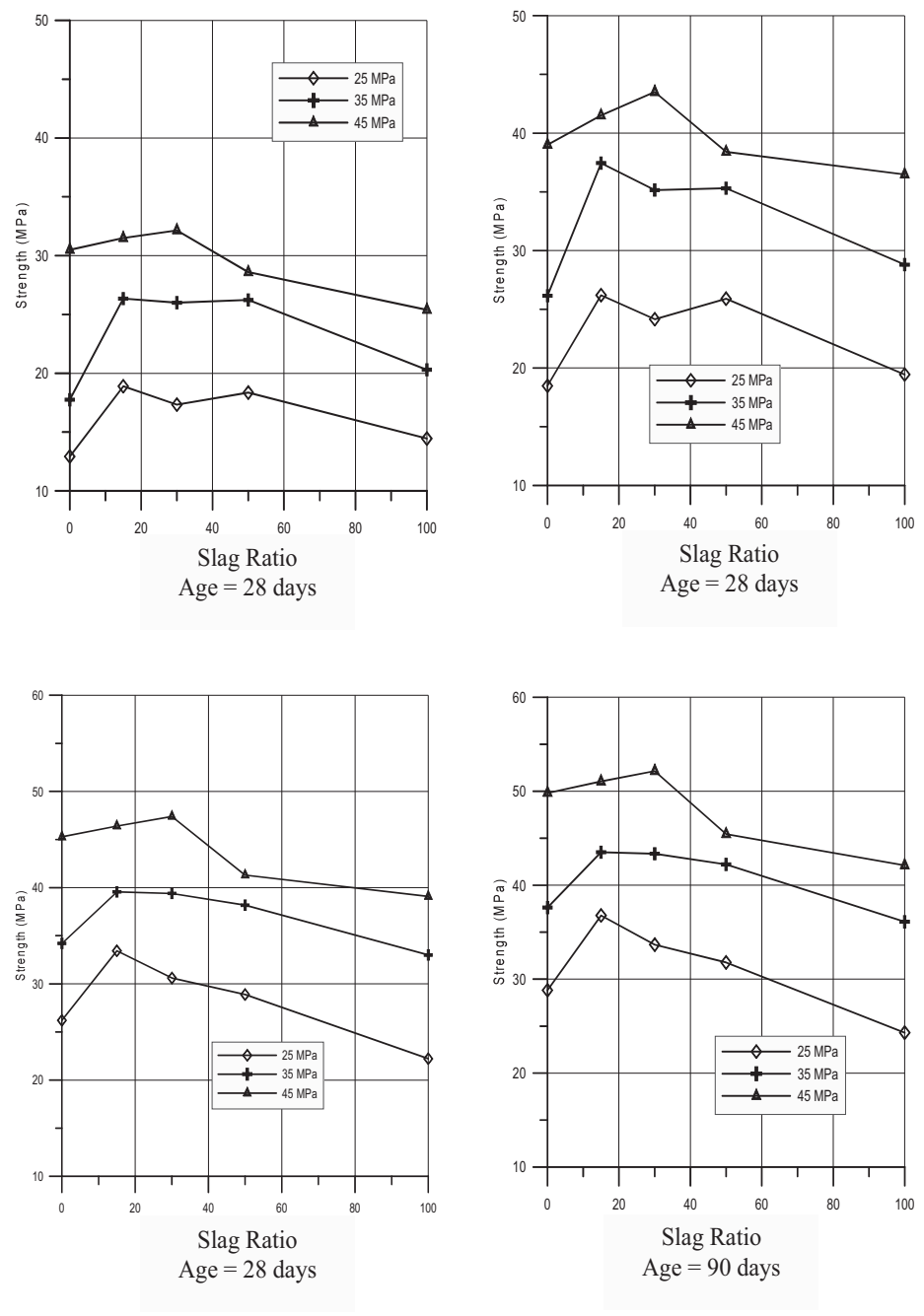


Fig. 3. Relationship between the slag ratio and the compressive strength of concrete at various ages.

**Tensile strength:** The results of flexural tensile strength of concrete are shown in Fig. 4. It is clear from all figures that the flexural tensile strength of concrete increases by the increase in slag ratio up to 50 %. However, the use of a 100 % sand replacement by slag was not beneficial when compared to the other replacements at the ages of 28 and 90 days. In all replacements, the use of slag produced concrete of higher flexural tensile strength. The increase in the tensile strength is probably due to the higher angularity of the slag particles, which increases the paste-aggregate bond strength. However, the use of high replacements (above 50%) is not as beneficial as lower ones because of the increased fineness of the slag, which increases its demand for cement.

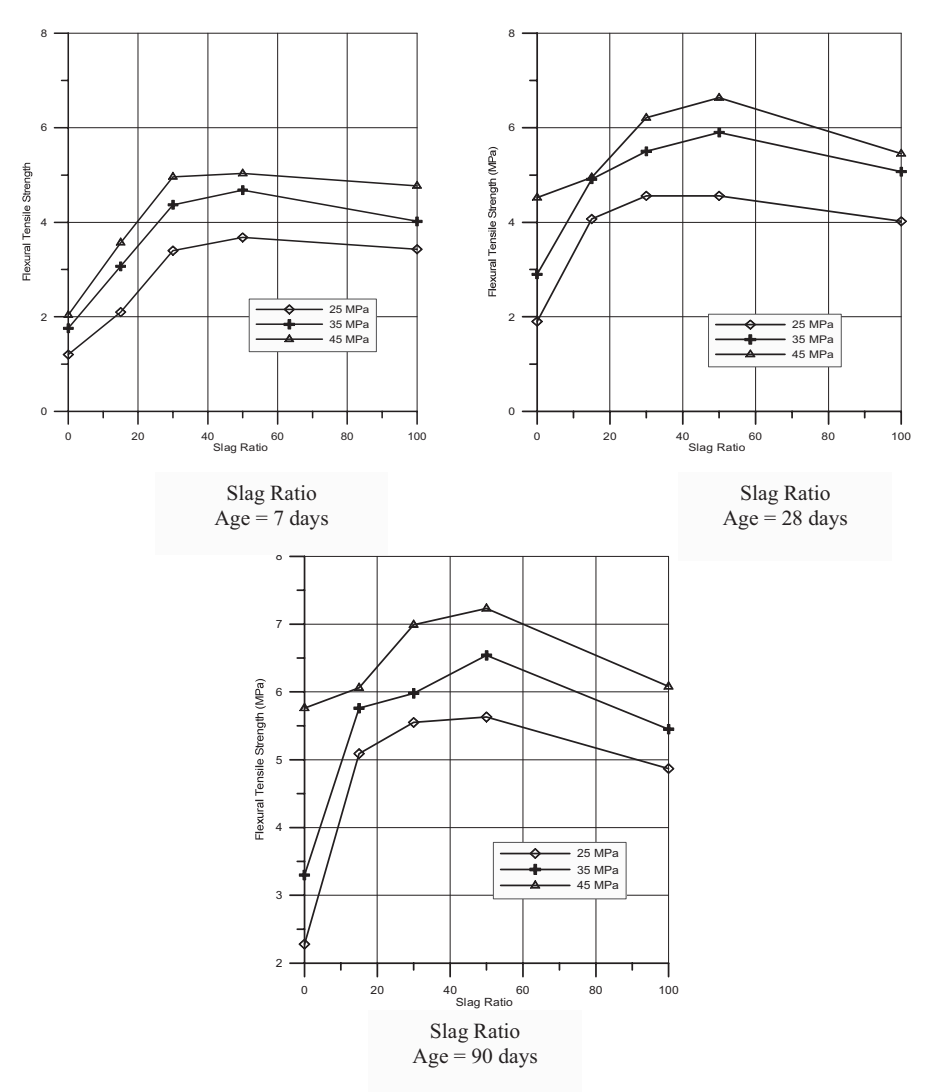


Fig. 4. Relationship between the siag ratio and the ratio of strength to the initial strength of concrete with no slag.

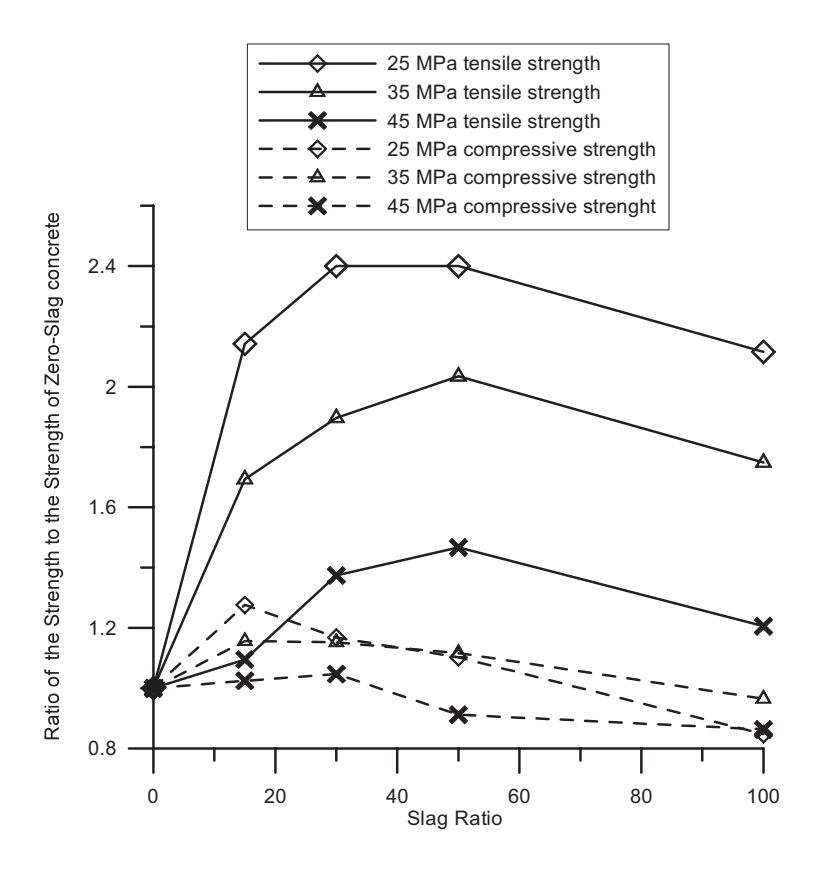


Fig. 5. Relationship between the slag ratio and the ratio of strength to the initial strength of concrete with no slag.

**General Observations:** Figure 5 shows the relationship of the strength of concrete to the strength of concrete containing no slag at the age of 28 days.

- a. Referring to the tensile strength plots in this Fig. 5, the following are observed:
- b. The use of steel slag increases the tensile strength of concrete by 1.4 to 2.4 times the strength of normal concrete, depending on the ratio used.
- c. The optimum value occurs when the sand is replaced by 25 to 50% sand-slag replacement.
- d. The lower the strength of concrete, the higher the ratio of steel slag concrete to that with no slag.
- e. All tensile strength values, including those with 100% sand replacement are always higher than concrete containing no slag.

Referring to the compressive strength plots in Fig. 5, the following are observed:

a. The use of steel slag increases the compressive strength of concrete by a maximum of 1.3 times the strength of normal concrete, depending on the ratio used. However, reduction in strength can occur beyond the 50% replacement.

- b. The optimum value occurs when the sand is replaced by 15 to 30% slag.
- c. The lower the strength of concrete, the higher the ratio of steel slag concrete to that with no slag.
- d. The compressive strength in all mixes containing 100% sand-slag replacement is always lower than strength for those mixes with no slag.

#### Conclusions and Recommendations

Based on the study presented in this research, the following conclusions and recommendations are drawn:

- 1. The use of steel slag as fine aggregate has a negative impact on the workability of concrete especially for replacement ratios above 50 %. However, this problem can be easily tackled by the use of admixtures.
- 2. Fine slag, known locally as "scrap", of low CaO can be utilized in normal concrete mixes for enhancement of both compressive and tensile strength hence eliminating one of the environmental problems created by the steel industry.
- 3. Best results for the enhancement of compressive strength are obtained when the replacement percentages are 15 to 30 %. Therefore, special care should be taken when designing mixes or when batching the material at site.
- 4. The lower the grade of concrete, the better the enhancement in compressive and tensile strength.
- 5. The use of steel slag in normal concrete mixes is beneficial for the enhancement of the tensile strength for all replacement ratios. However, the best results were obtained when the replacement percentage is about 50%. The use of steel slag increases the tensile strength of concrete by 1.4 to 2.4 times the strength of normal concrete, depending on the ratio used.

#### References

- Alizadeh R., Chini M., Ghods P., Hoseini M., Montazer Sh., M. Shekarchi M. (1996) "Utilization of electric arc furnace slag as aggregates in Concrete" Environmental Issue, CMI report Tehran. 1996.
- Asi I., Qasrawi H. and Shalabi F., 2005 "use of steel slag in engineering projects", Progress Report No. 1 submitted to United Iron and Steel Manufacturing Company.
- Geiseler, J. (1999) "Slag-approved material for better future, Proceeding of International Symposium on the Utilization of Metallurgical Slag (ISUS 99), Beijing, China.
- Kamal, M., Gailan, A. H., Haatan, A., Hameed, H. (2002), "Aggregate made from industrial unprocessed slag" Proceeding of the 6<sup>th</sup>. International Conference on Concrete Technology for Developing Countries, Amman, Jordan.

- Manso J., Gonzalez J and Polanco J. "Electric furnace slag in concrete" (2004), Journal of Materials in Civil Engineering, ASCE, November/December, pp639-645.
- Maslehuddin M., Alfarabi M., Shammem M., Ibrahim M. and Barry M. (2003), "Comparison of properties of steel slag and crushed limestone aggregate concretes", Construction and Building Materials, Vol.17, pp 105-112
- Neville A. and Brooks J. (2002), "Concrete Technology", 2nd edition, Longman, UK. Neville A. M. (1996), "Properties of Concrete", 4<sup>th</sup>. Edition, Longman, UK.
- Shekarchi, M., Alizadeh, R. Chini, M., Ghods, P. Hoseini, M. and Montazer, S. (2003), "Study on electric arc furnace slag properties to be used as aggregates in concrete," CANMET/ACI International Conference on Recent Advances in Concrete Technology, Bucharest, Romania.
- Shekarchi M., Soltani M., Alizadeh R., Chini M, Ghods P., Hoseini M., Sh. Montazer Sh.(2004) "Study of the mechanical properties of heavyweight pre-placed aggregate concrete using electric arc furnace slag as aggregate" International Conference on Concrete Engineering and Technology Malaysia.

#### Flexural and Shear Behavior of RC Beams Strengthened With CFRP Strips or Mat

#### Seleem S. E. Ahmad

Engineering Materials Department, Faculty of Engineering, Zagazig University, Egypt email: sse\_ahmad@yahoo.com

#### **Abstract**

This paper presents results obtained from an experimental investigation of reinforced concrete beams strengthened in flexure and shear using externally epoxy bonded carbon fiber strips or fabric. Three series concrete beam models were built and tested under three-point bending load. The beams were classified into three series according to the expected mode of failure: tension failure, TF, compression failure, CF, and shear failure, SF. One beam for each series was used as a control beam without strengthening. Three different methods of strengthening were used for each series.

Significant reductions in deflection, curvature, and structural ductility were observed as the RC beam strengthened by CFRP. The yielding load of the RC beam is increased up to 25% as the beam strengthened with CFRP strips in tension at bottom. No significant effect was marked on the behavior of the compression failure beams as they strengthened by the suggested techniques in this work. The cross play mat CFRP is more effective than CFRP strips as they were used in strengthening of the RC beam in shear.

**Key Words**: Flexural behavior; carbon fiber reinforced polymer; failure mode of RC, strengthening techniques, mechanical behavior.

#### Introduction

The technique of bonding steel plates using epoxy adhesives is recognized as an effective and convenient method for repair and strengthening of existing reinforced concrete structures. However the problems associated with the steel corrosion, handling, undesirable formation of weld and de-bonding lead to the need for alternative materials and further research in this field. Carbon fiber reinforced polymer (CFRP) can be used to rehabilitate or restore the strength of weakened structural element. High strength to weight ratio, resistance to electro-chemical corrosion and good fatigue strength of CFRP composites offer a viable alternative to bonding of steel plates. The flexural and shear capacity of concrete members, also, may be increased through the external bonding of CFRP sheets and fabric (Al-Amery and Al-Mahaidi, 2006; Anil 2006 and Toutanji and et al., 2006).

The effect of CFRP sheets on the strength of concrete beams was experimentally investigated (Grace and et al., 1999, Saadatmanesh and Ehsani, 1991). The failure modes and the techniques used in analyzing these modes were reviewed (Buyukozturk and Hearing 1998) for concrete beams retrofitted with FRP materials. The influence of externally bonded GFRP laminates on the failure mechanisms of flexural and shear of both damaged and undamaged concrete beams has been studied experimentally in (Hanna and Jones 1997). Results of experimental tests have been reported (Chaallal and et al., 1998) for the shear strength of concrete beams strengthened with epoxy-bonded unidirectional CFRP strips. The effect of FRP plates on the crack inclination angle and the shear capacity of concrete beams have been studied analytically (Malek and Saadatmanesh 1998).

This paper summarizes the results of the experimental testing of 12 simply supported beams strengthened with different arrangements of CFRP. The beams were classified into three series according to the expected mode of failure: tension failure, TF, compression failure, CF, and shear failure, SF. One beam for each series was used as a control beam without strengthening. Three different methods of strengthening were used for each series. The main objective of the study given herein is to examine experimentally the efficiency and effectiveness of the supposed methods of strengthening.

#### **Experimental Program**

**Geometry of Test Beams:** To understand the behavior under load of beams strengthened with CFRP strips or fabrics, three series (TF, CF, and SF) of tests consisting of four beams each were carried out under three-points bending load. All beams were identical in size,  $1600 \times 250 \times 150$  mm. Series TF consisted of four beams: TF0, TF1, TF2 and TF3, with 7 stirrups of 6 mm diameter /m. The internal reinforcement was two 13 mm diameter bars in compression and two 10 mm diameter in tension. Series CF consisted of four beams: CF0, CF1, CF2 and CF3, with 7 stirrups of 6 mm diameter /m. The internal reinforcement was two 16 mm diameter bars in tension and two 8 mm diameter in compression. Series SF consisted of four beams: SF0, SF1, SF2 and SF3, with 4 stirrups of 6 mm diameter /m. The internal

reinforcement was two 10 mm diameter bars in compression and two 10 mm diameter in tension. The reinforcement and dimensions details are shown in Fig. 1.

**Material Properties:** The concrete of the three series was designed for 28-day cube strength of 30 MPa. The internal reinforcing bars were hot-rolled steel with average measured yield strength of 350 MPa and a tensile strength of 520 MPa. The stirrups were made of mild steel with yield strength of 280 MPa and a tensile strength of 365 MPa. The main properties of steel and concrete are given in Table 1.

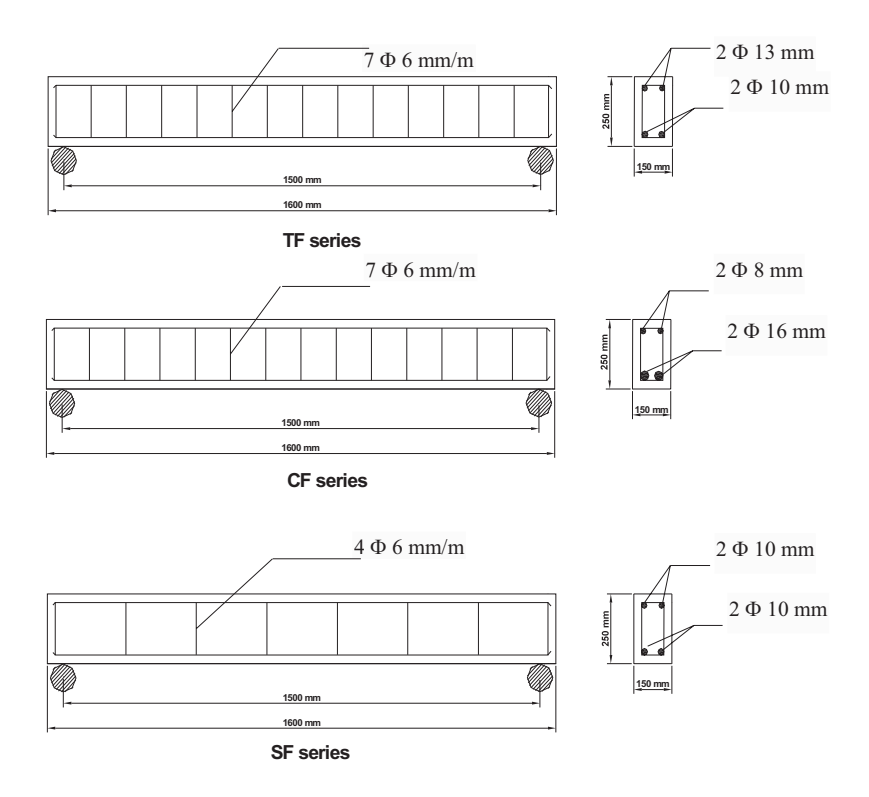


Fig. 1. The reinforcement and dimensions details of the test specimens.

**Table 1. Properties of the Used Materials** 

Duonauty	Internal steel		CFRP	Epoxy adhesive	Concrete
Property	stirrups	main	strips	adhesive	Concrete
Density, Kg/m <sup>3</sup>	7800	7800	1500	1650	2300
Modulus of elasticity, GPa	206	206	165	13	23
Tensile yield strength, MPa	280	350	2800	>25	-
Compressive yield strength, MPa	280	350	-	>100	30
Elongation at failure (%)	23	16	1.7	-	-

The fabric consisted of carbon fibers set at 90 degrees in the longitudinal and the transverse directions so as to obtain a flexible weave to match the shapes of the backings. Unidirectional carbon fiber strips 70 mm wide and 1.2 mm thick, were used in this study. The fabric and unidirectional strips were from SIKA Inc. in Egypt. The main characteristics of the carbon fiber, as supplied by the manufacturer, are given in Table 1. The adhesive used for bonding the strips and fabrics to the concrete surfaces was a two-component epoxy resin named Sikadur-30. The two components were mixed mechanically with a helicoidally whisk until the mixed product was of uniform color. The characteristics of the adhesive, as supplied by the manufacturer, are given in Table 1. Before bonding the strips and fabrics, the concrete surfaces were subjected to moist sandblasting and hydraulic scouring. Initially, the concrete surfaces were coated with a layer of adhesive of uniform thickness to obtain a good surface impregnation. The strips and fabric, cut to the required size, were then applied to the moist resin using a flexible roller.

Strengthening Details and Test Rig: Three different methods of strengthening were used for each series. In the TF series the beams were strengthened by bonding CFRP strips on the bottom face of the beams, on the tension zone side of the beams and on the tension and compression zones side of the beams. In the CF series the beams were strengthened by bonding CFRP strips on the bottom face of the beams, on the compression zone side of the beams and on the tension and compression zones side of the beams and on the tension and compression zones side of the beams. In the SF series the beam were strengthened by bonding a cross play fabric mat on the zone of maximum shear stresses (the outer third of the beam), bonding vertical strips on the zone of maximum shear stresses (the outer third of the beam) and bonding a diagonal strips with 45 degree on the zone of maximum shear stresses (the outer third of the beam). The strengthening details are shown in Fig. 2.

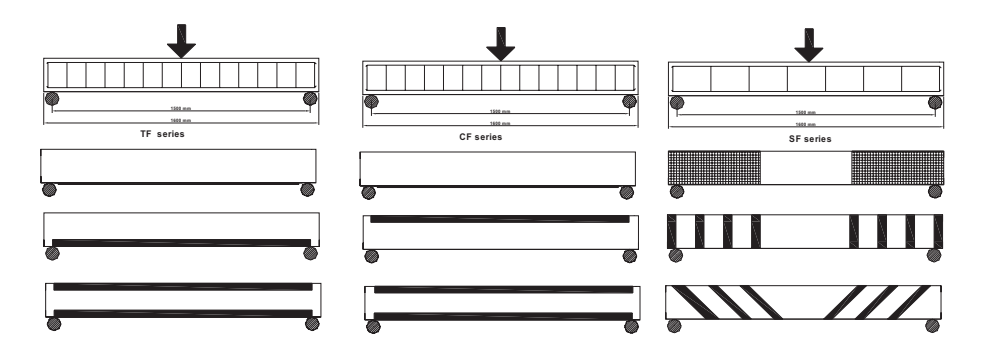


Fig. 2. Strengthening details of the tested specimens.

Each test beam was loaded as shown in Fig. 2. Loads were measured directly from the test machine. The mid span deflections were measured using digital strain gauge of accuracy 0.001 mm. The applied load and the resulting mid span deflection were recorded at load increment of 5 KN.

#### **Tests Results and Discussion**

**Control Beams:** The strength and deformation capacity of the control test specimens varied significantly depending on the area of internal reinforcing steel. The measured response of the control specimens, without strengthening, is shown in Fig. 3.

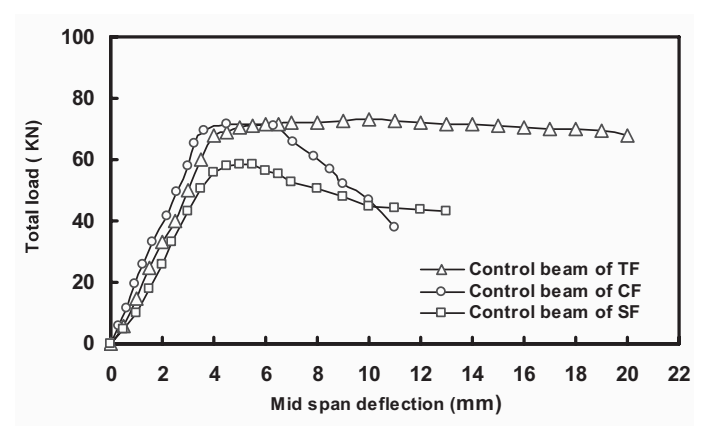


Fig. 3. Total applied load versus mid span deflection of control beams.

The response of the control beams was essentially similar before the concrete cracking and the steel yielding. The control beams of TF, CF and SF showed approximately linear response between the applied load and mid span deflection up to load of 68, 69.9 and 56 KN respectively (yielding load in each specimen). After yielding, all control beams showed a nonlinear response between the applied load and mid span deflection. The degree of nonlinearity was varied according to the expected mode of failure. From the load deflection curves of control beams in Fig. 3, it could be observed that the initial stiffness and yield load of CF specimens are higher than those of TF specimens, and SF specimens. This result can be attributed to the differences between the total areas of internal steel in each beam. After yielding, the stiffness of the CF specimens was abruptly decreased as compared to the stiffness of the TF and SF specimens.

#### Tension Failure Beams, TF

A comparison between the behavior of TF beams and control beam is given in Fig. 4. The response of the TF beams was initially similar to the control beams up to the steel yielding with slightly increase in the stiffness of the strengthened beam. Moreover, the yielding loads of the strengthened beams were enhanced. The yielding loads for the beam strengthened in tension at bottom, the beam strengthened in tension and compression at side and the beam strengthened in tension at side are about 85 KN, 79 KN and 74.5 KN respectively; while the yielding load of the control beam is about 68 KN. This means that the strengthening techniques which used in this work enhanced the yielding load of the tension failure beams by 25%, 16% and 9% respectively. This result can be attributed to the high efficiency of the strengthening in tension at bottom due to the higher closing effect of the CFRP strips for the predictable micro cracks.

The results in Fig. 4 clearly show a higher decreasing in the stiffness after yielding for the beam strengthened in tension at bottom as compared to other beams. This observation can be explained as a result of differences in the mode of failure. The beam strengthened in tension at bottom failed due to peeling of concrete cover. The cracks initiated from the end of CFRP strip, then proceeded at about 45° angles up to the internal longitudinal steel, then continuing horizontally through the concrete at the level of the reinforcing steel (Plate 1).

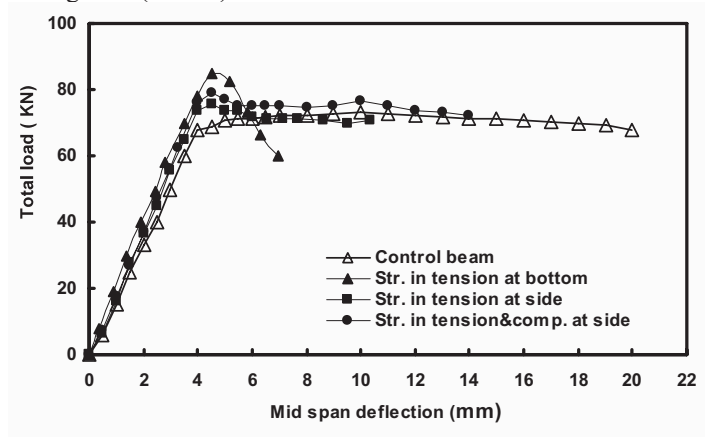


Fig. 4. Total applied load versus mid span deflection of control and strengthened beams for TF group.



Plate 1. Peeling failure mode for the beam strengthened in tension at bottom.

Plate 1 shows peeling failure mode for this beam. The other two beam failed by similarly crack patterns. First crack usually occurred at a slight load than unplanted beam. Initially, the cracks were vertical, as would be expected for flexural cracks, but later they would bend over in the shear regions.

**Compression Failure Beams (CF):** The measured response of the CF specimens strengthened with different configurations of CFRP strips shown in Fig.5. In this figure, the response of the corresponding control specimen is also given. The response of the strengthened specimens was essentially the same as the response of control beam before the concrete cracking. Moreover, the strengthened specimens tends to be a slightly stiffer than the control specimen after cracking especially for the strengthened beam in tension and compression at side (Plate 2).

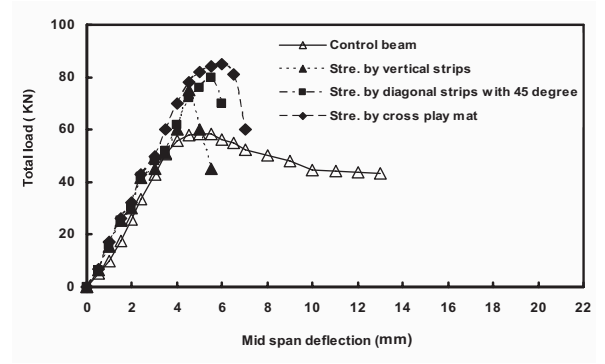


Fig. 5. Total applied load versus mid span deflection of control and strengthened beams for CF group.



Plate 2. Failure mode for the beam strengthened in compression at side.

Plate 2 shows the failure mode of the strengthened beam in compression at side. All the strengthened beams in compression failure group failed when the CFRP strips debonded from the surface of the concrete. This was approximately a sudden mode of failure. The strengthened CF concrete beams fail due to the term of separation of CFRP strips. Separation of CFRP strips take place from the concrete surface at mid span and extend towards the supports. A crushing of concrete at the mid span loading point was

observed in the specimen shown in Plate 2. Some of flexural cracks were also observed in the specimen strengthened in tension and compression at side. Bond between the CFRP Strips and the concrete is of critical importance to the effectiveness of externally bonded CFRP strips. If this interfacial bond is compromised before CFRP sheets rupture, sheet-debonding failure occurs. Such a failure mode diminishes the strengthening potential of an externally bonded CFRP sheet.

**Shear Failure Beams (SF):** The experimental load/mid span deflection curves for control and strengthened beams are shown in Fig. 6 for the shear failure group, SF. The pattern of the curves in Fig. 6 indicates that the control beam has a maximum load of 56 KN and fail after a moderate sufficient warning. The pattern of curves in Fig. 6 indicates that the strengthened beams by vertical strips has a maximum load of 72 KN (i.e. 28% increasing as compared to the control beam) and fails without sufficient warning. A similar behavior was observed for the strengthened beam by diagonal strips with 45°. This beam has a maximum load of 80 KN (i.e. 42% increasing as compared to the control beam). These two beams fail due to debond and separation of CFRP strips followed by shear failure. Flexural and shear cracks are observed in the two beams without crushing of concrete at loading point.

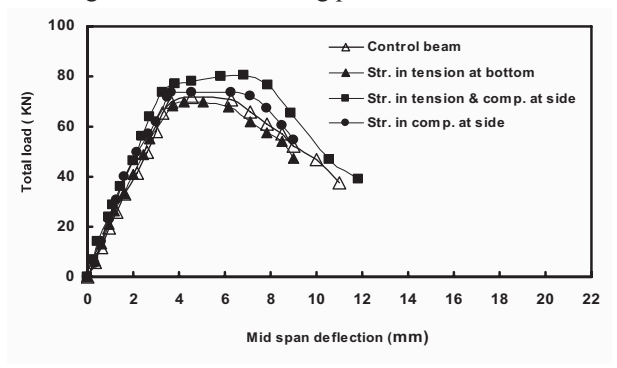


Fig. 6. Total applied load versus mid span deflection of control and strengthened beams for SF group.

On the other hand, the beam strengthened by cross play mat has a maximum load of 85 KN (i.e. 51% increasing as compared to the control beam) and fails after a slightly sufficient warning as compared with the other two beams. Only flexural cracks were observed in this beam which indicates the existence of strong bond between the concrete and surface of the CFRP mat. Plate 3 shows the failure mode of this beam.



Plate 3. Failure mode for the beam strengthened in shear by cross play mat.

#### Conclusions

The following conclusions are drawn based on the experimental studies carried out under this work:

- 1. The yielding load of the RC beam is increased up to 25% as the beam strengthened with CFRP strips in tension at bottom.
- 2. No significant effect was marked on the behavior of the compression failure beams as they strengthened by the suggested techniques in this work.
- 3. The cross play mat CFRP is more effective than CFRP strips as they used in strengthening of the RC beam in shear.

#### References

- Al-Amery R., and Al-Mahaidi R., (2006) "Coupled flexural–shear retrofitting of RC beams using CFRP straps", Composite Structures, 75, PP 457–464.
- Anil O., (2006) "Improving shear capacity of RC T-beams using CFRP composites subjected to cyclic load", Cement & Concrete Composites, 28 PP 638–649.
- Buyukozturk O., and Hearing B., (1998) "Failure behavior of pre-cracked concrete beams retrofitted with FRP", Journal of Composites for Construction ASC, 2(3), PP 138-144.
- Chaallal O., Nollet M.J., and Perraton D., (1998) "Shear strengthening of RC beams by externally bonded side CFRP strips", Journal of Composites for Construction ASCE, 2(2), PP 111-114.
- Grace N. F., Sayed G.A., Soliman A.K., and Saleh K.R., (1999) "Strengthening reinforced concrete beams using fiber reinforced polymer (FRP) laminates", ACI Struct. J., 96(5), PP 865-874.
- Hanna S., and Jones R., (1997) "Composite warps for aging infrastructure: Concrete beams", Engineering Failure Analysis, 4(3), PP 215-225.
- Malek A., and Saadatmanesh H., (1998) "Ultimate shear capacity of reinforced concrete beams strengthened with web-bonded fiber-reinforced plastic plates", ACI Struct. J., 95(4), PP 391-399.
- Saadatmanesh H., and Ehsani M.R., (1991) "RC beams strengthened with GFRP plates. I: Experimental study", J. Struct. Engrg. ASCE, 117(11), PP, 3417-3433.
- Toutanji H., Zhao L., and Zhang Y., (2006) "Flexural behavior of reinforced concrete beams externally strengthened with CFRP sheets bonded with an inorganic matrix", Engineering Structures, 28, 2006, PP 557–566.

# Repair Work at the Tower-Concrete Structure on the Batllava Lake

Naser Kabashi, Faculty of Civil Engineering, Prishtine, Kosovo Cene Krasniqi, Faculty of Civil Engineering, Prishtine, Kosovo Fisnik Kadiu, Faculty of Civil Engineering, Tirane, Albania

#### Abstract

Numerous buildings originally constructed for a specific use are required to undergo extensive repair as a result of different external conditions during the work life. This paper presents the details of the repair work on the reinforced concrete tower structure of the Batllava Lake. The main objective of this project is to strengthen concrete structure after the displacements caused by water-ice during the winter which has brought the water-leakages in the tower. The project included stopping the water leakages with injections (including the expansion materials) and strengthening of the structure in general. This paper also discusses the special materials used and the characteristics that made them most suitable for this kind of repair work.

**Key Words**: Concrete, repair, concrete rings, expansion materials, reinforcement.

#### Introduction

The current situation of the Tower on lake Batllava and the paramount importance of this building was the reason to analyze and to solve the problematic situation that came about. This paper is based on the current situation of construction, our experience in repair works and the experience with the materials used for this kind of work. The paper presents the problems and the situation as they were before and after the repairing works, allowing thus to see the differences. During the repair works, we also took care of statically strengthening of construction, always having in mind the priority importance of the facility.

### **Function of Tower**

Lake Batllava is a source of drinking water for four hundred thousands inhabitants of Prishtina, the capital city of Kosova. The tower is constructed on the dam of this artificial lake. Its main function is to receive water from three levels of the lake and convey it to the water treatment facility, and then through the pipeline system for consumption. The tower is approximately 40m deep with 35m under the water level (Fig. 1).

#### **Causes of Deterioration**

During the winter of 2004, the lake and its surrounding area fell under the influence of an extremely cold weather conditions and the lake froze in depth of about 0.6m. The movement of ice blocks formed these conditions caused displacement in the structure, creating cracks in the bottom of tower. This caused leakage of water inside the tower causing damage in the machinery and made it impossible to access them for maintenance (Fig. 2a and b).



Fig.1. General view of the tower in the Lake Batllava.

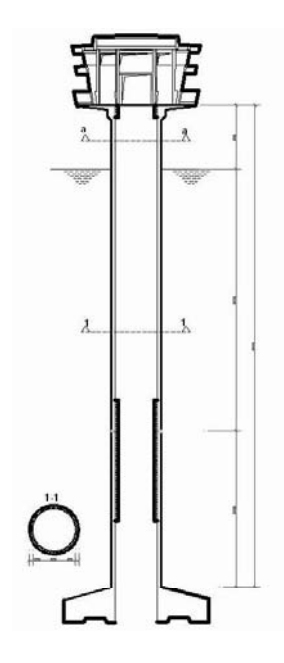




Fig.2a. Elevation of the tower.

Fig.2b. Water leakage in tower before repair.

# **Design Criteria**

The ice forces are the main factor causing cracking, and the following briefly presents the basic calculations to evaluate these effects (Fig. 3).

# Hydrostatic forces

The hydrostatic force is calculated as:

$$W_{\text{stat}} = \frac{1}{2} \gamma_u H^2 \tag{1}$$

Where  $\gamma_u$  is the water density taken as 10 kN/m<sup>3</sup>, H is the height the water level, and  $W_{stat} = 0.5 \times 10 \times 40^2 = 8000 \text{ kN/m}$ 

### Ice forces-static force

The static force from ice action is calculated as:

$$F_{ice,stat} = 150 \div 220 \frac{kN}{m^2} \text{ or}$$

$$W_{ice,stat} = d \times F_{ice,stat} \frac{kN}{m^2} F_{ice,stat} = 200 \frac{kN}{m^2}$$
(2)

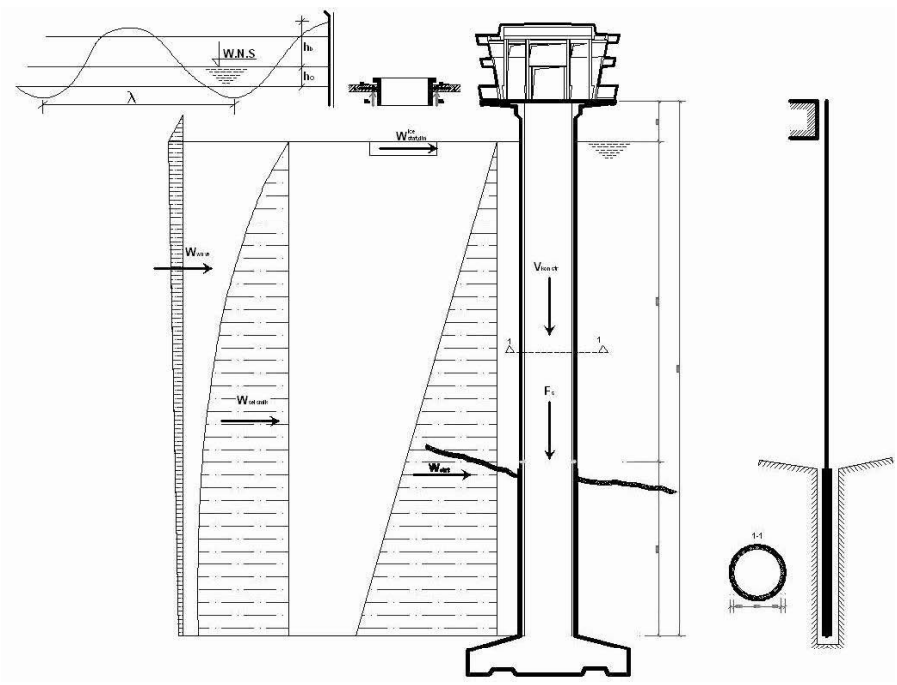


Fig.3. The basis for calculations of ice forces.

# Ice force-Dynamic force

The ice dynamic force is calculated as:

$$W_{ice,din} = K_a \times V \times d \times \sqrt{F_{ice}} (kN)$$
(3)

Using the relevant conditions the result it will be

$$W_{ice.din} = 29.4 \times 0.6 \times 1.0 \times \sqrt{8} = 52,92 \text{ kN/m}$$

Also during the calculations we used the following forces:

- -Wave force: 
$$W_{\text{wave}} = 560 \text{ kN/m}$$
 (4)

- - Seismic force from water 
$$W_{\text{seiz}} = 3067.9 \text{ kN/m}$$
 (5)

- - Seismic force from ice blocks 
$$W_{\text{seiz,ice-part}} = 29,88 \text{ kN/m}$$
 (6)

- - Seismic force from construction 
$$V_{kons} = 1.57 \circ 40 \circ 25 = 1570.8 \text{ kN}$$
 (7)

Based on these force components we calculate the construction and solve the methodology of reinforcement, and type of pre-stressing. Assuming the need for repair is not derived from inadequate strength; however, there is some controversy about the required structural performance for many repairs.

Evolution of the repair system with regard to the structural stability is considered and presented further below:

Usually it is taken for granted that the structural performance of the structure would be the same as was before deterioration. The order of the repair can be designed specifically to accommodate the redistribution of loads.

### Repairing Works

The main problem before starting the repairing works was to stop the water leaking inside. The pressure of the water was very powerful and it was almost completely inaccessible. The materials to be used had to meet several requirements:

- High adherence to the substrate;
- Shrinkage must be low;
- Creep should be similar to that of concrete;
- The strength of material should be similar to that of concrete.

#### Selection of Materials

The repair materials used in this project were manufactured by MAPEI in Italy. The following table will present their main characteristics:

Table 1. Main Characteristics and Constituent of used Materials

Base of materials	Constituents	Reaction	Commercial
			product
Inorganic cement-	High strength cement	Compensated shrinkage	Lamposilex
based material (no	and special admixture	Quick setting	
traditional mortars)	(aluminate cement,	High mechanical	
	expansive agents)	strength in short time	
Organic based	Epoxy resin	High fluidity	Resfoam
material (resins and	Polyurethane	Penetrations	1KM
polymers)	Polyester resin	Waterproofing the	
		cracks	

# **Preparation Work**

The first step was the removal of the concrete in critical positions up to about 10 cm depth in locations where the reinforcement steel was exposed. After that, sponges were used to stop the water leakage on the critical length and to decrease the water pressure. The water leakage was adjusted in a few draining pipes (Fig.4). Parallel to this operation, Lampsilex was used to close the cracks, and to control the water flow. This step is illustrated in Fig.4.





Fig. 4. Preparing works and using of Lamposilex, as a water stopping material.

The next step was to waterproof the structure by injecting Resfoam 1KM by inserting a piston pump through the special packers into the structures. Upon contact with water, this material formed a semi-rigid waterproof polyurethane foam. This exercise was successful in closing the small cracks and consequently stopped the water leakage. The result is presented in Fig.5.





Fig. 5. Using the Resfoam 1KM for the injection with the packers.

Stopping the water leakages created better condition for further work in strengthening the critical locations.

# **Strengthening of Structure**

The design of the repair work aimed at improving the strength and stability of the structure to a level similar to that of a new structure. The strengthening was accomplished by casting reinforced concrete rings, which were stuck in the old concrete in a way that they create a new structure (see Fig 6).

Technical data of the ring: Length: 4.0 m

Depth: 0.25 m

Steel reinforcement: Based on the static calculations

Concrete: SCC (C 35/45)

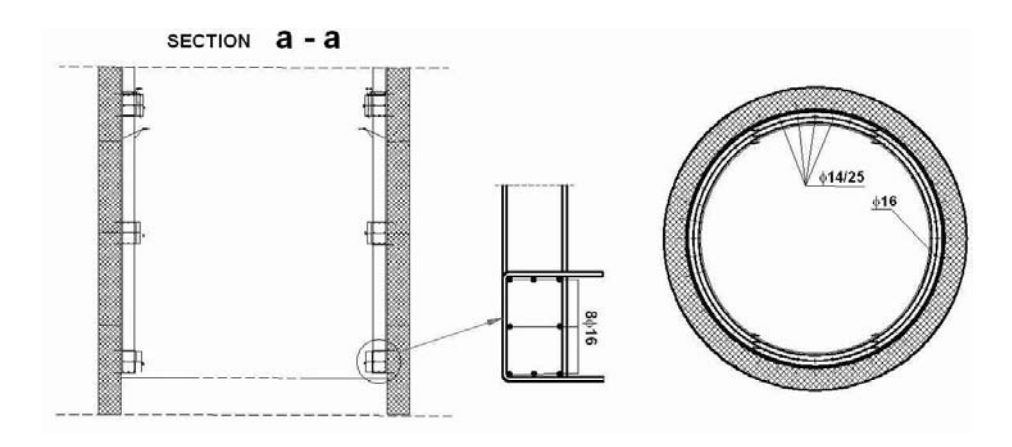


Fig. 6. Primary ring – the critical ribbon.

Another smaller ring was constructed at the top of structure in order to connect the main ring with the other parts of structure on the top. The connection elements-cables (reinforcement steel) for pre-stressing are inclined relative to the main ring and oriented towards the crown top ring. The pre-stressing was done when the concrete strength had achieved the desired values. Details of the top ring are presented in the Fig.7.

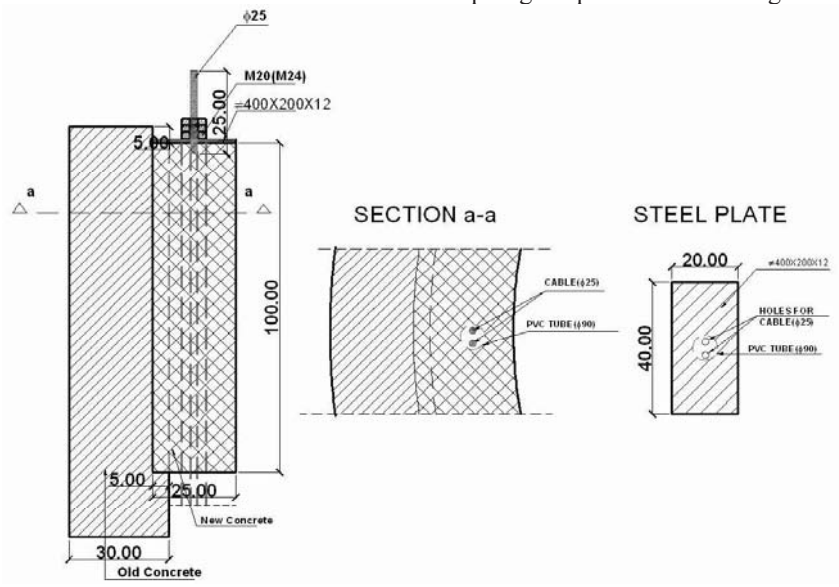


Fig. 7. Construction details of top ring.

Before laying of the new concrete, traces of old grouts, oil, grease, paint and other worn-out materials and substances were removed from the surface. The next step was cleaning to improve the bond between the two layers of concrete, by washing with water under pressure. After that surface was coated with a thin liquid mortar of Cement and Planicrete. Details of this mortar are presented in the Table 2.

Table 2. Concrete Surface Treatment between Two Layers

Type	Material	Mechanism of Action	Properties	Thickness
Coating	Cement-	Anti-carbonation and	Improved the	5 mm
	based	chloride barriers	connection between	
			concrete layers.	

Fresh concrete had to travel down a distance of thirty-five meters and segregation was a serious concern. Self Compacting Concrete (SCC) was used and the concrete was successfully cast without noticeable segregation. The situation after concreting is shown in Fig.8.





Fig. 8a. During the concreting.

Fig.8b. After concreting.

## **Controls After Execution**

The final hardened condition of the repair work was determined by application the following test, and the relevant results.

**Table 3. Properties of Hardened Concrete** 

Characteristics	Test	Parameters
Compressive strength	Rebound hammer	C 35/45
Adhesion	Pull-off	>1.5 MPa
Shrinkage cracking	visual	ok
Delamination	Hammer tapping	ok
Resistively	Wenner test	ok
Voids	Ultrasonic test	ok
Permeability to water	Penetration test	ok

The results confirmed the quality execution of works and the behavior of the used materials. Finally, the pre-stressing of cables-reinforcement steel is done based on the percent of elongation of steel. The structure is considered like a new structure, incorporating the old and new concrete.

#### Conclusions

Structural strengthening of concrete and repairing is an art form that has evolved into a complex science. It involves the use of conventional and new materials, as well as new techniques applied for several cases. We must recognize that strengthening design and detailing is much more complex than new construction. In addition to dealing with the unknown actual structural state, is the degree to which new materials are added to an existing structural state.

This paper presents the state of the structure before, after the repairing and strengthening, and compares both situations. The Tower is now utilized fully and safely; it is completely dry inside and the machinery operates without breakdowns, which resulted from the wet conditions reigning before the repairing.

The main thing to do was to stop the water leakages, only from inside, because it was impossible to do anything from the outside because of the deep waters. The methodology used in these works was genuine and tailor-made to the conditions of the specific site and the works were performed step by step in a sequence. The materials used were produced by "MAPEI"- Italy and offered wider options compared with materials used before in our region. Also in the critical ribbon we increased the rigidity of structures, in this case to make sure of the inclination of the structures, and prestressing would make it possible for the structure to behave identically to a new one.

#### References

- 1. REHABCON: Strategy for maintenance and rehabilitation in concrete structures (2000).
- 2. Concrete repair guide: Reported by ACI Committee 546 (2004)
- 3. Jakob Sustersic; Franci Kavcic; Bojan Grum; Sanacija Betonskih Objektov(2004); Ljubljana, Slovenia.
- 4. Build 365: Concrete, repairing materials and protective coating.
- 5. Build 368: Concrete, repair materials: Capillary absorption.
- 6. MAPEI Concrete Repair Materials.
- 7. EN 206:2000, Concrete-Part 1 : Specification, performance, production and conformity.
- 8. EN 1543. Product and systems for the protection and repair of concrete structures. Measurement of bond strength by pull-off.
- 9. NISTIR 6042. Predicting the performance of concrete repair materials (1999).
- 10. Johan Wilberg: Bond strength between repair material and substrate in concrete patching repairs (2003).
- 11. N. Kabashi: Used the local materials to produce the HPC; (2006), Ljubljana.
- 12. Product guide-Concrete repair-"CLAN" (2003).

# Repairs and Rehabilitation of Town Hall-Calcutta

S.K. Manjrekar and R.S. Manjrekar

Sunanda Speciality Coatings Pvt. Ltd., Mumbai, India

#### Abstract

The historical heritage Town Hall was built in the year 1813 by the East India Company to serve as a meeting place for large gatherings and recreations; it was a showpiece building no visitor could fail to notice. Built in Tuscan-Doric order of the Palladian style it has two storeys above a brick vaulted foundation. This beautiful heritage building over the years had fallen into a state of bleakness and dereliction and needed major restoration to bring back its original glory.

This paper highlights the various aspects covered, technical expertise involved in selecting an effective rehabilitation scheme, limitations in the conventional schemes, selecting the specialised construction chemicals etc used during the preservation of this heritage structure which today stands a proud and rejuvenated monument in the city of Calcutta, in India.

#### Introduction

The historical heritage Town Hall was built in the year 1813 by the East India Company to serve as a meeting place for large gatherings and recreations. It was a showpiece building no visitor could fail to notice.

The historical importance of the structure together with the patriotic sentiments the citizens of Calcutta had for this structure both called for its restoration back to its original dignity. This beautiful heritage building had once lived and breathed history and hosted momentous meetings and men of courage. But over the years it had fallen into a state of bleakness and dereliction and needed major restoration to bring back its original glory.

A functionally sound and sensible facelift was necessary and was carried out as per the procedures explained here.

## **Background**

The Town Hall of Calcutta forms an integral part of the socio-political history of the Modern Bengal. Built in Tuscan-Doric order of the Palladian style, it has two storeys above a brick vaulted foundation. A structure built by the East India Company by raising funds through public lottery was completed in 1813. Colonel John Garstin, the then Chief Engineer of Bengal was entrusted with the design and construction of this structure.

The purpose of constructing this hall was to create a public space where one could hold meetings and formal receptions and display marvels of the English worthies. The building served as a place for public meetings, large gatherings and recreations even though it was constantly under repairs from the day it was constructed.

Initially "The Town Hall" Committee managed the hall; thereafter the management of the hall underwent periodic changes and finally in 1867, the hall became the property of the Municipality (later on Corporation) of Calcutta.

The hall has witnessed a galaxy of Indians attending meetings within its portals. It has housed the historic public gathering for the protest against the division of Bengal in 1905, the felicitation of Shri Rabindra Nath Tagore after his winning the Nobel Prize in 1813. It also held the celebration of Tagore's 70th birthday.

The post independence period saw the Town Hall being gradually converted into the Municipal Magistrates Court and other offices of the Calcutta Municipal Corporation. A part of it was also occupied by the Municipal Service Commission and the Public Service Commission. As a result of such random occupations in pre- and post-independence era, some of the inherent structural defects became more acute. Right from its inception the Town Hall was structurally weak and the patchwork repairs from time to time only added to its problem. Decades of impudent interference with the structure and cluttering of the halls with offices reduced the beautiful historic building into a dilapidated structure. It was almost on its way to destruction.

### **Initial Survey and Findings**

Structurally, the town Hall was built with brick and wood. It was a two storied structure above a brick vaulted foundation. The Ground Floor was about 23 feet high containing a marble hall and few smaller rooms. The upper floor was 30 feet in height. The building on the whole was a solid rectangular block with two protruding porticos on the South and North. A series of grand steps from the road in the front (Esplanade Road) led to the collonaded front portico while a second entry from the rear side used to serve the way for carriage ways.

The building demonstrates a load bearing structure with brick masonry of 975 mm thick and circular columns 775 mm thick. The mortar principally was lime, sand and brick dust. The average thickness of plaster was 20 mm. The Central Hall has two rows of 22 columns each in the East-West direction. The Basement has been constructed with barrel vaults spanning between the walls and the columns with a cross vault running along the central axis in the North-South direction.

The wooden beams of the first floor had sagged and could no longer take the load of the first floor. As a result, a series of cast iron pillars were placed along the brick columns to support the first floor.

Consequently, the Main Hall on the ground floor had become a jungle of columns and beams at the floor level making it unworthy of holding any large gatherings. The brick vaults in the foundation were in poor conditions as moisture content in them were high and huge cracks had developed in several places due to the load of the large marble statues on the ground floor and some cast iron supports. The fourteen skylights were made of wooden frames with wired glass louver. The main source of leakage was from the skylights as the lower frames had rotted and gave away. The glass louvers had broken allowing free access to rain water thereby damaging the wooden floor; below many of the skylights turned soft and spongy from continuous water absorption. The roof slab had several levels and waterproofing and large part of the roof was leaking and the seepage water got absorbed in the wall and columns. Also, it was severely damaged exposing the rusted reinforcement bars where portions of the roof slab had come off.

The original roof waterproofing was done with lime terracing which became undulated in the course of time. As a result, pockets of accumulated rainwater all over the roof terrace started the slow disintegration of the lime terracing which does not have the binding strength for retention over a large area. The rain water pipes were placed arbitrarily along the parapet wall damaging the cornices and the terracotta motifs on the exterior wall. These and several other detail findings were placed before a Technical Recommendations Committee and recommendations were formulated.

#### Recommendations

A thorough inspection of the building was done by removing small pieces of plaster, paint and other material. Measured drawings were prepared. Lists of material to be used were made. After a complete assessment of the damage, a statement was prepared giving priority to certain items and estimates were drawn up for various options for

restoration of each item. Each item was evaluated against time and cost. Some items were kept for the second phase of restoration.

Finally, it was decided to include the following items taking into consideration the budget:

- 1. Roof waterproofing
- 2. Structural strengthening
- 3. Grouting of polymers (in foundation & superstructure)
- 4. Replacement of external and internal plaster
- Restoration of doors and windows
- 6. Restoration of the steps leading to the front portico
- 7. Restoration of the wooden staircase leading to the first floor mezzanine
- 8. Restoration of the fourteen skylights at roof level
- 9. Repair and upgradation of toilets
- 10. Replacement of drainage and sewerage lines
- 11. Realignment of rain water lines
- 12. Removal of old electric lines
- 13. Upgradation of landscaping
- 14. Addition of a gate and railing in the front

All above referred areas were dealt with great details to get the serviceable and rejuvenated structure. However, in this paper only the first four items in which special introduction of state-of-the-art polymer technology is involved are considered with respect to their methodology, properties and the mechanism.

## 1. Roof Waterproofing:

Conventional ways of waterproofing the structure are like brickbat coba followed by IPS. Brickbat coba is generally used to provide a slope to the treatment and IPS layer works as an impermeable treatment by itself, which also assumes the slope of brickbat coba. The brickbat coba is not otherwise supposed to be waterproof, but on the contrary is absorbent which accumulates the water. On saturation, the brickbat coba attempts to transfer the water further, which generally penetrates into the slab, and penetrates more easily if the same is porous or full of cracks.

In order to take care, polymeric cementitious waterproof coatings are preferred world over. These systems have better adhesion to the surfaces and can tolerate to an extent the deficiencies of the surface like slight wetness and microdusting etc. The thickness of these coatings also is 8 to 10 times more than pure polymer coatings.

Another practical approach adopted is to incorporate the water-based polymers in the IPS itself. This increases the water impermeability of the IPS and at the same time decreases the extent of shrinkage cracks due to increase in the flexural strength of the matrix. Additionally, the use of polymers in cement concrete/mortar is found to increase the adhesion of the concrete mortar to the surface. Considering the above facts the specifications adopted were as follows.

### **Specifications:**

- 1. Existing Tarfelt treatment including loose base material was removed.
- 2. Pockets of loose sub base were repaired with brickbats and 1:4 cement sand plaster with addition of 5% POLYALK EP (Polymeric Mortar Modifier).
- 3. Waterproof plaster was provided at the parapet. The plaster was finished smooth and grooves of 5 mm were provided at a grid of 1.2 X1.2 meters-rounding to be provided at the junction of parapet wall with usual notching detail at 200 mm high dado
- 4. Plaster was cured and roof was ponded with water 100 mm high for 7 days.
- 5. The ponded water was removed and 5 mm grooves were filled with polymer mortar putty of 2:5:15 ratio of POLYALK EP: Cement: Sand with 0.4 water cement ratio.
- 6. The roof was allowed to dry for 7 days without curing.
- 7. Waterproof coatings were applied with POLYALK WP (Polymeric cementitious waterproof coating): Cement in the ratio 1:1.5 by weight and kept agitated by stirring continuously in container. Two coats of this were applied at an interval of not less than 4 hours. Refer Table 1 for results of waterproofing surface coatings of POLYALK WP tested as per DIN 1048.
- 8. After two days of final coat, mist curing was provided by spray or gunny bags for 2 days, then air cured for 15 days at the end of which water was ponded again up to 100 mm height for testing.
- IPS was carried out, admixed with water-based polymers @ 2% by weight of cement.

Table 1. Results of Waterproofing Surface Coatings of POLYALK WP 15 cm Concrete Cubes: DIN Results

Temperature of conducting test: 30°C Duration of test: 5 days

Test pressure: (as per DIN 1048): 1 bar for 48 hours 3 bars for 24 hours

7 bars for 24 hours

Sr. No	Permeability	Age at Testing	Remarks
1.	12 mm	33 days	Chemical POLYALK WP applied in
	11 mm		single coat and then cubes were
	07 mm		cured by sprinkling water through
			sponge kept on top face of the cube.
2.	35 mm	37 days	Chemical POLYALK WP applied in
	35 mm		single coat and then cubes were not
	48 mm		cured.
3.	0 mm	42 days	Chemical POLYALK WP applied in
	0 mm	Ţ	double coat and then cubes were
	0 mm		cured.

## 2. Structural Repairs:

Carbonation is one of the principle causes of corrosion and it brings about various physical changes in the quality of concrete. However, it affects the alkalinity of the concrete by bringing it down considerably. Generally, the pH of good concrete which is in the vicinity of 12.5 to 13 comes down to around 9. This loss in pH causes the reinforcing steel to be susceptible to corrosion. The carbonation plane moves into the concrete from the outer surface as a result of external attack and it is dependent upon the moisture content of the concrete. This plane moves rapidly when relative humidity is between 50 to 70 percent<sup>1</sup>. One can find out the depth of carbonation from a formula  $d = Kc\sqrt{t}$  where, d = the depth of the carbonation reaction plane in mm, after time t, years. Coefficient of carbonation Kc is related to the permeability of the concrete, the amount of available free time, relative humidity and the carbon dioxide (other related gases in case of polluted environments) content of the given environment.

As reported<sup>2</sup> in this case study, the carbonation attack was seen to be upto 70 mm depth which was associated with highly undesirable low pH in the range of 5 to 8.0. Half cell readings also were fairly negative of -450 to -600 mv. These data corroborated well with the physical state of the structure. Thus, ascertaining the extent of corrosion and carbonation proved to be very useful first step in the sequence of repairs.

### Removal of Diseased/Loose Concrete:

The next step consisted of the process of removal of diseased/loose concrete and the removal of corrosion products from the steel and preparing the surface for further applications. It needs to be mentioned here that howsoever effective the materials are, the basic surface treatment plays very important role in the efficacy of the repair operation. In addition, it is very important to see that the surrounding good concrete is not damaged. In this case chipping was done by hammers, which is most widespread method of concrete removal if the deterioration is deeper than 15 mm or more. ACI Committee 546<sup>3</sup> also stresses on proper selection of chipping tools, which will avoid the damage of surrounding concrete.

### Why Rusticide Should be Used?

Corrosion products of embedded reinforcement steel cannot be removed by use of a mere stiff wire brush. If an attempt is made to remove the same by sand blasting, chances are that along with the corroded portion, additional un-corroded cross section of steel together with adjacent concrete are lost. Hence, corrosion products are best removed by chemicals like phosphating agents, rust converters etc. The next important step is to ensure that the corrosion products on the steel are removed effectively. For this, it is reported that the mechanical means prove quite inadequate. Hence, it is always correct to use the chemical rust remover-cumconverter material. The application of this material does not reduce the section of steel (like in sand blasting) after having removed the loose oxidation scales. It, in fact, consolidates the left over section. This treatment also helps in resisting the

corrosion to an extent, though subsequent process of pacifying the steel is very essential. Hence, rusticide, which is a phosphate-based rust remover and converter was used for removing the corrosion <sup>4,5</sup>.

# Why Polyalk Fixoprime Should be Used?

Rust removing agents, besides offering removal of rust, offer some degree of protection from further corrosion. However, this protection is not enough to protect the steel for great lengths of time since it is vulnerable to further corrosion as the concrete cover gets carbonated or when the ratio of chloride ions to hydroxyl ions gets disturbed as a result of chloride attack. In such cases, additional protection preferably by polymer-cementitious co-matrix (generally known as corrosion inhibitors) on the steel is quite effective. These coatings are useful in constantly maintaining a high alkalinity next to the steel inspite of fall in pH of cover concrete due to environmental attack. This treatment in the form of coating needs to be given only to the exposed steel surface. Neither chemical cleaning nor rust converting processes are permanent relief from corrosion. Hence, a protective barrier film of POLYALK FIXOPRIME which is corrosion inhibiting alkaline acrylic based polymeric coating was applied on the reinforcement steel <sup>6,7</sup>.

## **Need of a Bond Coat of Polyalk EP:**

In several cases, where traditional repairs are executed by re-plastering or mere concrete jacketing or even guniting, it is often seen that the new concrete/mortar mass separates from the old concrete. This obviously happens due to dissimilar behavior patterns of the old, already set concrete and the subsequent new concrete or mortar, which is undergoing stresses and strains while stiffening, mainly due to shrinkage.

Bonding polymers which are based on polymer latexes, when used along with cement, give equally excellent adhesion both to old concrete as well as the new one<sup>8</sup>. There is substantial reduction in cost too and the one-pack nature of the polymer keeps the tackiness of the surface for a long time. It also helps to keep the conditions around the exposed concrete generally alkaline, thereby preventing corrosion of steel and carbonation of the adjacent concrete. Hence, a bonding coat of POLYALK EP was applied on the surface.

# **Use of Polymer Modifdied Mortar in Concrete - POLYALK EP:**

Providing a new cover to a repairable structure should be done only wherever necessary and the temptation to expose the entire surface – even if a part of it is unaffected strong concrete, should be avoided. Judicious removal of diseased concrete is therefore essential. If the replacement is done by unmodified concrete, it can deteriorate due to carbonation and chemical attacks.

In addition to above reported properties, studies of comparative photomicrographs have shown that the addition of polymer emulsions to concrete results in bonding of the latex to the aggregates and helps in bridging the cracks as they form. As a result, the polymer relives the internal macro stresses, retards the formation and enlargements of cracks and increases the concrete's overall strength<sup>10</sup>. Moreover, as the voids and cracks are bridged by the polymer, it results in substantially reducing the penetration of moisture and corrosion chemicals. The indicative properties of the polymers used in these mortars are given in Table 2. Hence polymer modified mortar with POLYALK EP was effectively used on this site.

Table 2. Properties of Polymer Cement Mortars9

Sr.	Properties	Properties			Polymer/Cement ratio (on Wt/Wt basis)		
No.	Troperties	0	0.2	0.4			
		Dry	0.07	2.0	3.4		
1	Adhesion to concrete, N/mm <sup>2</sup>	Wet	0.03	1.0	1.4		
	, and the second	Wet	0.00	1.4	2.1		
2	A 11:2	Dry	0.0	2.0	1.6		
2	Adhesion to steel, N/mm <sup>2</sup>	Wet	0.0		1.3		
2	T	Dry	3.0	6.0	4.3		
3	Tensile strength, N/mm <sup>2</sup>	Wet	1.8		3.9		
4	Compressive strength, N/mm <sup>2</sup>	Dry	56.0	50.0			
5	Flexural strength, N/mm <sup>2</sup>	Dry	7.1		10.6		
3	riexurai strengui, iv/iiiii	Wet	5.8		9.6		
	Effects of chemicals on dry flexural strength after six months immersion, N/mm <sup>2</sup> - Untreated  - 10%potassium hydroxide  - 10% magnesium sulphate  - 5% lactic acid  - 5% hydrochloric acid  Effects of extremes of temperature N/mm <sup>2</sup> - untreated  - after 6 frees/ thaw cycles at 18°C ( in 10% brine)  - after 1 year at 70°C		7.2 6.1 4.3 5.9 0.0 7.1 0.0	13.2 12.3 13.2 8.0 2.2 10.6 10.4			
8	Adhesion to concrete (dry), N/mm <sup>2</sup> - untreated - after 6 months at 70°C		0.1	3.4 2.6			
9	Shrinkage to concrete (dry), N/mm <sup>2</sup> - water-cement ratio - percent shrinkage		0.40 0.07	0.34 0.02	0.30 0.01		
10	Water penetration, g/ m <sup>2</sup> /24 hours		46.9	38.1	1.9		
11	Water penetration with Revinex 29Y 40 in mortar, Kg/ m <sup>2</sup> /24 hours		100.0	35.0	0.0		

### **Specifications:**

- 1. Surface to be repaired was prepared properly by cleaning and washing thoroughly.
- 2. In case of R.C.C. structure proper anti corrosive treatment to reinforcement using RUSTICIDE (*Phosphate-based rust remover and converter*) was done using a soft brush.
- 3. Then after drying; application of rust passivation coating was prepared using POLYALK FIXOPRIME (*Corrosion Inhibiting alkaline acrylic-based polymeric admixture*): Cement in the ratio 1:2 and applied on the reinforcement by brush.
- 4. Before applying the Repair Mortar the damaged surface was coated with Polymer Cement slurry primer (Bond Coat) of POLYALK EP (*Single-coat co-polymeric admixture*): Cement in the ratio 1:1 by using a stiff brush.
- 5. The Repair Mortar was then prepared using POLYALK EP: Cement: Quartz Sand (Graded) in the ratio 1:5:15 restricting the water Cement ratio to 0.35 to 0.4. The mortar had to be in dough like consistency and press applied by hand on the primed surface.
- 6. The thickness of Repair Mortar was not to exceed 20 mm at a time.
- 7. Extra thickness required repetition of the above procedure of Bond coat.

# 3. Grouting With Polymer (in Foundation and Super Structure):

# **Use of Polymer in Grouting**

There are many advantages of polymer latex-cement comatrix systems over conventional grouting systems <sup>11</sup>. These are as follows:

- Being water-based, it is quite compatible with cement and can work in wet conditions.
- 2. Since it is a polymer and cement together, it can display the properties of both cement and polymer i.e. one can have the desirable compression properties from cement and flexural properties from the polymer.
- 3. It is already polymerized system and hence on drying there would not be a volume change due to shrinkage.
- 4. Cement is structurally a good material and if dispersed properly with the right water-cement ratio it can give excellent results. However, in plain cement injections, w/c ratio has to be kept very high to provide workability and hence cement can no more work as a structural material. In case of polymer latexes, w/c ratio can be controlled without loss in workability. Hence grouted areas get an additional parameter of compression along with mere filling of the voids.
- 5. The total comatrix has excellent flexural and hence tensile parameters which will additionally reinforce the grouted area.
- 6. Finally, as compared to any other grout with similar parameters these systems are very economical since they use cement as one of the components.

Refer to Table 3 for comparison of Compressive and Flexural strength of PCGs with plain cementitious grouts under identical workability.

Table 3. Comparison of Compressive and Flexural Strength of PCGs with Plain Cementitious Grouts under Identical Workability (Testing Age –28 Days)

Proportions of PCGs used		Flexural	Compression	Mode	
Polymer	Cement	Silica	strength in	strength in	of
latex		sand	kg/cm <sup>2</sup>	kg/cm <sup>2</sup>	curing
1	2.5	-	183	320	
1	2.5	-	183	320	Water
1	2.5	-	188	328	w ater
1	2.5	-	190	330	
Aver	age streng	th	186	324.5	
1	2.5	-	316	260	
1	2.5	-	320	256	Air
1	2.5	-	324	264	All
1	2.5	-	320	256	
Aver	Average strength		320	259	
1	2.5	1	150	220	
1	2.5	1	166	225	Air
1	2.5	1	164	225	All
1	2.5	1	160	222	
Aver	Average strength		160	223	
-	1	2	83.3	160	
-	1	2	83.3	160	Water
-	1	2	84.0	162	vvater
-	1	2	85.0	162	
Average strength		83.9	161		

# **Specifications:**

- 1. Injection holes were drilled to at least 100 mm depth in joints of masonry and pipes were embedded and the holes were suitably sealed.
- 2. Trial grouting was carried out with 1:2 Cement, Silica sand, Water slurry using a static head or pump not exceeding 2.5 Kg/sqcm.
- 3. In case the trial grout did not indicate substantial penetration of grout then grouting with 1 part of Polymer POLYALK EP (*Polymeric mortar modifier*), 2.5 parts of Cement and 1 part of Silica sand was admixed and grouting operation was conducted.
- 4. Refer Table 3 for comparison of Compressive and Flexural strength of PCGs with plain cementitious grouts under identical workability.

### 4. Internal Plaster And External Plaster:

# **Internal Plaster:**

The original mortar in the brickwork and plaster was lime mortar with finish in shell lime. There was dampness in the walls and columns at ground floor up to a certain height, and some cracks were formed. In portions the brickwork had also

deteriorated. Hence, the requirement was to strengthen the masonry by grouting, and repair the damaged brickwork.

a. Trials were conducted using existing mortar. The lime plaster was cut from the walls, thoroughly ground and scrammed. This was mixed in the following proportions with cement and sand:

1:2:4 Cement: Lime: Sand and 1:3:4 Cement: Lime: Sand.

- b. The second proportion of 1:3:4 was found to be more suitable for use in the plaster of the superstructure columns and brickwork.
- c. For mortar, 250 ml of Super Plasticizer SUNPOLICRETE NGT was added per bag of cement mixed with adequate water.
- d. The same was followed for the external plaster also.

### **External Plaster:**

- a. For external plasters joints in brickwork were raked out and cracks were repaired by grouting as mentioned above and washed thoroughly.
- b. After slight drying of the walls, Bonding of Polymer Cement slurry was applied using POLYALK WP (*Polymeric Water proofing solution*) mixed 2% by weight of cement.
- c. Plaster was carried out as mentioned by adding 250 ml SUNPOLICRETE NGT (Super plasticizer) per bag of cement.

Other Specifications for Restoring the Architectural Beautification and Utilities were also framed based on the idea of maintaining the dignity and heritage of the structure.

#### Gift to the Nation

The Homage Trust had a unique gift to be handed over to the people of Calcutta and the nation as a whole. The complete Repairs and Restoration of this Heritage structure on completion was handed over to the Calcutta Municipal Corporation on the auspicious day of Bengali New Year during a function.

Sunanda Speciality Coatings Pvt. Ltd., Mumbai, under the able guidance of Dr. S. K. Manjrekar with his expertise of Material Science was amongst the prominent members who shared this challenging task of Structural Restoration. The Project Consultant Mr. Arup Sarbhadhikari was also instrumental in restoring this structure back to its original heritage face.

## Note:

Polyalk EP Polymeric Mortar Modifier.

Polyalk WP Polymeric Cementitious waterproof coating.

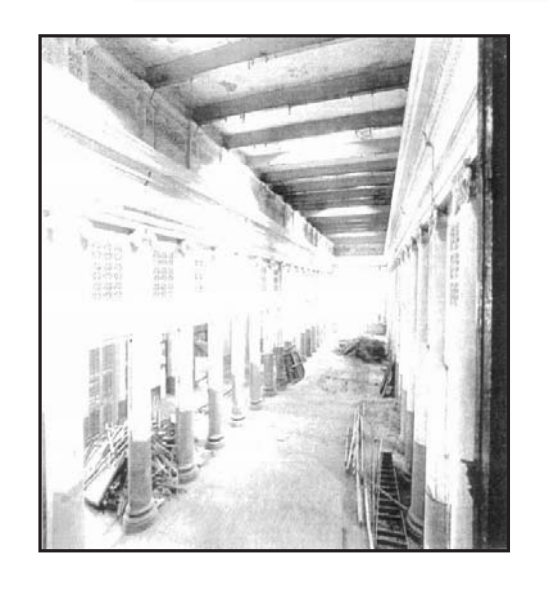
Rusticide Phosphate Based solution for Rust Remover & Convertor.
Polyalk FP Corrosion Inhibiting alkaline acrylic-based Polymeric admixture.

Sunpolicrete NGT Naphthalene based Super-Plasticizer.

#### References

- 1. SMOLCYK, H.G., Physical and chemical phenomena of carbonation, *Proceedings RILEM International symposium on carbonation of concrete*, Cement and Concrete Association, Wexham Springs, UK, 1976, pp.10.
- 2. BAHADURPURKAR, M.G., GODBOLE, U.B. Major structural repair to GKG bridge at Andheri, *National Conference on Corrosion Controlled Structure*, Indian Society of Structural Engineers, 1999, pp.345.
- 3. Guide for repair of concrete bridge superstructures, ACI 546.1 lr-80, American Concrete Institute, Detroit, 1980, pp.20
- 4. CAIMS JOHN and ABDULLAHRAMLI, *ACI Materials Journal*, Vol.91, no.4, July-August 1994.
- 5. SIEELY CARROL N. and KELLY THOMAS ENP., Concrete surface preparation coating and lining and inspection, *National Association of Corrosion Engineers*, Houston 1991.
- 6. BRETT, M.A. and BRETT, A.O., *Electro-chemistry methods and application*, Oxford University Press, 1993 pp.361.
- 7. MANJREKAR, S.K., MANJREKAR R.S. and NAIR P.R.C. Role of polymer Cement-inhibitor comatrix in corrosion control of reinforcing steel, *The Indian Concrete Journal*, July 1996, Vol 70, No.7, pp 389-392.
- 8. *CEB/FIP Model Code for Concrete Structures*, 3<sup>rd</sup> Edition, Comite Eurointernational du Beton / Federation Internationale de la Precontrainte, Paris, 1978, pp.348
- 9. OHAMA Y. Study of properties and mix proportioning of polymer modified mortars for buildings (in Japanese), Report on the Building Research Institute, No.65, Tokyo, Japan, 1973.
- 10. BULLOCK, R.E., Factors influencing concrete repairs materials, *Concrete International: Design and construction*, Vol 2 No.9, September 1980, pp.67-68
- 11. Manjrekar, S.K. Manjrekar, R.S., "Use of Polymers and Inorganic Chemicals for Groutings in Concrete and their Cost Implications". Presented at the Proceedings of Sixth International Conference on Structural Faults and Repair, Westminster Central Hall, London, July 4, 1995.

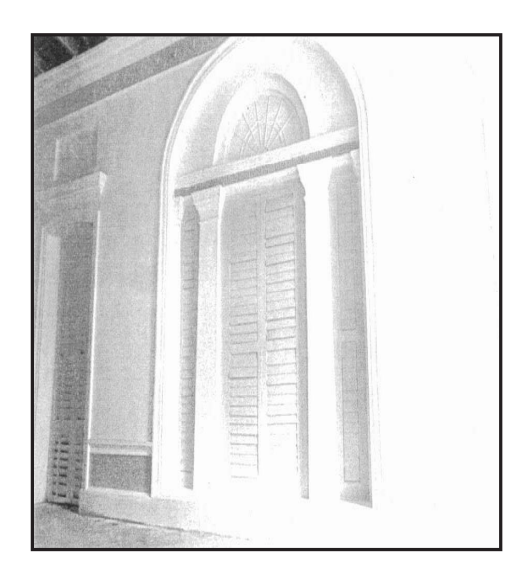
# INTERNAL ROW OF COLUMNS IN CENTRAL HALL





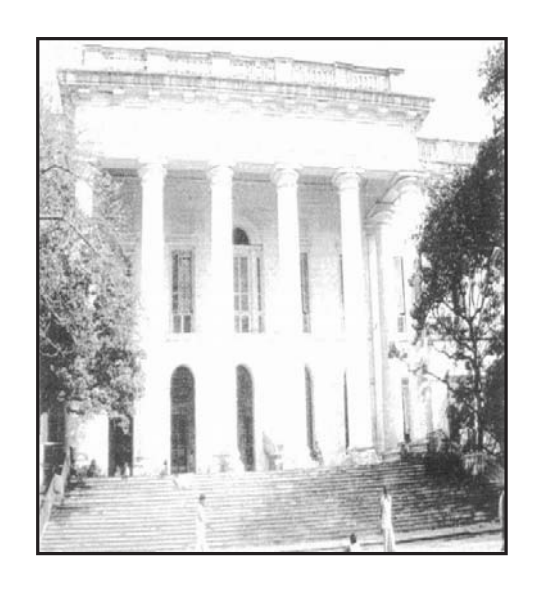
BEFORE AFTER

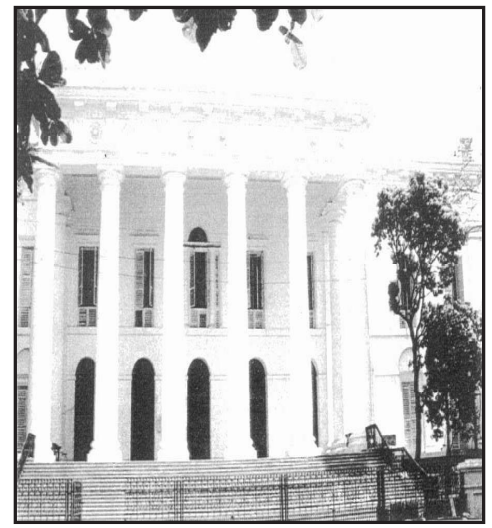




**VIEW OF THE DECORATIVE INTERNAL WINDOW** 

# **FRONT ELEVATION**

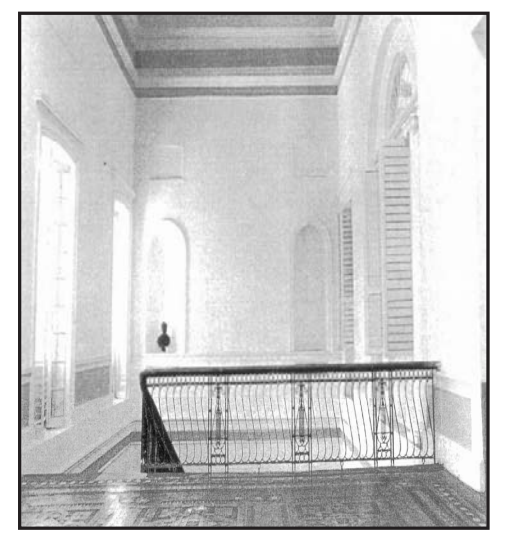




BEFORE AFTER

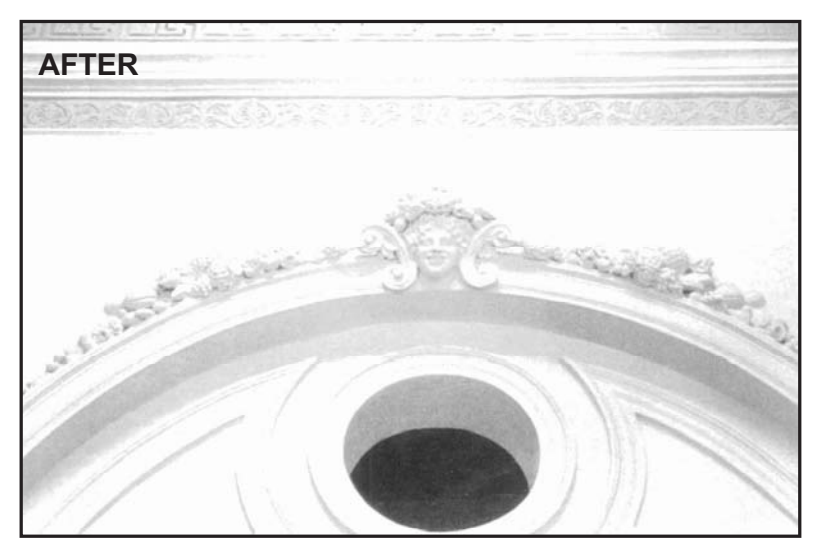
# **VIEW OF THE INTERNAL STAIRCASE**





BEFORE AFTER





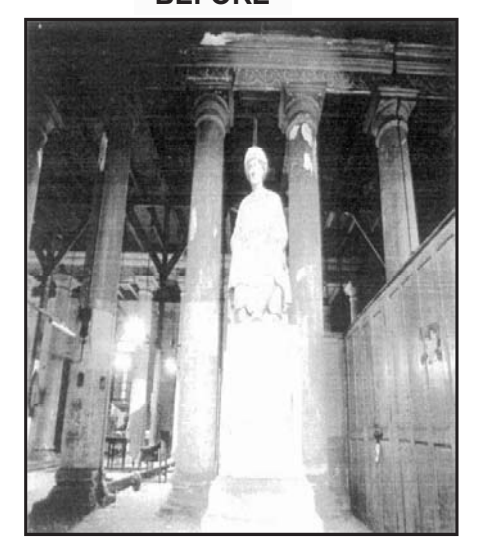
**VIEW OF THE DECORATIVE MOTIF** 

# **INTERNAL STAIRCASE**

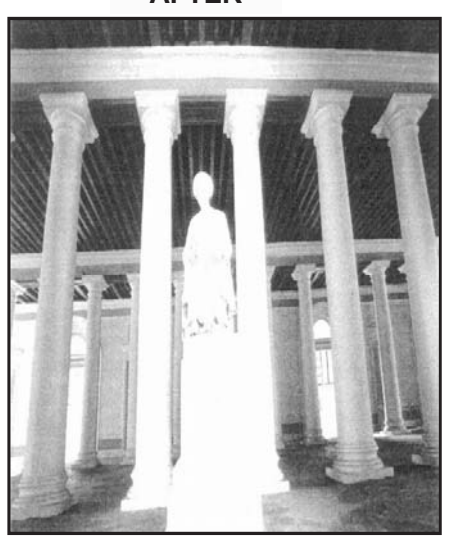




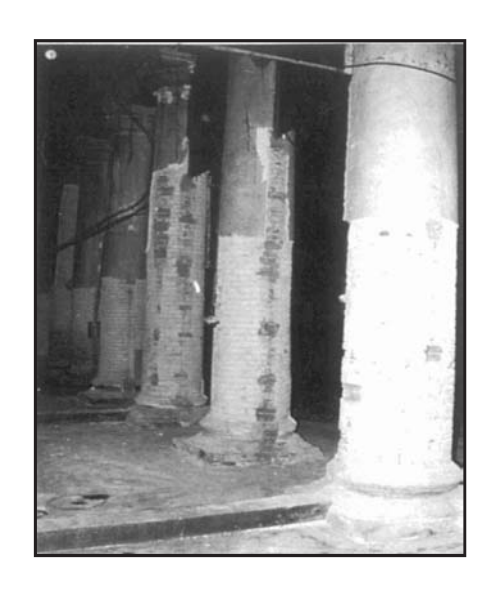
**BEFORE** 



**AFTER** 



VIEW OF THE STATUES ON THE GROUND FLOOR



**DAMAGED COLUMNS** 

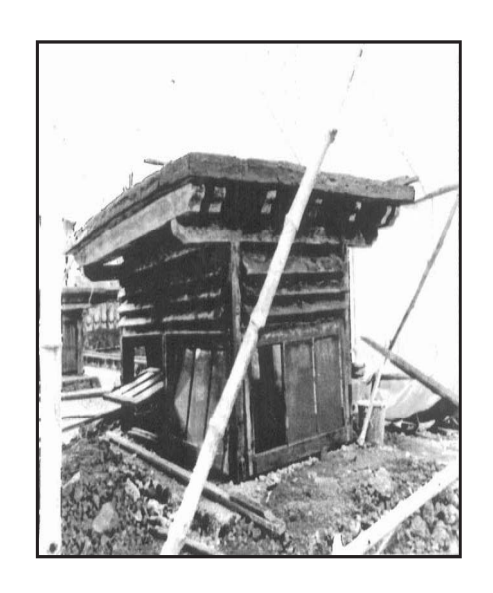
**DAMAGED DOORS/WINDOWS** 



DAMAGED COLUMNS ON FIRST FLOOR







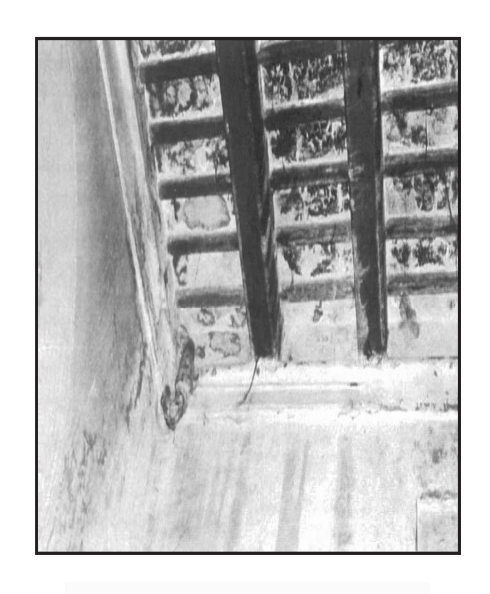
**DAMAGED SKYLIGHT** 



RAIN WATER FALLING ON THE FRONT PORTICO



LEAKAGES FROM RAIN WATER PIPES



**DAMAGED SLAB** 

# **Enhancing the Structural Behavior of Reinforced Concrete Beams Using FRP Systems**

#### Hisham Abdel-Fattah

Department of Civil Engineering, College of Engineering, University of Sharjah, Sharjah, UAE

#### Sameer Hamoush

Civil and Architectural Engineering Department, North Carolina A&T State University, USA

#### Abstract

Fiber Reinforced Plastic (FRP) Composites retrofit systems are developed to enhance the structural performance of deficient reinforced concrete beams. First, the paper highlights the design of the FRP systems and secondly, systems with promising results will be used to upgrade deficient beams. Structural evaluation for retrofitted beams is performed to evaluate the ductility and strength performance. As a part of design of the FRP systems, an experimental program was conducted on small test specimens to determine the stress strain response of a various FRP system fiber configurations. Three fiber orientations,  $0^{\circ}$ ,  $\pm 22.5^{\circ}$ , and  $\pm 45^{\circ}$ ; and two fiber material types, glass and carbon were evaluated in a vinylester resin. The performance of these small test coupons was used to fabricate and evaluate 16 sets of FRP systems for various combination of fiber types and orientation angles. The 16 sets provided the stress-strain relationship of each of the FRP systems. This stress strain model was incorporated into a numerical model of a retrofitted reinforced concrete section to establish moment curvature behavior.

#### Introduction

Rehabilitation of existing reinforced concrete beams built prior to the year 1970, appears to be both technically feasible and a cost effective option to replacement. It has been shown in previous studies<sup>1-5</sup> that jacketing using reinforced concrete and steel plates enhances the ductility and strength of the sections, as well as increasing the shear strength. However, it was also shown that the labor and construction time associated with these rehabilitation systems limits the versatility of these techniques, especially when column size varies and specialized fabrication is required. Using FRP systems<sup>6-10</sup> with a non-linear stress-strain response as reinforcement of concrete sections, particularly in the frame connection application, requires an accurate nonlinear analysis of concrete members to evaluate the resultant structural responses. A better understanding of the composite FRP concrete section is critical for the optimal implementation of these retrofit systems.

### **Design of Overlay Composites**

Designing of FRP upgrading systems to enhance the strength with sufficient ductility is the focus of this paper. It is well known that upgrading for strength can be achieved with any appropriate area of known FRP system. But the challenge is to ensure sufficient ductility as provided by steel reinforcement. The background for the design approach of the FRP architecture for the ductility requirement was based on the study of metallic materials. The studies showed that a Ramberg-Osgood equation can be used to accurately model a nonlinear material response. This equation has been used to successfully model the response of steel and aluminum and covers both the linear and fully elastic-plastic responses. Therefore, a similar approach is taken to establish the nonlinear response of the composite FRP systems in this investigation.

The proposed equation used to model the stress-strain response of the composite FRP material is:

$$\varepsilon = \left(\frac{\sigma}{E}\right) + \left(\frac{\sigma}{R}\right)^n \tag{1}$$

In Equation 1, E is the elastic modulus. The constants n and R are the Ramberg-Osgood constants. The value of n is usually large (15 or higher) for elastic materials and approaches one for elastic-perfectly plastic materials. Both R and n are established by fitting the equation to the experimental data. The elastic modulus can be found using the linear part of the stress-strain curve. Validation of the stress strain response for the carbon and glass fabric composites was accomplished by series of tension test data and implementing the equation described above to evaluate the constants E, R and n. To generalize the results as a function of  $\pm \theta$ , additional testing will need to be conducted so that the fiber performance characteristics can be optimized to achieve the required ductility, strength and stiffness. However, the two test series at the bounds can be used to prove this proposed methodology as well as more generalized equations developed at a later time if this proves to be effective. This effort is described in the following sections.

During this investigation, a series of small coupon standard tension tests were conducted on  $0^{\circ}$ ,  $\pm 22.5^{\circ}$  and  $\pm 45^{\circ}$  fiber bias woven fabric glass and carbon composites made with vinyl ester resin. It should be noted that the orientation of the principal fiber weaving direction relative to load direction is termed the bias. For instance, a  $0^{\circ}$  fiber bias in woven composites denotes that the load direction is parallel to the weft or weaving direction. Theoretically, in most fiber mat materials, the material properties in the  $0^{\circ}$  and  $90^{\circ}$  bias directions are the same. The complete stress-strain performance of these materials was recorded to ultimate failure and used to establish a stress-strain relationship for each of the materials. The stress strain response of a  $0^{\circ}$  fiber bias laminate material exhibits a linear stress-strain behavior up to failure. However, the  $\pm 22.5^{\circ}$  and  $\pm 45^{\circ}$  bias fiber laminate materials typically have a nonlinear response. For a given weave pattern and fiber configuration, the  $0^{\circ}$  and  $\pm 45^{\circ}$  bias cases usually represent the extremes of stress-strain behavior expected for that material over a variety of loading configurations, while all other  $\pm \theta$  (example  $\pm 22.5^{\circ}$ ) responses fall in between these two extreme cases.

Figure 1 shows the equation fit to test data for the  $\pm 45^{\circ}$  glass fabric composite. Figure 2 shows the equation fit to test data for the  $\pm 22.5^{\circ}$  carbon fabric composite. The fitted equation parameters are listed in Table 1 below. This table also includes the data for steel. Note that the modulus of steel is much higher than that of the composites. The table also includes the failure strains used as a limit for the analysis.

Table 1. Material Properties of the Composite Fiber Systems

Composite	Lay Up	E MPa	Strain at Failure	R MPa	n
Class/Vinyloston	0	28,000	1.25 %	520	20.0
Glass/Vinylester	$\pm 45$	12,000	11.00 %	260	4.10
Carbons/Vinylester	0	49,000	1.00 %	740	20.0
	± 45	37,000	1.15 %	510	12.0
	$\pm 45$	12,000	11.00 %	340	3.25
Steel		210,000		625	1.50

A generalization of constants "n and R" with the limited amount of data reported is not appropriate since the relationship between the bias of these constants cannot be found with only three data points. More experimental testing data, particularly for intermediate values of  $\pm \theta$  is needed to develop generalized equations for the Ramberg-Osgood Constants (n and R) as a function of the fiber orientation angle  $\theta$ .

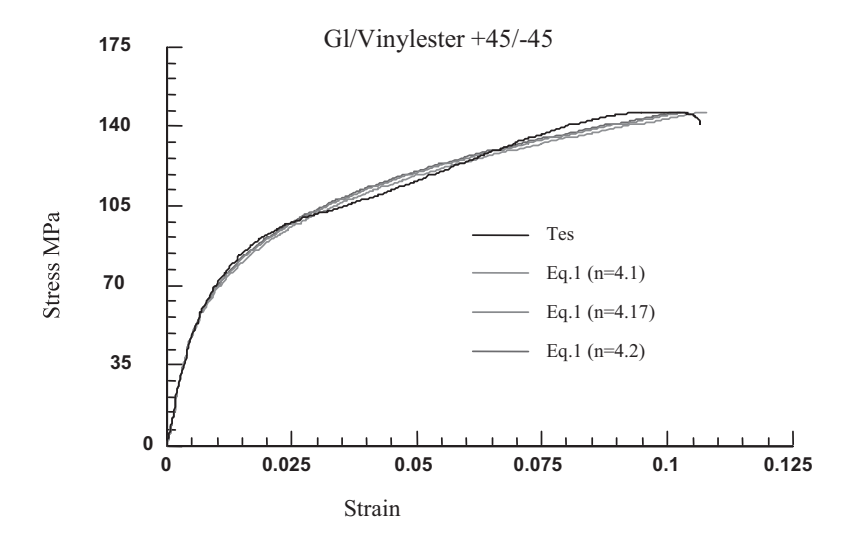


Fig. 1. Comparison of tension test and equation fit for glass fiber at  $45^{\circ}$  bias.

## **Experimental Evaluation of FRP Retrofitting Systems**

Based on the above model, it appears that the two important lay-ups of the FRP systems are the  $0^{\circ}/90^{\circ}$  for strength and  $\pm 45^{\circ}$  for ductility purpose. A series of test experiments were developed to study the combination of the lay-ups and fiber types.

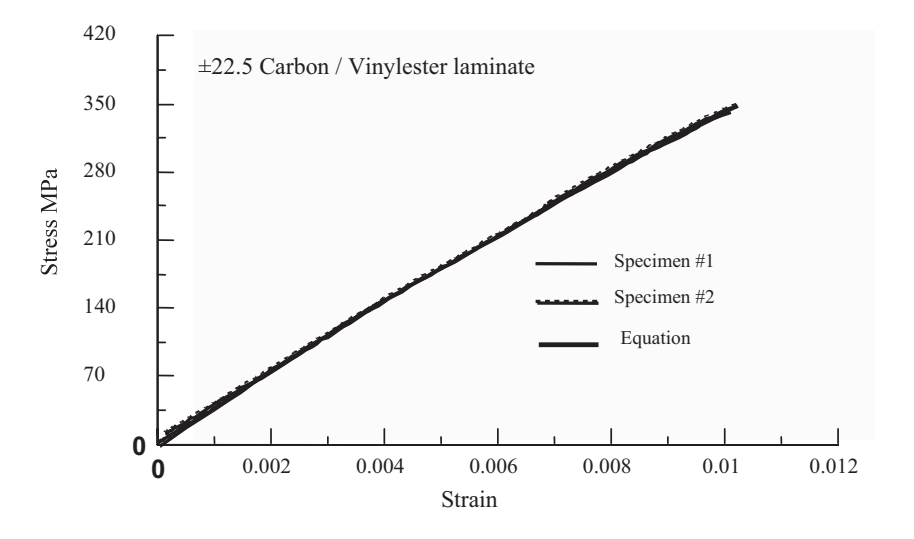


Fig. 2. Tension test data and fitted equation for  $\pm 22.5^{\circ}$  carbon fiber.

Table 2 shows the properties of the fiber used in the investigation. While  $\pm 22.5^{\circ}$  does not have any significant effects on the strength and ductility, only lay-ups  $0^{\circ}/90^{\circ}$  and  $\pm 45^{\circ}$  were used in the testing program. Table 3 shows summary of testing variables. Each set of Table 3 consists of three repetitions. The resin used was ATLAC 580-05 Vinyl Ester in room temperature curing. Summary of the experimental program is shown in Table 2. The fiber balance was maintained for all specimens of the experimental program. Also, it must be mentioned that the thickness of the bending test specimens was doubled to provide extra flexural rigidity for meaningful tests.

Table 2. Properties of the Fibers Used in the Experimental Program

Composite Material	Glass BFG 2532	Carbon W-5-322
Ultimate Tensile Strength	345 MPa	480 MPa
Elongation at Ultimate Strength	1.25 %	1.0 %
Modulus of Elasticity	28,000 MPa	48,000 MPa
<b>Design Thickness</b>	0.27 mm / layer	0.33 mm/ layer

Table 3. Testing Program for the FRP Configuration Architecture

Set No	Outer Layers	Inner Layer	No. of Specimens	Type of Test	Specimen Size (mm)
1	0/90° Glass	±45° Glass	3	Axial Ten.	25 x 1.40 x 305
2	0/90° Carbon	±45° Carbon	3	Axial Ten.	25 x 1.40 x 305
3	0/90° Glass	±45° Carbon	3	Axial Ten.	25 x 1.40 x 305
4	0/90° Carbon	±45° Glass	3	Axial Ten.	25 x 1.40 x 305
5	±45° Glass	0/90° Carbon	3	Axial Ten.	25 x 1.40 x 305
6	±45° Carbon	0/90° Glass	3	Axial Ten.	25 x 1.40 x 305
7	±45° Glass	0/90° Glass	3	Axial Ten.	25 x 1.40 x 305
8	±45° Carbon	0/90° Carbon	2	Axial Ten.	25 x 1.40 x 305
9	0/90° Glass	±45° Glass	3	Flexure	25 x 2.80 x 203
10	0/90° Carbon	±45° Carbon	3	Flexure	25 x 2.80 x 203
11	0/90° Glass	±45° Carbon	3	Flexure	25 x 2.80 x 203
12	0/90° Carbon	±45° Glass	3	Flexure	25 x 3.00 x 203
13	±45° Glass	0/90° Carbon	3	Flexure	25 x 2.80 x 305
14	±45° Carbon	0/90° Glass	3	Flexure	25 x 3.00 x 305
15	±45° Glass	0/90° Glass	3	Flexure	25 x 2.80 x 305
16	±45° Carbon	0/90° Carbon	3	Flexure	25 x 2.80 x 305

The purpose of the tension specimens was to obtain the stress strain behavior including the ultimate stress and strains, while the flexural teats were to validate the Elastic Modulus of Elasticity for each configuration.

The tensile tests were performed using MTS testing machine equipped with strain-controlled strokes. The axial stress and axial strain were obtained by a Data Acquisition system connected to the testing apparatus. The tensile tests indicated two types of behavior for the tested FRP architectures. Specimens with 0/90° carbon and  $\pm 45^{\circ}$  glass failed in a progressive nature where the carbon failed first, followed by the glass failure. The stress strain shows a sudden change in the slope of the cures. This point identified as an apparent yield point. FRP architecture with out the above combination behaved nonlinearly up to failure. Figure 3 shows the stress/strain for specimens with an apparent yield point while Fig. 4 shows the stress/strain relationship for specimens without an apparent yield point.

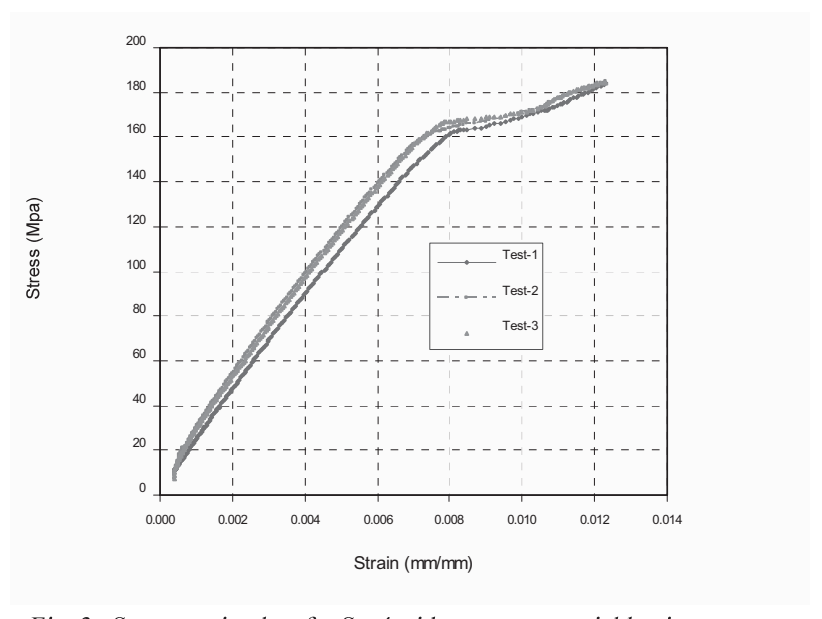


Fig. 3. Stress strain plots for Set 4 with an apparent yield point.

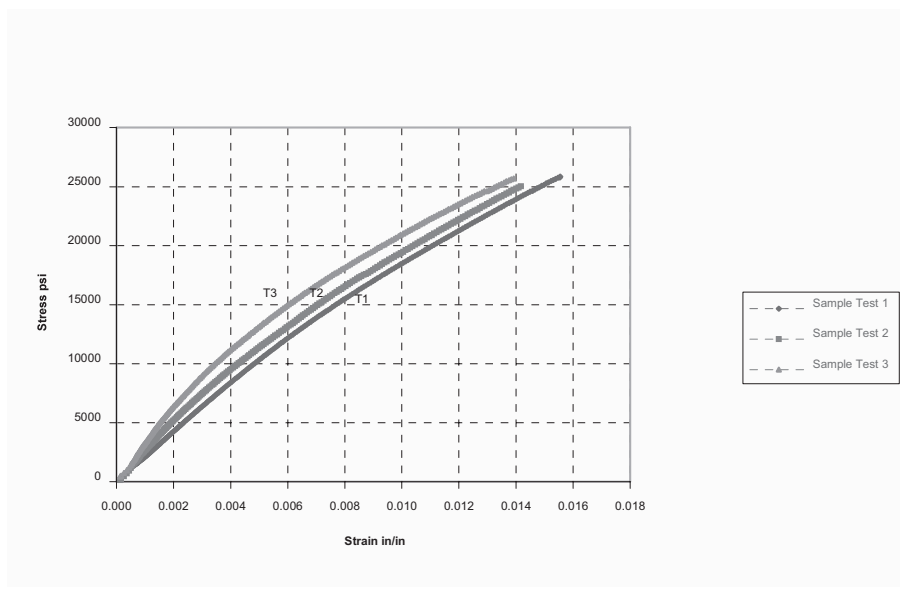


Fig. 4. Stress strain plots for Set 1 without an apparent yield point.(psi = 0.0069 MPa).

A flexural testing program was conducted to evaluate the flexural rigidity of specimens with the same fiber architectures as those of the specimens used for the tensile tests. The purpose of these tests is to validate the stiffness values obtained from the tension tests. Using four point loading conditions, the setup for the flexural tests.

Figure 5 shows the load deflection curve for specimens with an apparent yield point while Fig. 6 shows the behavior for specimens without an apparent yield point.

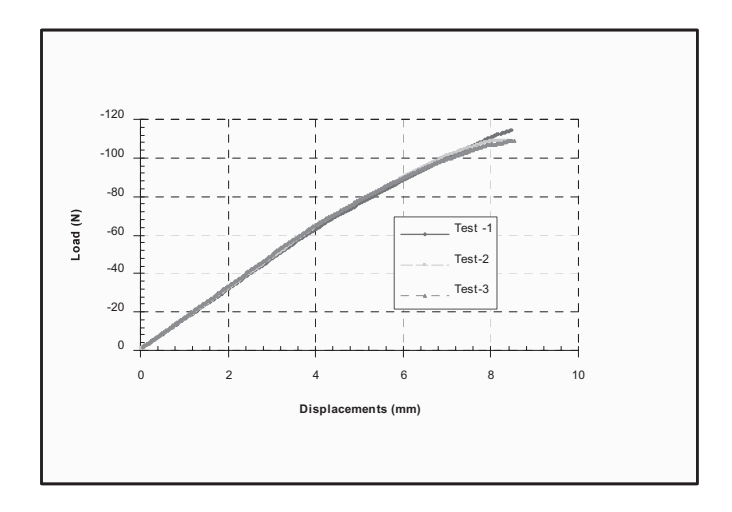


Fig. 5. Load deflection for Set 9 with an apparent yield point.

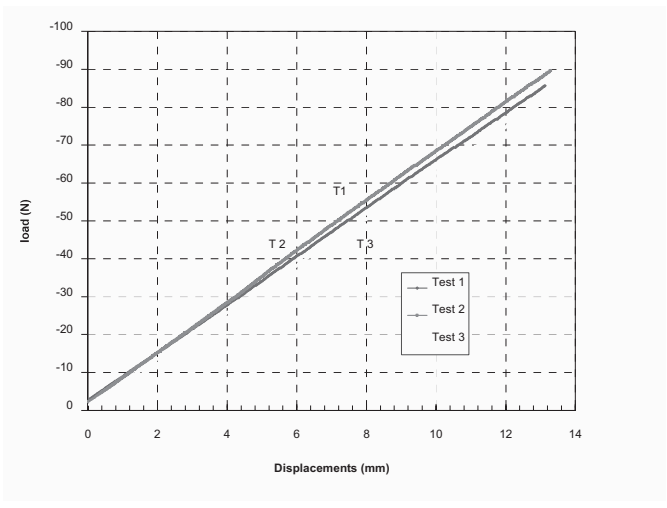


Fig. 6. Load deflection for Set 9 without an apparent yield point.

The summary of the testing program is shown in Table 4. The table shows the failure stresses, failure strain and the modulus of elasticity for all fiber architectures used. By examining Table 4, it can be noted that the combination $\pm 45^{\circ}$  carbon/ $0/90^{\circ}$  glass gives the highest strains at failure. The combination  $0/90^{\circ}$  carbon/ $\pm 45^{\circ}$  carbon gives the maximum strength with the least failure strain.

Table 4. Summary of the testing results for various FRP architectures.

Set No.	Outer Layers	Inner Layer	Failure Stresses	Elastic Modulus E <sub>1</sub>	Failure Strains
1.0	0.000.01		(MPa)	(MPa)	(mm/mm)
1,9	0/90° Glass	±45° Glass	172	17.2	0.014
2,10	0/90° Carbon	±45° Carbon	296	43.1	0.01
3,11	0/90° Glass	±45° Carbon	131	17.2	0.018
4,12	0/90° Carbon	±45° Glass	186	29.0	0.013
5,13	±45° Glass	0/90° Carbon	172	18.6	0.0135
6,14	±45° Carbon	0/90° Glass	186	17.9	0.02
7,15	±45° Glass	0/90° Glass	152	14.5	0.017
8,16	±45° Carbon	0/90° Carbon	193	32.4	0.012

## Structural Performance of Beams Reinforced With Various FRP Systems

An analytical investigation of the moment-curvature response of a typical 12"x 24" (300x600 mm) concrete beam reinforced with 2 #9 ( $A_s = 2 \text{ in}^2$ , (2580 mm<sup>2</sup>)) steel reinforcing bars in the tension side (bottom) was undertaken in this investigation. The

chosen reinforced concrete section has a reinforcement ratio,  $\rho$ , of 0.008 and this steel amount is about  $0.25*\rho_{balanced}$ . For this investigation, the concrete compressive strength was assumed to be 4 ksi (27.6 MPa) and Grade 60 steel was used.

A computer program was developed to evaluate the curvature of the section for every strain increment in the concrete. The ultimate concrete compression strain was assumed to be 0.003 and this strain was incremented in steps of 0.0006. The computer code performed a numerical integration to determine the concrete force based on the concrete stress distribution. The program enforced force and moment equilibrium at each strain increment through an iterative approach. In the model, the ultimate strain of 0.003 was chosen as recommended by the ACI318-2002 but the model is capable to adopt a higher value for the ultimate strain if desired.

The strain, stress, and force distributions were used to develop a moment curvature relationship for the typical concrete section and used as a reference to compare the performance of similar sections after they had been upgraded with various FRP configurations. Based on internal load equilibrium and the assumption that plane sections remain plane after the load application, the strain in the reinforcements was evaluated for every strain increment in the concrete.

The predicted moment curvature response of the section reinforced with the  $\pm 0^{\circ}$  carbon fiber is shown in Figure 7. Also shown in this plot is the moment curvature response of the concrete section if it had been reinforced using the current ACI concrete code (having two # 9 rebar at the bottom). It can be noted from Fig. 7 that using a FRP with a linear stress strain relationship does not produce a ductile response as required by the ACI Code.

Similarly, using glass fibers with a linear response of stress-strain behavior, the required glass fiber area is  $2.44 \text{ in}^2$  to meet the same strength requirements. It can be seen in all cases that the  $90/0^{\circ}$  bias fiber orientation does not produce sections with as much ductility as the steel reinforced sections. Figure 8 shows the response of a section reinforced with: (1) 2 # 9,  $as_s = 2 \text{ in}^2$ , (2)  $\pm 45^{\circ}$  class fibers (required area is  $9 \text{ in}^2$  (645 mm²)) and (3)  $3.5 \text{ in}^2 0/90^{\circ}$  carbon  $/\pm 45^{\circ}$  glass with an apparent yield point.

Examining the results summarized in Figs. 7 and 8 indicate that using a  $\pm$  45° bias in the fiber lay-up results in a significant increase in the FRP cross sectional area needed to upgrade the strength of deficient concrete sections to meet today's standards. Furthermore, the failure of the concrete section is controlled by ultimate concrete strain (0.003) which occurs long before the fiber reaches its ultimate strength and thus underutilizes the ductility inherent in this material. The architecture of 0/90° carbon /  $\pm$ 45° glass improves but the failure strains much lower than that of the steel or fibers with  $\pm$ 45° orientation.

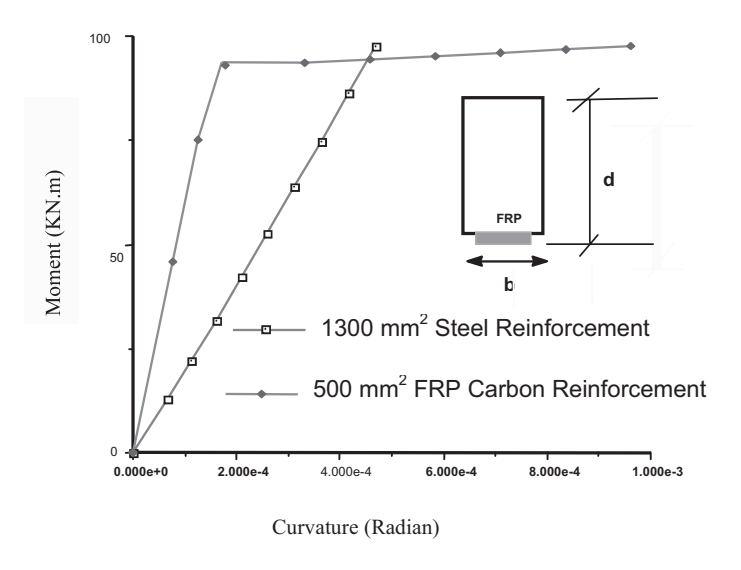


Fig. 7. Moment Curvature Behavior of Linear Carbon Fiber Materials (0° Bias)

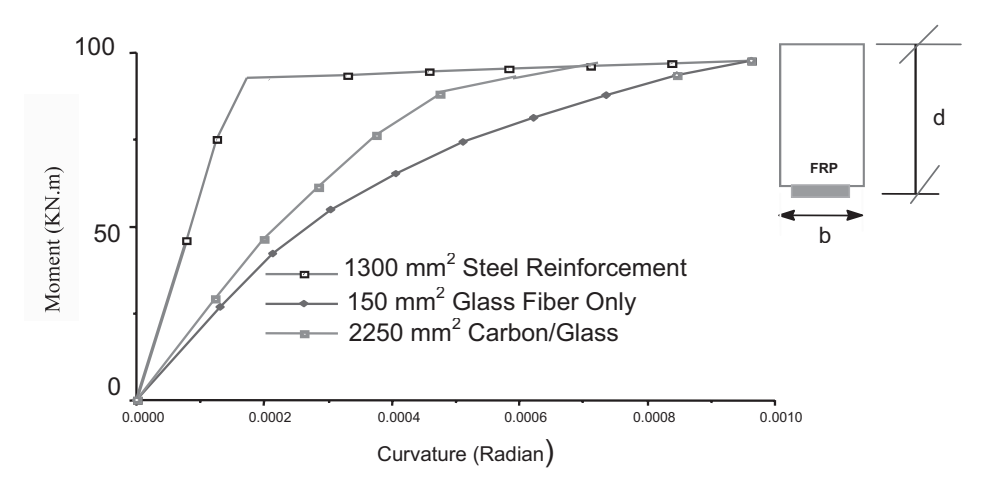


Fig. 8. Moment Curvature Behavior of Linear Glass Fiber Material (0° Bias)

## **Conclusions and Recommendations**

The study presented in this report was focused on the evaluation of interior concrete frame connections with continuity steel deficiency. The numerical analysis conducted in this study focused on evaluating the application of FRP systems to these connections in an effort to improve the ductility and upgrade the strength of these connections to the current concrete code recommendations. A FORTRAN program numerical model was developed to perform the analysis of concrete sections reinforced with various FRP systems.

In addition, the investigation allowed the following conclusions to be made:

- 1. The presented study provides guidelines for selecting the FRP materials and fiber orientation for upgrading deficient beams with specified requirements.
- The testing configurations of the fiber architectures and two fiber types provide sufficient data to understand the stress strain relationship of sections reinforced by various FRP systems.
- 3. In selecting the FRP systems, there is a direct relationship between the code defined ductility requirements and the fiber area required to upgrade for the strength. As the ductility requirement increases the fiber bias angle, there is an accompanying increase in the fiber cross sectional area necessary to meet the flexural strength requirements.
- 4. Using more than one FRP material to upgrade the section improves the ductility performance. It appears that in a hybrid system, the rigid materials (0/90° carbon) will fail first, followed by the failure of the more flexible materials (±45° glass). This behavior is important since it has a great effect of the composite materials patch design and is expected to provide the best approach in achieving the optimal ductile failure of the reinforced concrete section

The study performed is at the initial stage and more comprehensive study is required to fully implement the new FRP system and develop a robust design algorithm. Also, the final evaluation of the repair system should be validated by a well-constructed experimental program to provide total validation of the repair systems analyzed.

#### References

- Ghobarah A., Aziz Tarek S., and Biddah Ashraf, 1997, "Rehabilitation of reinforced Concrete Frame Connections Using Corrugated Steel Jacketing," ACI Structural Journal / May-June, pp. 283
- 2. Scott Robert H., 1996, "Intrinsic Mechanism in Reinforced Concrete Beam-Column Connection Behavior," ACI Structural Journal, May-June, , pp 336346.
- 3. Bidda Ashraf, Ghobarah A., and Aziz Tarek S., 1997, "Upgrading of Non ductile Reinforced Concrete Frame Connection," Journal of Structural Engineering, ASCE/August, pp. 1001.
- 4. Alcocer Sergio M. and Jirsa James O., 1993, "Strength of Reinforced Concrete frame Connections Rehabilitations by Jacketing," ACI structural journal/May-June, pp. 249.

- Lou Y.H, Durrani A.J., Bai Shaoliang, and Yuan Jixing, 1994, "Study of Reinforcing Detail of Tension Bars in Frame Corner Connection," ACI Structural Journal/July-August, pp. 486.
- Ibell, Tim and Silva, Pedro, "Design of Continuous FRP Strengthened Concrete Structures Allowing Moment Redistribution." International SAMPE Symposium and Exhibition, V. 49 SAMPE 2004 Conference proceedings. May 16-20, 2004, pp. 2939-2951.
- 7. Hakan, Nordin and Bjorm, Taijsten, "Testing of Hybrid FRP Composite Beam in bending," Composite Part B: Engineering, V35, n1, January 2004, pp 27-33.
- 8. Henrik, Thomsen, "Failure Mode Analysis of Reinforced Concrete Beams Strengthened in Flexure with Externally Bonded Fiber Reinforced Composites," Journal of Composites for Construction, V8, No. 2, March/April, 2994, pp 123-131.
- 9. Wang, Y.C and Chen C.H. "Analytical Study on Reinforced Concrete Beams Strengthened for Flexure and Shear with Composite Plates," Composite Structures, v59, No. 1, January 2003. pp 137-148.
- Soudki, K. "Guide for the Design and Construction of Externally Bonded FRP Systems for Strengthening Concrete Structures," Proceedings of the 2005 Structures Congress and the 2005 Forensic Engineering Symposium 2005. 2005, pp. 1627-1633.

# The Behaviour of Geopolymer Paste and Concrete at Elevated Temperatures

B. Toumi, University of Ouem El Bouaghi, Algeria
Z. Guemmadi, University of Constantine, Algeria
H. Houari, University of Constantine, Algeria
H. Chabil, University of Constantine, Algeria

#### **Abstract**

High Performance Concrete (HPC) is mainly used for special purpose every time when a needed concrete quality cannot be obtained by ordinary concrete for the most part in tunnels, bridges, high-rise buildings and in nuclear reactors. It is exposing to high temperatures and mainly the risk of the sudden spalling under elevated temperatures, whereby pieces of hardened concrete explosively dislodge, has to be clearly understood. After a brief introduction of high temperature effects in concrete, we present the behavior of fly ash-based concrete at elevated temperatures. Samples were heated up to 700°C to evaluate strength loss due to thermal damage. The results of differential thermal expansion analysis between the aggregates and paste show that after exposure to elevated temperatures the effect of thermal expansion and contraction behavior of paste and aggregates in the two-phase concrete material leads to massive degradation of the load resistance.

**Key Words:** High strength concrete, High temperatures, Spalling, Fly ash, Thermal expansion, Contraction, Massive degradation.

#### Introduction

Unlike ordinary concrete, if high performance concrete is exposed to fire-condition, it may have a different tendency and feature of spalling due to the compact structure of HPC, which makes it more difficult to transport vapor and moisture. Very high vapor pressure may occur close to the surface. This means that there is a greater risk that HPC spall, compared with ordinary concrete. In ordinary concrete (OC) the vapor can easily be transported to the surface and the moisture towards the inner part. However, the moisture concentration can at last be too large and explosive spalling of 20-40 mm concrete cover can occur. So it is of great importance to find different ways of decreasing the risk and tendency of spalling for HPC. One measure is to choose a concrete mix with various additives to improve the permeability and the pore structure. When surface spalling of fire-exposed concrete structures occur smaller or greater parts disappear and the reinforcement cover may vanish leading to direct heating of the reinforcement and a rapid decrease of load-bearing capacity. Sometimes the spalling can be very comprehensive and cause an immediate failure of the structure. The spalling can be explosive or a calm process.

Increased tendency for surface spalling is caused by:

- High moisture content
- Dense concrete (HPC)
- Compressive stress from external load and pre-stress
- Rapid temperature rise

Three primary mechanisms can be identified, which separately or in combination can cause surface spalling:

- Vapor pressure
- Thermal stresses
- Structural transformation of aggregate

For these reasons, new materials like geopolymer seem to have more advantage use in high performance concretes.

## **Definition of Geopolymer**

The term 'geopolymer' was first introduced by Davidovits in 1978 to describe a family of mineral binders with chemical composition similar to zeolites but with an amorphous microstructure. He also suggested the use of the term 'poly(sialate)' for the chemical designation of geopolymers based on silico-aluminate<sup>1,2</sup>.

Unlike usual Portland cements, geopolymers do not form calcium silicate-hydrates (CSHs) for matrix formation and strength, but utilize the polycondensation of silica and alumina precursors and a high alkali content to attain structural strength. Therefore, geopolymers are sometimes referred to as alkali activated alumina silicate binders<sup>3</sup>.

Geopolymers, also called polysialates, are a class of amorphous aluminosilicate materials formed near ambient temperatures<sup>4, 5</sup>. These materials, similar to cements, exhibit a fast setting and an exceptional hardness and strength. These inorganic

polymers materials are synthesized by reaction of a strongly alkaline silicate solution and an aluminosilicate source at near-ambient temperature. For this fact, geopolymer cements are based on an aluminosilicate structure while traditional cements are composed of portlandite [Ca(OH)2] and calcium silicate hydrate (C-S-H) phases.

The aluminosilicate materials are much more resistant to chemical attack and they do not have calcinations step. The physical and chemical properties of geopolymer make them potentially suited for use in refractory applications and as waste immobilization matrices.<sup>6,7</sup>

## Materials Used and Laboratory Investigations

Fly Ash: Fly ash used in this study was low-calcium (ASTM Class F)

**Aggregates:** Local crushed limestone-type aggregates, comprising 0/3mm, 0/8mm and 8/15 mm coarse aggregates and fine aggregates, in saturated surface dry condition, were used.

**Alkaline Liquid:** The alkaline liquid used was a combination of sodium silicate solution (Na2O= 13%, SiO2=29%, and water=58% by mass) and sodium hydroxide solution. (NaOH) with 96%-98% purity. The NaOH solids were dissolved in water to make the solution.

**Super Plasticizer:** In order to improve the workability of fresh concrete, high-range water-reducing naphthalene based super plasticizer was added to the mixture. The mixture proportion for concrete is given in Table 1.

**Table 1. Concrete Mixture Proportions** 

Materials	Mass (kg/m <sup>3</sup> )	
Coarse aggregates:	8/15	300
Coarse aggregates.	3/8	380
Fine sand	630	
Fly ash	400	
Sodium silicate solutio	100	
Sodium hydroxide soluti	42	
Super Plasticizer	5	

**Curing of Test Specimens:** After casting, the test specimens were heat-cured at 60°C for 24 hours<sup>8</sup>. After demolding, the specimens were left to air-dry in the laboratory until the day of test.

**Furnace characteristics and specimens heating:** The internal dimensions of the furnace compartment, which is completely closed (except for two 20 mm diameter holes that allow thermocouples to be placed), are 240 mm x 240 mm x 240 mm. The maximum operating temperature of this furnace is 1100°C with a power rating of 40kW. This furnace is controlled by a programmable microprocessor temperature

controller attached to the furnace power supply with feedback temperature from a Type K thermocouple located in the furnace compartment.

Temperature measurements were accomplished by placing a 0.8 mm Type K thermocouple into the specimen's central core (50 mm  $\pm 1 \text{ mm}$  from the surface). An identical thermocouple was attached to the specimen's surface. Thermocouples were inserted until they contacted the bottom of the holes, and the remaining opening of the holes was filled with cement mortar.

This initial heating study was carried out with a heating rate of 10EC/min, which was the maximum controllable rate of rise provided by the furnace. The study was run with a maximum core target temperature for the specimen's core of 300EC. This required the furnace to be operated at a maximum temperature of 325EC and an exposure time of at least 5 hours.

The specimens were exposed to a standard RABT curve developed in Germany as a result of a series of test programmes such as the Eureka project for a period of 2 hours and a highest temperature of 700°C.

In the RABT curve, the temperature rise is very rapid up to 1200°C within 5 minutes. The duration of the 1200°C exposure is shorter than other curves with the temperature drop starting at 30 minutes for car fires. The drop off for train fires only starts at 60 minutes. The 110 minutes cooling period is applied to both fire curves.

The failure criteria for specimens exposed to the RABT-ZTV time/temperature curve is that the temperature of the reinforcement should not exceed 300°C. There is no requirement for a maximum interface temperature.

#### **Results and Discussion**

**Compressive strength:** Compressive strength tests on samples (100 mm x 100 mm x 100 mm) were carried out at room temperature after cooling down from the treatment temperatures. As shown in Fig. 1, compressive strength has no significant decrease until 500°C; after that it became 30% less important at 700°C. Until this temperature there was no spalling observed but specimens cracked probably due to the disintegration of the limestone aggregate.

**Bending-tensile strength:** The same optimum-effect as that of the compressive strength test was determined in bending-tensile strength tests.

Mercury Intrusion Porosimetry: A plot of cumulative intrusion volume versus pore diameter is shown in Fig. 2. The majority of the intrusion volume occurs between 0.1-  $0.01 \mu m$ .

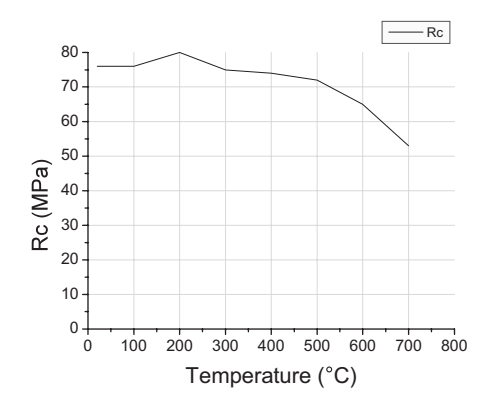


Fig. 1. Compressive strength versus temperature.

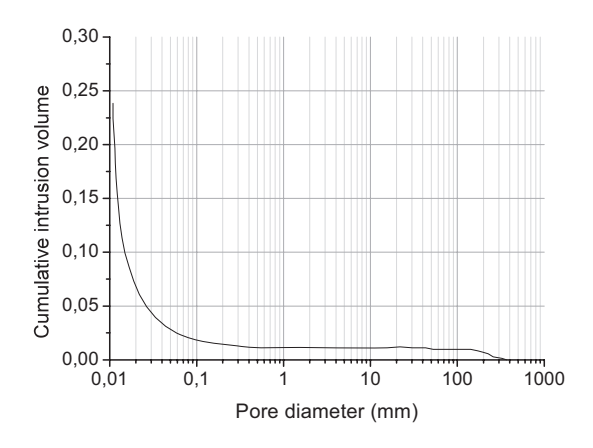


Fig. 2. Cumulative intrusion volume versus pore diameter.

In HPC on the basis of the standard Portland cement, there is a transition layer between the aggregate grain and hardened cement. The thickness of the layer ranges from 20 to  $100~\mu m$ ; the layer microstructure and composition differ from that of hardened cement. The contents of Ca(OH)2 and ettringite are higher. There are often Ca(OH)2 particles oriented along the aggregate particles. The porosity of the transition layer is larger than that of the hardened cement and a porosity gradient with the decreasing character in the direction away from the aggregate particles could be observed. More than 60% of the reaction water (Fig. 3) evaporates before  $100^{\circ}\text{C}$  without causing any damaging stress.

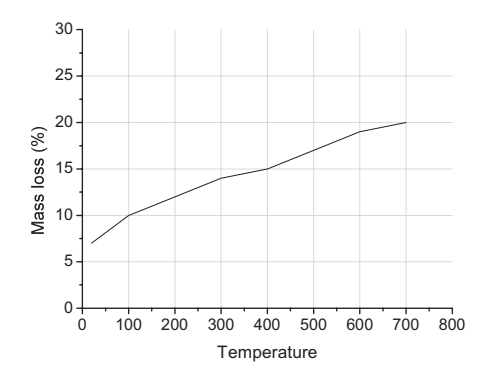


Fig. 3. Mass loss versus temperature.

#### **Conclusions**

If HPC, without any additives like polypropylene and with a water binder ratio less than about 0.32, is exposed to the standard fire exposure, ISO 834, it is characterized by a successive spalling of 5-10 mm thickness and the longer fire duration, the deeper its spall. Total spalling may lead to the collapse of the structure which usually results in grave consequences including losses of properties or casualties. The effect of high temperatures on the properties of geopolymer mortars was investigated in the temperature range of 100 to 700 °C; in this interval of temperature no spalling was observed.

A geopolymer material exposed to the action of high temperatures loses a substantial part of its strength that drops to 30 % of its original value. The strength already starts dropping at a temperature of 250 °C and it remains practically the same at higher firing temperatures. The lowest values of the residual strength were observed in the temperature range of 600 to 700 °C; they were due to the presence of the melt that started forming. The values of the residual strength after the firing were rather higher than those characterizing the materials on the basis of Portland cement.

In comparison to the concrete made of Portland cement, in geopolymer concrete there is no transaction boundary between geopolymer and aggregate that can be detected by a direct measurement of the geopolymer compositions in the proximity of the aggregate itself. The geopolymer, on the basis of fly ashes, is a porous material in which the porosity is very similar in the region of nano-pores, regardless of the conditions of their preparation.

#### References

 Davidovits, J. (1988a). Soft Mineralogy and Geopolymers. Paper presented at the Geopolymer '88, First European Conference on Soft Mineralogy, Compiegne, France.

- 2. Van Jaarsveld, J. G. S., van Deventer, J. S. J., & Lukey, G. C. (2002a). The effect of composition and temperature on the properties of fly ash-and kaolinite-based geopolymers. *Chemical Engineering Journal*, 89(1-3), 63-73.
- 3. Roy, D. M. (1999). Alkali-activated cements Opportunities and Challenges. *Cement & Concrete Research*, 29(2), 249-254.
- 4. Davidovits, J. Geopolymers-inorganic polymeric new materials. Journal of Thermal Anal., 1991, Vol. 37, p. 1633-1656.
- 5. Davidovits, J. "Synthetic Mineral Polymer Compound of the Silicoaluminates Family and Preparation Process, US Pat. No. 4,472,199, Sept. 18, 1984.
- 6. Perera, D. S., Nicholson, C. L., Blackford, M. G., Fletcher, R. A., and Trautman, R. L., J. Ceram. Soc. Jap., 2004, 112, S1-S4.
- Perera, D. S., Blackford, M. G., Vance, E. R., Hanna, J. V., Finnie, K. S., and Nicholson, C. L., Mat. Res. Soc. Proc., 2004, Sci. Basis Nucl. Waste Man. XXVIII, 824, CC8, 35.
- 8. Hardjito, D., Wallah, S. E., Sumajouw, D. M. J., & Rangan, B. V. (2005a). Fly Ash-Based Geopolymer Concrete. *Australian Journal of Structural Engineering*, *Vol.* 6(1), 77-86.

# **Mechanical Properties of Recycled Aggregate Concrete**

## Khaldoun Rahal

Associate Professor, Civil Engineering Department, Kuwait University, Kuwait

#### **Abstract**

This paper reports the results of an experimental study of some of the mechanical properties of recycled aggregate concrete (RAC) as compared to those of conventional normal aggregate concrete (NAC). Ten mixes of concrete with target compressive strength ranging from 20 to 50 MPa were cast using normal and recycled aggregates. The selected mix proportions are typically used by producers of ready-mix concrete in Kuwait. The development of the cube compressive strength and the indirect shear strength at ages of 1, 3, 7, 14, 28 and 56 days are reported. The results show that the 28-days cube compressive strength and the indirect shear strength of recycled aggregate concrete were on the average 90% of that of a natural aggregate concrete with the same mix proportions. The trends in the development of compressive and indirect shear strength in recycled aggregate concrete were similar to those in natural aggregate concrete.

#### Introduction

The environmental impact of the production of the raw ingredients of concrete such as cement and coarse and fine aggregates is considerable (1-3). The scale of the problem makes it prudent to investigate other sources of raw materials in order to reduce the consumption of energy and the available natural resources and to achieve a more "green" concrete.

In Kuwait, the environmental impact of the production of coarse aggregate led the local authorities in 1997 to ban this production from local quarries, and led suppliers to import coarse aggregates at larger cost from nearby countries such as the United Arab Emirates. This significantly affected the cost of concrete, and increased the variation in properties of the available aggregates.

Crushing concrete to produce coarse aggregate for the production of concrete is one common means for achieving a more environmentally friendly concrete. In Kuwait, two possible sources of concrete for re-use as coarse aggregate are from demolition of existing buildings, and reject concrete from ready-mix plants. A large number of building structures which were constructed 25 to 40 years ago in Kuwait have completed their service life and are being demolished for replacement with new and taller structures, especially as the real-estate business has improved in recent years. Moreover, a certain quantity of the concrete produced by the ready-mix plants is usually returned before placing, mainly due to delays during placing, high initial slump and overestimation of required quantity by the clients. Depending on the type of concrete supplied (wet mix versus dry mix) and the adequacy of the management, most local ready mix suppliers dispose between 1% and 2% (with limited cases where this ratio is below 0.2%) of the concrete produced. The yearly consumption in Kuwait currently exceeds 5 million m<sup>3</sup> and is expected to increase. Reject concrete can hence be estimated at about 100,000 metric tonnes. In the past decade, a significant portion of the reject concrete was disposed in unauthorized locations such as on the side of the roads leading to the ready mix plants. Lately, the local authorities have strictly enforced the ban on unauthorized disposal, but the fine charged was set at 50 Kuwaiti Dinars only (about 130 euros). Even though the relatively low fine deterred the larger part of the illegal disposal, more appropriate measures need to be taken especially as the disposal of waste in municipal landfills remain free of charge.

The mechanical properties as well as the durability characteristics of RAC must be investigated to ensure a proper use of the recycled material. There have been reports from numerous studies concerned with the mechanical properties (1-5, 7, 9) and durability aspects (6-8) of RAC. However, properties using local materials need to be investigated in order to gain better confidence in the adequacy of the new material for local use. This paper reports the results of an experimental investigation of some of the mechanical properties of RAC made of locally available materials in Kuwait.

## **Recycled Aggregates**

Demolished concrete was obtained from two sites in the Hawally region in Kuwait. Large parts from beams were transported to the labs and broken by workers into smaller pieces with sizes smaller than 70 mm. Those pieces were then crushed using a jaw crusher to sizes smaller then 20 mm and then sieved. Table 1 gives some of the measured properties of the aggregates used. In accordance with a common industry practice, stones retained in 9 mm, 12 mm in. and 19 mm sieves were maintained to be used in the mix.

Table 1. Properties of the Aggregates Used

Aggregate	Water Absorption (%)	Specific gravity (SSD)	Specific gravity (oven dried)	Chloride content (% of cement mass)
Natural	0.68	2.86	2.84	0.14
Recycled	3.47	2.39	2.31	0.30

## **Experimental Program**

Five different mix designs commonly used by ready-mix producers in Kuwait for concrete with target strength between 20 and 50 MPa were used. Table 2 gives the details of the mix proportions. The water-cement ratio ranged from 0.40 for 50 MPa concrete to 0.65 for 20 MPa concrete. It is customary in Kuwait to refer to the compressive strength in kg/cm², and this is maintained in this paper. For example, K300 refers to a concrete with cube compressive strength of 300 kg/m², which is nearly equal to 30 MPa.

Five mixes were cast using conventional natural aggregates. Similar mixes were cast using recycled aggregates, giving a total of 10 mixes. The amount of water reducers added to the mixes was adjusted to obtain a slump of about 50 to 60 mm. Twenty five 100-mm cubes were cast in steel moulds from each mix. Transporting and crushing the concrete to produce the aggregate was cumbersome and time-consuming, and hence the smaller 100-mm cubes were used instead of the standard 150-mm cubes. In addition, three 150-mm cubes were cast to measure the indirect shear strength. The development of the compressive strength was monitored by testing the cubes at 1, 3, 7, 14, 28 and 56 days of age.

Table 2. Concrete Mix Proportions (kg/m<sup>3</sup>)

Class	K200	K250	K300	K400	K500
Target 28-days cube strength	20	25	30	40	50
[MPa]					
Cement (Type I)	360	380	400	420	460
Water (+liquid super plasticizer)	234	190	192	181	184
w/c	0.65	0.50	0.48	0.42	0.40
Sand [kg/m <sup>3</sup> ]	705	705	705	705	705
Coarse aggregate (9 mm)	500	500	500	500	500
Coarse aggregate (12 mm)	340	340	340	340	340
Coarse aggregate (19 mm)	260	260	260	260	260

The test set up illustrated in Fig. 1 was used to test the indirect shear strength of the 150 mm cubes. This indirect test resembles the push-over tests to a large extent, except that the cubes are easier to cast. The vertical failure plane is subjected to significant shear stresses, and can be considered an adequate method to obtain comparative results that can form the basis of a more detailed study using beam test specimens.

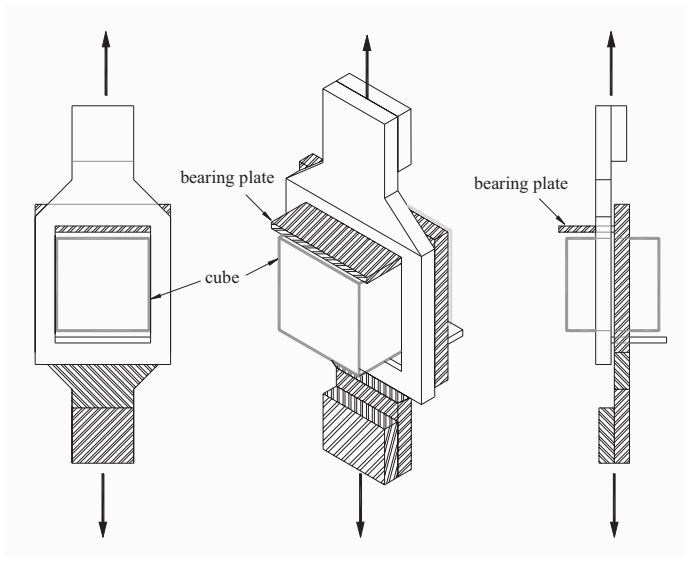


Fig. 1. Setup of indirect shear test.

#### **Discussion of Test Results**

The test results are summarized in Tables 3 and 4, and the following sections discuss these results of the study, with emphasis on the comparison between the behavior of RAC and NAC. It is to be noted that the density of RAC was on the average 2250 kg/m<sup>3</sup>, which was about 3.6% less than the observed 2330 kg/m<sup>3</sup> density of NAC.

**Effect of water-cement ratio:** Tables 3 and 4 summarize the test results. Figure 2 shows the relationship between the 28-days cube compressive strength and the water-cement ratio for the RAC and NAC. The figure shows that the target strength was achieved at 28-days for both types of concrete, except for the K400 RAC and K500 RAC mixes which were respectively 1.4% and 7% less than target.

Figure 3a shows the relationship between the 28-days cube compressive strength and the water-cement ratio for the RAC and NAC. Table 3 and Fig. 3 show that the target cube strength was achieved at 28-days for both types of concrete, except for the K400 RAC and K500 RAC mixes where the average strengths were respectively 1.4% and 7% lower than the target strength. As expected, the strength of RAC was slightly lower than the conventional concrete made from similar mix proportions. On the average, the RAC cube strength was 88.4% of that of the conventional concrete.

Figure 3-b shows a similar relationship between the 28-days indirect shear strength and the water-cement ratio. On the average, the RAC cube strength was 87.7% of that of the conventional concrete. This ratio is similar to that of the cube compressive strength. The shear strength of the K300 concrete was unexpectedly close to that of the K400 concrete. Otherwise, the trend in the graph is typical of the effect of water on the strength. Figure 3 shows that higher strength can be achieved by reducing the water to cement ratio in RAC. Judging by the age of the demolition concrete used to produce the RA, it is likely that this concrete had a lower strength and a higher water to cement ratio than the concrete achieved in this study. Hence though the compressive strength of RAC is affected by the strength and water to cement ratio of the original concrete, it is not limited to that strength as an upper value.

The figure also shows similar relations between the strength and w/c for both concrete. As expected, the strength of the RAC was slightly smaller than the conventional concrete made from similar mix proportions. Figure 3 shows the relationship between the cube strength of the two concrete. On the average, the RAC strength was 88.4% of that of the conventional concrete.

Table 3. Average Results from Cube Compression Tests (MPa)

Measured Property	Type	No. of	Concrete Class				
		tests	K200	K250	K300	K400	K500
Strength at 1 day	RAC	3	4.3	5.60	6.30	8.97	10.1
	NAC	3	5.6	7.33	8.77	10.2	13.7
Strength at 3 days	RAC	3	10.7	13.4	16.4	18.5	21.5
	NAC	3	12.5	16.3	18.9	23.4	29.2
Strength at 7 days	RAC	3	15.0	18.9	22.7	26.5	27.8
	NAC	3	17.0	21.2	24.7	32.5	37.3
Strength at 14 days	RAC	3	18.0	22.5	27.2	35.2	41.5
	NAC	3	19.9	25.9	31.2	41.1	46.5
Strength at 28 days	RAC	10	20.3	29.2	32.2	39.4	46.5
	NAC	10	22.7	32.3	36.0	46.0	53.5
Strength at 56 days	RAC	3	21.6	30.7	33.4	42.7	51.2
	NAC	3	23.3	33.3	37.0	48.3	57.6
Standard Deviation of 28	RAC	10	0.53	0.96	0.77	0.85	1.48
days strength	NAC	10	0.95	0.80	0.84	0.99	1.00
Coefficient of variation of	RAC	10	2.61	3.27	2.41	2.16	3.17
28-days strength (%)	NAC	10	4.18	2.47	2.33	2.14	1.87

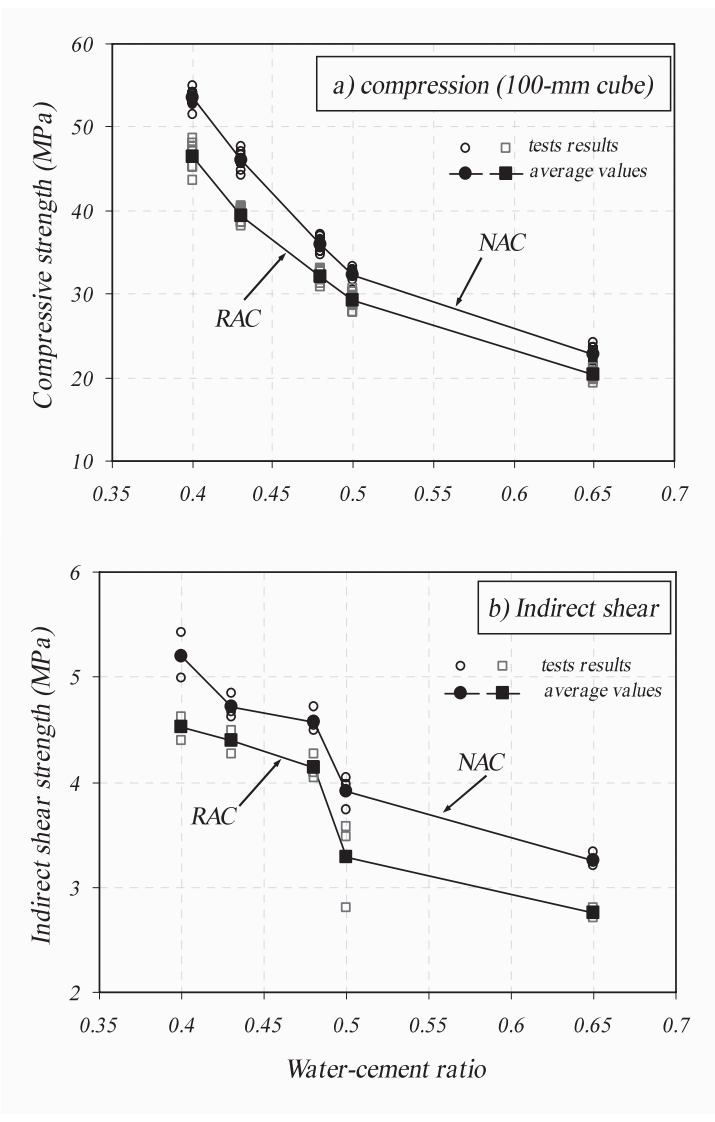


Fig. 2. Variation of 28-days cube compressive strength and indirect shear strength with water-cement ratio.

Table 4. Average Results from Indirect Shear Tests (MPa)

Age of	Type	No. of	Concrete Class				
test		tests	K200	K250	K300	K400	K500
(MPa)							
1 day	RAC	3	0.6	0.7	0.8	1.0	1.1
	NAC	3	0.8	1.0	1.2	1.4	1.5
3 days	RAC	3	1.4	1.8	2.2	2.4	2.6
	NAC	3	1.6	2.0	2.4	3.2	3.3
7 days	RAC	3	2.0	2.6	3.1	3.3	3.6
	NAC	3	2.3	2.9	3.4	3.7	4.0
14 days	RAC	3	2.6	3.3	3.8	3.9	4.2
	NAC	3	2.9	3.6	4.2	4.3	4.6
28 days	RAC	10	2.8	3.3	4.1	4.4	4.5
	NAC	10	3.3	3.9	4.6	4.7	5.2
56 days	RAC	3	3.1	3.6	4.4	4.6	4.8
	NAC	3	3.5	4.1	4.7	4.9	5.5

**Development of Compressive Strength:** Figure 2 shows the development of the cube strength starting between 1 to 56 days of age. The figure shows similar trends in strength development. In comparison with RAC, conventional natural aggregate concrete gained relatively larger percentage of its 28-days strength in the first 7 days. At 14 days and later age however, RAC gained a larger percentage of its strength, including the period after the 28-days of age.

Variability in Test Results of 28-days Strength: For each of the ten mixes, ten cubes were tested at 28-days to study the possible variability in strength. Table 2 reports the average, standard deviation and coefficient of variation for the ten mixes. Except for the K200 mixes, the coefficient of variation in RAC was slightly larger than in conventional concrete.

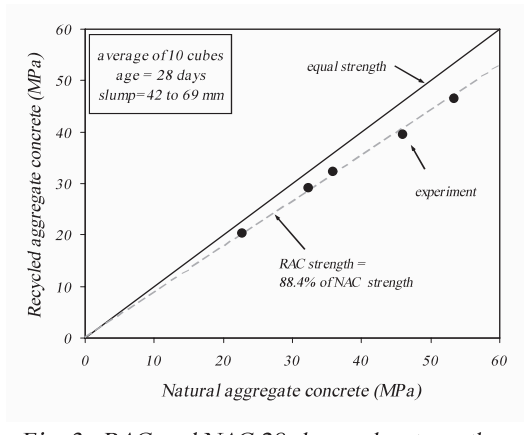


Fig. 3. RAC and NAC 28-days cube strength.

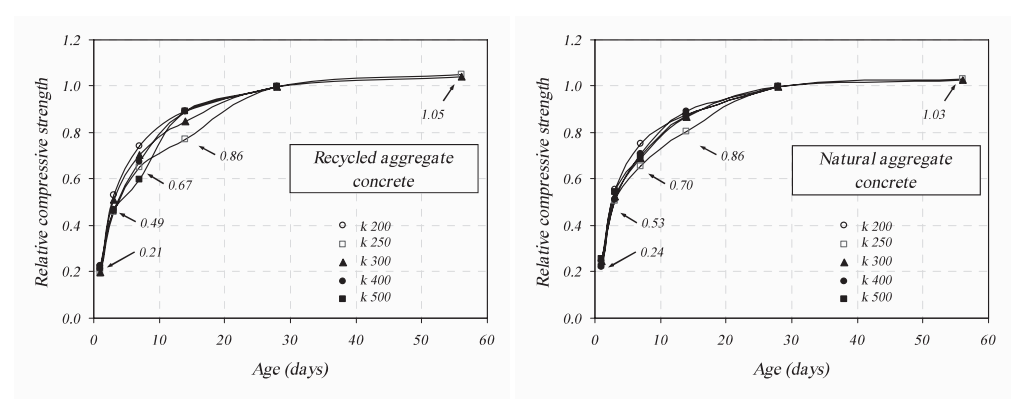


Fig. 4. Strength development in RAC and NAC.

## **Conclusions**

Based on the experimental results, the following can be concluded:

- 1. The 28-days target compressive strength for all five mixes were achieved except for the 40 and 50 MPa RAC where the observed strength was slightly lower than that of the target strength.
- 2. The cube compressive strength of RAC was on the average 88.5% of that of a conventional NAC with similar mix proportions and slump. The slump was maintained by adjusting the amount of water reducers in the mix.
- 3. On the average, the 56-days cube strength was 5% and 3% higher than the 28-days strength for RAC and conventional NAC respectively.
- 4. RAC and conventional NAC showed similar trends in strength development, with relatively faster strength gain in conventional concrete up to 7-days age.
- 5. The 28-days cube strength in RAC showed a scatter slightly larger than that in conventional NAC. The coefficient of variation ranged from 2.2% to 3.3% with an average of 2.7% for RAC and between 1.9% and 4.2% with an average of 2.6% for conventional NAC.
- 6. There has been no evidence of difference in secant stiffness of RAC and NAC. The ACI equation over-estimates the secant stiffness of both materials produced in this study.

## Acknowledgement

The research reported in this paper was supported by Kuwait University, Research Grant EV03/04. This support is gratefully acknowledged.

#### References

- 1. Buck, A.D., 'Recycled Concrete as a Source of Aggregate,' ACI Journal, 1977, Vol. 74, No. 5, pp. 212-219.
- 2. Hansen, T.C. and Narud, H., 'Strength of Recycled Concrete Made from Crushed Concrete Coarse Aggregate,' Concrete International, 1983, No. 1, pp. 79-83.
- 3. Hansen, T.C. and Hedegard, S.E., 'Properties of Recycled Aggregate Concrete as Affected by Admixtures in Original Concretes,' ACI Journal, 1984, Vol. 81, No. 1, pp. 21-26.
- 4. Forster, S.W., 'Recycled Concrete as Aggregate,' Concrete International, 1986, Vol. 8, No. 10, pp. 34-40.
- 5. Tavakoli, M. and Soroushian, P., 'Strengths of Recycled Aggregate Concrete Made Using Field-Demolished Concrete as Aggregate,' ACI Materials Journals, 1996, V. 93, No. 2, pp. 182-190.
- 6. Tavakoli, M. and Soroushian, P., 'Drying Shrinkage Behavior of Recycled Aggregate Concrete,' Concrete International, 1996, Vol. 18, No. 11, pp. 58-61.
- 7. Rashwan, M.S. and AbouRizk, S., 'The Properties of Recycled Concrete,' Concrete International, 1997, Vol. 19, No. 7, pp. 56-60.
- 8. Hadjieva-Zaharieva, R., Ramos-Quebaud, M., Wirquin, E. and Buyle-Bodin, F., 'Opportunities for Implementation of Recycled Aggregates in Production of Durable Concrete in Building Construction,' Cement and Concrete Technology in the 2000's, Second International Symposium, Istanbul, Turkey, pp. 361-381.
- 9. Abdelfattah, A. and Tabsh, S., 'Feasibility of Using Recycled Concrete in The United Arab Emirates', 2003 ICPCM Conference, Cairo, Egypt, pp. 82-90.
- 10. Al-Fadala, K. B., 'Recycling concrete Waste into Hot Mix Asphalt,' Master's Project Report, Department of Civil Engineering, Kuwait University, 2003, 61 pp.
- 11. ACI 318-02, 'Building Code Requirements for Reinforced Concrete (ACI 318-02) and Commentary (ACI 318R-02),' American Concrete Institute, Detroit, 2002, 443 pp.
- Ahmad, S.H. and Shah, S.P., 'Structural Properties of High Strength Concrete and its Implications for Precast Prestressed Concrete,' PCI Journal, Nov.-Dec. 1985, pp. 92-119.

# **Properties of Recycled Aggregate Concrete**

Ali Al-Harthy, Ramzi Taha, Abdullah Al-Saidy and Salim Al-Oraimi Department of Civil and Architectural Engineering, College of Engineering, Sultan Qaboos University, P.O. Box 33 Al-Khaudh 123, OMAN

#### **Abstract**

Demolition of deteriorated and old concrete structures results in large amounts of concrete waste that usually occupies valuable landfill areas. Moreover, environmental and economic factors are increasingly encouraging a higher value utilization of demolition debris. The opportunity for using recycled building waste and recycled aggregate concrete (RAC) in new concrete construction projects has been a subject of intensive research for many years and some countries in the Western world and Japan have made a good progress in the utilization of recycled construction materials. Unfortunately, the use of recycled construction debris has received very little attention in the Arabian Gulf countries. If proven feasible, it could mean that thousands of tons of concrete waste would eventually be cleared for use in RAC. In this study, a number of laboratory tests on recycled coarse aggregates were carried out to investigate the strength and durability of RAC. The variables that were considered in the tests include some physical properties of the recycled aggregates (RA), such as density and absorption. RAC specimens containing 10% to 100% replacement of normal aggregate by RA were prepared. The compressive strength and absorption characteristics of RAC were determined. The results indicate that the strength of concrete made from RA is not adversely affected when RA are used in lieu of normal coarse aggregates. In addition, concrete strength will generally increase with an increasing replacement of normal aggregates by RA content of up to 30% and then will subsequently decrease with any further increase in RA. Increasing replacement by RA was found to decrease the workability due to the high absorption characteristics of RA. In general, the absorption characteristics of RAC was found to increase with increasing amounts of RA.

## Research Studies on Recycled Aggregates Concrete

Most researchers in the period from 1945 to 1977 have found that the marked difference between recycled concrete and normal concrete is the higher water absorption in recycled concrete (Nixon, 1977; Hasaba et al., 1981; Hansen and Narud, 1983). This is attributed to absorption by cement paste adhered to the old aggregates. This adhered mortar could affect deformation properties of RAC such as elasticity, creep and shrinkage. Drying shrinkage has been found to be greater in recycled concrete. The compressive strength in recycled concrete was found somewhat lower than the normal concrete. Concrete which are produced with recycled coarse and fine aggregates tend to be harsh and unworkable because fine recycled aggregates consist of angular particles (Huisman and Briston, 1982). The density of recycled aggregates is somewhat lower than the density of original aggregates due to a relatively low density of the old mortar which is attached to original aggregates particles (Hasaba et al., 1981; BCSJ, 1978; Ravinrarajah and Tam, 1985). Several studies (Nixon, 1977; Ravinrarajah and Tam, 1985) have shown that recycled concrete aggregates produced from all but poorest quality concrete can be expected to pass ASTM and BS requirements of the Los Angeles abrasion loss percentage, British Standard crushing value, as well as 10% fines value even for production of concrete wearing surface.

Some reported results (Huisman and Briston, 1982) show a compressive strength reduction of concrete of 15% when few impurities of lime plaster, soil, wood, gypsum, asphalt or paint are added to the recycled concrete.

In the laboratory it is found that compressive, tensile, and flexural strength of recycled aggregate concrete can be equal to or higher than that of the original concrete (Hansen and Narud., 1983; BCSJ, 1978; Mukai et al., 1978). However, in practice and often in the laboratory, strengths of recycled aggregate concretes are found to be lower than those of corresponding original concretes (Nixon, 1978; Buck, 1977; Malhotra, 1978).

Unlike the situation in Europe and North America, there has been very limited appreciation of recycled materials in the construction industry in the middle-east. A study showed promising results for engineering applications (Akmal and Tabsh, 2003). Ryu (2002) studied the effect of the recycled aggregate on interfacial property, permeability and strength characteristics of the concrete. These were evaluated in order to examine the relationship between the recycled aggregate and the performance of the hardened concrete. The experimental results showed that the recycled aggregate has a significant effect on the overall properties of concrete. The permeability increases as the w/c ratio increases. The strength characteristic of the concrete is not affected by the quality of the recycled aggregate.

The application of building rubble collected from damaged and demolished structures is an important issue in every country. After crushing and screening, this material can serve as recycled aggregate in concrete. A series of experiments using recycled aggregate of various compositions from building rubble was conducted by (Chen et al., 2002). Test results showed that the building rubble could be transformed into useful recycled aggregate through proper processing. Using unwashed recycled aggregate in concrete will affect its strength. The effect will be more obvious at lower water/cement

ratios. When the recycled aggregate was washed, these negative effects were greatly improved. This is especially true for the flexural strength of the recycled concrete.

Katz (2003)used crushed concrete having a 28-day compressive strength of 28 MPa at ages 1, 3 and 28 days to serve as a source of aggregate for new concretes, simulating the situation prevailing in precast concrete plants. The properties of the recycled aggregate and of the new concrete made from it, with nearly 100% of aggregate replacement, were tested. The test result showed the properties of the RAC at different ages were quite similar and the concrete made with 100% RA was weaker than concrete made with natural aggregates at the same w/c ratio.

The concept of using recycled aggregate for making concrete is slowly but definitely gaining popularity. Research is in progress to make this technology feasible.

Tavakoli et al., (1996) determined the compressive, splitting, and flexural strength of recycled coarse aggregate concrete and compared with those of concrete made using natural crushed stone. The properties of the aggregate were also compared. Test results indicated that the strength characteristics of recycled aggregate concrete are influenced by key factors, such as the strength of the original concrete, the ratio of coarse to fine aggregate in the original concrete, the ratio of top size of aggregate in the original concrete to that of the recycled aggregate, and the Los Angeles abrasion loss and water absorption of recycled aggregate. These factors also influence the effect of water-cement ratio, aggregate top size, and dry mixing on the strength characteristics of recycled aggregate concrete.

Buyle-Bodin et al. (2002) evaluated the main risks for the durability of concrete made of industrially produced recycled aggregates. A characterization of recycled aggregates is performed and their peculiarities are highlighted. Comparison between the behavior of RAC and that of ordinary natural aggregate concrete was carried out. The influence of both the composition and the curing conditions is discussed. The durability study is focused on the assessment of parameters representing the porous structure and concrete characteristics. Because of the high total water/cement ratio of RAC, their flow properties control their durability. It is established that RAC are characterized by significantly higher water absorption and air permeability. The diffusion of the carbon dioxide is faster, too. This leads to a weaker resistance of RAC to environmental attacks. Since the main durability problems are caused by the fine recycled fraction, its use needs to be restricted. Another way to increase RAC durability seems to be the extended curing in wet environment.

Zaharieva et al. (2003) compared the water permeability, air permeability and surface permeability of recycled aggregate concrete (RAC) with those of a control concrete made with natural aggregate. The study shows that the permeation properties of RAC depend on mix-design, conditions of curing and drying of samples. Relationships between permeability and other physical characteristics of concrete such as water absorption capacity and diffusivity are discussed. According to the criteria existing for ordinary concrete made with natural aggregate, RAC could be classified as being of moderate quality rather than poor quality. The testing methodology shows that some of

the techniques used to measure the permeability of RAC need to be modified in order to properly relate with the distinctive characteristics of this material.

## **Experimental Details**

In this study, recycled aggregate concrete (RAC) samples were cast using recycled aggregates produced in the laboratory. These RA were obtained by processing concrete specimens made of normal aggregates. Three concrete mixes were considered: high strength concrete mix (H) with a water-to-cement ratio (w/c) of 0.4; a medium strength concrete mix (M) with w/c of 0.6 and a low strength concrete mix (L) with a w/c of 0.7. Table 1 shows the mix proportions for each mix type.

Concrete prisms  $(1000 \times 100 \times 40 \text{ mm})$  made of normal aggregates were cast from mix proportions show in Table 1. These prisms were cured in air for 14 days to obtain satisfactory properties of concrete. At the age of 28 days, the prisms were fed in a jaw-crushing machine to process the recycled aggregates. The prisms were broken into smaller pieces by the crushing machine and the processed aggregates were sieved and cleaned to remove the dust particles.

**Table 1. Mix proportions of Normal Concrete Mixes** 

Constituent	Mix #1(H)	Mix #2 (M)	Mix #3 (L)
Water-Cement Ratio (w/c)	0.4	0.6	0.7
Water	$240  (kg/m^3)$	$216  (kg/m^3)$	$217 (kg/m^3)$
Cement	600 (kg/m <sup>3</sup> )	$360  (kg/m^3)$	$310  (kg/m^3)$
Sand	$670  (kg/m^3)$	$550 (kg/m^3)$	$750  (kg/m^3)$
Coarse Aggregate (20mm)	602 (kg/m <sup>3</sup> )	690 (kg/m <sup>3</sup> )	674 (kg/m <sup>3</sup> )
Coarse Aggregate (10mm)	401 (kg/m <sup>3</sup> )	584 (kg/m <sup>3</sup> )	450 (kg/m <sup>3</sup> )

Physical properties of the recycled coarse aggregates such as particle size distribution, specific gravity and absorption were determined. The concrete tests included slump tests to measure the workability, concrete compressive strength and the initial surface absorption of the concrete. The strength properties of the concrete were obtained for ages 14, 28 days, and 90 days.

In each mix of the recycled aggregate concrete (RAC), normal coarse aggregates were replaced with different percentages of recycled aggregates. The details of the different mixes are shown in Table 2. The strength of the original concrete from which the recycled aggregate is processed is also identified by a letter. For example, M/L mix is a medium strength (M) mix with RA from low strength (L) concrete. There were three types of different sources of recycled aggregates (H, M and L) in order to study the effect of strength of the original concrete on the properties of recycled aggregates concrete.

Table 2. RAC Mixes

Mix	% Recycled Aggregate (RA)					
	10	30	50	70	100	
H/H	$\sqrt{}$					
M/H		V				
M/M	V	V	V	V	V	
M/L		V				
L/H		√	V			
L/M		√	V			
L/ L	V	V	V	V	√	

#### Results

Figure 1 shows the grading of the normal and the recycled aggregates. As Fig. 1 shows, the aggregates meet grading requirements of ASTM C33.

The specific gravity and absorption tests were conducted for four different samples of 20mm aggregates. These samples were normal aggregates (N); recycled aggregates from high strength; recycled aggregates from medium strength concrete and recycled aggregates from low strength concrete. Table 3 shows the apparent specific gravity, bulk specific gravity and water absorption of 20mm aggregates from the normal and recycled aggregates. Table 3 shows that the apparent and bulk specific gravities for the recycled aggregates are slightly lower than the gravities of the normal aggregates. Table 3 also shows that the water absorption is much higher in recycled aggregates than in normal aggregates. The difference in water absorption is more than twenty times.

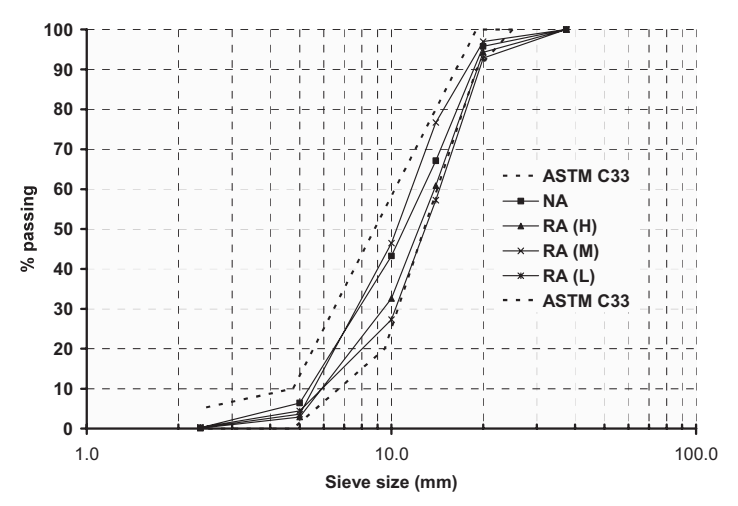


Fig. 1. Grain size distribution for the coarse aggregate.

Table 3. Specific Gravity and Absorption Test Results for Normal and Recycled Aggregates

Samples	Normal Aggregates	High Strength RA	Medium Strength RA	Low Strength RA
Apparent Specific Gravity	2.811	2.763	2.724	2.690
Bulk Specific Gravity	2.792	2.407	2.357	2.322
Absorption (%)	0.249	5.344	5.710	5.899

Figure 2 shows the slump measurements for all the mixes. It is clear that the workability decreases with increasing recycled aggregates contents.

The compressive strength test was conducted for normal aggregate concrete by using three specimens of 100 mm cube for each mix type. The ages of these specimens were 14, 28 and 90 days. Figure 3 shows the variations in compressive strength with respect to curing age.

The compressive strength test was conducted for recycled aggregate concrete by using also three specimen of 100 mm cube for each mix. The ages of these specimens were 14, 28 and 90 days. The normal aggregates were replaced by different amounts of recycled aggregates (10 to 100% replacement) for the three different strengths. The H/H mix is a RAC mix with w/c=0.4 and the RA is from a high strength normal concrete. The M/M mix is a RAC mix with w/c=0.5 and the RA is from a medium strength normal concrete. The L/L mix is a RAC mix with w/c=0.7 and the RA is from a low strength normal concrete. Figure 4 shows the 28-days compressive strength in the RAC mixes containing different replacement of normal aggregates by the recycled aggregates.

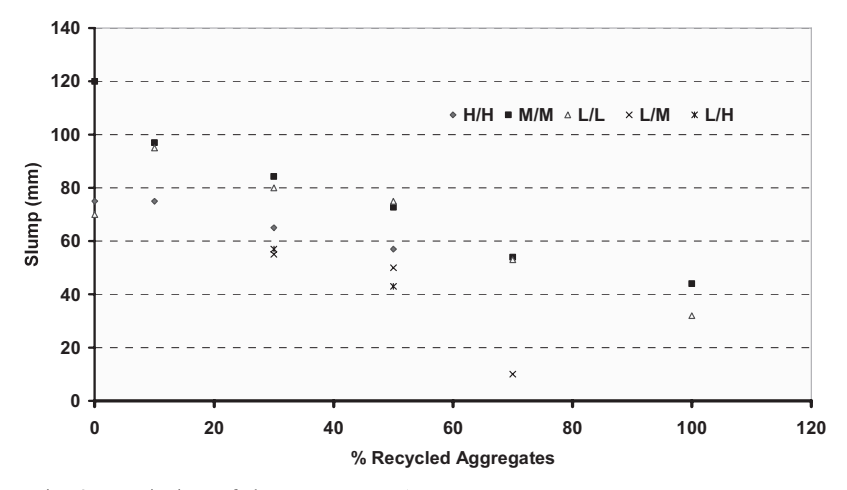


Fig. 2. Variation of slump versus RA contents.

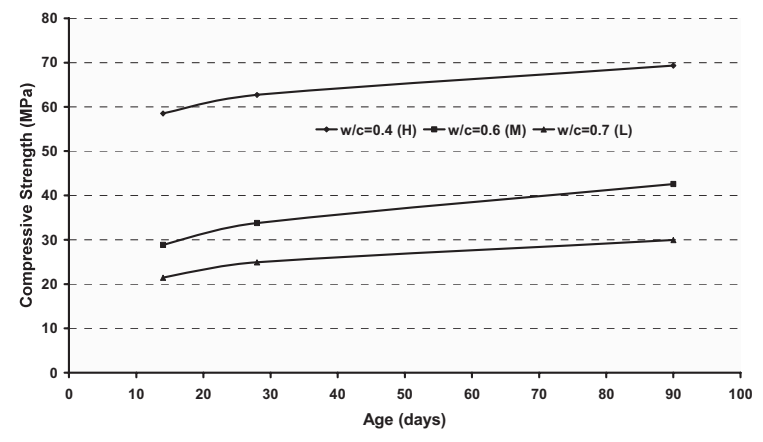


Fig. 3. Compressive strength for normal aggregate concrete vs. age.

The strength increases with increasing percentage replacement of recycled aggregate up to a limit ranging from 10% (H/H) to 30% (M/M and L/L) and then decreases with increasing recycled aggregates content. None of the strength of the recycled aggregates concrete was less than the normal aggregate concrete (control mix).

By using the prepared specimens of different strength mixes, the compressive strength test was carried out. In the mixes M/H and L/H, M/M and L/M and, M/L and L/L the used recycled aggregates were obtained from the crushing of normal aggregates concrete of high, medium and low strength, respectively. The observed results for strength are represented in Fig. 5. Figure 5 shows that the compressive strength of the RAC does not directly depend on the strength of the source of the recycled aggregates used in the mix.

The initial surface absorption test was conducted for normal aggregate concrete (control mix) by using three different specimens of 150 mm cube for each mix. The three specimens were cured for 28 days. The samples were then kept in the laboratory until the day of the initial surface absorption test. Figure 6 shows the average flow of the normal aggregate concrete for different water-cement ratio. The flow increases with the increase of the water-cement ratio for w/c=0.4 and w/c=0.6 and decrease with time. But the mix L (high w/c) indicates the minimum value.

The initial surface absorption test was conducted for recycled aggregates concrete by using three different specimens of 150 mm cube for each mix. The three specimens were cured for 28 days. The samples were then kept in the laboratory until the day of the initial surface absorption test. Figure 7 shows the variation of the surface absorption with RA contents for the three different concrete strengths. The flow generally increased with increase in RA contents from 10 to 50% for the H RAC samples and from 30 to 100% for L RAC.

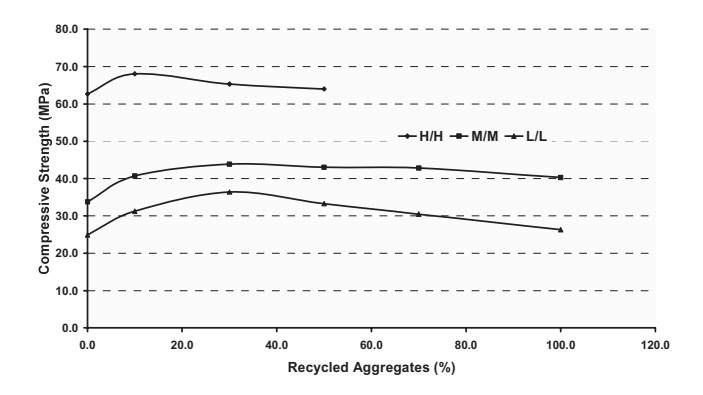


Fig. 4. Compressive strength for high strength RA concrete vs. % RA.

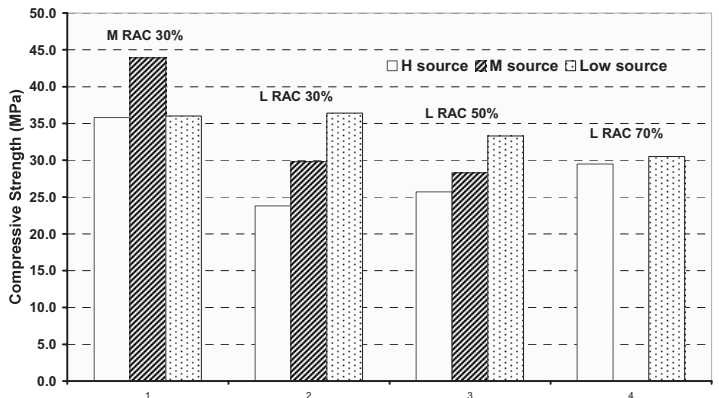


Fig. 5. Compressive strength for low, medium and high strength RAC made with different sources of RA.

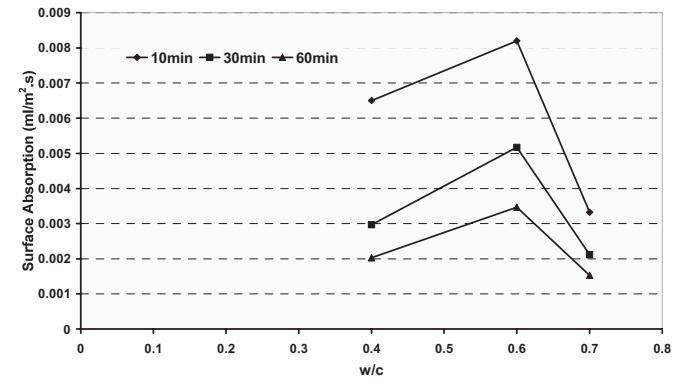


Fig. 6. Initial surface absorption for normal aggregate.

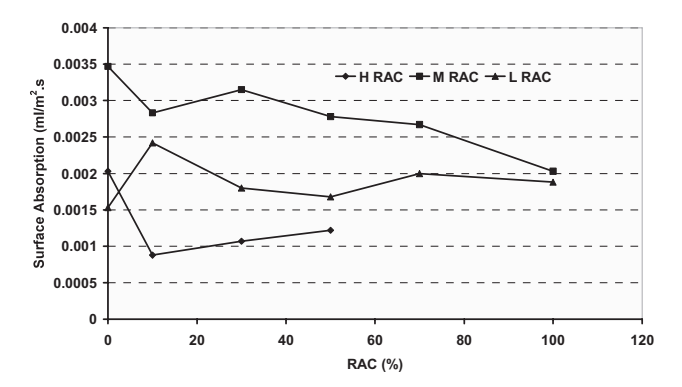


Fig. 7. Variation of surface absorption with RA contents.

#### **Conclusions**

This project studied the properties of concrete made with recycled aggregate. Workability, strength and initial surface absorption were considered. The main effects of the recycled aggregate on the properties of concretes are:

- 1. The workability decreases with increasing amount of recycled aggregates.
- 2. The strength of concrete made from recycled aggregate is not adversely affected when recycled aggregates are used in place of normal aggregates. The concrete strength was found to increase with increasing replacement by recycled aggregates up to 30% and then to decrease with increasing recycled aggregates replacement.
- 3. The strength of recycled concrete does not appear to depend on the strength of the original concrete from which the recycled aggregate is processed.
- 4. The water absorption of recycled aggregates concrete varies and is found to generally increase with increasing amount of recycled aggregates.

#### References

Akmal Abdelfattah; Sami W. Tabsh, Feasibility of using recycled concrete in the United Arab Emirates, ICPCM – A New Era of Building, Cairo, EGYPT, Feb. 18-20, 2003

B.C.S.J, Study on recycled aggregate and recycled aggregate concrete, Building Contractors Society of Japan, Committee on Disposal and Reuse of Concrete Construction Waste, Concrete Journal, 16, No. 7, pp 18-31, 1978.

Buck, A.D., Recycled concrete as a source of aggregate. ACI Journal, pp. 212-219, 1977.

Buyle-Bodin, F; Hadjieva-Zaharieva, R. Influence of industrial produced recycled aggregate on flow properties of concrete. Materials and Structure / Materiaux et construction, V 35, n253 Sep/Oct 2002, p504-509.

Chen How-Ji, Yen Tsong and Chen, Kuan-Hung. Use of building rubbles as recycled aggregates, Cement and concrete Reserch, V 33, n1, Jan 2003, p125-132.

- Hasaba, S., Kawamura, M., Trik, K., Drying shrinkage and durability of concrete made with recycled concrete aggregates, Japan Concrete Institute, Vol. 3,pp 55-60, 1981
- Hansen, T.C. and Narud, H., Strength of recycled concrete made from crushed concrete coarse aggregate. Concrete International –Design and Construction, Vol. 5, No. 1, pp 79-83, 1983.
- Huisman, C.L., and Briston, R.A., Recycled Portland cement concrete specifications and control, FHWA Proceedings of the National Seminar on PCC Pavement recycling and rehabilitation, 1982, St. Louis, Missouri, USA Federal Highway Report FHWA-TS-82-208.
- Kakizaki, M., Harada, M., soshiroda et al., Strength and elastic modulus of recycled aggregate concrete, Proceedings of the Second International RILEM Symposium on Demolition and reuse of concrete and masonry. 2: Reuse of Demolition Wastes (ed. Y. Kasai) Nihon Daigaku Kaikan, Japan, Chapman & Hall, London.
- Katz Amnon, Properties of Concrete made with recycled aggregate from partially hydrated old concrete, Cement and Concrete Reserch, V 33, n5, May 2003, p703-711.
- Malhotra, V.M., Use of recycled concrete as a new aggregate, Proceedings of Symposium on Energy and Resource Conservation in the Cement and Concrete Industry, CANMET, Report No. 76-8, Ottawa, 1978.
- Mukai, T., et. al., Study on reuse of waste concrete for aggregate of concrete. Energy and Resource Conservation in Concrete Technology, Japan-US Cooperative Science Programme, San Fransisco, 1979.
- Mukai, T., Kikushi, M., and Ishikiwa, N., Study on the properties of concrete containing recycled aggregates. Cement Association of Japan, 32<sup>nd</sup> Review, 1978.
- Nixon, P.J., Recycled concrete as an aggregate for concrete a review. RILEM TC-37-DRC. Materials and Structures (RILEM), Vol. 65, pp. 371-378, 1978.
- Nixon, P. J., Recycled Concrete as an Aggregate for Concrete, a Review, RILEM TC-37-DRC, Materials & Structures (RILEM), 65, p371-378, 1977.
- Ravinrarajah, R.S., and Tam, T.C., Properties of Concrete made with crushed concrete as coarse aggregates, Magazine of Concrete Research, Vol. 37, No. 130, 1985.
- Ryu, J.S, An experimental study on the effect of recycled aggregate on concrete properties, Magazine of Concrete Reserch, V54, n1, Feb 2002, p7-12.
- Tavakoli, Mostafa; Soroushin, Parviz. Strength of recycled aggregate concrete made using filed-demolished concrete as aggregate, ACL Materials Journal, V 93, n2, Mar/Apr 1996, p182-190.
- Zaharieva, Roumiana; Buyle-Bodin, Francois; Skoczylas, Frederic; wirquin, Eeric. Assessment of the surface permeation properties of recycled aggregate concrete. Cement and Concrete Composite, V 25, n2, Feb 2003, p223-232.

# Sustainability - A Duty and Science in the Concrete Industry

O. Kayali, School of Aerospace, Civil and Mechanical Engineering, University of New South Wales @ ADFA, Canberra, Australia, E-mail: o.kayali@adfa.edu.au

M. N. Haque, Department of Civil Engineering, College of Engineering & Petroleum, University of Kuwait, PO Box 5969, Kuwait, E-mail: Naseer@civil.kuniv.edu.kw

#### Abstract

The concrete industry, arguably being the most important of the building industries these days, provides a significant area for sustainable strategies. Materials that are consumed in making concrete provide the most important element of such strategies. Judicial use of cement coupled with the beneficial employment of certain so called 'industrial waste products' constitute the backbone of a sustainable concrete technology. The use of fly ash, ground granulated blast furnace slag (GGBFS), rice husk ash, condensed silica fume (CSF), and recycled concrete, bricks and other materials are all gaining varying degrees of acceptance from engineers and the society.

Careful design that considers long-term durability as a most important design criterion is an essential step in the direction of sustainability. Such design coupled with the use of 'waste' materials other than cement and natural aggregates can further enhance the durability as well as the sustainability of structures.

High performance concrete (HPC) is becoming the concrete of choice for rapidly emerging new and strong economies. This concrete is also the concrete that can provide the opportunity for sustainable design and material use. The materials that are used to produce high-strength-high-performance concrete often include waste products. Such inclusion is a significant contribution to sustainable industry. Nevertheless, one of the most important roles of the concrete engineer is to scientifically evaluate the use of such materials. As research publications abound with results showing benefits of certain materials whether from waste products or otherwise, it is the duty of the engineer to judge whether one or all of such materials should be used. A judgment, as this, needs to be based on the particular circumstances that dominate the building in question.

#### Introduction

Sustainability is a new dominant paradigm shift in Engineering and is pointing the way of the future. Among major concerns of sustainability is the fragility of the natural environment. Its aim in this regard is to arrest the negative impact of human activity. In its general meaning, sustainability embodies all the provisions necessary for excellent engineering solutions. Such solutions are those that contribute in a balanced measure to profitability, long-term community benefits and low environmental impact.

In this paper, the authors identify the issues that concern sustainability in the concrete industry. They then introduce and discuss the areas where the quest for sustainability can take a substantial advantage. The authors hope that the conclusions they have highlighted in this article will be heeded by those involved in the building industry especially at this time of extraordinary heated activity of concrete construction in the Gulf region.

# **Definition of Sustainability**

Rather than leave this term subject to different perceptions, it is preferred that a definition, broad as it may be, should be able to limit the scope in the argument for sustainability, especially as far as building activities are concerned. Dictionaries give the meaning of sustainability as the ability to be maintained. Dictionaries further define the term in ecological perspective as 'exploiting natural resources without destroying the ecological balance of an area'. We consider that these definitions very well describe the problem that we are facing in the concrete industry. That is the questions that are presented in this regard are:

- 1. Can the concrete industry be maintained at the current pace?
- 2. Can this industry be controlled to certain defined limits by which the ecological balances are maintained?

To discuss and then attempt to answer these questions, we need to examine certain facts. These facts relate to the particular concrete industry.

#### **Cement Production**

It is estimated that in the year 1900, 10 Mt of cement were produced globally. This quantity is estimated to have produced 40 M cubic metres of concrete (Aitcin, 2000). It is estimated that the world population in 1900 was 1.650 billion. That is, 0.024 m³ of concrete was the average per person. In contrast, a 2004 estimate puts cement production at 1.7\*10° tonnes per year (Gartner, 2004), producing 6 billion m³. That is at the average of 1 m³ per person. Cement production has increased by 170 times. World population has increased by 3.9 times. The average cement consumption of each person on earth has increased from 6.25 kg per year to 268 kg per year. The average concrete consumption per person increased, by approximately 42 times. Aitcin has cited Scheubel and Nachtwey (Scheubel and Nachtwey, 1997) who did a very interesting study relating the consumption of cement to per capita income. They found that cement consumption peaks at 600 kg per capita when the income is at US \$10,000

to US \$13,000 per capita. Cement consumption declines for the increased income after that. Since the increase in consumption is rapid within the lower income categories, it is therefore expected that it in the emerging economies, in other words, the developing countries, that will lead consumption figures. This, of course is an extremely interesting phenomenon of socio-economic dimensions but it is beyond the scope of this paper.

To date, information from the cement industry in the UAE illustrates that cement grinding capacity will surge by ca. 37% in 2007 and by an even higher ca. 51% in 2008, settling at 35.4 million tons per annum, prior to leaping a further 14% in 2009 to record 40.5 million tons per annum(Menareport, 2006).

The UAE currently faces a shortage of cement production by about 5 million tonnes per year with a current production capacity of 11 million tonnes per annum which is set to increase by 3 to 4 million tonnes per annum by 2007. According to a report, the estimated consumption of cement in the Gulf is more than 40 million tonnes and would increase tremendously in the next three years as the investment in key sectors will be around \$ 8 billion in the coming three years (Anon, 2006). In 2005, cement consumption in the UAE was 14 Mt, at the rate of 2920 kg per capita. This is more than 10 times the average world consumption (TAIB, 2006).

The amount of  $CO_2$  emission from cement industry varies between 0.82 tonnes per tonne of cement, when the estimate is made by those from within the industry itself (Gartner 2004; Strategic Industry Leaders 2006) to 1 tonne  $CO_2$  per tonne of cement, when the estimate is made by other researchers (Malhotra, 1999). It is however certain that  $CO_2$  emission that is produced from cement manufacture exceeds 0.82 tonnes per tonne of cement. There are estimates that  $CO_2$  emissions from cement manufacture alone amount to 10% of the greenhouse gases (Anon, 1997). Much less pessimistic studies put this figure at 5% (Hendriks, Worrell et al., 1998).

In 2002, the World Business Council for Sustainable Development, (WBCSD) recommended the reduction of CO<sub>2</sub> emissions from cement manufacture processes by 30% by 2020 and by 60% by 2050 (The United Kingdom Parliament 2002). A study by Eco Securities made for the United Nations Environment Programme Finance Initiative (ECOSECURITIES, 2005) placed cement industry in the high risk category when it comes to the impact of climate change and GHG emission policies on the industry and thus on lending institutions. Holdren has found that stabilizing the atmospheric concentration of CO<sub>2</sub> requires reduction in CO<sub>2</sub> emission to a fraction today. The moderate projection of global CO<sub>2</sub> emission is that by the year 2100 it will reach 20 GtC (giga tons of carbon) per year (Holdren, 2003). Holdren postulated that stabilizing atmospheric CO<sub>2</sub> will need to have a target of about 7 GtC per year by the year 2100. This target and the maintenance of a steady decline rate may eventually lead to an ideal target of 3-4 GtC by the year 2200. That level would only bring back the level of CO<sub>2</sub> in the atmosphere to that of twice the level of pre-industrial concentration.

#### The Share of Concrete Production

According to the report of the US Department of Energy, concrete production accounts to 12% of the CO<sub>2</sub> emissions associated with cement and concrete industry (Choate

2003). Therefore, one should always add such figure to the figures allocated for cement production alone. The factors contributing to this are mainly quarrying and transportation of aggregates and the rest of the manufacturing processes and transportation of finished product. It is of interest to note that the report shows that cement and concrete industry in the United States operates at only 40% thermal efficiency.

From all of this, it can be concluded that:

- Cement manufacture and concrete production is a major contributor to GHG emissions.
- 2. The level of CO<sub>2</sub> emission as contributed by the cement industry is not sustainable.
- 3. Measures must be taken by the industry to address this issue and drastically reduce the CO<sub>2</sub> share of cement and concrete.
- 4. Democratic governments, under various national and international influences, are implementing policies that will enforce reductions in GHG emissions.
- 5. Cement and concrete industry groups will have to heavily invest in R&D in order to be able to meet minimum targets of reductions while staying viable as profit generating ventures.

### So, What Can Be Done?

The finding that has been mentioned above regarding the inefficiency of cement and concrete manufacturing is of course of extreme importance. However, we will only limit our discussion to other aspects in the raw materials of concrete and to the aspects of the finished product. These aspects, we believe, are what we as concrete and structural people can focus on, in order to contribute towards the aim of reducing GHG emissions. The following paragraphs include brief identification of such aspects.

# 1. Creation of Durable Concrete:

The Romans used all natural cementitious materials to build concrete roads, concrete water aqueducts, amphitheatres, temples and bridges. Many of their structures are still used till this day for very much the same purpose (Herring and Miller, 2002). The Roman Empire stretched over many climates, yet their concrete was durable. It withstood freezing and thawing cycles as well as alkali-aggregate reactions. It was not high-strength concrete, but it certainly was, and still is, high performance concrete.

Building with durable concrete means not to have to rebuild again and not to need more cement. This is apart from the savings made on repair and all the indirect sources of CO<sub>2</sub> emission that result from employing such activities. But may be we need to go a bit further in being inspired by the ancient Romans. One of the reasons for their concrete to last such a very long time is that it did not contain steel reinforcing rods. Another reason is the fact that they often used small pre-cast elements, sometimes with crude shape and sometimes with perfectly molded shapes and sizes. Such practice created concrete that did not crack due to temperature and humidity changes. Had they used steel bar reinforcement, they would have had to

increase the strength of their concrete and reduce its permeability. They would have employed large elements, and eventually would have got similar problems to what we have today.

# *The questions here are:*

Are we ready to rethink about some of our practices that have been taken for granted? Can we re-invent concrete practices such that we depend more on small, lightweight and un-reinforced elements? These authors believe we can, provided that people in three related institutions work consciously together towards this purpose. These are the architects, the structural engineers and the academics.

But, even if we did not introduce such drastic change, we need to look at our practices and its consequences which are detrimental to durability.

Several good ready-mix concrete firms suffer from the common problem of variability of results. The first author happened to assist researching this problem and found out a great deal of reliance on concrete-mystery thinking. That is, the consideration that the concrete will somehow be fine no matter what. Day to day variation in grading, moisture content and type of aggregate affect workability which often gets treated by an operator's quick decision, often increasing the water content, thus obstructing its durability characteristics.

Steel reinforcement is another major area where attention must be given. In particular, attention should be given to the detailing. The congestion of bars and the availability of adequate cover are extremely important aspects that cannot be ignored. Detailing must not be left to the site foreman to sort it out. Such a practice often leads to very little or absolutely no cover. The result would be accelerated deterioration and often great repair cost or even demolition and rebuilding.

# 2. Using Less Cement:

In 1980, Bryant Mather published an article in Concrete International titled "Use Less Cement" (Mather, 1980). In which he warned against the effects of too much cement in mass concrete that can cause thermal stresses. In 2000, he published another article under the same title. In the latter, Mather pointed out the fact that even in sections like pavements and bridge decks, too much cement content causes increased cracking due to shrinkage and thermal effects (Mather, 2000). He further demonstrated that if strength was not required for load carrying capacity, then other problems of durability may be addressed by different means suitable for the particular durability issue.

The idea that strength will cover all possible issues and faults is a mistaken one. A student of the first author once requested a 32 MPa concrete for a research that needed a large pour and when the results came out he discovered that the concrete was a 55 MPa grade. The student was advised to repeat the test with 32 MPa only. When the student informed the 'reputable' contractor of the results, the contractor was proud of the fact that he usually gets much more than the target. Some

contractors find it easier and cheaper to give much higher strengths than to be dragged into disputes later on. No wonder we have cracks in the concrete.

# 3. Replacing a Small or Large Portion of Cement with other Supplementary Cementitious Materials:

Nowadays, there are several powdery materials that fit into this category. To limit the scope of this paper, we will focus on three materials that have gained a great deal of popularity in recent years. These are: condensed silica fume, fly ash and ground granulated blast furnace slag.

Without going into great details about the properties and characteristics of these materials, we will briefly highlight certain points regarding each.

**Condensed Silica Fume:** Silica fume is a byproduct of the reduction of high-purity quartz with coal in electric furnaces in the production of silicon and ferrosilicon alloys. Silica fume consists of very fine particles with a surface area in the order of 20,000 m<sup>2</sup>/kg. On average its particles are approximately 100 times smaller than cement particles. Its extreme fineness and high silica content make it a highly effective pozzolanic material (ACI, 1987; Luther, 1990).

It is true that silica fume significantly improves a number of properties in concrete. The main reason why it does this lies in two main facts. Firstly, its extremely fine size, and secondly, its pozzolanic activity. As to the first fact, the very fine size makes it possible for the particles of silica fume to adhere to the surfaces of aggregates far easier than cement particles. This results in filling up of the weakest part of concrete which is the interfacial zone. Moreover, it efficiently reduces or eliminates bleeding. Thus, it reduces porosity, especially around aggregates. Therefore, its use improves durability. The pozzolanic activity adds the benefit that the particles of silica fume react with the calcium hydroxide product of hydration to form calcium silicate hydrates. Thus adding to the strength of concrete especially in the zones where the concrete is weakest at the paste/aggregate interface.

Nevertheless, the use of silica fume should not exceed 10% of cement mass. Otherwise such use becomes counterproductive. Also the quantity of silica fume, if used, should not be less than 5% of the cement mass otherwise it becomes an inefficient, though expensive material. Therefore, the benefits reaped out of silica fume are in fact very much related to the presence of the aggregates. This conclusion has been confirmed when neat paste was subjected to testing with and without silica fume replacement (Scrivener, Bentur et al., 1988). If less than 5% is used, there would not be enough particles of the silica fume to cover the aggregates. If more than 10% is used, the pozzolanic reaction of silica fume would hinder the normal long term Portland cement hydration development due to the early pozzolanic reaction of silica fume that creates a barrier between the 'still not totally hydrated' cement particles (Hooton, 1993).

At the same time, the use of silica fume nearly always necessitates the use of superplasticizer. This is because silica fume causes a large demand for water due to

its large surface area. The superplasticizer effect was found to be enhanced by the silica fume inclusion to the extent that no additional water is needed and therefore, the workability is maintained at the same level of w/c ratio with and without the silica fume (Ollivier, Carles-Gibergues et al., 1988).

Silica fume causes acceleration in the hydration process. This may result in increasing the heat produced (Roy 1987). The acceleration in hydration is further enhanced if there is a combination of silica fume and GGBFS (Larbi, Fraay et al., 1990).

It is seen from this very brief presentation of silica fume, that its use can be enormously beneficial from the point of view of creating a durable concrete that possesses very low permeability. Yet, it is very important to note the limitations whereby such use should be constrained. Otherwise, this use in itself may produce negative effects.

**Fly Ash:** This is a by-product of the coal fired power industry. The classification of fly ash as being type F or type C depends upon the source of the coal. Generally type F comes from bituminous coal and contains high amount of silica. Type C fly ash is generally derived from sub-bituminous coal and lignite. Type C is usually rich with lime. Type F fly ash is the one that is most commonly used in concrete and is known to possess pozzolanic properties.

So far fly ash has been largely considered as a waste product. However, the attitude towards fly ash has shifted quite significantly from considering it a waste material toward considering it as a valuable asset. The reasons behind this important shift are greatly due to continuous research in the area of using this material as a cement replacement.

It has been proven that fly ash can improve workability and durability. Moreover, because of the improved workability, a lower water demand results in enhancing strength while using less cement and thus producing lower heat at hydration. The volume of research conducted on fly ash and its effects is enormous. It is also not free from contradictions and controversy. Yet, the overall picture that emerges is a positive one. Because of the increasingly positive image that emerges from the advantages of using fly ash, we can understand the push to use as much as possible of it. This trend has produced what is now called 'high volume fly ash replacement'. There is no doubt that if we can substitute cement by large amount of fly ash, we can achieve several environmental benefits. Obviously, one benefit is getting rid of the accumulating fly ash that can be a hazard if inhaled or if it contaminates the water table.

Investigations into the use of high volume class F fly ash together with low portland cement content have produced favorable results as far as strength and durability are concerned (Langley, Carette et al., 1989; Poon, Lam et al., 2000). Malhotra has shown that up to 60% of the cement can be replaced by fly ash of class F or C and still give excellent strength and durability results (Malhotra, 1994). It has been reported that high volume fly ash concrete showed exceptionally low permeability

to water and chloride ions (Mehta, 1999). Ravina clearly illustrated that concretes with fly ash as partial replacement of sand have had higher compressive strength and modulus of elasticity than plain concretes without fly ash even when the portland cement content was 15% less than that of the concrete that contained fly ash. He related the effects to the densification and microstructural modification of the hardened cement paste (Ravina, 1998).

These research works are no doubt correct and very well conducted. However, we should not be tempted to choose their results out of context. We must not forget that a great deal of research occurs in ideal conditions of mixing, compaction and above all curing. This is absolutely understandable since we often want to scientifically study, analyse and compare several parameters. The problem is that in practice, things often happen quite differently. Curing is seldom done as desired, let alone being continued beyond 7 days. Research results on the effects of variation of temperature and humidity conditions during the initial curing period abound. They point to important differences in the behavior of fly ash concrete between real and lab work.

The problem associated with fly ash is mainly due to its slow pozzolanic activity between the calcium hydroxide produced from the hydration of portland cement and alkali soluble silicates or "glass" content of fly ash (Owens, 1979). At normal temperatures, the pozzolanic reaction is slow and no significant changes are observed after the initiation of hydration. To achieve the desired concrete properties studies (Al-Amoudi, Rasheeduzzafar et al, 1991) indicated prolonged moist curing to ensure adequate early strength development. However, some researchers (Haque, 1998) recommend initial curing of 7-days as a condition for the concrete blended with supplementary cementitious materials. While this recommendation is correct for commonly practiced concrete production including relatively low amounts of fly ash, it is wrong to try to extrapolate such recommendation to 'unusual' concrete with high volume fly ash content.

We have very recently obtained results of an extensive research conducted on high volume fly ash replacement concrete, which was cured under conditions that resemble realistic circumstances in the Middle East. These results point to the necessity of paying great deal of attention to the importance of prolonged curing if high volume fly ash is contemplated. If, we take only half of the fact about the good effects of high volume fly ash replacement, we may easily end up with concrete with high permeability where its steel reinforcement would corrode in a very short period. Publications of these results, which will appear soon, will show that chloride penetration in concrete that contains more than 50% fly ash replacement is very significant. In places where chloride contamination is expected, we need to be very cautious. This does not mean in any way that we should not go for high volume fly ash substitution. What we are stating is that when we do this, we must give a special treatment to this concrete especially in the processes of compaction and curing. So, in relation to our topic of sustainability, we realize that the important issues are:

- 1. To use as little as possible of cement.
- To use as much as possible of fly ash instead of cement and where possible, instead of sand.
- 3. To still be able to produce concrete that is durable for the design life of the structure.

In effect, these are the issues that are most crucial in the sustainability quest of concrete production.

The only way to realize an optimization of these issues is through knowledge of the limitations of the material and the influences of local practices and the only way of applying such knowledge is through engineers on the job who have been very well trained and have become very much aware of the necessity f accommodating the particularities of the materials and working and environmental conditions.

GGBFS: Ground Granulated Blast Furnace Slag (GGBFS or BFS) is a by product of the steel industry. The BFS is a latent hydraulic material which has chemical composition intermediate between that of pozzolanic material and Portland cement. The BFS acts as hydraulic cement when mixed with water in the presence of OPC. BFS is being used in the construction of dams and massive projects because of its low heat of hydration. Wet Sleddale Dam in Cumbria was constructed with 70% replacement of cement by BFS in the year 1966. After 35 years of exposure to acidic environment, the dam continues to perform extremely satisfactorily (Connell, 1998). BFS was also used in the marine project in the construction of the causeway linking the two nations of Saudi Arabia and Bahrain with 72% replacement of cement by BFS and it has been performing satisfactorily (Ingerslev, 1989).

Again, studies abound when it comes to the effects of BFS replacing cement. There is no doubt that great benefits can be reaped as far as the quality of the concrete when BFS is used. This is apart from the obvious benefits that result from using less cement. And again, the importance of giving due consideration to the particularities of the place, the structure, work force abilities and the environment can not be too much emphasized.

#### 4. Replacements to Natural Aggregates:

The bulk constituent of concrete is that of the aggregates. The concrete industry, in general, does not show a great deal of concern regarding the availability of aggregates. Yet, studies in various parts of the world have started to appear and point to the increasing scarcity of the material (Vagt,1995; Anon, 2003). Added to this, much of the landscape in developed and developing countries is being scarred as a result of quarrying for aggregates.

In Kuwait, natural aggregates are of excellent quality, yet in 1984 a study has warned of their eminent depletion (Kayyali, 1984). Nevertheless, concrete structures in the Gulf region that were constructed using excellent aggregates did not escape a rapid deterioration. It can be foreseen that when countries like Kuwait and

her neighbours, which witness today an unprecedented phenomenon in building boom, experience shortages in good quality aggregates, inferior material will be used instead. Added to this is the rush for completion due to various reasons, we can expect the deterioration phenomenon to manifest on a very large scale. Repairs and reconstruction mean further consumption of raw materials, further consumption of cement and further emission of green house gases.

It is thus understandable that a comprehensive treatment of the issue of concrete materials must include protection from deterioration. This also means that the aggregates which make up the bulk of concrete must be of good quality.

There has been quite a strong movement towards using alternatives for natural materials, and rightly so. Recycled crushed concrete, crushed bricks and blocks, bottom ash, blast furnace slag, and a large range of natural and artificial lightweight aggregates are now available. In the context of our discussion here, such alternatives should be assessed according to the situation at hand. Nevertheless, researchers still need to evaluate the durability performance of each type of aggregates so as to provide the industry with the necessary information that help in making decisions concerning materials use.

#### 5. The New Concretes:

Several new innovative concrete related products have appeared quite recently. Some of these products are already sustainability-oriented. Some other products, though have not been invented with sustainability as criterion, do have a positive impact on sustainability. Also there are some products that were invented with the aim of producing ultra high strength concrete. These solve many problems in construction and add a wealth to architectural possibilities. Nevertheless all such products need to be carefully evaluated from the sustainability view point.

In the following paragraphs, we will try to summarise recent developments in this regard.

Reactive powder concrete: Though the idea was not totally new, Richard and Cheyrezy were able in 1995 to present a fully structured and cohesive description of Reactive Powder Concrete as completely new breakthrough in concrete production (Richard and Cheyrezy, 1995). This concrete describes a family of ultra high strength concretes that range in compressive strength from 170 MPa to more than 800 MPa. The flexural strength ranges from 30 to 140 MPa. Briefly, these concretes depend upon elimination of the skeletal structure of concrete that comprises the large aggregates and sand. Instead, they employ extra fine sand and crushed quartz together with silica fume and super plasticizer. This technology makes it possible for the fine constituents to fill as much as possible in the available space without being bound and hindered by a skeletal structure that contains pores which can never be filled. The making of such concrete may also involve application of pressure and or heat. Furthermore, the incorporation of fine steel fibres may be utilized to further enhance ductility.

It is evident that such concrete can revolutionize the concrete building industry. Without trying to be exclusive, this concrete would produce much smaller sections, eliminate steel reinforcement, enhance durability and may end up costing less in spite of its high initial cost. Obviously, concrete of this sort lends itself more readily to the processes of pre-casting.

Elimination of steel bar reinforcement and utilizing pre-casting procedures would no doubt significantly reduce deterioration problems mainly due to corrosion of reinforcement and the strict methods of production. Using thinner sections and lighter construction results in less cement needed, lower dead loads, shallower foundations, larger usable spaces and more elegant structures. Elimination of large aggregates solves aggregate shortage problems in many locations. All these effects are positive from the point of sustainability.

The production and use of this type of concrete in the Gulf region can definitely be a viable option. We are not concluding that it should be the only option. But, we strongly believe that the initial high cost of producing this concrete would be more than compensated by having a durable construction in this fast growing part of the world.

**Geopolymers:** It seems that we owe a great deal of our cement and concrete heritage today to ancient Romans (Herring and Miller, 2002) and even to earlier people in Mesopotamia (Roy, 1999). Not only did they discover pozzolanic materials but also they found the way to activate it simply by mixing it with slaked lime (Herring and Miller 2002). Doing so, they actually produced concrete with extraordinary excellent durability. At present, we are revisiting their work and reinventing it.

Geopolymers is a commonly used name for alkali-activated cements. Simply, it has been found that the addition of alkalis like calcium hydroxide, sodium hydroxide or potassium hydroxide to fly ash activates the material accelerating the pozzolanic reaction. The result is an amorphous aluminosilicate gel where the structure has the ability to absorb and lock potentially deleterious ions (Quanlin and Naiqian, 2005) and also can resist volume changes (Palomo, Grutzeck et al., 1999).

We have here only very lightly touched on the subject of geopolymers. However, in the context of this paper, it suffices to say that fly ash when activated in this manner can produce a hardened paste that possesses mechanical strength of nearly 60 MPa. It is only sufficient to remember that fly ash production is around 800 Mt per year (Fernandez-Jimenez and Palomo, 2005). Development of this sort has the potential of: (a) providing a large consumption outlet for fly ash. (b) making concrete from less and less cement; and (c) producing much more durable concrete.

Having stated that, it is not a matter of simply bringing materials and mixing them together to produce the desired results. We need to combine experimentation, chemical knowledge, further research into crystalline formations and developments resulting from such activation, long-term research into possible effects of variation in temperature and humidity on durability, volume changes and mechanical

properties. But very importantly, engineers and researchers need to be aware of the problems that a concrete structure is likely to face in order that the solution offered meets the required performance.

Concrete-Polymer-Composites: Advances in polymer development and uses are immense. It has been forecast that within 15 years, polymers in construction will be the most important element in polymer production and market (Van Gemert, Czarnecki et al., 2005). This is however, a typical case of the need for the cooperation and thorough understanding of the situation in which such materials may be used. Knowledge of the properties and differences between various types of material is necessary before employing materials of this sort. Promises of the marketing agencies are not enough and cannot replace scientific understanding of the properties and their suitability for the situation at hand. A wise use of these composites has the potential of saving substantial cost to the industry and the nation. This is because these materials can protect from serious deterioration and thus are invaluable in the quest for sustainable construction industry.

Other Developments and Materials: In the following paragraph, we will attempt to very briefly describe some other developments that are promising as far as sustainability is concerned.

Self Compacting Concrete - This is a new generation in the concrete family. The importance of producing very low w/c paste with self compaction property has been presented since the superplasticizers made the pronounced impact on the concrete industry (Diamond and Gomez-Toledo, 1978). The technology has taken off more significantly in the 90's and is now becoming a very popular method (Persson, 2001). Briefly, the technology employs the use of fillers and potent superplasticizers as in the case of high performance concretes. But in addition, it uses specifically viscosity enhancing admixtures and may use air entraining agents as well. The resulting concrete is that which flows freely and needs no compaction. It can be easily appreciated that such concrete is an excellent solution for modern high rise buildings that need pumping the concrete during construction. Moreover, due to the dispensability of compaction, cost savings and noise elimination has been a substantial gain economically and environmentally. This technique has also produced uniformity of concrete elements in addition to excellent durability. This development therefore is rightly considered a valuable contribution to sustainable industry. It has also given rise to enhance the synergetic research in what has been called "smart admixtures" which produce the desired behaviour in the composite material.

New Generation of Lightweight Aggregates - Very recently manufacturing lightweight aggregates from fly ash has gained another step forward in the development of aggregates that possess excellent adhering properties with the paste matrix. This aggregate, produced concrete of high performance which exceeded that of granite concrete of equal amount of cement (Kayali, 2005). This has dispelled the previously held belief that connects strength to high density. It can be realized that advances in this respect are quite promising in getting rid of fly ash accumulation while producing lighter, stronger and more durable structures.

#### **Conclusions**

- 1. Durability of concrete is one of the most important factors, if not the most important, in the attempt to arrive to sustainable stage in concrete construction.
- 2. Cement manufacture is a major contributor to the greenhouse gases. Efforts should be directed to reduce the need for this manufacture.
- 3. Alternative materials that may replace cement include industrial by-products like silica fume, fly ash and blast furnace slag. All of these carry enormous benefit to the concrete industry in general and sustainability in particular.
- 4. Extracting natural aggregates for the concrete industry cannot be sustainable in the long run. Recycling aggregates, crushed bricks, crushed blocks, crushed concrete and lightweight aggregates made from waste products are alternatives that should be given due importance.
- 5. New polymer materials that serve to create concrete polymer composites carry the promise to become major building materials in the future. Such materials provide solutions to durability issues especially when used in repair and pre-cast industries. Though they may be expensive, their use may prove one good solution to the issue of sustainable building.
- 6. Looking beyond the current culture in concrete should be researched and discussed. This is now possible with the advent of new materials that allow very strong composites to be produced. In view of these new developments, can the tradition of reinforcement be revisited?
- 7. Academics and engineers need to realize the importance of the element of sustainability. Revision to programmes in civil engineering should, in the opinion of these authors, be done to include sustainability as an important part of materials study as well as design.
- 8. The developments in new materials put emphasis on the necessity to deeply understand the functions and limitations of any new suggested material that is being marketed for the use in concrete. This again highlights the need for revisiting civil engineering courses of the structure stream in order to include deeper study and appreciation of the chemical and physical characteristics of materials of construction.

#### References

ACI, A. C. (1987). "Silica Fume in Concrete." ACI Materials Journal 84(March-April): 158-166.

Aitcin, P.C. (2000). "Cements of yesterday and today: Concrete of tomorrow." Cement and Concrete Research 30(9): 1349-1359.

Al-Amoudi, O. S. B., Rasheeduzzafar, et al. (1991). "A Reply to a Discussion by M.N. Haque and O.A. Kayyali of the Paper "Carbonation and Corrosion of Rebars in Salt Contaminated OPC/PFA Concrete"." Cement and Concrete Research 21(5): 956-957.

Anon (1997). "Co<sup>2</sup> emissions from cement manufacture have been undersetimated." Applied Catalysis B: Environmental 13(2): N12-N13.

Anon (2003). World construction aggregates. T. F. Group.

Anon (2006). Dh1.5 billion cement plant to be set up. Khaleej Times. Dubai.

- Choate, W. T. (2003). Energy and Emission Reduction Opportunities for the Cement Industry. U. S. D. Energy. Columbia.
- Connell, M. (1998). "The Long-Term Performance of High Slag Concrete." Concrete 32(6): 30-31.
- Diamond, S. and C. Gomez-Toledo (1978). "Consistency, setting, and strength gain characteristics of a "low porosity" Portland cement paste." Cement and Concrete Research 8(5): 613-621.
- ECOSECURITIES (2005). Global Climate Change: Risk to Bank Loans. New York, ECO Securities-United Nations Environment Programme Finance Initiative: 80 pp.
- Fernandez-Jimenez, A. and A. Palomo (2005). "Composition and microstructure of alkali activated fly ash binder: Effect of the activator." Cement and Concrete Research 35(10): 1984-1992.
- Gartner, E. (2004). "Industrially interesting approaches to "low-CO<sup>2</sup>" cements." Cement and Concrete Research
- H. F. W. Taylor Commemorative Issue 34(9): 1489-1498.
- Haque, M. N. (1998). "Give it a Week 7 days Initial Curing." Concrete International 20(9): 45-48.
- Hendriks, C. A., E. Worrell, et al. (1998). Emission reduction of greenhouse gases from cement industry. 4th International Conference on Greenhouse gas control technologies, Interlaken, Austria, IEA GHG R&D Programme, UK.
- Herring, B. and S. Miller (2002). "The Secrets of Roman Concrete." Constructor (September): 13-16.
- Holdren, J. P. (2003). U.S. Climate Policy Post Kyoto. The Convergence of U.S. National Security and the Global Environment, The Aspen Institute Congressional Program.
- Hooton, R. D. (1993). "Influence of silica fumereplacement of cement on physical properties and resistance to sulphate attack, freezing and thawing, and alkali-silica reactivity." ACI Materials Journal 90(2): 143-151.
- Ingerslev, L. C. F. (1989). "Precast Concrete for the Bahrain Causeway." Concrete International 11(12): 15-20.
- Kayali, O. (2005). lightweight fly ash aggregates for high strength concrete. Innovation and Sustainability of Structures in Civil Engineering, Nanjing, China, South East University.
- Kayyali, O. A. (1984). "Study of Aggregates used for concrete in Kuwait." Trasportation Research Record(989): 26-33.
- Langley, W. S., G. G. Carette, et al. (1989). "Structural concrete incorporating high volumes of ASTM Class F fly ash." ACI Materials Journal (American Concrete Institute) 86(5): 507-514.
- Larbi, J. A., A. L. A. Fraay, et al. (1990). "The chemistry of the pore fluid of silica fume-blended cement systems." Cement & Concrete Research 20(4): 506-516.
- Luther, M. D. (1990). High-performance silica fume (microsilica)- Modified cementitious repair materials. 69th annual meeting of the Transportation Research Board.
- Malhotra, V. M. (1994). CANMET investigations dealing with high-volume fly ash concrete. Advances in Concrete Technology. V. M. Malhotra. Ottawa, Canada, CANMET: 445-482.
- Malhotra, V. M. (1999). Role of Supplementary Cementing Materials in Reducing Greenhouse Gas Emissions. Infrastructure Regeneration and Rehabilitation

- Improving the Quality of Life through Better Construction, A Vision for the Next Millenium, Sheffield, Sheffield Academic Press.
- Mather, B. (1980). "Use Less Cement." Concrete International 2(10): 22-24.
- Mather, B. (2000). "Use Less Cement." Concrete International 22(11): 55-56.
- Mehta, P. K. (1999). "Advancements in concrete technology." Concrete International 21(6): 69-76.
- Menareport (2006). UAE industry entering transitional phase report No. 204326, Albawaba Media and Technology Group.
- Ollivier, J. P., A. Carles-Gibergues, et al. (1988). "Activite' pozzolanique et actionde remplissage d'une fumee de silica dans les matrices de beton de haute resistance." Cement & Concrete Research 18(3): 438-448.
- Owens, P. L. (1979). "Fly ash and its usage in Concrete." Concrete 13(7): 21-26.
- Palomo, A., M. W. Grutzeck, et al. (1999). "Alkali-activated fly ashes: A cement for the future." Cement and Concrete Research 29(8): 1323-1329.
- Persson, B. (2001). "A comparison between mechanical properties of self-compacting concrete and the corresponding properties of normal concrete." Cement and Concrete Research 31(2): 193-198.
- Poon, C. S., L. Lam, et al. (2000). "Study on high strength concrete prepared with large volumes of low calcium fly ash." Cement and Concrete Research 30(3): 447-455.
- Quanlin, N. and F. Naiqian (2005). "Effect of modified zeolite on the expansion of alkaline silica reaction." Cement and Concrete Research 35(9): 1784-1788.
- Ravina, D. (1998). "Mechanical properties of structural concrete incorporating a high volume of class F fly ash as partial fine sand replacement." Materials and Structures 31(3): 84-90.
- Richard, P. and M. Cheyrezy (1995). "Composition of Reactive Powder Concrete." Cement and Concrete Research 25(7): 1501-1511.
- Roy, D. M. (1987). Hydration of blended cements containing slag, fly ash, or silica fume. Meeting of Institute of Concrete Technology, Coventry, UK.
- Roy, D. M. (1999). "Alkali-activated cements Opportunities and challenges." Cement and Concrete Research 29(2): 249-254.
- Scheubel, B. and W. Nachtwey (1997). Development of Cement Technology and its Influence on the Refractory Kiln Lining. Refra Kolloquium, Berlin.
- Scrivener, K. L., A. Bentur, et al. (1988). "Quantitative characterization of the transition zone in high strength concretes." Advances in Cement Research 1(4): 230-237.
- StrategicIndustryLeaders (2006). Punching Above Its Weight. Canberra, Department of Industry, Tourism and Resources.
- TAIB (2006). GCC Equity Research, Fujairah Cement Industries Co.
- The United Kingdom Parliament (2002). Supplementary Memorandum by the British Cement Association. Minutes of Evidence. S. C. o. S. a. Technology. London.
- Vagt, O. (1995). Mineral Aggregates. Canadian Minerals Yearbook, 1995. C. M. Yearbook: 14 pp.
- Van Gemert, D., L. Czarnecki, et al. (2005). "Cement concrete and concrete-polymer composites: Two merging worlds: A report from 11th ICPIC Congress in Berlin, 2004." Cement and Concrete Composites 27(9-10): 926-933.

# Use of Limestone's Filler to Improve the Quality of Algerian Concretes and Cement Paste

Z. Guemmadi, University of Constantine, Algeria
G. Escadeillas, LMDC INSA-UPS Toulouse, France
B. Toumi, University of Ouem El Bouaghi, Algeria
H. Houari, University of Constantine, Algeria

#### Abstract

In Algeria, more than thousand aggregate crushing stations produce annually about 68 million tons of aggregates, essentially of calcareous nature. Unfortunately, more than 20% of the manufactured sands are unsuitable for use as construction sands because of their high fines content that largely exceed the current standard maximum limit of 12%. Similarly, the limestone fillers, which also result from the limestone rocks crushing process, are regarded as inadequate residues and hence unexploited.

To improve the situation, it is important to improve all the aggregates and sands with a high filler content and more particularly sands and the limestone fillers itself. This has a favourable effect not only on the economy of the country but also the environment.

This paper shows the influence of the characteristics of Algerian limestone fine (proportioning, fineness) on the physical properties, the mechanical performance and durability of cement pastes made with different water to binder ratios. Obtained results show that the replacement of part of cement by these limestone fillers can significantly improve the mechanical resistance, the workability, as well as the durability. This study also shows that the limestone fillers not only have a physical effect but also an improved chemical activity by producing new hydrated compounds such as the carboaluminates.

**Key Words:** Limestone fillers, Cement paste, Fineness, Mechanical resistance, Carboaluminate

#### Introduction

The production of building materials is typically accompanied by formation of secondary products (limestone fillers) or waste which has a direct impact on the environment and affects the quality of sands. The best way of minimizing their impact on the environment is finding a means to reuse the secondary product in a beneficial way.

The term 'fillers' refers to rock particles (added to a binder) obtained by fine milling or crushing. In certain countries, limestone additions have been used for decades as partial cement replacement. Limestone fillers are generally added directly at the cement production plant. Research on the influence of limestone additions on the properties of hydrated cement-based materials indicates that their action is primarily physical in nature (Hewlett, 1997). However, evidence of reaction with the aluminates-bearing phases usually found in cement systems has been reported (Neville, 1996). Calcite fines have also been used as a replacement for gypsum in Portland cement (EN 197-1, 2000). It has been shown that limestone additions can accelerate the hydration of the calcium silicate components of cement (Voglis et al., 2005).

The use of limestone fines results in products that have acceptable mechanical properties (Hewlett, 1997, Vuk T et al. 2001). These additions also have beneficial rheological effects (Hewlett, 1997). The positive effects of limestone addition can explain why regulations worldwide have permitted its addition to cement. However, depending on the country, the amount permitted varies from 0% to 35%. Debate on acceptable amounts of limestone addition to cement continues. The wide variety of practical cases of contact where concrete structures are directly in contact with chemically aggressive salt solutions and the expensive maintenance and repair of damaged structures account for the global interest in the durability of cement-based materials.

In the Western countries (in France, for example, the law of July 13, 1992 relating to the waste disposal and environmental protection), the disposal of solid wastes, such as rubble, in refuse tips are strictly illegal. In Algeria, more than 20% of the manufactured sand in more than thousand plants that produce annually a total of 68 million tons of aggregate is not suitable for use as construction sand because of its fines content being higher than 12% (current normative limit). In the same way, limestone fillers, resulting from the process of crushing limestone rocks, are regarded as unusable residues and thus not exploited.

In civil engineering, the promotion of rejected quarry materials makes it not only possible to contribute to protecting the environment, but it also constitutes an attractive field of research about general execution of the solid waste treatments and the development of more economic hydraulic binders. To increase the production of cements with mineral additions (other than traditional additions of fly-ash, silica fume, slag....) several investigations were carried out throughout the world in order to develop the use of the limestone fines (EN 197-1, 2000).

The various results show that the limestone fillers added to cement can have several roles:

- A filling role by correcting the size distribution of the fine elements of cement (Escadeillas, 1986).
- A rheological role by their capacity fluxing on the interstitial paste (Voglis et al., 2005, Guemmadi, 2002, Escadeillas, 1986).
- A chemical and physical role by increasing compressive strength and improvement of durability (Guemmadi, 2002).
- A chemical and physical role by formation of carboaluminates, germs that fix the hydrate (Hewlett, 1997, Guemmadi, 2002, Escadeillas, 1986).

The development of Portland-composite cements, using traditional and up-to-date mineral additions, is considered the state of art in cement production. The initial aim was the reduction of cost but further objectives have been added, such as the improvement of performance, the energy saving, the use of conventional raw material or industrial by-products and the ecological benefits (Hewlett et al., 1997, EN 197-1, 2000) and to have many benefits, both technical and economical (Hewlett et al., 1997, Voglis, et al.; 2005).

The European Standard EN 197-1 identifies four types of Portland-limestone cement containing 6–20% limestone (types II/A-L and II/A-LL) and 21–35% limestone (types II/B-L and II/B-LL), respectively (Voglis, et al.; 2005).

The use of Portland-limestone cements seems to have many benefits, both technical and economical (Neville; 1996, Tsivilis S et al., 2002, Ramachandran, 1988). It is expected that the future world production of Portland-limestone cement will be continuously increased. The wide use of limestone cement requires a thorough knowledge of the cement and concrete properties.

As far as the limestone cement is concerned, the research work is focused on three areas: The first one is the effect of limestone on the cement performance (Ramachandran, 1988, Ciach et al., 1971). The second one deals with the participation of limestone in the hydration reactions of clinker (Helmuth, 1980, Guemmadi et al., 2002), while the third one is the production process and specifically the intergrading of clinker and limestone (Guemmadi, 2002). Although there is a disagreement on specific issues, the knowledge level is satisfactory and continuously extended. It is thus essential to know the effects of the limestone fillers according to their contents and their smoothness on the cementing matrices and specifically on the hydraulic cement pastes.

Thus, the objectives of this research are:

- To present and examine the main part of the rheological and mechanical performances of cement pastes comprising Algeria limestone fillers in function the rate and finenesses.
- 2. To determine the optimum substitution rate of cement by limestone fillers.
- 3. To determinate the evolution of porosity by mean of mercury porosimeter.

# **Experimental Program**

**Principle of the study:** The objective of the study consists of making various cement pastes starting from cement CPA-CEM I and then substitute a part of this cement by limestone fillers having various finenesses. The parameters of study are:

- Content of fines: 0%, 5%, 10%, 15%, 20%, 25%, 30% and 40% (substitutions in mass).
- Fineness of fines: F5, F10, F15 and F29 respectively with the fillers diameter of 15 μm, 10 μm, 15 μm and 29 μm.
- Water to binder ratio: 0.24, 0.26 and 0.28

#### **Materials Used**

**Cement:** Cement used is CPA-CEMI. It comes from the cement factory of Tebessa. The clinker shows good chemical and mineralogical characteristics. The laser grading analysis reveals a distribution of the various particle-size ranges of grains between 1 and 100 m, a median diameter of 8 m and a specific area of 2900 cm²/g (use m²/kg or mm²/kg as per SI standards). The X-rays diffractogram of anhydrous cement is shown in Fig. 1. The chemical, mineralogical composition and characteristics of cement used are presented in Tables 1 and 2

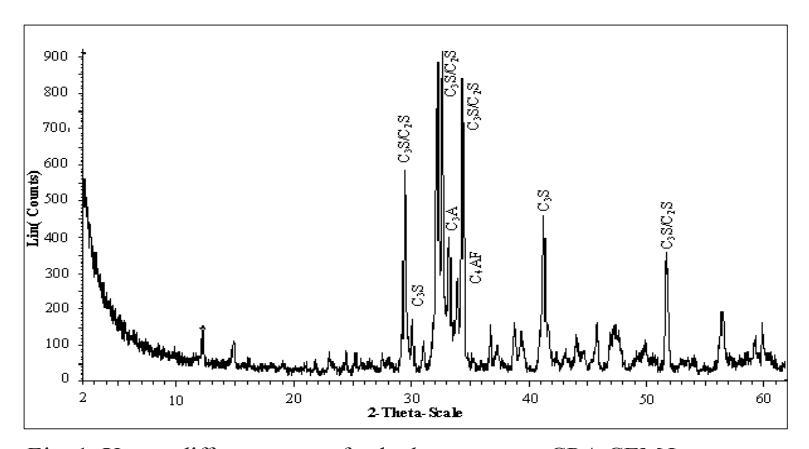


Fig. 1. X-rays diffractogram of anhydrous cement CPA-CEM I.

Table 1. Chemical and Mineralogical Analysis of Cement, %

	Chemical composition									
SiO <sub>2</sub> Fe <sub>2</sub> O <sub>3</sub> Al <sub>2</sub> O <sub>3</sub> CaO MgO SO <sub>3</sub> Cl Na <sub>2</sub> O PF										
20.01	2.97	4.65	64.01	0.62	2.15	0.015	0.24	4.34		
	Mineralogical composition									
(	$C_3S$ $C_2S$				C <sub>3</sub> A C <sub>4</sub> A			F		
61.3 15.9			8.0		9.6					

**Table 2. Cement Characteristics** 

Characteristic	Units	Type of cement CPA (CEMI)
Apparent bulk density	$kg/m^3$	1100
Absolute density	$kg/m^3$	3100
Normal consistency	%	25
Beginning of setting	h and min	2 h 15 min
End of setting	h and min	3 h 15 min
Shrinkage at 28 days	μm / m	810

**Filler:** The fillers come from the giant carrier E.N.G (national enterprise of aggregate). They are of limestone nature having a higher content of CaCO<sub>3</sub> of 98% (analysis by XRD Fig. 2). The filler F5, F10, F15 and F29 differed mainly by their median diameters which are presented in Table 3. The characteristics of these fillers are gathered in Table 4.

Table 3. Value of Blaine Specific Area and Median Diameters of Fillers

Filler	F5	F10	F15	F29
Specific area (cm <sup>2</sup> /g)	5400	3100	2800	2640
Median diameters (µm)	5	10	15	29
Apparent bulk density (kg/m <sup>3</sup> )	810	870	980	1030
Absolute density (kg/m <sup>3</sup> )	2700	2700	2700	2700

**Table 4. Chemical Compositions of Fillers** 

SiO <sub>2</sub>	Fe <sub>2</sub> O <sub>3</sub>	Al <sub>2</sub> O <sub>3</sub>	CaO	MgO	$SO_3$	NaCl	PF
0.58	0.02	0.06	55.85	0.06	0.07	0.56	43.80

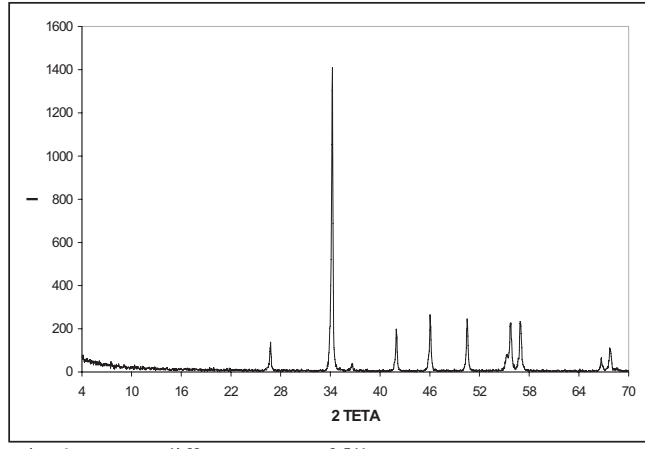


Fig. 2. X-rays diffractogram of filler.

Laser grading of cement and filler is shown in Fig. 3

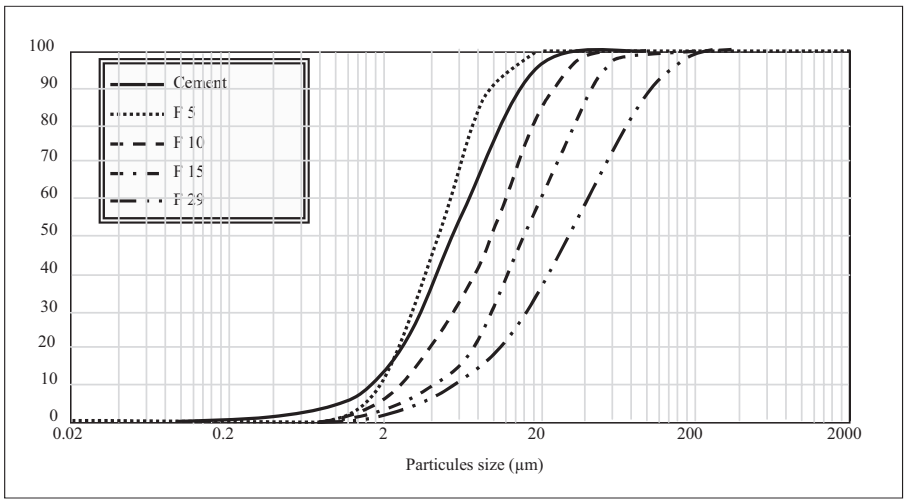


Fig. 3. Laser grading of cement and filler.

**Water:** For the paste mixing, drinking water was used. Its quality is in conformity with the standard regulations (NF P18 404). The results of the chemical analysis of water are shown in Table 5.

Table 5. Chemical Analysis of Water

Ca	Mg	Na	K	Cl	$SO_4$	CO <sub>2</sub>	NO <sub>3</sub>	Insol.	PH
116	36	80	3	140	170	305	5	786	7.9

# Fabrication of Specimen and Methodology of Testing

Production and mixing of the pastes study were carried out according to standard NFP 18-403. The first pastes obtained were used for the determination of normal consistency and the rheological study. Others pastes were carried out for the investigation of the performances of the hardened state. The release from the mould is made after 24h. The test-tubes obtained were preserved in a wet chamber HR=95%  $\pm$  5% and T=20°C until the testing ages of 2, 7, 28, 90 days and 9 months.

The tests were carried out on four series of pastes. Each series corresponds to one of the fillers F5, F10, F15 or F20 added to cement CPA-CEMI to proportions of 0%, 5%, 10%, 15%, 20%, 25%, 30% and 40% and ratios W/C=0.24, 0.26 and 0.28 respectively.

#### Results and Discussions

**Consistency:** The normal consistency of cement CPA-CEMI without addition (Fig. 4) is reached for 25% of water content. For added filler to cement (Fig. 5), one can

observe that up to 15%, limestone fine F5 and F10 play the role of one flux. Beyond this percentage these fines have a thickening effect. Fines F15 and F20 have a weak effect with mean consistency.

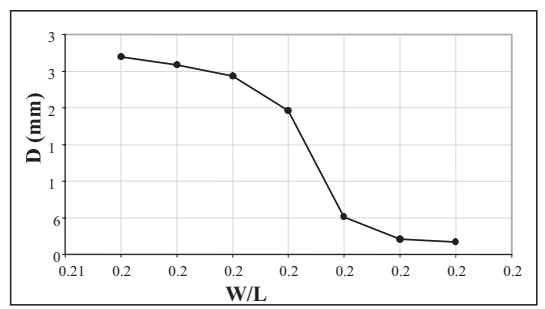


Fig. 4. Consistence of CPA-CEMI cement paste.

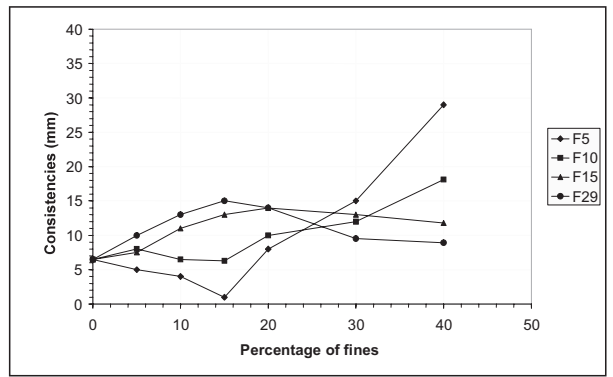


Fig. 5. Consistencies of the cement paste as function of percentage of substitution.

**Setting time:** The influence of substitution rates of limestone fine is weak to mean in the beginning and end of setting times in the interval 0% to 20% (Figs.6 and 7). Beyond this value, fines F15 and F20, the time of beginning and the end of setting rise from 20 to 90 minutes so fillers play a retarding role on the setting time.

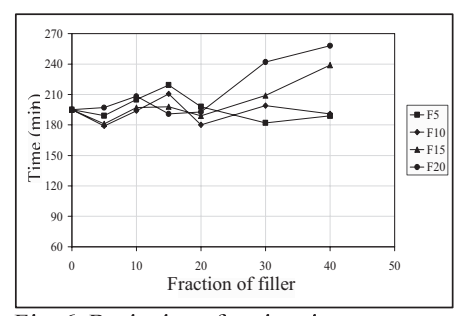


Fig. 6. Beginning of setting time

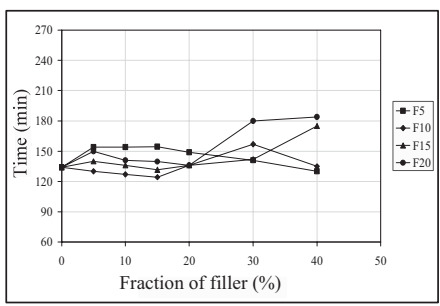


Fig. 7. End of setting time.

**Compressive strength:** The incorporation of fines having high specific area such as the fillers F5 and F10 (Fig. 8) considerably improves the compressive strengths especially for values of substitution of about 15%. Beyond this value, the resistance decreases by about 45% for the fillers F20 to 40% of substitution.

The finest fillers (F5) improve a better resistance in compression. Choosing these type of fillers, the optimal value of 15%, is particularly well highlighted. The increase in resistance can be explained, as shown by x-ray diffraction (Fig. 9), by the formation of the Carboaluminate which appears from the seven days. The formation of monocarboaluminates in the paste with 15% of F5 filler content is very important compared to the paste with F20 filler. The limestone fillers are thus active chemically and their activity influences the mechanical resistances of the binder.

**Tensile strength:** The tensile strength (Fig.10) is affected almost in the same way as compressive strength, except for the fines F5 and F10 for which the increase are more marked.

**Evolution of total porosity:** For the pastes without addition (100% cement), a very tightened porosity was noted in a marked principal peak, between 10 and 100, this peak is reduced by the incorporation of the very fine fillers F5 and F10 at a rate of 15%. So the hardened cement paste with 15% F5 filler seems as dense and homogeneous material which explains the improvement of the mechanical performances. In addition, for the addition of F5 fillers to 40%, several families of pores are observed, which points that this paste is more porous and have porosity coarser than that observed in the paste with 15%.

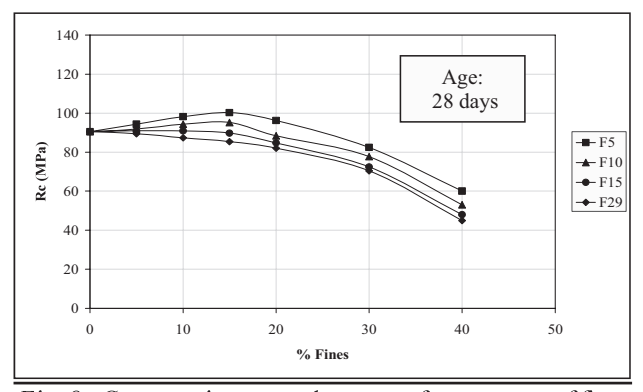


Fig. 8. Compressive strength versus of percentage of fines.

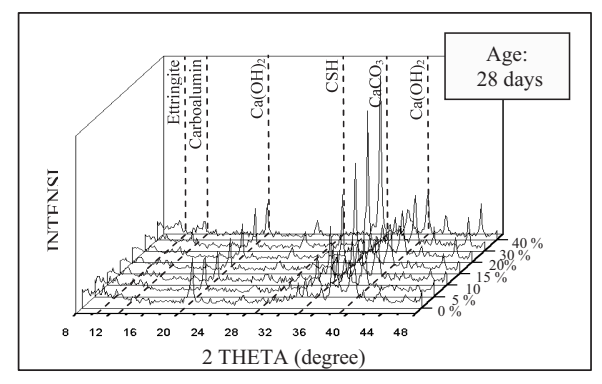


Fig. 9. X-rays diffraction of hardened cement paste.

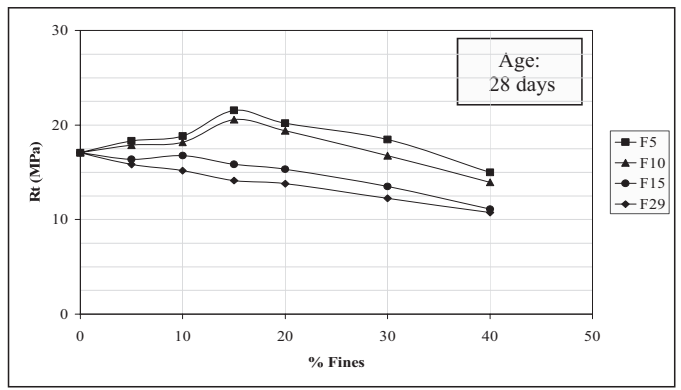


Fig. 10. Tensile strength versus of percentage of fines.

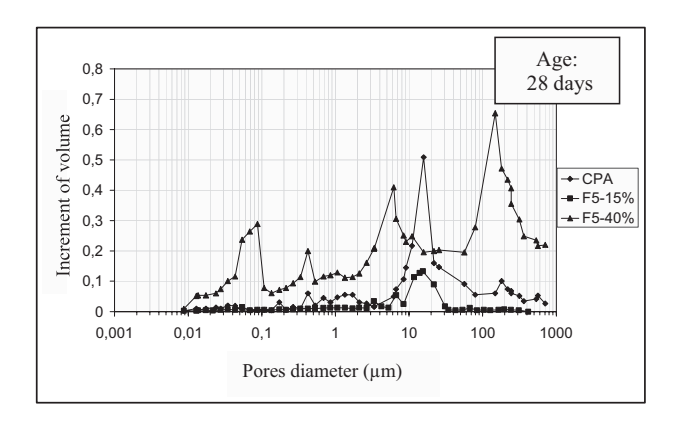


Fig. 11. Distribution of the pores according to the fine rate (F5 Fillers; W/C=0.24).

#### Conclusion

In Algeria, limestone fines resulting from crushing aggregates have for long been considered as unusable residues and one of principal causes of rejection in construction. However, they can have a beneficial role in the matrix cementing.

The various results obtained show well that the limestone fillers can play several roles:

- A filling role by offsetting the cement lack on fine elements in the grading curve.
- A rheological role by their dispersing capacity on the grains of cement which results in reduction in the water content at a constant hardness.
- A chemical and physical role by formation of carboaluminates, crystal nuclei (with acceleration of the hydration).
- The variation of smoothness of the fillers practically does not have a significant influence on the demand for water.
- The influence of the fillers is marked favourably when their content is lower than 25%.
- Porosity of the pastes decrease with the addition of the limestone fillers up to 15% beyond that point an increase is observed either for fine smoothness and W/C ratio.

The present study, confirms that with filler contents of 15%, the mechanical performances of the cement pastes are clearly improved.

The hardness of the cement pastes with this percentage of fine is slightly affected.

The fineness of limestone fine has a considerable role in the improvements of the rheological and mechanical performances of the cement pastes due to the formation the new compounds such as the carboaluminates (Guemmadi, 2002, Escadeillas, 1988).

#### References

- Brown P. W., Franz E., Frohnsdorff G. and Taylor H.F.W. N., "Analysis of the aqueous phase during early C3S hydration". Revue Cement and Concrete Research, V14, pp 257-262. Edition Pergamon 1986.
- Ciach T. D., Gilott J. E., Swenson E. G., Sereda P. J. "Microstructure of Calcium Silicate Hydrates". Revue Cement and Concrete Research No.1, pp13 25. Edition Pergamon, 1971.
- Escadeillas G.: "Les ciments aux fillers calcaires: Contribution a leur optimisation par l'étude des propriétés mécaniques et physiques des bétons fillérisés". Thèse Doctorat de l'Université Paul SABATIER, Toulouse, 1988.
- European Committee for Standardization, Cement: Composition, Specifications and Conformity Criteria, Part 1: Common Cements, EN 197-1, EN/TC51/WG 6 rev., 2000.
- Guemmadi Z., Toumi B. Houari H.: "Behavior of limestone sand based concrete with variable filler content", International Congress Challenges of concrete Construction, pp12, Dundee, Scotland, 5 11 September 2002.

- Guemmadi Z., Toumi B. Houari H: "The Optimal Filler Content Giving the Best Performances of Concrete" Session 1 First International Conference & Fourth Exhibition, pp 32-41, September 29-October 1, Kuwait, 2003.
- Guemmadi Z., Houari H.: Influence de l'ajout de fines calcaires sur les performance des bétons dans l'Est Algérien". Annales du Bâtiment et des Travaux Publics. n° 6. Pp 23-32. 2002.
- Hewlett P. Lea's Chemistry of Cement and Concrete,4th ed. England, John Wiley & Sons: 1997.
- Helmuth R.A., "Structure and Rheology of Fresh Cement paste". Proceedings. International Conference on the Chemistry of Cement V7, pp 6-30. Paris, 1980.
- Negro A.et Stafferi L., "Application du Microscope électronique à balayage à l'étude du ciment et des produits d'hydratation". 2éme Partie : Pâte et mortiers. Revue. Matériaux De Construction, n° 686, pp 112-116. Edition Dunod, 1974.
- Neville M. "Properties of Concrete, 4th & final ed. England, Addison Wesley Longman Limited; 1996.
- Ramachandran VS: "Thermal analysis of cement components hydrated in the presence of calcium carbonate". Thermochim Acta 1988;127:385–94.
- Tsivilis S, Chaniotakis E, Kakali G, Batis G. Portland limestone cements: An analysis of the properties of limestone cements and concrete. Cem Concr Comp 2002; 24:371–8.
- Voglis N., Kakali G., Chaniotakis E., S. Tsivilis., "Portland-limestone cements: their properties and hydration compared to those of other composite cement" Cem Concr Comp27 (2005) 191–196.
- Vuk T, Tinta V, Gabrovek R, Kaucic V. "The effects of limestone addition clinker type and fineness on properties of Portland cement" Cem Concr Res 2001;31(1):135–9.

# Influence of Different Admixtures on the Mechanical Behavior of Two-Stage (Pre-Placed Aggregate) Concrete

Hakim S. Abdelgader\*, Ahmed E. Ben-Zeitun and Abdurrahman A. Elgalhud
\*Al-Fateh University,
P O Box 83038,
Tripoli, Libya.
Email: hakimsa@poczta. onet. pl

#### Abstract

The hypothesis of two-stage concrete is different from conventional concrete because the particle-to-particle contact of coarse aggregate shrinkage is lower than normal concrete. The important aspect of two-stage (pre-placed aggregate) still remains unclear in its strength. Either by experiment or by theory the strength of two-stage (pre-placed aggregate) concrete has been described in different ways. Since no reliable data is available showing the strength of two-stage (pre-placed aggregate) concrete. It is necessary to investigate its strength at different mixes. This paper deals with the effect of different admixture on the mechanical behavior of two-stage (pre-placed aggregate) concrete. This paper presents also the experimental results of pre-placed, crushed aggregate concreted with thirty-sex different grout mixture proportions. A total of 360 concrete cylinders were tested in unconfined compression and splitting tension at 28 days. On the basis of these results a relationship between the tensile strength and the compressive strength of two-stage (pre-placed aggregate) concrete is statistically derived.

#### Introduction

Two-stage (pre-placed aggregate) concrete differs from normal traditional concrete not only in the method of placement but also in it<sup>s</sup> content of a higher proportion of coarse aggregate. It may be regarded as a "skeleton concrete" as the coarse aggregate effectively rests against one another and the remaining void is filled with grout [1]. Because of the initial point-to-point contact of the coarse aggregate, as placed, the modulus of elasticity of two-stage (Pre-placed Aggregate) concrete is very high [2].

While concreting the mass structures (of at least 0. 5 m in size), in the open air and especially under water in places hard to reach (e.g. in zones of great thickness of reinforcement), and where there is enough stone aggregate, it is profitable to apply two-stage concrete. Two-stage (pre-placed aggregate) concrete is also useful in the manufacture of high density concrete for atomic radiation shielding where steel and heavy metallic are used as coarse aggregate [3].

As concrete technology develops, basic grouts composed of only cement, sand and water can be modified to produce structural concrete more effectively. Such grouts may be modified chemically by using suitable admixtures or mechanically by using a specially designed high-speed mixer. But there has been no precise information on the either possibility to modify grout in the manufacture of two-stage (pre-placed aggregate) concrete [4].

According to ACI Committee 304 1R, strength could be increased through the use of high-range water-reducing admixtures, silica fume, and or other admixtures, but neither research nor performance data are available [3].

This paper deals with the effect of different admixture (superplasticiser, expanding admixture and superplasticiser + expanding admixture) on the mechanical behavior of two-stage (pre-placed aggregate).

#### Materials and Test Procedures

**Fine Aggregate:** The fine aggregate used in the manufacture of grout was a natural beach sand from Zlietn quarry (nearly 150 km east of Tripoli city) with specific gravity 2.63 and the maximum greatest size 1.18 mm according to specification. The grading of the fine aggregate obtained from the sieve analysis is shown below in figure 1.

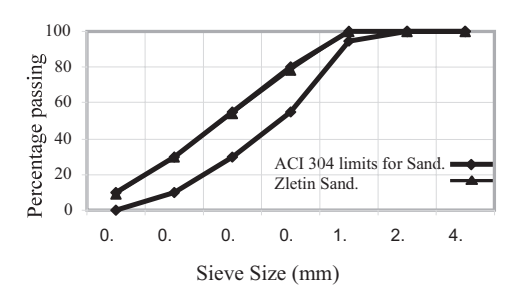


Fig. 1. Grading of fine aggregate.

**Admixtures:** The superplasticiser used in the grout was naphthalene-formaldehyde derivative of trade name "Superplasticiser SikaMent-163" and was mixed at the rate of 2% by weight of cement. The expanding agent of trade name "Intraplast-Z" was aluminum powder based admixture, which was used at the rate of 2% by weight of cement.

**Cement:** There is no special type of cement to make grout for two-stage concrete. The cement used throughout the experiments was ordinary Portland cement Type I with 28-days compressive strength of 41 MPa and Blaine fineness of 3497 cm<sup>2</sup>/g.

**Coarse Aggregate:** The coarse aggregate used in these experiments was angular basalt aggregate; the source of the stone aggregate is obtained from "Abou-Arogub region quarry" 40 km south of Tripoli. Maximum sizes of angular coarse aggregate approximately 38mm, which is less than one third (1/3) of the mould width (Fig. 2). Physical properties of coarse aggregates are shown in Table 1.

Table 1. Physical Properties of Coarse Aggregat
---

FINES	CRUSHING	SPECIFIC	VOID	WATER	ABRASION
KONTENT	VALUE	GRAVITY	RATIO	ABSORPTION	VALUE
%	%	%	%	%	%
2.47	20.74	2.69	47.18	1.96	23.81

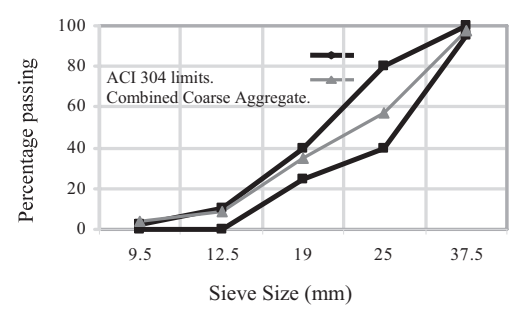


Fig. 2. Grading curve of coarse aggregate.

A total of 360 cylinder specimens, five samples for each grout proportion (three w/c and three c/s ratios) with and without admixture were cast. The dimensions of these specimens were 150 mm in diameter and 300 mm in height. The cylinder specimens were tested to obtain the compressive strength and tensile strength (split test) of two-stage (pre-placed aggregate) concrete. Tests were conducted to determine the 28-day compressive strength and tensile strength measured by split test. After one day of casting the concrete specimens were removed from the cylinders and immersed in water tank for seven days. All cylinder specimens were then stored in the laboratory at constant temperature and relative humidity.

### **Grout Mix Preparation And Concrete Specimen**

The selection of sand-cement and water-cement ratios are more critical in two-stage concrete than in normal concrete, because the amount of sand and water control the fluidity of grout, an essential requirement in the manufacture of two-stage concrete. With a certain proportion of sand, cement and water, it may be possible to cast normal concrete but it may not be at all possible to grout two-stage concrete at that proportion. It is therefore necessary to use trials to obtain a suitable mix for each particular condition of grout mix and coarse aggregate grading.

To establish suitable mix proportions for intrusion grouting using cement, sand, water without and with admixture (superplasticiser, expanding admixture and superplasticiser + expanding admixture), several trial mixes were used in laboratory. The major criterion adopted to maintain the uniformity of grout was its consistency. To measure this consistency a flow cone and flow table were used as shown in Fig. 3 [3, 5].

Three different proportions of cement-to-sand 0.5:1, 1:1 and 1.5:1, with varying ratios of water-to-cement 0.38, 0.55 and 0.80 were tried out to determine the optimum mix proportions (Table 2). It is obvious higher economic results from a higher sand-cement ratio but the increase in sand content, as experienced, should not be such that it limits fluidity and reduces the strength of concrete. Tests on consistency as shown in Fig. 3 demonstrated that the higher sand-cement ratio of 1.5 required much more water.

For example, the water-cement ratio 0.38 in the plain grout (without admixture) at all cement sand ratios is the minimum ratio suitable for grouting; it was not possible to penetrate all voids in the aggregate skeleton, as it required higher pumping pressure to inject the grout. As a result, the concrete specimen has a honeycomb structure with partial binding of the aggregate skeleton. Grout containing admixture at w/c ratio of 0.38, on the other hand, filled all voids and created a smooth surface of the sides and ends of each cylinder [6].

**Table 2. Mix Proportions of Grout** 

WATER-CEMENT	CEMENT-SAND	UNIT QUANTITIES, kg	
RATIO, W/C	RATIO, C/S	CEMENT	SAND
	0.5	295	590
0.38	1.0	421	421
	1.5	525	350
	0.5	282	564
0.55	1.0	407	407
	1.5	508	338
	0.5	265	530
0.80	1.0	396	396
	1.5	490	326





a. Flow Cone

b. Flow Table (Meter)

Fig. 3. Fluidity equipments.

# **Analysis and Discussion of Results**

**Compressive Strength of TSC**: The compressive strength fc of two-stage concrete was tested with and without admixture at 28 days. On the basis of the results a relation for fc has been assumed, but it can be also calculated according to the design algorithm presented [7]. For the compressive strength of two-stage concrete (fc) an empirical equation was calculated using the following formulae:

$$f_c = A + (B) \times w/c + (C) \times (w/c)D + (E) \times c/s [MPa]$$
(1)

Where:  $f_c$  stands for the estimated compressive strength of two-stage concrete, w/c is the water-to-cement ratio and c/s is the cement-to-sand ratio.

Table 3. Regression Coefficients of Equation 1

TYPE OF GROUT	A	В	C	D	E	CORRELATION COEFFICIENT
Without admixture*	-3.67	11.20	3.96	-1.79	3.70	0.883
Superplasticiser	43.90	-32.55	-3.27	-1.68	2.42	0.944
Expanding admixture	-14.31	-39.83	68.45	0.47	2.63	0.891
Expanding admixture + Superplasticiser	-25.70	-87.70	126.75	0.52	1.88	0.660

<sup>\*</sup>Does not include water/cement ratio = 0.38 at all cement sand ratios

The experimental results from equation 1 clearly reveal that the compressive strength of two-stage concrete without admixture is not almost equal to that of compressive strength with admixture (superplasticiser) with the same water to cement and cement to sand ratios. The reason for lower strength is due to the lower sand content in two-sage concrete and the amount of water per unit volume of grout was however higher. In other words the fluidity of the grouting was high.

The compressive strength of two-stage concrete was increased as compared to the strength without admixture when the superplasticiser was used. But when compared to the cement/sand ration at constant water/cement ratio, the compressive strength of two-stage concrete slight increase. The possible reason for the slightly increase in strength

might be associated with the bleeding of water in grout as observed through a transparent cylinder tube. This was also evidenced by the loss of grout-aggregate bond under side of aggregate particles on examination of the fractured specimens [8, 9].

According to [10] the quality two-stage (pre-placed aggregate) concrete depends not only on the strength of grout but on its ability to expand while a fluid and removes the traces of bleed water that collect under aggregate particles. With this idea that an expanding admixture, a blend of special metallic aluminum powder expansion agent, was used in the grout. The strength data, from equation 1, shows that using the expanding admixture the compressive strength of two-stage concrete was significantly increased. The compressive strength without any admixture equation 1, at 28 days, was 15.7 MPa while using expanding admixture the compressive strength increased to 18 8 MPa at constant w/c and c/s ratios. This is to be expected in two-stage concrete because of the expanding behaviour of the admixture. The generated hydrogen gas, on the other hand, leads to an increase in the amount of air-voids in the unrestrained grout cylinder, which accounts for a reduction in compressive strength. It is therefore concluded that the compressive strength of a grout, particularly when admixture is used, is not a satisfactory index of the compressive strength of two-stage concrete in which the grout is employed.

Superplasticizer and expanding admixture were used together. Among the four types of grout (Table 3), the compressive strength equation 1 was found to have the highest strength. This could be due to:

- Higher fluidity of grout using superplasticizer (that enables the grout to fill all the voids between aggregate particles).
- Expansion effect of grouts using expansion admixture to minimise bleeding and settlement of grout.

It was found that the 28 day compressive strength of two-satge concrete with admixture (expanding admixture) was 16.5 MPa at water/cement ratio =0.55 and cement/sand ratio=0.50. Whereas the compressive strength with admixture together (superplasticizer and expanding admixture) at the same grout was found 19.6 MPa.

# **Tensile Strength of TSC**

The split tensile strength of TSC was investigated at 28 days. The split tensile strength is calculated according to ASTM C 496, as follows:

$$f_t = \frac{2P}{\pi HD} \tag{2}$$

Where:  $f_t$  splitting tensile strength; P = maximum applied load; and H and D = length and diameter of the specimen, respectively.

The test results on tensile strength of two-stage concrete in the two series (with and without admixture) are high. The values of tensile strength for grout proportion are estimated by equation 3. No cause was apparent for the relatively high tensile strength. However, it is believed that the amount of coarse aggregate content, method of

placement and the greater mechanical interlocking among the particles could be responsible for the high tensile strength.

Failure in splitting tension was restricted principally due to the line of split and occurs through the mortar and coarse aggregate.

$$f_t = A + (B) \times w/c + (C) \times (w/c)D + (E) \times c/s \quad [MPa]$$
(3)

Where:  $f_t$  stands for the estimated splitting tensile strength of two-stage concrete, w/c is the water-to-cement ratio and c/s is the cement-to-sand ratio.

CORRELATION TYPE OF GROUT C E A В D **COEFFICIENT** Without admixture\* -0.251.26 0.67 -1.29 0.51 0.833 Superplasticiser -12.75 |-25.27 | 39.03 | 0.50 0.39 0.860 Expanding admixture -11.54 | -23.20 | 36.12 0.52 0.48 0.960

-7.41 | -1.37

-1.39

0.42

0.855

**Table 4. Regression Coefficients of Equation 3** 

9.82

# Compressive and tensile strength of TSC

Expanding admixture

+ Superplasticiser

A number of formulas have been suggested for the relationship between the compressive strength and the tensile strength of two-stage concrete. The results of this investigation show an important feature. It appears that there is a good correlation between the compressive strength and tensile strength of two-stage concrete. As the compressive strength increases with grout the tensile strength was also found to increase in the same manner. In the present work, however, the following formula was developed by regression analysis to relate splitting tensile strength ( $f_i$ ) to the compressive strength ( $f_i$ ). The relationship between the compressive strength and the tensile strength of different grout proportions are shown in Figures 4, 5, 6 and 7.

$$f_t = A + (B) \times f_c + (C) \times (f_c)D$$
 [MPa] (4)

Where:  $f_t$  splitting tensile strength and  $f_c$  compressive strength.

**Table 5. Regression Coefficients of Equation 4** 

TYPE OF GROUT	A	В	C	D	CORRELATION COEFFICIENT
Without admixture	-49.67	-0.44	38.63	0.15	0.724
Superplasticiser	39.97	0.36	-32.28	0.10	0.800
Expanding admixture	-4.30	-0.30	1.82	0.658	0.721
Expanding admixture + Superplasticiser	162.65	1.15	-132.28	0.108	0.680

<sup>\*</sup>Does not include water/cement ratio = 0. 38 at all cement sand ratios

The limit values of the compressive strength  $(f_c)$  in equation (4) are:

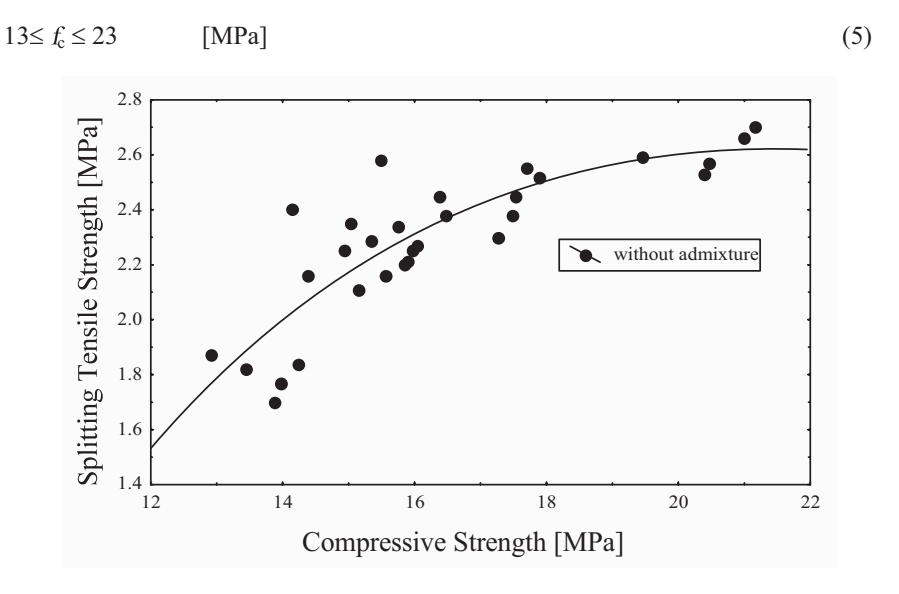


Fig. 4. Split tensile strength versus compressive strength of two-stage concrete.

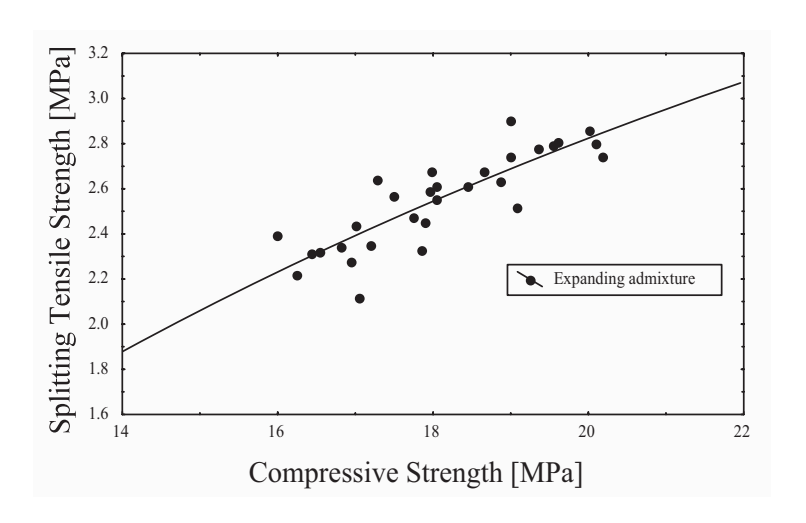


Fig. 5. Split tensile strength versus compressive strength of two-stage concrete.

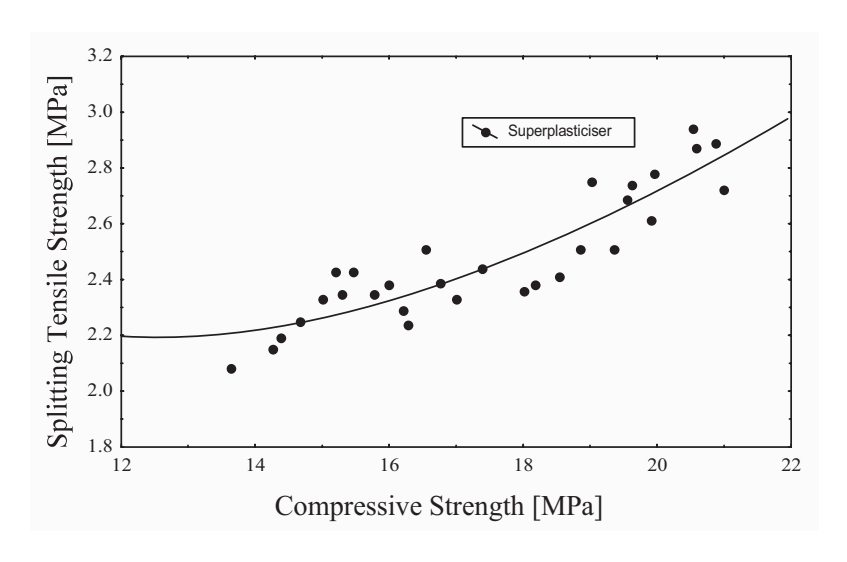


Fig. 6. Split tensile strength versus compressive strength of two-stage concrete.

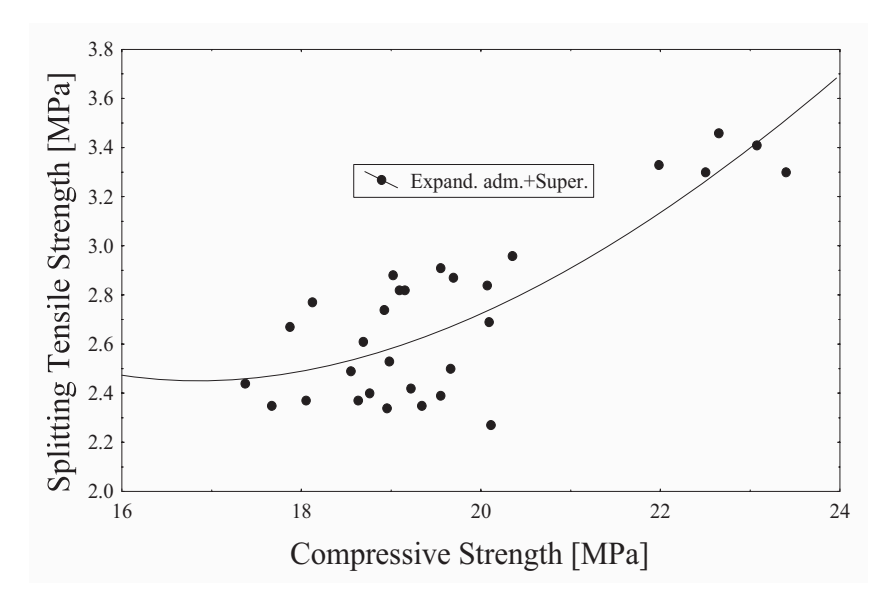


Fig. 7. Split tensile strength versus compressive strength of two-stage concrete.

#### **Conclusions**

- 1. To establish a suitable mix proportion for grout, the flow-cone test by itself was not sufficient to provide a suitable answer, particularly when admixture was used. Depending upon grading of aggregate and grouting equipment, it was found that the manufacture of grout and its pumpability should be best judged by personal experience based on trials.
- 2. As the method of placement in two-stage (pre-placed aggregate) concrete is entirely different from that of normal concrete, a suitable admixture is necessary for the requirement of pumpability of grout. The expanding admixture use was found to be the most suitable admixture as it provided higher fluidity with minimum bleeding.
- The compressive strength of two-stage concrete was tested with and without admixture at 28 days for all grout proportions. On the basis of the results a correlation between compressive strength and grout proportions was statistically derived.
- 4. The splitting tensile strength of two-stage concrete was found high at all grout proportions. The relationship between tensile and compressive strength suggests that the tensile strength of TSC increase with an increase in compressive strength.
- 5. The fractured specimens of two-stage concrete in compression showed numerous cracks around its surface. It showed extensive lateral expansion in the form of bulging, prior to the failure, though in general it was not sudden and explosive. It was also noticed that a large proportion of failures occurred by cracking through the aggregate particles.
- **6.** The modification that could be useful in improving strength is to change the admixture doses. Although this has not been investigated, it seems that reducing the admixture doses to half, the compressive strength of two-stage concrete could be improved. This would not only reduce the amount of air-voids in concrete but would also lower the cost of the admixture.

#### References

- 1. King, J. C., (1959), "Concrete by intrusion grouting, Handbook of Heavy Construction", Edited by Stubbs, F. W. Jr., McGraw-Hill, New York.
- 2. Abdelgader H. S., Górski J., (2003), Stress-strain relations and modulus of elasticity of two-stage concrete. Journal of Materials in Civil Engineering ASCE, 2003, 15, No. 4, pp 329-334.
- 3. ACI Committee 304, (2005), Guide for the use of pre-placed aggregate concrete for structural and mass concrete applications. Reported by American Concrete Institute ACI Committee 304. Re-approved 2005.
- 4. Abdelgader H. S., Górski J., (2002), Influence of grout proportions on modulus of elasticity of two-stage concrete. Magazine of Concrete Research, 2002, Vol. 54, No. 4, pp 251-255.

- 5. Abdelgader, H. S., (1996), Effect of quantity of sand on the compressive strength of two-stage concrete. Magazine of Concrete Research, 1996, Vol. 48, No. 177, pp 353-360.
- 6. Elgalhud, A. A., (2006), Influence of some types of admixtures on the mechanical properties of two-stage concrete at the Long Term, Master's Thesis, Civil Engineering Department Al- Fateh University, Tripoli, Libya, March 2006.
- 7. Abdelgader, H. S., (1999), How to design concrete produced by a two-stage concreting method. Cement and Concrete Research, 1999, Vol. 29, No. 3, pp 331-337.
- 8. Abdelgader H. S., Ben-Zeitun A. E., (2004), Effect of grout proportions on tensile strength of two-stage concrete measured by split and double-punch tests. Structural Concrete, 2004, Vol. 5, No. 4, pp. 173-177.
- 9. Abdelgader H. S., Ben-Zeitun A. E., Saud A. F., and Elgalhud A. A., (2006), Mechanical behavior of two-stage (pre-placed aggregate) concrete. Proceedings of the 10th Arabic Engineering Conference, 13-15 November 2006, Kuwait.
- 10. King, J. C., (1967), Strength evaluation and quality control of pre-packed concrete. American Concrete Institute, 1967, Vol. 64, pp 744.

# Recent Practices of Analysis and Design of High-Rise Buildings in Kuwait (Case Study)

#### Tarek Anwar Awida

Assistant Professor, Structural Engineering Dept., Faculty of Engineering, Ain Shams Univ., Cairo, Egypt. email: TarekA@keoic.com

#### Abstract

The main concern of this paper is to provide an overview of the current analysis and design methodology for reinforced concrete high-rise buildings. A case study of residential complex consisting of two new 30-floor towers located in Kuwait city is presented to demonstrate the most significant factors to be considered to ensure the building is designed to have sufficient strength to withstand ultimate (factored) gravity (dead plus live) and lateral (wind plus seismic) loading and sufficient stiffness to limit deformations and lateral drift to be within the acceptable range to verify the occupancy comfort level. Building code procedures based on general assumptions, are usually but not always conservative, and do not provide accurate wind loads because of exposure conditions, directional properties of the wind climate, complex geometry shapes, torsion, aerodynamic interactions, and load combinations. Wind tunnel tests, which are capable of more accurate load definitions, have become faster and more economical as a result of improved analysis and design methodologies. Finally, recommendations for analysis and design of reinforced concrete residential high-rise buildings in Kuwait are introduced.

#### Introduction

In the last decade developers and authorities in Kuwait, recognized the need to allow for more building heights due to many reasons. Some of these reasons are the enormous demand in the local market for office and residential areas, availability of the financial resources in safe and good economic conditions after the Gulf War II and the aim to develop Kuwait city following Dubai model. In the time being, many high-rise buildings were already found in Kuwait city and many more are under design or construction. This situation forced the structural engineering professions in Kuwait to expand their knowledge and advance their design and construction skills and techniques.

The case study of residential complex in Kuwait city presented here is considered a good practical example to be studied and reported. It is an existing complex in the Gulf road including car park in the basement level and podium level for landscape occupying the whole plot area. Above ground, there are two buildings with different heights ranging from five to eighteen floors. The existing building was constructed since 1978. The developers plan to construct two 30-story towers within the plot area and in close proximity to the existing buildings to be benefited from the new regulations. Partial demolition of some areas in both basement and podium level will be done to allow for the new construction. The slenderness ratios for the new towers are about 8-to-1 and 4-to-1 due to the very tight space available. As a preliminary rule of thumb, assume for tall and slender structures that either increasing the mass or the stiffness will reduce the acceleration. Concrete structures, more readily than steel structures, can often utilize the increase in mass to also increase the stiffness, thereby providing a double benefit. For this reason, the future of concrete for mega-structures looks bright, especially now that extremely high concrete strengths are available.

As a structure becomes taller, lighter or more slender, the possibility of excessive accelerations of the upper floors during relatively common wind events becomes more likely. The building occupants are usually sensitive to acceleration and its change rather than displacement and velocity. Acceptability criteria for accelerations are not currently codified. General guidelines do exist that are generally accepted by the wind engineering community. Threshold curves are available to give limits for human behavior. A dynamic analysis is required to allow the predicted response of the building to be compared with the threshold limits. Lower acceleration levels are used for residential buildings rather than office or commercial occupancies.

The main concern of this paper is to provide full description for the analysis, design and construction considerations for these towers. ETABS software (Extended Three Dimensional Analysis of Building Systems) which originally developed by Computer and Structure Incorporation (CSI) is used for conducting analysis and design of the structure using partial and complete 3-D models. The main structural system used is a combination between reinforced concrete core, shear walls and columns to resist both lateral and gravity loads. Floor slabs are used as cast-in-situ traditional and post-tension (PT) slabs. Lateral wind loads used in the design are estimated as specified in the codes and using the wind tunnel laboratory tests. The wind-induced accelerations are computed in the highest occupied levels to ensure the residential occupancy comfort.

Finally, recommendations for analysis and design of reinforced concrete residential high-rise buildings in Kuwait are introduced.

# **Existing Site Conditions**

The existing development was constructed since about 28 years near the Gulf road in Kuwait city. The foot-print of the site is occupied entirely by a single level basement, which is used for car parking and electrical/mechanical rooms. The ground (podium) level external area comprises mostly entrance pathways and landscaping which are supported on the reinforced concrete waffle slab which forms the roof of the basement. Rising above the ground (podium) floor, there are two existing buildings, the elevations of these buildings are stepped back, and the height varies from five to around eighteen levels above the ground floor. These buildings are constructed in reinforced concrete and are supported by a 1.50 meters thick raft. Isolated footings with 1.50 meters thick below the columns connected by 300mm thick raft are used for parking area outside the existing buildings. A settlement strip (between the raft inside and outside the buildings) is introduced. It is specified in the AS-Built drawings as "to be casted after construction of the 11<sup>th</sup> floor level".

An investigation study for the existing buildings to verify the structural conditions was done and found that the different structural elements are fairly in good conditions and no indications for any major structural problems had been noticed. The study reported that the developer proposal to add two new towers is feasible from the structural point of view due-to-the fact that foundation and podium level slabs around the existing buildings can be separated without negative effects on the remaining structure stability. In addition, the study recommended special care and detailing to maintain the old and new basement properly sealed to prevent water leakage (*Awida*, 2002).

#### **Proposed New Structure**

The new structure will comprise two 30-storey towers and commercial shops within the plot. One of the new towers shall be used for residential apartments and the other one for serviced (hotel) apartments. Due to the restricted size of the site, together with municipality set-back regulations these towers will be in close proximity to the existing buildings. The locations of these new towers in plan are selected to allow for maximum outward gulf views and inward natural light, while maintaining privacy. The tower elevations are designed to be integrated with the existing buildings elevations. A strip of 800mm fair face concrete is maintained in each floor level and the rest of the floor height is used as stone cladding for both towers to match with the existing buildings. Each tower is serviced by a mechanical floor located at the 19<sup>th</sup> floor. The architects and engineers worked hand in hand to develop the building form and the structural system, resulting in towers that efficiently respond to the wind, while maintaining the integrity of the design concept. Figure 1 shows a perspective view of the new towers and the existing buildings. The slenderness ratios of the new towers are about 8-to-1 for tower (A) and 4-to-1 for tower (B) due to the very limited space available. The partial demolition of the existing basement and ground structure shall be required to allow for the new construction works. The demolition line in the foundation level is selected to be within the settlement strip while the same in the podium level is selected to be within the existing expansion joints location. This helps to keep the structural stability of the remaining part of the structure unaffected by the demolition works.



Fig. 1. Perspective of new towers and existing buildings.

# **Structural System Description**

With wind being the critical factor in the design of high-rise buildings, structural simplicity and constructability were also the key objectives of the design. The resulting system can be referred to central core/shear walls and columns located at the building perimeter. The closed core walls provide an extremely stiff torsional restraint. The vertical supporting structural elements (columns/walls) shall be constructed utilizing high performance concrete (f<sub>c</sub>'=50 MPa) to minimize its sizes. Perimeter concrete beams with 800mm deep connecting the edge columns are used in each floor, thus allowing the columns to participate in the resistance of lateral loads as well as redistribution of gravity loads. The gravity load redistribution in addition to an estimated modifier for columns cross sectional area shall balance the stress level in the vertical elements and minimize the effects of differential shortening, an especially significant factor in the high-rise buildings (*Fintal*, 1987).

A combination of traditional and post-tension (PT) cast-in-situ concrete slabs is used for the floor slab system. PT slabs are selected because of the following reasons:

- PT slab provides lighter structure for long spans by significant amount compared to the traditional slab and this reflected in less sizes of columns, walls and foundation.
- PT slab provides reduction of construction cycle.
- PT slab provides flexibility for architectural layout changes from floor to floor without changing the structural framing.
- PT slab provides flexibility for service slab openings without drop beams or slab thickening.

Figures 2 and 3 introduce the typical structural framing plans for tower A and tower B respectively. The result is a very elegant and efficient structure which utilizes the gravity load-resisting system to effectively assist in the resistance of lateral loads.

#### Wind Tunnel Test and Results

To assess the dynamic response of a structure using a model of the structure in a wind tunnel, it is necessary for the design team to provide the laboratory with the following information: the location and shape of the structure; the mass distribution in the structure; the fundamental periods (torsional and in the two major orthogonal axes); and the deformation curves and the damping anticipated. An aeroelastic model of the structure can then be constructed and tested. This model must simulate the flexibility, damping, and mass of the prototype structure to provide detailed information on the movement of the structure as well as the dynamic loads generated by this motion. The construction and testing of such a model is time-consuming and expensive. Should initial results indicate revisions to the structure, the model must be revised and tested again (*Grossman*, 1990).

The objectives of the wind tunnel test in our case study are to:

- Provide an assessment of the wind loading relevant to the design of the superstructure and building foundations for the proposed towers, taking into account the dynamic effects.
- Provide an assessment of the wind induced building motions and aerodynamic stability for the proposed towers in terms of their potential to cause occupant discomfort at the highest occupied levels.

The basic wind speed considered in this study (mean hourly wind speed at h=10.0 meters in open country terrain with roughness height of 0.03 is used as 23.0 meter/second), corresponds to 28 meter/second, fastest mile, consistent with the UBC-97 approach. Three-second gust wind speed at h=10.0 meters in open country terrain with a roughness height of 0.03 is used as 35.1 meter/second, consistent with the ASCE-02 approach.

A 1:300 scale model of the proposed towers was constructed for conducting a wind tunnel study to measure and determine the overall wind loads acting on the two structures. Fluctuating static wind loads were measured on the proposed towers A and B for a full range of wind directions. Figure 4 shows the model used for wind tunnel testing at laboratory. The wind specialist conducted dynamic analysis using structural and dynamic properties. The main conclusions of this study are:

- Peak magnitude instantaneous dynamic base loads have been estimated.
- Floor-by-floor peak dynamic loads were estimated and load cases extrapolated to account for the non-simultaneous action of the individual peak floor-by-floor load components.
- The highest peak combined accelerations (for a structural damping level of 1.5%) produced in response to wind loading are calculated and found do not exceed accepted acceleration thresholds for residential occupancy comfort for 1, 5 and 10 years return period wind speeds.

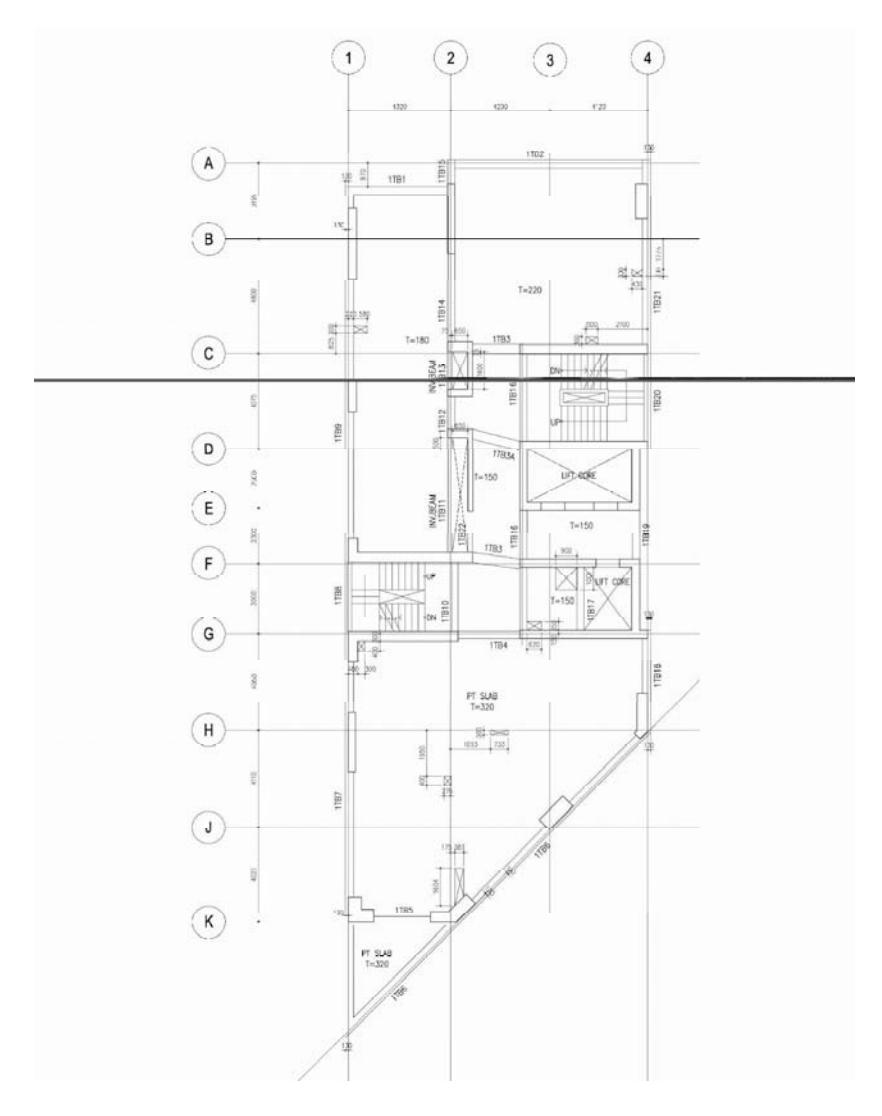


Fig. 2. Typical structural framing plan for tower (A).

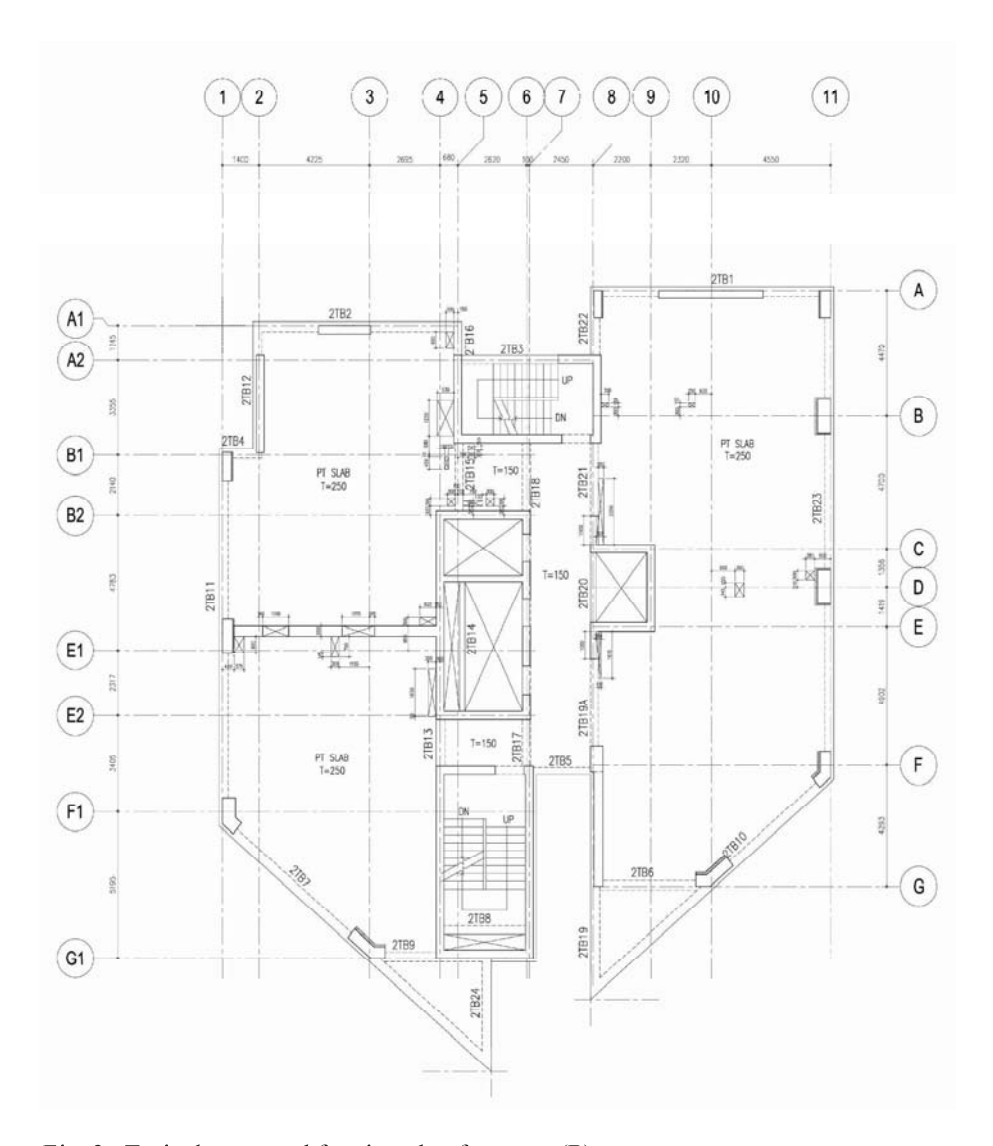


Fig. 3. Typical structural framing plan for tower (B).

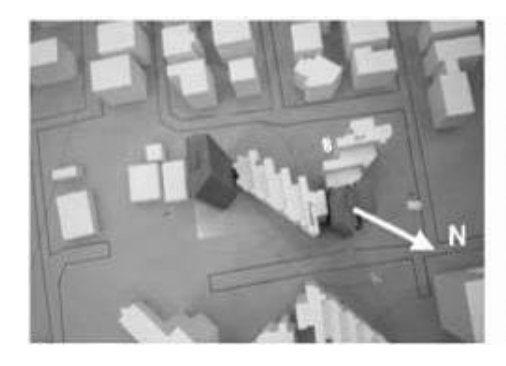




Fig. 4. The model used for the wind tunnel testing at laboratory.

# Structural Analysis and Design

Three-dimensional structural models were built for the two towers using ETABS software (Extended Three Dimensional Analysis of Building Systems) (ETABS 2005). Both gravity (dead and live) and lateral (wind and seismic) loads are applied to the model. Wind loads as specified in ASCE-02 code in two perpendicular directions are considered. In addition, ten wind load cases recommended by wind tunnel studies are subjected to the model. Seismic zone (1) coefficients are used as specified in UBC-97 code for Kuwait city and as recommended in the soil investigation report. All load combinations as per code requirements for both serviceability and strength design studies are taken into consideration in the analysis.

The stiffness (EI) values for flexure members used in the analysis for the strength design method, where factored loads are used, are considered as cracked sections as per the coefficients recommended in ACI code (ACI 2005). In case of serviceability study, where service unfactored loads are used, to predict deflections, vibrations, building periods and drift, modified (EI) values are used. The estimated wind induced forces in wind tunnel laboratories and a second order analysis should be computed based on service loads. Estimated modifiers for the columns' cross sectional areas are used to balance the stress level in the vertical supporting elements in order to minimize the effects of differential elastic shortening, an especially significant factor in high-rise buildings. These area modifiers are estimated based on the output of summation of gravity loads for individual 3-D structural model of the different building floors compared to the same of the complete building model. Design of reinforced concrete supporting elements (columns and shear walls) was conducted using ETABS. High performance concrete with cylindrical compressive strength 50MPa was used for columns and walls in both towers while concrete with cylindrical compressive strength of 35MPa was used for foundation, slabs and beams. Complete detailed design for traditional slabs was introduced in the Tender Documents while only slab thickness was specified for post-tension (PT) slabs and the detailed design was assigned to the specialist contractor subject to engineer's approval prior to construction.

Tower A is 12.64 meters wide and 104.65 meters height above ground. The slenderness ratio is about 8.30 (i.e. more than 5). For this reason, wind-induced forces based on

UBC-97 code are not applicable and ASCE-02 code is used in addition to wind tunnel test results. This tower is considered sensitive to dynamic effects and many design revisions were made in order to maintain the serviceability values such as building drift and acceleration within the acceptable range (*Grossman*, 1990). Reinforcement percentage for columns in tower A ranges from 2% up to 3.70% and shear walls vertical reinforcement ranges from 1.40% for 300mm thick wall to 2.50% for 400mm thick walls at basement level. The high percentage of reinforcement in shear walls for tower A is expected due to building slenderness ratio.

Tower B is 23.25 meters wide and 105.70 meters height above ground. The slenderness ratio is about 4.60. This means that this tower is less sensitive for dynamic effects compared to tower A. In this case, either UBC-97 or ASCE-02 codes can be used for estimating the wind-induced forces in addition to wind tunnel test results. Reinforcement percentage for columns in tower B is ranging from 1.30% up to 3.05% except one column (4.50%) and most of shear walls have vertical reinforcement 1.40% with 300mm thick walls at the basement level.

# **Foundation Design**

Site preparation will consist of partial demolition of existing construction at the location of the new towers, nominal dewatering to lower ground water below the anticipated foundation level and installation of underpinning system (proposed to be scant piles) to limit movements of the existing building foundations. The soil investigation reported that the estimated settlements for the new towers foundation as isolated raft would be excessive and some additional load would be applied to the new raft from the existing view of the planned different foundation level. Accordingly, the new towers should be supported on a piled foundation. The cast-in-situ concrete bored piles were found the most appropriate pile type as per the site circumferences. Pre-production pile tests were recommended to be undertaken, in order to confirm the estimated capacities in the preliminary soil investigation report. Such tests should consist of compression and uplift tests and should consider three times working load or failure to reassess and modify the pile design where appropriate. It is agreed by all the project parties to consider the pile design, (pile diameter, length and reinforcement), as a design and built contract using the pile load test results and the design criteria prepared by the engineer to expedite the design and construction process for foundation.

Analysis and design for foundation and piles load distribution are conducted using SAFE software (Slab Analysis by Finite Element method) (*SAFE*, 2005) originally developed by Computer and Structures Incorporation (CSI) using the Columns data and loadings imported from ETABS model for the different load cases. The design value of pile service capacity for each pile group is determined and specified in the Tender Documents to allow the specialist contractor to design the pile diameter, length and reinforcement.

# **Construction Bid Packaging Strategy**

The project management team establishes a bid packaging strategy for the construction works in order to:

- Ensure the full coordination between the different contractors.
- Ensure the contractors qualifications for the different specialty works and confirm quality level.
- Minimize/reduce the impact to the current users (tenants) of the existing buildings.
- Idealize the construction time and cost.

The different Bid Packages (BP) can be summarized as follows:

# **BP#1: Re-routing of existing services:**

This package contains relocation of the existing services located at the new towers construction areas at basement and externally at podium to allow for other packages to start construction works.

## **BP#2: Demolition and piling works:**

In this package, it is intended to encompass the design and execution of the demolition, excavation, secant piles, de-watering, shoring and pile works. It is a specialty trade design and built contract focused on piling and associated works.

# BP#3: Civil, architectural, finishing, interior and conveying systems:

This package involves the construction of all items related to the basement, podium and super-structure within towers A and B areas.

# BP#4: Mechanical and electrical works:

This package combines all the mechanical and electrical works within the towers A and B areas. The full coordination among the different contractors (BP#3 & BP#4) should be done during all the construction activities.

# BP#5: Commercial area and landscape works:

The demolition of the existing facilities at podium level outside the towers areas and construction of the new commercial area and hard/soft landscape and service parking works are included in this package scope of work.

#### Conclusions and Recommendations

A case study of reinforced concrete residential complex in Kuwait city is presented as a good practical example to be studied and reported for the benefit of the structural engineering professions in Kuwait. An extensive description for the structural analysis, design and construction procedure is introduced through out this paper. The main recommendations concluded from this study are as follows:

- Structural engineering professions for design and construction in Kuwait need to expand their sphere of knowledge in order to fulfill the requirements of the expected increase of office and residential high-rise buildings in Kuwait.
- The selection of the structural system for high-rise buildings should consider the efficiency of resisting both gravity (dead and live) and lateral (wind and seismic) loads. The architects and engineers should work hand in hand to develop the building to maintain safety and integrity of the design concept from day one of the project design.
- Structural analysis and design of reinforced concrete high-rise buildings should be
  done using efficient and professional software designed for such type of buildings
  (3-D static and dynamic analysis). The most significant factors to be considered
  in the analysis and design are elastic shortening of columns, an accurate
  estimation for the wind-induced forces as specified by codes and/or using wind
  tunnel test results (if needed), flexure stiffness modifiers in ultimate and service
  conditions and P-Delta analysis.
- Serviceability study to predict deflections, building periods, drift and accelerations in the highest occupied levels should be conducted to confirm that they are within the acceptable limits and to verify the occupancy comfort.

# References

- 1. ACI 318-05, (2005), Building Code Requirements for Structural Concrete and Commentary, American Concrete Institute (ACI), Framington Hills., USA
- 2. Awida, T. A. (March 2002), Partial demolition and Extension of Kuwait Medical College Building, ASCE J. Arch. Engrg., Vol. 8, Issue 1, PP2-6.
- 3. 'ETABS' software Plus version 9.0.4 (1984-2005), Extended Three Dimensional Analysis of Building Systems, Computers and Structures Incorporation (CSI), University Avenue, Berkeley, California, USA.
- 4. Fintal, M., Ghosh, S. K. and Iyengar, H. (1987), Column Shortening in Tall Structures-Predictions and Compensation, Portland Cement Association (PCA), Skokie, Illinois, USA.
- 5. Grossman J. S. (1990), Slender Concrete Structures-The New Edge, ACI Structural Journal, Vol. 87, No. 1, PP39-52.
- 6. 'SAFE' software version 7.3.5 (1978-2005), Slab Analysis by Finite Element method, Computer and Structures Incorporation (CSI), University Avenue, Berkeley, California, USA.

# Shear Strengthening of Reinforced Concrete Beams Using Near-Surface Mounted Conventional Reinforcing Bars and CFRP Rods

Khaldoun N. Rahal
Civil Engineering Department
Kuwait University, Kuwait
email: rahal@civil.kuniv.edu.kw

#### **Abstract**

This paper presents the preliminary results of an experimental investigation of the shear behavior of reinforced concrete beams strengthened using near-surface mounted (NSM) Carbon Fiber Reinforced Plastic (CFRP) rods and conventional reinforcing bars (rebars). Two T-beams reinforced in the transverse and longitudinal directions were cast and tested in a four-point loading setup at a shear span to depth ratio of 3. One beam acted as a control beam, while the other was strengthened with NSM vertical reinforcement. The beam had two test regions, one strengthened with CFRP rods, while the other with NSM conventional rebars. It was observed that the strengthening increased the cracking shear by 23% and the shear capacity by 37% for rebars and 47% for CFRP rods. The widths of the diagonal cracks were significantly reduced. The results show the advantages of using the NSM strengthening technique.

#### Introduction

Strengthening of existing reinforced concrete beams is often required for various reasons. Design for larger loads and restoration of the capacity due to under-design, error in construction or deterioration caused by corrosion require increasing the flexural as well as the shear capacity of a beam. On the other hand, beams suffering from inadequate concrete strength due to difficulties during concrete production and/or construction require more shear than flexural upgrade due to the more significant dependence of the shear capacity on the concrete quality and strength.

Innovative composite materials such as Fiber Reinforced Polymer (FRP) have been used in the rehabilitation of existing reinforced concrete structures since the early 1950s (Rubinsky and Rubinsky, 1954). Reinforced concrete structures can benefit from the high specific modulus and strength, lightweight, resistance to corrosion, and ease of installation of FRP. The 1980's brought an increase in use of FRP in RC elements subjected to severe chemical attack [ACI 440R-96, 1996].

For shear strengthening, the vast majority of research on FRP has been on the use of laminates e.g. Deniaud and Cheng, 2001; Khalifa et al., 1998. These unidirectional sheets are very efficient in strengthening beams and easy to install. However, they are susceptible to bond failure because of the relatively high shearing stressing at the interface with the concrete and the difficulty in strengthening their bonding using mechanical anchoring [Khalifa et al., 1998].

One of the alternatives is to use NSM strengthening. This method was proven successful with conventional reinforcing bars in negative bending moment regions in slabs and beams because FRP laminates would be subjected to the unfavorable effect of finishing and wear and tear. The work on the use of FRP rods for shear strengthening is limited (Shehata et. al., 2000, De-Lorenzis and Nanni, 2001).

On the other hand, FRP materials are significantly expensive than conventional rebars, and while laminates are commercially available in Kuwait, rods are available only by special orders. NSM conventional reinforcing bars can be considered a possible alternative to NSM rods because it is commercially available in Kuwait, it costs only a fraction of the cost of the FRP rods, its long-term durability performance is understood, and it could provide a solution to the low bond resistance of the FRP rods. This paper presents the preliminary results of an experimental study aimed at gaining a better understanding of the potential of using NSM CFRP rods and conventional steel bars to strengthen reinforced concrete beams in shear.

# **Experimental Program**

Figure 1 shows details of the two T-beam specimens tested. The beams were 3.25 meters long and 500 mm deep, and contained longitudinal and transverse reinforcement. The target concrete strength was 30 MPa. One of the beams was not strengthened to act as a control specimen. The second beam had two test regions as shown in the figure. The west (left) side was strengthened with conventional  $\rho$ 8 rebars spaced at 200 mm, while the east (right) side was strengthened with  $\rho$ 8 mm FRP rods spaced at 200 mm.

Hence, two test results were obtained. The shear span was 1290 mm, giving a shear span to depth ratio of 3.

The longitudinal reinforcement was four  $\emptyset 22$  mm bars and the effective depth was 430 mm. With a flexural compression zone within the relatively wide flange (380 mm), the longitudinal reinforcement ratio is about 0.93%, which is a practical value. The transverse reinforcement was  $\emptyset 6$  mm spaced at 200 mm. This corresponds to about 1.88 times the minimum transverse reinforcement required by the ACI code [2005] for the 30 MPa target concrete strength. This is also a very practical level of reinforcement. The properties of the reinforcing bars and the FRP rods are given in Table 1. The properties of the concrete and a summary of the results are given in Table 2.

Table 1. Properties of Reinforcing Steel and CFRP Rods

Size	$f_{v}$	$f_u$
	(MPa)	(MPa)
ø6 mm	338	442
ø8 mm	427	507
ø 10 mm	433	610
ø 22 mm	446	705
ø8 mm FRP		1900‡

<sup>\*</sup>supplied by manufacturer

The concrete was supplied by the Kuwait British Readymix Company, and the observed  $f_c$  was close to the target strength as shown in Table 2. The compressive strength of the cylinder was about 85% of the strength of the 150-mm cube. The 28-days cylinders and cubes ( $f_c$  and  $f_{cu}$  respectively) results shown in Table 2 are calculated as the average values from three standard cylinder samples, while the cylinder and cube strength on the day of test ( $f_{cy}$  and  $f_{cu}$  respectively) are calculated as the average of two sample specimens each.

The epoxy used to bond the strengthening reinforcement was manufactured locally in Kuwait by Al-Ghanim Industries, and is suitable for anchor bolts. It was designed for use on vertical and overhead surfaces, and its strength was determined by the manufacturer to be 90 MPa.

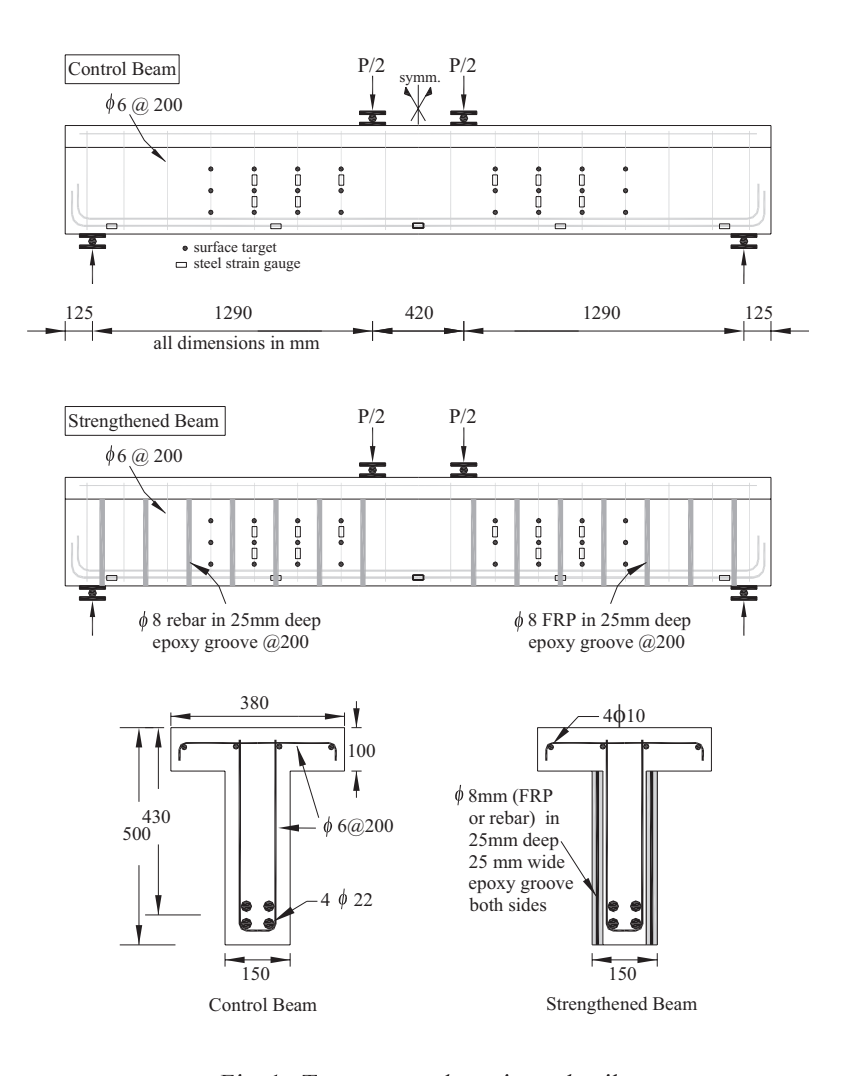


Fig. 1. Test setup and specimen details.

Table 2. Properties of Concrete and Summary of Results

Specimen/	f'c*	f'cu *	Age at test	$f_{cy}^{\dagger}$	$f_{cu}^{\dagger}$	V <sub>cr</sub>	Vexp
Test	(MPa)	(MPa)	(days)	(MPa)	(MPa)	(kN)	(kN)
region							
Control	32.9	38.8	220	37.6	44.5	65	150
B90-F200			270			80	205
B90-R200	32.9	38.8	270	37.3	43.9	80	220

\*tested at 28 days, average of three samples

<sup>‡</sup>tested same day as beam specimen, average of two samples

# **Instrumentation, Casting of Concrete**

The ends of the tensile longitudinal bars were bent past the supports to provide better development. Electrical resistance strain gauges were attached to the longitudinal and transverse reinforcement as shown in Fig. 1. The concrete was poured into the formwork and was compacted using mechanical vibrators. After casting, the beams and a group of the control cubes and cylinders were cured at room temperature using wet burlap covered by plastic sheets. Other samples were prepared to be tested after 28 days as per ASTM C39-99. The curing of the beams and the samples was stopped two to four days before testing to allow for painting and placement of the beam on the loading frame. Surface strain gauges were attached on the surface of the concrete as shown in Fig. 1 to measure strains at various load stages.

## **Testing Setup**

Figure 1 shows the load and support arrangements. Four 25 mm thick and 120 mm long steel plates were used at the location of the loading and supports. The vertical load was applied using a 570 kN actuator, and the load was conveyed to the two locations shown in Fig. 1 using a thick spreader plate. The vertical deflections were measured at midspan. In addition, the horizontal elongation at the ends of the beams was measured to ensure the roller supports allowed the beam to elongate without restraint in the longitudinal direction.

# **Strengthening and Test Procedures**

The strengthening was carried out before the application of the load on the beams. Grooves 25 mm deep and 25 mm wide were cut on the vertical sides of the web, and extended from the bottom of the web till the bottom of the flange. Similar to the procedure used by De Lorenzis and Nanni [2001], the epoxy was placed to half the depth of the grooves, and the bars or rods were installed and pressed gently into the epoxy. Then the groove was fully filled with epoxy. The epoxy was allowed two days to cure before testing the beam.

The load was applied in stages which ranged from 10 to 20 kN. After each loading, the load was maintained constant while measurements were recorded, cracks measured and marked, and photographs were taken. When the weaker side of the strengthened beam reached its ultimate shear capacity, the load was released, and the failing half of the beam strengthened using top and bottom plates and external rods. Then the loading was restarted.

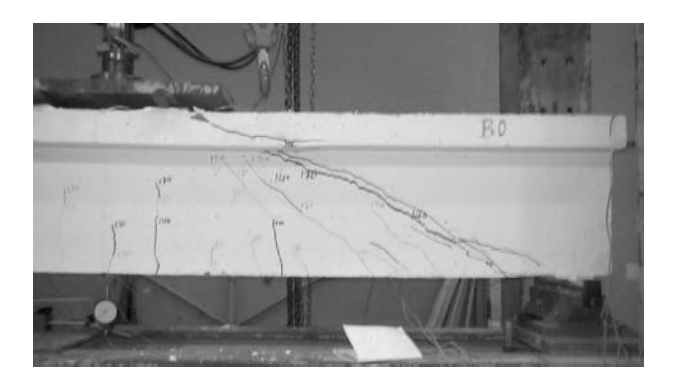


Fig. 2. Test region of the control beam at ultimate capacity.

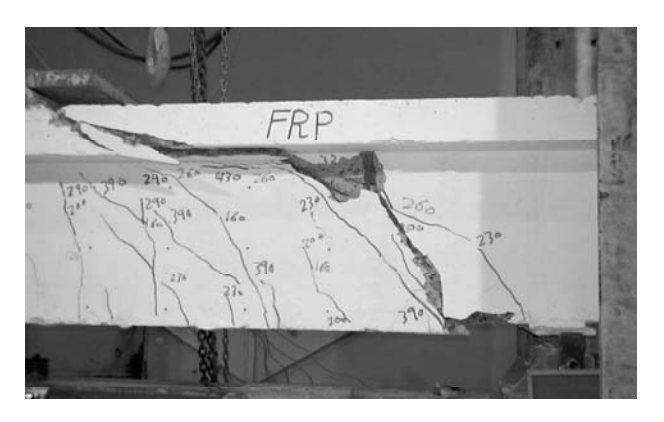


Fig. 3. FRP strengthened test region at ultimate capacity.



Fig. 4. Test region strengthened with conventional bars at ultimate capacity.

# **Test Results**

Figure 2 shows one side of the control beam after it had reached the ultimate strength, while Figs. 3 and 4 show the sides strengthened with FRP rods and conventional rebars respectively. The control beam showed a typical shear failure. The test regions strengthened with FRP rods and with conventional bars showed a typical development of shear cracks but the final critical crack was considerably steeper than usual because it was a combination of two previously developed cracks. The FRP pulled out about 100 mm below its upper end, at the location where the major crack intercepted the rod. On the other hand, the rebars used in strengthening suffered with limited signs of pullout. Strains measured in the transverse direction on either side of the rebars showed values larger than the yielding stress of the strengthening rebars.

Figure 5 shows the load-midspan deflection in the two specimens. The curve in the strengthened beam was not measured after the unloading which followed the failure of the side strengthened with conventional rebars. The figure shows that the strengthening increased the strength considerably, and allowed the strengthened beam loading to approach its flexural failure load. The longitudinal reinforcement near midspan yielded, but its strain hardening reserve strength allowed it to resist higher load, causing the beam to fail in shear.

Table 2 gives the observed cracking and the ultimate shear force in the three test regions. It is noted that these values do not include the self weight of the beams. The cracking force on either side of each specimen was the same. The table shows that the strengthening increased the cracking force by 23%. A more significant increase was observed in the ultimate shear load, where NSM conventional bars and FRP rods increased the strength by 37% and 47% respectively. It is to be noted that the ACI code equations [ACI 2005] calculates a 66 kN cracking shear force (shear observed in control beam is 65 kN), and an ultimate shear force of 107 kN (shear observed in control test is 150 kN). If the  $\theta$ 8 rebars were internal and properly anchored, the ACI equations calculate an ultimate shear force of 199 kN (shear observed in test region strengthened by conventional rebar is 205 kN).

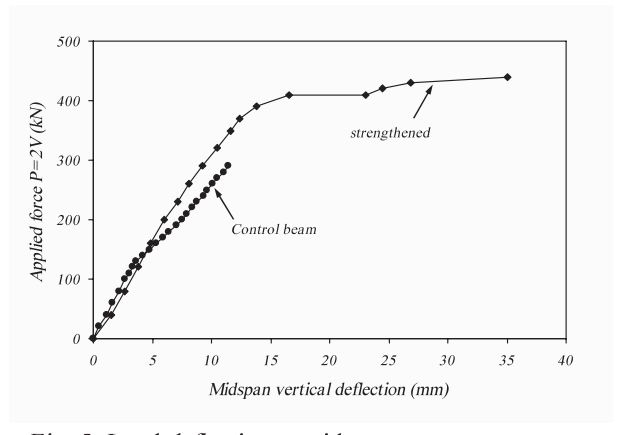


Fig. 5. Load-deflection at midspan.

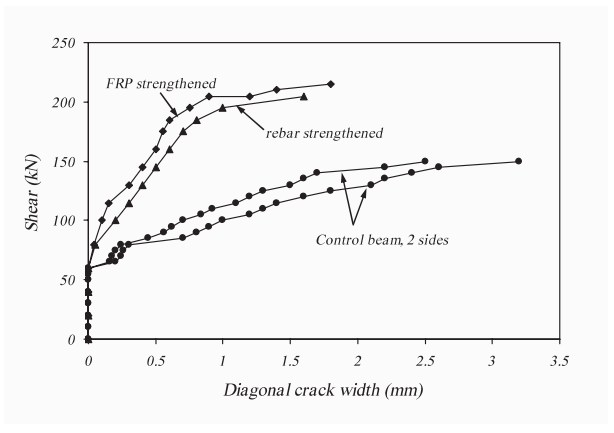


Fig. 6. Applied shear force versus diagonal crack width.

Figure 6 shows the diagonal crack width measured near mid-height of the specimens. The NSM bars and rods improved the crack control in the beams. It is noted that the behavior of the two sides of the strengthened beams was very similar inspite of the considerable difference in stiffness between the rebars and the rods.

#### **Conclusions**

The use of NSM conventional reinforcing bars and NSM CFRP rods to strengthen reinforced concrete beams in shear was investigated. The experimental results showed a significant increase in cracking and in ultimate capacity and a significant reduction in the width of the diagonal cracks in the strengthened test regions. The CFRP rods caused a 47% increase in shear capacity in comparison with a 37% increase for conventional bars, but the CFRP failed by pullout of one of the rods and the surrounding concrete, including the epoxy used to bond the rods inside the grooves. Further testing is underway to investigate the effect of changing the inclination and the spacing of the strengthening reinforcement.

#### Acknowledgement

The research presented in this paper was made possible by a generous support from Research Administration at Kuwait University, grant EV05/05. This support is gratefully acknowledged. The experiments were conducted under the supervision of Eng. Hatem Rumaih, whose contribution is also acknowledged.

#### Notations

 $f'_c$  = cylinder compressive strength of concrete at 28 days (ASTM C 39-99)

 $f'_{cu}$  = cube compressive strength of concrete at 28 days

 $f_{cu}$  = cube compressive strength at day of test  $f_{cy}$  = cylinder compressive strength at day of test

 $f_v$  = yield strength of reinforcing steel

 $f_u$  = ultimate strength of reinforcing steel

P = applied total load on specimen V = applied shear force in test region

 $V_{cr}$  = observed cracking shear force in test region  $V_{exp}$  = observed ultimate shear force in test region

#### References

- ACI Committee 318, 2005, "Building Code Requirements for Reinforced Concrete and Commentary ACI 318M-05," American Concrete Institute, Detroit, 436 pp.
- ACI 440R-96, 1996. "State-of-the-Art Report on Fiber Reinforced Plastic (FRP) Reinforcement for Concrete Structures", American Concrete Institute, Detroit, 65 pp.
- De Lorenzis, L. and Nanni, A., 2001. "Shear Strengthening of Reinforced Concrete Beams with Near-Surface Mounted Fiber-Reinforced Polymer Rods", ACI Structural Journal, V. 98, No. 1, Jan.-Feb., pp. 60-68.
- Deniaud, C. and Cheng, J.J., 2001. "Shear Behavior of Reinforced Concrete T-Beams with Externally Bonded Fiber-Reinforced Polymer Sheets," ACI Structural Journal, V. 98, No. 3, pp. 386-394.
- Khalifa, A., Gold, A, Nanni, A and Abdel Aziz, M.I., 1998. "Contribution of Externally Bonded FRP to Shear Capacity of Flexural Members," ASCE Journal of Composites for Construction, V. 2, No. 4, pp. 195-203.
- Rubinsky, I.A. and Rubinsky, A., 1954. "An Investigation into the Use of Fiber-Glass for Pre-stressed Concrete," Magazine of Concrete Research, V.6, pp. 71-78.
- Shehata, E., Morphy, R. and Rizkalla, S., 2000. "Fiber Reinforced Polymer Shear Reinforcement for Concrete Members: Behavior and Design Guidelines," Canadian Journal of Civil Engineering, V. 27, pp. 859-872.

# Modeling of Cost-Effective Residential Houses in Kuwait

<sup>1</sup>Hasan A. Kamal, <sup>1</sup>Shaikha A. Al-Sanad, <sup>1</sup>Saud F. Al-Otaibi and <sup>2</sup>Shaikha F. Al-Fulaij

<sup>1</sup>Building and Energy Technologies Department, and <sup>2</sup>Quantitative Methods and Modeling Department, Kuwait Institute for Scientific Research, Kuwait

#### Abstract

The construction industry is a major sector in Kuwait's economy. This industry is rapidly expanding since the last few years. The majority of buildings in Kuwait are made of concrete frame structures. More that 90% of the conventional buildings are residential and individual houses. The single type houses are the most dominant residential houses. In Kuwait, two main systems are available for the householders to own a house. The first system is to build their own house which will enforce them abide by all processes of construction such as design, supervision and construction. The advantage is building a house that meets the owner's needs. The second system is to buy an already constructed house with the advantage of saving time and effort of construction but the house may not meet all the owner's requirements. Residential houses in Kuwait are known to be expensive, compared to other countries in the region. The cost of those houses is affected by the construction systems, technologies and materials. Another major factor that contributes to increase in the cost of residential houses is improper space utilization of the houses, which is influenced by lack of understanding of the actual needs and social habits.

A study is conducting to investigate the current practices for construction of residential buildings in Kuwait. The main factors that affect the cost of such buildings are identified. This paper will emphasize on the different aspects related to enhancing the cost of houses. A mathematical model will be developed for cost-effective houses in Kuwait. The model will take into consideration the current practices of building materials and space distributions. Simulation method will be used for cost estimation of houses counting for the existed uncertainties in the cost of materials and other aspects. Accordingly, the optimal cost-effective residential houses in Kuwait will be estimated.

**Key Words**: Construction, Building, Cost, Model, Simulation.

#### Introduction

In Kuwait, individually owned houses are the dominating residential buildings, which comprise around 85% of the total number of buildings. The government provides a respectable support to the Kuwaiti residents for owning their houses. Efforts for finding methods to reduce the cost of houses will significantly impact the residents and national expenditure of the construction sector. Taking into consideration the cost of land in Kuwait, a house is measured as the top investment-consuming aspect of individual's considerations.

It is important for individuals to accurately estimate the cost of houses before commencement of the construction. The allocation budget for building a house must be properly utilized by owners (individuals). Cost estimation of a house is the process of establishing the expected cost required to complete a house in accordance to the design drawings and specifications, prior to commencement of construction. During the design phase of a house, it is necessary for the owners, who lack knowledge of construction to understand the factors that affect the construction cost. Those factors could be related to the design and space utilization of the house, materials used and construction system.

# Background

# Construction Practice of Residential Houses

Building houses in Kuwait is considered costly, compared to the houses in the neighboring countries in the region. The building materials and system technology is the main cause of the high cost. Almost all residential houses are constructed of concrete. The frame system is constructed with reinforced concrete, then the walls are filled with masonry to construct internal and external partitions (Al-Khayyat et al., 1989). Most of the building materials are imported and manpower is locally trained by practice.

Construction of residential houses in Kuwait is guided by three different methods. The design and construction of houses for the three methods is categorized as: 1) design and construction by the governmental Public Authority for Housing Welfare (PAHW), 2) design and construction by private construction companies and 3) a land and loan system by the government that allows individuals to design and construct their own houses.

For individually built residential houses, owners usually take the responsibility to design the house based on their expected needs and requirements. From previous experience, the designed systems and materials normally tend to be over-designed. The built-up spaces, in some cases, are not properly utilized. Therefore, exaggeration in space utilization and distribution add more cost to the house.

#### Cost Estimation

Cost is a major criterion for the parties of any project contract. Housing projects is one type of such projects. It is important to accurately and precisely estimate the cost of a house in the pre-construction stage and after completing the design drawings. Owners

need this information for managing the overall budget of house construction. Contractors also need this information for determining their profits. Several cost estimation techniques are used for construction projects based on designers' experience and the available information from previously executed and related projects.

Several cost estimation methods are used for the different phases of a project. In order to know the cost of project phases or activities, a breakdown of the cost and quality of each item used is determined. For concrete framing systems, it is essential to know the items contributing to the cost of the systems during the design phase of a house. This information will assist designers to estimate and optimize the cost of the house.

The cost of housing structures in current practices is impacted significantly by the design of the house and the selected materials specified for constructing (Mohamed and Celik, 2002). The cost of a house, for example, include the structural framing system, concrete works, site works, walls, mechanical system, electrical system, finishing, and general requirements.

## Uncertainty

Uncertainty comprises of cost estimation of housing projects as the cost of buildings materials and manpower varies during the house construction cycle. The source of uncertainty is present in the actual cost of the needed materials and manpower. Several factors affect the material cost, for example, the local market price fluctuation due to supply and demand, quality, etc. The quality is the main source for manpower cost.

Principle sources of uncertainty include variations in items and subsystem performance, inaccurate data, insufficient information, lack of experience. The uncertainties in construction management relate to scheduling uncertainty, cost uncertainty, and technological uncertainty (Shtub et al., 1994). The market price fluctuation of building materials is considered as a source of uncertainty of the exact cost of building materials. This uncertainty will influence the accuracy of the total cost estimation of houses.

## Simulation Methods

Simulation methods have been used in the last decades due to the vast advancement in the computational methods. Simulation can be defined as the process of conducting experiments on a model (mathematical or physical) instead of direct application on a real system. A model is a representation of the real system for the purpose of studying its performance. The uncertainty or randomness inherent in the model elements is incorporated into the model. The experiments are designed to account for this uncertainty. It is important in the simulation method to accurately represent the system under study. The simulation accuracy increases as the number of simulation cycles increases, which is a costly and time-consuming process especially for large systems (Ayyub and McCuen, 1997). Monte Carlo simulation is the most common simulation method. The Monte Carlo simulation deals with non-probabilistic system architecture using probabilistic method to probabilistically assess the output variable of interest.

# **Objectives**

The main objectives of this paper are as follows:

- To investigate the current practice for construction of residential houses in Kuwait.
- To determine the aspects contributing to the cost of residential houses.
- To propose a simulation model for cost-effective houses in Kuwait.

#### Method for Cost Estimation of Residential Houses

#### Factors Affecting the Cost of Houses

Several factors directly or indirectly affect the cost of houses. Those factors are, for example, cost of design process, material cost, workmanship cost, finishing quality cost, social-technical needs for Kuwaiti families that are incorporated in the design, space distribution, etc. In order to clearly understand the quantification process and cost calculation for cost of houses, the Bill of Quantity (BOQ) documents for many housing projects in Kuwait are collected.

The items that are included in the design and construction of those houses are identified and classified. They can be divided into two main types, frame system cost and finishing cost. The frame systems of the houses are all constructed in a skeleton system using reinforced concrete members. The finishing cost includes the cost of all materials used to complete the construction upto its final stage, except the concrete frame.

In order to simplify the cost estimation process, the items that are used in the frame system and finishing costs are re-categorized into eight types. Each type includes the cost of material used, in addition to the workmanship cost. As per collected data, the cost of each type is calculated in Kuwaiti Dinars per square meter of the house built-up area, KD/m<sup>2</sup>. The eight types of cost items used for estimating the cost of a house are defined as: 1) general requirement, 2) site work, 3) concrete work, 4) masonry work, 5) thermal and moisture protections, 6) doors and windows, 7) finishing works and 8) electro-mechanical services.

The General requirements include the administrative works of the project. The site survey and excavation works at the beginning of the project is included in the site work. The concrete work item contains the works conducted for the concrete framing system. The masonry work includes all block items for constructing walls and partitions. All items of water and thermal proofing of roofs, foundations and structural walls are included under thermal and moisture protections.

The doors and windows work include design, supply and installation of all doors and windows in the house. The finishing works include all plaster work, false ceiling, ceramic tile, marble and painting of walls and ceiling work. The electrical and mechanical works of the houses that include supply and installation are provided in the Electro-mechanical services.

# Mathematical Model

In order to estimate the cost of a residential house, the design of the house must be completed and details of drawings are prepared. The items used in constructing the houses are identified. The price of each item is determined based on the market rate. According to the house design and prepared drawings, the built-up areas that are related to the above items are calculated. The total cost of the house is then estimated based on the rates collected and areas calculated from the drawings. The calculation process is explained in Eq. 1 and defined as

$$TC = \sum_{i=1}^{n} (MC_i)(A_i)$$
 (1)

where TC is the total cost of a house,  $MC_i$  is the cost of material item i,  $A_i$  is the built-up area of item i of the house and n is the number of materials.

# Simulation Application

Monte Carlo simulation method is used to estimate the cost of houses. The simulation program depends on the collected data of the market price for each factor contributing to the cost of houses as previously explained. A probabilistic method is used to rationally estimate the house cost. Uncertainty exists in the cost of most items of houses. Therefore, the range of price cost per square meter of built-up area for each type of cost item is assumed. The probabilistic parameters for those items called random variables, are determined such as the probability density function, mean and standard deviation.

The direct Monte Carlo simulation approach consists of drawing samples of the random variables according to their corresponding probability density functions and, then, feeding the samples back into the performance function (Kamal 2001). Drawing and feeding the samples of the random variables process is repeated for *N* time's simulation cycles (Kamal and Al-Rasheed, 2006).

The mean of the total cost of a house is defined as

$$\mu(TC) = \frac{\sum_{j=1}^{N} TC_j}{N}$$
 (2)

where  $\mu(TC)$  is the mean value of the total cost of a house,  $TC_i$  is the total cost simulation cycle j, and N is the number of simulation cycles.

$$COV(TC) = \frac{\sigma(TC)}{\mu(TC)}$$
(3)

where COV(TC) is the coefficient of variation of the total cost of a house,  $\sigma(TC)$  is the standard deviation of the total cost and  $\mu(TC)$  is the mean of the total cost.

# **Case Study: Residential House without Basement**

## Description

A residential house in Kuwait was selected as a case study for estimating the construction cost. The house is a three-story concrete building designed by an individual owner and constructed by a locally selected contractor. The area of the house land is 400 m². Based on the blue print of the house, the total built-up area of the house is 972 m² including ground, first, second and top floors. Detail of built-up area distribution of each floor is shown in Table 1.

Table 1. Distribution of Built-Up Areas in the Selected House

Description	Built-up Area (m²)
Ground Floor	350
First Floor	277
Second Floor	345
Top Floor	68
Total	972

# Residential House Cost Based on BOO Rates Method

According to the Bill of Quantity rates of this residential house, the total cost of each item is calculated. The calculation is also based on the built-up area for each type and item. Table 2 lists the cost breakdown of each of the eight types and items used in constructing the house. The total construction cost of the building is equal to K.D.106,191. The cost of square meter of built-up area including all costs of construction equals to K.D.109 (One hundred nine Kuwaiti Dinars per square meter of total built-up area). This value is the outcome of dividing the total cost (K.D.106,191) by the total built-up area (972 m²).

The ratio (cost percentage) of each construction material type of items is shown in Figure 1. The items are sorted in descending order showing that the concrete works contribution is 31% to the total cost of the house, finishing work 20%, electromechanical services 18%, masonry 10%, doors and windows 8%, thermal and moisture protection 5%, site work 4% and general requirements 4%.

Table 2. Cost Breakdown of Construction Types and Items

Description	Cost K.D.
General Requirements	4,000
Site Works	4,593
Concrete Works	32,530
Masonry Works	10,858
Thermal and Moisture Protection	5,120
Doors and Windows	8,320
Finishing work	21,330
Electromechanical services	19,440
Total	106,191

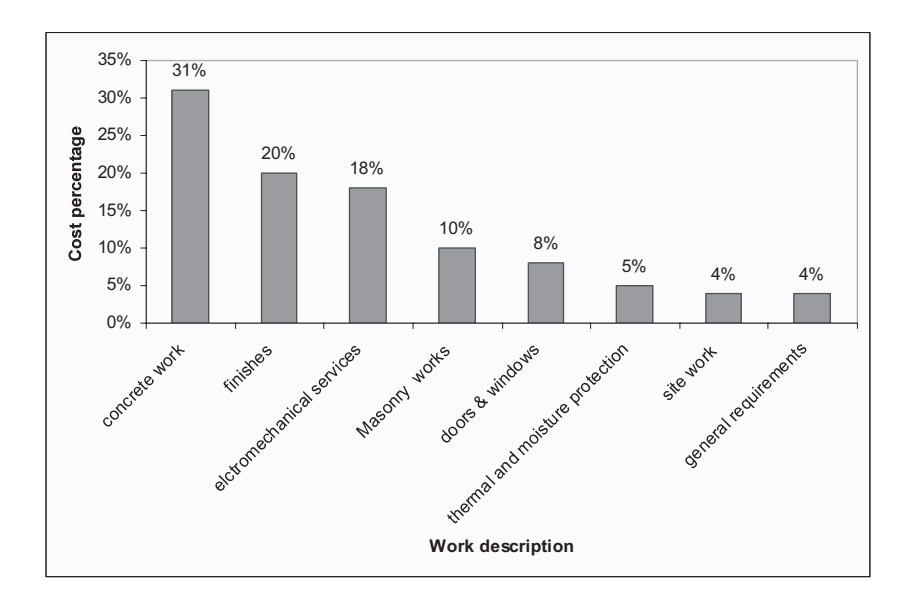


Fig. 1. Cost ratio (percentage) of construction items.

# Cost Estimation Based on Simulation Method

The Direct Monte Carlo simulation method is used to estimate the cost of the house. The built-up area is as above and equals to 972 m<sup>2</sup>. The probabilistic parameters for the material types and items are estimated. The estimation is based on the market price rate and expert opinion. As listed in Table 3, the probability distribution function for all items is assumed normal. The mean and standard deviation of each item is determined. The Electro-mechanical services item is assumed constant and equals to K.D. 15,000 for a three-floor house with a land area close to 400 m<sup>2</sup>.

A computer program code is developed to conduct the Monte Carlo simulation method for estimating the total cost of the house using the probabilistic parameters listed in Table 3. Samples of material items are drawn using the listed parameters for each simulation cycles. The computer program was operated five times for the following simulation cycles, 10, 100, 1000, 10000 and 100000. For each run, the mean, standard deviation and coefficient of variation was calculated for the total cost of the house using equations. 2 and 3, respectively. Table 4 lists the results of the simulation method. For each square meter of built-up area, the average cost the house in K.D. is calculated to be around K.D.107.

Table 3. Estimated Probabilistic Characteristics for the Cost of all Items in K.D.

Items	Distribution Type	Mean (µ)	Std Dev (σ)
General requirement	Normal	5.5	2.5
Site works	Normal	5.0	2.0
Concrete works	Normal	33.0	15.5
Masonry works	Normal	11.5	4.0
Thermal and moisture protection	Normal	5.25	2.5
Doors and windows	Normal	9.0	3.5
Finishes	Normal	22.0	15.0
Electro-mechanical services	Constant	15,000	-

Table 4. Monte Carlo Simulation Results for the House Cost In K.D.

No. of Cycles	Mean (µ)	Std Dev $(\sigma)$	COV
10	111,723	2,8452	0.255
100	104,045	24,033	0.231
1,000	103,366	22,203	0.215
10,000	103,500	22,151	0.214
100,000	103,881	21,848	0.210

## Discussions

From the two methods of estimation for the cost of the house, it is an easy process to normalize the house cost in K.D. per square meter of the total built-up area. This estimation is an indication of the cost that is affected by the quality of materials used for the finishing works. The total cost of the house using the BOQ rates is calculated as to K.D.106,191 while the total house cost using the simulation is K.D.103,881 for 100,000 simulation runs. The difference is around 2%. As shown in Table 4, the accuracy of simulation is slightly improved by increasing the number of simulation cycles, reduction in COV values. The estimated cost of the rate of square meter with respect to the total

built up area is almost the same for both traditional and simulation methods, 107 KD/m<sup>2</sup> and 106.5 KD/m<sup>2</sup> respectively.

#### Conclusions

A study was conducted to estimate the cost of residential houses in Kuwait. The current practices of construction of residential house are investigated. It is observed that individuals who construct their own houses from design to construction phases have exaggerated in designs and, therefore, increase the cost of the house. Another observation is that the distribution of spaces of those houses is not utilized properly. This leads to improper utilization of the house budget.

Different aspects contributing to the cost of a house are determined based on material items used in construction. The concrete works of the construction indicated the highest budget consumption of houses, for internal finishing works, electro-mechanical services, masonry works, doors and windows, thermal and moisture protection, site work, and general requirements, respectively.

The unit cost in K.D. per unit area of built-up area is calculated in this study and is an appropriate indication to estimate the total cost of construction of houses. The total cost of both traditional and simulation methods are estimated. Both costs are useful to estimate the budget.

The computer program developed for the simulation method provides flexible method for estimating a house cost. The 'What-If' technique can be used to change the simulation parameters (material items) in order to measure their impact on the total cost of a house. This technique will provide a methodology for helping individuals to construct cost-effective houses that meet their needs within the initially allocated budget.

# References

- Al-Khayyat, H.; N. Qaddumi; M. Al-Shaleh; and D. Atawneh (1987) "Investigation of building systems in housing projects", (BM-22/4). Kuwait Institute for Scientific Research, Report N. KISR2426, Kuwait.
- Ayyub, B., and McCuen, R., 'Probability, Statistics, and Reliability for Engineers', CRC Press LLC, 1997.
- Kamal, H.A., 'Simulation-Based Reliability Assessment Methods of Structural Systems', *Ph.D. Dissertation*, University of Maryland at College Park, 2001, 268 pp.
- Kamal, H. A., and Al-Rasheed, K. A. "Simulation-based Cost Estimation of Structural Concrete Systems in Kuwait," The International Conference on Civil Engineering Infrastructure Systems, American University of Beirut, Beirut, Lebanon, June 12-14 2006.
- Mohamed, A., and Celik, T., 'Knowledge-based System for Alternative Design, Cost Estimating and Scheduling', *Knowledge Based Systems*, 15, 2002, 177-188.
- Shtub, A., Bard J.F. and Globerson, S., 'Project Management: Engineering, Technology, and Implementation', Prentice-Hall, Inc., 1994, 634 pp.

# **List of Authors**

Antoine E. Naaman Professor of Civil Engineering University of Michigan Ann Arbor, U.S.A.

email: naaman@engin.umich.edu

A. A. Maghsoudi
Assistant Professor
Civil Engineering Department
Kerman University
Kerman, Iran
email: maghsoudi.a.a@mail.uk.ac.ir

A. A. Shahin
Fayoum University
Faculty of Engineering
Civil Engineering Department
Fayoum, Egypt

A. Chateauneuf Laboratory of Civil Engineering University Blaise Pascal Clermont, France

A. R. Khaloo Civil Engineering Department Sharif University of Technology Azadi Ave, P.O.Box 11365-9313 Tehran, Iran email: khaloo@sharif.edu

A. Serag
Fayoum University
Faculty of Engineering
Civil Engineering Department
Fayoum, Egypt

Abdullah Al-Saidy Department of Civil and Architectural Engineering, College of Engineering Sultan Qaboos University P. O. Box 33 Al-Khaudh 123 Sultanate of Oman

Abdullateef M. AlKhaleefi Civil Engineering Department College of Engineering and Petroleum Kuwait University Kuwait email: khaleefi@civil.kuniv.edu.kw Abdurrahman A. Elgalhud Al-Fateh University P O Box 83038, Tripoli, Libya.

Adnan S. Masri Associate Professor of Civil Engineering Beirut Arab University Lebanon

Ahmed E. Ben-Zeitun Al-Fateh University P O Box 83038, Tripoli, Libya

Ali Abdul-Jaleel Research Associate Building and Energy Technologies Dept. Kuwait Institute for Scientific Research P.O. Box 24885 13109 Safat Kuwait

Ali Al-Harthy Dept. of Civil & Architectural Eng. College of Engineering Sultan Qaboos University P.O.Box 33 Al-Khaudh 123 Sultanate of Oman

Aman Mwafy Mid-America Earthquake Centre University of Illinois at Urbana-Champaign Illinois, U.S.A

Amr S. El-Deeb Ain Shams University Cairo, Egypt

Amr S. Elnashai Mid-America Earthquake Center Department of Civil & Environmental Engineering University of Illinois at Urbana-Champaign Urbana, IL 61801, U.S.A.

Amr W. Sadek Building and Energy Technologies Dept. Kuwait Institute for Scientific Research P.O. Box 24885 13109 Safat Kuwait B. Toumi University of Ouem El Bouaghi Algeria

Cene Krasniqi
Faculty of Civil Engineering
Prishtine,
Kosovo

Daniel A. Kuchma Mid-America Earthquake Center Dept. of Civil & Environmental Eng. University of Illinois at Urbana-Champaign Urbana, IL 61801, U.S.A.

F. Faraji M. Sc. Student of Metallurgy Engineering Department Kerman University Kerman, Iran, email: ftmfji@yahoo.com

Faisal Shalabi Assistant Professor The Hashemite University Jordan

Farzad Arabpour Dahooei Concrete Research & Education Center (ConREC) P.O.Box: 15875- 4498 Tehran, Iran email: info@aciiranchapter.org

Fisnik Kadiu Faculty of Civil Engineering Tirane, Albania

Fouad. A. Kasti Dar Al-Handasah Verdun St. P.O. Box: 11-7159 Beirut 1107 2230, Lebanon email: Fouad.kasti@dargroup.co

G. Escadeillas LMDC INSA-UPS Toulouse France Ghassan K. Al-Chaar Construction Engineering Research Laboratory University of Illinois U.S.A

H. Chabil University of Constantine Algeria.

H. Houari University of Constantine Algeria.

H. Kamal Building and Energy Technologies Dept. Kuwait Institute for Scientific Research P.O. Box 24885 13109 Safat Kuwait Email: hkamal@safat.kisr.edu.kw

Hakim S. Abdelgader Al-Fateh University P O Box 83038 Tripoli, Libya email: hakimsa@poczta.onet.pl

Hisham Abdel-Fattah Department of Civil Engineering College of Engineering University of Sharjah P. O. Box 27272 Sharjah, UAE

Hisham Qasrawi Senior Lecturer The Hashemite University, Jordan email: qasrawi2@yahoo.com

Hisham S. Basha Associate Professor of Civil Engineering Beirut Arab University Lebanon

Ibrahim Asi Associate Professor The Hashemite University Jordan Issam E. Harik
Raymond Blythe Professor of Civil
Engineering & Program Manager,
Structures and Coatings
Kentucky Transportation Center,
University of Kentucky
Lexington, KY 40506-0281, U.S.A
email: iharik@engr.uky.edu

J. Kwok MMFX Technologies Corporation Irvine

California, U.S.A.

Jun Ji Mid-America Earthquake Center Department of Civil & Environmental Engineering University of Illinois at Urbana-Champaign Urbana, IL 61801, U.S.A.

K. Demagh Department of Civil Engineering University of Batna Algeria

K. M. Othman
Fayoum University
Faculty of Engineering
Civil Engineering Department
Fayoum, Egypt

Khaldoun Rahal Associate Professor Civil Engineering Department Kuwait University, Kuwait email: rahal@civil.kuniv.edu.kw

M. A. A. El Aziz Fayoum University Faculty of Engineering Civil Engineering Department Fayoum, Egypt

M.N. Haque
Department of Civil Engineering
College of Engineering and Petroleum
University of Kuwait
PO Box 5969, Kuwait
email: Naseer@civil.kuniv.edu.kw

Moetaz M. El-Hawary Research Scientist Building and Energy Technologies Dept. Kuwait Institute for Scientific Research P.O. Box 24885 13109 Safat Kuwait email: <a href="mailto:mhawary@safat.kisr.edu.kw">mhawary@safat.kisr.edu.kw</a>

Mohammad A. Sabra MSE, Beirut Arab University, Lebanon

Naser Kabashi Faculty of Civil Engineering Prishtine, Kosovo

Nayef Z. AlMutairi Civil Engineering Department College of Engineering and Petroleum Kuwait University, Kuwait

O. Kayali School of Aerospace Civil and Mechanical Engineering University of New South Wales @ ADFA Canberra, Australia email: o.kayali@adfa.edu.au

O. Salah Zamil Holding Group Kingdom of Saudi Arabia

Oh-Sung Kwon Mid-America Earthquake Center Dept. of Civil & Environmental Eng. Univ. of Illinois at Urbana-Champaign Urbana, IL 61801, U.S.A.

R. S. Manjrekar Chairman and Managing Director Sunanda Speciality Coatings Pvt.Ltd. Mumbai, India

Ramzi Taha Department of Civil and Architectural Engineering, College of Engineering Sultan Qaboos University P.O.Box 33 Al-Khaudh 123 Sultanate of Oman Robert David Hossell Grace Construction Products Dubai, UAE

S. Faza MMFX Technologies Corporation Irvine, California, U.S.A.

S.A.Taheri Civil Engineering Department Sharif University of Technology Azadi Ave, P.O.Box 11365-9313 Tehran, Iran email: ataheri@mehr.sharif.ir

S.K.Manjrekar Sunanda Speciality Coatings Pvt. Ltd. Mumbai, India

Salim Al-Oraimi
Dept. of Civil and Architectural Eng.
College of Engineering
Sultan Qaboos University
P.O.Box 33 Al-Khaudh 123
Sultanate of Oman

Sameer Hamoush Civil and Architectural Engineering Department North Carolina A&T State University Greensboro, NC 27411, U.S.A.

Saud F. Al-Otaibi Associate Research Scientist Building and Energy Technologies Dept. Kuwait Institute for Scientific Research P.O. Box 24885 13109 Safat Kuwait Seleem Saleh El sayed Ahmad Associate Professor Department of Engineering Materials Faculty of Engineering Zagazig University, Egypt email: sse ahmad@yahoo.com

Shaikha A. Al-Sanad Building and Energy Technologies Dept. Kuwait Institute for Scientific Research P.O. Box 24885 13109 Safat Kuwait

Shaikha F. Al-Fulaij Quantitative Methods and Modeling Department, Kuwait Institute for Scientific Research P.O. Box 24885 13109 Safat Kuwait

Tarek Anwar Awida Assistant Professor Structural Engineering Department Faculty of Engineering Ain Shams University Cairo, Egypt. email: TarekA@keoic.com

Z. Guemmadi University of Constantine Algeria

Ziad M. Mousa MSE Beirut Arab University Lebanon



شركة مجموعة فورفيلمز للطباعة Four Films Printing Group

> ماتف: Tel: 965 4820150 www.fourfilms.com